

Return To
SCIENCE AND TECHNOLOGY DIVISION
Library of Congress

DECLASSIFIED
By authority Secretary of

SEP 7 1960

Def memo 2 August 1960

LIBRARY OF CONGRESS

LC REGULATION: BEFORE SERVICING
OR REPRODUCING ANY PART OF THE
DOCUMENT, ALL CLASSIFICATION
MARKINGS MUST BE CANCELLED.

Return To
SCIENCE AND TECHNOLOGY DIVISION
Library of Congress

4613

DECLASSIFIED
By authority Secretary of

SEP 7 1960

Defense memo 2 August 1960


LIBRARY OF CONGRESS

SUMMARY TECHNICAL REPORT
OF THE
NATIONAL DEFENSE RESEARCH COMMITTEE

LC REGULATION: BEFORE SERVICING
OR REPRODUCING ANY PART OF THIS
DOCUMENT, ALL CLASSIFICATION
MARKINGS MUST BE CANCELLED.

This document contains information affecting the national defense of the United States within the meaning of the Espionage Act, 50 U. S. C., 31 and 32, as amended. Its transmission or the revelation of its contents in any manner to an unauthorized person is prohibited by law.

This volume is classified ~~SECRET~~ in accordance with security regulations of the War and Navy Departments because certain chapters contain material which was ~~SECRET~~ at the date of printing. Other chapters may have had a lower classification or none. The reader is advised to consult the War and Navy agencies listed on the reverse of this page for the current classification of any material.



Manuscript and illustrations for this volume were prepared for publication by the Summary Reports Group of the Columbia University Division of War Research under contract OEMsr-1131 with the Office of Scientific Research and Development. This volume was printed and bound by the Columbia University Press.

Distribution of the Summary Technical Report of NDRC has been made by the War and Navy Departments. Inquiries concerning the availability and distribution of the Summary Technical Report volumes and microfilmed and other reference material should be addressed to the War Department Library, Room 1A-522, The Pentagon, Washington 25, D. C., or to the Office of Naval Research, Navy Department, Attention: Reports and Documents Section, Washington 25, D. C.

Copy No.

239

This volume, like the seventy others of the Summary Technical Report of NDRC, has been written, edited, and printed under great pressure. Inevitably there are errors which have slipped past Division readers and proofreaders. There may be errors of fact not known at time of printing. The author has not been able to follow through his writing to the final page proof.

Please report errors to:

JOINT RESEARCH AND DEVELOPMENT BOARD
PROGRAMS DIVISION (STR ERRATA)
WASHINGTON 25, D. C.

A master errata sheet will be compiled from these reports and sent to recipients of the volume. Your help will make this book more useful to other readers and will be of great value in preparing any revisions.

SUMMARY TECHNICAL REPORT OF DIVISION 6, NDRC

VOLUME 12

DECLASSIFIED

By authority Secretary of

SEP 7 1960

Defense memo 2 August 1960

LIBRARY OF CONGRESS

DESIGN AND CONSTRUCTION OF CRYSTAL TRANSDUCERS

LC REGULATION: BEFORE SERVICING
OR REPRODUCING ANY PART OF THIS
DOCUMENT, ALL CLASSIFICATION
MARKINGS MUST BE CANCELLED.

OFFICE OF SCIENTIFIC RESEARCH AND DEVELOPMENT
VANNEVAR BUSH, DIRECTOR

NATIONAL DEFENSE RESEARCH COMMITTEE
JAMES B. CONANT, CHAIRMAN

DIVISION 6
JOHN T. TATE, CHIEF

WASHINGTON, D. C., 1946



NATIONAL DEFENSE RESEARCH COMMITTEE

James B. Conant, *Chairman*

Richard C. Tolman, *Vice Chairman*

Roger Adams	Army Representative ¹
Frank B. Jewett	Navy Representative ²
Karl T. Compton	Commissioner of Patents ³
Irvin Stewart, <i>Executive Secretary</i>	

¹*Army representatives in order of service:*

Maj. Gen. G. V. Strong	Col. L. A. Denson
Maj. Gen. R. C. Moore	Col. P. R. Faymonville
Maj. Gen. C. C. Williams	Brig. Gen. E. A. Regnier
Brig. Gen. W. A. Wood, Jr.	Col. M. M. Irvine
	Col. E. A. Routheau

²*Navy representatives in order of service:*

Rear Adm. H. G. Bowen	Rear Adm. J. A. Furer
Capt. Lybrand P. Smith	Rear Adm. A. H. Van Keuren
Commodore H. A. Schade	

³*Commissioners of Patents in order of service:*

Conway P. Coe	Casper W. Ooms
---------------	----------------

NOTES ON THE ORGANIZATION OF NDRC

The duties of the National Defense Research Committee were (1) to recommend to the Director of OSRD suitable projects and research programs on the instrumentalities of warfare, together with contract facilities for carrying out these projects and programs, and (2) to administer the technical and scientific work of the contracts. More specifically, NDRC functioned by initiating research projects on requests from the Army or the Navy, or on requests from an allied government transmitted through the Liaison Office of OSRD, or on its own considered initiative as a result of the experience of its members. Proposals prepared by the Division, Panel, or Committee for research contracts for performance of the work involved in such projects were first reviewed by NDRC, and if approved, recommended to the Director of OSRD. Upon approval of a proposal by the Director, a contract permitting maximum flexibility of scientific effort was arranged. The business aspects of the contract, including such matters as materials, clearances, vouchers, patents, priorities, legal matters, and administration of patent matters were handled by the Executive Secretary of OSRD.

Originally NDRC administered its work through five divisions, each headed by one of the NDRC members. These were:

- Division A — Armor and Ordnance
- Division B — Bombs, Fuels, Gases, & Chemical Problems
- Division C — Communication and Transportation
- Division D — Detection, Controls, and Instruments
- Division E — Patents and Inventions

In a reorganization in the fall of 1942, twenty-three administrative divisions, panels, or committees were created, each with a chief selected on the basis of his outstanding work in the particular field. The NDRC members then became a reviewing and advisory group to the Director of OSRD. The final organization was as follows:

- Division 1 — Ballistic Research
- Division 2 — Effects of Impact and Explosion
- Division 3 — Rocket Ordnance
- Division 4 — Ordnance Accessories
- Division 5 — New Missiles
- Division 6 — Sub-Surface Warfare
- Division 7 — Fire Control
- Division 8 — Explosives
- Division 9 — Chemistry
- Division 10 — Absorbents and Aerosols
- Division 11 — Chemical Engineering
- Division 12 — Transportation
- Division 13 — Electrical Communication
- Division 14 — Radar
- Division 15 — Radio Coordination
- Division 16 — Optics and Camouflage
- Division 17 — Physics
- Division 18 — War Metallurgy
- Division 19 — Miscellaneous
- Applied Mathematics Panel
- Applied Psychology Panel
- Committee on Propagation
- Tropical Deterioration Administrative Committee

NDRC FOREWORD

DECLASSIFIED

By authority Secretary of

plicated in the Summary Technical Report of NDRC, the monographs are an important part of the story of these aspects of NDRC research.

In contrast to the information on radar, which is of widespread interest and much of which is released to the public, the research on subsurface warfare is largely classified and is of general interest to a more restricted group. As a consequence, the report of Division 6 is found almost entirely in its Summary Technical Report, which runs to over twenty volumes. The extent of the work of a Division cannot therefore be judged solely by the number of volumes devoted to it in the Summary Technical Report of NDRC: account must be taken of the monographs and available reports published elsewhere.

Any great cooperative endeavor must stand or fall with the will and integrity of the men engaged in it. This fact held true for NDRC from its inception, and for Division 6 under the leadership of Dr. John T. Tate. To Dr. Tate and the men who worked with him—some as members of Division 6, some as representatives of the Division's contractors—belongs the sincere gratitude of the Nation for a difficult and often dangerous job well done. Their efforts contributed significantly to the outcome of our naval operations during the war and richly deserved the warm response they received from the Navy. In addition, their contributions to the knowledge of the ocean and to the art of oceanographic research will assuredly speed peacetime investigations in this field and bring rich benefits to all mankind.

The Summary Technical Report of Division 6, prepared under the direction of the Division Chief and authorized by him for publication, not only presents the methods and results of widely varied research and development programs but is essentially a record of the unstinted loyal cooperation of able men linked in a common effort to contribute to the defense of their Nation. To them all we extend our deep appreciation.

VANNEVAR BUSH, Director
Office of Scientific Research and Development

J. B. CONANT, Chairman
National Defense Research Committee

AS EVENTS of the years preceding 1940 revealed more and more clearly the seriousness of the world situation, many scientists in this country came to realize the need of organizing scientific research for service in a national emergency. Recommendations which they made to the White House were given careful and sympathetic attention, and as a result the National Defense Research Committee [NDRC] was formed by Executive Order of the President in the summer of 1940. The members of NDRC, appointed by the President, were instructed to supplement the work of the Army and the Navy in the development of the instrumentalities of war. A year later, upon the establishment of the Office of Scientific Research and Development [OSRD], NDRC became one of its units.

The Summary Technical Report of NDRC is a conscientious effort on the part of NDRC to summarize and evaluate its work and to present it in a useful and permanent form. It comprises some seventy volumes broken into groups corresponding to the NDRC Divisions, Panels, and Committees.

The Summary Technical Report of each Division, Panel, or Committee is an integral survey of the work of that group. The first volume of each group's report contains a summary of the report, stating the problems presented and the philosophy of attacking them, and summarizing the results of the research, development, and training activities undertaken. Some volumes may be "state of the art" treatises covering subjects to which various research groups have contributed information. Others may contain descriptions of devices developed in the laboratories. A master index of all these divisional, panel, and committee reports which together constitute the Summary Technical Report of NDRC is contained in a separate volume, which also includes the index of a microfilm record of pertinent technical laboratory reports and reference material.

Some of the NDRC-sponsored researches which had been declassified by the end of 1945 were of sufficient popular interest that it was found desirable to report them in the form of monographs, such as the series on radar by Division 14 and the monograph on sampling inspection by the Applied Mathematics Panel. Since the material treated in them is not du-

FOREWORD

A TRANSDUCER, as described in this volume, is a device capable of converting electrical energy into sound energy when used as a projector, and capable of converting sound energy into electrical energy when used as a receiver. Although in an echo-ranging set the transducer serves this dual purpose, in many other applications, the transducer is employed as a sound projector only or as a sound receiver only. In practically all of the many military applications of underwater sound, a transducer of one type or another is required. It was appropriate, therefore, that adequate provision should be made for research upon the physical principles underlying transducer design.

It is possible to construct transducers employing any one of a number of different physical principles. However, it is believed that the most satisfactory structures for sonar applications utilize either the magnetostriction effect exhibited by certain magnetic materials such as nickel and certain of its alloys, or the piezoelectric effect exhibited by certain crystals, such as quartz, Rochelle salt, and ammonium dihydrogen phosphate.

The research undertaken by the Division was principally concerned with transducers of these two types. The results of studies pertinent to the design of magnetostriction transducers and materials are reported by Dr. Sabine of the Harvard University Underwater Sound Laboratory in Volume 13 of this series. This volume

reports the results of studies of transducer design involving the piezoelectric effect. It should be recognized that the research of the Division summarized in these volumes was a continuation or expansion of previous work, and supplemented other research in progress.

Prior to the war both British and U. S. service laboratories had developed effective transducers for incorporation in echo-ranging sets and for use in other equipment. During the war period, the Navy continued its research both in the Naval Research Laboratory and through support and sponsorship of research and development by industrial organizations. The total research and development effort was therefore very considerable and very substantial advance was made.

The preparation of this report was undertaken by members of the U. S. Navy Electronics Laboratory (the Division's San Diego Laboratory, UCDWR, until March 1945), and the Division is grateful to the authors and to the Navy for making possible the completion of this report after the San Diego Laboratory was transferred to Navy direction. The transducer research program received constant support from the Navy and splendid cooperation between the various agencies engaged in research and development was secured for cordial interchange of information.

JOHN T. TATE
Chief, Division 6

PREFACE

THIS VOLUME seeks to give an account of the present state of transducer theory and of the art of transducer construction. Although a serious effort has been made by its authors to describe the work and thinking of other laboratories, it is inevitable that such a volume will be biased toward the home laboratory. Because they are better known to the present authors, the techniques practiced by and transducers built by the University of California Division of War Research [UCDWR] are given more space than those of other laboratories.

The general level of the book is variable. Some sections, such as those on construction techniques, can be read by anyone having only a slight technical background. Others require an extensive training in theoretical physics in order to appreciate their content. This is particularly true of the basic discussion in Chapter 2. However, since the various portions are not interdependent, the book should be generally useful to all engaged in the transducer art.

This volume has many authors and the various chapters must be regarded as a contribution from the author or authors listed. The editor has refrained from altering them in any way and, as a result, some discontinuity of style may be noticed. As the final writing coincided in time with the conclusion of UCDWR's activities and with the resulting dispersion of personnel, it has not been possible to check the interchapter references as closely as would be desired. The mathematical sections have not had the advantage of being smoothed by classroom use and may present undue difficulty to the reader.

Shortly after the beginning of UCDWR it became clear that the work in both fundamental research and engineering development would require special transducers. It seemed more expedient to establish a group, the Transducer Laboratory, within its organization than to attempt to have such units built outside. It was fortunate, indeed, that the publication of the excellent book by W. P. Mason, *Electromechanical Transducers and Wave Filters*, came when it did, for it has served as a textbook for many

of the UCDWR scientists who were learning the art. Some early work was done, prior to the establishment of the Transducer Laboratory, by D. K. Froman, A. M. Thorndike, C. H. Kean, and G. E. Duval on the properties of X-cut Rochelle salt crystals. This study was useful in that it confirmed and extended the known data on this material.

The need for transducers early in World War II was so great that it was not possible to devote the time or manpower to the desired fundamental studies of piezoelectricity and elasticity which were needed to give a firm basis for transducer design procedures. UCDWR was forced for nearly two years to build transducers by cut-and-try methods and profit as best it could by experience gained with them.

Not until late 1943 was it possible to make a reassignment in personnel at UCDWR so that a research group could be set up within the Transducer Laboratory. The members of this group operated under the general assignment to learn whatever they could about transducers. Some of this knowledge came from visits and conferences with other transducer groups throughout the country, the remainder from theoretical and experimental research in San Diego. This volume is a compilation of such accumulated information.

G. D. Camp, who was in charge of the research group just mentioned, was responsible for the arrangement of this volume and in general guided the work of the group which obtained much of the original data given herein. T. F. Burke, Jr., one of the original members of the Transducer Laboratory, originated many of the design procedures which have been used by UCDWR. B. G. Eaton, F. M. Uber, and F. X. Byrnes have all made plentiful contributions; Eaton has done much work on directivity patterns and has made laboratory studies on many phases of the transducer art. Uber, in the short time he was with UCDWR, made many investigations in methods of attaching crystals to various surfaces and devised production controls for cemented joints. He is solely responsible for the introduction of the Cycle-Welding technique for the attachment of crystals to rub-

ber. Byrnes has been engaged in the design of several of the UCDWR transducers and in methods of matching electronic circuits to them.

The editor desires to acknowledge the importance of the roles played by many others who, while not authors of this volume, have through their work very largely made it possible. Special mention is made of G. A. Argabrite who relieved the undersigned as head of the Transducer Laboratory in the early months of its growth and remained its leader throughout the war. There is scarcely a phase of the work of this group which has not profited by his active enthusiasm. D. C. Kalbfell, as a member of the research group, was concerned significantly with the electronic equipment associated with transducers. He is particularly to be mentioned for his studies of impedance bridges. R. Bellman did much of the original theoretical work in Chapter 3. H. W. Hunter did valuable work on all phases of transducer construction being particularly concerned with their ruggedness or resistance to shock. K. M. Burton, as foreman of the transducer shop, by his painstaking efforts made transducer construction more reliable. C. E. Green, F. L. Paul, and Miss M. C. MacKenzie conducted many laboratory experiments for the research group. The many mathematical and numerical calculations involved in the development of some of the conclusions presented in this volume were done by a group of mathematicians consisting of Mrs. A. J. Keith, Mrs. O. W. Wilt and Mrs. F. C. Herreshoff.

Most particular mention must be made of the Calibration Laboratory of UCDWR whose task it was to assay the performance of all units

designed by the Transducer Laboratory. C. J. Burbank headed this group and together with J. H. Martin, head of the Sweetwater Calibration Station, and the latter's predecessor, D. H. Ransom, offered on the basis of their calibrations many useful suggestions to the transducer designers. Without the able help of this group little could have been accomplished by the Transducer Laboratory.

As the manuscript of this volume neared completion, D. J. Evans, assisted by C. A. Young and L. A. Cartwright undertook the mechanical task of assembling illustrations, paging, and numbering, which constitute the final, most tiresome labors. The art work for illustrations in Chapter 8 was done by S. F. Simonet. Also contributing to Chapter 8 were Théron Lambert, G. W. Banks, and V. G. McKenny.

Finally, the excellent cooperative spirit with which members of UCDWR were always received by the Bell Telephone Laboratories, the Brush Development Company, the Submarine Signal Company, and the Naval Research Laboratory has been very helpful throughout World War II. To mention a few of the gentlemen in these companies who have been particularly stimulating one must include A. C. Keller, W. H. Martin, and W. P. Mason of the Bell Telephone Laboratories; A. L. Williams, W. R. Burwell, Frank Massa, and Harry Shaper of the Brush Development Company; H. J. W. Fay and I. C. Clement of the Submarine Signal Company; and H. C. Hayes and E. B. Stephenson of the Naval Research Laboratory.

F. N. D. KURIE
Editor

CONTENTS

CHAPTER		PAGE
1	General Survey by <i>Glen D. Camp</i>	1
2	The Phenomenological Theories of Linear Dissipative Elec- trics, Dielectrics, and Piezoelectrics by <i>Glen D. Camp</i>	30
3	Properties of the Component Parts of Crystal Transducers by <i>Richard Bellman, T. Finley Burke, Glen D. Camp, Bourne G.</i> <i>Eaton, and Fred M. Uber</i>	73
4	Properties of Assembled Crystal Transducers by <i>T. Finley</i> <i>Burke, Glen D. Camp, and Bourne G. Eaton</i>	127
5	Electronic Systems and Matching Networks by <i>Francis X.</i> <i>Byrnes</i>	211
6	Design Procedures by <i>T. Finley Burke</i>	230
7	Design Adjustment by <i>T. Finley Burke</i>	255
8	Construction Techniques and Equipment by <i>Fred M. Uber</i> .	267
9	Research Techniques and Apparatus by <i>T. Finley Burke,</i> <i>Francis X. Byrnes, and Bourne G. Eaton</i>	358
	Glossary	381
	Bibliography	383
	Contract Numbers	387
	Index	389



Chapter 1

GENERAL SURVEY

By Glen D. Camp

1.1

INTRODUCTION

THIS VOLUME REPRESENTS an attempt at a unified account of present knowledge relevant to the design and construction of crystal transducers; some account of the work of other laboratories has been given, but this is by no means complete.

The basic purpose of underwater transducers is to generate and receive sonic signals in water. These signals may be used for the detection of submerged objects, the control of devices, interference with the operation of enemy devices, and underwater communication. These applications are discussed here only to the minimum extent necessary to understand the various transducer characteristics needed.

Underwater transducers are functionally equivalent to radio and radar antennae. Acting as a transmitter, an electric signal sets a part of the transducer, which is often called the "motor," in motion and thus produces an outgoing signal. As a receiver, the process is reversed: an incident sonic signal sets the motor in motion, producing an electric signal at the terminals. Both transducer and antenna are inert systems, requiring an external driver or receiver amplifier; both are coupled to a field, the former elastic and the latter electromagnetic; and in both, the field exists and is propagated in a medium, one being an elastic fluid, water, and the other, empty space or the "ether."

In crystal transducers the fundamental physical phenomenon, whereby energy is converted from one form to another, is *piezoelectricity*. Historically, this phenomenon is divided into the *direct* and *inverse* effects. The direct effect is the production of an electric field in a crystal when deformed, and was discovered by the Curie brothers in 1880; it is the effect that makes a receiver possible. The inverse effect is the distortion of a crystal when exposed to an electric field, and makes a transmitter pos-

sible. These effects are not independent but, like all reversible processes, are inextricably connected by a reciprocity principle. In fact, the next year after the Curies discovered the direct effect, Lippman predicted the existence of the inverse effect, on the basis of their discovery and the thermodynamic laws of reversible processes. His prediction was verified by the Curies that same year, although this discovery might have been delayed many years if the prediction had not suggested what to look for.

Piezoelectricity, in common with magnetism, dielectrics, etc., has been studied from two quite independent points of view. The first is *molecular* piezoelectricity, which is concerned with the fundamental interactions which cause the phenomenon. The second is *phenomenological* piezoelectricity, in which one ignores the fundamental cause completely but seeks to obtain a correct *description* of the behavior of macroscopic crystals.

In this volume, we are completely unconcerned with the molecular aspect of piezoelectricity. A macroscopic crystal is regarded as a given thing, having certain complicated properties susceptible to gross experimental study. Our only concern with piezoelectricity is to understand these macroscopic properties sufficiently well to enable us to use crystals for a specific purpose.^a While piezoelectricity is the basic phenomenon which permits a crystal transducer to function, we are also deeply concerned with other branches of physics which become involved when one attempts to put the basic phenomenon to a useful purpose. In fact, in few branches of applied physics is the theory

^a This remark refers solely to the contents of this volume. Research in molecular piezoelectricity at Brush Development Company and Bell Telephone Laboratories led, in the midst of World War II, to the almost complete displacement of Rochelle salt by ammonium dihydrogen phosphate, the latter having many advantages over the former. It is possible that continuation of this work might lead to crystals still better suited to the construction of transducers.

more complicated, the phenomena more diverse, the experimental procedures more difficult, or the techniques more critical. Nearly all prewar research was done on highly idealized cases with the emphasis on pure piezoelectricity. Quite properly, for the purposes of that research, every effort was made to eliminate just those complicated interactions which play an essential role in the performance of a practical transducer. Here we must take an entirely different attitude: we must recognize that this idealized approach is only an important first step and we should attempt, by a closely related program of theoretical and experimental research and field tests, to learn what factors interfere with the minute motions of crystals and how to control these motions sufficiently to put them to practical use.

For our present purpose, a crystal is an object such that, if a properly oriented piece is cut from the mother bar, equipped with suitable electrodes and properly mounted and protected, it will serve to generate or receive a sonic signal. As will develop later, rectangular plates cut at certain angles from mother bars of Rochelle salt [RS] or ammonium dihydrogen phosphate [ADP], and designated as 45° X-cut and 45° Y-cut RS and 45° Z-cut ADP (see Figure 1), are the only types of cut crystals that have so far found extensive practical application in underwater transducers in the United States. Quartz has been effectively used in England, but only because an adequate supply of the above synthetically grown crystals was not available there. For reasons to be discussed later, the use of 45° X-cut RS is now regarded as a regrettable expedient to be tolerated only in very special and rare circumstances. The use of 45° Y-cut RS has greatly declined, but is still of sufficient importance to warrant inclusion. This volume therefore deals with 45° Y-cut RS and 45° Z-cut ADP almost exclusively, touching only briefly on 45° X-cut RS for small hydrophones on long cables where a preamplifier cannot be used.

In dealing with these rectangular plates of RS or ADP we are here concerned (1) with tests for verifying that they are properly oriented and that they satisfy certain other standards; (2) with the best sizes and shapes for

a particular application; (3) with the best ways of mounting and protecting them; (4) with their coupling to the water; (5) with the effects produced, how these depend upon frequency, and the response to pulse excitation. We are concerned also with the improvement and standardization of the numerous techniques, both experimental and constructional, which are involved, and with the design of suitable electronic drivers for transmitters and suitable amplifiers for receivers (the electric circuit characteristics of crystal transducers are sufficiently specific and critical to warrant special study of this electronic problem). Above all, we are concerned with knowing how, as far as is at present possible, to produce a transducer which will serve a specific purpose in a specific device and which will be practical to manufacture in quantity.

Crystal transducers are devices with a sharply limited domain of useful applicability. Their performance is not sufficiently flexible to allow one intended for one purpose to serve well for another. Only by a thorough knowledge of the factors which influence their behavior, together with a clear understanding of the effects which it is desired to achieve, can one hope to produce a transducer which will be satisfactory for a given service. In fact, the first list of desirable characteristics almost invariably contains features which are contradictory. Only after careful consideration of all aspects of the problem, in the light of all available knowledge, is it usually possible to reach a workable compromise between desired and realizable characteristics.

While this circumstance arises, to a considerable extent, from inadequate knowledge and techniques, a part of it is intrinsic to the crystal itself and can be alleviated only by an entirely different line of research, namely, finding a crystal with more suitable properties. As previously stated, this volume makes no attempt to follow this attack. The ideal toward which we work is therefore to remove all unsatisfactory features which are extrinsic to the crystal so that the final result is limited only by the properties of the best available crystals, always taking account of the practicality of manufacture. Much progress has been

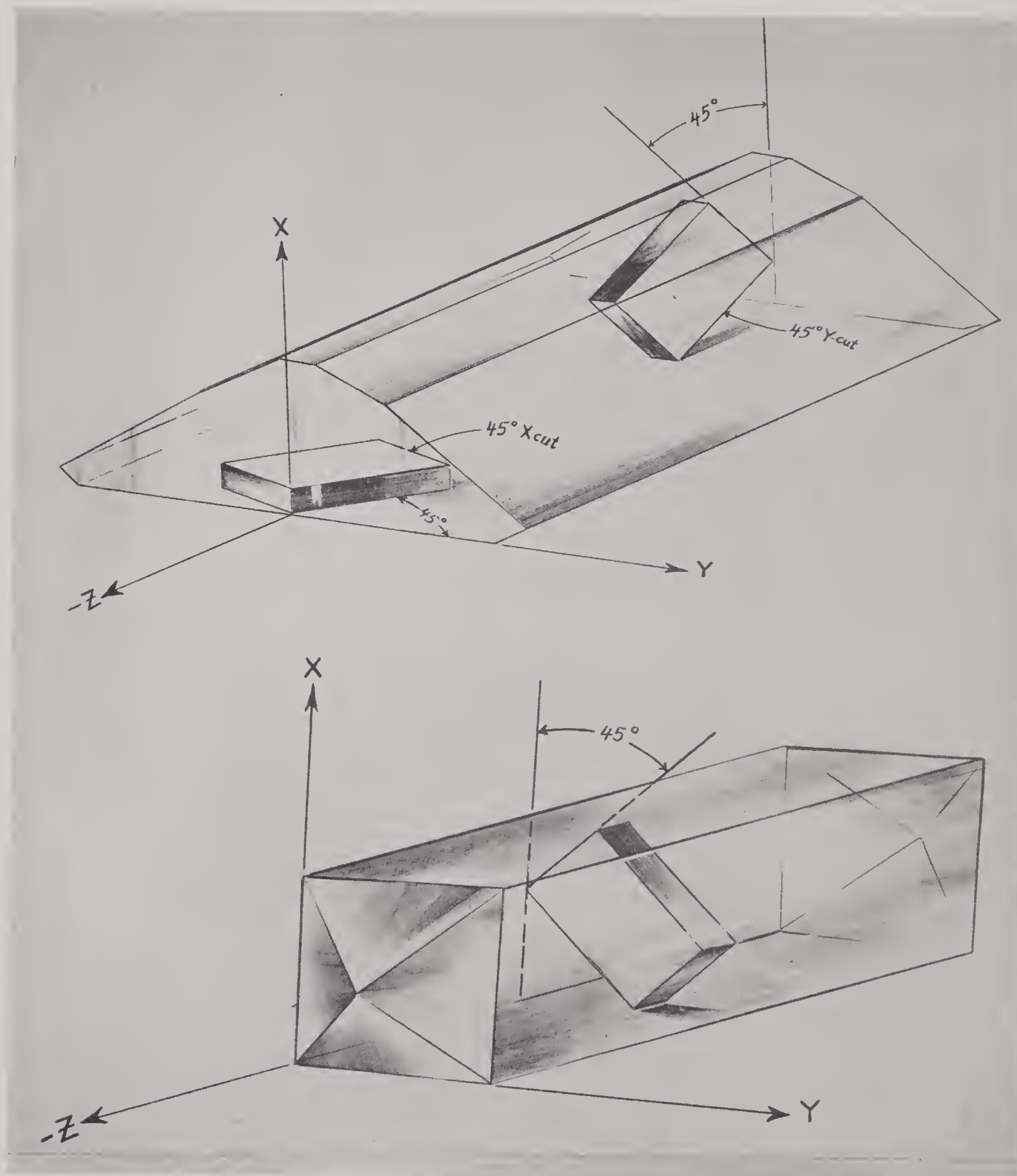


FIGURE 1. Orientation of rectangular plates of 45° X-cut and Y-cut RS (top) and 45° Z-cut ADP (bottom), in the mother bars.

made in this direction, but there is still much to be done.

It will pay us to pause here to summarize the foregoing basic considerations and to define as sharply as possible the purpose, scope, and limitations of this volume.

1. Underwater crystal transducers are devices which use the piezoelectric effect to convert electric and sonic signals reciprocally. They have a variety of applications, discussed in this volume only to the minimum extent necessary to understand the origin of specifications.

2. Piezoelectricity has molecular and phenomenological aspects. Only the latter, sufficient for the purpose of this volume, is discussed here; however, further study of the molecular aspects, which has already made a great contribution in developing ADP, might make further contributions. Only rectangular plates of 45° Y-cut RS and 45° Z-cut ADP are extensively treated here, these sufficing for the great majority of underwater crystal transducers at present.

3. Although piezoelectricity is the basic, necessary phenomenon, other branches of physics play essential roles in the behavior of crystal transducers. These are complicated and critical.

4. The characteristics of crystal transducers are not very flexible, and they must therefore be designed and built to serve a specific purpose and will usually not serve well in a service for which not intended.

5. The overall purpose of this book is to present, in as thorough a form as possible, a complete account of all aspects of present knowledge of the problem of producing underwater crystal transducers which will serve a specified purpose, the ultimate goal being a finished product which is practical to manufacture in quantity, and which will do a specified job in service.

1.2

TYPICAL UNITS

Underwater crystal transducers are built in a wide variety of external shapes, sizes, and internal constructions. Some idea of external

shapes and sizes will be gained from Figure 2. A brief identification of the units follows.

1. An early Bell Telephone Laboratories unit, built for a particular research application, which operates in the supersonic frequency band and may be used either as a receiver or as a transmitter.

2. A Brush Development Company unit, used for listening in the sonic frequencies. Its unusual shape results from its containing a parabolic reflector which focuses the sound on a small crystal assembly.

3. The University of California Division of War Research [UCDWR] CQ8Z, the transmitter-receiver of QLA sonar, a device which was manufactured in considerable quantity (considering its large size) and assisted U. S. submarines in evading mines. It went through several modifications and the model shown, the latest, has many interesting features. Perhaps the most unusual is the high degree of acoustic isolation between the transmitting and receiving motors, which makes the "crosstalk" level very low. (See Chapter 6.)

4. The UCDWR JB has a spherical shape and general external appearance very similar to several Submarine Signal Company transducers, but the internal construction is quite different.

5. The UCDWR GD case was used for a number of different units all practically identical in external appearance, but differing widely in internal construction. An example of these is the GD-16 (see Figure 34).

6. The UCDWR BE is an example of an unusual shape made necessary by the application to which the transducer was put. Sound is radiated through the curved part of the case.

7. The UCDWR BG, later and improved model of the UCDWR BE. This is shown in detail in Figure 35.

8. The UCDWR KC is an excellent transducer which was produced in considerable quantity during World War II. The case is made of very thin metal in a streamlined shape, except for top and bottom members which are made heavier for strength and isolation. Despite the thinness of the wall, it is amply rugged for its purpose.

9. This Submarine Signal Company unit con-

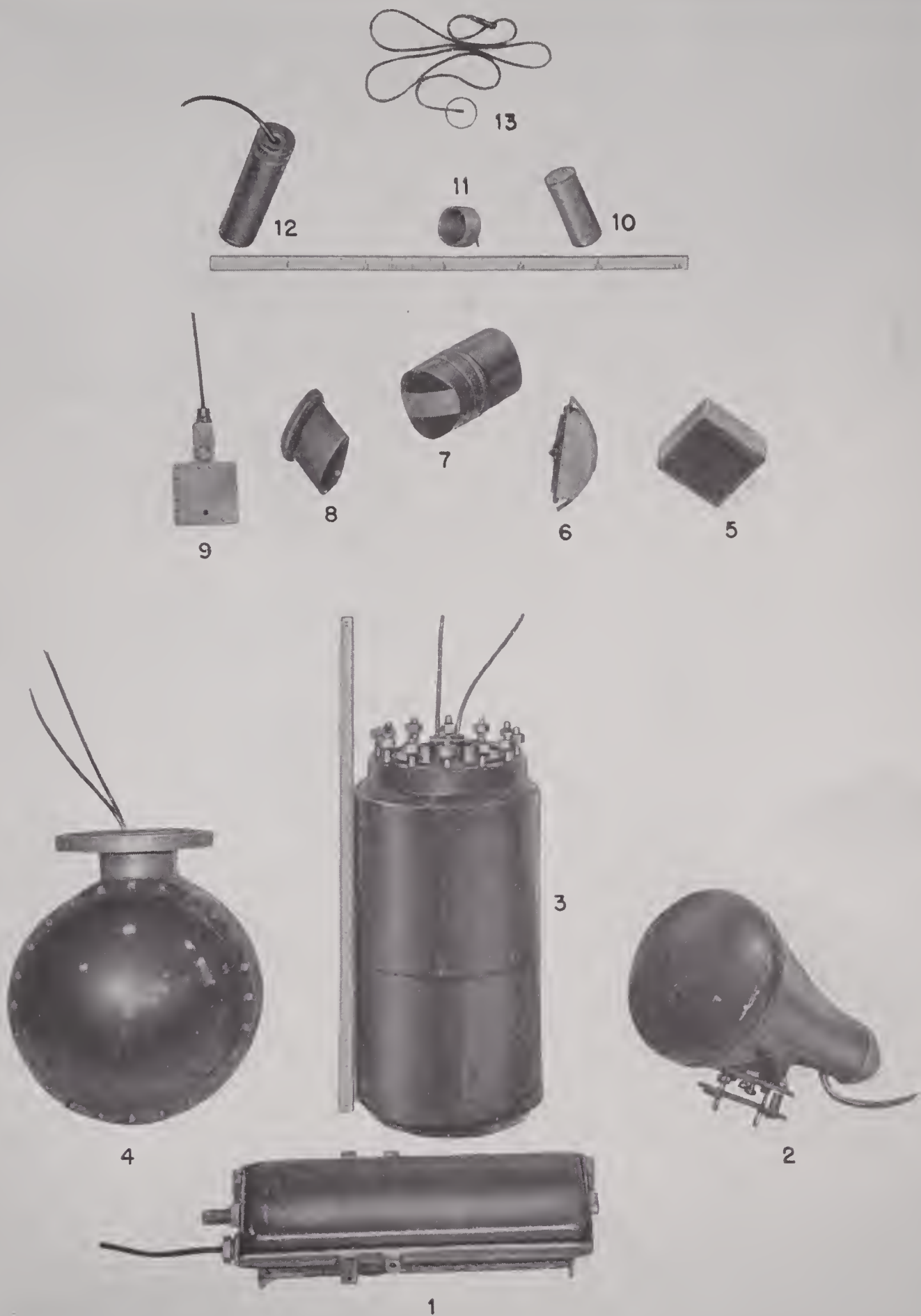


FIGURE 2. Typical crystal transducers, illustrating comparative sizes and shapes. (See text for explanation.)

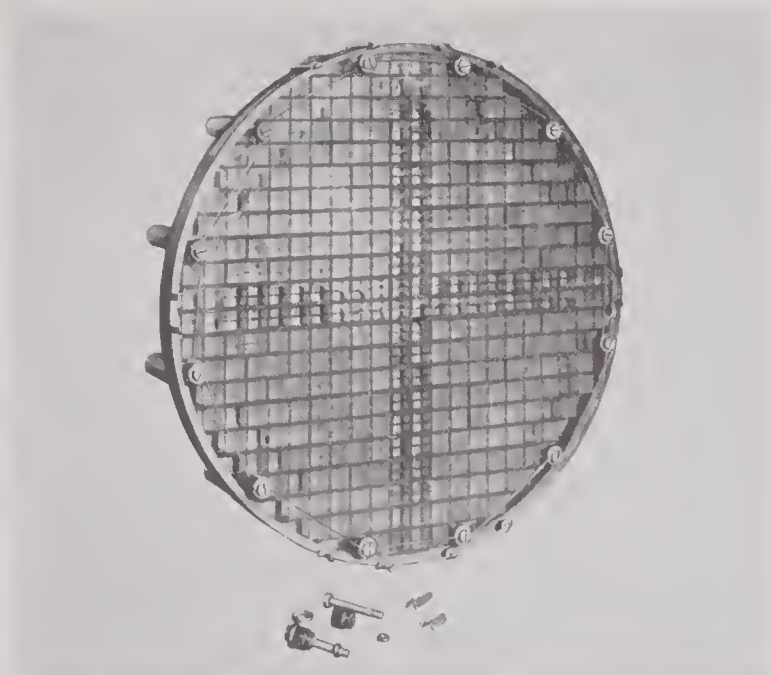


FIGURE 3. The crystal array of a typical transducer. The individual crystal blocks are separated by isolating material and bound together as a single unit in a frame. All the crystal blocks are not the same size so as to regulate the shape of the beam pattern. This unit is intended for operation at supersonic frequencies. (Bell Telephone Laboratories D172735 modified QB transducer.)



FIGURE 5. The assembly of Figure 7 mounted in its case not yet entirely closed. The right side of the case is made of qc rubber through which supersonic sound passes freely. (Bell Telephone Laboratories D172735 modified QB transducer.)



FIGURE 4. Another view of the same unit shown in Figure 3. This is the completed "motor" or vibrating element of the transducer. The crystals are on the right side of a metal plate which has been cut up into a number of resonating bars whose purpose is to modify the resonant frequency of the unit. The crystal array is attached to this backing plate by means of a cement or glue. (Bell Telephone Laboratories D172735 modified QB transducer.)

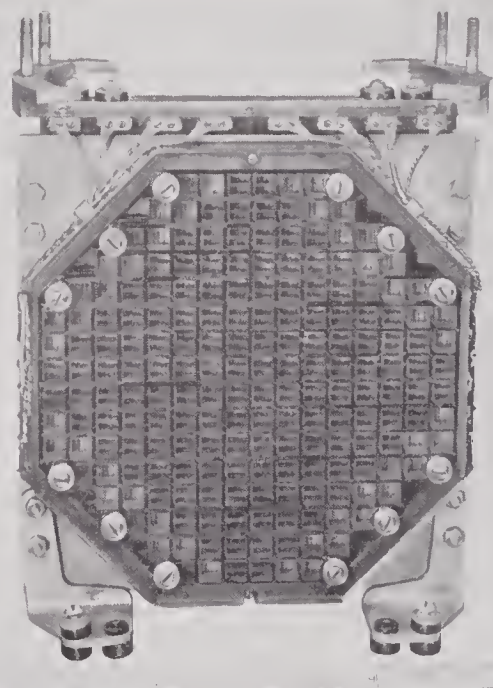


FIGURE 6. The motor of a transducer showing octagonal array of crystals cemented to the backing plate, the outermost crystals being twice as large as those in the central section to control the shape of the directivity pattern. The vertical lines, visible under some of the larger crystals, are grooves in ceramic wafers which are cemented between the crystals and the backing plate for voltage insulation.



tains an unusual motor, consisting of a number of Benioff blocks, the theory of which is discussed in Chapter 3.

10. The UCDWR CY4 is a simple stack motor, sealed in an olive can. It was also produced in large quantities during World War II.

11. The UCDWR EP is a "window-coupled" unit, the crystals being Cycle-Welded on the inside to the rubber window. More details on an earlier model of this transducer are shown in Figures 36 and 37.

12. The UCDWR CD or CJ is a stack motor in a rubber sleeve, strengthened by a perforated tube. These were used in Navy model OAS and OAU practice targets for training purposes.

13. The UCDWR probe microphone or acoustic ammeter is a late model of a device for

studying the motion of a surface. The active element is a minute crystal at the tip, enclosed in a circle in the picture. The cable, which contains a guard shield, goes to a cathode-follower amplifier.

Several of these units will be studied in some detail in later parts of this volume. For the present, it may be useful to give a general idea of the internal construction of typical transducers. The views of assembled and disassembled units shown in Figures 3 to 40 should be sufficiently self-explanatory for the present.

The purpose of this section is to make evident the broad range of shape, size, and other properties required to produce transducers which will satisfactorily perform the wide variety of functions demanded in service.

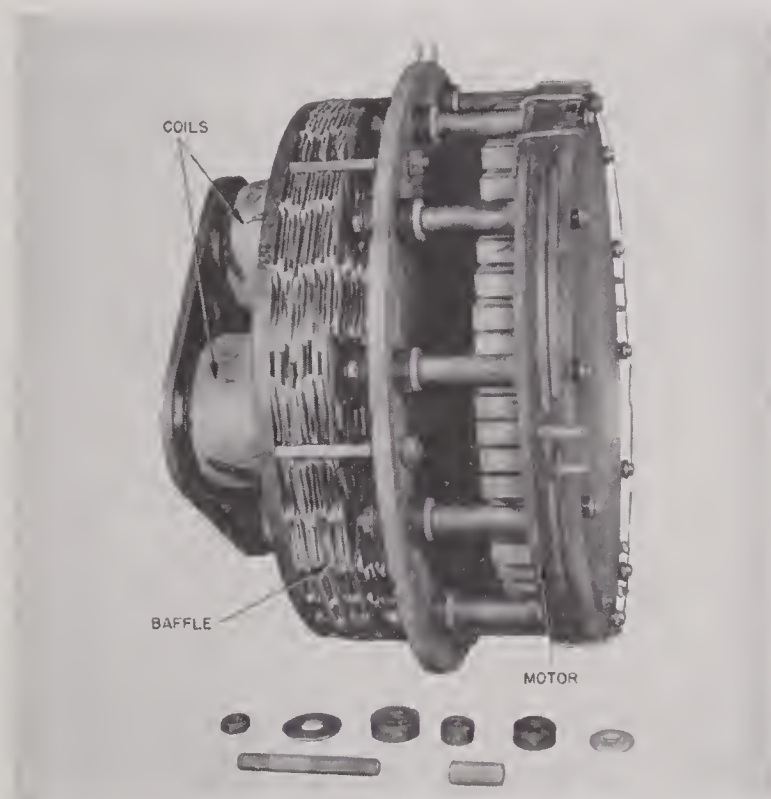


FIGURE 7. The motor of Figure 4 is shown here attached to a baffle which also carries a coil assembly. This assembled unit is ready to be put in a case which will subsequently be filled with castor oil to provide a path for sound from the motor through the case to the surrounding water. The purpose of the baffle, which is a good absorber of sound at supersonic frequencies, is to suppress backward radiation from the resonating bars. The coils modify the electrical characteristics of the unit to match it to its driving amplifier. (Bell Telephone Laboratories D172735 modified QB transducer.)



FIGURE 8. The completely assembled transducer. The qc rubber sound window is still on the right. The unit has now been filled with castor oil and is ready for use. The flange at the top will be used to attach it to a shaft protruding through the bottom of a ship. The lead which connects the crystal motor to the rest of the electronic system will enter the ship through this shaft. (Bell Telephone Laboratories D172735 modified QB transducer.)

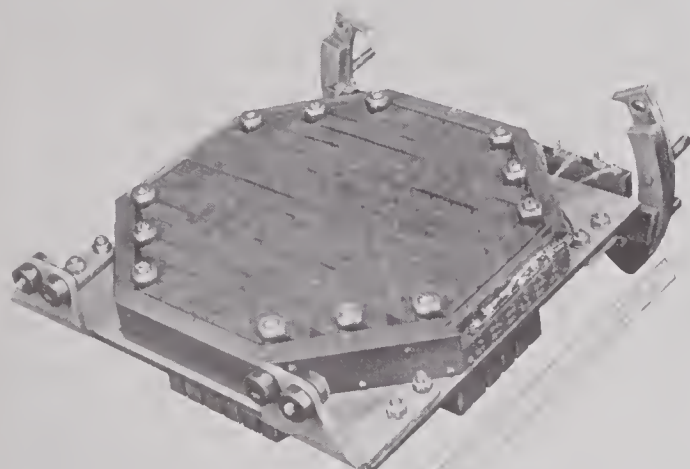


FIGURE 9. Another view of the transducer motor shown in Figure 6.

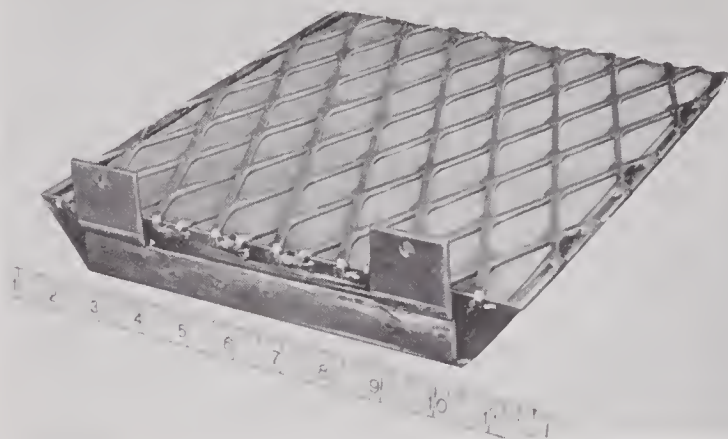


FIGURE 11. The baffle for the transducer of Figure 6. This is mounted immediately behind the resonating bars shown in Figure 10 to absorb sound radiated in this undesired direction. It consists of closely spaced sheets of fine mesh metal gauze in an expanded metal frame. The sound absorption mechanism is viscous friction of castor oil, moving in the many narrow passages formed by the metal gauze. (Bell Telephone Laboratories D171932 MCC transducer.)

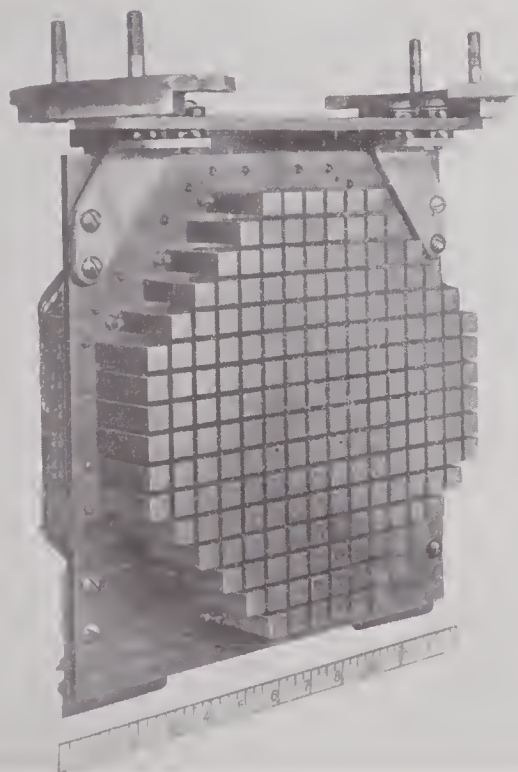


FIGURE 10. The reverse side of the backing plate of the motor in Figure 6. This plate has been cut so that each crystal block is backed by its own resonating bar. The cuts are intended to allow each bar to vibrate independently of the others. (Bell Telephone Laboratories D171932 MCC transducer.)



FIGURE 12. The completed transducer shown in Figure 11. The darker section is the qc rubber sound window through which sound is radiated. The cables and mounting flange may be seen at the top of the case. (Bell Telephone Laboratories D171932 MCC transducer.)

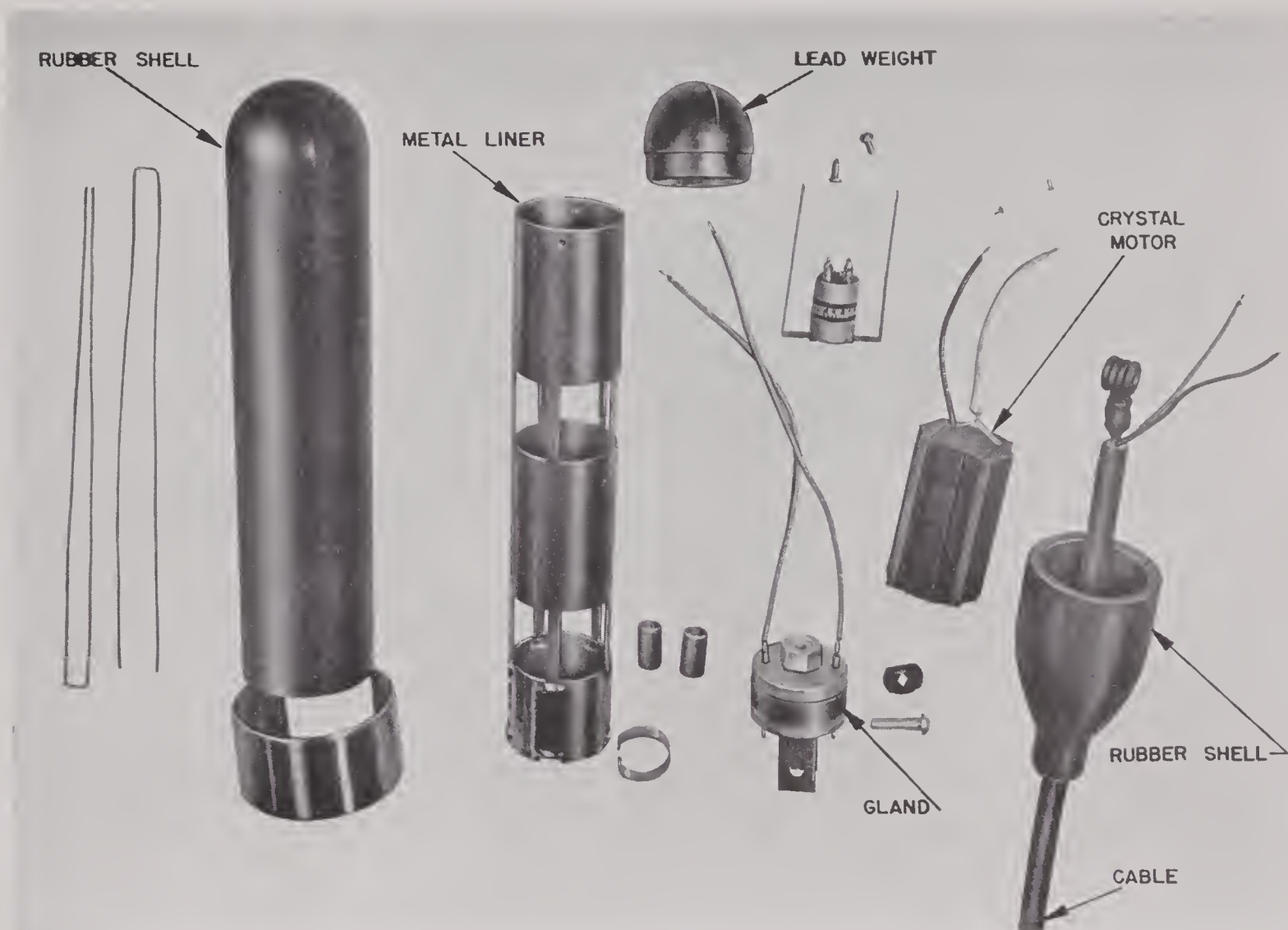


FIGURE 13. Disassembled nondirectional hydrophone. The crystal motor shown in Figure 15 is mounted inside a metal liner through holes in which the sound reaches the active ends of the crystals. This liner has a lead weight attached to keep it upright. The whole assembly fits in a two-piece rubber shell, the lower part of which is filled with castor oil. (Brush Development Company AX83 hydrophone.)



FIGURE 14. The completely assembled Brush Development Company AX83 hydrophone. It is supported by its cable and hangs in the water with its long axis vertical.

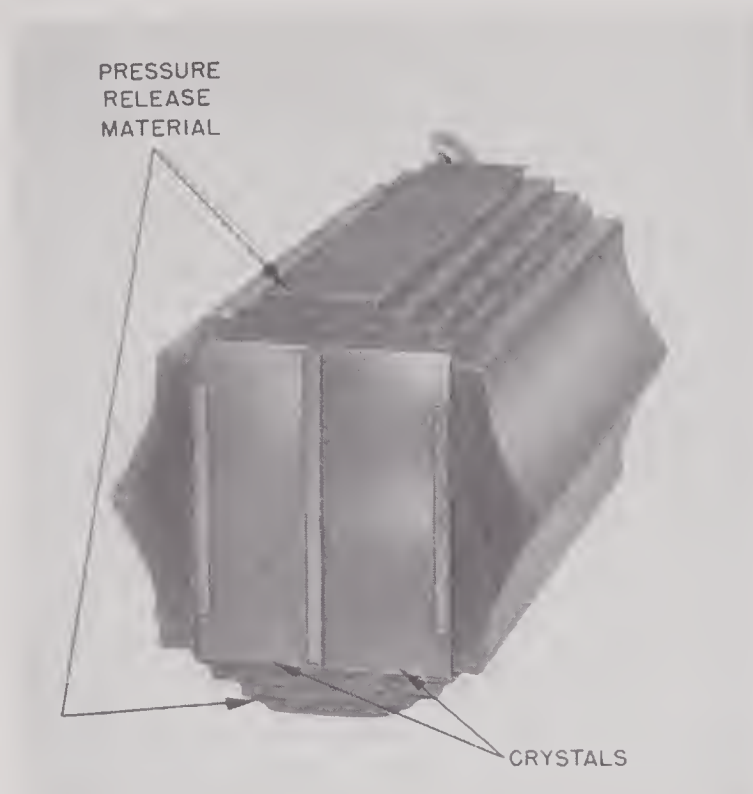


FIGURE 15. The motor of a nondirectional hydrophone designed for operation in the sonic frequency band. Two quite large crystals have their two active ends exposed but their active sides are covered by pressure release material. (Brush Development Company AX83 hydrophone.)

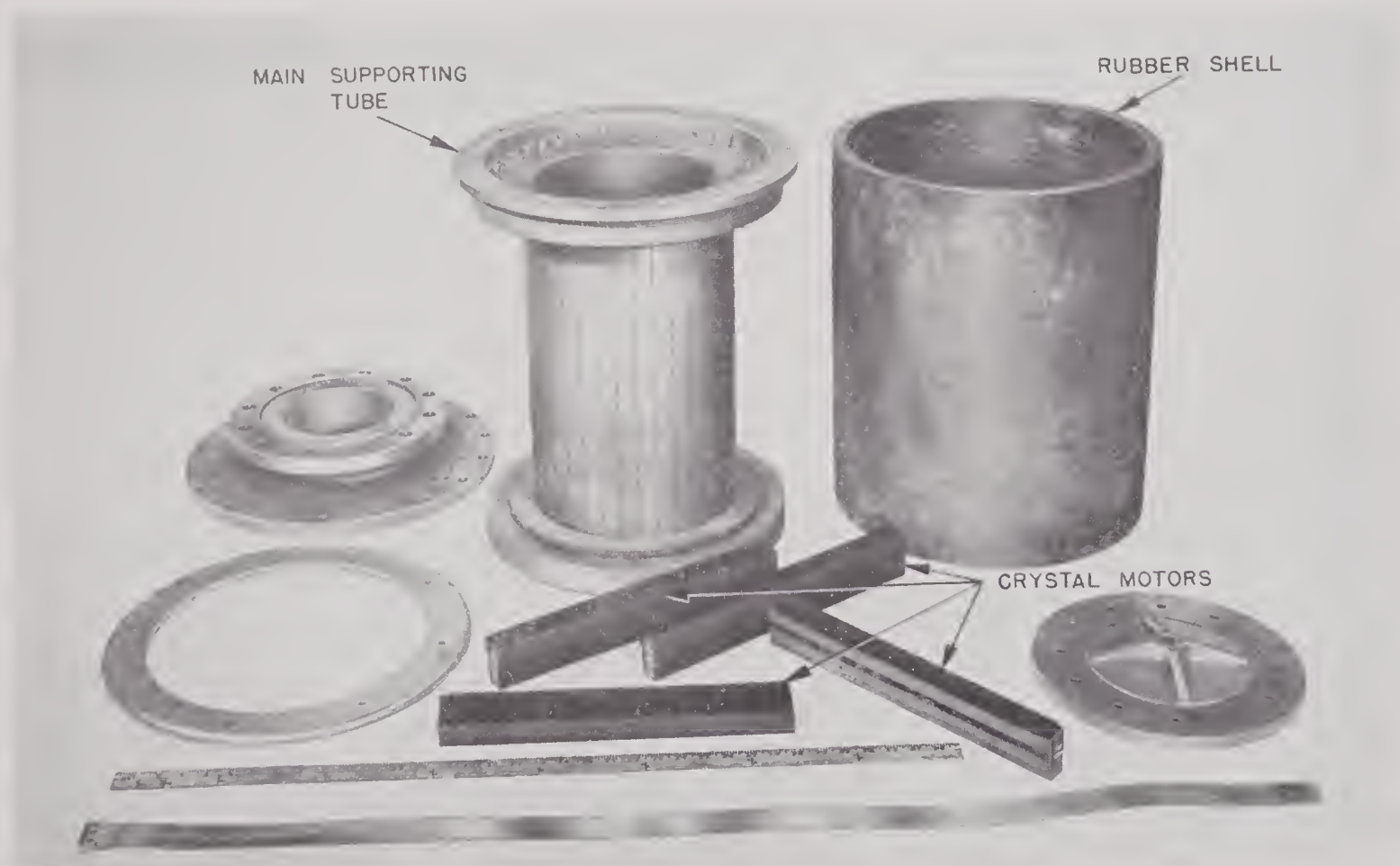


FIGURE 16. This transducer has several vertical strip motors immersed in castor oil in the space between the metal tube and the rubber shell. Separate leads are brought out from each motor. (Brush Development Company AX89 transducer.)



FIGURE 17. Another view of the Brush Development Company AX89 transducer with the crystal motors in place. The crystal blocks in these motors are thicker at the upper and lower ends to control the shape of the directivity pattern.



FIGURE 18. The completely assembled Brush Development Company AX89 transducer. The rubber shell is sealed to the main metallic structure by clamping bands. The slight bulge in the rubber is caused by the pressure of the castor oil. This unit was designed to be used as a transmitter in the supersonic frequency band.

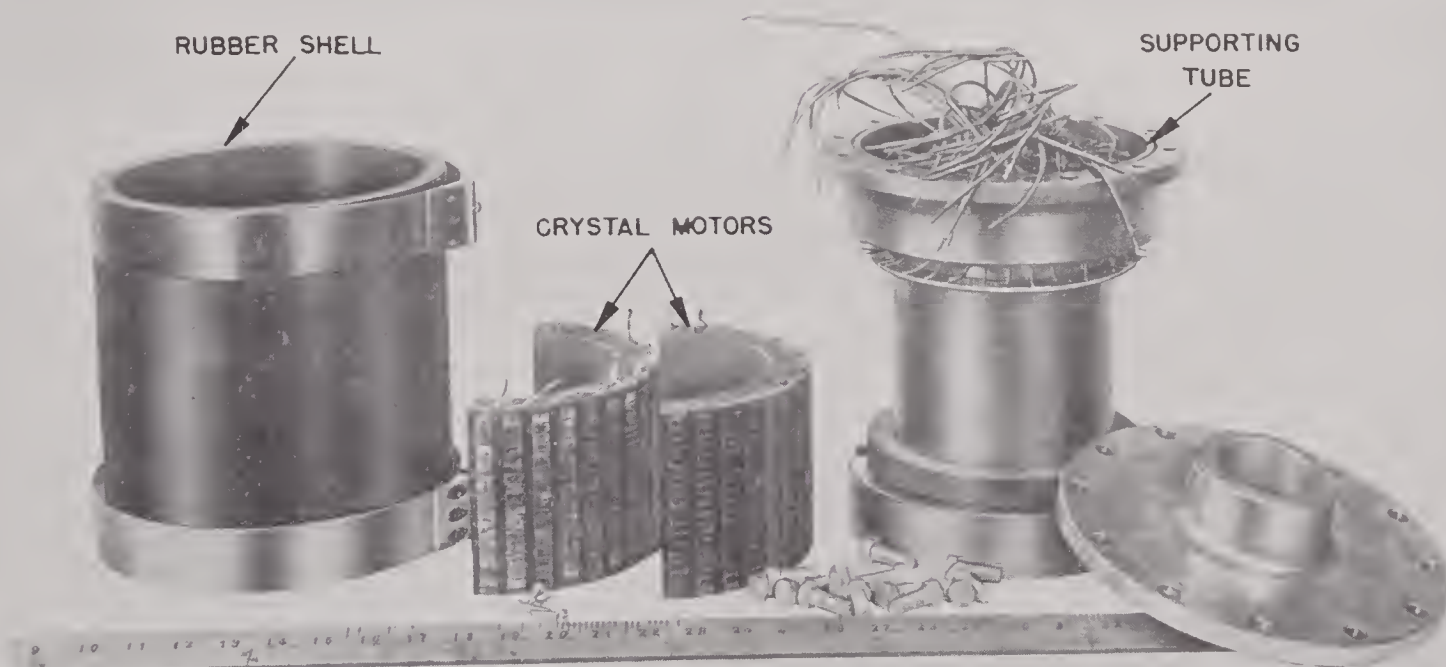


FIGURE 19. A transducer similar to the one shown in the preceding figures. Here the crystals are nested in pressure-release material and are mounted in a manner similar to that shown in Figure 17. (Brush Development Company AX104 transducer.)

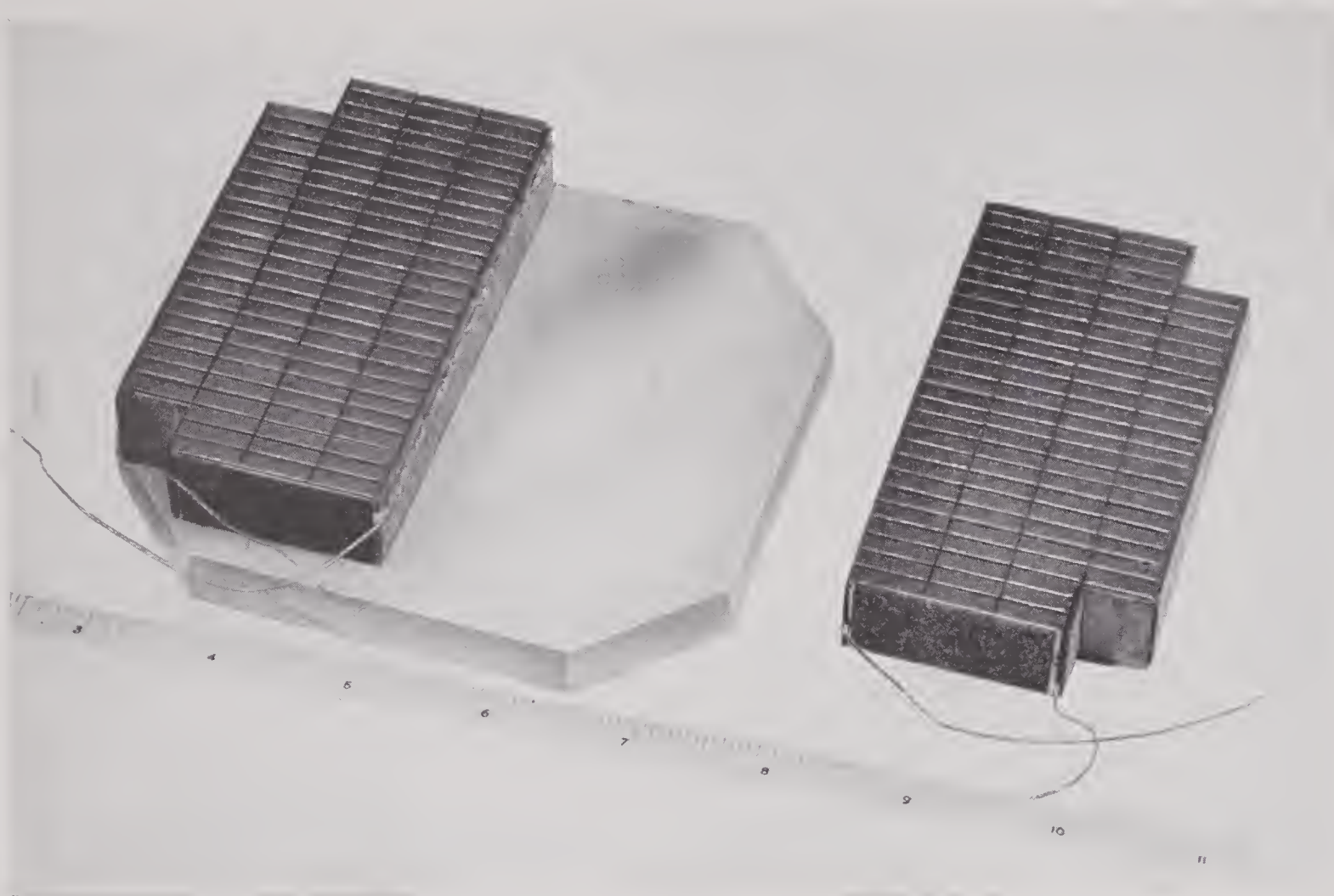


FIGURE 20. The partly assembled motor of the Brush Development Company AX124 transducer. The crystal array is built in two sections, with pressure-release material separating and surrounding each block of crystals, and then cemented to a glass backing plate.

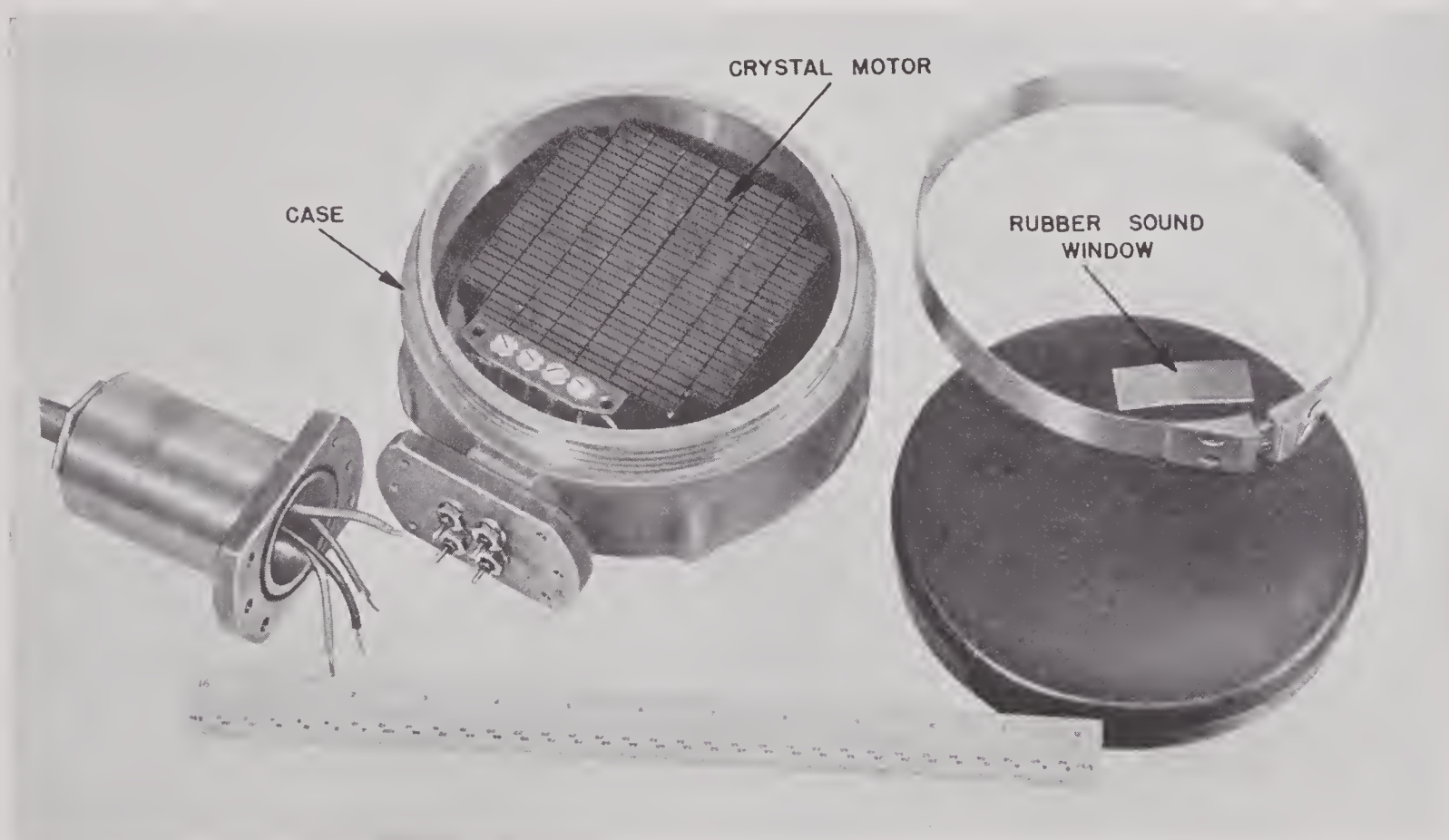


FIGURE 21. The motor of Figure 20 shown in its case. The rubber sound window will be attached to this case by means of the clamping band and the unit will then be filled with castor oil. This transducer was designed as a transmitter of sound in the supersonic frequency band. (Brush Development Company AX124 transducer.)



FIGURE 22. A large transducer designed for transmission at supersonic frequencies. The conical assembly of the individual motors will give a slight uptilt to the beam. One of the separate motors may be seen in the foreground. Both the crystals and their backing bars are cemented together in a shell of pressure-release material. This unit is similar in construction and purpose to those shown in Figures 17 and 19. (Brush Development Company AX132 transducer.)



FIGURE 23. The completely assembled Brush Development Company AX132 transducer.

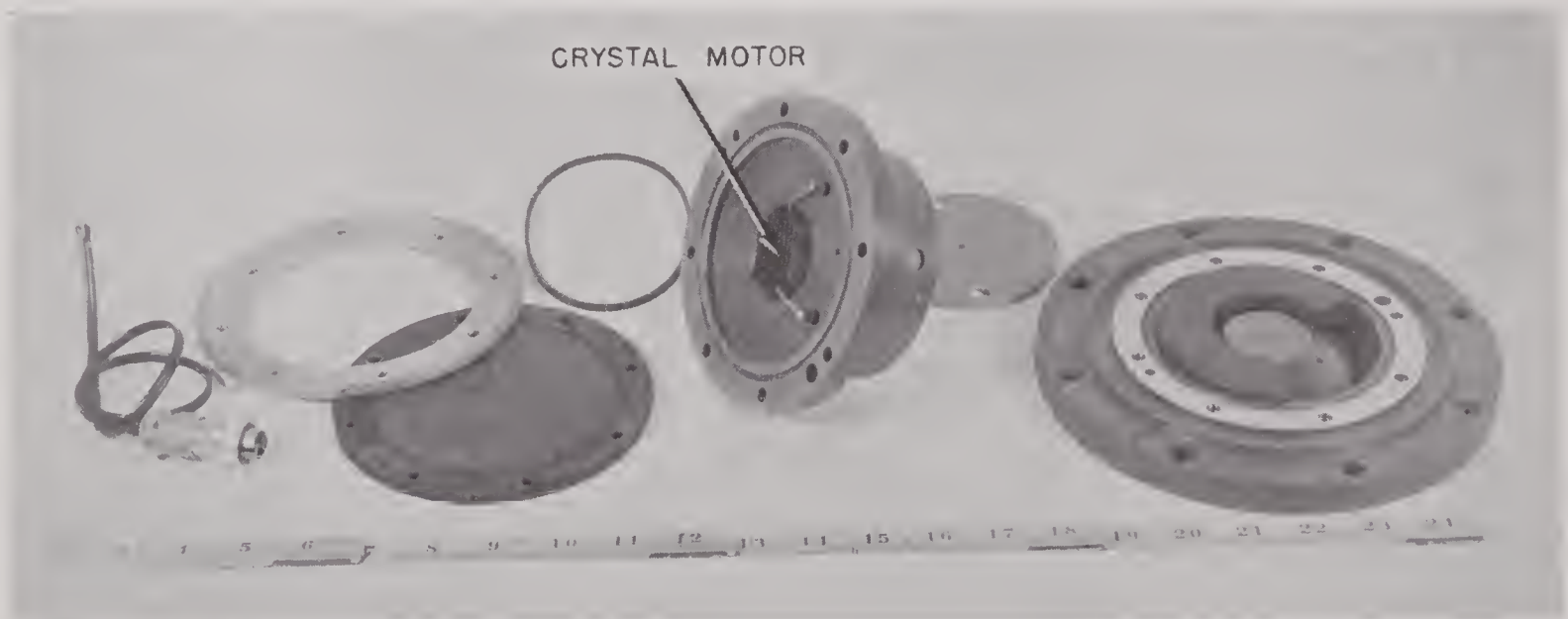


FIGURE 24. A disassembled hydrophone. The small block of crystals may be seen mounted in the middle of the main casting. (Brush Development Company AX133-5 transducer.)

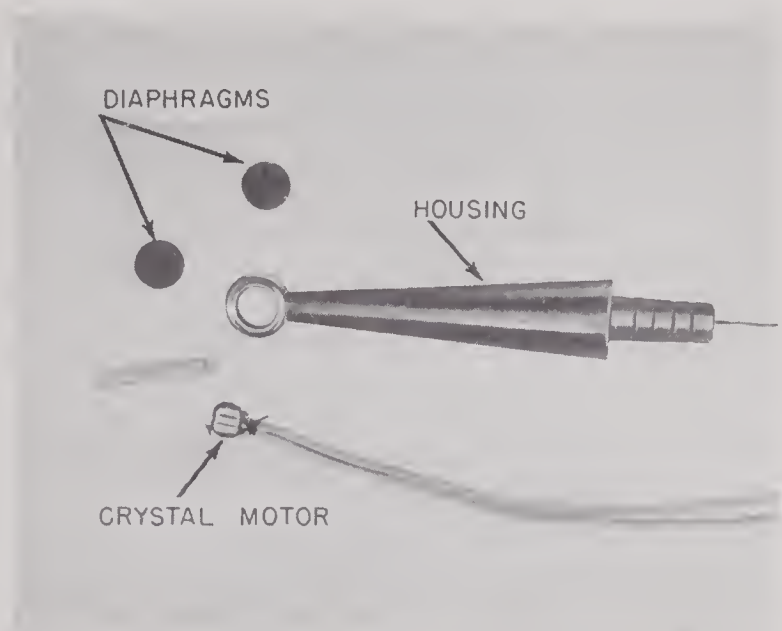


FIGURE 25. Parts of a small calibration hydrophone. The stack of three tiny crystals is mounted in the eye of the brass housing. The two copper diaphragms are cemented over this eye and the whole structure is covered first by copper and then by chromium plating. (Brush Development Company C11 hydrophone.)



FIGURE 27. Another hydrophone of the same general construction as shown in Figures 13 to 15. (Brush Development Company C22-A2 hydrophone.)

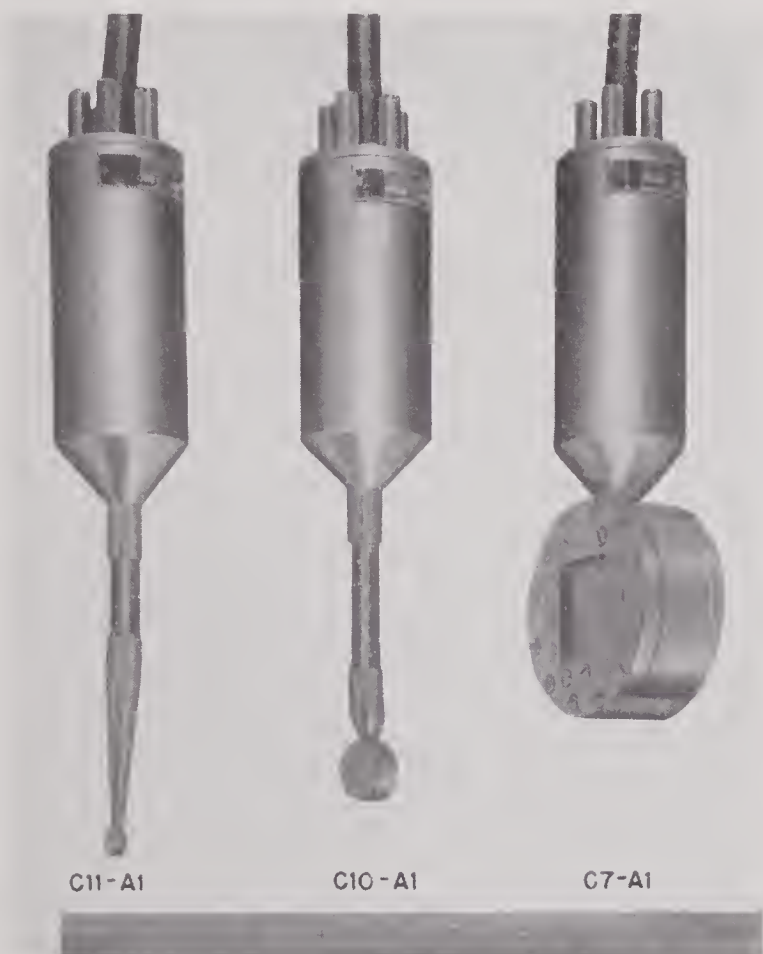


FIGURE 26. Three calibration hydrophones. From left to right, each is designed for progressively lower frequency. The one at the extreme left is shown disassembled in Figure 25. (Brush Development Company C11, C10, and C7 hydrophones.)

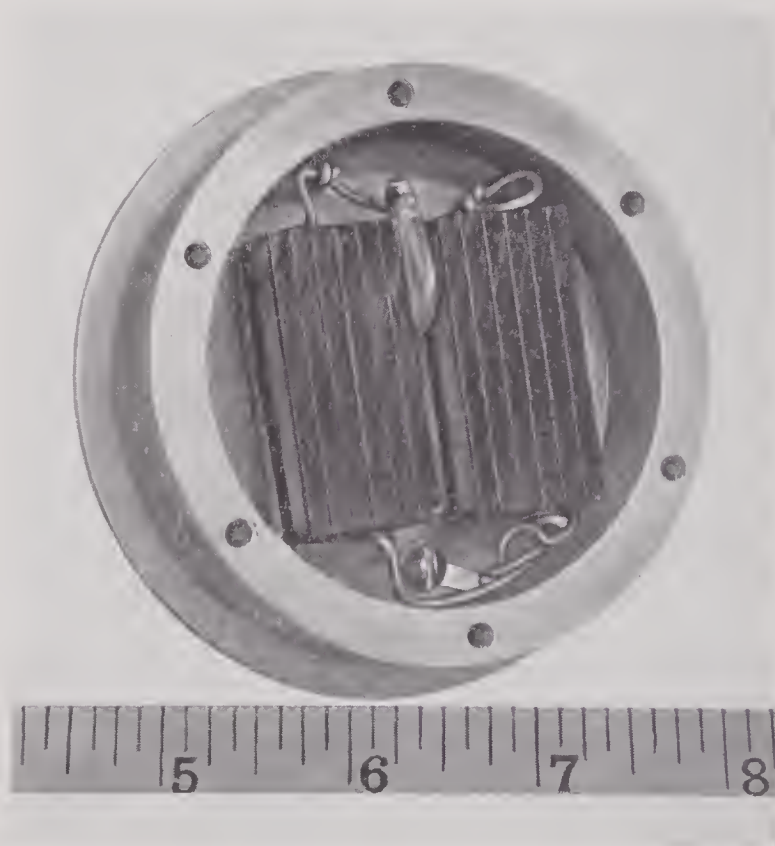


FIGURE 28. A small hydrophone. This unit is interesting because the crystals are mounted "on their side." (Brush Development Company C45 transducer.)

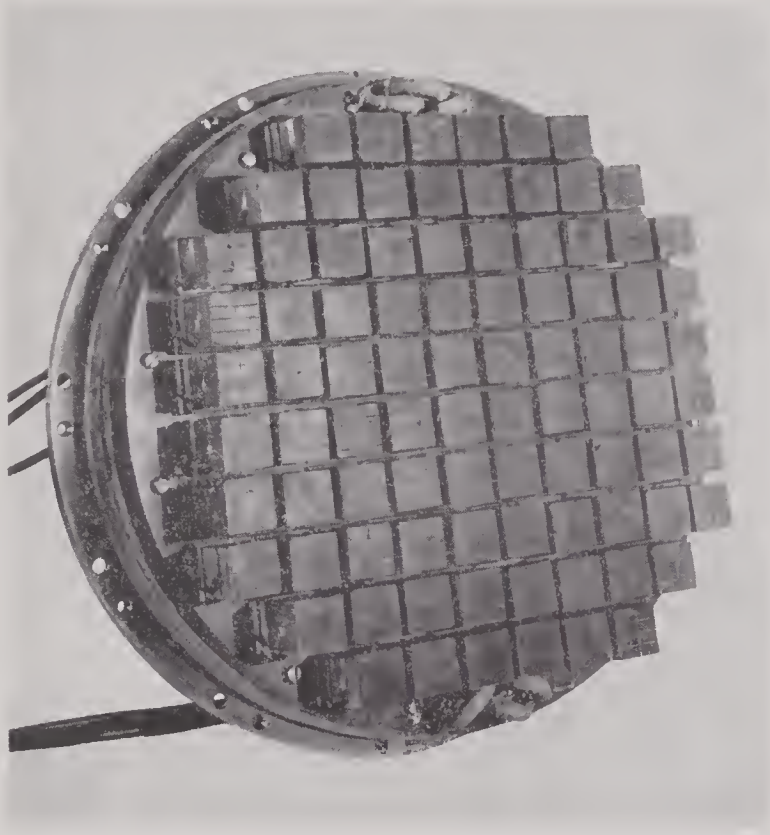


FIGURE 29

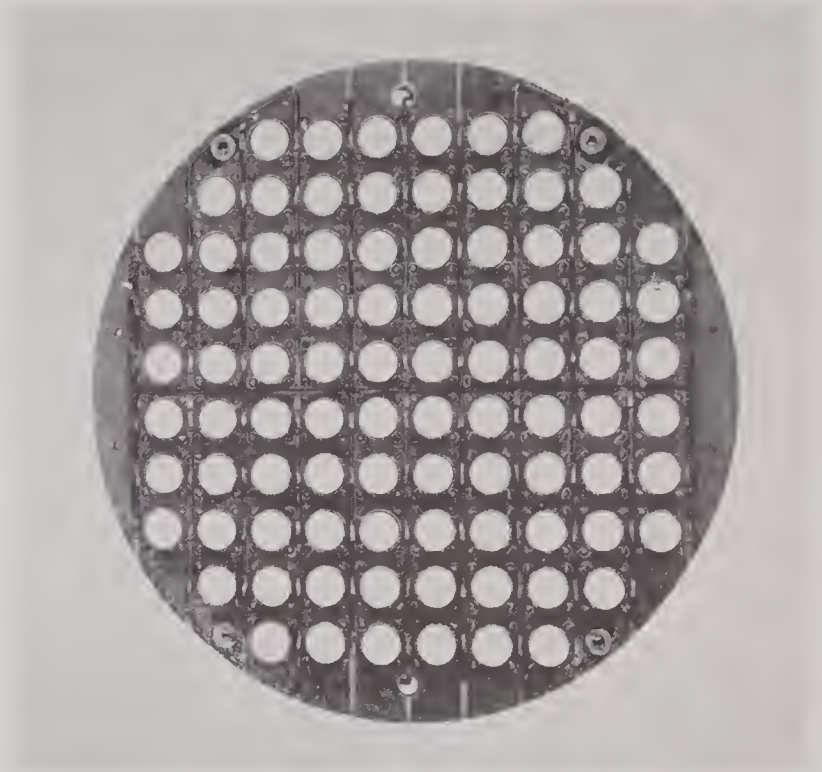


FIGURE 30

Crystal array of NRL transducer is shown in Figure 29 with larger crystals around the edge to shape directivity pattern. Each block of crystals is cemented to a square backing plate carrying a cylindrical resonator rubber mounted in a small cylindrical case so that the resonator is surrounded on all sides by pressure-release material (air). For repair, each unit can be removed without disturbing the others. (See also Figure 13 of Chapter 3.) Figure 30 shows the back of the motor with the cups around each resonator. Unsoldering two leads and removing four screws releases any unit. (NRL.)

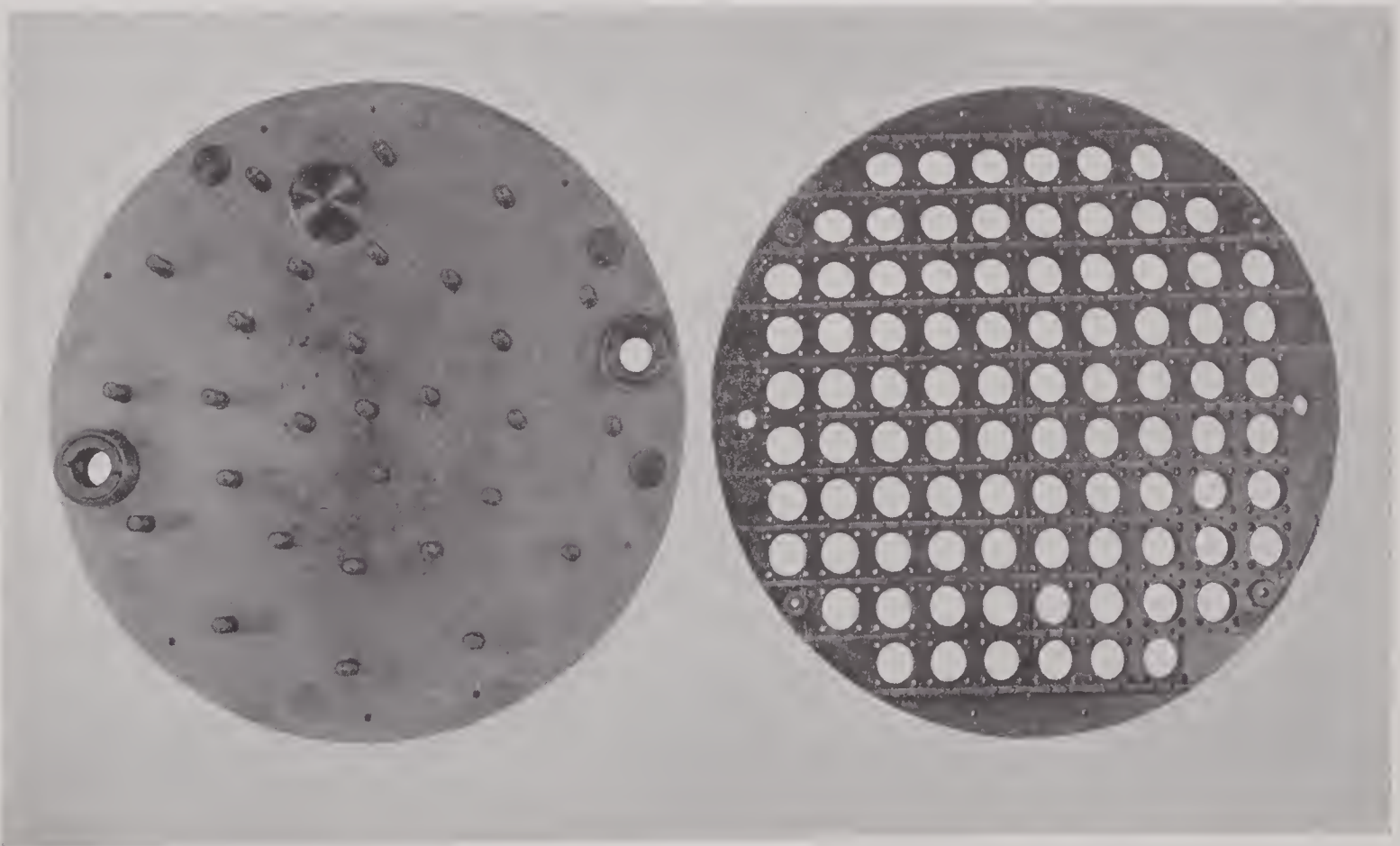


FIGURE 31. Right, bakelite disk to which the separate units are attached, including left, part of a rubber sandwich used to seal the portion of the transducer containing castor oil from the remainder. (NRL.)

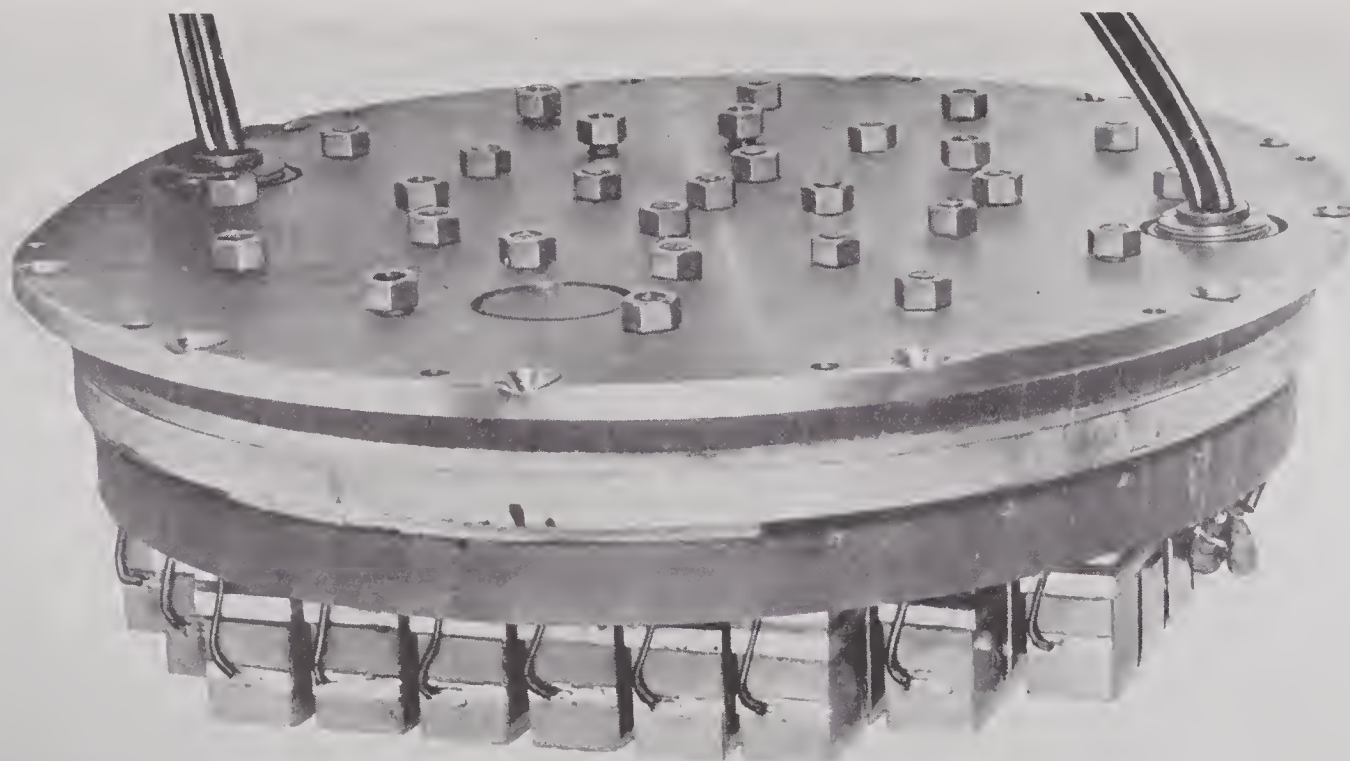


FIGURE 32. Completely assembled motor mounted on rubber sandwich ready for insertion in case. Tightening the various bolts compresses the rubber so that the section of case containing the crystals may be oil-filled. (NRL.)

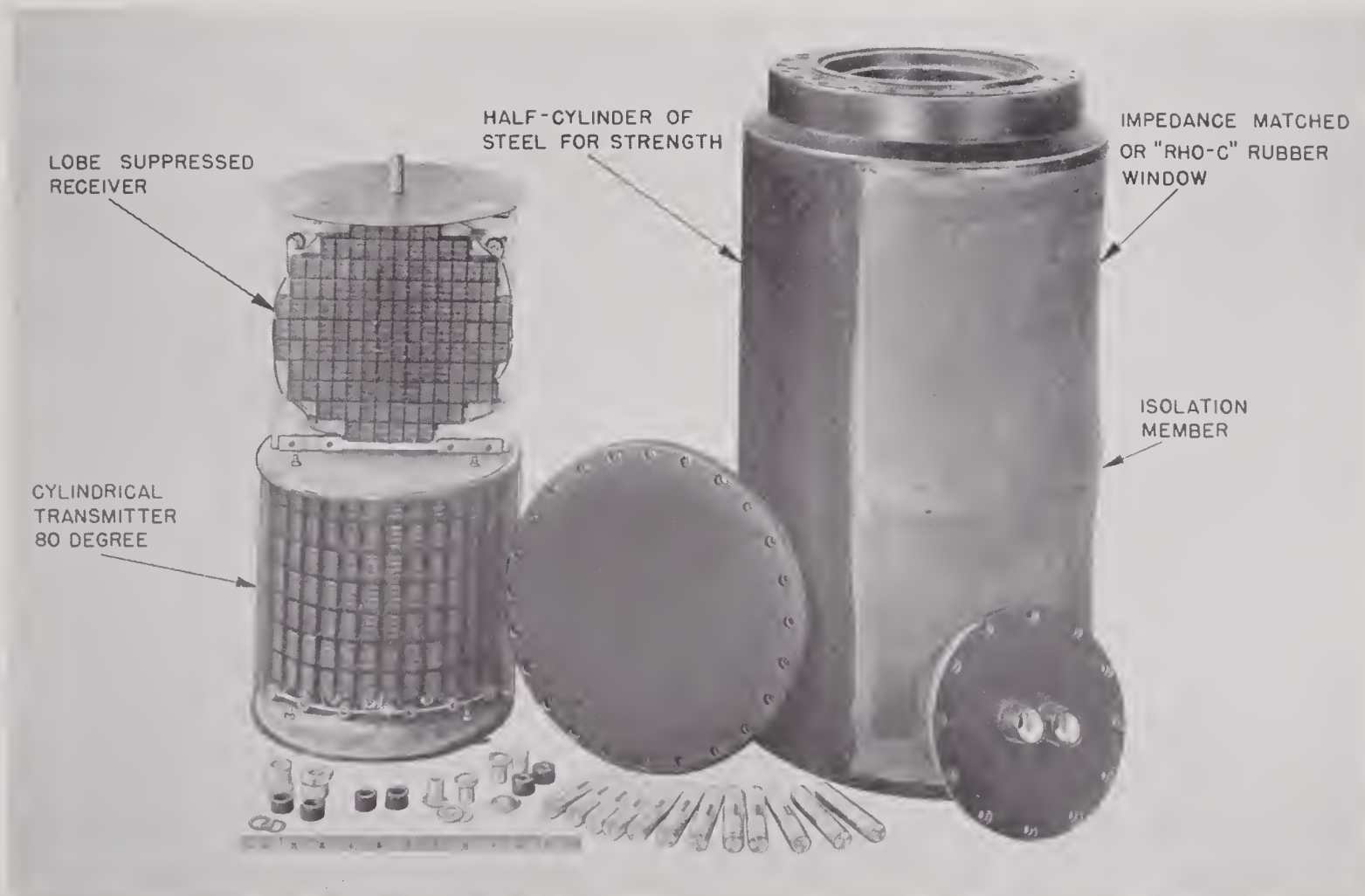


FIGURE 33. Transducer with two separate motors used in sonar system which radiates continuously. The receiver (upper motor) is flat, producing a sharp directivity pattern (Figure 43), whereas the transmitter (lower motor) is cylindrical, producing a broad pattern (Figure 44). A baffle between the two minimizes the sound fed from the transmitter to the receiver. (Assembled transducer, item 3, Figure 2.) (UCDWR CJJ78256.)

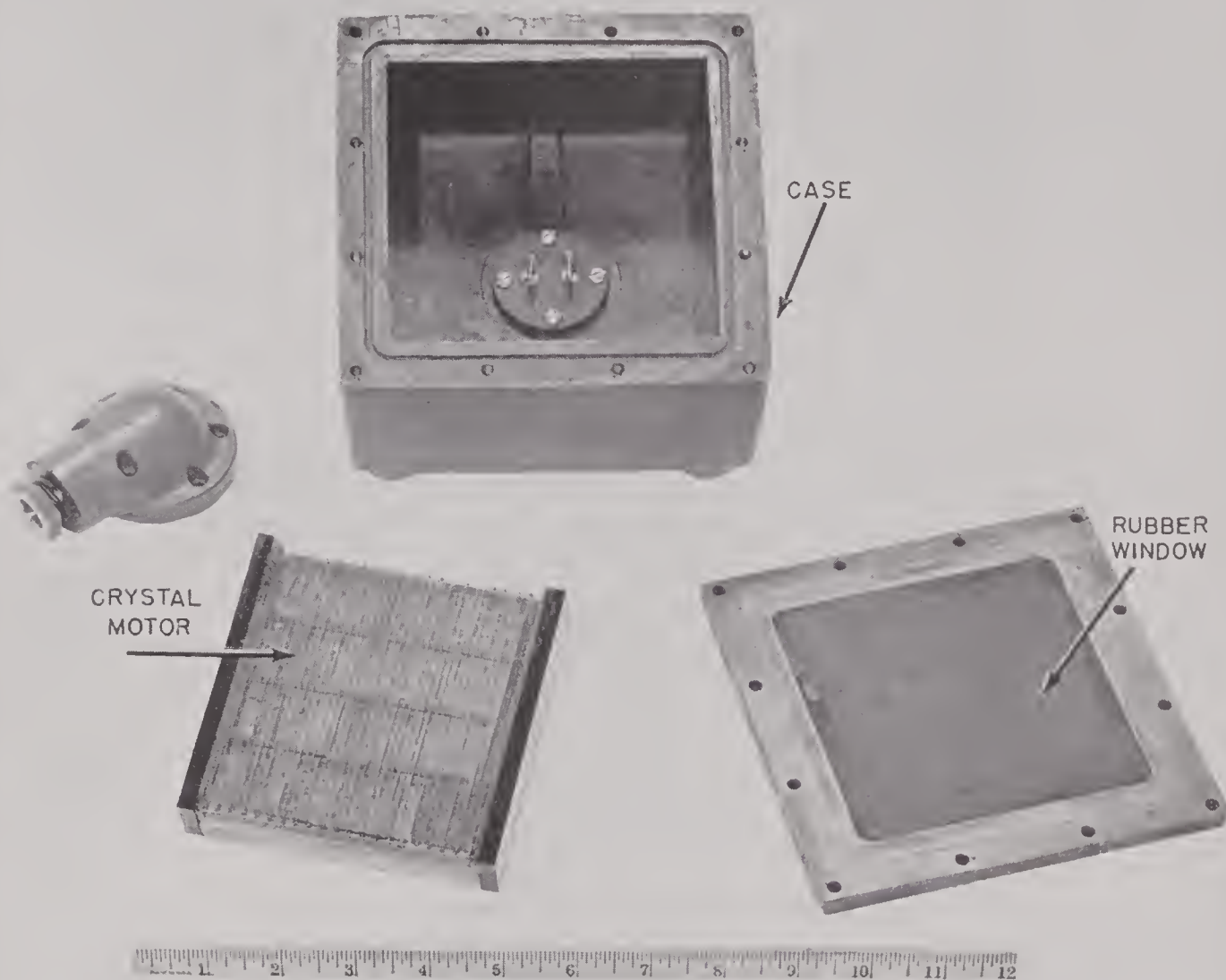


FIGURE 34. A high-frequency transducer having a motor in which the crystals are mounted "on their side" on a steel porcelain-covered backing plate. This motor is mounted in the case by nesting it in pressure-release material. The rubber window bonded into a metal frame is shown at the right. (UCDWR GD16 transducer.)

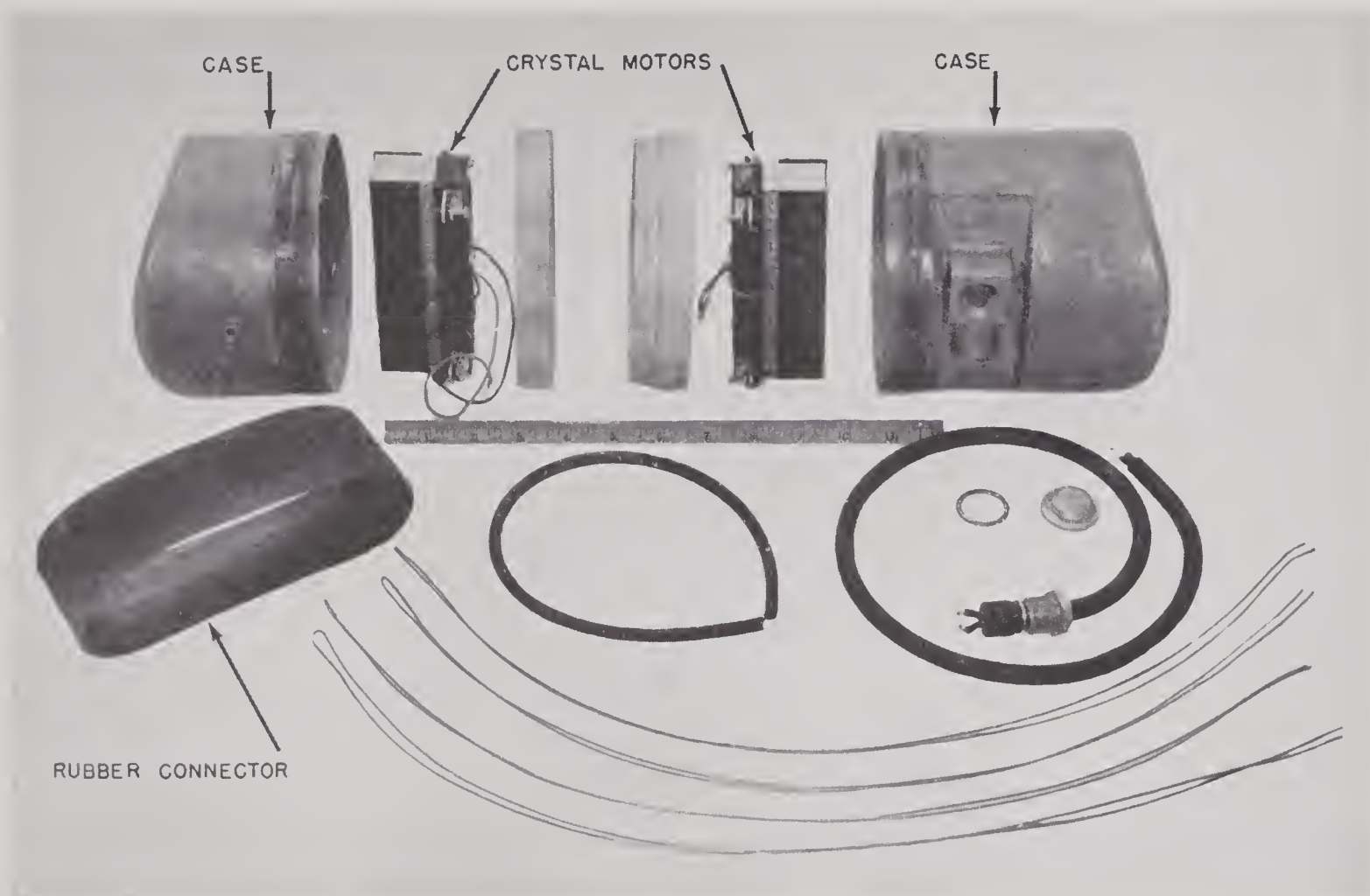


FIGURE 35. Extreme design occasioned by difficult specifications. Vibrating faces of the two motors are narrow in a horizontal plane and wide in a vertical plane. Motors are mounted in two thin metal cases connected by belt of rubber. The metal is sufficiently thin to transmit sound without appreciable attenuation. The result is a transmitter whose pattern is nearly circular in the horizontal plane and comparatively narrow in the vertical plane. (UCDWR BG2 transducer.)

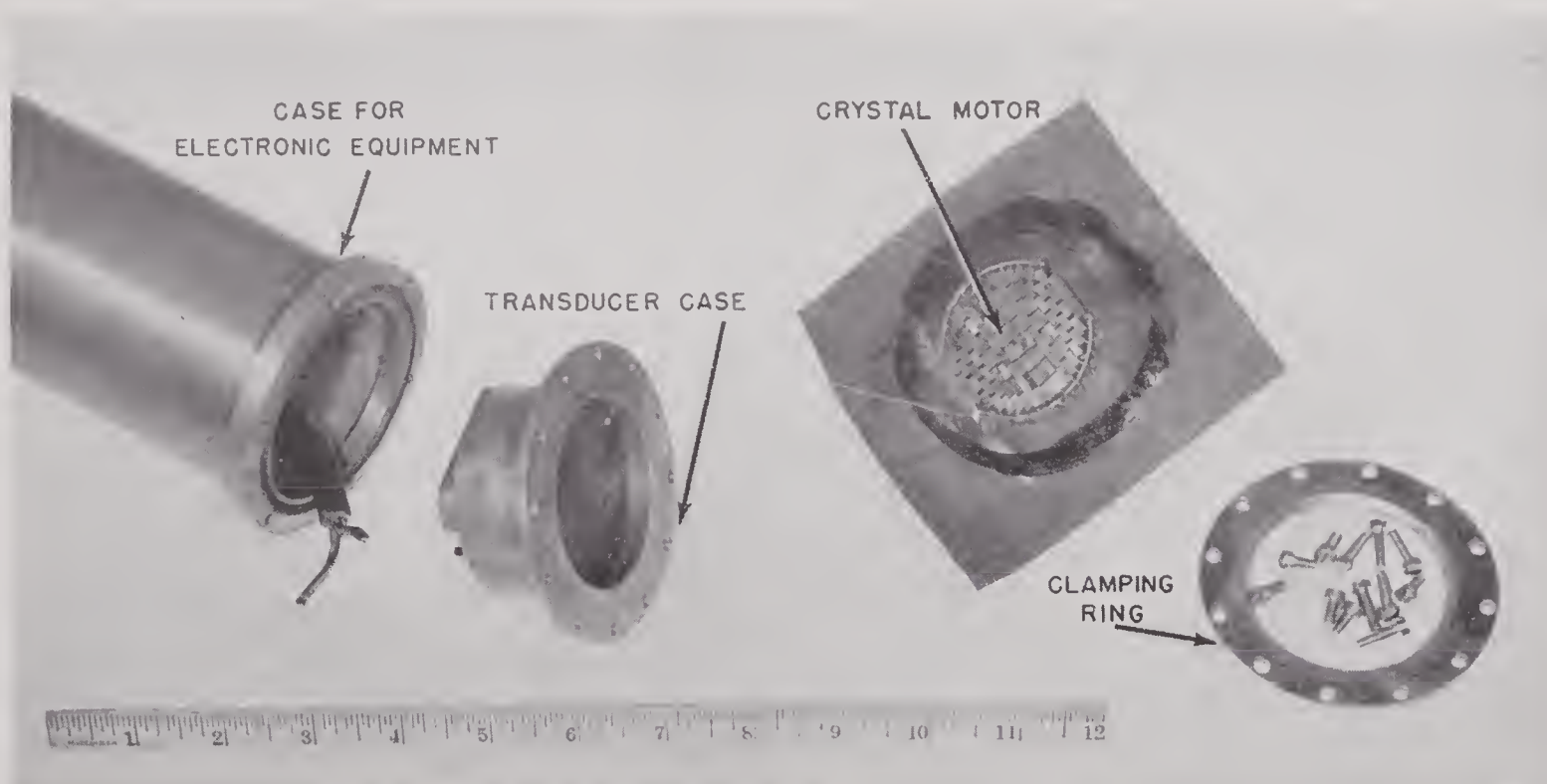


FIGURE 36. Small high-frequency transducer used in a hand-held echo-ranging device. Crystals are Cycle-Welded to rubber sheet in direct contact with the water. No backing plate. Since the crystals are coupled very directly through the thin rubber sheet with the water, this transducer is air-filled, not oil-filled. (UCDWR EP transducer.) Item 11, Figure 2 shows more advanced version of unit.

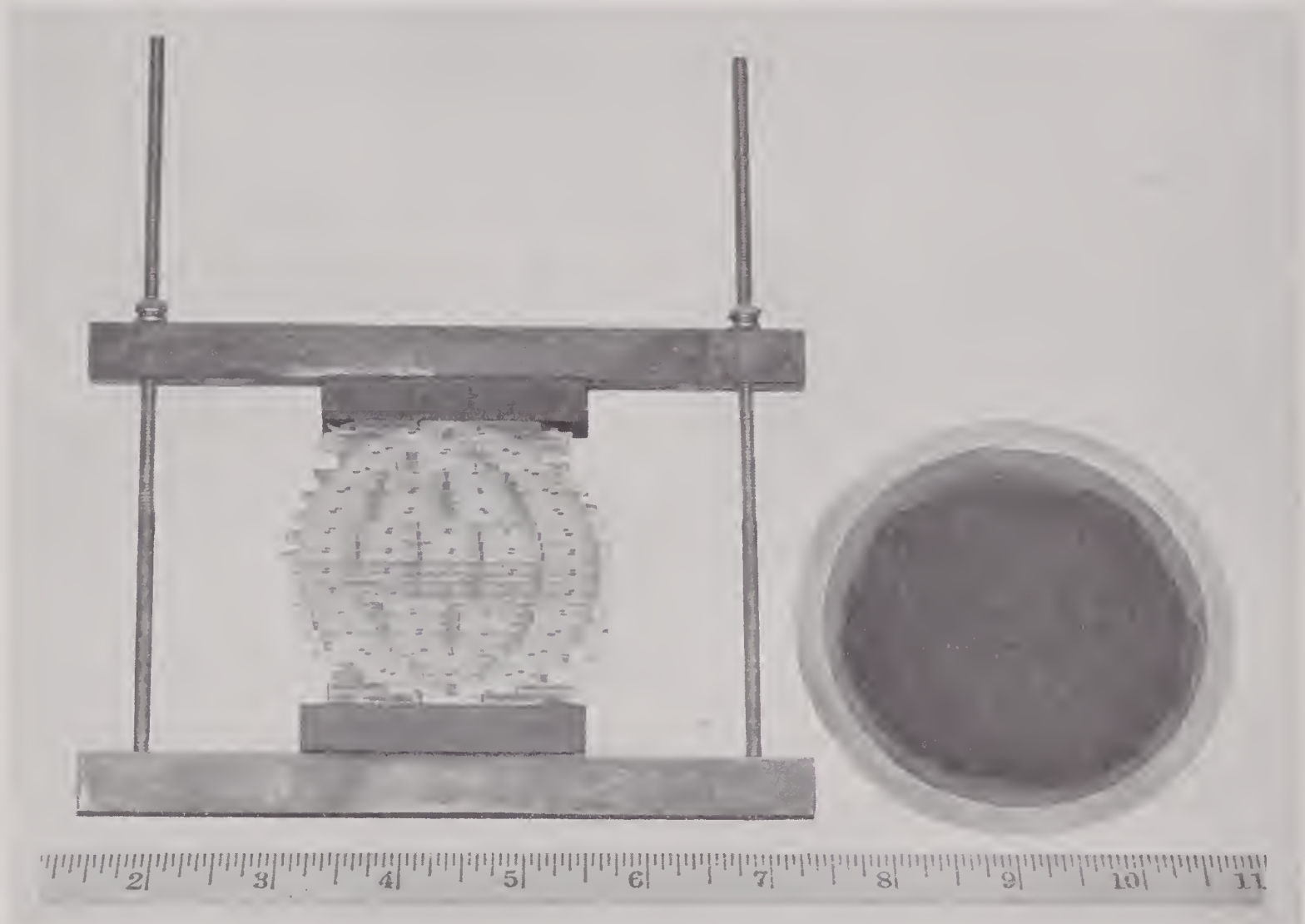


FIGURE 37. A step in the assembly of the UCDWR EP Transducer. The crystal array has been built up and is shown in its clamp at the left. The rubber diaphragm in an aluminum frame has been prepared for Cycle-Welding. The polarizing marks on the crystal in the array are to guide the assembler so that the crystals will be properly oriented to vibrate in phase.

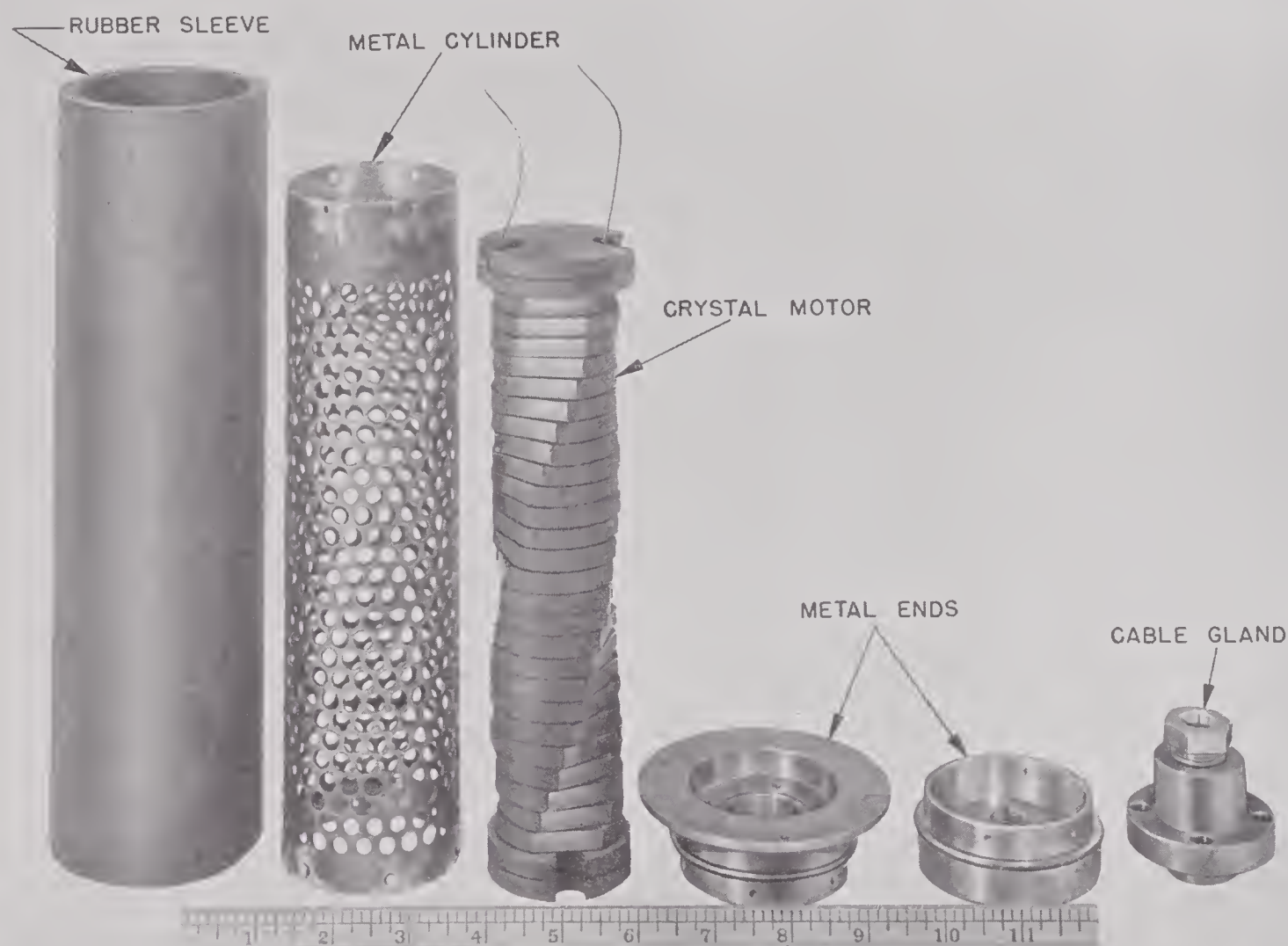


FIGURE 38. A transducer designed to have a uniform directivity pattern in the horizontal plane and a sharp pattern in the vertical plane. The crystal motor consists of a spiral "stack" cemented to pressure-release material except on the active ends. The motor is mounted inside a perforated shell which is covered by a rubber sleeve and filled with castor oil. (UCDWR CD transducer.) This is item 12 of Figure 2.



FIGURE 39. This transducer was required to meet very stringent specifications. Not only was its shape and size specified, but it was necessary that it withstand severe shock tests and that its frequency band be extremely large. For this latter reason, two separate motors have been made by Cycle-Welding crystals to a length of pressure-release material which is then wrapped around the central arbor. This unit, on being covered by the rubber sleeve, is castor-oil-filled. (UCDWR Type CCU10Z.)





FIGURE 40. The interior of another transducer designed to withstand extreme shock. Rows of crystals are Cycle-Welded to a rubber sleeve which has strengthening metal inserts in it. The unit is air-filled. (UCDWR CCU6Z transducer.)

1.3

CALIBRATION DATA

In evaluating the performance of completed crystal transducers, certain standardized, routine calibration tests are in common use. There are many technical questions involved in the selection of apparatus and procedures for these tests and in determining their accuracy, which are not considered in this volume.^{1, 2}

The purpose of this section is merely to enumerate these tests, as an indication of the type of information which may readily be obtained from a calibration laboratory.

In the performance of calibration tests, the transducer is regarded as a "black box," elastically coupled to the water and electrically accessible through two or more leads. While it is, therefore, not always simple to interpret the results in terms of internal properties, the results of these tests are nevertheless of the utmost importance.

1.3.1

Ideal Medium

Calibration tests should be made so as to depend as little as possible on the properties

of the medium and its surroundings. For example, every precaution should be taken to eliminate effects arising from surface and bottom reflections, bubbles, and obstacles. The ideal is to obtain the characteristics of the unit in an infinite homogenous medium which is completely described, for our purposes, by its phase velocity and density. The effects produced by a transducer in an actual medium then constitute a transmission problem, and are not considered in this volume.³

1.3.2

Directivity Patterns

One important property of a transducer, when acting as a transmitter, is the manner in which transmitted energy is distributed in direction; or, when acting as a receiver, the dependence of its sensitivity on the direction of the incident radiation.

The pressure produced by the unit acting as a transmitter, at sufficiently great distances (i.e., in the radiation field), can be shown to be given by $T(\theta, \phi)/r$, in which θ , ϕ , and r refer to a polar coordinate system with origin inside the unit. The function T , after multiplication by a normalizing factor to make it 1 in the direction of some suitably chosen axis, is called the *pressure directivity pattern* and may be a complex number; its absolute square is the intensity directivity pattern.

If a plane wave of fixed amplitude is incident upon the unit from various directions, the potential difference developed across the terminals is $R(\theta, \phi)$, and this function, after normalization, is called the pressure directivity pattern of the unit as a receiver; its absolute square is the intensity pattern. It is shown in Chapter 4, on the basis of very general assumptions, that the normalized T and R functions are identical; that is, the intensity-directivity pattern of a transducer should be the same whether it acts as a transmitter or a receiver. This has been experimentally verified repeatedly, so that now it is customary to measure either $|T|$ or $|R|$, whichever is more convenient.

The directivity pattern of a transducer is usually plotted on a decibel scale, so that the quantity given is $10 \log |T|^2$ or $10 \log |R|^2$, usually adjusted to 0 db in the direction of the

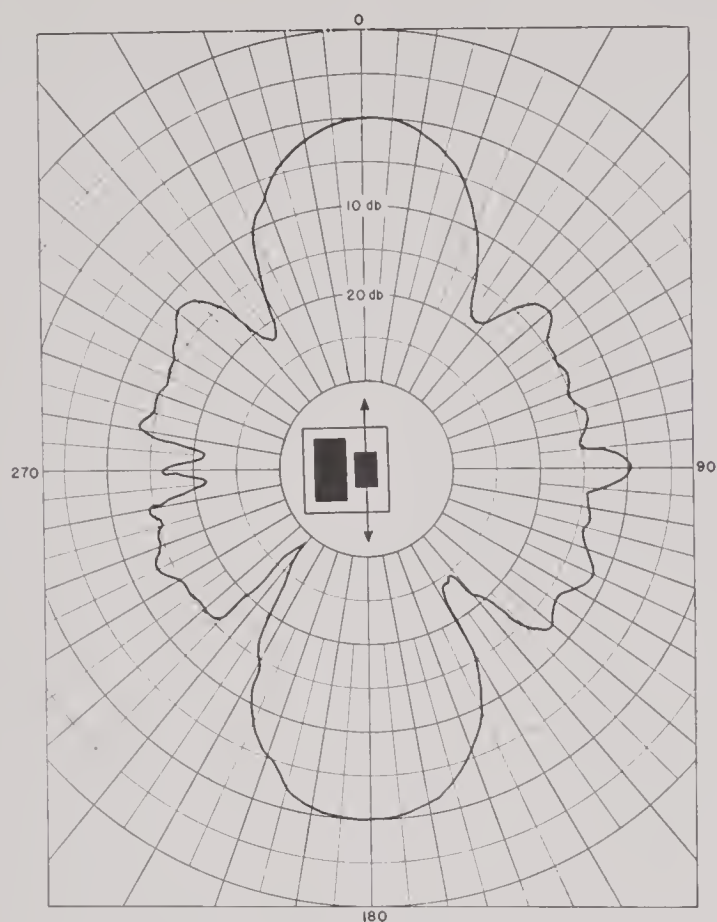


FIGURE 41. Directivity pattern of the top motor of a transducer, similar to that shown in Figure 39, in a plane through the vertical axis. The radiation upward and downward is only about 15 db below maximum. Frequency 60 kc; test distance, 20 feet; depth 9 feet. (UCDWR CCU8Z transducer.)

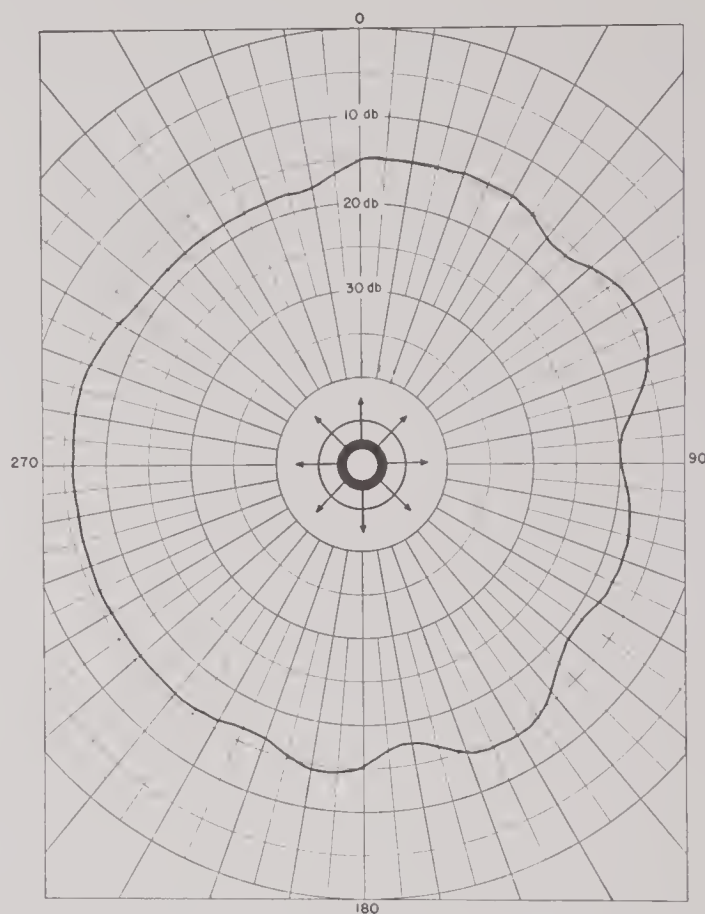


FIGURE 42. The horizontal directivity pattern of the unit shown in Figure 41. The maximum variation from uniformity is about ± 3 db, which was not important for its application. (UCDWR CCU8Z transducer.)

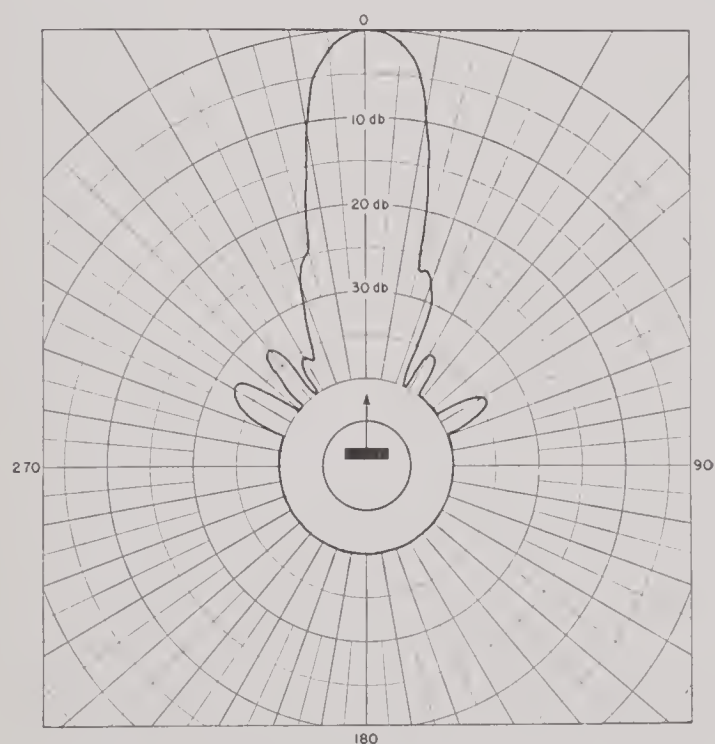


FIGURE 43. Directivity pattern of the receiver section of the unit shown in Figure 33, at 42 kc. The small side lobes are particularly to be noted. Except for two bulges on the main lobe at about -25 db, there are no side lobes greater than -30 db. Test distance, 20 feet; depth, 9 feet. (UCDWR CJJ78256 transducer.)

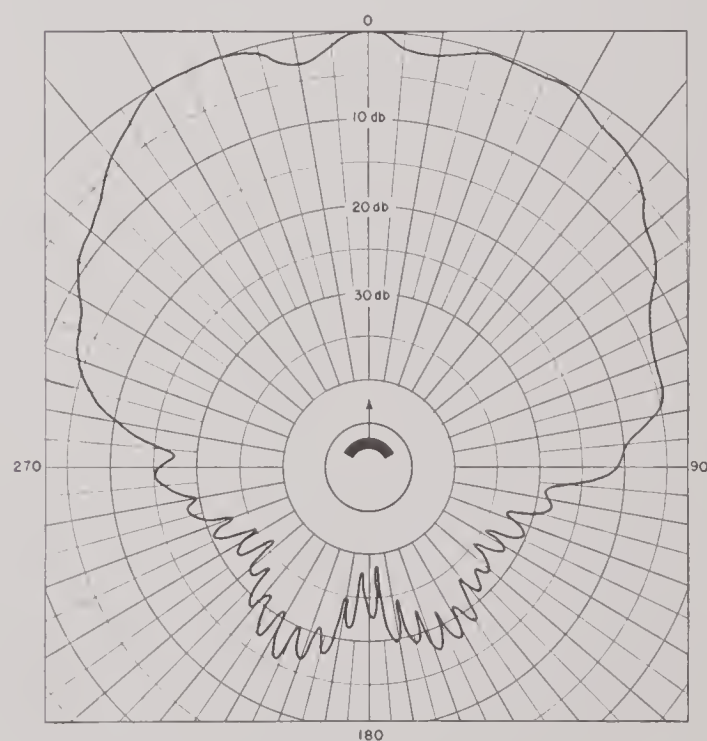


FIGURE 44. Directivity pattern of the transmitter section of the transducer shown in Figure 33. The application of curving the crystal array to get a broad beam is illustrated here. The typical diffraction pattern around the back portion is characteristic of units of this type.

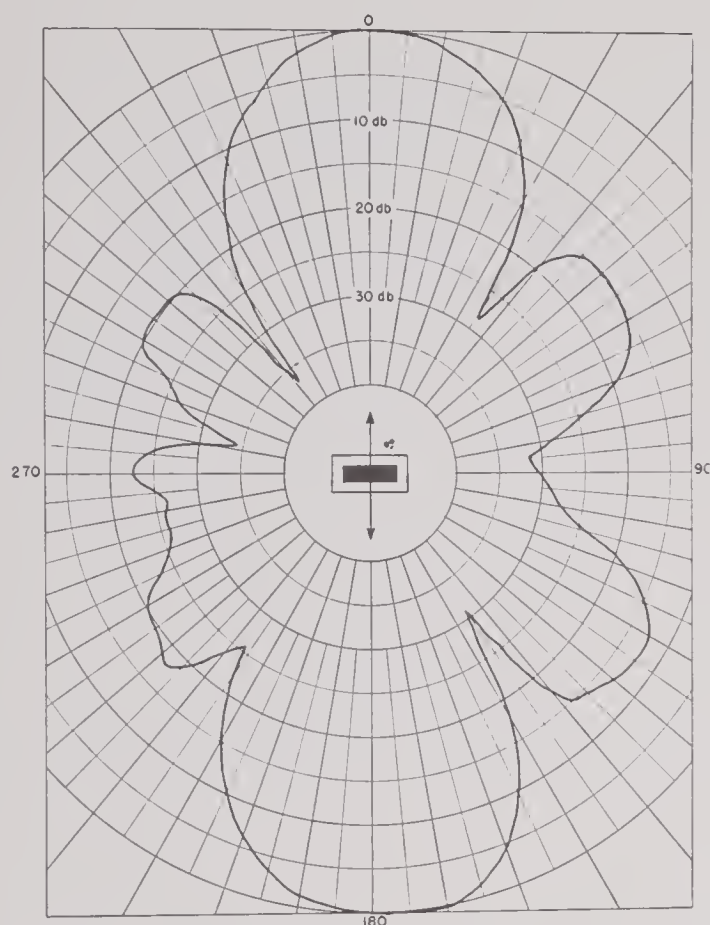


FIGURE 45. The directivity pattern of a unit whose motor is long and narrow, taken in a plane containing the long axis. The side lobes are not well suppressed, one being as high as -12 db. Frequency, 20 kc; test distance, 12 feet; depth, 9 feet. (UCDWR CY4 transducer.)

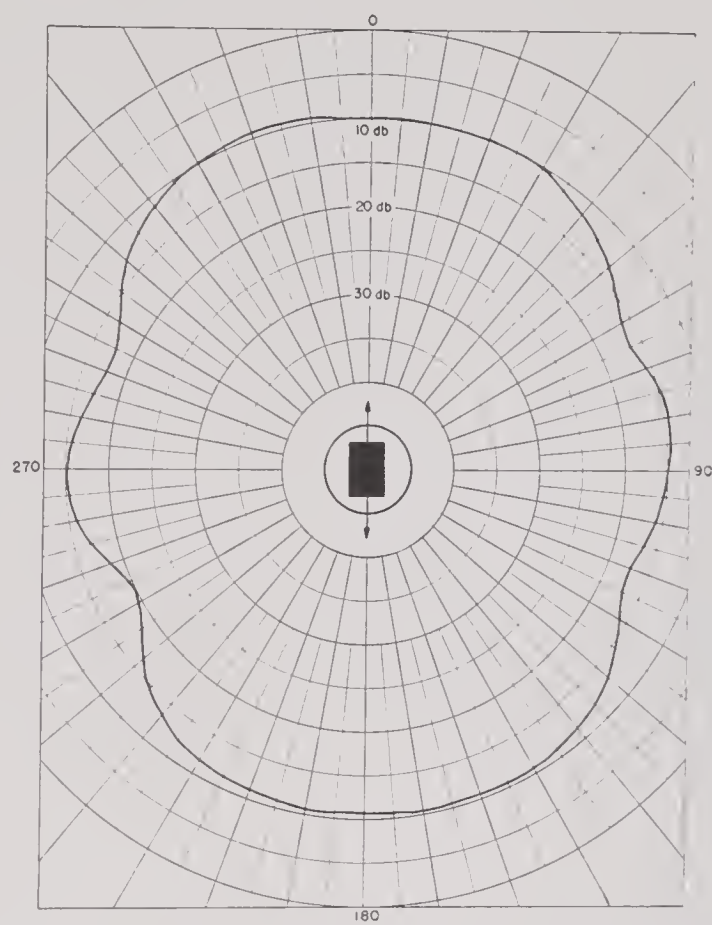


FIGURE 46. The directivity pattern of same unit as in Figure 45 in a plane perpendicular to the long axis. The short dimension of the crystal yields a roughly uniform pattern. Frequency, 20 kc; test distance, 12 feet; depth, 9 feet. (UCDWR type CY4 transducer.)

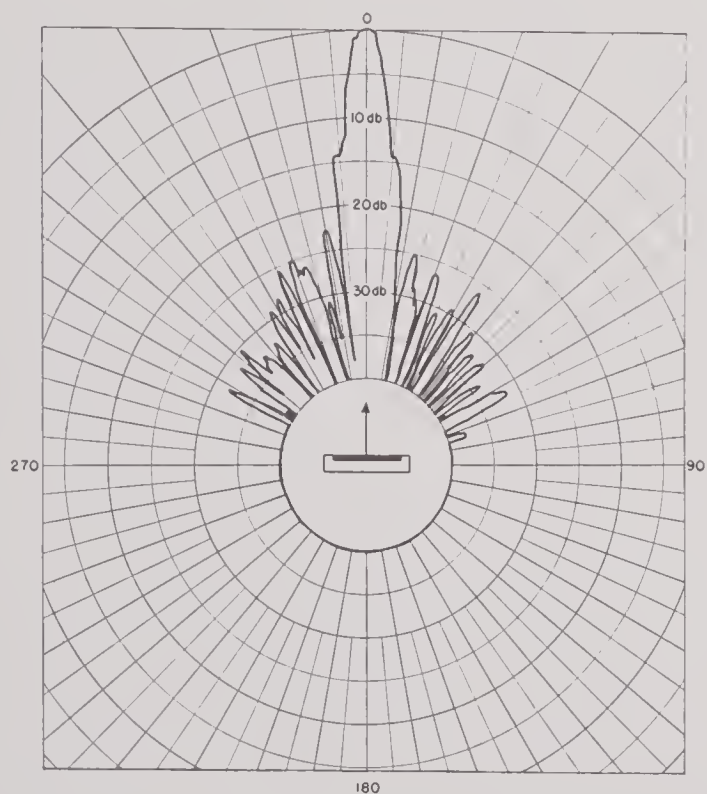


FIGURE 47. The directivity pattern of a unit designed for sharpness in one direction and breadth in the perpendicular shows very narrow beam with reasonably good suppression of side lobes. Frequency, 90 kc; test distance, 20 feet; depth, 9 feet. (UCDWR FE2Z transducer.)

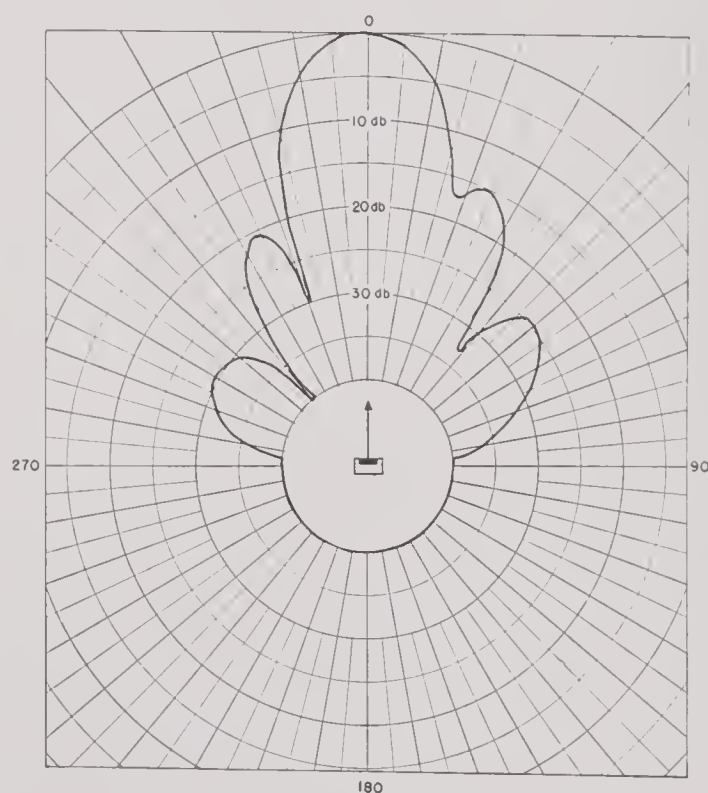


FIGURE 48. The directivity pattern of the same unit as in Figure 47 but in a plane perpendicular to the preceding. The pattern, as was desired, is found to be much broader and no effort was made to suppress the side lobes. Frequency, 90 kc; test distance, 20 feet; depth, 9 feet.

axis. The pattern will, in general, be down in all other directions, because the axis is usually chosen in the direction of maximum intensity (and sensitivity). Patterns of a few UCDWR units, in specified planes and at specified frequencies, are shown in Figures 41 to 48. The factors which influence directivity patterns, and their theoretical calculation from given data, are discussed in Chapter 4.

The total energy radiated by a transducer actuated by a given signal is a necessary quantity if one wishes to know the efficiency of the unit. The total power radiated is the integral of the intensity over any sphere completely surrounding the transducer, and this is usually expressed in terms of the intensity on the axis at some standard distance and the integral of $|T/T_{\text{axis}}|^2$ over the unit sphere. This latter integral divided by the total solid angle, is known as the *directivity factor*:

$$\text{directivity factor} = \left(\frac{1}{4\pi} \right) \int d\omega \left| \frac{T}{T_{\text{axis}}} \right|^2,$$

in which $d\omega$ is an element of solid angle. Ten times the logarithm of the directivity factor is called the *directivity index*.

Thus the directivity factor of a spherically symmetric unit is 1 and its index is 0 db. If the pattern of a unit consists of one principal lobe which is conical (i.e., axially symmetric) together with a number of minor lobes, then the directivity factor is readily obtained from the

angle θ at which the pattern is down 3 db:

$$\text{directivity factor} = \sin^2 \left(\frac{\theta}{2} \right).$$

This equation assumes the source is uniformly driven, in an infinite baffle, etc., but is quite adequate for most transducers (see Section 4.4).

For example: a pattern $\pm 10^\circ$ wide at the -3 db points has a directivity factor of approximately 0.0076 and an index of -21 db. If $\theta \leq 30^\circ$ the error in the directivity factor caused by setting $\sin \theta = \theta$ is less than 10 per cent.

1.3.3

Responses

There are a number of properties of a transducer which go under the general name of "responses." For a transmitter, the response is the intensity, usually expressed in decibels, on the axis for any of a number of different conditions of drive, such as constant voltage across the transducer terminals, constant current into a specified length of specified cable, and out of a real amplifier. It is important to notice that the response is meaningless unless the conditions of drive are carefully specified. Responses are usually given as a function of continuously increasing frequency for given conditions, such as a current of 10 ma into the unit, or 1 w of available power; however, the variation of fre-

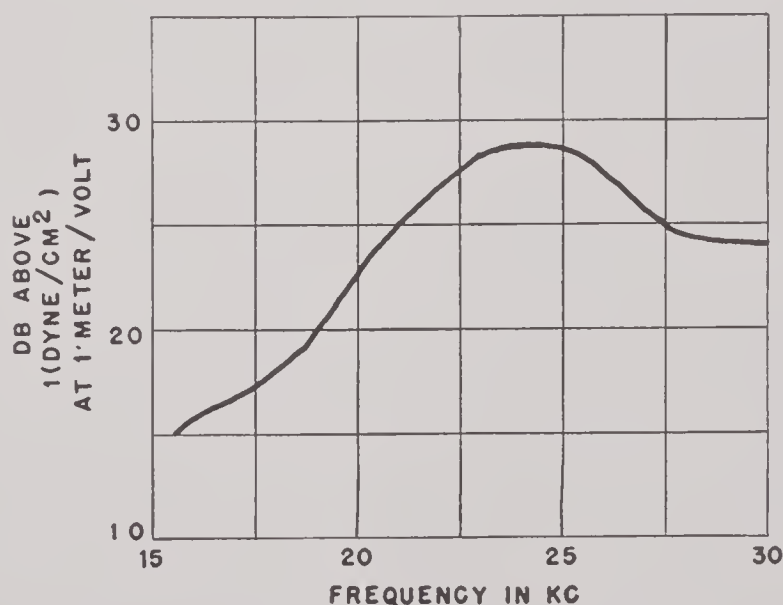


FIGURE 49. Transmitter response of the same transducer whose patterns were shown in Figures 45 and 46. In this case, constant voltage is applied to the transducer terminals. Test distance, 10 feet; depth, 9 feet. (UCDWR CY4 transducer.)

quency is not essential, as one might, for example, give the response at a single frequency as a function of the power input, to determine whether the system is linear.

The receiver response of a unit is some measure of the electric signal for a sound wave of given intensity, incident along the axis and for specified conditions of termination of the receiver (for example, open-circuit voltage across the terminals, open-circuit voltage at the end

of some definite length of cable, output at the terminals of a built-in preamplifier).

The transmitter and receiver responses of several UCDWR units, under stated conditions, are shown in Figures 49 to 51.

Factors influencing the responses of a unit are extremely complicated, depending upon the most intimate details of the internal structure. The control and improvement of responses form an important part of our subject matter.

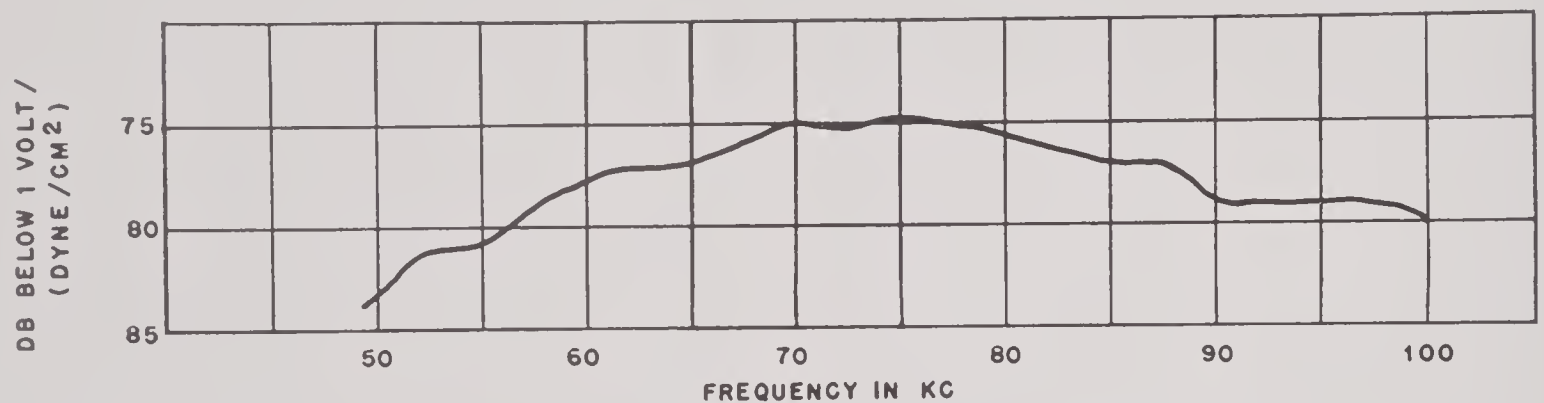


FIGURE 50. The frequency response as a receiver of a broad band transducer. Here the open circuit voltage across the transducer terminals is plotted against the frequency, and it will be noted that between 57 and 100 kc the response is uniform within $\pm 2\frac{1}{2}$ db. Test distance, 10 feet; depth, 9 feet. (UCDWR XCCZ4 transducer.)

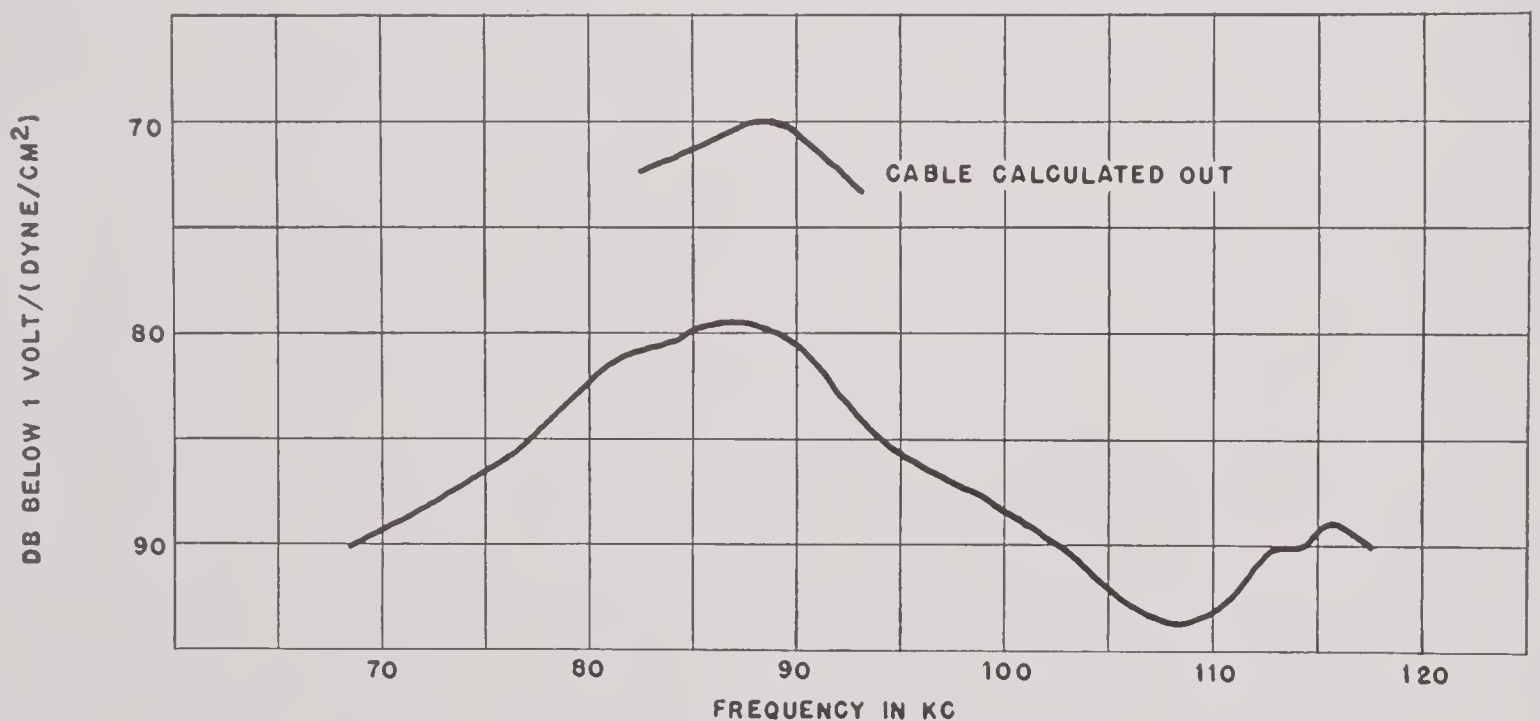


FIGURE 51. Frequently a transducer is designed for a service in which only a very short length of cable, say 2 or 3 feet, is needed, but in order to calibrate it, a much longer piece must be attached. A knowledge of the impedance of the cable and transducer permits a correction to be made for the cable. This is the open circuit voltage of a transducer, acting as a receiver, measured at the end of 35 feet of cable. Near 90 kc, the region of interest, a correction has been applied. The corrected response is about 10 db higher. Test distance, 20 feet; depth, 9 feet. (UCDWR FE2Z transducer.)

1.3.4

Impedances

Still regarding the transducer as a black box, we can make electrical measurements at the terminals and thus determine the *series-equivalent impedance* as a function of frequency. This impedance, which depends upon the elastic as well as the electric properties of the system, is merely the complex impedance, at each frequency, of the simple circuit to which, for the purpose of calculating total current, it is equivalent.

The cable usually consists of three conductors, the two leads to the crystals, and a shield, and the black box is therefore an inert three-terminal network. For routine tests, it is customary to make measurement on the two leads to the crystals, and in this case it is important to specify sharply what disposal is made of the shield. The most common arrangement is to ground the upper end of the shield, leave the lower end free, and drive through the leads from a transformer whose center tap is grounded. The series impedances of several UCDWR units are shown in Figures 52 to 55.

Impedance data, provided the conditions under which they are taken are carefully noted, serve two valuable functions. First of all, they are of immediate and practical importance in designing associated electronic systems. Second, they supply valuable information for determining the effect of various constructional features and for verifying theoretical treatments.

1.4

POWER LIMITATIONS

If the power input to the electric terminals of a transducer is increased, the sonic output will increase proportionately, at least for a while. The practical question now arises: "Under various circumstances, what factors establish the ultimate upper limit to the power which can be radiated?"

No categorical answer can be given to this question, and the best information on the subject is summarized in Chapter 4. For the present, it must suffice to mention a few of the possibilities. In certain units having a self-con-

tained power supply, the limiting factor will be the available power and the efficiency of the unit. If unlimited power is available, the limit may be set by electrical breakdown within the system, by cavitation of the elastic medium, and perhaps otherwise. No certain instance is known in which the failure of a unit, working into water, was caused by dynamic fracture of the crystals. Such cases have, it is true, been reported; however, it seems likely that these failures had other causes such as undetected fracture from rough handling followed by electrical breakdown of the damaged crystal due to high-voltage puncture.

The electrical breakdown properties of a unit can be improved by careful attention to details of construction, and some units have been operated near resonance up to 2,500 v across ADP crystals $\frac{1}{4}$ in. thick, or about 4.0 kv per cm. These same units are subjected to a routine manufacturing test of 4,400 v at 60 c, or about 7.0 kv per cm.

Cavitation is, roughly speaking, analogous to boiling induced by lowering the pressure. However, there is some evidence to suggest that metastable states are involved, and that the previous history of the medium, vaporization nuclei, and perhaps other factors make the subject much more complicated than a simple thermodynamic treatment would imply. These factors are discussed more fully in Chapters 3, 4, and 6.

1.5

APPLICATION

The many and varied applications of crystal transducers are not the direct concern of this volume, and no attempt is made to discuss this subject exhaustively. However, we must mention briefly certain aspects of their application in order to understand the nature of the specifications toward which we must work.

Let us first roughly divide all applications into *listening* and *echoing*. Listening, except in very special cases, will be done over a broad band, and a suitable receiver must therefore have a response which is reasonably flat over a considerable range of frequency. The signal-to-noise ratio is usually determined by factors

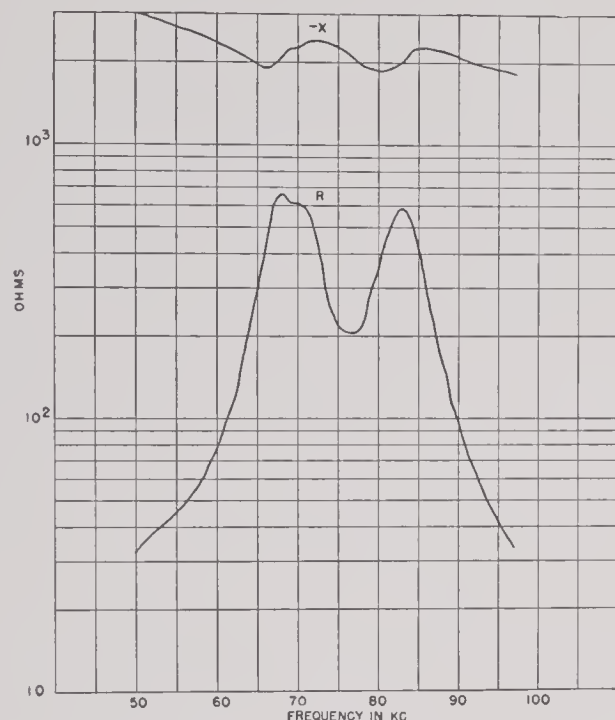


FIGURE 52. The complex series equivalent impedance, $R + jX$, of a transducer similar to that shown in Figure 39; for convenience, the negative of the reactance is plotted. The two motors are connected in parallel, leading to double maxima in the resistance and the negative reactance. The cable was compensated during the measurement by an equal cable in another leg of the bridge. (UCDWR CCU8Z transducer.)

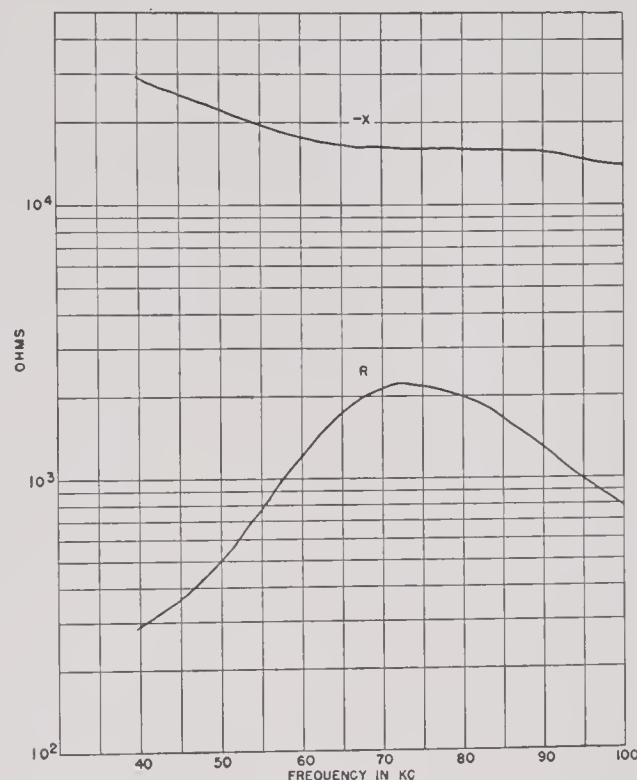


FIGURE 53. The complex impedance of the transducer whose response was shown in Figure 49. Comparison shows that the maximum resistance and the maximum response both occur at about the same frequency. (UCDWR XCCZ4 transducer.)

beyond the control of the designer, and therefore it will do no good to increase the energy-collecting area of the unit beyond a certain point; therefore, the size of a receiver is almost always determined by the desired directivity pattern. Two distinct types of directivity patterns will serve most purposes: one will either wish the receiver to collect signals coming from any and all directions (thereby also accepting noise from all directions), whereupon the directivity pattern will approach a sphere; or else, one will desire to receive signals only from within a rather restricted cone, either to improve the signal-to-noise ratio or to determine direction, or both. In this last case the directivity pattern should consist of one main lobe with the side lobes reduced as much as possible (see Chapter 4).

Echoing falls into two classes, single and band frequency. The first corresponds to transmitting long wave trains (pings), and the second includes both frequency modulation and short pings. The first requires that the response be as high as possible at a single frequency and

is not greatly concerned with the behavior at other frequencies, while the latter requires a fairly flat response over a band. Directivity patterns will vary from narrow single lobes to broad patterns, depending on the particular application, how much reverberation and noise can be tolerated, etc.

If a separate transmitter and receiver are used, the consideration determining the characteristics of the receiver are similar to those in listening, except for the frequency range. In some applications, one unit serves both as transmitter and receiver, and here the desired properties of the transmitter must usually take precedence.

One of the most important properties of a transmitter is the amount of power that it can radiate either continuously or in intermittent pings, depending on the application. The factors determining the ultimate power output of a unit are quite complicated and, in so far as they are understood, are discussed in Chapters 3, 4, and 6.

In some cases, factors outside the control of

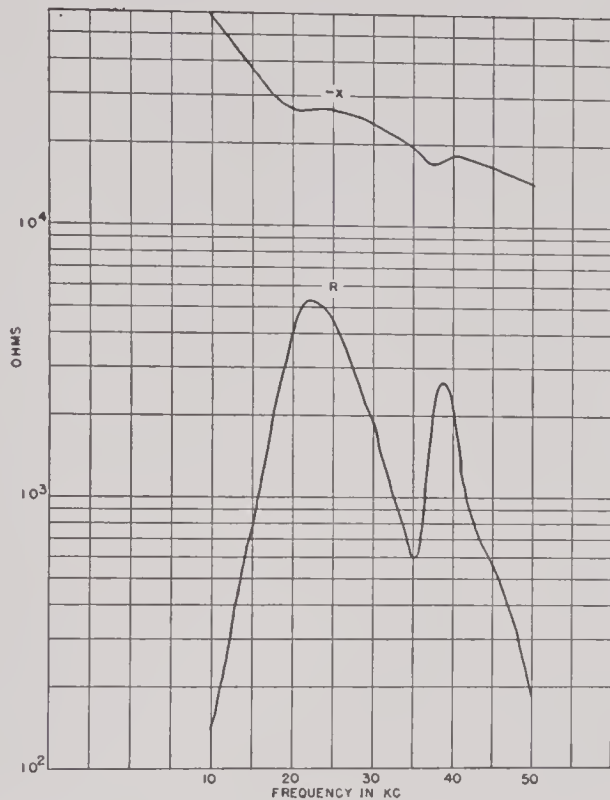


FIGURE 54. The complex impedance of the transducer whose response was shown in Figure 50. Here again it is noted that the maximum response and the maximum resistance occur at approximately the same frequency. The second peak is the second resonance of the *same* crystals, as distinguished from the first resonances of two different sets of crystals shown in Figure 52. (UCDWR CY4 transducer.)

the designer may determine the type of electronic gear which must be used; for example, certain units may require a self-contained battery-operated power supply, and in this case the efficiency of the unit may become extremely important. As a general rule, however, the associated electronic equipment should be designed to the transducer rather than the reverse, since electronic systems are more flexible than crystal transducers. If for any reason this cannot be done, then it is of the utmost importance to know the characteristics of the electronic system with which the transducer must work.

Finally, the type of service to which the transducer will be exposed must be taken into account. For example, a unit may be required

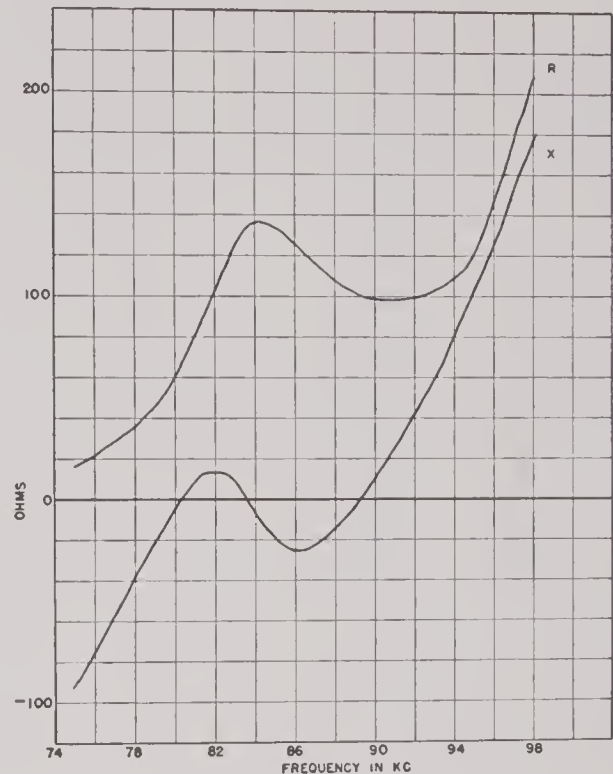


FIGURE 55. Frequently a matching network is installed inside the case of a transducer between the cable and the crystal motor to alter its response. This is the complex impedance of the unit whose response is shown in Figure 51. It will be noted that the maximum resistance now occurs at a somewhat lower frequency than the resonance shown in that figure. Note also that the sign of the reactance has not been reversed and that the ordinates are linear rather than logarithmic. (UCDWR FE2Z transducer.)

to go very deep in the water, whereupon both the effects of pressure and of operating the unit from a long cable must be taken into account. Again, the system may be exposed to shock of one kind or another and its mechanical ruggedness therefore becomes a matter of prime importance.

* * *

The purpose of this chapter has been to survey briefly some of the general problems that arise in the design of crystal transducers. The rest of this volume is devoted to a detailed study of these problems and attempts to indicate the state of knowledge of the subject at present.

Chapter 2

THE PHENOMENOLOGICAL THEORIES OF LINEAR DISSIPATIVE ELASTICS, DIELECTRICS, AND PIEZOELECTRICS

By Glen D. Camp

CRYSTAL TRANSDUCERS involve such a multiplicity of physical phenomena that, without a theory to correlate experimental data, these data would appear as a hopeless jumble. Therefore, before attempting a detailed study of crystal transducers, the theories of elastics, dielectrics, and piezoelectrics are here developed from more basic laws of physics. Elasticity is required for itself, to elucidate the properties of backing plates, to study viscous dissipation mechanisms, etc. Furthermore, a linear dissipative piezoelectric system is a superposition of an elastic and a dielectric system, both anisotropic and both occupying the same region, with coupling between the two. It is instructive to develop the theories of the uncoupled systems separately and then couple them.

The first section is devoted to pure elasticity; after developing the general linear anisotropic theory, it is specialized to yield the theory of isotropic solids and viscous and nonviscous fluids. The second section is devoted to the theory of linear anisotropic dielectrics.

In the third section, coupling is established between these two systems, yielding the theory of linear piezoelectricity. Dissipation of several types is introduced, since these phenomena are important in crystal transducers. The section closes with a study of the symmetry properties of *Rochelle salt* [RS] and *ammonium dihydrogen phosphate* [ADP].

The general reciprocity theorem, and the rigorous equivalent circuit for a linear dissipative piezoelectric system, are deduced in the fourth section.

A variational principle, rigorously equivalent to the basic boundary-value problem of linear dissipative piezoelectric systems, is developed in the fifth section. This variational principle is used to solve the boundary-value problem for rectangular plates of 45° Y-cut RS and 45° Z-cut ADP. The solution is obtained first in the Mason approximation, and later in a higher

approximation which includes some additional effects of practical importance.

2.1

ELASTICS

The linear approximation to the theory of elasticity is adequate for all our work, a very fortunate circumstance since the theory becomes extremely complicated in higher order. The proof that the linear approximation is adequate depends partly on results obtained later but will be outlined here.

Consider a crystal radiating into water at a single frequency. The displacement amplitude is approximately $u = U \sin 2\pi x/\lambda'$ in which x is measured from the nearest node (or virtual node, if there is none in the crystal), λ' is the wavelength in the crystal, and U is the maximum amplitude at the real or virtual loop at $x = \lambda'/4$. The strain is du/dx which has its maximum value $2\pi U/\lambda'$ at $x = 0$. If $x = L'$ is a face at which the crystal is radiating into water, then the intensity is

$$I = \left(\frac{\rho c^3}{2} \right) \left(\frac{2\pi U}{\lambda} \right)^2 \sin^2 \frac{2\pi L'}{\lambda'}.$$

We can therefore express the maximum strain in terms of the intensity,

$$\left(\frac{2\pi U}{\lambda'} \right) = \left(\frac{\lambda}{\lambda'} \right) \left(\frac{2I}{\rho c^3} \right)^{\frac{1}{2}} \csc \frac{2\pi L'}{\lambda'},$$

which is of order 10^{-5} if the crystal is resonant ($L' = \lambda'/4$) and $I = 0.3$ w per sq cm per sec, the so-called steady-state cavitation level in sea water (see Section 4.8). Even if an intensity of 10^4 times "cavitation" could be achieved, and if L' were only $(1/2)^4$ of its resonant value, so that the crystal was operating four octaves away from its resonant frequency, then even under these conditions, which are absurdly extreme since voltage breakdown would occur long before they could be achieved, the maxi-

mum strain would be only 10^{-2} . It is therefore valid, in all applications, to neglect squares and products of strain components compared to the strain components themselves, the error so incurred being considerably less than 1 per cent.

2.1.1 Physical Principles

There are two basic physical principles which make the formulation of a phenomenological theory of elasticity feasible. First, the displacement of the particles in any region is a superposition of a random thermal agitation together with a (relatively) slowly varying and orderly displacement. The wavelengths associated with elastic vibrations, even for very high frequencies, are very large compared with the average distance between atoms^a and this permits us to treat an elastic medium as a continuum, the variation in thermal motion being reflected primarily in the temperature dependence of the density, elastic moduli, etc. The dissipation corresponding to the conversion of the orderly displacement into thermal agitation in crystals, steel, etc., is so small compared to the losses in a practical transducer that we neglect it entirely (e.g., the mechanical Q of the resonance of a free crystal is greater than 2,000, one drop of castor oil on the surface reduces this to a few hundred, and in a completed transducer in water it is of order 5). Thus we may treat all substances as continua, and, furthermore, crystals, steel, and most other metals, glass, etc., may be regarded as dissipationless. The latter is not true of many plastics such as synthetic rubber.

Second, molecular forces are of extremely short range compared to the shortest wavelengths encountered, the range being of the order of the molecular diameter. This means that the elastic effect of these forces, which is their average over a time long enough to smooth out the random thermal agitation but still short compared to the period, is equivalent to a system of internal stresses acting across every sur-

face in the medium. These stresses are generated by a point (derivative) operator acting upon the displacements, whereas if the range of molecular forces was comparable with the wavelength, a finite-distance (integral) operator would be involved, enormously complicating theoretical treatments.

The elastic behavior is determined by an array of experimentally determined moduli, no attempt being made to calculate these elastic constants from molecular interactions. In the present linear approximation, the maximum number of distinct moduli is 21 (see Section 2.1.4) and any symmetry reduces this number. The problem which we must solve is to find the motion from these given moduli and from the geometry and the density of an elastic system, together with interactions with other systems. We must first develop the kinematics of continua.

2.1.2 Displacement and Strain

We choose a Cartesian^b coordinate frame xyz fixed with respect to the undisplaced position of our elastic body.¹ To take advantage of tensor notation, we shall use x_m with $m = 1, 2, 3$, interchangeably with xyz according to

$$x_1 = x, x_2 = y, x_3 = z. \quad (1)$$

A displacement takes the material in the immediate neighborhood of x_m to a new point \bar{x}_m given by

$$\bar{x}_m = \bar{x}_m(x_1, x_2, x_3) = x_m + u_m. \quad (2)$$

The coordinates \bar{x}_m of displaced points still refer to the original frame, which is fixed with respect to the undisplaced position of the body.

The three quantities u_m are the Cartesian components of the displacement of each particle, measured from a local origin which is just the undisplaced position of the same particle. This displacement will, in general, be different at each point both in magnitude and direction, and will therefore be a function of xyz ; in kinetic problems, it will also be a function of time.

^b Since the field equations are obtained in tensor form, their transformation to other frames is a simple matter.

^a Even at 100 mc, the wavelength in air at STP is 3×10^{-4} cm, while the mean distance between molecules is of order 3×10^{-7} . In water the wavelength is greater and the separation is smaller, the corresponding figures being 1.5×10^{-3} and 3×10^{-8} cm.

Since to each point in the undisplaced body there corresponds a unique point in the displaced body, and conversely, the Jacobian of the transformation which generates the displacement, equation (2), must be neither zero nor infinite. Neglecting squares of the dimensionless quantities du_m/dx_n , the Jacobian is

$$J\left(\frac{\bar{x}, \bar{y}, \bar{z}}{x, y, z}\right) = J\left(\frac{\bar{x}}{x}\right) = \left|\left(\delta_{mn} + \frac{du_m}{dx_n}\right)\right| \simeq 1 + \text{div } \mathbf{u}, \quad (3)$$

in which δ_{mn} is the Kroneker delta, 1 if $m = n$, 0 otherwise.

If we follow the motion of all the material that was within some region R bounded by a closed surface S , then, owing to the displacement, this material will at a later time be in some displaced region \bar{R} bounded by \bar{S} . The total momentum belonging to this material is then given by

$$\int_{\bar{R}} \rho(\bar{x}, \bar{y}, \bar{z}) \dot{\bar{x}}_m(\bar{x}, \bar{y}, \bar{z}) d\bar{x} d\bar{y} d\bar{z}, \quad (4)$$

in which $\dot{\bar{x}}_m$ is the velocity of the material at $\bar{x}\bar{y}\bar{z}$, the displaced point which came from xyz . Now since there is a unique transformation connecting $\bar{x}\bar{y}\bar{z}$ and xyz , this integral can be transformed back into one over the undisplaced region R . In this transformation, $\dot{\bar{x}}_m$ becomes just $\dot{x}_m(xyz)$, and while there is a correction necessary to ρ , this correction is exactly compensated by the Jacobian factor (see next paragraph) and, hence, the momentum becomes

$$\int_R \rho \dot{x}_m dx dy dz. \quad (4')$$

By similar arguments, we can calculate any other quantity associated with an arbitrary region \bar{R} which is generated by the displacement of a region R (e.g., kinetic energy and potential energy). As the only examples of cases in which the deviation of the Jacobian from 1 must be taken into account, we may calculate the change in density and the related quantity, the dilatation. By our definition of \bar{R} ,

it contains exactly the same particles as R , and hence contains the same mass

$$m = \bar{m} = \int_R \rho dx dy dz = \int_{\bar{R}} \bar{\rho} d\bar{x} d\bar{y} d\bar{z} \quad (5)$$

$$= \int_R \bar{\rho} J\left(\frac{\bar{x}}{x}\right) dx dy dz.$$

Now since equation (5) is valid for any arbitrary region, we have

$$\bar{\rho} = \frac{\rho}{J(\bar{x}, x)} \simeq \rho(1 - \text{div } \mathbf{u}). \quad (6)$$

The dilatation, defined as the increase in volume per unit volume of a very small undisplaced region [i.e., the limit of $(\bar{V} - V)/V$], can be calculated directly from equation (6) by taking advantage of the equality of masses, or as follows:

$$\begin{aligned} \bar{V} - V &= \int_{\bar{R}} d\bar{x} d\bar{y} d\bar{z} - \int_R dx dy dz \\ &= \int_R [J\left(\frac{\bar{x}}{x}\right) - 1] dx dy dz. \end{aligned} \quad (7)$$

For a small enough region, the bracket may be taken outside of the last integral in equation (7), whereupon the remaining integral becomes just V , and we have

$$\lim \frac{(\bar{V} - V)}{V} = J\left(\frac{\bar{x}}{x}\right) - 1 \simeq \text{div } \mathbf{u}. \quad (8)$$

Thus $\text{div } \mathbf{u}$ is the fractional increase in the volume at each point, consistent with equation (6) which shows that, neglecting second-order terms, it is also the fractional decrease in the density.

We may summarize the foregoing by noticing that to calculate any quantity associated with a region R or the corresponding displaced region \bar{R} , we may in our approximation ignore the distinction between the two regions if the quantity is first or higher order (momentum, kinetic, or potential energy), and only need to observe the distinction if we wish to calculate the first-order correction to a 0th-order quantity (mass, volume).

To complete our study of the kinematic aspects of displacements, we must now develop the well-known result that the most general infinitesimal displacement may be regarded as the superposition *at each point* of a rigid translation, a rigid rotation, and a deformation which distorts every small sphere into an ellipsoid. The local translation is just u_m , and the local rotation and deformation are determined by the antisymmetric and symmetric parts of the tensor du_m/dx_n , respectively. These local displacements fit together to form a displacement of the

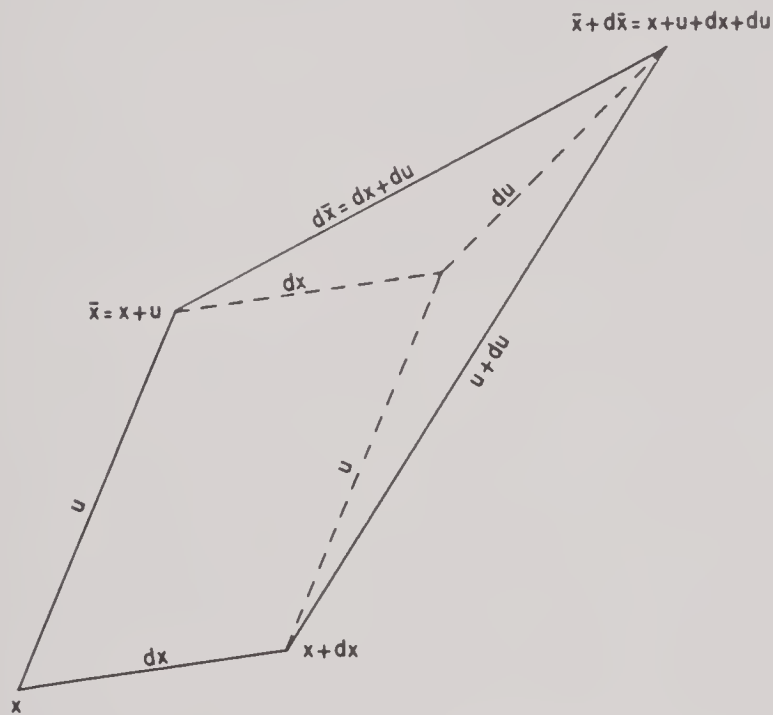


FIGURE 1. Illustration of displacement and strain.

whole body without fracture precisely because they are generated by a continuous vector field u_m through its derivative tensor, and, hence, there are differential identities connecting the local displacements at neighboring points.

Referring to Figure 1, consider all those particles which, in the unstrained state, lie on dx between x and $x + dx$ (subscripts are dropped in this discussion, but all quantities are tensors). The displacement takes x to $\bar{x} = x + u$ and $x + dx$ to $(\bar{x})_{x+dx} = x + dx + u + du$. Thus, the particles on dx are translated by u and the translated vector d is rotated and extended by du to form $d\bar{x}$, according to^c

^c The notation $,n$ is the commonly used abbreviation for d/dx_n . Also, the Einstein convention is used, whereby repeated indices are automatically summed over, unless the contrary is specifically stated, without writing a summation sign.

$$d\bar{x}_m = \frac{d\bar{x}_m}{dx_n} dx_n = (\delta_{mn} + u_{m,n}) dx_n. \quad (9)$$

We now separate $u_{m,n}$ into its symmetric and antisymmetric parts, both of which are tensors:

$$\begin{aligned} u_{m,n} &= s_{mn} + a_{mn} \\ s_{mn} &= \frac{u_{m,n} + u_{n,m}}{2} \\ a_{mn} &= \frac{u_{m,n} - u_{n,m}}{2} \end{aligned} \quad (10)$$

The matrix $(1 + u)$ in equation (9) differs only by the small matrix u from the identity, so that neglecting second-order small quantities,

$$\begin{aligned} (1 + u) &= (1 + s + a) \\ &\simeq (1 + s)(1 + a) \\ &\simeq (1 + a)(1 + s), \end{aligned} \quad (11)$$

$$\begin{aligned} d\bar{x}_m &= (\delta_{mp} + s_{mp})(\delta_{pn} + a_{pn}) dx_n \\ &= (\delta_{mp} + a_{mp})(\delta_{pn} + s_{pn}) dx_n. \end{aligned} \quad (12)$$

Equation (12) asserts that $d\bar{x}$ is generated from dx by applying the matrices $(1 + a)$ and $(1 + s)$, and that the order is immaterial so long as we neglect second-order terms. Now $(1 + a)$ is the matrix of an infinitesimal rigid rotation, while $(1 + s)$ carries a sphere into an ellipsoid. The rotation is given by

$$\theta = \frac{1}{2} \text{curl } u. \quad (13)$$

The equation of the ellipsoid, referred to a frame parallel to our fundamental frame but with origin at \bar{x} , is obtained as follows: we consider all elements dx of some constant length r and ask upon what surface their ends lie after the displacement. We already know that their initial ends all move by u to \bar{x} , and their length and direction is given by equation (12). Solving equation (12) and forming the square of the length of dx , we have

$$dx_m \simeq (\delta_{mn} - u_{m,n}) d\bar{x}_n, \quad (14)$$

$$\begin{aligned} dx_m dx_m &= r^2 \\ &= d\bar{x}_p (\delta_{mp} - u_{m,p}) (\delta_{mn} - u_{m,n}) d\bar{x}_n \\ &= d\bar{x}_p (\delta_{pn} - 2s_{pn}) d\bar{x}_n. \end{aligned} \quad (15)$$

Equation (15) asserts that a quadratic form in the $d\bar{x}$ is a constant r^2 , and this is an ellipsoid because the principal values of $1 - 2s$ are all positive since all components of s are small compared to 1; physically, a hyperbola would correspond to rupture.

Now from equation (15), or more directly

from equation (12), after discarding the rigid rotation (since it does not change the length of dx), we see that the principal values of \bar{r}/r , the ratio of the length of $d\bar{x}$ to that of dx , are 1 plus the principal values of s , and the extensions in the three principal directions are therefore

$$\bar{r} - r = r(\text{principal values of } s). \quad (16)$$

Thus, the principal values of s are the principal strains and s_{mn} is therefore called the strain tensor. Anticipating a later application, it should be emphasized that only s contributes to the deformation of an element dx , and, hence, only this part of $u_{m,n}$ can occur in the potential energy density.

In nearly all works on elasticity, the strain is specified by a matrix e_{mn} whose diagonal elements are identical with s_{mn} but whose off-diagonal elements are just twice as large. Unlike s_{mn} , e_{mn} is not a tensor,^{2, 3a} and this causes dissymmetry in the equations of motion (see Section 2.1.3) and complicates the transformation of these equations to other frames of reference. Despite these disadvantages, long usage has firmly established the e_{mn} in elastic theory, and it is necessary to know the distinction between them and the strain tensor s_{mn} .

2.1.3 Stresses; Equations of Motion

As remarked in Section 2.1.1, the forces with which one part of an elastic body act upon another have a very short range and therefore, on a macroscopic scale, are equivalent to a system of stresses over every surface inside the body. The force on an element of area dS must be proportional to dS and, except in fluids, must also depend upon its orientation. Every surface element dS has two normals pointing in opposite directions and we shall say that dS belongs to that part of the material lying on the side toward which the normal is taken. Now choose an element whose normal points in the direction of the positive x axis and call the components of whatever force acts upon it,

$$-P_{xx}dS, -P_{yx}dS, -P_{zx}dS. \quad (17)$$

The minus signs are chosen to agree with conventions used in most works of elasticity and it

should be noted that the components of the stress normal to the surface, P_{xx} , is positive for a tension and negative for a pressure. The tangential components of the stress P_{yx} and P_{zx} will, in general, vanish only for a fluid. When we say that the above are the components of the force acting upon dS , we mean that they give the force with which the material on one side acts upon the material on the side to which dS belongs. Equation (17) so far applies only to a dS belonging to the material on its positive side, but the force on the material on the negative side is just the reaction and can therefore be obtained by reversing the sign of each component.

Now take two other elementary surfaces of the same area dS , one with its normal pointing in the positive y direction the other in the positive z direction. Call the forces on these elements

$$\begin{aligned} &-P_{xy}dS, -P_{yy}dS, -P_{zy}dS, \\ &-P_{xz}dS, -P_{yz}dS, -P_{zz}dS. \end{aligned} \quad (18)$$

The unit normals to these three surfaces are respectively $(1,0,0)$, $(0,1,0)$, and $(0,0,1)$. Letting n_s stand for any of these normals, all the above relations can be condensed into the single expression

$$-P_{rs}n_s dS. \quad (19)$$

Furthermore, by letting n_s take values $(-1,0,0)$, etc., equation (19) also gives the reactions correctly.

This looks like the contraction of a second-rank tensor with the unit vector which determines the orientation of an arbitrary dS and, since there is nothing special about the direction of the coordinate frame, we suspect that this is a general relation. This is, in fact, true, and it can be shown that unless the stress on an arbitrary element is given by the above formula for all orientations of dS , the acceleration of an element of volume would be infinite, since only then will the total force over the surface of a small region go to zero like the volume instead of the area.^{2a}

That P_{rs} is actually a tensor follows from the fact that $-P_{rs}n_s$ is the force per unit area, a vector, for arbitrary n_s ; that is, contracting P_{rs} with an arbitrary vector gives a vector, and this

is only true of a tensor. Furthermore, it can be shown that unless P_{rs} is symmetrical, the couple acting on a small closed region will go to zero only like the cube of its linear dimensions while the moments of inertia go to zero like the fifth powers of these dimensions and, hence, the angular acceleration will be infinite.^{2a} Thus, we conclude that the stresses are represented by a symmetric second-rank tensor. We have not yet shown how to calculate its components, but we know that it can depend only on the strain tensor, the symmetric part of $u_{m,n}$, together with material constants.

The resultant of all these surface forces, acting over the closed surface S bounding a region R , will be equivalent to a total force, acting on the material in R , of amount

$$-\int_S P_{rs} n_s dS = \int_R \left(\frac{dP_{rs}}{dx_s} \right) dV \quad (n_s \text{ inward}), \quad (20)$$

in which the transformation from a surface to a volume integral is made with Gauss's flux-divergence theorem. Since equation (20) is valid for any arbitrary region R , we see that the resultant of the surface stresses is a body force of (dP_{rs}/dx_s) per unit volume.

The equation of motion of an arbitrary infinitesimal element of volume may now be obtained by taking the time derivative of the total momentum, equation (4), again taking advantage of the arbitrariness of R to drop the integral sign,

$$(\rho dV) \ddot{u}_r = \left(\frac{dP_{rs}}{dx_s} \right) dV + B_r dV, \quad (21)$$

in which B_r is the force per unit volume arising from any external fields (e.g., gravitation). These three equations become propagation equations for the displacement components u_m as soon as we have established a relation between the stress and strain tensors.

2.1.4 Energy Density; Generalized Hooke's Law

Let us now consider a body which is in equilibrium under the action of surface forces and, perhaps, a body force density B_r , both arising from some external agency. If we now

cause the surface and body forces to vary in such a way that the displacement receives a small arbitrary variation, we can, on the one hand, calculate the work done by the external agency and, on the other, the increase in potential energy, the latter provided we assume a potential energy density.

The deformed body will possess a certain amount of potential energy which is distributed throughout it with some volume density W . This potential energy density function W must depend only upon the strain tensor s_{mn} , together with certain phenomenological constants characteristic of the material, and it must be a positive definite function of this strain tensor (i.e., vanish only if every component of the strain tensor vanishes, and be positive otherwise). The simplest function of this type is a quadratic form in the s_{mn} and since these are small quantities, all higher-order terms may be neglected. We therefore have

$$W = \left(\frac{1}{2} \right) c_{pqrs} s_{pq} s_{rs}. \quad (22)$$

In equation (22), the stiffness moduli c_{pqrs} must form a fourth-rank tensor, because W must be a scalar for arbitrary values of the tensor s_{pq} ; this determines the manner in which they change when referred to a new coordinate frame (see Section 2.3). Since the s_{pq} are symmetric in pq , the c_{pqrs} must be symmetric under an interchange of p with q and also r with s , so that only six values of the pairs pq and rs can give distinct components. Furthermore, exchange of the pairs pq and rs does not alter W , and hence must not alter the tensor. It therefore has at most as many distinct elements as a symmetric sixth-rank matrix, namely 21. Any symmetry will reduce this number.

Now let us suppose the body, or any region within it, to be in static equilibrium under the combined action of surface forces of amount F_r per unit area and body forces of amount B_r per unit volume. The work done by these forces, corresponding to an arbitrary infinitesimal variation of the displacement, must be equal to the increase in potential energy, and we therefore have

$$\int_S F_r \delta u_r dS + \int_R B_r \delta u_r dV = \int_R \left(\frac{dW}{ds_{pq}} \right) \delta s_{pq} dV. \quad (23)$$

For equilibrium, the surface forces must balance those arising from the stresses, $F_r = P_{rs}n_s$ (outward normal). This enables the surface integral to be replaced by one over the volume, giving

$$\int_R \left(B_r + \frac{dP_{rs}}{dx_s} \right) \delta u_r dV + \int_R P_{rs} \delta u_{r,s} dV = \int_R \left(\frac{dW}{ds_{pq}} \right) \delta s_{pq} dV. \quad (24)$$

The external body forces B_r combined with the internal dP_{rs}/dx_s must be in equilibrium, otherwise, by equation (21), there will be an acceleration, and hence the first integral in equation (24) is zero. Because of the symmetry of P_{rs} , $\delta u_{r,s}$ may be replaced by $\delta s_{r,s}$ and hence, since the region R is arbitrary, we are left with

$$P_{pq} = \frac{dW}{ds_{pq}} = c_{pqrs} s_{rs}. \quad (25)$$

Equation (25) states that the stresses to first approximation are linear functions of the strains, which is a generalization of Hooke's law. We could have started from this assumption and deduced the potential energy density. The symmetry would then have come from the integrability conditions.

If we insert the above values of the stresses into the equations of motion, equation (21), we have three field equations which govern the propagation of the displacement at all interior points. If, as is usually the case, the B_r are zero, then equation (21) represents the propagation of waves in a crystalline medium having no sources.

To get a completely determinate system, we need know only two more things: the numerical values of the elements of the stiffness tensor and the conditions which exist at the boundaries, the latter discussed in the next section. The determination of the elastic moduli for any particular substance, together with their transformation to other axes, is discussed in Section 2.3 on piezoelectrics. Here we shall have other phenomenological tensors that require consideration, and shall also have to discuss their transformation to the matrix form, more convenient for detailed calculations as distinguished from general theoretical treatments.

2.1.5

Boundary Conditions

To obtain a determinate problem, the equations of propagation must be supplemented by boundary conditions which may take a variety of forms. These are of the utmost importance, since to falsify the boundary conditions corresponds to assuming the existence of external forces which are not actually operating. The principal types of boundary conditions are as follows.

1. Block. Over some external surfaces of the system it may be assumed that some rigid fastening prevents all displacement. This is, of course, an idealization since nothing is rigid if we go to a high enough frequency, but it may be a satisfactory approximation in certain cases.

2. Free. If a surface is in contact with air the boundary condition is that the stresses over that surface shall be zero.

3. Driven. A surface may be exposed to certain external driving forces (receiver). The boundary condition in this case is that the external forces shall match those arising from the internal stresses.

4. Impedance. In later work we will have occasion to assume impedance boundary conditions and, even though the numerical values of the (usually complex) surface impedances may be very difficult to evaluate, we shall find this to be a very valuable means of representing certain physical situations. If a part of the external surface looks into an inert medium to which it is elastically coupled then we may expect reactions which are linear functions of the displacement and its time derivatives, corresponding to dissipative and reactive loads. We need only find the steady-state solutions in the frequency range of interest, since other solutions can be built up from these by Fourier integrals. We therefore introduce a normal and a tangential specific acoustic impedance,^d and match the normal component of the internal stress with the normal impedance times the normal velocity, and the tangential component with the tangential impedance times the tangential velocity.

^d The tensor formulation of boundary conditions involving a tangential as well as a normal impedance is discussed in reference 4.

It should be noticed that the impedance boundary condition includes the blocked and free conditions as special cases, corresponding to infinite and zero impedance respectively.

2.1.6

Isotropic Solids

The isotropic solid is a special case defined by the condition that there are no preferred directions within it. Its stiffness tensor must therefore be the same in all Cartesian frames.

The transformation of the various material tensor under rigid rotation of the Cartesian axes is discussed in Section 2.3.3, where the piezoelectric and dielectric tensors are treated in addition to the elastic tensor. Using the methods of that section, together with the requirement of complete symmetry, one readily concludes that the stiffness tensor for an isotropic solid is

$$c_{pqrs} = \lambda \delta_{pq} \delta_{rs} + \mu (\delta_{pr} \delta_{qs} + \delta_{qr} \delta_{ps}), \quad (26)$$

in which λ and μ have been chosen so as to agree with the notation of Love.^{2b}

In this section we are concerned with pure elasticity (as distinguished from piezoelectricity), primarily in rods and plates. The theory of rods is contained in that of crystal plates (see Section 2.5.3), and is most conveniently handled by the equivalent circuit representation as given in Chapter 3. One merely short circuits the condenser and uses the simplifications arising from the isotropic c_{pqrs} given above; this amounts to setting the thickness and width Poisson ratios equal, and the shear Poisson ratio ϵ_s to zero.

The pure thickness vibration of plates is identical in theory to that of rods, the only difference being that the thickness modulus replaces Young's modulus, the former being about a third larger for steel. For calculating the resonant frequency, this is important; however, for calculating a steel backing plate to be a good block, it is of no consequence, since the characteristic impedance of steel is so high that even a one-eighth wave plate is a good block.

However, plates also vibrate in flexure, and here the situation is complicated and of practical importance since any nonuniformity in a

crystal motor will tend to excite these flexural modes. This matter is discussed in Chapter 3.

2.1.7

Nonviscous Fluids

FIELD EQUATIONS; BOUNDARY CONDITIONS

In a nonviscous fluid, the stress arises solely from the dilatation, the rigidity modulus μ being zero,

$$P_{pq} = \lambda u_{r,r} \delta_{pq} = -p \delta_{pq}, \quad (27)$$

$$p = -\lambda u_{r,r} = -\lambda \operatorname{div} \mathbf{u}. \quad (28)$$

The propagation equation is

$$\rho \ddot{u}_r = P_{rs,s} = -p_{,r} = \lambda (\operatorname{div} \mathbf{u})_{,r} \quad (29)$$

$$\rho \ddot{\mathbf{u}} = -\nabla p = \lambda \nabla \operatorname{div} \mathbf{u}. \quad (30)$$

The boundary conditions at any surface are

$$P_{pq} n_q = -p n_p = F_p, \quad (31)$$

in which F_p is the force per unit area exerted on the boundary surface by external agencies. They are of course contradictory unless F_p is normal to the surface, since a nonviscous fluid cannot support a tangential stress.

STEADY STATE

Only the steady-state problem is of interest in this volume since, even if one could handle the general time-dependent problem, its solution would be useless since only the steady-state motion of crystals is considered. The usual method of Fourier integral representation is, of course, available for the study of short pings.

There are two steady-state conventions in common use. One uses $\exp(i\omega t)$ for the time factor, as in most works on electric circuit theory. A plane wave traveling in the positive x direction, $\exp(i\omega t + ikx)$, therefore has a propagation vector which points in the opposite direction to that in which the wave travels. To avoid this, Morse⁵ and others use $\exp(-i\omega t)$ whereupon k is positive for a wave traveling in the positive direction; likewise, Hankel and Heine functions of the *first* kind represent *outgoing* waves. This latter convention is followed in this volume when discussing elastic waves in *fluids*, whereas the positive time-exponent convention, $\exp(+i\omega t)$, is used when discussing crystals, etc., where the equivalent circuit rep-

resentation urges conformity with electric circuit theory. If the positive exponent is used (crystals), an inductive or mass reactance is positive, a condenser or spring reactance is negative; the use of the negative exponent (fluids) reversing the signs of these reactances. Therefore, when combining results using two different conventions, it is necessary to make a qualitative check to be sure that the reactances have the proper signs.

The propagation equations for the pressure are readily obtained by taking the divergence of equation (30), and using equation (28),

$$(\nabla^2 + k^2)p = 0 \quad (\text{except at a source}), \quad (32)$$

$$k^2 = \frac{\omega^2}{c^2}, \quad c = \left(\frac{\lambda}{\rho} \right). \quad (33)$$

The pressure then serves as a velocity potential,

$$\mathbf{v} = \frac{\nabla p}{i\omega\rho}. \quad (34)$$

The boundary conditions which must be appended to yield a determinate problem may take a variety of forms. The simplest is that the pressure shall be zero over a given surface (free surface); another is that the normal component of velocity shall be zero; these are both included in the impedance boundary condition

$$p = Z(\mathbf{v} \cdot \mathbf{n}), \quad (35)$$

in which Z is the normal specific impedance.

In addition to the boundary conditions at inert surfaces, there must also be a source or active surface, otherwise all amplitudes are zero.

NEUMANN BOUNDARY-VALUE PROBLEM; GREEN'S FUNCTIONS

In the present state of knowledge of crystal transducers, the mechanical coupling between crystals and the impedance loads on their faces are very imperfectly known. There is therefore nothing to be gained at present by trying to take account of the impedance presented to the individual crystals by the radiation field even if one knew how to do this extremely complicated calculation. One must rather try to determine the general rules governing the dependence of this impedance on crystal spacing and velocity distributions over the face.

The most important practical problem in transducer design studies is therefore a Neumann problem⁶; to find the pressure in an infinite fluid region when the normal component of this velocity is given at each point on a closed surface (the transducer). At the present time, no general solution to this problem is known (even for the simplest of all surfaces, a sphere). Nevertheless, it will be seen that valuable results are obtained by using certain approximate solutions; these approximations are the basis of all present calculations of directivity patterns and the radiation impedance seen by a transducer.

The problem to be solved is

$$(\nabla^2 + k^2)p = 0 \quad (\text{outside the transducers}), \quad (36)$$

$$\mathbf{v} \cdot \mathbf{n} = \left(\frac{dp}{dn} \right) / ik\rho c \quad (\text{given on transducer}), \quad (37)$$

$$p \text{ outgoing, like } D(\theta, \phi) \exp \frac{ikr}{r} \text{ as } r \rightarrow \infty. \quad (38)$$

There are two general attacks on this problem: If the transducer surface is simple enough (sphere, long cylinder), one can obtain a formal solution in the form of an infinite series of characteristic functions. This method is applied in Chapter 4 to get some very useful approximate results. The other is the Green's function method which leads to the rigorous form of the Huygens-Fresnel principle to be discussed here.

A Green's function of the above problem is defined as any function of the form

$$g(1, 2) = g_0(1, 2) + W(1, 2), \quad (39)$$

$$g_0(1, 2) = \exp \frac{ikr_{12}}{r_{12}}, \quad (40)$$

$$r_{12} = |\mathbf{r}_2 - \mathbf{r}_1|, \quad (41)$$

in which $W(1, 2)$ is a solution of equation (36) at *every* point outside the transducer; that is, it has no singularities (sources) outside the transducer (and hence must have some inside, since no function can satisfy equation (36) in all space). Physically, a Green's function represents the field produced by a point source (first term on right) in the presence of some unspecified kind of reflection from the transducer (and perhaps other surfaces in the general problem,

but not here, since the transducer is assumed to be in an infinite medium).

Outside the transducer, $g(1,2)$ satisfies

$$(\nabla_1^2 + k^2)g(1,2) = 0, \text{ except at } \mathbf{r}_1 = \mathbf{r}_2. \quad (42)$$

Multiplying equation (42) by $p(1)$, and equation (36) (evaluated at \mathbf{r}_1) by $g(1,2)$, and taking the difference, one has

$$\text{div}_1 [p(1)\nabla_1 g(1,2) - g(1,2)\nabla_1 p(1)] = 0, \quad (43)$$

this being valid at every point outside the transducers and outside a small sphere surrounding \mathbf{r}_2 . Converting this to a surface integral over the transducer and the sphere, and letting the sphere shrink to zero, one has the rigorous Huygens-Fresnel principle

$$p(2) = \left(\frac{1}{4\pi}\right) \int_{\text{transducer}} dS_1 \left[\frac{p(1)dg(1,2)}{dn_1} - \frac{g(1,2)dp(1)}{dn_1} \right]. \quad (44)$$

This is valid for all Green's functions, including the known $g_0(1,2)$; however, it is not a solution of the problem because it contains not only dp/dn , known on the surface, but also the unknown $p(1)$.

If $g(1,2)$ is the *rigid* Green's function, that is, if $W(1,2)$ represents the waves reflected from a rigid transducer, then

$$\frac{dg_r(1,2)}{dn_1} = 0 \quad (\text{on transducer}), \quad (45)$$

and the unknown $p(1)$ falls out [but one now has $g_r(1,2)$, which is unknown],

$$p(2) = - \left(\frac{ik\rho c}{4\pi} \right) \int dS_1 g_r(1,2) v_n(1). \quad (46)$$

No entirely satisfactory approximation to $g_r(1,2)$ is at present known, even for a sphere, despite the fact that this subject has been intensively studied by Rayleigh and others,^{7,8} but some very useful semiquantitative conclusions can be reached by the study of special cases.

One would like to be able to calculate the pressure corresponding to a given velocity distribution over the transducer surface: at points *on* the surface, to get the impedance seen by the transducer at each surface point; and at points *far away* compared to the wavelength or the longest dimension of the transducer, whichever is larger, to calculate the directivity pattern and as an alternate method of estimating

the order of magnitude of the resistive part of the impedance.

Most transducers must have dimensions of the order of a few wavelengths, in order that suitable directivity patterns can be obtained. Thus, they fall in the critical region between the long and short wave limits; nevertheless, it is helpful to study these limiting cases.

First consider $g_r(1,1')$ for two points \mathbf{r}_1 and \mathbf{r}_1' both on the surface. This surface-surface Green's function yields a formal expression for the impedance,

$$\frac{p(1')}{v_n(1')} = - \left(\frac{ik\rho c}{4\pi v_n(1')} \right) \int dS_1 v_n(1) g_r(1,1'). \quad (47)$$

It will be shown in Chapter 4 that, in the long wave limit, only the volume-velocity radiates appreciably, and hence only the average normal velocity sees an appreciable resistive component of radiation impedance. We are not interested in the reactive component because it will merely shift the resonance frequency slightly, and hence we are not interested in the surface-surface Green's function in the long wave limit.

In the short wave limit (that is, wavelength small compared to the radius of curvature or the smallest distance on the surface in which the normal velocity changes appreciably, whichever is smaller), each element of surface will behave essentially like an infinite plane. The impedance must therefore approach a pure resistance of ρc and hence the Green's function evidently approaches $(-4\pi/ik\rho c)$ times a delta function of the two surface points.

The special case of a sphere throws light on how short the wavelength must be before this is a good approximation. Let the pressure and the surface velocity be expanded according to

$$p(\mathbf{r}) = \sum p_{nm} \left[\frac{h_n(kr)}{h_n(ka)} \right] P_n^m(\cos \theta) \exp im\phi, \quad (48)$$

$$v(\mathbf{a}) = \sum v_{nm} P_n^m(\cos \theta) \exp im\phi, \quad (49)$$

$$h_n(z) = \left(\frac{\pi}{2z} \right)^{1/2} H_{n+1/2}(z). \quad (50)$$

Then the pressure and velocity coefficients are connected by

$$p_{nm} = \rho c \zeta_n(ka) v_{nm}, \quad (51)$$

$$\zeta_n(z) = \frac{ih_n(z)}{h'_n(z)}, \quad (52)$$

in which, because of equation (51), the ζ_n are called *modal* impedances in ρc units; it should

be noticed that they are independent of the azimuthal quantum number. Using equation (51) to replace the p_{nm} in equation (48), one has

$$p(\mathbf{r}) = \rho c \sum \zeta_n(ka) v_{nm} \left[\frac{h_n(kr)}{h_n(ka)} \right] P_n^m \exp im\phi. \quad (48')$$

In the short wave limit, ka is large, and it can be shown that the ζ_n , as n increases, are very close to unity up to $n \simeq ka$, where they rise very suddenly to a large maximum in absolute value, after which they fall to zero very rapidly. Now suppose that the velocity distribution is such that the v_{nm} are negligible beyond $n = n_1 < ka$; then the sum can be broken at n_1 and the ζ_n all set equal to 1, whereupon, on the surface, one has

$$p(\mathbf{a}) \simeq \rho c v_n(\mathbf{a}), \quad n_1 < ka. \quad (53)$$

The condition for validity of this result can be expressed in very simple physical terminology, related to similar results in physical optics. If the normal velocity can be built with negligible error using n 's only up to n_1 , this means that it changes by an appreciable fraction of itself in a distance of the order of $2\pi a/n_1$ or larger; the above inequality can be written as

$$\frac{2\pi a}{n_1} > \lambda, \quad (54)$$

and we see that on a sphere whose radius is a few wavelengths, the *details of the velocity are resolved if the wavelength is small compared to the distance along the surface in which the velocity changes appreciably*. By replacing *radius* by *radius of curvature* one has a result expressed in general physical terms which make no reference to the specific properties of the sphere, and one therefore believes that the above is general; in confirmation of this, one finds the same result on a cylinder (see Section 4.2).

While the foregoing does not yield the radiation resistance in the intermediate cases, it furnishes a very useful criterion for determining whether the full ρc loading will be achieved in a particular case and how closely the individual crystals must be packed to avoid their resolution, with resultant scallop-edged patterns. These results are discussed more fully in Chapter 4; for the present, our conclusion concerning the surface-surface Green's function is that, as the wavelength decreases, it approaches a delta function, being very large at $\mathbf{r}_1' = \mathbf{r}_1$ and falling

rapidly to zero after $|\mathbf{r}_1' - \mathbf{r}_1|$ exceeds a wavelength or so, provided the radius of curvature of the surface is large compared to the wavelength.

Next, consider $g_r(1,2)$ for an \mathbf{r}_1 still on the surface but \mathbf{r}_2 very far away compared to the wavelength or the largest dimension of the transducer. Call this surface-distant Green's function

$$g_r(1,2) = \tau g_0(1,2), \quad (55)$$

in which τ depends upon wavelength, the geometry of the surface, and upon the direction of \mathbf{r}_2 but negligibly upon its magnitude (this latter is the essential definition of "distant"). If we knew the function τ , two useful calculations could be made: the directivity pattern and the total power radiated; from the latter, one can estimate the radiation resistance (see Chapter 4).

In the long wave limit, one readily concludes that σ approaches unity (its value for infinite space) by taking advantage of the symmetry of $g_r(1,2)$: instead of regarding $g_r(1,2)$ as the pressure at \mathbf{r}_2 caused by a source on the rigid surface at \mathbf{r}_1 , one regards it as the pressure at \mathbf{r}_1 caused by a source at \mathbf{r}_2 . Then by doing a simple scattering problem, one concludes that an obstacle small compared to the wavelength will very slightly perturb the incident wave field even on the surface of the obstacle (one should picture long waves slowly compressing a minute obstacle).

In the short wave limit, each point on the surface will act roughly like a rigid plane tangent at that point, provided the points are geometrically visible from one another.

Thus, the surface-distant Green's function approaches the two limits given by equation (55) and

$$\text{Long wave limit: } \tau \simeq 1, \quad (56)$$

$$\begin{aligned} \text{Short wave limit: } \tau \simeq 2 \text{ (if } \mathbf{r}_1 \text{ geometrically visible from } \\ \mathbf{r}_2), \\ \simeq 0 \text{ (if not).} \end{aligned} \quad (57)$$

As previously remarked, transducers tend to fall in the intermediate region between the long and short wave limits: if D is some characteristic dimension of the motor, directivity considerations usually make kD , or $2\pi D/\lambda$, any-

where from 1 up to 10 or 15. A careful study⁹ of the Green's function of the rigid sphere, extending Rayleigh's⁷ work, indicates that in this intermediate region the surface-distant Green's function is given better by the Kirchhoff directivity factor than by either equation (56) or (57),

$$\text{Intermediate region: } \tau \simeq (1 + \cos \alpha), \quad (58)$$

in which α is the angle at \mathbf{r}_1 between the outward normal and $(\mathbf{r}_2 - \mathbf{r}_1)$. It should be noticed that equation (58) is a compromise between equations (56) and (57).

The foregoing results are applied to the calculation of radiation resistance and directivity patterns in Chapter 4.

ENERGY DENSITY AND FLUX

The total elastic energy density and flux in a nonviscous fluid is

$$E = \frac{\rho \dot{\mathbf{u}}^2}{2} + \frac{1}{2} P_{pq} u_{p,q} = \frac{\rho \dot{\mathbf{u}}^2}{2} + \left(\frac{\rho c^2}{2} \right) (\text{div } \mathbf{u})^2, \quad (59)$$

$$S_p = -P_{pq} \dot{u}_q = -\rho c^2 \dot{u}_p (\text{div } \mathbf{u}). \quad (60)$$

The rate of increase of energy per unit volume should be equal to the convergence of the energy flux. One has

$$\begin{aligned} -\text{div } \mathbf{S} &= \rho c^2 (\dot{\mathbf{u}} \cdot \nabla \text{div } \mathbf{u} + \text{div } \dot{\mathbf{u}} \text{div } \mathbf{u}), \\ &= \left(\frac{d}{dt} \right) \left[\left(\frac{\rho \dot{\mathbf{u}}^2}{2} \right) + \left(\frac{\rho c^2}{2} \right) (\text{div } \mathbf{u})^2 \right] \\ &= \frac{dE}{dt}, \end{aligned} \quad (61)$$

in which $\Delta \text{div } \mathbf{u}$ is replaced by means of the propagation equation.

We must see what form these quantities and the conservation law, equation (61), take in steady state. First, an ambiguity from a strict mathematical viewpoint must be noted: In steady-state formalism, long usage has caused three distinct quantities to be represented by a single symbol, relying on context to distinguish them. Taking the pressure p as an example, this represents:

1. The actual time varying pressure, in excess of hydrostatic.
2. The complex time varying function p' whose *real part* is p .
3. The complex amplitude of p' , the quantity obtained by dropping the time-factor $\exp(-i\omega t)$, say p'' , a function of spatial variables only.

These quantities are related by:

$$p' = p'' \exp(-i\omega t), \quad (62)$$

$$\begin{aligned} p &= \Re p' = \Re p'' \cos \omega t + \Im p'' \sin \omega t, \\ &= |p''| \cos(\omega t - \text{phase } p''). \end{aligned} \quad (63)$$

The advantages arising from having a single symbol for these three quantities far outweighs the formal mathematical objection that they are actually distinct. However, one must be careful in forming second-degree quantities such as occur in the energy density and flux.

The energy flux in steady state is, from equation (60),

$$\begin{aligned} \mathbf{S} &= (\Re p)(\Re \mathbf{v}), \\ &= (p + \tilde{p}) \frac{\left(\frac{\nabla p}{ik\rho c} - \frac{\nabla \tilde{p}}{ik\rho c} \right)}{4}, \\ &= \left(\frac{1}{4ik\rho c} \right) (\tilde{p} \nabla p - p \nabla \tilde{p} + p \nabla p - \tilde{p} \nabla \tilde{p}). \end{aligned} \quad (64)$$

The last two terms go like $\exp(-2i\omega t)$ and $\exp(2i\omega t)$, respectively, and their time average is therefore zero. One is not ordinarily interested in the rapid variations in energy density and flux, and hence one keeps only the first two terms which are constant in time, using the same symbol.

$$\mathbf{S} = \left(\frac{1}{2ik\rho c} \right) \Im \tilde{p} \nabla p, \quad (65)$$

$$\begin{aligned} \text{div } \mathbf{S} &= \left(\frac{1}{2ik\rho c} \right) \Im (\nabla \tilde{p} \cdot \nabla p + \tilde{p} \nabla^2 p), \\ &= \left(\frac{1}{2ik\rho c} \right) \Im (\nabla \tilde{p} \cdot \nabla p - k^2 |p|^2). \end{aligned} \quad (66)$$

The first term is pure real; the second is also real if k is real, as it is in the absence of absorption, and hence $\text{div } \mathbf{S} = 0$. This is consistent with time-averaged conservation, since the time average of the energy density is of course independent of time.

The energy density is, from equation (59),

$$\begin{aligned} E &= \frac{\rho (\Re \mathbf{v})^2}{2} + \frac{(\Re p)^2}{2\rho c^2}, \\ &= \rho \frac{\left[\Re \left(\frac{\nabla p}{ik\rho c} \right) \right]^2}{2} + \frac{(p + \tilde{p})^2}{8\rho c^2}, \end{aligned} \quad (67)$$

$$\overline{E} = \frac{\nabla p \cdot \nabla \tilde{p}}{4k^2 \rho c^2} + \frac{|p|^2}{4\rho c^2}. \quad (68)$$

In a plane traveling wave, $\nabla p = i\mathbf{k}p$, in which case

$$\left. \begin{aligned} E &= \frac{|p|^2}{2\rho c^2} \\ S &= \left(\frac{|p|^2}{2\rho c} \right) \left(\frac{\mathbf{k}}{k} \right) = Ec \left(\frac{\mathbf{k}}{k} \right) \end{aligned} \right\} \begin{array}{l} \text{plane} \\ \text{traveling} \\ \text{wave,} \end{array} \quad (69)$$

in which, for convenience, the time-averaging symbol has been dropped.

If a sound field is caused solely by outgoing waves from a single transducer, as is the case in discussing the directivity pattern and energy radiated, both at distant points, then the radius of curvature is so large compared to the wavelength that equations (67) and (68) are applicable with negligible error. This is readily proven, and the error estimated (it is of order λ/r), by recalling that the entire field may be regarded as a superposition of terms of type

$$h_n(kr)P_n^m(\cos \theta) \exp(im\phi). \quad (71)$$

Differentiating this with respect to r and using the recursion and asymptotic formulas, one finds that

$$\frac{d}{dr} = ik \left[1 + \theta \left(\frac{1}{kr} \right) \right] \quad (72)$$

provided $n < kr$. This latter condition means that one is far enough out that the sharpest lobe, subtending an angle of order $2\pi/n$, has an arc distance along the wave front, $2\pi r/n$, large compared with the wavelength.

2.1.8

Viscous Fluids

Our interest in viscous fluids arises from two possible dissipation mechanisms within a transducer. The first is the generation of viscous shear waves by tangential motion of crystals. As will be shown below, these waves are absorbed in a very short distance (a fraction of a millimeter in castor oil); hence, they enter the theory as a tangential impedance, primarily on the lateral faces of crystals (see Section 2.5). The second is the partial conversion of longitudinal to shear waves, with complete absorption of the latter, at reflecting boundaries. While these mechanisms cannot be analyzed in detail because of the complicated interior geometry of

transducers, the order of magnitudes of the effects to be expected are deduced below.

STEADY-STATE BOUNDARY-VALUE PROBLEM

The stress in a viscous fluid¹⁰ has tangential as well as normal components, the latter depending upon the rate of strain, but otherwise having the same structure as that for an isotropic solid,

$$P_{pq} = \lambda \delta_{pq} u_{r,r} + \lambda' \delta_{pq} \dot{u}_{r,r} + \mu' (\dot{u}_{p,q} + \dot{u}_{q,p}). \quad (73)$$

It is customary to assume that λ' , the dilatational viscosity, is zero; however, Rayleigh¹¹ has called attention to the fact that the experimental basis for this assumption is scant.

The steady-state propagation equation is^e

$$-\rho \omega^2 \mathbf{u} = [\lambda - i\omega(\lambda' + \mu')] \nabla \operatorname{div} \mathbf{u} - i\omega \mu' \nabla^2 \mathbf{u}, \quad (74)$$

and the boundary conditions are, as in any elastic system, the equality of the flux of the stress with the external forces.

Introducing the usual scalar and vector potentials

$$\mathbf{u} = \nabla \phi + \operatorname{curl} \mathbf{A} \quad (\operatorname{div} \mathbf{A} = 0), \quad (75)$$

the above propagation equation separates, yielding

$$(\nabla^2 + k^2) \phi = 0, \quad (76)$$

$$k^2 = \left(\frac{\rho \omega^2}{\bar{\lambda}} \right), \quad \bar{\lambda} = \lambda - i\omega(\lambda' + 2\mu'), \quad (77)$$

$$(\nabla^2 + k'^2) \mathbf{A} = 0, \quad (78)$$

$$k'^2 = \left(\frac{i\omega \rho}{\mu'} \right). \quad (79)$$

The divergence condition on \mathbf{A} , applied to a plane wave, shows that \mathbf{A} represents transverse waves; similarly, ϕ represents longitudinal waves. The attenuation of longitudinal waves is negligible in the short distances involved in a transducer, so that we shall drop the imaginary part of k ; it should be noted that this causes the dilatational viscosity to fall out, but this does not necessarily mean that it is unimportant in transmission over large distances.

^e The time factor is taken as $\exp(-i\omega t)$. See Section 2.1.7.

The propagation vector for the transverse waves is

$$k' = \left(\frac{\rho\omega}{2\mu'} \right)^{\frac{1}{2}} (1 + i). \quad (80)$$

This has a phase of 45° , which means that a plane wave is down to $(1/e)$ th value in the $(1/2\pi)$ th fraction of a shear wavelength. This $(1/e)$ th absorption distance is the reciprocal of the imaginary part of k' ,

$$L' = \frac{1}{\Im k'} = \left(\frac{2\mu'}{\rho\omega} \right)^{\frac{1}{2}}, \quad (81)$$

which, for castor oil at 20 C and 10 kc, is only 0.02 cm.

TANGENTIAL IMPEDANCE

From the very short wavelength of shear waves we see that any plane a few millimeters in its smallest dimension may be regarded as infinite when considering specific tangential impedances. Thus the specific tangential impedance imposed on a crystal face separated from another surface by a viscous fluid may be estimated by considering a pair of infinite parallel planes, one of which is oscillating uniformly. Let the plane $z = z_1$ have a tangential displacement amplitude u_0 , the plane $z = 0$ being at rest and the space between filled with a viscous fluid. Then

$$A = (0, A_2, 0), \quad (82)$$

$$A_2 = - \frac{U_0 \cos k'z}{k' \sin k'z_1}, \quad (83)$$

$$P_{13} = -i\omega\mu U_0 k' \cot k'z_1, \quad (84)$$

$$Z_{13} = \frac{(P_{13})z_1}{(-i\omega U_0)}, \\ = \left(\frac{\mu'}{z_1} \right) \left(\frac{k'z_1}{\tan k'z_1} \right).$$

For very small z_1 , of the order of 10^{-3} cm, this is a resistance (μ'/z_1) of the order of a tenth of the radiation resistance, and since the lateral faces have a much greater area than the radiating faces, can be extremely important. A clear-cut example of this is found in an experimental UCDWR CY4 type transducer (see Chapter 6). If z_1 is one or two shear wavelengths, Z_{13} is an impedance $(\mu'/L')(1 - i)$, which has equal resistive and mass-reactive parts. Thus the resistance is μ/z_1 until z_1 be-

comes of the order of the $(1/e)$ th absorption distance and is then constant at (μ'/L') . The latter corresponds to a plane working into an infinite medium.

REFLECTION CONVERSION

A longitudinal wave obliquely incident upon a reflecting surface will produce tangential motion near this surface, and thus a part of the incident energy will be converted to viscous shear waves, which will be absorbed in a short distance.

To get some idea of the importance of this process, consider a plane longitudinal wave incident upon a rigid plane $y = 0$, at the angle θ . Reflected longitudinal and shear waves will be created, and these, combined with the incident wave, must make the normal and tangential displacement zero.

The potentials are

$$\phi_{\text{inc}} = \exp ik(x \sin \theta - y \cos \theta), \quad (85)$$

$$\phi_{\text{ref}} = r \exp ik(x \sin \theta_r + y \cos \theta_r), \quad (86)$$

$$A_{\text{ref}} = 0, 0, A \exp i(\alpha x + \beta y), \\ (\alpha^2 + \beta^2 = k'^2). \quad (87)$$

The displacements on the plane $y = 0$ are readily calculated to be

$$u_1 = ik(\sin \theta \exp ikx \sin \theta + r \sin \theta_r \exp ikx \sin \theta_r) - i\beta A \exp i\alpha x, \quad (88)$$

$$u_2 = -ik(\cos \theta \exp ikx \sin \theta - r \cos \theta_r \exp ikx \sin \theta_r) + i\alpha A \exp i\alpha x. \quad (89)$$

These must both be identically zero in x , and hence the exponents must all be the same. This yields

$$\theta_r = \theta, \quad (90)$$

$$\alpha = k \sin \theta, \quad (91)$$

$$\beta = (k'^2 - k^2 \sin^2 \theta)^{\frac{1}{2}} \simeq k', \quad (92)$$

and using these results in equations (88) and (89), one has

$$(1 + r)k \sin \theta = \beta A, \quad (93)$$

$$(1 - r)k \cos \theta = \alpha A. \quad (94)$$

Finally, eliminating A from these two equations, one has

$$r \simeq 1 - \frac{2\alpha \tan \theta}{\beta} \simeq 1 - \frac{2k \sin \theta \tan \theta}{k'}, \quad (95)$$

$$|r|^2 \simeq 1 - \left(\frac{2\mu'\omega}{\rho c^2} \right)^{\frac{1}{2}} \sin \theta \tan \theta. \quad (96)$$

The dimensionless quantity $(2\mu'\omega/\rho c^2)^{1/2}$ is of the order 7×10^{-3} for castor oil at 10 kc and 20 C, and thus we see that the reflected energy differs from the incident by less than 1 per cent at 45° incidence; even at 85° , the dissipation is only about 7 per cent of the incident energy. The approximate formula, equation (96), is valid until the second term on the right becomes of order 1, and we can see that this occurs only when the incident wave is within a degree or so of grazing incidence.

The reflection-conversion mechanism was at one time regarded by the writer as a possible cause of inefficiency in transducers. If the match to the water is so poor that the equilibrium energy density of the standing-wave pattern inside the transducer is large compared to that in the water just in front of the diaphragm, this mechanism might cause appreciable dissipation. In a well constructed transducer, however, the foregoing result makes it appear extremely unlikely that this mechanism is of any practical importance.

2.2

DIELECTRICS

Just as in the last section we discussed pure elasticity, in this section we will discuss the theory of pure dielectrics, reserving the coupling of such systems to the next section.

The theory of linear dielectrics is complicated, being analogous to that of diamagnetism. Certain cuts of RS are both nonlinear and strongly temperature dependent in the range of sea temperatures, and hence even more complicated. The practical use of such cuts is limited almost entirely to extremely small receivers, where it is important to get as large a capacitance as possible so that the capacitance between the two conductors will not shunt the signal too severely. No satisfactory theoretical treatment of such systems is known, and we shall therefore confine this discussion to dielectrics in which the polarization is a linear function of the components of the total electric field. This approximation is entirely adequate for Y-cut RS and all cuts of ADP, and therefore covers the great majority of all cases of practical interest.

2.2.1

Dipole Distribution

In this section we consider a continuous distribution of dipoles without specifying what causes these dipoles; for example, they might be the dipole distribution of an electret.

A dipole is the combination of equal positive and negative charges separated by a very small distance. The dipole moment, say \mathbf{m} , is a vector which points from the negative to the positive charge and its magnitude is the product of the positive charge by the separation of the two charges. If such a dipole is placed at a point \mathbf{r}_1 the potential at the point \mathbf{r}_2 is given by

$$\mathbf{m} \cdot \frac{\mathbf{r}_{12}}{r_{12}^3} = \mathbf{m} \cdot \text{grad}_1 \frac{1}{r_{12}}, \quad (97)$$

in which $\mathbf{r}_{12} = \mathbf{r}_2 - \mathbf{r}_1$, and r_{12} is its magnitude. A continuous distribution of dipoles of volume density \mathbf{P} therefore produces a potential given by

$$\begin{aligned} \phi_P(2) &= \int dV \mathbf{P}(1) \cdot \text{grad}_1 \frac{1}{r_{12}} \\ &= \int dV \left[\text{div}_1 \left\{ \frac{\mathbf{P}(1)}{r_{12}} \right\} - \left\{ \frac{\text{div}_1 \mathbf{P}(1)}{r_{12}} \right\} \right]. \end{aligned} \quad (98)$$

We must now characterize the \mathbf{P} distribution a little more precisely. First, we assume that \mathbf{P} goes to zero at infinity fast enough so that all integrals, involved in the entire discussion, converge. Second, we assume that \mathbf{P} is continuous and each of its components differentiable throughout all space, except for certain surfaces (closed or open) across which \mathbf{P} suffers finite discontinuities in magnitude, direction, or both; these surfaces are the boundaries between different materials in the system, crystal to air, crystal to electrode, etc. These conditions will be satisfied in any real physical problem.

The first term in the right member of equation (98) may be transformed to an integral over these surfaces. We divide all space into regions, as indicated in Figure 2, by auxiliary surfaces at all of whose points \mathbf{P} is continuous. We then have two types of regions: type R_1 , bounded wholly by surfaces across which \mathbf{P} is continuous (including the surface at infinity, where \mathbf{P} is zero) and type R_2 , partially bounded by a surface of discontinuity. These latter al-

ways occur in pairs, R_2 and R_2' , with the discontinuous surface as a common boundary.

Now the first term in the right member in equation (98) is the sum of the integrals over all these regions, which together fill all space.

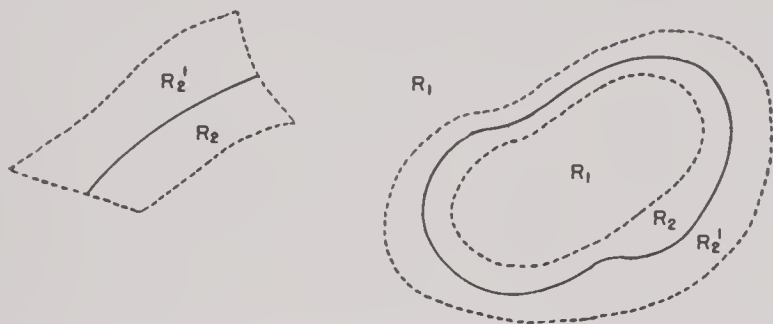


FIGURE 2. Auxiliary surfaces enclosing surfaces of discontinuity.

Using Gauss's flux-divergence theorem, this sum is the sum of the flux of \mathbf{P}/r_{12} out of each of these regions. The auxiliary surfaces always divide an R_1 - and an R_2 -type region and the contribution from them is therefore zero because \mathbf{P} is continuous and the flux out of every element dS of an R_1 is the negative of the flux out of the adjoining R_2 .

The integral is therefore just the total flux *into* the surfaces of discontinuity or, for better analogy with a result to be obtained for the second term, the negative of the total flux *out* of these surfaces. It is convenient to have a short name for the flux per unit area of a vector *out* of a surface, and we shall call it the surface divergence,

$$\text{surf div } \mathbf{F} = \mathbf{n} \cdot \mathbf{F} + \mathbf{n}' \cdot \mathbf{F}', \quad (99)$$

$$\text{surf div } \psi \mathbf{F} = \psi \text{ surf div } \mathbf{F} \quad (\text{if } \psi \text{ is continuous}), \quad (100)$$

in which \mathbf{n} and \mathbf{n}' are the two oppositely directed unit normals pointing out of the surface on its two sides and \mathbf{F} and \mathbf{F}' are the values of the vector on the two sides, differing at most by a finite vector. If the normal component of the vector is continuous, its surface divergence is zero. It should be noticed that the symmetry of equation (99) avoids all ambiguity as to signs.

The potential, equation (98), now becomes

$$\phi_P(2) = - \int dS \text{ surf div}_1 \frac{\mathbf{P}(1)}{r_{12}} - \int dV \left[\frac{\text{div}_1 \mathbf{P}(1)}{r_{12}} \right]. \quad (101)$$

This is the potential that would be produced in

vacuum by a surface and volume distribution of electric charges of density

$$\sigma_P(1) = - \text{surf div}_1 \mathbf{P}(1), \quad (102)$$

$$\rho_P(1) = - \text{div}_1 \mathbf{P}(1). \quad (103)$$

However, this charge distribution must not be confused with a free charge distribution that can move about in the material. It is the so-called bound charge and arises solely from lack of cancellation between neighboring dipoles. It is interesting to notice that the total of all this charge is zero,

$$q_P = - \int \text{surf div } \mathbf{P} dS - \int \text{div } \mathbf{P} dV = 0, \quad (104)$$

because, upon transforming the second integral into one over the surfaces of discontinuity, just as we transformed the exact divergence in equation (98), it exactly cancels the first term.

We must now examine the general properties of ϕ_P . First, it is everywhere continuous, because it can be regarded as the potential of the distribution given by equations (102) and (103) and only a doublet (or higher) layer can give a discontinuity to an electrostatic potential. Second, at every point not on a surface of discontinuity, it must satisfy Poisson's equation

$$\nabla^2 \phi_P = - 4\pi \rho_P = 4\pi \text{ div } \mathbf{P}. \quad (105)$$

Finally, the normal component of its negative gradient \mathbf{E}_P suffers a discontinuity at the surfaces of discontinuity given by

$$\text{surf div } \mathbf{E}_P = 4\pi \sigma_P = - 4\pi \text{ surf div } \mathbf{P}. \quad (106)$$

Introducing the electric displacement defined by

$$\mathbf{D}_P = \mathbf{E}_P + 4\pi \mathbf{P}, \quad (107)$$

all these relations are summarized by the simple results

$$\text{div } \mathbf{D}_P = 0, \quad (108)$$

$$\text{surf div } \mathbf{D}_P = 0, \quad (109)$$

$$\phi_P \text{ (continuous everywhere)}, \quad (110)$$

in which the last, equation (110), includes the more commonly used statement that the tangential component of \mathbf{E} is continuous and is, in fact, more stringent.

In conclusion, it should be emphasized that we have so far not developed a theory of dielec-

tics, because we have said nothing about the cause of \mathbf{P} . If the dipole distribution is given (e.g., a given electret which is not further polarizable), then equations (105) and (106) constitute a generalized Dirichlet boundary-value problem: a field equation with given non-homogeneous term, together with given values of the surface divergence of the field on certain surfaces.

We are not interested here in this case and it is mentioned only for contrast and to emphasize that we are at liberty to postulate any phenomenological relation between \mathbf{P} and other quantities without invalidating our present results. Two different postulates will in fact be made: one in the next section to get the linear theory of pure dielectrics, and a more general one in the following section as a step toward the linear theory of piezoelectricity.

2.2.2

Linear Dielectric

To get the theory of linear dielectrics, we now need to make just two additions to the previous section: to include the possibility of a volume and surface distribution of free charges, and to assume a relation between the polarization and the total electric field at any point. The potential of a volume and surface distribution of free charges is given by

$$\phi_f(2) = \int \frac{dS\sigma(1)}{r_{12}} + \int \frac{dV\rho(1)}{r_{12}}, \quad (111)$$

and by the same methods of the previous section, we obtain

$$\mathbf{D}_f = \mathbf{E}_f, \quad (112)$$

$$\text{div } \mathbf{D}_f = 4\pi\rho_f, \quad (113)$$

$$\text{surf div } \mathbf{D}_f = 4\pi\sigma_f, \quad (114)$$

$$\phi_f \text{ (continuous everywhere)}. \quad (115)$$

The potential of a superposition of dipoles and a volume and space distribution of free charges therefore satisfies

$$\phi = \phi_p + \phi_f \text{ (continuous everywhere)}, \quad (116)$$

$$\mathbf{E} = \mathbf{E}_p + \mathbf{E}_f = -\text{grad } \phi, \quad (117)$$

$$\mathbf{D} = \mathbf{D}_p + \mathbf{D}_f = \mathbf{E} + 4\pi\mathbf{P}, \quad (118)$$

$$\text{div } \mathbf{D} = 4\pi\rho_f, \quad (119)$$

$$\text{surf div } \mathbf{D} = 4\pi\sigma_f. \quad (120)$$

We now assume that the polarization is caused by the total field (*not* the field of the free charges only, because there can be no way of distinguishing between the two parts of the field by observations at a point),[†] and we therefore have some kind of a phenomenological equation of state,

$$\mathbf{P} = \mathbf{P}(\mathbf{E}). \quad (121)$$

The most complicated form of the general equation (121) which is susceptible to treatment, and fortunately one which gives a good description of a majority of dielectrics, is

$$\mathbf{P}_r = \chi_{rs}\mathbf{E}_s \quad \text{or} \quad \mathbf{D}_r = K_{rs}\mathbf{E}_s, \quad (122)$$

$$K_{rs} = \delta_{rs} + 4\pi\chi_{rs}, \quad (123)$$

in which the susceptibility and dielectric tensors χ_{rs} and K_{rs} , which will later be shown to be symmetric, are otherwise arbitrary so far as the theory is concerned. They must therefore be evaluated and shown by experiment to be constants for many substances (in any one frame).

Inserting equation (122) into equations (116) to (120) now gives a completely determinate Dirichlet problem if ϕ_f and σ_f are given. In our problems, ϕ_f is zero everywhere and σ_f is zero except on electrodes, and there its value is given (zero) only for an open-circuit receiver. Equation (120) must therefore be used to calculate σ_f , and we adjoin the boundary condition ϕ constant over all electrodes (given for a transmitter, to be calculated for a receiver). However, we are not yet ready to show how approximate solutions of these problems are found; we do not yet have the theory of piezoelectric problems, because we have as yet established no coupling between the elastic (see Section 2.2.1) and dielectric systems.

We now calculate the potential energy of the distribution of free charges and the induced polarization. Let us imagine that the free charges in a distribution, both volume and surface, to be increased slightly. The work done,

[†] Mason neglects the electric depolarizing field \mathbf{E}_p in treating crystal plates, together with a further depolarizing field of piezoelectric origin. We shall see later that in his approximation, this is justifiable; however, in higher approximation and even in first approximation for other shapes, the depolarizing fields should be included.^{3b, 12}

which is equal to the increase in potential energy, is given by

$$\delta W = \int \phi \delta \sigma_j dS + \int \phi \delta \rho_j dV. \quad (124)$$

It should be noticed that we do not include terms for the increment of the dipole distribution, because this increment is not independent but is determined by the increment to the free charges. The only way that an external system can do work is by bringing up further free charges, since to interfere with the polarization would be to violate equation (122).

In equation (124), we express the increments to the distributions in terms of \mathbf{D} , using equations (119) and (120), and then transform the surface integral to one over the volume.

$$\begin{aligned} 4\pi \delta W &= \int (-\operatorname{div} \phi \delta \mathbf{D} + \phi \operatorname{div} \delta \mathbf{D}) dV \\ &= \int \mathbf{E} \cdot \delta \mathbf{D} dV. \end{aligned} \quad (125)$$

This result is so far perfectly general, being independent of the special linear relation, equation (122). However, to integrate it, we must take advantage of this relation, obtaining

$$\begin{aligned} W &= \left(\frac{1}{8\pi} \right) \int \mathbf{E} \cdot \mathbf{D} dV \\ &= \left(\frac{1}{8\pi} \right) \int E_r K_{rs} E_s dV. \end{aligned} \quad (126)$$

This total work done by the mechanical forces which brought up the free charges is just the potential energy of the system. It should be noticed that it is the final distribution of these mechanical forces which *holds* the charges in position.

The localization of the energy in an electrostatic field has been the subject of considerable debate, but at least we see that we will get all the potential energy if we assume that it is distributed throughout space with a density $E_r K_{rs} E_s / 8\pi$. We notice that this is a quadratic form in the components of \mathbf{E} and can reach two conclusions from this fact: no system can be in equilibrium under the action of electrostatic forces alone (Earnshaw's theorem) and, hence, all the principal values of K_{rs} must be positive; also, if K_{rs} had an antisymmetric part, it would contribute nothing to the potential energy but would contribute a component to \mathbf{D} which would be perpendicular to \mathbf{E} , as shown by equation

(122), a component against which no work is done since it falls out of the potential energy; hence, K_{rs} must be symmetric and, with it, χ_{rs} .

Having separately developed the theory of linear elastic and dielectric systems, we are now ready to couple them and thus obtain the theory of linear piezoelectricity.

2.3

PIEZOELECTRICS

A piezoelectric system is an elastic and a dielectric system, both nonisotropic, occupying the same region. The essential feature that makes such a system so interesting and useful is that the two component systems do not function independently, but are coupled so that mechanical forces produce electric polarization and electric fields produce elastic deformations. Without this coupling, it would be impossible to convert electric energy to mechanical (transmitter) or mechanical to electric (receiver); with it, we have an *electromechanical transducer*.

This coupling can be included in the theory by taking over all of the fundamental relations of pure elasticity and pure dielectrics, but altering the elastic and dielectric equations of state and making corresponding alterations in the energy density, propagation equations, and boundary conditions. The strain and the stress tensors each have six distinct components, and the pure elastic (linear) equation of state, equation (25) of Section 2.1.4, furnishes just six linear relations between them, so that if either tensor is known the other may be calculated. Similarly, the electric displacement and the electric field each have three components and the pure (linear) dielectric equation of state, equation (122) of Section 2.2.2, supplies three linear relations between them, so that if either vector is known, the other may be calculated. Regarded together, there are eighteen distinct quantities between which nine equations of state have been assumed. In the absence of coupling, these nine relations fall apart into two sets: the six elastic and the three dielectric equations. This must be altered so that we still have nine relations between eighteen quantities, but they do not fall apart. It is a matter of con-

venience how we choose these relations; any nine quantities may be expressed in terms of the other nine, and the form used will depend on the particular application. New material constants will need to be introduced, corresponding to the piezoelectric coupling, and it will be shown that there are at most eighteen of these new constants, this number being reduced by any symmetry.

It should be emphasized that the potential is an internal field quantity^{3c} and that the relation between it and the voltage applied to the electrodes is established through the boundary conditions. This is a necessary variation from Mason's treatment since regarding the electric field as an externally given quantity corresponds to neglecting both the electric and mechanical depolarizing field and, although this is valid in lowest approximation and for certain types of geometry, it is not a generally valid approximation. Physically, this corresponds to the fact that the polarization at a point is caused by the field at that point, it being immaterial that part of this field is caused by free charge and part by polarization. One consequence of this variation is that the proper energy density of the vacuum field $E^2/8\pi$ will be included in the energy of the system, while Mason's expression for the total energy density vanishes if both the strain and the polarization vanish. We therefore have a problem involving four field quantities, the three components of the displacement u_m and the electric potential ϕ .

2.3.1 Energy Density and Equations of State and of Propagation

In Section 2.1.4, we obtained the potential energy density of a linear elastic system and derived the elastic equations of state by equating the work done, in an infinitesimal additional displacement, to the increase in total potential energy. Similarly, in Section 2.2.2, we calculated the potential energy density of a pure dielectric. We must now apply this same treatment to the piezoelectric case.

If the system is initially in static equilibrium under the combined action of external body and surface forces, together with the forces neces-

sary to hold any free charges in place, the work done in an infinitesimal displacement is

$$\int_R dV \left(P_{rs} \delta s_{rs} + \frac{E_m \delta D_m}{4\pi} \right). \quad (127)$$

The potential energy density must vanish if both the strain and the electric displacement vanish, and otherwise must be positive. Again, the simplest function satisfying these conditions is a quadratic form, and neglecting all higher-order terms, we have

$$W = \left(\frac{1}{2}\right) c_{pqrs} s_{pq} s_{rs} + \frac{D_r K_{rs}^{-1} D_s}{8\pi} + \frac{D_r f_{rpq} s_{pq}}{4\pi}, \quad (128)$$

in which the notation^g has been chosen so as to agree with Mason's.^{12a} The first two terms are the pure elastic and the pure dielectric energy, the first for an electrically shielded crystal ($\mathbf{D} = 0$), and the second for a mechanically blocked crystal ($s_{pq} = 0$), while the third term is the coupling energy. The new coefficients f_{rpq} form a third-rank tensor,^h symmetric in the last two indices and therefore having at most eighteen distinct components; if this tensor is zero, the systems separate and there is no electro-mechanical energy conversion; if small, high voltage is required to convert electric to mechanical energy.

The increase in potential energy corresponding to a variation of the strain and electric displacement is

$$\int_R dV \left\{ \left(\frac{dW}{ds_{pq}} \right) \delta s_{pq} + \left(\frac{dW}{dD_r} \right) \delta D_r \right\}. \quad (129)$$

Equating this to the work done, equation (127), and taking account of the arbitrariness

^g Compare equation (C.43) of reference 12 with equation (130) below. The above energy density is just $E^2/8\pi$ greater than Mason's equation (C.30).¹² This difference, the self-energy of the field, corresponds to taking the field into the system instead of regarding it as externally given.

^h See Section 2.3.3, where the connection between the tensor and matrix representation of all of the material constants, and their transformation properties, are discussed.

of the region R , we get for the generalized equation of state

$$\begin{aligned} P_{pq} &= \frac{dW}{ds_{pq}} = c_{pqrs} s_{rs} + \frac{D_r f_{rpq}}{4\pi}, \\ E_r &= \frac{4\pi dW}{dD_r} = f_{rpq} s_{pq} + K_{rs}^{-1} D_s. \end{aligned} \quad (130)$$

An alternate form of equation (130), more suitable for getting the field equations, is obtained by solving the second for D , and substituting into the first

$$\begin{aligned} P_{pq} &= \bar{c}_{pqrs} s_{rs} + \bar{f}_{rpq} E_r, \\ D_r &= -4\pi \bar{f}_{rpq} s_{pq} + K_{rs} E_s, \end{aligned} \quad (131)$$

$$\begin{aligned} \bar{c}_{pqrs} &= c_{pqrs} - \frac{f_{mpq} K_{mn} f_{nrs}}{4\pi}, \\ \bar{f}_{rpq} &= \frac{K_{rm} f_{mpq}}{4\pi}. \end{aligned} \quad (132)$$

Now in obtaining the equation of motion of an element of volume, equation (21) of Section 2.1.3, we had no occasion to inquire into the cause of the stress. It was sufficient that the force between neighboring parts of the system could be described by a stress tensor. Similarly, in obtaining the result that lines of induction begin only on free charges, equations (119) and (120) of Section 2.2.2, it was sufficient that the field be produced by a distribution of free charges and dipoles regardless of the origin of these distributions. Therefore, these relations are still valid provided the coupled equation of state, equation (131), is used; and the coupled propagation equation is therefore

$$\begin{aligned} \rho \ddot{u}_p &= \bar{c}_{pqrs} u_{r,s,q} - \bar{f}_{rpq} \phi_{,r,q} + B_p, \\ 4\pi \bar{f}_{rpq} u_{p,q,r} + K_{rs} \phi_{,s,r} &= -4\pi \rho_f, \end{aligned} \quad (133)$$

in which the change of s_{mn} to $u_{m,n}$ is possible because of the symmetry properties of the tensors \bar{c} and \bar{f} . These are four field equations governing the propagation of the four field quantities u_m and ϕ , if the body force and charge density are given. We have retained these quantities, even though they are zero in all our problems, because equation (133) may also be regarded as the *explicit* solution of the problem of what body force and charge density are necessary to support an arbitrarily assumed displacement and potential. This enables us to estimate the error in an approximate solution.

If we set \bar{f} to zero, equation (133) becomes

the propagation equation in pure elasticity and Poisson's equation in pure dielectrics, and the coupled system separates into two independent systems. If the coupling is made unilateral by setting \bar{f} to zero in the second equation, we have the approximation in which the field is regarded as externally given and only the mechanical depolarizing field is neglected. The resultant system will not obey the reciprocity principle.

2.3.2 The Linear Dissipative Piezoelectric Boundary-Value Problem

SURFACE DISSIPATION

We are now in a position to condense the foregoing results by formulating a boundary-value problem governing the behavior of a quite general linear dissipative piezoelectric system.

The time-dependent boundary-value problem is readily formulated, but its solution in any other case than steady state appears so hopeless that it is of doubtful practical value; accordingly, it is assumed that all quantities have time variations like $\exp(i\omega t)$, and only the amplitude problem is stated. However, transient problems can then be successfully attacked by the well-known Fourier integral method.

The fundamental field quantities are taken to be three displacement components $u_p(x, y, z, t)$ and the electric potential $\phi(x, y, z, t)$; this choice avoids adjoining differential identities which would be necessary if polarization, field, or electric displacement were used. It is permissible to ignore the magnetic field caused by variations in the electric field because, even at the highest frequency in practical use, the magnetic field so created is extremely small and the resultant inertia and dissipation introduced is negligible.

From these four fundamental field quantities, the stress and electric displacement, auxiliary field quantities, are derived according to

$$P_{pq} = \bar{c}_{pqrs} u_{r,s} - \bar{f}_{rpq} \phi_{,r}, \quad (134)$$

$$D_p = -4\pi \bar{f}_{prs} u_{r,s} - K_{pq} \phi_{,q}. \quad (135)$$

The use of the asymmetric derivative tensor $u_{r,s}$ instead of the symmetric strain tensor is

permissible since the symmetry of \bar{c}_{pqrs} and \bar{f}_{prs} selects only the symmetric part anyway.

The propagation equations, in steady-state form, are

$$\rho\omega^2 u_p + P_{pq,q} + B_p = 0, \quad (136)$$

$$\text{div } \mathbf{D} = D_{p,p} = 4\pi\rho_f. \quad (137)$$

These are four field equations for determining the four field quantities u_p and ϕ , and they require only boundary conditions to form a determinate problem. It is scarcely necessary to remark that all quantities are now complex amplitudes depending on spatial variables only.

The body force B_p and the free charge density are assumed to be zero in all problems treated in this volume, except that in the next section a complex dielectric constant is introduced, which corresponds to assuming a volume conductivity in insulating materials. These quantities are retained here because the propagation equations explicitly give the extraneous body force and free-charge density corresponding to an assumed displacement and potential, and hence enable the error in an approximate solution to be estimated.

Before the boundary conditions can be formulated, it is necessary to define the region. In doing this, it should be recalled that a piezoelectric system is actually a superposition of two systems, one elastic and the other dielectric, with coupling between the two. Hence the boundary-value problem contains those for pure elastic and pure dielectric systems as special cases provided we allow for discontinuous changes in all the material constants. For example, in a crystal transducer, \bar{f} falls suddenly to zero across crystal surfaces; likewise the \bar{c} and K tensors undergo discontinuous changes. Furthermore, it may be advantageous to exclude certain interior regions, occupied by Coreprene, etc., from the elastic domain, regarding them as energy sinks represented by a complex impedance over the bounding surface of the excluded region; however, it would be quite wrong to exclude these from the domain of the electric potential since some of these materials exhibit high dielectric dissipation.

We are therefore led to the region shown in Figure 3. The total region R is bounded externally by a conducting sheath and is held at

zero potential. It may extend to infinity; if not, it is regarded as terminated by a continuous distribution of mechanical generators exerting a force per unit area of amount \mathbf{F} and having internal impedance characterized by a specific acoustic stiffnessⁱ tensor S_{pq} , both of which may be functions of position on the surface and of frequency. The elastic region is R with the impedance regions excluded; the interactions across these surfaces are characterized by a stiffness tensor and, if any are active, by an \mathbf{F} just as with the external boundary; the elastic region will be designated as $R - Z$.

The metal conductors are closed regions assumed to have infinite conductivity. The potential is therefore constant within them, and the potential domain is therefore $R - c$; however, the interior of these conductors is a part of the *elastic* domain.

Finally, the whole region R will usually be separated into subregions in which the material is homogeneous (but not necessarily isotropic); a surface of discontinuity may correspond to a discontinuity in any of the material tensors \bar{c} , \bar{f} or K .

The boundary conditions to be adjoined to the above propagation equations, to form the complete boundary-value problem, are therefore

$$P_{pq}n_q = F_p - S_{pq}u_q \quad (138)$$

on impedance and external surfaces,

$$(P_{pq} - P'_{pq})n_q = 0 \quad (139)$$

on all surfaces of discontinuity,

$$n_p D_p = 4\pi\sigma_f \quad (140)$$

\mathbf{n} outward, on conductors,

$$(D_p - D'_p)n_p = 0 \quad (141)$$

on nonconducting surfaces of discontinuity,

$$\phi, u_m \quad (142)$$

continuous everywhere,

$$\phi = V_c \quad (143)$$

constants on and inside conductors.

INTERNAL VISCOUS AND DIELECTRIC DISSIPATION

The foregoing steady-state boundary-value problem includes the possibility of radiation or

ⁱ The representation of inert loads, both tangential and normal, by a stiffness tensor is discussed in reference 4.

true dissipation into impedance surfaces, but the interior of each medium has been regarded as conservative. This is a good approximation for crystals, steel, etc., since the internal dissipation in these materials is negligible compared to the radiation losses for a crystal working into water.

However, there are dissipation processes, known to be of practical importance, which cannot be represented by an impedance surface. These include dielectric losses, which may be serious in Corprene, and internal elastic dissipation in Corprene, rubber, etc. Accordingly, it seems advantageous to broaden the general theory to include these types of dissipation.

Dielectric dissipation can be included, in the steady state, by adding an imaginary term,

$$- \left(\frac{4\pi}{i\omega} \right) \sigma_{pq},$$

to the dielectric tensor, in which σ_{pq} is the conductivity tensor occurring in Ohm's law. This tensor is assumed to be symmetric, since any antisymmetric part would cause a current to flow without any corresponding dissipation. It is also assumed to be positive-definite, since otherwise certain directions of the field would correspond to negative dissipation.

Internal elastic dissipation can be included by adding to the stress a term linear in the strain *velocity*, an obvious generalization of the Stokes-Navier equation. In the steady state this becomes

$$\mu_{pqrs} \dot{s}_{rs} = i\omega \mu_{pqrs} u_{r,s}.$$

The viscosity tensor μ_{pqrs} is symmetric in the first two indices because otherwise the well-known requirement of symmetry of the stress tensor would be violated. It is symmetric in the second pair, because the strain is. Finally, unless it is symmetric with respect to exchange of the first and second pair of indices, there will be velocity dependent forces which, like the magnetic deflection of a charge, cause no dissipation; such forces are not considered here. Accordingly, the viscosity tensor is assumed to have the same symmetry properties as the elastic stiffness tensor.

Thus by allowing K_{pq} and \bar{c}_{pqrs} to become complex, but maintaining the same symmetry, the

possibility of internal viscous and dielectric losses is included in the foregoing boundary-value problem without changing its formal structure.

In the next section, this boundary-value problem, complete with boundary conditions as well as propagation equations, is shown to be derivable from a variation principle. Solutions are then obtained by the semidirect method, for the case of a rectangular crystal plate, first in the Mason approximation and then in a higher approximation which includes additional effects of practical importance.

2.3.3 Matrix Formulation; Transformation Under Rigid Rotation

In formulating the general theory of elastic, dielectric, and piezoelectric systems, we are led inevitably to the tensor analysis because certain sets of physical quantities (e.g., the components of the strain, the stress, the electric displacement, the elastic, dielectric, and piezoelectric constants) demand consideration as a whole just as, in a special case of this, a force demands consideration as a single physical influence even though we need three quantities to represent it.

There are several great, interrelated advantages to the tensor formulation:^j (1) the above simplification of concepts whereby, for example, we can think about *the* stress, instead of thinking of six quantities; (2) its treatment of all coordinate frames on an equal basis, thus freeing us from preoccupation with geometric details of a particular frame in general problems in which these details are irrelevant; (3) the *formal* simplicity of the transformation of a representation in one frame to that in another; (4) the great economy in notation which often enables the results of the lifework of great physicists to be developed and written down in a few pages, etc.

^j It is unfortunate that tensor analysis was not sufficiently developed to be more useful to W. Voigt³ in his great work on crystal physics. All through his long book (about 800 pages), one feels that he is searching for refinements to this valuable tool, refinements which came shortly afterwards through the work of Levi-Civita and others.

These advantages disappear to some extent when we attempt a specific calculation: a coordinate frame, having geometry as simply related to the system as possible, is chosen; it is inconvenient to make numerical arrays of the elastic constants, a fourth-rank tensor, etc. For these and other reasons, there are many advantages to the commonly used matrix formulation^k for specific applications. We must therefore develop this formulation and its connection with the tensor formulation, here restricting ourselves, however, to Cartesian coordinates.

The matrices involved are rectangular rather than square, several having only one row or one column. Taking advantage of the symmetry, there are at most only six distinct elements in the strain or stress tensor, twenty-one elastic, and eighteen piezoelectric constants, etc. These various quantities can be conveniently arrayed by using matrices which have at most six rows and columns, and we therefore introduce new indices a, b, c, \dots taken from the early part of the alphabet and always ranging from 1 to 6.

The stress tensor now becomes a matrix of six rows and one column (to avoid confusion with the polarization, it will be represented by X in this section).

$$X_{a.} = \begin{matrix} & a \\ & P_{11} & 1 \\ & P_{22} & 2 \\ & P_{33} & 3 \\ & P_{23} & 4 \\ & P_{31} & 5 \\ & P_{12} & 6 \end{matrix} \quad (144)$$

We shall also have occasion to write the transposed matrix,

$$X_{.a} = \begin{matrix} a & 1 & 2 & 3 & 4 & 5 & 6 \\ P_{11} & P_{22} & P_{33} & P_{23} & P_{31} & P_{12} \end{matrix} \quad (145)$$

The dot shows which index is absent and in most cases we can drop it. When writing these matrices without their indices, they become simply X and X^t in which the special superscript is not a running index but merely means "transposed."

In a similar way, the strains are arrayed as

^k The matrix formulation is developed by Bond.¹³ However, the connection between the tensor and matrix formulation is not developed.

one column or one row matrices. The transposed strain matrix is

$$s_{.a} = s_{11} \ s_{22} \ s_{33} \ 2s_{23} \ 2s_{31} \ 2s_{12} = s', \quad (146)$$

with a corresponding form for s itself. It should be noticed that the off-diagonal elements of the strain tensor are doubled to form the corresponding elements of the matrix.

It is convenient to have a condensed notation for showing the connection between the various tensors and the corresponding matrices. This can be done by introducing *connection* matrices, which are quantities having mixed indices,

$$X_{a.} = C_{apq} P_{pq}; \quad s_{a.} = D_{apq} s_{pq}, \quad (147)$$

$$\begin{aligned} C_{apq} &= \delta_{ap} \delta_{pq} + \left(\frac{1}{2}\right) p_{(a-3)pq} \\ &\quad (\text{not summed on } p), \\ D_{apq} &= \delta_{ap} \delta_{pq} + p_{(a-3)pq} \\ &\quad (\text{not summed on } p), \end{aligned} \quad (148)$$

in which p_{mpq} is a permutation matrix, 1 if mpq is any permutation of 123 and 0 otherwise, or

$$P_{mpq} = N_{mp} N_{pq} N_{qm}; \quad N_{rs} = (1 - \delta_{rs}).$$

The reciprocal connections, whereby the matrices are converted to tensors, are easily shown to be

$$P_{pq} = X_a D_{apq}; \quad s_{pq} = s_a C_{apq}, \quad (149)$$

$$C_{apq} D_{ars} = \frac{1}{2} (\delta_{pr} \delta_{qs} + \delta_{ps} \delta_{qr}), \quad (150)$$

so that C and D are reciprocally related.

Substituting these matrices into the energy density and equations of state, equations (128) and (130) of Section 2.3.1, they become

$$W = \frac{1}{2} s_a c_{ab} s_b + \frac{D_r K_{rs}^{-1} D_s}{8\pi} + \frac{D_r f_{ra} s_a}{4\pi}, \quad (151)$$

$$= \frac{1}{2} s^t c s + \frac{D^t K^{-1} D}{8\pi} + \frac{D^t f s}{4\pi},$$

$$X = c s + \frac{f^t D}{4\pi}, \quad (152)$$

$$E = f s + K^{-1} D,$$

$$\begin{aligned} c_{ab} &= C_{apq} c_{pqrs} C_{brs} = c_{ba}; \\ f_{ra} &= f_{rpq} C_{apq}. \end{aligned} \quad (153)$$

Thus, the elastic tensor c_{pqrs} becomes a 6 by 6 symmetric matrix, and the piezoelectric tensor f_{rpq} becomes a matrix of three rows and six columns. The dielectric tensor remains a 3 by 3 symmetric matrix, and the vectors E and D become matrices of three rows and one column.

It is extremely easy to manipulate these matrix equations, the only necessary precaution being to preserve the order of factors in each term, since multiplication is not necessarily commutative. For example, to obtain the

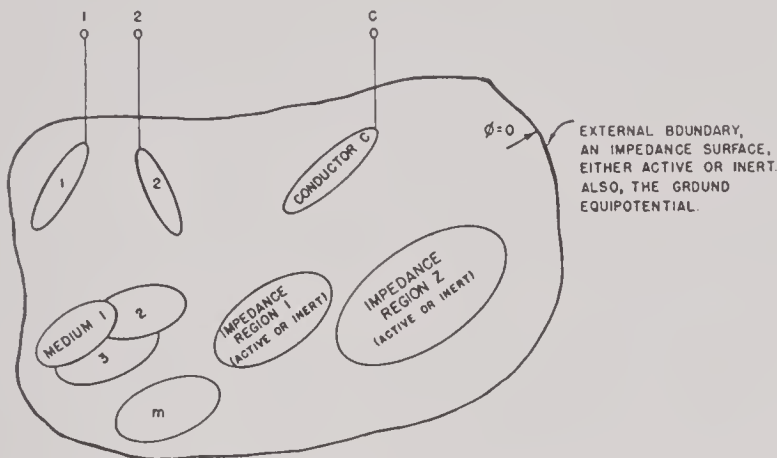


FIGURE 3. The domain in which the linear dissipative piezoelectric boundary-value problem is defined.

analogues of equations (131) and (132) of Section 2.3.1, we need only premultiply the second of equation (152) above by K , solve for D , and substitute into the first:

$$\begin{aligned} X &= \bar{c}s + \bar{f}'^t E, \\ D &= -4\pi \bar{f}s + KE, \end{aligned} \quad (154)$$

$$\begin{aligned} \bar{c} &= c - \frac{f' K f}{4\pi}, \\ \bar{f} &= \frac{K f}{4\pi}. \end{aligned} \quad (155)$$

We can now obtain the rotation transforms of the material constants in a form requiring, at most, the multiplication of 6x6 matrices, and therefore suitable for numerical calculations.¹ We first notice that the energy density, equation (150), separates into three terms, the first two of which we interpret as the proper energy of the elastic and dielectric systems, respectively, and the third as the coupling energy between these systems. This separation must be possible in every frame and hence each of these terms is a tensor of zero rank. Since the strain and displacement are matrices derived from tensors, the transforms of the material constants are uniquely determined by the transformation properties of these matrices.

¹ These relations are given by Bond,¹³ but there are some errors in this otherwise very valuable paper.

If the frame is rigidly rotated, the new coordinates are

$$x_p' = a_{pq} x_q \quad \text{or} \quad x' = ax, \quad (156)$$

in which a is orthogonal, $a^t = a^{-1}$. The transformation of the vectors E , D , and P follow the same law.

The transformation of the strain tensor, in the opposite direction to allow the old quantities in the energy density to be expressed in terms of the new, are

$$s_{pq} = a_{rp} a_{sq} s'_{rs}, \quad (157)$$

and by replacing the tensors by the corresponding matrices, we find

$$\begin{aligned} s_a &= T_{ba} s_b' \quad \text{or} \quad s = T^t s', \\ T_{ab} &= D_{bpq} a_{rp} a_{sq} C_{ars}. \end{aligned} \quad (158)$$

The matrix T has been defined as above so as to be identical to Bond's alpha.^{13a}

We now replace the old strain and electric displacement by the new, the former according to equation (158) and the latter according to equation (156) after inversion, $D = a^t D'$. The three terms in the energy density then become

$$s^t c s = s'^t c' s'; \quad c' = T c T^t. \quad (159)$$

$$D^t K^{-1} D = D'^t K'^{-1} D'; \quad K'^{-1} = a K^{-1} a^t. \quad (160)$$

$$D^t f s = D'^t f' s'; \quad f' = a f T^t. \quad (161)$$

These are explicit formulas for calculating the material constants in a rotated frame from those in the original frame. Although these calculations are bound to be laborious, the matrix formalism enormously shortens them, in fact, to such a point that a calculation that is otherwise not practically feasible, can be carried through in an hour or two. The steps in this calculation are as follows: Write out a and a^t ; calculate the elements of the 6x6 matrix T_{ab} ; then carry out the matrix multiplications indicated in equations (159), (160) and (161). These multiplications are made more easily, and the probability of mistakes reduced by ruling grids 6x6, 6x3, and 3x3 with quite large squares and then cutting the paper with no margins so that a prefactor may be fitted directly to a postfactor.

These transformations are of value even

when the numerical value of the constants are not known, because they enable us to calculate the proper orientation to make certain constants zero (e.g., so that a field normal to a plate will cause no shear stress) merely from a knowledge of the symmetry class of the crystal.

SYMMETRY REDUCTION OF THE MATRICES

Nearly all crystals possess some symmetry, that is, by performing certain rotations and/or reflections, the resultant is indistinguishable from the original, provided we ignore its finite size. Each symmetry class is characterized by some finite subgroup of the rotation-reflection group, the extremes being the completely asymmetric crystal, which admits only the identity, and the completely symmetric (isotropic) substance, which admits the entire continuous rotation-reflection group.

Corresponding to each symmetry class, there will be certain relations existing between the material constants such that the higher the symmetry, the fewer independent parameters are needed to determine all the others. Crystals from which practical transducers can be made represent a nice balance between too little and too much symmetry. If too little, their field-induced deformations will be so complicated that nothing resembling a piston motion can be obtained; if too much, all their piezoelectric constants vanish.

To determine the special structure of the matrices of a crystal of a known class, we need only transform the matrices in accordance with equations (159), (160), and (161) of Section 2.3.3, using all the distinct transformations of its particular subgroup, and in each case demand that the matrix be unchanged. In this section, the resultant reduction of the matrices of RS and ADP are calculated.

First, we must notice that while there are several different elastic matrices (c , the elastic matrix for zero electric displacement; \bar{c} , for zero field, etc.), they all have the same symmetry properties. The same remark applies to the various piezoelectric matrices (f , the strain-field matrix for zero electric displacement; \bar{f} , the stress-field matrix for zero strain, etc.) and to the various K matrices (K , the clamped

dielectric matrix for zero strain; K^F , the free dielectric matrix for zero stress, etc.). This can be proved as follows. Any two *tensors* having the same rank also have the same symmetry since they will transform in the same way under the rotation group corresponding to the particular symmetry of the crystal. The conditions from which the symmetry is determined will therefore be identical for both; the only question is therefore whether, in going over to the matrix representation, the same connection formulas are involved. This is true for c , \bar{c} , etc.; f , \bar{f} , etc.; K , K^F , etc. To illustrate a case in which it is not necessarily true, let us solve equation (152) of Section 2.3.3 for the strain:

$$s = c^{-1}X - \frac{c^{-1}f^t D}{4\pi}. \quad (162)$$

The compliance matrix c^{-1} can be expressed as a fourth-rank tensor just as c itself, and therefore has the same symmetry properties as c when so expressed. However, the connection formula is

$$c_{ab}^{-1} = D_{apq} c_{pqrs}^{-1} D_{brs} \quad (163)$$

which differs from equation (153) of Section 2.3.3 in using the D instead of the C connection matrix. Thus, while the matrices c^{-1} and \bar{c}^{-1} both have the same symmetry properties, these properties are not necessarily the same as those of c and \bar{c} . This difference goes back to the different way in which the strain and stress tensors are converted to matrices. If instead of putting a factor 2 on the off-diagonal elements of the strain tensor to get the last three elements of the strain matrix, equation (146) of Section 2.3.3, a factor $2^{1/2}$ had been put on the off-diagonal elements of *both* the strain and stress tensor, then the C and D connection matrices would be identical and this difference would disappear. In any event, we can always calculate c^{-1} from c , having first determined the symmetry properties of c ; and, for the particular symmetry of RS and ADP, c and c^{-1} actually have the same symmetry properties.

Having established the principles of symmetry reduction, we need only do detailed calculations for c , f , and K , deducing all other matrices from these. We first consider RS, since the symmetry group of ADP includes that of

RS, and we will thus simplify the calculations for ADP. RS belongs to the orthorhombic system, bisphenoidal (Bond's class 6). Its axes are mutually perpendicular and 180° rotation about any one leaves the properties unchanged. Only two axes of the rotation need be considered, since the third is the resultant of any two. We therefore require that all matrices be unchanged by either of the two rotations

$$a_1 = \begin{bmatrix} 1 & & \\ & -1 & \\ & & -1 \end{bmatrix}, \quad a_2 = \begin{bmatrix} & -1 & \\ & 1 & \\ & & -1 \end{bmatrix}. \quad (164)$$

The K matrix, transformed according to these two a 's, becomes (K and K^{-1} transform identically)

$$\begin{aligned} K'_1 &= a_1 K a_1^t = \begin{bmatrix} + & - & - \\ - & + & + \\ - & + & + \end{bmatrix}; \\ K'_2 &= a_2 K a_2^t = \begin{bmatrix} + & - & + \\ - & + & - \\ + & - & + \end{bmatrix}. \end{aligned} \quad (165)$$

For these diagonal a 's, the elements are not moved around but merely have their signs altered as indicated. Each of these transformed matrices must be identical with the untransformed, and hence all those elements which become negative upon transformation must actually vanish; hence we conclude that K is diagonal. Symmetry conditions can tell us nothing more about K , and actually all three of its elements are distinct for RS.

Before transforming f or c , we must obtain the T 's corresponding to the two a 's. These are easily shown to be represented, for diagonal a 's, by the supermatrix

$$T = \frac{I}{0} \mid \frac{0}{a}. \quad (166)$$

The transforms of f , according to equation (161) of Section 2.3.3, are therefore

$$\begin{aligned} f' &= afT^t = \begin{bmatrix} a & 0 \\ 0 & 0 \end{bmatrix} \begin{bmatrix} g & h \\ & \end{bmatrix} \begin{bmatrix} I \\ & a^t \end{bmatrix} \\ &= \begin{bmatrix} ag & aha^t \\ 0 & 0 \end{bmatrix}, \end{aligned} \quad (167)$$

in which a is to be given its two values a_1 and a_2 , and g and h are temporary notations for the

left and right 3x3 matrices into which f may be broken for convenient treatment. For ag to be the same as g for both a 's, it is necessary that $g = 0$. Also, we see that h transforms just like K above, and hence must be diagonal.

Turning now to c , we have

$$\begin{aligned} c' &= TcT^t = \begin{bmatrix} I & 0 \\ 0 & a \end{bmatrix} \begin{bmatrix} p & q \\ q & r \end{bmatrix} \begin{bmatrix} I & 0 \\ 0 & a^t \end{bmatrix} \\ &= \begin{bmatrix} p & qa^t \\ aq & ara^t \end{bmatrix}, \end{aligned} \quad (168)$$

in which p , q , and r are temporary notations for the 3x3 matrices into which c may be broken. Now we see that q transforms just like g above, and hence must be zero. Furthermore r transforms like h and hence must be diagonal.

c_{11}	c_{12}	c_{13}		
c_{12}	c_{22}	c_{23}		
c_{13}	c_{23}	c_{33}		
			c_{44}	f_{14}
			c_{55}	f_{25}
			c_{66}	f_{36}
			f_{14}	k_{11}
			f_{25}	k_{22}
			f_{36}	k_{33}

FIGURE 4. Symmetry-reduced matrix of RS.

The c , f , and K matrices for RS, arrayed for convenience in a 9x9, are therefore as shown in Figure 4 (all elements not shown are zero).

We now turn to ADP which has higher symmetry, being a member of the tetragonal system, scalenohedral (Bond's class 11). Like RS, its axes are mutually perpendicular and each is digonal, so that its matrices are reduced at least as much as those of RS. However, it has the additional symmetry of a tetragonal rotation-reflection axis (always taken as the z axis), such that rotation by 90° around this axis, together with reflection across a plane perpendicular to it (xy plane), leaves it unaltered. Only one of these 90° rotation-reflections need be used, since all the others have

been taken into account because of the three digonal axes. The a and T matrices are

$$a = \begin{bmatrix} 0 & 1 & 0 \\ -1 & 0 & 0 \\ 0 & 0 & -1 \end{bmatrix} \quad T = \left[\begin{array}{c|c} A & 0 \\ \hline 0 & a \end{array} \right], \quad (169)$$

in which A is the matrix each of whose elements is the square of the corresponding element of a (not to be confused with the matrix a^2).

Transforming K , already diagonal because of the digonal axes, we find

$$aKa' = \begin{bmatrix} K_{22} & & \\ & K_{11} & \\ & & K_{33} \end{bmatrix}, \quad (170)$$

so that we conclude that $K_{22} = K_{11}$.

c_{11}	c_{12}	c_{13}		
c_{12}	c_{11}	c_{13}		
c_{13}	c_{13}	c_{33}		
			c_{44}	f_{14}
			c_{44}	f_{14}
			c_{66}	f_{36}
			f_{14}	κ_{11}
			f_{14}	κ_{11}
			f_{36}	κ_{33}

FIGURE 5. Symmetry-reduced matrix of ADP.

Transforming f , with the left 3x3 already zero and the right diagonal, we find that the A part of T does not enter, and hence we have

$$h' = aha', \quad (171)$$

which is the same as the transformation of K above and hence $f_{14} = f_{25}$.

Finally, the new c is given by

$$\begin{aligned} c' = TcT' &= \left[\begin{array}{c|c} A & \\ \hline & a \end{array} \right] \left[\begin{array}{c|c} p & 0 \\ \hline 0 & r \end{array} \right] \left[\begin{array}{c|c} A & \\ \hline & a' \end{array} \right] \\ &= \left[\begin{array}{c|c} ApA & 0 \\ \hline 0 & ara' \end{array} \right]. \end{aligned} \quad (172)$$

Recalling that r is already diagonal, we see that

$c_{44} = c_{55}$. To find the significance of $ApA = p$, we must do the multiplication, obtaining

$$\begin{aligned} ApA &= \begin{bmatrix} 0 & 1 & 0 \\ 1 & 0 & 0 \\ 0 & 0 & 1 \end{bmatrix} \begin{bmatrix} c_{11} & c_{12} & c_{13} \\ c_{12} & c_{22} & c_{23} \\ c_{13} & c_{23} & c_{33} \end{bmatrix} \begin{bmatrix} 0 & 1 & 0 \\ 1 & 0 & 0 \\ 0 & 0 & 1 \end{bmatrix} \\ &= \begin{bmatrix} c_{22} & c_{12} & c_{23} \\ c_{12} & c_{11} & c_{13} \\ c_{23} & c_{13} & c_{33} \end{bmatrix}, \end{aligned} \quad (173)$$

and hence we conclude that $c_{22} = c_{11}$ and $c_{23} = c_{13}$.

The c , f , and K matrices for ADP, arrayed in a 9x9, are therefore as shown in Figure 5.

The foregoing Figures 4 and 5 give all the independent parameters necessary to specify RS and ADP, but of course give no information as to the numerical values of these parameters. The constants are referred to the crystallographic (mutually perpendicular) axes; in the next section, we will rotate these matrices so that they are suitable for studying 45° Y-cut RS and 45° Z-cut ADP.

MATRICES FOR ROTATED CUTS

The symmetry-reduced matrices of RS and ADP obtained in the previous section refer to the (mutually perpendicular) crystallographic axes. In this section we obtain these same matrices referred, however, to rotated axes. The rotations are 45° around the Y axis for RS and 45° around the Z axis for ADP.

First consider ADP, since it is simpler. The a and T matrices for a 45° rotation around the Z axis are

$$\begin{aligned} a &= \begin{bmatrix} c & s & 0 \\ -s & c & 0 \\ 0 & 0 & 1 \end{bmatrix} \\ T &= \left[\begin{array}{ccc|ccc} \frac{1}{2} & \frac{1}{2} & 0 & 0 & 0 & \sigma \\ \frac{1}{2} & \frac{1}{2} & 0 & 0 & 0 & -\sigma \\ 0 & 0 & 1 & 0 & 0 & 0 \\ \hline 0 & 0 & 0 & c & -s & 0 \\ 0 & 0 & 0 & s & c & 0 \\ -\frac{1}{2}\sigma & \frac{1}{2}\sigma & 0 & 0 & 0 & 0 \end{array} \right]. \end{aligned} \quad (174)$$

in which c and s are abbreviations for the sine and cosine of 45° (or -45°) and σ is the sign of s , +1 if the rotation is counterclockwise, -1 if clockwise.

The detailed calculations involve a straight-

forward application of equations (159), (160), and (161) of Section 2.3.3, but are a little long and hence only the results are given, arrayed in a 9x9 in Figure 6 (elements not shown are zero).

The unprimed quantities in Figure 6 are those of Section 2.3.3 and refer to the crystallo-

c'_{11}	c'_{12}	c'_{13}			σ'_{36}
c'_{12}	c'_{11}	c'_{13}			$-\sigma'_{36}$
c'_{13}	c'_{13}	c'_{33}			0
		c_{44}		$-\sigma'_{14}$	
		c_{44}		σ'_{14}	
		c'_{66}			
		σ'_{14}		K_{11}	
		$-\sigma'_{14}$		K_{11}	
σ'_{36}	$-\sigma'_{36}$	0			K_{33}

FIGURE 6. Matrix for 45° Z-cut ADP.

graphic axes. The primed quantities, expressed in terms of the unprimed, are

$$\begin{aligned} c'_{11} &= \frac{c_{11} + c_{12}}{2} + c_{66} \\ c'_{12} &= \frac{c_{11} - c_{12}}{2} - c_{66} \\ c'_{66} &= \frac{c_{11} + c_{12}}{2} \end{aligned} \quad (175)$$

We now see that there is no difference between +45° and -45° Z-cut ADP plates, if properly oriented, and that we may therefore take $\sigma = +1$. If we rotate either plate 180° around its x or y axis (plate, not crystallographic), it becomes indistinguishable from the other. This is exactly what is done, in polarizing crystals, if a small longitudinal compression shows the wrong polarity. The identity of these two cuts is a consequence of the tetragonal rotation-reflection axis, and we must therefore be prepared for a more complicated situation in RS since it does not have this symmetry.

Turning now to RS, the a and T matrices for a 45° rotation around the Y axis are

$$\begin{aligned} a &= \begin{bmatrix} c & 0 & -s \\ 0 & 1 & 0 \\ s & 0 & c \end{bmatrix} \\ T &= \begin{array}{ccc|ccc} \frac{1}{2} & 0 & \frac{1}{2} & 0 & -\sigma & 0 \\ 0 & 1 & 0 & 0 & 0 & 0 \\ \frac{1}{2} & 0 & \frac{1}{2} & 0 & \sigma & 0 \\ \hline 0 & 0 & 0 & c & 0 & s \\ \frac{1}{2}\sigma & 0 & -\frac{1}{2}\sigma & 0 & 0 & 0 \\ 0 & 0 & 0 & -s & 0 & c \end{array} \quad (176) \end{aligned}$$

Applying these, in accordance with equations (159), (160) and (161) of Section 2.3.3, to the c , f , and K matrices arrayed in Figure 4, we obtain the corresponding matrices in the rotated frame. The results are given in Figure 7 below, arrayed in a 9x9. The primed quantities, expressed in terms of the elements of the unrotated matrices, are

$$\begin{aligned} c'_{11} &= \frac{c_{11} + c_{33} + 2c_{13}}{4} + c_{55}, \\ c'_{12} &= \frac{c_{12} + c_{23}}{2}, \\ c'_{13} &= \frac{c_{11} + c_{33} + 2c_{13}}{4} - c_{55}, \\ c'_{15} &= \frac{c_{11} - c_{33}}{4}, \\ c'_{25} &= \frac{c_{12} - c_{23}}{2}, \\ c'_{44} &= \frac{c_{44} + c_{66}}{2}, \\ c'_{46} &= \frac{c_{66} - c_{44}}{2}, \\ c'_{55} &= \frac{c_{11} + c_{33} - 2c_{13}}{4}, \\ f'_{14} &= \frac{f_{14} - f_{36}}{2}, \\ f'_{34} &= \frac{f_{14} + f_{36}}{2}, \\ K'_{11} &= \frac{K_{11} + K_{33}}{2}, \\ K'_{13} &= \frac{K_{11} - K_{33}}{2}. \end{aligned} \quad (177)$$

The matrices of Figures 6 and 7 are not convenient for comparison of the properties of rectangular plates of 45° Z-cut ADP and 45° Y-cut RS, because the xyz frame is differently oriented with respect to the edges of the plates in the two cases. By rotating the frame, to which

ADP. For the limited purposes of this volume, therefore, it seems best to carry out the calculation without assuming numerical values but having used only the very general symmetry arguments to deduce the general structure, and then to evaluate the significant combinations of these elements by experiments intimately related to the actual motion of a crystal in an underwater transducer. Thus, Figure 9 is solely

c_{11}	c_{12}	c_{13}		c_{16}		f_{31}
c_{12}	c_{11}	c_{13}		c_{16}		$-f_{31}$
c_{13}	c_{13}	c_{33}		c_{36}		0
			c_{44}	c_{45}	f_{14}	$-f_{15}$
			c_{45}	c_{44}	f_{15}	$-f_{14}$
c_{16}	c_{16}	c_{36}		c_{66}		
			f_{14}	f_{15}	k_{11}	k_{12}
			$-f_{15}$	$-f_{14}$	k_{12}	k_{11}
f_{31}	$-f_{31}$	0				k_{33}

FIGURE 9. Matrix of 45° Y-cut RS, including those of 45° Z-cut ADP as a special case.

an indication of structure deduced from symmetry.

2.4 RECIPROCITY; EQUIVALENT CIRCUIT

The reciprocity principle is the basis of the absolute calibration of standard transducers and is, in addition, a very valuable design tool.^m It has been repeatedly verified experimentally, within a decibel or so, for crystal transducers constructed with 45° Y-cut RS and 45° Z-cut ADP. Since there is no evidence of any trend to the discrepancies, it is assumed that these arise from experimental error, and the principle is therefore regarded as valid.

It therefore becomes important, as a check on the theory as so far developed, to determine if this principle is one of its consequences. The theory is summarized by the boundary-value

^m See Chapter 4 on some applications of the reciprocity principle to design.

problem of Section 2.3.2, and it will now be shown that the principle is a direct consequence of this boundary-value problem.

In a practical transducer, the external case is usually metal except for a rubber window, and hence very little of the electric field escapes; this is especially true in salt water or, in fact, any natural body of water except perhaps a very pure mountain lake. Consequently, the external bounding surface in Figure 3 of Section 2.3.2 may be any surface from that just enclosing the transducer to the surface at infinity. Also, there is nothing to prevent the region R from containing two or more transducers, since the number of conductors is not specified; in fact, any one of the elastically excluded impedance regions could be a transducer, since it was not assumed that these regions were homogeneous or that they contained no conductors.

Now let the continuous distribution of force and impedance over the impedance surfaces, including the external surface, be replaced by a large number of pistons, numbered 1, 2, . . . π . . . , each very small compared to the shortest wavelength under consideration so that the active force (per unit area) and stiffness may be regarded as constant over each piston. This approximation may be made arbitrarily good, and it avoids the occurrence of integral equations.

Assuming that all material constants and the surface stiffnesses on each piston are known, the behavior of the system is completely determined by the potential amplitudes V_c at which each conductor, and the force $F_{p\pi}$ (per unit area) at which each piston, is driven. The generalized displacements corresponding to these generalized forces may clearly be taken as the charge q_c on each conductor and the average displacement of each piston (multiplied by the area of the piston, for convenience),

$$4\pi q_{c''} = \int_{c''} dS n_p D_p \quad (n_p \text{ outward}), \quad (178)$$

$$U_{p''\pi''} = \int_{\pi''} dS u_{p''}. \quad (179)$$

Eliminating explicit reference to the details of the internal motion, these generalized dis-

placements are linear functions of the generalized forces

$$q_{c''} = C_{c''c'}V_{c'} + C_{c''p'\pi'}F_{p'\pi'}, \quad (180)$$

$$U_{p''\pi''} = C_{p''\pi''c'}V_{c'} + C_{p''\pi''p'\pi'}F_{p'\pi'}. \quad (181)$$

The coefficients are generalized compliances and are functions of the material constants, the piston stiffnesses, the geometry of the system, and the frequency. Their interpretation is as follows. $C_{c''c'}$ is the free-piston capacitance matrix; $C_{c''p'\pi'}$ is the short-circuit response to external forces; $C_{p''\pi''c'}$ is the free-piston transmitter response; and $C_{p''\pi''p'\pi'}$ is the short-circuit response to mechanical drive.

Our problem is to show that it is a consequence of the boundary-value problem that the above compliance matrix is symmetric and hence that the above set of equations is circuit-like and subject to all the general circuit theorems. The impedance matrix is $(1/i\omega)$ times the reciprocal of this compliance matrix; its existence is assured by the physical consideration that by forcing definite charge and displacement amplitudes upon the system, determinate potentials and forces must result and hence the above set of equations must be solvable for $V_{c'}$ and $F_{p'\pi'}$.

The proof that this symmetry is a consequence of the boundary-value problem is closely analogous to that for a pure dielectric or a pure elastic system. One considers the special solution $u_p(c), \phi(c)$ corresponding to unit potential amplitude on one conductor, zero on all others, and zero forces on all pistons. As c ranges over all conductors, this yields a set of free-piston solutions. Similarly, one considers the solution $u_p(p'\pi'), \phi(p'\pi')$ corresponding to the p' -component of the force on the π' -piston being unity, all other components on this and all other pistons, and all potentials, being zero. This yields a set of grounded-conductor solutions.

By superposition of these special solutions, one obtains the general solution

$$u_p = u_p(c')V_{c'} + u_p(p'\pi')F_{p'\pi'}, \quad (182)$$

$$\phi = \phi(c')V_{c'} + \phi(p'\pi')F_{p'\pi'}. \quad (183)$$

The auxiliary field quantities corresponding to each of the special solutions are called $D_p(c)$, $F_{pq}(c)$, etc., and these quantities obey the same superposition rule.

It is now readily shown that the elements of the compliance matrix are given by

$$C_{c''c'} = \left(\frac{1}{4\pi} \right) \int_{c''} dS n_p D_p(c'), \quad (184)$$

$$C_{p''\pi''p'\pi'} = \int_{\pi''} dS u_{p''}(p'\pi'), \quad (185)$$

$$C_{c''p'\pi'} = \int_{c''} dS n_p D_p(p'\pi'), \quad (186)$$

$$C_{p'\pi'c''} = \int_{\pi'} dS u_{p'}(c''). \quad (187)$$

It must be shown that the antisymmetric part of equations (184) and (185) are zero, the first with respect to exchange of the indices c'' and c' , and the second with respect to exchange of the pairs $p''\pi''$ and $p'\pi'$; and that the electro-mechanical coupling compliances, equations (186) and (187), are equal. This is straightforward but a little long, and will therefore be done in detail only for $C_{c''c'}$; this, together with an outline for the others, will illustrate the method so that the others can be readily treated.

Since $\phi(c'')$ is unity on c'' , and zero on all other conductors including the ground, one can insert it under the integral in equation (184) and then extend the integral over all conductors and the external surface. The resultant flux out of all conductors after antisymmetrizing, can then be transformed to a volume integral,

$$4\pi(C_{c''c'} - C_{c'c''}) = - \int_{R-c} dV [D_p(c')\phi(c'') - D_p(c'')\phi(c')],_{p'}. \quad (188)$$

The divergence of D_p is zero, so that two terms fall out in expanding the divergence bracket; also the result vanishes inside the conductors because there is no electric field there, and hence the region of integration may be extended to include the interiors of the conductors, which are a part of the elastic domain. Expressing D_p in terms of the strain and field, the two bilinear forms in the field cancel and one is left with

$$C_{c''c'} - C_{c'c''} = -\bar{f}_{prs} \int_{R-Z} dV [u_{r,s}(c')\phi_{,p}(c'') - u_{r,s}(c'')\phi_{,p}(c')], \quad (189)$$

in which the removal of the interior impedance regions is permissible because \bar{f} vanishes there.

If the system were nonpiezoelectric, this would complete the proof, since the \bar{f} tensor would then be zero. However, we now eliminate $\bar{f}_{prs}\phi_{,p}(c')$ and $\bar{f}_{prs}\phi_{,p}(c'')$ with the stress equation. A pair of bilinear forms in the strains cancel, and one is left with

$$C_{c''c'} - C_{c'c''} = - \int_{R-Z} dV [F_{rs}(c'')u_{r,s}(c') - F_{rs}(c')u_{r,s}(c'')]. \quad (190)$$

The first term inside the bracket is

$$[F_{rs}(c'')u_r(c')]_{,s} - F_{rs,s}(c'')u_r(c'). \quad (191)$$

Eliminating the divergence of the stress tensor with the propagation equation, the second term of equation (191) becomes

$$-\rho\omega^2 u_r(c'')u_r(c').$$

The resultant dot product of the two displacements is symmetric and hence falls out upon exchange of the indices, and we are left with an exact divergence which, upon being converted to a surface integral over the impedance surfaces and the external boundary, that is, over all the pistons, yields

$$C_{c''c'} - C_{c'c''} = \sum_{\pi} \int dS n_p [P_{pq}(c'')u_q(c') - P_{pq}(c')u_q(c'')]. \quad (192)$$

Now $P_{pq}(c''$ and $c')$ are the stresses, corresponding to free-piston solutions, and hence their flux across the pistons are from the boundary conditions, $u_p(c''$ or $c')S_{pq}$; the above bracket therefore becomes the difference of two bilinear forms in $u_c(c')$ and $u_q(c'')$ and, since S_{pq} is symmetric, vanishes.

In treating equation (185), one replaces $u_{p''}(p'\pi')$ by

$$u_p(p'\pi') [P_{pq}(p''\pi'')n_q + S_{pq}u_q(p''\pi'')], \quad (193)$$

and extends the integral over all pistons; this is permissible since the bracket is zero on every piston except π'' and is zero there unless p is p'' , in which case it is one. Then the stiffness term falls out upon exchange and the remaining exact flux can be converted to a volume integral over $R - Z$. The divergence is expanded, the displacement propagation equation used, and

the stress expressed in terms of the strain and field. This latter brings out an \bar{f} which, vanishing inside the impedance regions, allows the region to be extended from $R - Z$ to R . Having served its purpose, the \bar{f} tensor is eliminated with the equation for the electric displacement; the result is an exact divergence which can be converted to a surface integral over all conductors, and here the special $\phi(p''\pi'')$ and $\phi(p'\pi')$ vanish.

In treating equations (186) and (187) one finds it most convenient to bring equation (186) to an integral over the pistons, by methods similar to those described above, whereupon it becomes identical to equation (187).

The foregoing shows that a linear dissipative piezoelectric system, governed by the boundary-value problem of Section 2.3.2, has the equivalent circuit shown in Figure 10.

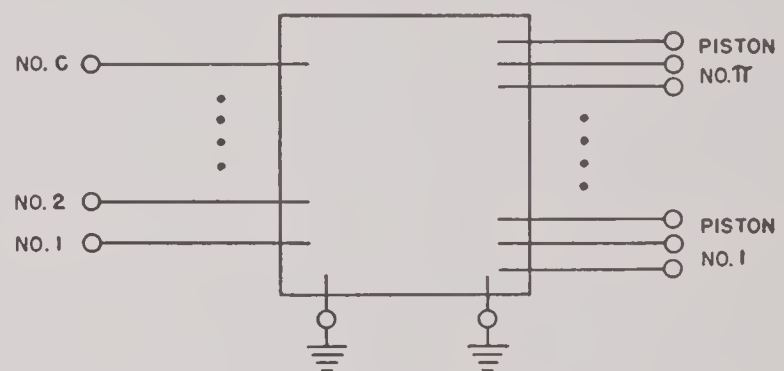


FIGURE 10. The rigorous equivalent circuit for a linear dissipative piezoelectric system.

2.5 AN EQUIVALENT VARIATIONAL PRINCIPLE

2.5.1 The Steady-State Boundary-Value Problem

The steady-state solution of the above boundary-value problem is adequate for our purposes, since the transient behavior can be determined by superposition of steady states. This problem is defined by

$$\rho\omega^2 u_p + P_{pq,q} = 0 \quad (\text{in the crystal}), \quad (194)$$

$$\text{div } \mathbf{D} = 0 \quad (\text{in all space}), \quad (195)$$

$$P_{pq}n_q + S_{pq}u_q = F_p \quad (\text{over surface of crystal}), \quad (196)$$

$$\text{surf div } \mathbf{D} = 4\pi\sigma \quad (197)$$

(on every surface of discontinuity),

$$\phi = (\text{constant on electrodes,} \quad (198)$$

continuous everywhere),

in which the displacement, strain, etc., are complex amplitudes. The complex tensor S_{pq} acts on the displacement instead of the velocity, and may be conveniently called the "stiffance"; it is just $i\omega Z_{pq}$, in which Z_{pq} is the ordinary (velocity) impedance tensor. Its value for various surfaces and frequencies is a set of parameters to be experimentally determined a posteriori; for the present, we need only assume that it is symmetric and has only two distinct principal values, the normal and tangential specific acoustic (displacement) impedances, as discussed previously.

The solution of this problem by the characteristic function method is hopelessly complicated, since, to mention only one complication, the characteristic values will be solutions of some set of simultaneous complex transcendental equations.

2.5.2

Variational Principle

If, however, we can find a variation principle equivalent to this problem, we can use the powerful *direct method*, of which the well-known Rayleigh-Ritz method of treating conservative systems is a special case. This method has many advantages, the most important being that we can use our qualitative understanding of a physical system to guide us in the choice of trial solutions.

The derivation of the equations of motion of a dissipative system from a variation principle was first accomplished many years ago by Bateman,^{14,15} but the great power of this method for treating complicated practical problems does not seem to have been appreciated. Some extensions of Bateman's valuable contribution, with applications to various acoustic problems, will shortly be published elsewhere.

Leaving aside the arguments which lead us to choose the following variation principle, consider the integral

$$I = \int dV (\rho\omega^2 \frac{u_p u_p}{2} - W') \quad (199)$$

$$+ \int dS [F_p u_p - \frac{1}{2} u_p S_{pq} u_q - (\phi - V)\sigma],$$

$$W' = \frac{1}{2} s' \bar{c} s - \frac{E' KE}{8\pi} + s' \bar{f}' E. \quad (200)$$

The variational principle $\delta I = 0$ will be shown to be equivalent to the boundary-value problem governing the behavior of a transmitter, and it will lead to an equivalent circuit for this case. The equivalent circuit for a receiver will then be obtained by reciprocity considerations (see Chapter 3).

The volume integral extends over all space, but only the terms in the electric field will make contributions outside the crystal because \bar{c} and \bar{f} and the displacements are zero there; the surface integral extends over all surfaces of discontinuity, but here again only the electric-field terms will make contributions outside the crystal.

The total integral I is a complex number whose value depends upon our choice of ϕ , u_p , and σ since we assume that all constants, the external surface force density F_p (zero for a transmitter), and the potentials V on all metal surfaces, are given. It will now be shown that amongst all functions ϕ , u_p , and σ , that set which gives I a stationary value satisfies equations (194) to (198), so that demanding that the first variation of I (under arbitrary variations of ϕ , u_p , and σ) shall vanish is equivalent to the complete boundary-value problem. This stationary value is of course not an extremal, since there is no meaning attached to the extremal of a complex function; but neither does Hamilton's principle correspond to an extremal, and yet its usefulness is well known.

The first variation of I is

$$\delta I = \int dV (\rho\omega^2 u_p \delta u_p - \delta W') \quad (201)$$

$$+ \int dS [F_p \delta u_p - \delta u_p S_{pq} u_q - \sigma \delta \phi - (\phi - V) \delta \sigma].$$

The function W' is simply related to, but not identical with, the energy density W . It is easily shown that its variation is given by

$$\delta W' = P_{pq} \delta u_{p,q} + \frac{D_r \delta \phi_{,r}}{4\pi}. \quad (202)$$

Inserting these values into equation (201), and doing two partial integrations according to

$$\begin{aligned} P_{pq} \delta u_{p,q} &= (P_{pq} \delta u_p)_{,q} - P_{pq,q} \delta u_p, \\ \text{and} \quad \delta \phi_r D_r &= \text{div} (\mathbf{D} \delta \phi) - \delta \phi \text{div} \mathbf{D}, \end{aligned}$$

we find

$$\begin{aligned} \delta I &= \int dV \left[\delta u_p (\rho \omega^2 u_p + P_{pq,q}) + \delta \phi \text{div} \frac{\mathbf{D}}{4\pi} \right] \\ &+ \int dS \left[\delta u_p (F_p - S_{pq} u_q - P_{pq} n_q) \right. \\ &+ \left. \delta \phi (\text{surf div} \frac{\mathbf{D}}{4\pi} - \sigma) - (\phi - V) \delta \sigma \right]. \quad (203) \end{aligned}$$

We see that the principle $\delta I = 0$ for arbitrary variations of ϕ , u_p and σ is exactly equivalent to equations (194) to (197), and we may therefore apply the direct method to I , equation (199). It is to be emphasized that the equations of state are assumed, so that P_{pq} and D_r are expressible in terms of the derivatives of the field quantities, but that the propagation equations and *all* boundary conditions, except, of course, equation (198), are consequences of the variational principle $\delta I = 0$. Thus, σ , whose integral over the electrodes is the "displacement" conjugate to the externally driven potentials V , is varied independently and the variational principle makes it match $\text{surf div} \mathbf{D}/4\pi$ on the electrodes.

In applying the direct method to I , we should assume a trial value for ϕ out to infinity, or more correctly, out to the grounded closed conductor consisting of the case with rubber windows electrically closed by sea water. Such a treatment would not only take account of flux fringing near the edges of the crystal plate, but also of stray capacitances and dielectric losses shunting the crystal electrodes. However, it is not clear what to assume for the external potential, and hence we resort to another expedient.

Suppose the entire problem were solved, so that we knew the external electric displacement, \mathbf{D}_0 . Let

$$\begin{aligned} J &= \int_{\text{crystal volume}} dV (\rho \omega^2 \frac{u_p u_p}{2} - W') + \int_{\text{all crystal surfaces}} dS (F_p u_p - \frac{1}{2} u_p S_{pq} u_q) \\ &+ \int_{\text{plated surfaces}} dS \sigma (V - \phi) + \int_{\text{unplated surfaces}} dS \phi \left(\frac{\mathbf{n} \cdot \mathbf{D}_0}{4\pi} \right), \quad (204) \end{aligned}$$

in which \mathbf{n} is the outward normal to the crystal.

Then, under arbitrary variations of u_p , ϕ , and σ as before, but *not* varying \mathbf{D}_0 , δJ is given by

$$\begin{aligned} \delta J &= \int_{\text{crystal volume}} dV \left[\delta u_p (\rho \omega^2 u_p + P_{pq,q}) + \delta \phi \left(\frac{\text{div} \mathbf{D}}{4\pi} \right) \right] \\ &- \int_{\text{all crystal surfaces}} dS \delta u_p (S_{pq} u_q + P_{pq} n_q - F_p) \\ &+ \int_{\text{plated surfaces}} dS \left[\delta \sigma (V - \phi) + \delta \phi \left(\frac{-\mathbf{n} \cdot \mathbf{D}}{4\pi} - \sigma \right) \right] \\ &+ \int_{\text{unplated surfaces}} dS \delta \phi \mathbf{n} \cdot \frac{(\mathbf{D}_0 - \mathbf{D})}{4\pi}. \quad (205) \end{aligned}$$

The principle $\delta J = 0$ now yields the proper propagation equations and boundary conditions but contains the unknown vector \mathbf{D}_0 in the last term of equation (205).

It can be shown that the error arising from dropping the entire last term is negligible in the case of 45° Y-cut RS and 45° Z-cut ADP, if the electrodes fully cover the electrode faces. It should be noticed that $\delta J'$ the result of dropping the last term in equation (205), is not the exact variation of any integral, since it can be obtained by dropping \mathbf{D}_0 in J , equation (204), taking the variation, and adding to this a term

$$\int_{\text{unplated surfaces}} dS \delta \phi \left(\frac{\mathbf{n} \cdot \mathbf{D}}{4\pi} \right), \quad (206)$$

to cancel what is left of the last term of equation (205). This addendum is not an exact variation since \mathbf{D} depends upon the derivative of the displacement and potential.

We are therefore left with only one error of consequence, which arises from the fact that the σ deduced from equation (205) is the surface density only on the face of the electrode in contact with the crystal. Thus we will make an error in computing the current amplitude onto the electrodes. However, this error will correspond almost exactly to the effect produced by a pair of condensers, one from each electrode to the case. The error in this correspondence is of the same order as the error in neglecting the last term of equation (205).

Therefore, when we finally deduce an equivalent circuit, we need only insert these condensers to get a very accurate equivalent circuit for

the single crystal. The capacitances of these condensers is not given by equation (205) but they can be measured and, unless restricted space requires the electrodes to come quite close to metal parts of the case, are not of great practical importance. In any event, their effect can be taken into account.

2.5.3 Solution of the Boundary-Value Problem

The boundary-value problem governing the motion of a loaded piezoelectrical crystal was formulated in Sections 2.3.1 and 2.3.2. In Sec-

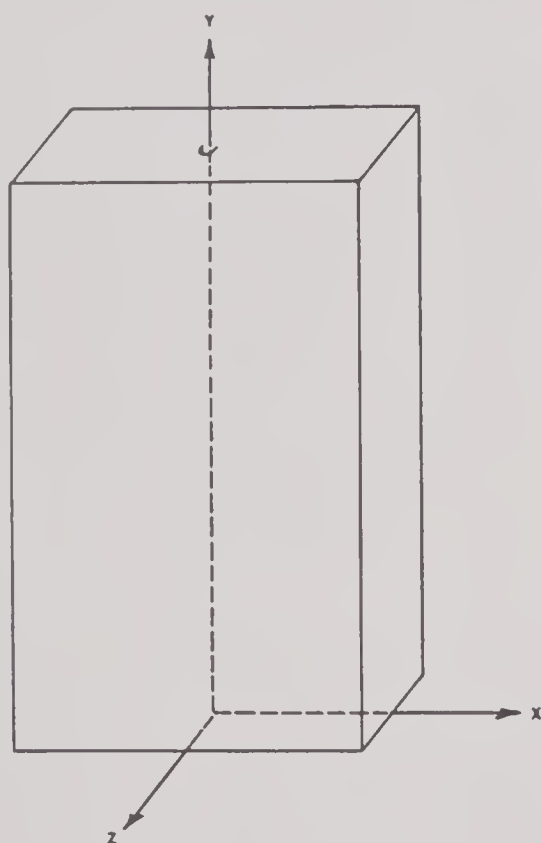


FIGURE 11. Coordinate frame.

tion 2.5.2, a variational principle rigorously equivalent to this boundary-value problem was presented.

This variational principle will now be applied to a single rectangular plate of 45° Y-cut RS or 45° Z-cut ADP. The solution is first obtained in the Mason approximation, and in the next section, in a higher approximation.

Consider a rectangular plate of 45° Y-cut RS or 45° Z-cut ADP, referred to the xyz frame to which the matrices of Section 2.3.3, Figure 9, refer. This coordinate frame, shown in Figure

11, permits 45° Y-cut RS and 45° Z-cut ADP to be treated in one calculation, when the appropriate matrices are used.

The displacement and the potential is assumed to be expansible in a power series in the lateral coordinates x and z , with coefficients that are arbitrary functions of y ,

$$\begin{aligned} u &= u_0 + u_{10}x + u_{01}z + u_{20}x^2 + u_{11}xz + u_{02}z^2 + \cdots, \\ v &= v_0 + v_{10}x + \cdots, \\ w &= w_0 + w_{10}x + \cdots, \\ \phi &= \phi_0 + \phi_{10}x + \cdots. \end{aligned} \quad (207)$$

The usefulness of the Mason approximation, which will be shown to be equivalent to such an expansion in which only u_{10} , v_0 , and u_{01} are different from zero, is sufficient evidence that there is a significant domain in which the above expansion is valid. Physically, one would expect the expansion to converge rapidly if the thickness and width are small fractions of the longitudinal wavelength as deduced from the Mason approximation, and the ratio of thickness to width is sufficiently small so that the parallel-plate condenser approximation is good.

On the other hand, there is ample experimental evidence to show that errors of serious practical significance to the design of transducers occur if one does not save a few of these terms. In order to gain some idea of the complexity of the motion of crystal plates, it will be helpful to study Figures 12 and 13, which are photographs of the distributions of silicon carbide dust which develop when the crystals are driven at various frequencies, in air.

In Figure 12, all the crystals are driven at or near their lowest (free-free) resonance. A study of these photos brings out three important points: (1) even near resonance, the motion is more complicated than that envisaged in the Mason approximation; (2) the motion of RS is considerably more complicated than that of ADP, as suggested by the more complicated matrices of RS compared to ADP (see Figures 6 and 7 of Section 2.3.3); and (3) the motion of both RS and ADP becomes more complicated as the width-length ratio increases.

In Figure 13, the crystals are driven at or near their second, third, and fourth resonances. The photos give only a partial idea of the enormous complexity of the motion. For exam-



A 45° Z-CUT ADP $1\frac{1}{2} \times 1 \times \frac{1}{4}$ IN.



B 45° Y-CUT RS $1\frac{1}{2} \times 1 \times \frac{1}{4}$ IN.



C 45° Z-CUT ADP $\frac{1}{4}$ IN. STEPS IN LENGTH AND WIDTH



D 45° Y-CUT RS $\frac{1}{4}$ IN. STEPS IN LENGTH AND WIDTH

FIGURE 12. Silicon carbide dust patterns of 45° Z-cut ADP and 45° Y-cut RS at their fundamental resonances.



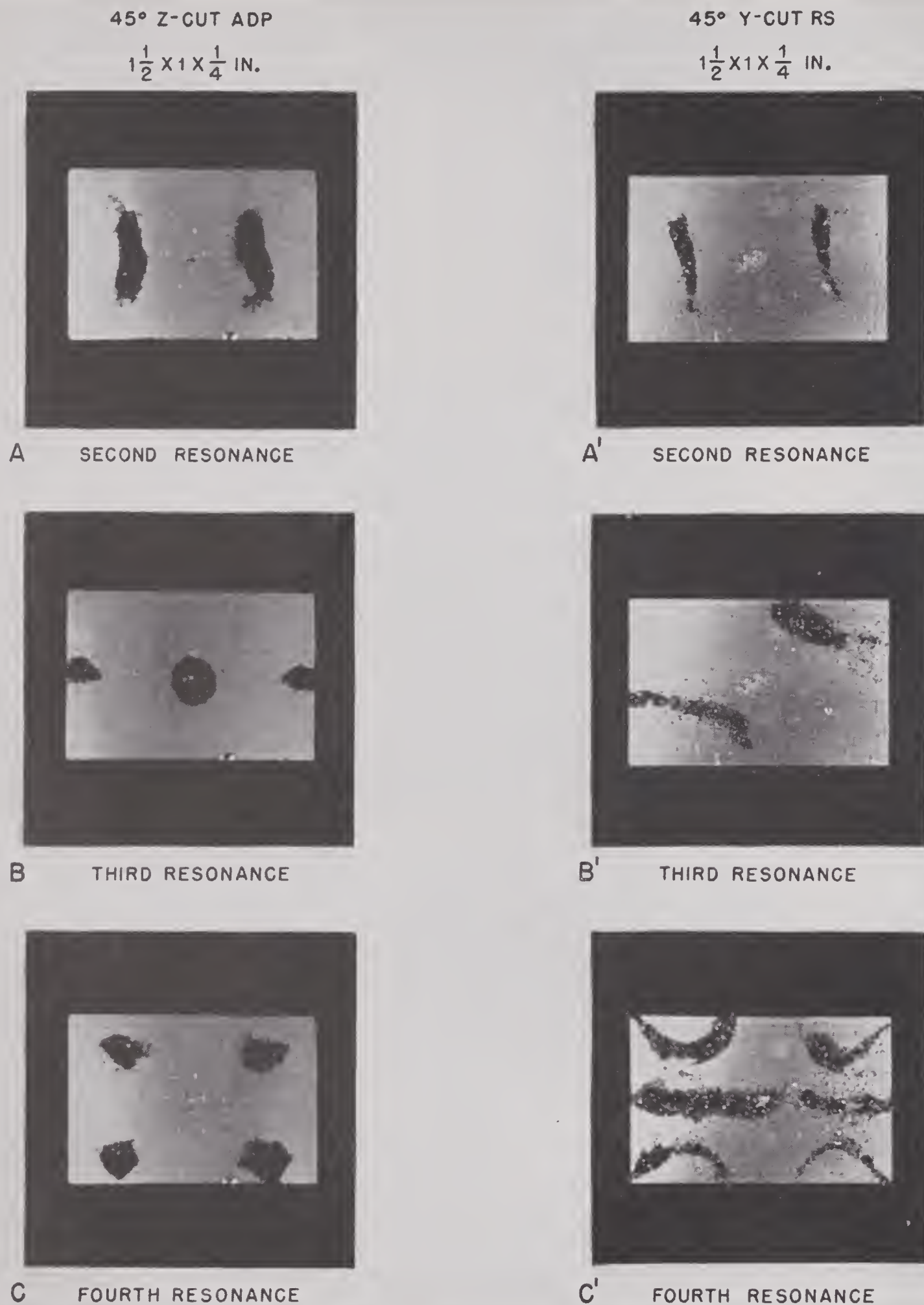


FIGURE 13. Silicon carbide dust patterns on electrode faces at higher resonances.

ple, the circular distributions in Figures 13B and 13C are actually vortices of silicon carbide dust, circulating continuously. To treat crystal plates near these higher resonances, one will presumably need to keep several terms of equation (207).

In order to understand the physics of the calculation which follows, it is helpful to study the modes of motion that would result if all but one of the displacement terms, in the expansions of equation (207), were zero. An indication of these motions is given in Figures 14A, 14B and 14C, and one sees that a free crystal could not vibrate in any one of these modes; that is, they are not normal modes. In fact, it would require an intricate system of blocks and external stresses to make any one term a normal mode. Since no single term is a normal mode, we must expect to find that, to some approximation not yet known, certain sets of these terms will be rigidly coupled together by sets of quantities which are generalizations of Poisson's ratio. This notion is very helpful in suggesting an attack on the equations obtained by applying the variational principle of Section 2.5.2 to the expansions of equation (207).

Our general procedure is as follows. Entering the variational principle with equation (207), one can perform all x and z integrations explicitly and thus obtain a variational principle in which the volume and surface Lagrangians are expansions in the moments of all ordersⁿ of an x, z -section, with coefficients which are functions of y only. Thus, the four field quantities u, v, w , and ϕ , functions of three variables, have been replaced by an infinite set of field quantities u_0, u_{10} , etc., which are, however, functions of only one variable, y . One advantage of the variational principle is now seen more clearly: we could deduce the coupled equations satisfied by the u_0, u_{10} , etc., from the fundamental field equations, but we would not know how to weight the successive equations. The variational equation weights these field equations, in a unified way, with successively higher-order moments of the cross section and we are thus able to make a consistent approximation. It is advantageous to refer to this procedure of

replacing the dependence upon some of the independent variables by an expansion in an independent set of functions, while keeping the dependence upon other variables in field quantities, as the *semidirect* method. This method stands midway between the original variational principle, which merely generates the field equations (and, in the present case, the boundary conditions), and the complete direct method invented by Ritz.

MASON APPROXIMATION, WITH A MODIFICATION

We will gain considerable facility with the variational treatment, and also test the method, by first showing that it gives the right answer in the Mason approximation. Accordingly, we assume that the principle longitudinal mode (v_0) is coupled only to Poisson motions in the two lateral directions, and that the potential is that of an infinitely thin parallel-plate condenser,

$$\begin{aligned} u &= u_{10}x = Ux \\ v &= v_0 = V \\ w &= w_{01}z = Wz \\ \phi &= \phi_{01}z = \Phi z \end{aligned} \quad (208)$$

Inserting these trial functions into the variational principle together with the assumption that σ , the surface charge density, depends upon y only and merely reverses sign in going from one electrode to the other, one finds

$$\begin{aligned} \frac{\delta J'}{A} &= \int_{y_1}^{y_2} dy \cdot \left\{ \delta U(\rho \omega^2 \bar{x}^2 U - \bar{c}_{11}U - \bar{c}_{12}V' - \bar{c}_{13}W + \bar{f}_{31}\Phi) \right. \\ &\quad - \delta U' \bar{c}_{66} \bar{x}^2 U + \delta V \rho \omega^2 V - \delta V' P \\ &\quad + \delta W(\rho \omega^2 \bar{z}^2 W - \bar{c}_{13}U - \bar{c}_{13}V' - \bar{c}_{33}W) \\ &\quad - \delta W' \bar{c}_{44} \bar{z}^2 W + \delta \Phi \left[\frac{K_{33}\Phi}{4\pi} - \bar{f}_{31}(U - V') - \sigma \right] \\ &\quad + \delta \sigma \left(\frac{\Delta}{2z_1} - \Phi \right) \left. \right\} - (\delta VNV)_1 - (\delta VNV)_2 \\ &\quad + (\delta \Phi \bar{f}_{15} \bar{z}^2 W')_2 - (\delta \Phi \bar{f}_{15} \bar{z}^2 W')_1. \end{aligned} \quad (209)$$

$$P = \bar{c}_{11}V' + \bar{c}_{12}U + \bar{c}_{13}W + \bar{f}_{31}\Phi. \quad (210)$$

All impedances have been neglected except the normal reaction at the two ends of the crystal, here represented by the normal stiffances N_1 and N_2 .

Without doing the possible partial integra-

ⁿ Because of the rectangular shape, all odd moments fall out in our present problem.

tions on the $\delta U'$ and $\delta W'$ terms, we further specialize U and W so that the coefficients of δU and δW vanish, obtaining

$$\begin{aligned}\bar{c}_{11}U + \bar{c}_{13}W &= f_{31}\Phi - \bar{c}_{12}V' + \rho\omega^2\bar{x}^2U, \\ \bar{c}_{13}U + \bar{c}_{33}W &= 0 - \bar{c}_{13}V' + \rho\omega^2\bar{z}^2W.\end{aligned}\quad (211)$$

This is solved in 0th order (i.e., neglecting \bar{x}^2 and \bar{z}^2), the result placed in the right member,

To dispose of the $\delta U'$ and $\delta W'$ terms, we use the solution of equation (212) only to 0th order, so as to consistently keep terms only up to the second-order moments. The $\delta U'$ term then becomes

$$-\delta U'\bar{c}_{66}\bar{x}^2U' = -\delta V''\bar{c}_{66}\epsilon_x^2\bar{x}^2V'', \quad (215)$$

with a similar result for the $\delta W'$ term. This

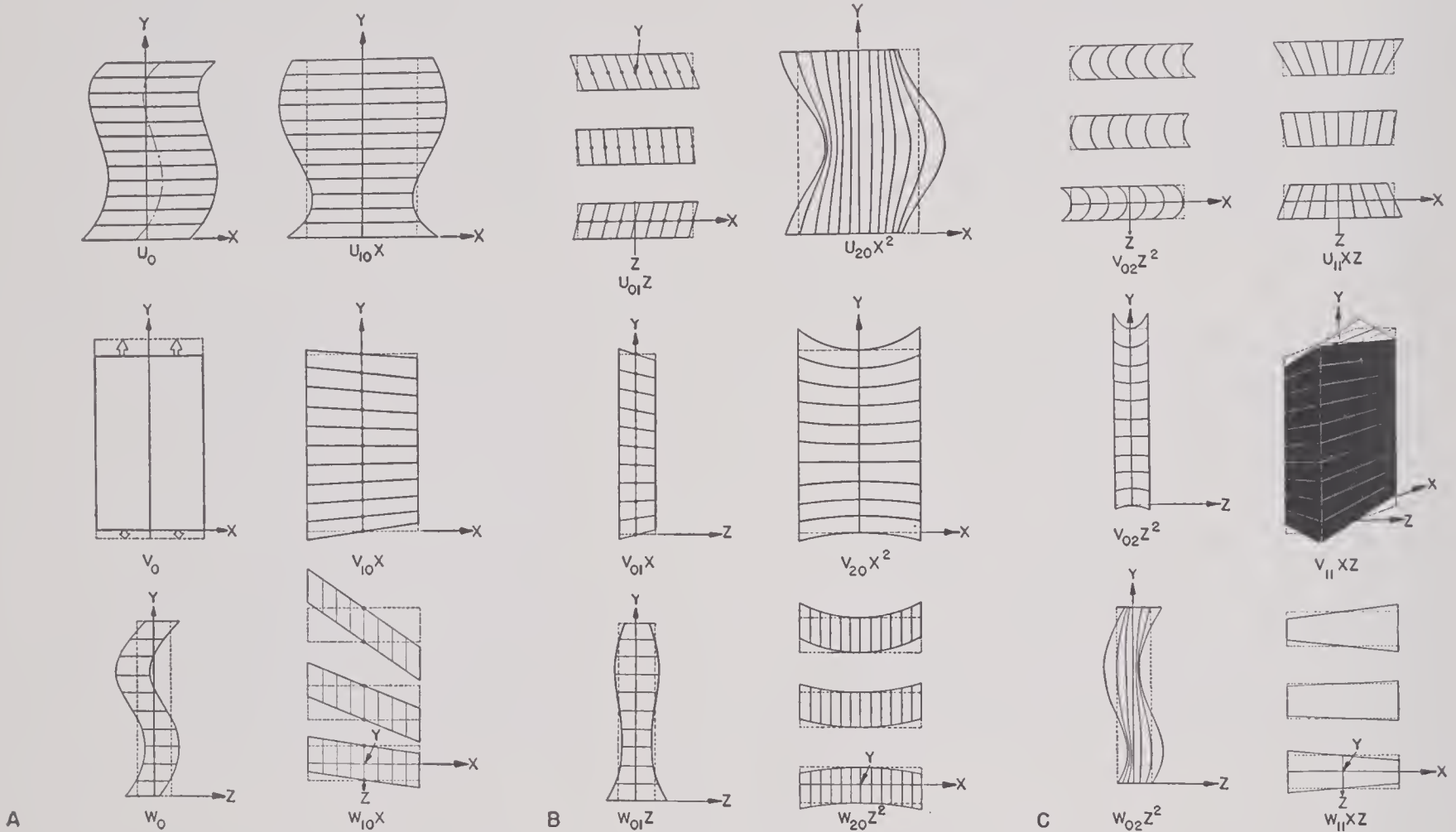


FIGURE 14. Motions corresponding to individual terms of equation (207).

and thus a second approximation is obtained, which neglects terms in the fourth-order moments. Only the linear combination P , which represents the effective stress in the y direction, is involved in this problem if we save only second-order moments, and this is

$$P = YV' + F\Phi, \quad (212)$$

$$Y = \bar{c}_{11} - \bar{c}_{12}\epsilon_x - \bar{c}_{13}\epsilon_z - \rho\omega^2(\epsilon_x^2\bar{x}^2 + \epsilon_z^2\bar{z}^2), \quad (213)$$

$$F = [1 + \epsilon_x + \rho\omega^2(\epsilon_x A_{11}\bar{x}^2 + \epsilon_z A_{13}\bar{z}^2)]\bar{f}_{31}, \quad (214)$$

in which A_{11} and A_{13} are elements of the reciprocal of the matrix of equation (211), and ϵ_x and ϵ_z are the Poisson ratios in the x and z directions.

term combines with the δV term because, in 0th approximation

$$\begin{aligned}V'' &= -k_0^2 V \\ k_0^2 &= \frac{\rho\omega^2}{Y_0}.\end{aligned}\quad (216)$$

The surface $\delta\Phi$ terms combine with the volume term, since Φ has been assumed independent of y . However, these surface terms are completely negligible in all practical cases; it is fortunate that they are negligible because, owing to the assumed form of the trial displacements and potential, they destroy reciprocity, so that if they had any appreciable effect, a

more complicated set of trial functions would be needed.^o

Doing the partial integration on the $\delta V'$ term, one obtains for the field equations and boundary conditions

$$\rho^+ \omega^2 V + P' = 0, \quad (217)$$

$$\sigma = K_{33}^+ \frac{\Phi}{4\pi} - FV', \quad (218)$$

$$\rho^+ = \rho \{ 1 - k_0^2 (\epsilon_x^2 \bar{x}^2 \bar{c}_{66} + \epsilon_z^2 \bar{z}^2 \bar{c}_{44}) \}, \quad (219)$$

$$K_{33}^+ = K_{33} + 4\pi A_{11} \bar{f}_{31}^2, \quad (220)$$

$$P_2 + N_2 V_2 = 0, \quad (221)$$

$$-P_1 + N_1 V_1 = 0. \quad (222)$$

First, if we neglect \bar{x}^2 and \bar{z}^2 , these are exactly Mason's^{12b} equations, in a different notation. Second, we see that, keeping the second-order moments, they are identical in form with Mason's equations but their physical implication is quite different because the various coefficients are now functions of frequency.

The identity in form allows us to use the Mason equivalent circuit for calculations, merely using the frequency dependent parameters instead of his constant parameters. It will be advantageous now to come to a physical understanding of equations (217) to (222), and equation (213). For this purpose, it is advantageous first to put equation (217) in a different form, one which is not as convenient for calculations, but which allows us to see what it means:

$$-\rho^{++} \omega^2 V - Y_0 V'' = (\epsilon_x^2 \bar{x}^2 \bar{c}_{66} + \epsilon_z^2 \bar{z}^2 \bar{c}_{44}) V'', \quad (223)$$

$$\rho^{++} = \rho \{ 1 + k_0^2 (\epsilon_x^2 \bar{x}^2 + \epsilon_z^2 \bar{z}^2) \}. \quad (224)$$

In equation (223), the first term is the kinetic reaction arising from all inertial effects, and from equation (224) we see that the effective density is greater than the actual by an amount which expresses the relative inertial effect^p corresponding to the two Poisson motions which are necessary to relax the lateral stresses. This effect is of considerable practical importance in

crystal transducers. The second term of equation (223) is the ordinary internal body force arising from internal variations of the longitudinal stress.

The right member of equation (223) is very interesting. The variational principle gives us the solution of the problem corresponding to the given driving forces together with any other extraneous forces necessary to maintain any constraints implied by the form assumed for the trial displacements. The trial functions include a shear strain supported by no surface forces; therefore the solution contains a *fictitious* body force to support this shear strain.

We therefore conclude that equation (223) is incorrect, in second order, for the problem of interest, because it contains only a part of the terms containing second-order moments. Thus, the foregoing treatment, although giving the very important lateral inertia term correctly, is valid only in the Mason approximation in which all second-order moments are neglected.

APPROXIMATION INCLUDING ALL SECOND-ORDER MOMENTS

To include all terms containing second-order moments, we take more terms in the trial functions. The details of this calculation are quite lengthy, and hence only the essential points will be given here.

First, we assume that tangential and normal stiffnesses act over all faces. The problem is greatly simplified, without losing the essential features, if we assume that the stiffnesses have the same value at all points on the *lateral* faces, so that the lateral stiffness is specified by the normal and tangential characteristic values N and T .

On the ends we assume normal stiffnesses N_1 and N_2 which, except for the factor $i\omega$ (necessary to convert an impedance to a stiffness), are identical to the radiation impedances assumed by Mason. For the present, we neglect the tangential stiffnesses on the ends because these bring in a new kind of term and destroy the simple result to be proven, that without these terms we can use the Mason circuit by merely allowing certain parameters to vary with frequency, width, etc. The error so intro-

^o These terms arise from the fringing of the electric displacement corresponding to a small shear strain in the assumed displacements. Reciprocity is restored if higher terms of V are included. See Section 2.4.

^p This effect, in isotropic systems, was discovered by Pockhammer.^{2c, 16, 17}

duced is a term which vanishes with the second moment and this is likely to be of practical importance in only one case, that in which one face is cemented to a backing plate by a cement so rigid as to seriously oppose tangential motion. The theoretical study of this case, perhaps of considerable importance, is not contained in this volume.

We keep all effects not considered in the Mason approximation only to the lowest order in which each occurs. Subject to this, and the neglect of tangential stiffances on the end faces as noted above, we keep all terms in the variational integral involving second-order moments, but drop all higher moments (because of the symmetry of a rectangle, the third-order moments vanish so that we are dropping fourth and higher moments).

To be sure of getting all second-order moments, we must keep cubic terms in the expansions of the displacement and potential, since these latter are differentiated once to get the strains and electric displacement. Actually, on account of the symmetry structure of the matrices of RS and ADP, the 45° cuts, and the symmetry of a rectangular plate, the cubic terms enter only to a very slight extent.

Instead of a simple power series expansion, it is found convenient to expand in a set of *orthogonal* functions $X_\alpha Z_\beta$ of x and z , defined by

$$X_\alpha = 1, x, \frac{(x^2 - \bar{x}^2)}{2}, \frac{(x^3 - 3x\bar{x}^2)}{6}; \quad (\alpha = 0 \text{ to } 3), \quad (225)$$

and similarly for Z_β . In addition to being orthogonal, vanishing like the α th and β th power of the width and thickness, respectively, these functions have the additional property, very convenient for calculation, that

$$\frac{dX_\alpha}{dx} = X_{\alpha-1}; \quad \text{with } X_{-1} = 0, \quad (226)$$

and similarly for dZ_β/dz . As a convenience to notation, we use the same symbols u_0, u_{10} , etc., as in the previous section, although they now have slightly different meanings.

The foregoing refers only to the expansion of the displacement. It can be shown that an adequate form for the potential, and one more

convenient for calculation since it simplifies so nicely on the electrodes, is

$$\phi = \phi_1 z + (z^2 - z_1^2)(\psi_0 + \psi_{10}x + \psi_{01}z). \quad (227)$$

Finally, the surface charge density is expanded according to

$$\sigma^\pm = \sum_{\alpha=0} \sigma_\alpha^\pm X_\alpha \quad (228)$$

on the $\pm z_1$ plates, in which the various coefficients are functions of y only. As seen at a glance from the only term in the surface Lagrangian which involves σ , all σ_α^\pm above $\alpha = 0$ fall out completely.

Finally, although the variational principle will yield the result, we can save some trivial complications by assuming at the outset that ϕ_1 is actually independent of y and that $\sigma_0^\pm = \pm\sigma_0$.

These trial functions are now inserted into the modified principle $\delta J' = 0$. The labor of forming this expression is greatly reduced by using the Einstein summation convention, whereby $u_{\alpha\beta} X_\alpha Z_\beta$ represents the sum of all terms as α and β range from 0 to 3; the derivative recursion formulas, equation (226) and the ortho-normality conditions satisfied by X_α and Z_β .

Examining the variational equations one finds that they are linear algebraic to the present approximation, except for the one governing v_0 . Also, the algebraic set falls apart into subsets, which greatly simplifies their solution. Thus certain of the displacement coefficients are linear combinations of a particular one and the electric field ϕ_1 , while others satisfy linear homogeneous equations with nonvanishing determinant. Physically, this means that certain motions, in the present approximation, are rigidly coupled to others by a generalization of a pantograph mechanism, the coupling constants being an array of quantities which are a generalization of Poisson's ratio; others, satisfying the homogeneous equations, form a separate physical system free to vibrate independently, but are not excited in this order.

An example of a homogeneous set is

$$\begin{aligned} \bar{c}_{44}(v_{01} + w'_0) + \bar{c}_{45}(u_{01} + w_{10}) &= 0, \\ \bar{c}_{45}(v_{01} + w'_0) + \bar{c}_{55}(u_{01} + w_{10}) &= 0. \end{aligned} \quad (229)$$

Since no subdeterminant of the \bar{c} matrix can

vanish (the strain energy is positive-definite), one concludes that the parentheses are zero.⁴

Another set takes the form

$$\begin{aligned}\bar{c}_{11}u_{20} + \bar{c}_{13}w_{11} + \bar{c}_{16}(u'_{10} + v_{20}) &= -\bar{c}_{12}v'_{10}, \\ \bar{c}_{13}u_{20} + \bar{c}_{33}w_{11} + \bar{c}_{36}(u'_{10} + v_{20}) &= -\bar{c}_{13}v'_{10}, \\ \bar{c}_{16}u_{20} + \bar{c}_{36}w_{11} + \bar{c}_{66}(u'_{10} + v_{20}) &= -\bar{c}_{16}v'_{10}.\end{aligned}\quad (230)$$

Using the abbreviations \bar{C} for the 3x3 matrix, and u_2 and \bar{c} for the 3x1 matrices with elements u_{20} , etc., and \bar{c}_{12} , etc., equation (230) becomes $\bar{C}u_2 = -\bar{c}v'_{10}$. The solution of this is $u_2 = -\epsilon v'_{10}$, in which ϵ is a 3x1 satisfying

$$\bar{C}\epsilon = \bar{c}. \quad (231)$$

The three elements of ϵ will be called ϵ_w , ϵ_t , and ϵ_s , the subscripts meaning width, thickness, and shear. If the elements \bar{c}_{16} and \bar{c}_{36} of C , which couple compressional and shear strains, are zero (as they are for ADP but not RS), then ϵ_w and ϵ_t are the ordinary Poisson ratios used by Mason. The ϵ 's are therefore generalizations of the Poisson ratios.

Another set, also involving ϵ and one which allows the physical meaning of this matrix to be more clearly seen, is

$$\begin{aligned}\bar{c}_{11}u_{10} + \bar{c}_{13}w_{01} + \bar{c}_{16}v_{10} &= -\bar{c}_{12}v'_0 - \bar{f}_{31}\phi_1 + O(\bar{x}^2), \\ \bar{c}_{13}u_{10} + \bar{c}_{33}w_{01} + \bar{c}_{36}v_{10} &= -\bar{c}_{13}v'_0 + 0 + O(\bar{x}^2), \\ \bar{c}_{16}u_{10} + \bar{c}_{36}w_{01} + \bar{c}_{66}v_{10} &= -\bar{c}_{16}v'_0 + 0 + O(\bar{x}^2),\end{aligned}\quad (232)$$

which yields

$$u'_1 = -\epsilon v'_0 + (\bar{C}_{11}^{-1}, \bar{C}_{12}^{-1}, \bar{C}_{13}^{-1})\bar{f}_{31}\phi_1 + 0(\bar{x}^2),$$

in which \bar{C}_{11}^{-1} means $(\bar{C}^{-1})_{11}$, etc., the designated element of the reciprocal matrix. It is interesting to notice that the same matrices \bar{C} , \bar{c} and ϵ connect u_2 to v'_{10} and u_1 to v'_0 .

Now if \bar{c}_{16} and \bar{c}_{36} are zero, equation (232) is the same as that which couples the Poisson "breathing," u_{10} and w_{01} , to the principal longitudinal motion v_0 , together with the equation $v_{10} = 0$. However, it is seen that v_{10} is also coupled to v_0 in RS. Thus the electrode faces vibrate between two limiting parallelograms in the case of RS, but not in ADP.

Taking account of all the algebraic equations, one finds that u_0 , w_0 , $(u_{01} + w_{10})$, v_{01} , $(v_{02} + w_{01})$ and $(u_{02} + w_{11})$ are all zero. The values of other secondary displacement coefficients may become important when sufficiently detailed experimental data are available, and are

readily calculated; however, for the present purpose, it is sufficient to use the relations to reduce the system down to a perturbed v_0 problem. Two other items of this reduction should be mentioned: First, in many of the terms of type $\delta u_{\alpha\beta}' Q$, the quantity Q vanishes by virtue of the algebraic relations, but some terms of this type remain; in all cases except the $\delta v'_0$ term, these are not partially integrated, but transformed to underived variations with the aid of the generalized Poisson relations and the solution of the 0th-order problem. Second, the auxiliary potential quantities ψ_0 , ψ_{10} , and ψ_{01} are all zero in this approximation.

Having disposed of all the algebraic relations, one is left with a propagation equation and boundary conditions for v_0 (hereafter called V), and an "equation of state" giving the charge density in terms of V' and Δ , the potential difference between the plates. These are

$$\rho^+ \omega^2 V + Y^+ V'' = 0, \quad (233)$$

$$P_2^+ + N_2 V_2 = 0, \quad (234)$$

$$-P_1^+ + N_1 V_1 = 0, \quad (235)$$

$$\sigma_0 = \frac{K^+ \Delta}{4\pi t} - F^+ V'. \quad (236)$$

The auxiliary quantities here introduced are defined by

$$\rho^+ = \rho \left\{ 1 - \epsilon_s^2 k^2 \bar{x}^2 - \left(\frac{2T}{Y} \right) \left(\frac{w+t}{k^2 w t} \right) \right\}, \quad (237)$$

$$\begin{aligned}Y^+ &= Y \left\{ 1 - k^2 \bar{x}^2 (\epsilon_w^2 + \epsilon_s^2) + \bar{z}^2 \epsilon_s^2 \right. \\ &\quad \left. + \left(\frac{N}{Y} \right) \left[w(\epsilon_w^2 + \epsilon_s^2) + t \epsilon_s^2 \right] \right\},\end{aligned}\quad (238)$$

$$P^+ = YV' + \frac{F^+ \Delta}{t}, \quad (239)$$

$$\begin{aligned}F^+ &= \bar{f}_{31} \left\{ 1 + \epsilon_w + \bar{x}^2 (\epsilon_w C_{11}^{-1} + \epsilon_s C_{31}^{-1}) \right. \\ &\quad \left. \left(\rho \omega^2 - \frac{6N}{w} \right) + \bar{z}^2 \epsilon_t C_{21}^{-1} \left(\rho \omega^2 - \frac{6N}{t} \right) \right\},\end{aligned}\quad (240)$$

$$K^+ = K_{33} \left\{ 1 + \left(\frac{\bar{f}_{31}^2 C_{11}^{-1}}{K_{33}} \right) \left[1 + O(\bar{x}^2) \right] \right\} \simeq K, \quad (241)$$

$$k = \frac{\omega}{c}, \quad c = \left(\frac{Y}{\rho} \right)^{\frac{1}{2}}. \quad (242)$$

in which w and t are the width and thickness of the plate, and ρ^+ , etc., is the perturbed pa-

⁴ Throughout this section, "zero" means "contributes terms to $\delta J'$ of order \bar{x}^4 or higher."

parameter corresponding to q , etc. The quantity designated as $O(\bar{x}^2)$ in equation (241) is of no importance in ADP or RS, and is therefore not written out.

These equations define a boundary-value problem identical in structure with Mason's, the different physical results arising solely from the dependence of the quantities ρ^+ , Y^+ , F^+ , and K^+ on frequency, width, and thickness, and the stiffnesses T and N . This is a very convenient circumstance, since it allows the valuable concepts and results obtained by Mason to be taken over, merely applying a correction term here and there.

Concerning the confidence which should be placed in the validity of this treatment, the following remarks are pertinent:

1. The final results are consequences of well-known and accepted principles of physics together with a variational principle which has been shown to be an alternate expression of these principles.

2. The Mason theory, which has been the foundation of all design work, is contained in the final result as the special case in which the dimensionless quantities $k^2\bar{x}^2$, $k^2\bar{z}^2$, T/Yk^2t ,

and Nw/Y are negligibly small compared to 1.

3. By setting T/Yk^2t and Nw/Y to zero, but keeping the conservative \bar{x}^2 and \bar{z}^2 terms, the finite-width correction to the resonant frequency is correctly given, as will be shown in Chapter 3.

It is therefore believed that the foregoing results lay the basis for a much more detailed understanding of crystal transducers than is at present available. Before full use can be made of this new theory, a carefully planned program of experimental work to evaluate the parameters T and N , especially their imaginary (dissipative) parts, will be necessary; the pressure of work during World War II did not permit this.

However, some of the consequences of this theory can be discussed on the basis of available experimental data, and certain further conclusions can be tentatively reached concerning the qualitative character of dissipation. In Section 2.4, it was shown that the above boundary-value problem is representable by an equivalent circuit, and in Chapter 3 those aspects of the theory which are at present capable of experimental examination are discussed.

Chapter 3

PROPERTIES OF THE COMPONENT PARTS OF CRYSTAL TRANSDUCERS

By *Richard Bellman, T. Finley Burke, Glen D. Camp, Bourne G. Eaton, and Fred M. Uber*

IN THIS CHAPTER, an attempt is made to come to as thorough an understanding as possible of the properties of the component parts of crystal transducers, and to study the couplings introduced between these parts when they are assembled into a completed unit.

The first section begins with what one sees, a "black box" with a few feet of cable, and systematically dissects it, laying the parts aside for study in later sections. Wherever feasible, the qualitative properties of these parts will be briefly mentioned; also, an attempt is made to catalog the couplings between parts as they are separated. At the close of this section, one will have not only a collection of component parts requiring further study, but also a qualitative picture of the primary motivating element, the crystal, obscured by a number of electric and mechanical shunts. Each of these shunts is an obstacle to delivering power to, or collecting a signal from, the crystals.

The remaining sections of this chapter are devoted to a detailed study of the parts themselves.

3.1 DISSECTION OF A TRANSDUCER

3.1.1 Electronic System

Starting with a complete sonar system, we first detach the electronic system, leaving only the upper end of a cable of two or more conductors above water. The electronic system may be a simple driver (transmitter), a simple amplifier (receiver), or a much more complicated system for various special applications. Although not properly a part of the crystal transducer, it is extremely important that the electronic system and the transducer be properly matched. The design of electronic systems for use with crystal transducers is discussed later (see Chapter 5).

3.1.2

Cables

By removing the packing gland, the cable is disconnected from the transducer terminals. The cable is a three-conductor system, two leads surrounded by a shield. In all except extreme applications, the cable will be a very small fraction of an (electromagnetic) wavelength, and we can treat it as a simple six-terminal net-

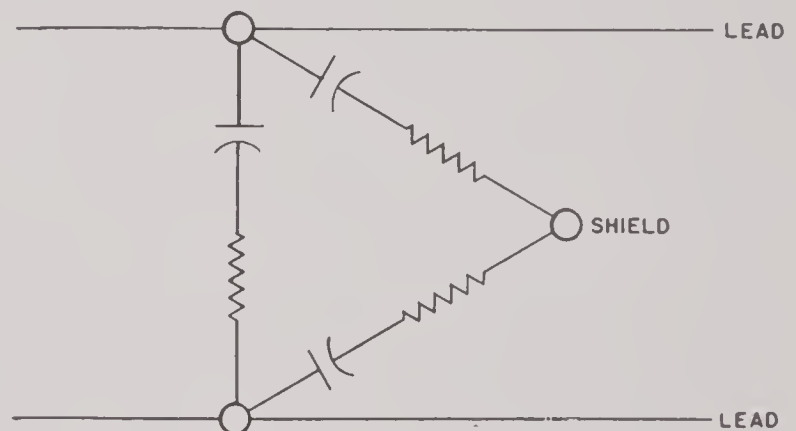


FIGURE 1. Approximate circuit for a shielded cable.

work. Neglecting small resistive drops in the leads themselves, we can reduce this network to the three-terminal network shown in Figure 1. Numerical data on the capacitances and dissipation factors for each of the elements are given later (see Chapter 5).

3.1.3

Matching Network

A crystal transducer having any appreciable dissipation or radiation resistance is capacitive at all frequencies, and therefore a coil can always be found which will make the impedance purely resistive at least at one frequency; because of the frequency dependence of the reactance, it is sometimes possible to tune a transducer at as many as three nearby frequencies. The coil is the simplest type of matching networks and in many respects is the best (see Chapter 5). In any event, the most complicated matching network is a four-terminal system

composed of inert elements, and its function is to perform an impedance transformation between the cable and what we shall refer to as the stripped transducer. The combination of cable and matching network is shown in Figure 2. The question mark indicates the necessity of

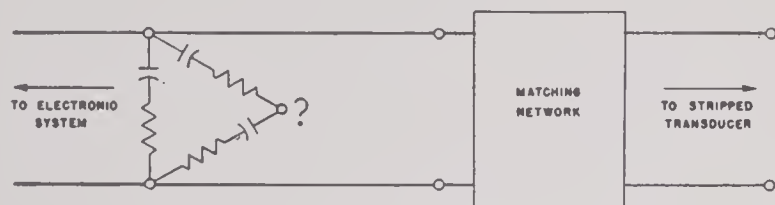


FIGURE 2. Cable and matching network.

making some definite disposition of the shield, the most usual disposition being to ground the upper end and leave the lower end disconnected.

3.1.4

Preamplifier

A small receiver has low capacitance and therefore high impedance, and the capacitive shunts between the leads and to the shield of the cable may appear essentially as a dead-short across the output terminals of the receiver. To circumvent this situation, a preamplifier is sometimes built into the case of the transducer. We shall regard everything between the cable leads and the leads to the crystal motor as a preamplifier, even though it may contain an inert matching network also. Then the most general preamplifier is an *active* four-terminal network whose function is both to perform an impedance transformation and to raise the level. The design of such systems is discussed later (see Chapter 5).

3.1.5

Cases

Depending on the detailed construction of the transducer, we now either remove a rubber sleeve or take off a rubber window molded into a metal ring, etc., remove^a the crystal motor, drain out any coupling fluid (e.g., castor oil),

^a Window-coupled units are an exception since the crystals are cemented to the inner face of the window.

and define everything left as the case, including the window or sleeve. The case serves a number of functions: it prevents the crystals and electric leads from getting wet, it protects the crystals from mechanical shock, and it serves as a means of support to the motor and other parts. It consists of a hollow shell, various supporting brackets, and cavities for containing matching networks and preamplifiers. Also, we shall include any materials such as Airfoam rubber or Corprene, used for acoustic isolation in the case. We must consider the case from two separate points of view, electric and acoustic.

The case is usually metal and is grounded by contact with sea water. We must therefore consider the capacitances of all terminals to the case, together with their associated dissipation factors. The magnitude of these effects depends upon the geometry and the materials which find themselves in electric fields, and in most well-designed transducers may be neglected; however, it is important to discuss them in order that this desirable end may be achieved.

In considering the elastic aspects of the case, we shall have to include any coupling fluid (e.g., castor oil). We must concern ourselves with cavity resonances within the oil, couplings from the motor to the case through various brackets and the oil, etc., and it is clear that the whole matter is extremely complicated. We have been unable to make any useful theoretical treatments of this problem, even of the crudest sort, to serve as a qualitative guide, and our results are fragmentary and primarily empirical.

The ideal solution would be to make all couplings zero, except that from the primary face of the motor to the water via the window. Two distinct attempts at this have been made; the window-coupled gas-filled unit, in which the crystals see negligible impedance except on their primary radiating faces which look into water through a window usually made of rubber; and the attempt to isolate acoustically all but the primary radiating faces of the crystal with Airfoam rubber, Corprene, etc.

Isolation of the secondary faces of the crystals is important for at least three reasons: (1) to reduce dissipation of energy, (2) to prevent "holes" in the response caused by excitation of parasitic modes, and (3) to reduce cross talk

if there are two motors in one case. No general solution of this problem has been found, but some instances are mentioned in Chapter 7.

3.1.6

Bare Motor

The bare motor consists of all the crystals together with any backing or fronting plates or bars to which they are attached. Electrically, it is a three-terminal network consisting of the two leads to the crystal and the backing plate, as shown in Figure 3. If the backing plate is glass or other nonconducting material, it is only a two-terminal network.

With respect to the motor, we are in a more favorable position than in studying cases: several theoretical problems have been roughly solved; all of these are, of course, idealized, but they furnish valuable guidance to experi-

isotropic elastic system and will possess a sharply defined spectrum of normal modes. If the geometry is sufficiently simple, we can calculate these normal modes with high precision and, in any event, we can map them and determine their resonant frequencies with the aid of the probe microphone (see Section 3.4).

3.1.8

Crystal Blocks

In the assembly of motors, blocks of two or more crystals are often used and it is therefore important to know to what extent the properties of such blocks differ from those of single crystals. In general, the results are just what would be expected; if the lateral dimensions of the assembled blocks are small compared to the longitudinal dimensions, the behavior closely follows that of a single crystal, assuming good cement joints. However, as soon as these dimensions approach equality with the longitudinal dimensions, undesired modes of motion begin to become important, and this sets an upper limit to the practical size of blocks.

3.1.9

Single Crystal Plates

We finally reach the primary active component of a transducer, the single crystal plate. This is susceptible to quite precise theoretical treatment and to detailed experimental examination (see Section 3.2).

3.1.10

Summary

The results of our dissection may now be summarized as follows: Electrically, a complete sonar system is represented as shown in Figure 4. The circle with a question mark indicates the necessity of making some definite disposal of the transducer end of the shield; the dotted line indicates the most usual disposition, which is to leave it free or, in other words, to connect it to ground through a very small capacitance. References are given to the quantitative discussions of each part of this circuit; for the present, we should merely observe that

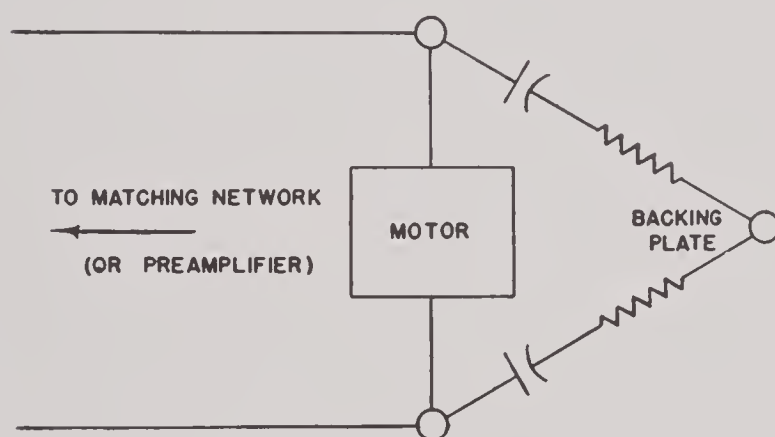


FIGURE 3. Circuit for bare motor.

mental investigation. Experimentally, we can make a very thorough examination of the motor, electrically with the three-terminal impedance bridge, and mechanically with the probe microphone (see Chapter 9). Results of these investigations are summarized later.

3.1.7

Backing Plates or Bars

We now begin a more detailed dissection, studying the parts of the bare motor itself; here we find systems of sufficient simplicity to enable quite accurate results to be obtained, both theoretically and experimentally. Whatever its shape, a backing plate or bar is a well-defined

the leads from the electronic system to the motor are shunted electrically in a number of ways.

It should be emphasized that this figure is a correct representation only of the electric circuit. The motor is connected mechanically to the case through its supports and any coupling fluid such as castor oil. If we knew how to replace Figure 4 by an *equivalent* circuit, these cou-

plings would appear as shunts across various elements in the more detailed equivalent circuit of the motor. In either case, the outgoing radiation is represented by the power consumed by a resistor inside the equivalent circuit of the motor, or, if the unit acts as a receiver, the incoming radiation is represented by a generator in series with the above resistor. We now see that this resistor or generator is shunted by a maze of electrical and mechanical impedances.

The balance of this chapter is devoted to a detailed study of the component parts qualitatively discussed above.

3.2

SINGLE CRYSTAL PLATES

The most thorough understanding of the properties of single crystal plates is not, by

itself, adequate for a satisfactory understanding of crystal transducers, because of the many other important effects; however, it is an essential first step.

In Chapter 2, the fundamental piezoelectric relations were derived and the boundary-value problem governing a loaded single rectangular crystal plate of finite width and thickness was solved to the next approximation beyond that

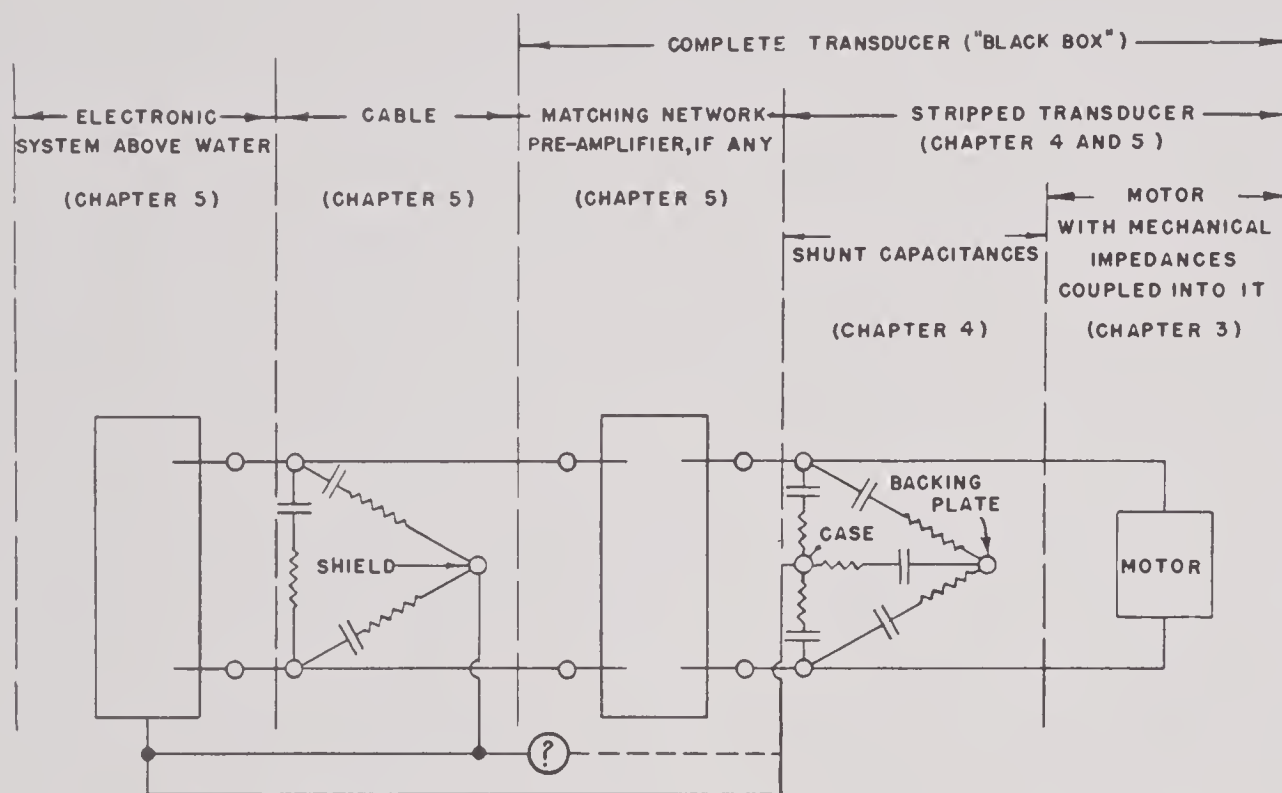


FIGURE 4. Electric circuit for a complete transducer, with references to discussions of various parts.

given by Mason,¹ by a semidirect variational method. The solution was left in the form of a one-dimensional boundary-value problem, identical in structure to Mason's, but having correction terms added to the various parameters.

In this section, the equivalent circuit corresponding to the solution of this perturbed boundary-value problem is deduced, some features of this circuit are analyzed, and the crystal constants significant to transducer design are evaluated. These constants are evaluated by experiments intimately related to the manner in which crystals are used in transducers, whereas some of the constants appearing in the literature depend upon a correct theoretical understanding of high-order shear modes; in view of the complicated motions which are possible at high frequency, as shown by the silicon carbide dust pictures in Figure 13 of Section 2.5.3,

the utmost caution is necessary in interpreting measurements on the higher modes. A secondary advantage of the procedure here used to evaluate the constants, from the limited viewpoint of this volume, is that one does not need to bother with a large number of constants which are of negligible importance in transducer design.

3.2.1 Equivalent Circuit of a Loaded Rectangular Crystal

In Chapter 2, it was shown that the motion of a rectangular plate of Rochelle salt [RS] or ammonium dihydrogen phosphate [ADP] is governed, to the next approximation beyond that given by Mason, by the one-dimensional boundary-value problem defined by equations (233), (234), (235), and (236) of that chapter.

The solution of this boundary-value problem, with the two ends at $y = 0$ and $y = L$, is

$$V = V_1 \cos k^+ y + \frac{(V_2 - V_1 \cos k^+ L) \sin k^+ y}{\sin k^+ L}, \quad (1)$$

$$k^+ = \left(\frac{\rho^+ \omega^2}{Y^+} \right)^{\frac{1}{2}} \\ = k \left\{ 1 + \frac{k^2(\epsilon_w^2 \bar{x}^2 + \epsilon_t^2 \bar{z}^2)}{2} - \left(\frac{T}{Y} \right) \frac{(w+t)}{k^2 wt} \right. \\ \left. - \left(\frac{N}{4Y} \right) \left[w(\epsilon_w^2 + \epsilon_s^2) + t\epsilon_t^2 \right] \right\}, \quad (2)$$

$$k = \frac{\omega}{c}, \quad c = \left(\frac{Y}{\rho} \right)^{\frac{1}{2}}. \quad (3)$$

The boundary values V_1 and V_2 of equation (1) are determined by the boundary conditions equations (234) and (235) of Chapter 2; and the charge q on the positive electrode is obtained by integrating the charge density, equation (236). One thus has three linear equations from which q , V_1 , and V_2 can be determined if the potential difference Δ is known,

$$Y^+ k^+ (-V_1 \csc \theta^+ + V_2 \cot \theta^+) + N_2 V_2 \\ = -\frac{F^+ \Delta}{t}, \quad (4)$$

$$Y^+ k^+ (-V_1 \cot \theta^+ + V_2 \csc \theta^+) - N_1 V_1 \\ = -\frac{F^+ \Delta}{t}, \quad (5)$$

$$q = C^+ \Delta - F^+ w (V_2 - V_1), \quad (6)$$

$$\theta^+ = k^+ L, \quad C^+ = \frac{K^+ w L}{4\pi t} \simeq \frac{K w L}{4\pi t} = C. \quad (7)$$

These equations are now transformed as follows: the displacements are replaced by velocities, according to $I = \dot{q} = i\omega q$, etc.; the stiffnesses are replaced by the corresponding impedances, according to $N_2 = i\omega z_2$, etc.; and fictitious electric currents I_1 and I_2 are introduced, proportional to the outward velocity of each end of the crystal,

$$I_1 = \phi^+ (-\dot{V}_1), \quad I_2 = \phi^+ \dot{V}_2, \quad (8)$$

$$\phi^+ = -F^+ w. \quad (9)$$

Finally, multiplying equations (4) and (5) by the radiation area wt and dividing by ϕ^+ , equations (4), (5), and (6) become

$$\left(\frac{Z_c^+}{i} \right) (I_1 \csc \theta^+ + I_2 \cot \theta^+) + Z_2^+ I_2 = \Delta, \quad (4')$$

$$\left(\frac{Z_c^+}{i} \right) (I_1 \cot \theta^+ + I_2 \csc \theta^+) + Z_1^+ I_1 = \Delta, \quad (5')$$

$$\frac{(I - I_1 - I_2)}{i\omega C} = \Delta, \quad (6')$$

$$Z_c^+ = \left(\frac{Y^+ k^+}{\omega} \right) \left(\frac{wt}{\phi^{+2}} \right) = z_c^+ \left(\frac{wt}{\phi^{+2}} \right), \quad (10)$$

$$(Z_1^+, Z_2^+) = (z_1, z_2) \left(\frac{wt}{\phi^{+2}} \right). \quad (11)$$

Large Z , with various subscripts, is here used for equivalent electric impedances, and small z for *specific* acoustic impedances. The factor wt/ϕ^{+2} converts a specific acoustic impedance to an electric impedance. The characteristic impedance of the crystal is

$$z_c^+ = \left(\frac{Y^+ k^+}{\omega} \right), \\ = \rho c \left\{ 1 - k^2 \left[\left(\epsilon_w^2 + 2\epsilon_s^2 \right) \bar{x}^2 + \epsilon_t^2 \bar{z}^2 \right] \right. \\ \left. - \left(\frac{T}{Y} \right) \frac{(w+t)}{k^2 wt} \right. \\ \left. + \left(\frac{N}{4Y} \right) \left[w(\epsilon_w^2 + \epsilon_s^2) + t\epsilon_t^2 \right] \right\}. \quad (12)$$

It is now readily verified that equations (4'), (5'), and (6') are the Maxwell equations for the three-mesh equivalent circuit shown in Figure 5. Furthermore, this circuit is identical in structure to the Mason equivalent circuit, and the parameters differ only by correction terms

which, although small, are of great practical importance.

It should be noted that by shorting the condenser in Figure 5, and using the proper parameters, one has the equivalent circuit for a

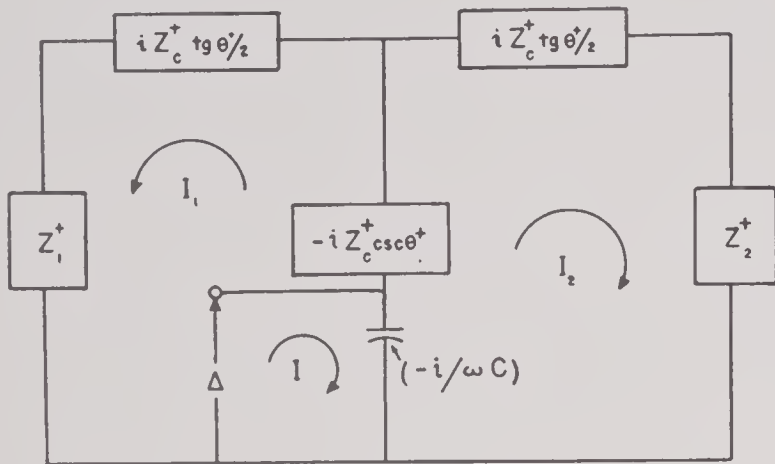


FIGURE 5. Equivalent circuit for a loaded rectangular crystal plate, to the next approximation beyond that given by Mason.

nonpiezoelectric plate, e.g., a backing rod. If the rod is driven by a force at either end, this force goes in series with Z_1^+ or Z_2^+ .

3.2.2 Equivalent Circuit in Two Cases

DEFINITIONS

There are two special cases which are extremely important, first, because they closely approximate the actual situation in three important classes of transducers (backing plate; inertia drive and symmetrical drive), and second, because they are important in the experimental determination of crystal constants, the impedance of cemented joints, etc. These are defined as follows:

Case I. Approximate Block. One of the terminating impedances (Z_1^+) is large while the other (Z_2^+) is small. A more precise meaning is given to "large" and "small" in the analysis which follows; for the present, it may be remarked that this condition is very well approximated over the practical operating band if one end of the crystal is cemented, by a good joint, to an approximately quarter-wave backing plate or bar, and the other looks into water or a lower impedance. Examples are University of California Division of War Research [UCDWR] types CQ, JB, GA, etc.

Case II. Approximate Free-Free. Both terminating impedances are "small." This condition is closely approximated in transducers of two classes: the inertia drive and the symmetrical drive.

MECHANICAL ARM

The series equivalent of the two parallel arms is

$$\frac{\left(iZ_c^+ \tan \frac{\theta^+}{2} + Z_1^+\right)\left(iZ_c^+ \tan \frac{\theta^+}{2} + Z_2^+\right)}{\left(2iZ_c^+ \tan \frac{\theta^+}{2} + Z_1^+ + Z_2^+\right)} \quad (13)$$

Making the above approximations, one has for series equivalent of the two parallel arms

$$\text{Case I: } (t + Z_2^+) - \frac{(t + Z_2^+)^2}{Z_1^+} \quad (14)$$

if $|t|, |Z_2^+| \ll |Z_1^+|$,

$$\text{Case II: } \frac{1}{2}t + \frac{1}{4}(Z_1^+ + Z_2^+) \quad (15)$$

if $|Z_1^+|, |Z_2^+| \ll |t|$,

in which t is used as a temporary abbreviation for $iZ_c^+ \tan (\theta^+/2)$.

Combining this with the $\csc \theta^+$ term, one has the circuit shown in Figure 6, which has only one mechanical arm. The values of the impedance of the mechanical arm in the two cases, together with two trigonometric identities used to obtain these results, are

$$\begin{aligned} -\csc \theta^+ + \tan \frac{\theta^+}{2} &= -\cot \theta^+, \\ -\csc \theta^+ + \frac{1}{2} \tan \frac{\theta^+}{2} &= -\frac{1}{2} \cot \frac{\theta^+}{2}, \end{aligned}$$

$$\text{Case I: } Z_b^+ = -iZ_c^+ \cot \theta^+ + Z_2^+ - \frac{(iZ_c^+ \tan \frac{\theta^+}{2} + Z_2^+)^2}{Z_1^+}, \quad (16)$$

$$\text{Case II: } Z_f^+ = -\frac{1}{2}iZ_c^+ \cot \frac{\theta^+}{2} + \frac{1}{4}(Z_1^+ + Z_2^+). \quad (17)$$

These approximations are valid if the inequalities of equations (14) and (15) are satisfied; therefore, to determine the significance of these inequalities, we need to find the order of magnitude of $Z_c^+ \tan (\theta^+/2)$ over the practical operating band, in each of the two cases. For the purposes of this rough estimate, it is permis-

sible to ignore the imaginary part of θ^+ , which is small; whereupon the mechanical or constant-voltage resonance (frequency of minimum impedance of the mechanical arm) occurs near $\theta = \pi/2, 3\pi/2$, etc. in Case I and near $\theta = \pi, 3\pi$, etc., in Case II. These values make $\tan \theta^+/2 = 1$ in Case I and infinity in Case II, both results being favorable to satisfying the inequalities. Thus, *very near* to the respective

valid and, with them, the approximate impedances given in equations (16) and (17), if

$$\text{Case I: } |Z_c^+|, |Z_2^+| \ll |Z_1^+|, \quad (14')$$

$$\text{Case II: } |Z_1^+|, |Z_2^+| \ll |Z_c^+|. \quad (15')$$

A more careful analysis shows that these conditions are also sufficient for the validity of the above approximations at the higher resonances; for, although the band width of validity decreases as we go to higher resonances, the band width of practical operation also decreases.

The characteristic impedances of water or rubber, ADP or RS crystals, and steel are approximately in the ratio 1 to 4 to 26. Hence, we see that in Case I, even an eighth-wave steel backing bar or plate is such an excellent block that we make negligible error by dropping even the first-order correction term in equation (16), *provided the cemented joint has a high impedance*. Conversely, this correction term can be used to evaluate the impedance of cemented joints by observing the discrepancy between the resonance frequency and that for a perfect clamp (see Section 3.3); in this case, the other end of the crystal is made to look into air ($Z_2^+ = 0$), and the numerator of the correction term, evaluated at resonance, becomes simply $-Z_c^{+2}$. In Case II, if Z_1^+ and Z_2^+ are the impedances of water, then the inequality equation (15') is well satisfied so long as we save the first-order correction term $1/4 (Z_1^+ + Z_2^+)$.

RESISTANCE AND REACTANCE

We can now reach suggestive tentative conclusions concerning the internal dissipation, since this can be evaluated except for two (frequency-dependent) parameters, the imaginary parts of T and N ; this leaves us in ignorance of the magnitude of the effect and how this varies with frequency, but enables us to determine its dependence on other quantities.

The internal dissipation resistance is the real part of the cotangent terms in equations (16) and (17). Both Z_c^+ and θ^+ have small imaginary parts which are readily separated by using the addition theorem for the cotangent. Since the imaginary parts of Z_c^+ and θ^+ are both small, we see that they contribute only a second-order correction to the intrinsic reactance;

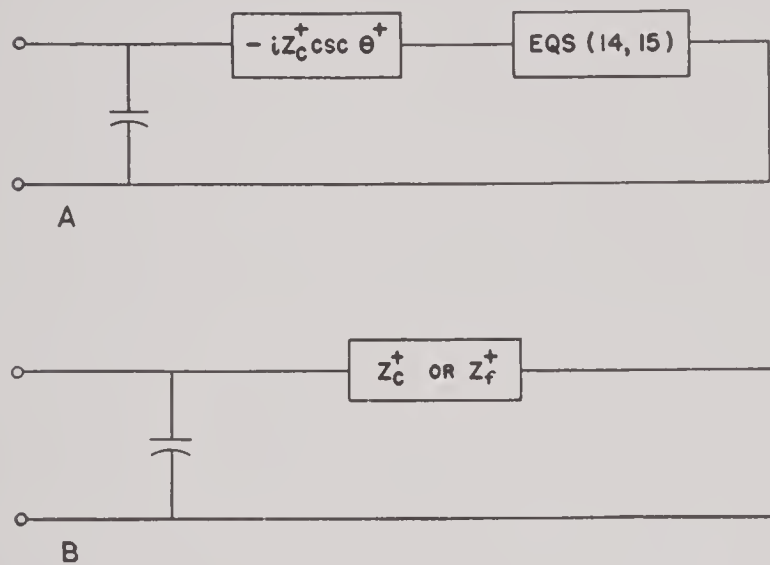


FIGURE 6. Equivalent circuit for Cases I and II. A. Circuit with cosecant term separated out. B. Circuit with cosecant term combined as given by equations (16) and (17).

resonances, the inequality for Case I requires that $|Z_c^+|$ and $|Z_2^+|$ be small compared to $|Z_1^+|$, while that for Case II is satisfied by any finite Z_1^+ and Z_2^+ .

However, we need to know the conditions for validity of these inequalities over the practical operating band, which is determined largely by the Q of the mechanical arm. First, consider only the lowest resonance in each case. Then, in Case I the inequality will be improved by going to lower frequency; going to higher frequency, $\tan (\theta^+/2)$ will have become only 2.4 at a frequency 1.5 times resonance, which is much wider than the band width determined by the Q of the mechanical arm (see Section 3.2.2, Constant-Voltage Band Width). Turning to Case II, we see that if the frequency is as low as 0.5, or as large as 1.5, times the resonant value, then $\tan (\theta^+/2)$ will have fallen only to unity.

Thus, in a band centered at the respective first resonances and wider than the practical operating band, the above inequalities will be

since other second-order terms have been dropped, this one must also be dropped to obtain a consistent approximation and hence the intrinsic reactance is obtained by replacing Z_c^+ and θ^+ by their real parts in the two cotangent terms. The intrinsic resistance, however, gets a first-order term from both Z_c^+ and θ^+ . The $1/Z_1^+$ term in Case I is also dropped, since this term is needed in only two instances: (1) the cement joint does not have high impedance, a situation which can and should be avoided by good technique (see Section 3.3), or (2) to evaluate the impedance of cemented joints, in which case precautions are taken to make T and N negligibly small.

The impedances given by equations (16) and (17), with the intrinsic terms separated into their reactive and resistive parts and the $1/Z_1^+$ term dropped, then become

Case I:

$$Z_b^+ = -i(\Re Z_c^+) \cot(\Re \theta^+) + R_b^+ + Z_2^+. \quad (16')$$

Case II:

$$Z_f^+ = -\frac{1}{2}i(\Re Z_c^+) \cot\left(\frac{\Re \theta^+}{2}\right) + R_f^+ + \frac{(Z_1^+ + Z_2^+)}{4}, \quad (17')$$

$$R_b^+ = R_T^+ \csc^2(\Re \theta^+) + R_N^+ G_N(\Re \theta^+), \quad (18)$$

$$R_f^+ = \frac{1}{4}R_T^+ \csc^2\left(\frac{\Re \theta^+}{2}\right) + R_N^+ G_N\left(\frac{\Re \theta^+}{2}\right), \quad (19)$$

$$R_T^+ = \left(\frac{\Im T}{\omega}\right) (r_w^{-1} + r_t^{-1}) \left(\frac{wt}{\phi^{+2}}\right), \quad (20)$$

$$R_N^+ = \left[\left(\frac{\Im N}{\omega}\right) r_w(\epsilon_w^2 + \epsilon_s^2) + r_t \epsilon_t^2\right] \left(\frac{wt}{\phi^{+2}}\right), \quad (21)$$

$$G_N(\alpha) = \left(\frac{\alpha}{2}\right)^2 \csc^2 \alpha + \left(\frac{\alpha}{2}\right) \cot \alpha, \quad (22)$$

in which \Re denotes the real, \Im the imaginary, part of the indicated quantity. The sign (+) on the resistances R_N^+ and R_T^+ arises solely from the occurrence of the factor (wt/ϕ^{+2}) which converts mechanical impedance to equivalent electric impedance.

It is readily shown that the squared cosecant and G_N functions vary negligibly over the practical operating bands, whether these are centered at the first or higher resonances, and

hence equations (18) and (19) may be evaluated at resonances for all practical purposes,

$$R_b^+ = R_T^+ + n^2\left(\frac{\pi}{4}\right)^2 R_N^+, \quad (18')$$

$$R_f^+ = \frac{R_T^+}{4} + n^2\left(\frac{\pi}{4}\right)^2 R_N^+. \quad (19')$$

Even without knowing the values of $\Im T$ and $\Im N$, some interesting tentative conclusions can be reached by studying equations (18') and (19'). First, let us see if they make reasonable predictions in instances where the results can be checked by simple considerations.

A symmetrically loaded crystal may be regarded as two approximately blocked crystals in parallel, since each half acts as a quarter-wave backing bar for the other half. An inertia drive can be similarly regarded, except that the radiation resistance is halved. Therefore, the predicted ratio of loss to radiation resistance for a blocked and a symmetrically loaded crystal should be the same, and an inertia drive should be half this. In verifying this, one must notice that the shape factors, based on actual dimensions, will be twice as great in the blocked as in the symmetrically loaded or inertia drive case; thus the dependence of R_T^+ and R_N^+ on these shape factors must be taken into account. We therefore have for the ratio of loss to useful resistance,

blocked:

$$\frac{(R_{Tb} + n^2\left(\frac{\pi}{4}\right)^2 R_{Nb})}{R_2}, \quad (23)$$

symmetrically loaded:

$$\frac{\left[\frac{2R_{Tb}}{4} + n^2\left(\frac{\pi}{4}\right)^2 \frac{R_{Nb}}{2}\right]}{\left(\frac{R_2}{2}\right)} = \text{Equation (23)}, \quad (24)$$

inertia drive:

$$\frac{\left[\frac{2R_{Tb}}{4} + n^2\left(\frac{\pi}{4}\right)^2 \frac{R_{Nb}}{2}\right]}{\left(\frac{R_2}{4}\right)} = \text{Twice equation (23)}, \quad (25)$$

and we see from equations (23), (24), and (25) that the theory gives sensible results in this case. The signs (+) have been dropped in equations (23), (24), and (25), since in form-

ing the ratios, the transformation factor (wt/ϕ^{+2}) falls out and one is left with the corresponding ratios of mechanical resistances.

Next, consider the dependence upon n . For any one type of drive, consider the problem of radiating energy at a *given* frequency, so that T and N will be unchanged, but comparing the efficiency of doing this with the first ($n = 1$) and the second ($n = 3$) resonances. Keeping the frequency constant will require that the crystals working at their second resonance be about one-third as long as those working at their first resonance; however, this reduction will alter the radiating area in the same proportion as the lateral area, and hence we conclude, from equations (18') and (19'), that the ratio of tangential loss to useful radiation will be the same for $n = 3$ as for $n = 1$, while the ratio of normal loss to useful radiation will be about nine times as great.

This is physically reasonable, and hence gives further confidence in the essential correctness of the variational treatment, as may be seen as follows: Consider first the normal loss. The dimensionless Poisson "breathing" ratios are easily shown to be $(w/L)\varepsilon_{\mu}\theta^{+}$ and $(t/L)\varepsilon_{\mu}\theta^{+}$, constant except for the factor θ^{+} . Hence, the loss must go up like θ^{+2} , that is, like n^2 . One might, of course, try to terminate the lateral faces with an N so small as to make this loss still negligible, but certainly there is nothing gained, from the viewpoint of efficiency, in using higher resonances.

The tangential motion, although more complicated the higher the resonance used, depends on the average value of $\sin^2 (\Re\theta^{+})$, always over an integer number of quarter cycles, and hence should be independent of n , as it is from the theory.

With regard to the dependence of R_T^{+} and R_N^{+} , that is $\Im T$ and $\Im N$, on frequency, and arrangement of crystals and other obstacles inside a transducer, only some qualitative conjectures can at present be made, since there is very little experimental data available and the problem is too complicated to obtain a reliable theoretical estimate.

The tangential impedance arises from the generation of viscous shear waves and these have an extremely short wavelength and are

absorbed in a very short distance (of the order of a fraction of a millimeter in castor oil at room temperature). Accordingly, we may expect to get some very reliable estimates by considering an infinite plane vibrating tangentially and looking into a fixed plane at distance D . This situation is discussed in Section 2.1.8 and one concludes that if D is greater than about one millimeter, the effect is probably unimportant, but that it may become extremely important if crystals with relative tangential motion are separated by a smaller distance. An isolated but very impressive experimental result supports this viewpoint in the case of a modified UCDWR-type CY4 transducer.^b The tangential impedance T is independent of frequency for small D and varies as $\omega^{1/2}$ for large D . This latter function of ω changes by less than 10 per cent over the practical operating band, and hence we conclude that the frequency dependence of R_T^{+} is probably not very important. However, the temperature dependence of R_T^{+} would be expected to be strong, since it is proportional to the square root of the viscosity for large D and to the viscosity itself for small D .

The variation of R_N^{+} is much more difficult to estimate. It presumably depends upon the standing-wave pattern established inside a transducer, which can vary with extreme rapidity as the frequency varies, together with the dissipation mechanisms which absorb energy from these standing waves. A very crude semiquantitative discussion of this very complicated problem is given elsewhere,² but it is doubtful that one will come to any practically useful conclusions in this matter without further experimental study.

MECHANICAL RESONANCE AND ANTIRESONANCE

The mechanical resonance frequencies for the two cases can be estimated as follows. Assuming that Z_2^{+} in Case I, and both Z_1^{+} and Z_2^{+} in Case II, are purely resistive, the resonant frequencies are given by

$$\text{Case I:} \quad \Re\theta^{+} = \frac{n\pi}{2}, \quad (26)$$

$$\text{Case II:} \quad \Re\theta^{+} = n\pi, \quad (27)$$

in which $n = 1, 3, 5$, etc., for the first, second,

^b See Section 7.4.

third, etc., resonance in both cases. Now, neglecting any reactive part in T and N , one has

$$\begin{aligned}\Re\theta^+ &= kL \left[1 + \frac{k^2(\epsilon_u^2 \bar{x}^2 + \epsilon_t^2 \bar{z}^2)}{2} \right], \\ &= kL \left[1 + \left(\frac{k^2 L^2}{24} \right) (\epsilon_u^2 r_w^2 + \epsilon_t^2 r_l^2) \right],\end{aligned}\quad (28)$$

in which r_w and r_l are the ratios of width to length and of thickness to length, respectively. Putting the 0th approximation for kL into the correction term, and inverting, one has a generalization, to the anisotropic case, of the Rayleigh frequency formula

Case I:

$$f_r L = n \left(\frac{c}{4} \right) \left[1 - \left(\frac{n^2 \pi^2}{96} \right) (\epsilon_u^2 r_w^2 + \epsilon_t^2 r_l^2) \right], \quad (29)$$

Case II:

$$f_r L = n \left(\frac{c}{2} \right) \left[1 - \left(\frac{n^2 \pi^2}{24} \right) (\epsilon_u^2 r_w^2 + \epsilon_t^2 r_l^2) \right], \quad (30)$$

in which the relation $k = 2\pi f/c$ has been used. It should be noticed that equation (29) can be deduced from equation (30) by thinking of the blocked crystal as a free-free crystal of twice the length; then this equation reads

Case I:

$$f_r(2L) = n \left(\frac{c}{2} \right) \left\{ 1 - \left(\frac{n^2 \pi^2}{24} \right) \left[\epsilon_u^2 \left(\frac{w}{2L} \right)^2 + \epsilon_t^2 \left(\frac{t}{2L} \right)^2 \right] \right\}. \quad (29')$$

It is seen that the effect of the lateral inertia correction increases with increasing n , in such a way that the successive resonances fall farther and farther below the simple 1, 3, 5, etc., ratios predicted without this term. Quantitative verification of this is given in the next section.

The mechanical antiresonant frequencies are given by equations (29) and (30) by setting $n = 0, 2, 4$, etc. These are extremely difficult to observe in the laboratory since the condenser is shunted by a very high mechanical impedance: one needs a very delicate probe microphone; however, they are readily observed in the responses of complete transducers (see Chapter 4).

It is scarcely necessary to emphasize that these equations are valid only if the diminuend

in the correction bracket is small compared to 1; however, this covers all practical cases.

These equations are used in the next section to determine the crystal constants c , ϵ_u , and ϵ_t ; from the first of these and the density, one obtains the characteristic impedance for a narrow and thin plate.

CONSTANT-VOLTAGE BAND WIDTH

The band width for *constant-voltage drive* can now be estimated from equations (16') and (17'); this is an important design parameter, but it should be emphasized that it is not the actual band width realized in practical transducers, since this latter depends upon the matching network and amplifier used. In accordance with general usage, the *half-width* is defined as the change in frequency δf required to reduce the power dissipated in the radiation resistance to *half* its resonance value, and the band width is twice this quantity. In this calculation, it is assumed that the radiation impedances [Z_2^+ in Case I, $\frac{1}{4}(Z_1^+ + Z_2^+)$ in Case II] are purely resistive, an assumption which is justified by observing that any reactive part, if varying slowly, can be combined with the intrinsic reactance, the primary effect being to shift the resonance frequency slightly.

The half-breadth in $\Re\theta^+$ is first calculated from equation (16') and (17'). For this purpose, it should be noticed that Z_c^+ depends upon $\Re\theta^+$ only in its correction term, and this latter is therefore evaluated at resonance. Furthermore, one keeps only the first-order departure of the reactance from its zero value at resonance, verifying the validity of this and the previous approximation a posteriori. The half-breadth in $\Re\theta^+$ is then determined by the condition that the reactance is equal to the resistance,

Case I:

$$(\Re Z_c^+ \csc^2 \Re\theta^+)_r \delta \Re\theta^+ = R_b^+ + R_2^+, \quad (31)$$

Case II:

$$\frac{1}{4} \Re Z_c^+ \csc^2 \left(\frac{\Re\theta^+}{2} \right)_r \delta \Re\theta^+ = \frac{1}{2} R_f^+ + \frac{1}{4} (R_1^+ + R_2^+). \quad (32)$$

Now $(\delta \Re\theta^+ / \Re\theta^+)_r = \delta f / f_r$ since the correc-

tion factors to $\Re\theta^+$, evaluated at resonance, cancel. Therefore

Case I:

$$\left(\frac{2\delta f}{f_r}\right) = \left(\frac{1}{Q_M}\right) = \left(\frac{4}{n\pi}\right) \frac{(R_b^+ + R_2^+)}{(\Re Z_c^+)_r}, \quad (33)$$

Case II:

$$\begin{aligned} \frac{(2\delta f)}{f_r} &= \left(\frac{1}{Q_M}\right) \\ &= \left(\frac{4}{n\pi}\right) \frac{\left[R_f^+ + \frac{(R_1^+ + R_2^+)}{2}\right]}{(\Re Z_c^+)_r}. \end{aligned} \quad (34)$$

In the above ratios of equivalent electrical quantities, the conversion factor wt/ϕ^{+2} cancels out, leaving the ratio of mechanical quantities; however, the dependence of Z_c^+ on width remains, and increases the band width somewhat.

From equations (33) and (34) one sees that a blocked and symmetrically loaded crystal has the same fractional band width, about one-third for a high-efficiency unit, increasing with internal losses; an inertia drive crystal ($R_1^+ = 0$) has about half this fractional band width, also increasing with losses. The corresponding mechanical Q 's are 3 or less and 6 or less, respectively. One other important conclusion is that the fractional band width decreases as the order of the resonance increases, being only about one-third as large at the second resonance as at the first, etc. This result is readily observable, and for most applications is a serious objection to using higher resonances.

ELECTRICAL ANTIRESONANCE; TRANSFORMATION RATIO

Referring to Figure 6, one sees that at some frequency above the mechanical resonance, the mechanical arm will become inductive by an amount sufficient to form a resonant loop with the condenser. At this frequency, f_a , the total series equivalent impedance seen at the electric terminals will be large (infinite in a lossless system), so that this loop resonance will appear at the electric terminals as an electric antiresonance.

This effect is considerably obscured if there is a resistance as large as that corresponding to the crystal working into water, but in an efficient transducer will appear as a wiggle in

the series equivalent reactance (see Section 3.2.2). For a free-free crystal in air, the effect is very marked, and the observed difference between the mechanical resonance and the electric antiresonance enables the transformation ratio between electric and acoustic impedances, ϕ^{+2} , and hence the piezoelectric constant F^+ , to be determined. Only this case will be discussed here.

The total admittance of the free-free crystal in air, in which case Z_c^+ and θ^+ are real, is

$$i\omega C + \left(\frac{2i}{Z_c^+}\right) \tan \frac{\theta^+}{2}, \quad (35)$$

and this is zero at the electric antiresonance. Evaluating all quantities in equation (35) at resonance, except the rapidly varying tangent term, one has

$$\omega_r C - \frac{4}{(Z_c^+)_r (\theta_a^+ - \theta_r^+)} = 0, \quad (36)$$

$$\frac{(\theta_a^+ - \theta_r^+)}{\theta_r^+} = \frac{(f_a - f_r)}{f_r} = \frac{4}{(\omega Z_c^+)_r C n \pi}, \quad (37)$$

$$\begin{aligned} (f_a - f_r)L &= \frac{2L(\phi^{+2})_r}{n\pi^2 C wt(z_c^+)_r} \\ &= \frac{8(F^{+2})_r}{n\pi K(z_c^+)_r}. \end{aligned} \quad (38)$$

The quantities $(F^{+2})_r$ and $(Z_c^+)_r$ depend upon n and the shape factors w/L and (t/L) . Neglecting this variation for the moment, that is, considering only very narrow crystals, we see that the theory predicts that the product $(f_a - f_r)L$ for any fixed n will be constant for crystals of all lengths, and that its values for the successive antiresonances are in the ratio 1, $1/3$, $1/5$, etc.

These and the more general predictions of equation (38) are compared with experiment in Section 3.2.3, where some but not all these predictions are verified. The discrepancy occurs primarily in the predictions at the higher antiresonances and since, as has previously been remarked, there are several reasons why it is unsatisfactory to operate a transducer very far from its first resonance, it is believed that this failure of the theory is not important from the viewpoint of this volume. A possible explanation of this partial failure of the theory, in the face of its close agreement with more signifi-

cant experimental results, is offered in Section 3.2.3.

LOW-FREQUENCY LIMIT

At a sufficiently low frequency, a crystal becomes stiffness controlled. This limiting case is the basis of the experimental determination of the dielectric constant K_{33} and also shows very simply why the open-circuit response of a hydrophone approaches a constant as the frequency is reduced.

In this limit, far below resonance, the reactances become so large that all resistances may be neglected. A further simplification is that the finite width corrections become negligible, so that θ^+ becomes simply $\omega L/c$; all signs (+) may therefore be dropped, i.e., the Mason approximation is valid.

The radiation reactances, Z_2 in Case I, Z_1 and Z_2 in Case II, also become negligible, even in comparison with the $\tan (\theta/2)$ terms, as will now be shown. The $\tan (\theta/2)$ term becomes approximately

$$i\rho c\left(\frac{\theta}{2}\right)\left(\frac{\omega t}{\phi^2}\right) = i\left(\frac{\rho L}{2}\right)\omega\left(\frac{\omega t}{\phi^2}\right), \quad (39)$$

which is the reactance of the mass of half the crystal. The radiation reactance is roughly that of the mass of a parallelepiped constructed on the radiating face and extending outward a distance of the order of the smaller of the two dimensions of this face t . The volume of this parallelepiped is ωt^2 , and hence the radiation reactance is smaller than that arising from the mass of the crystal by a factor of order t/L . The radiation resistance is smaller by another factor of order (t/L) .

In spite of the stiffness of the whole crystal, there is still a definite meaning attached to blocking one end, Case I: the number 1 end is blocked if I_1 is small, compared to I_2 . If Z_1 arises from a backing bar of length L_b , then its reactance is approximately $i\rho_b L_b \omega (\omega t/\phi^2)$, and the ratio of the currents is

$$\frac{I_1}{I_2} \simeq \frac{\left(\frac{\rho L}{2}\right)}{\left(\rho_b L_b + \frac{\rho L}{2}\right)} \simeq \left(\frac{\rho}{\rho_b}\right)\left(\frac{L}{2L_b}\right). \quad (40)$$

Since the density of backing material, usually steel, is greater than that of the crystal, any

ordinary backing plate will make the above ratio small compared to 1; this is the definition of Case I. In Case II, since both Z_1 and Z_2 are negligible compared to the $\tan (\theta/2)$ terms, this current ratio is 1.

We therefore have the cosecant stiffness term in series with (Case I) $iZ_c \tan (\theta/2)$ or (Case II) $(i/2)Z_c \tan (\theta/2)$. The impedances of these combinations are

Case I:

$$-iZ_c \cot \theta = \left(\frac{-iZ_c}{\theta}\right)\left(1 - \frac{\theta^2}{3} + \cdots\right), \quad (41)$$

Case II:

$$-\left(\frac{iZ_c}{2}\right)\cot \frac{\theta}{2} = \left(\frac{-iZ_c}{\theta}\right)\left(1 - \frac{\theta^2}{12} + \cdots\right). \quad (42)$$

At sufficiently low frequency these differ negligibly, and in the limit the mechanical arm be-

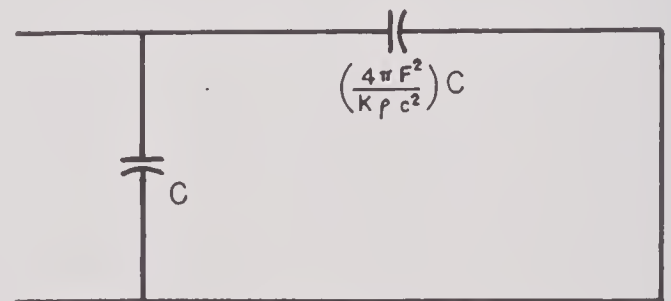


FIGURE 7. Equivalent circuit for Cases I and II, in the low-frequency limit.

comes a constant condenser of capacitance $(L/cZ_c) = (4\pi F^2/\rho c^2)(\omega L/4\pi t)$ in both cases, so that the effect is to increase the purely electric dielectric constant by $(4\pi F^2/\rho c^2)$. The circuit is shown in Figure 7.

The fractional error in the reactance of the mechanical arm is of order $\theta^2/3$ and $(\theta/2)^2/3$ in Cases I and II, respectively, and since the resonance frequency corresponds to $\theta = \pi/2$ and $\theta = \pi$, respectively, we see that the percentage error is the same in the two cases at any given fraction of the respective resonance frequencies. This error is about 20 per cent at half, and less than 1 per cent at one-tenth, of the resonance frequency. The error in the series-equivalent reactance is considerably smaller, since the mechanical condenser is much smaller than the electrical.

The ratio of the mechanical to the electrical condenser, for Case I, is

$$\left(\frac{L}{cZ_cC}\right)\left(1 + \frac{\theta^2}{3} + \dots\right) \simeq \left(\frac{4\pi F^2}{K\rho c^2}\right)\left[1 + \left(\frac{\pi^2}{12}\right)\left(\frac{f}{f_r}\right)^2 + \dots\right], \quad (43)$$

and the right member of equation (43) is also valid for Case II, since it is expressed in terms of the ratio of the actual to the resonant frequency. The dimensionless crystal constant $4\pi F^2/K\rho c^2$ is shown in Section 3.2.3 to be of the order of a tenth for both RS and ADP, and hence a small correction must be applied to capacitance measurements even at very low frequencies to get the blocked dielectric constant. This dielectric constant is evaluated in Section 3.2.3.

The equivalent circuit of a hydrophone, in the low-frequency limit, is obtained from Figure 7 by inserting a generator in the mechanical arm. The open-circuit emf of this generator is proportional to the pressure amplitude of the incident sound wave and, in the low-frequency limit, its internal impedance is negligible. The circuit then becomes a condenser potential-divider and the open-circuit voltage across the electric condenser is therefore independent of frequency. The *voltage*-transfer factor is approximately equal to the capacitance ratio, equation (43). However, what one wants is the transfer factor which converts *pressure* to open-circuit voltage, and this involves another ϕ so that one ultimately finds that the open-circuit response, in volts per unit incident pressure, is proportional to F as one would expect, rather than to F^2 . The details of these matters are discussed in Chapter 4, the present brief discussion being intended only to show one application of the circuit for the low-frequency limit.

SERIES-EQUIVALENT IMPEDANCE

The series-equivalent impedance of the parallel electrical and mechanical arms can be measured with precision by a suitable bridge. The value deduced from the equivalent circuit is

$$Z_s = \frac{(-i/\omega C)(R + iX)}{[R + i(X - 1/\omega C)]}, \quad (44)$$

in which R here includes both loss and radiation resistance, X is the total equivalent reactance

of the mechanical arm, and the signs (+) are to be understood. These two quantities are defined by equations (16') and (17') for the two cases.

The real and imaginary parts of this impedance are

$$R_s = \left(\frac{1}{\omega^2 C^2 R}\right) \left[1 + \frac{(X - 1/\omega C)^2}{R^2}\right]^{-1}, \quad (45)$$

$$X_s = \left(-\frac{1}{\omega C}\right) D(\omega), \quad (46)$$

$$D(\omega) - 1 = \left(\frac{1}{\omega CR}\right) \left[\frac{(X - 1/\omega C)}{R}\right] \left[1 + \frac{(X - 1/\omega C)^2}{R^2}\right]^{-1}, \quad (47)$$

in which $D(\omega)$ is the distortion factor by which the impedance of the condenser must be multiplied to obtain the actual series-equivalent reactance.

The factors $1/\omega^2 C^2 R$ and $1/\omega CR$ are slowly varying compared to $(X - 1/\omega C)$, and hence these will first be regarded as constants. The error arising from this assumption is not great, and will be eliminated later.

The quantity $(X - 1/\omega C)$ is the reactance around the mesh formed by the electrical and mechanical arms, and therefore vanishes at the resonance frequency of this mesh, that is, at the electrical antiresonance. Neglecting any radiation reactance, it is

$$\text{Case I: } X - \frac{1}{\omega C} = \Re Z_c^+ \cot \gamma \theta - \left(\frac{L}{cC\theta}\right), \quad (48)$$

$$\text{Case II: } X - \frac{1}{\omega C} = -\frac{1}{2} \Re Z_c^+ \cot \frac{\gamma \theta}{2} - \left(\frac{L}{cC\theta}\right), \quad (49)$$

in which $\gamma = (\Re \theta^+ / \theta)_r$ is the reciprocal of the frequency-depression factor, at resonance; it is evaluated at resonance because it differs from 1 only by small quantities whose variation over the operating band is a second-order small quantity.

Expanding the mesh reactance near the antiresonance frequency, one can readily show that only the first-order term is of any importance and one therefore has for

$$\text{Case I: } \frac{X - 1/\omega C}{R} \simeq \frac{\gamma \Re Z_c^+}{R} (\theta - \theta_a). \quad (50)$$

Ignoring the slight departure of the f_r/f_a from 1 in the coefficient, this is just

$2Q_M(f - f_a)/f_a$, and the same result holds in Case II provided the proper Q_M is used.

Putting equation (50) into equations (45), (46), and (47), with the slowly varying quantities evaluated at resonance, one has

$$R_s = R_{\max}(1 + x^2)^{-1}, \quad (51)$$

$$R_{\max} = \frac{1}{\omega_r^2 C^2 R}, \quad (52)$$

frequencies, decreasing with increasing R , and has the same fractional band width as the constant voltage response, both being $1/Q_M$. The distortion factor $D(\omega)$ indicates that the series-equivalent reactance approaches the condenser value between the resonances, being less just below f_a and greater just above.

Recalling that the slowly varying quantities $1/\omega CR$ and $1/\omega^2 C^2 R$ were evaluated at reso-

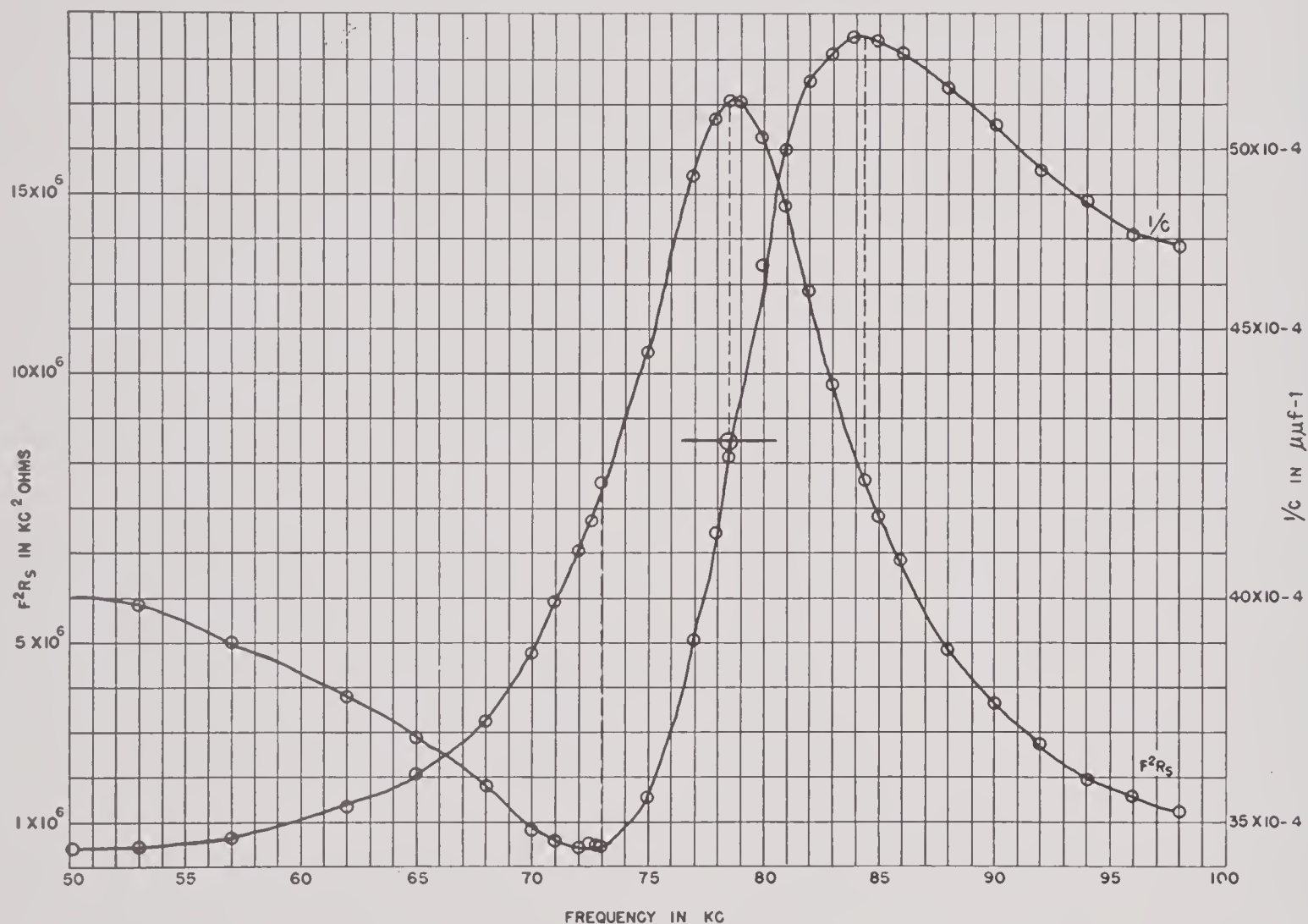


FIGURE 8. $f^2 R_s$ and $(1/C)$ for CCU10Z-1 transducer (0.773" motor).

$$D(\omega) = 1 + \left(\frac{1}{Q_E} \right) x(1 + x^2)^{-1}, \quad (53)$$

$$x = \frac{2Q_M(f - f_a)}{f_a}. \quad (54)$$

These results are valid for both cases, provided the proper Q 's are used. The quantity Q_E is $\omega_r CR$ and, neglecting finite width corrections, is related to Q_M by

$$Q_M Q_E = \frac{K \rho c^2}{2\pi F^2}. \quad (55)$$

The series-equivalent resistance has a maximum value of $(1/\omega_r^2 C^2 R)$ at the antiresonance

nance, we now see that the actual variation of these quantities will skew the R and D curves, slightly moving the extrema toward lower frequencies, lifting the parts of the curves below, and lowering the parts above, f_a .

For practical design purposes, the foregoing treatment is adequate, but in checking the theory, it is convenient to plot $f^2 R_s$ and $(-\omega X_s)$, the latter being the reciprocal of the series-equivalent capacitance as read directly from the bridge. According to the theory, these should be $1/(1 + x^2)$ and $[1 + (1/Q_E)x/(1 + x^2)]$,

except for a scale factor. These quantities are plotted for two transducers in Figures 8 and 9. Three features worthy of note are the symmetry of the curves, the occurrence of the maximum f^2R_s at the midpoint of $(-\omega X_s)$ and the occurrence of the extrema of $(-\omega X_s)$ at very nearly the same frequencies as the half-value frequencies of f^2R_s .

having the symmetry of RS or any higher symmetry.

The performance of a transducer at higher resonances is inferior in many respects to its performance at the first resonance; therefore, while this formula for $n = 1$ has very important practical application to design, its predictions for larger n 's are not directly signifi-

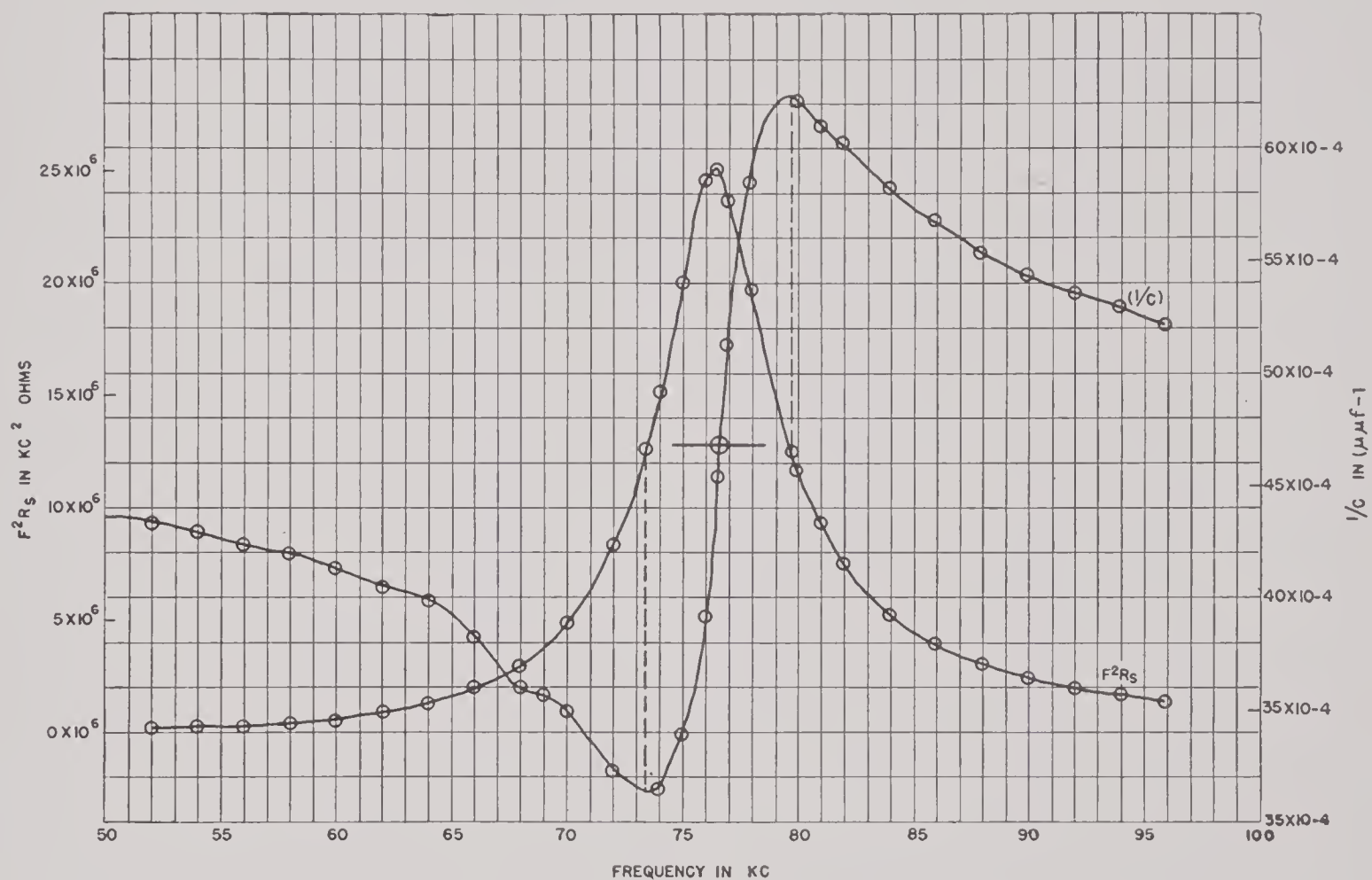


FIGURE 9. f^2R_s and $(1/C)$ for CCU10Z-2 transducer (high-frequency motor).

3.2.3 Evaluation of Crystal Constants

YOUNG'S MODULUS, CHARACTERISTIC IMPEDANCE AND WIDTH POISSON RATIO

From equation (30) of Section 3.2.2, the resonance frequencies of a free-free crystal are given by

$$\frac{f_r L}{n} = \left(\frac{c}{2} \right) \left[1 - \left(\frac{n^2 \pi^2}{24} \right) (\epsilon_w^2 r_w^2 + \epsilon_t^2 r_t^2) \right], \quad (56)$$

in which n is the modal number, with values 1, 3, 5, etc. This is the generalization of the Rayleigh formula for the resonance frequencies of a rod of finite width, for an anisotropic rod

cant. However, it is extremely important to test the validity of the general theory in as many ways as possible, and the various order resonances offer an excellent opportunity for this.

Accordingly, the resonance frequencies of about 60 45° Z-cut ADP rectangular plates, with evaporated gold electrodes, have been measured. The results are given in Figure 10, in which $f_r L/n$ is plotted against r_w^2 . Each point represents a group of 2 to 6 crystals having the same dimensions. The frequencies were measured with a Western Electric 17B oscillator which had been checked against a Bendix CRR heterodyne frequency meter, and other precau-

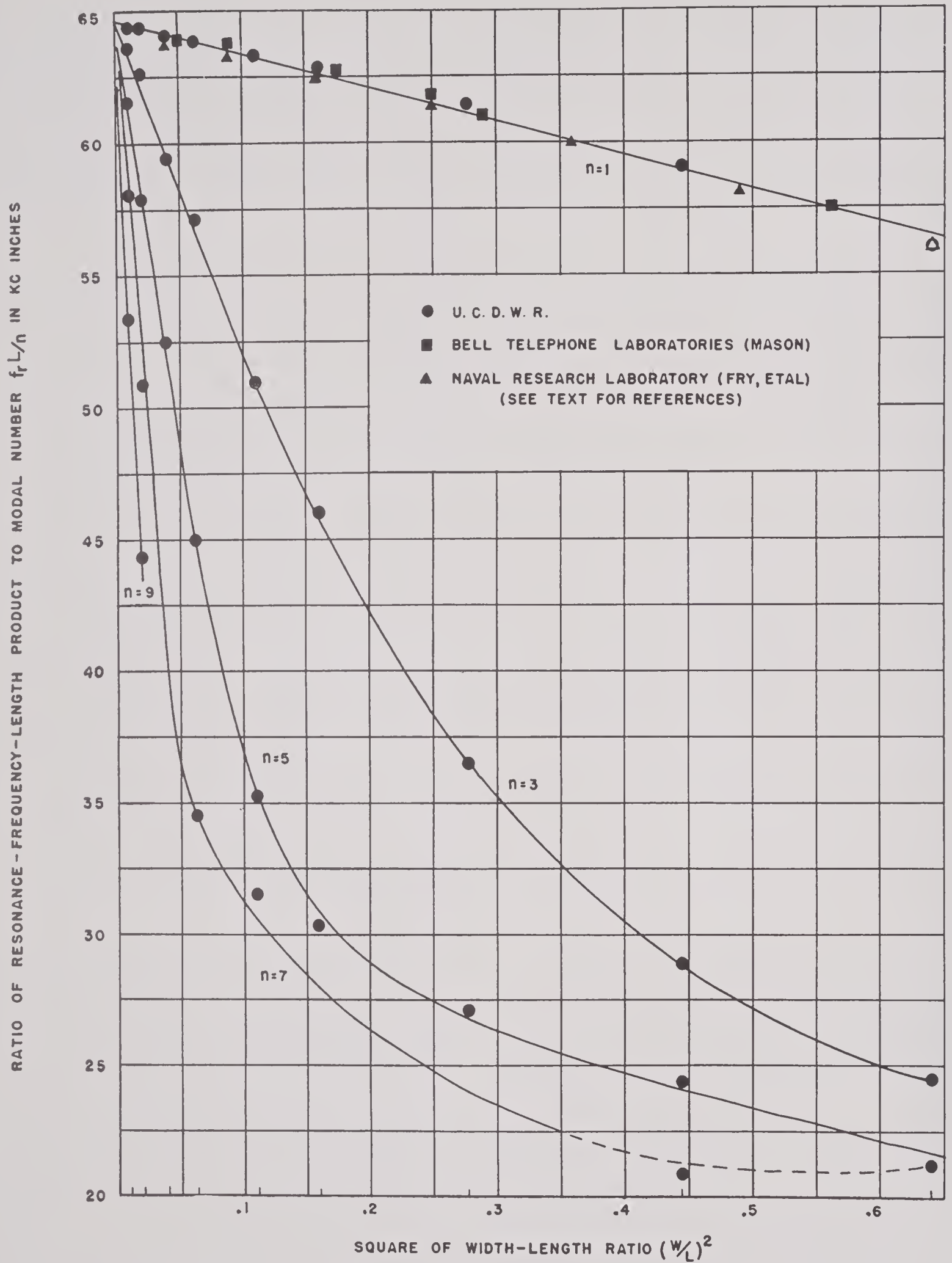


FIGURE 10. Dependence of resonance frequencies of ADP on length, width-length ratio, and modal number.

tions were taken to reduce error. The 1-db breadth of the resonances was less than 15 c for all crystals. The dispersion of the points from the linear part of each curve, which presumably includes the effect of all random errors, is about 0.5 per cent.

The thickness-length ratio varied, the largest value being 0.2. The effect of thickness on the resonance frequencies was less than the experimental dispersion from a smooth curve; we therefore conclude that the thickness Poisson motion is of negligible importance for the range of thickness-length ratios used in practical transducers. This conclusion is supported by results given in Section 3.3, where a rough estimate of 0.2 is obtained for ϵ_t . This very rough value indicates that the thickness correction term is

$$\left(\frac{n^2\pi^2}{24}\right)\epsilon_t^2 r_t^2 \simeq (7 \times 10^{-4}) n^2. \quad (57)$$

Thus, the lack of any measurable dependence for $n = 1$ and 3 is readily understood. For $n = 5$ and 7, however, the fractional effect of the largest thickness ratio 0.2 should be about 2 and 4 per cent if the above value of ϵ_t is correct, whereas no such effect was observed. Two possible explanations of this suggest themselves: first, ϵ_t may be smaller than the above rough value and, second, the error in these measurements may be greater for $n = 5$ and 7. This latter view is supported by the greater irregularity of the points on the curves for the higher n 's. In any event, this is a matter of higher precision rather than general principle, and certainly the thickness effect is not of any great practical importance.

The general structure of these curves is in excellent agreement with equation (56), out to values of r_t^2 where the fractional correction becomes of order $1/3$. Beyond this, higher-order terms become important enough to introduce curvature. It should be emphasized that this curving in no way casts doubt upon the validity of the variational principle from which the perturbed equivalent circuit was deduced, but is an anticipated consequence of the approximations made in applying that principle, since terms in the square of the fractional correction were dropped. Furthermore, it should be noticed

that for $n = 1$, the only n of practical importance in design, the departure from a straight line is negligible.

According to equation (56), the intercept of these curves is $c/2$, which is about 64.7 kc-in. We therefore obtain

$$\text{ADP: } c = 3.29 \times 10^5 \text{ cm/sec.} \quad (58)$$

Combining this with the density of ADP, 1.80 g per cu cm, one has for the characteristic impedance at zero width

$$\text{ADP: } z_c = \rho c = 5.92 \times 10^5 \text{ g/cm}^2 \text{ sec.} \quad (59)$$

Equation (56) predicts that the initial slopes of these lines, neglecting the thickness term, are

$$-\left(\frac{c}{2}\right)\left(\frac{n^2\pi^2}{24}\right)\epsilon_w^2. \quad (60)$$

In Table 1, the measured slopes, and the slopes divided by n^2 are given. In view of the great range of the slope, the constancy of the last column is regarded as good.

TABLE 1. Slopes and slopes/ n^2 , from Figure 10.

n	Slope, kc-in.	(Slope/ n^2), kc-in.
1	12.9	12.9
3	125.0	12.6
5	325.0	13.0
7	630.0	12.9
9	1070.0	13.2
Average 12.9 ± 0.3 extreme		

From equation (60), together with the figures in Table 1, one obtains

$$\text{ADP: } \epsilon_w = 0.7. \quad (61)$$

We know of no data on the higher resonances of free-free 45° Z-cut ADP plates to compare the foregoing results, but BTL³ and NRL⁴ have given data^c on the first resonance.

NRL makes no mention of any thickness effect, and the width effect agrees quite well with our data, as shown by triangles on the line for $n = 1$ in Figure 10.

BTL finds a small thickness effect, as indicated by Figure 11; however, the effect for

^c This work contains valuable material on transducer design, but the approach is so different from ours that we have not been able to study it thoroughly in the time available. It would undoubtedly repay a careful study.

$r_t = 0.2$, the largest value used in obtaining Figure 10, is about equal to the dispersion of the points and therefore, as previously remarked, our data is not sufficiently accurate to resolve the effect. By plotting the intercepts of Figure 11, one gets a value of about 0.3 for ϵ_t ; this is higher than the rough estimate of 0.2 previously mentioned, but one would need to study the original data to decide if the difference is significant. A curious feature of BTL's

value of ϵ_w (0.7) is over 4 times as large as an early value (0.17) given by Mason.⁵ Mason has since indicated in conversation that the value given in the quoted memo is low, but has not indicated by how much.

From the standpoint of determining the resonance frequency of 45° Z-cut plates for design purposes, the discrepancy is unimportant because, regardless of interpretation, the data given in Figure 10 can be used empirically.

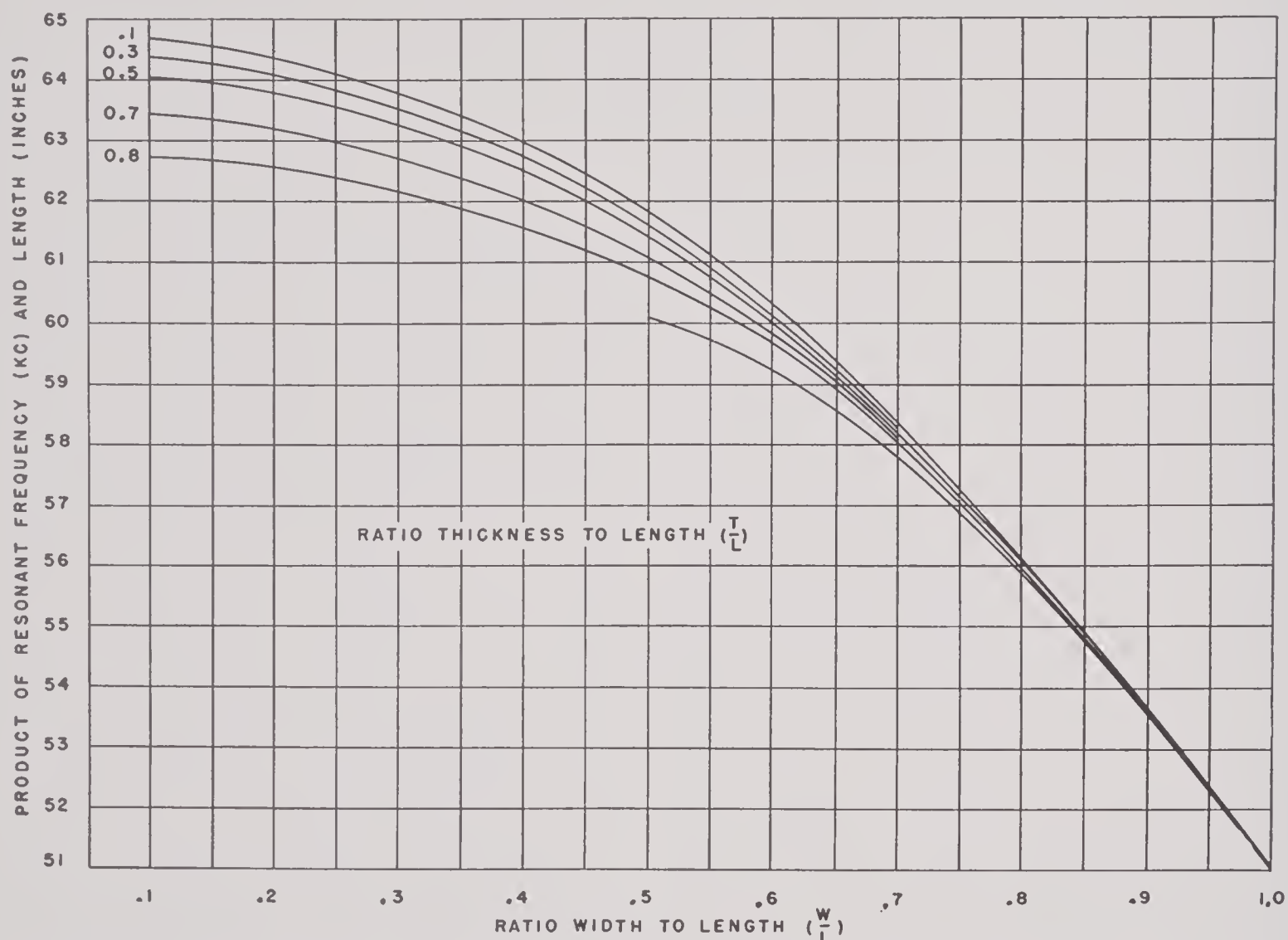


FIGURE 11. 45° Z-cut ADP crystals, product of resonance frequency and length against ratio of width to length for various ratios of thickness to length. (From BTL Drawing BA262699.)

curves is their congruence for all r_t as r_w approaches 1. This implies that the resonance frequencies of a thin square plate and a cube are the same, a result which is difficult to understand.

BTL's data for $r_t = 0.1$ agree quite well with ours, as indicated by the squares in Figure 10.

Despite the good agreement of the frequency depression data for the first resonance, our

However, it is extremely important that the theory be in good order, and we therefore feel that the original data, from which the quoted memo was prepared, should be carefully re-studied. It seems possible that the enormous discrepancy may arise in some way from the indirect method used to determine ϵ_w , involving several different cuts and shear modes with resonance frequencies up to a megacycle; how-

ever, it is then hard to understand why there is such close agreement on the Young's modulus. In a field as complicated as this, and thinking only in terms of the restricted purpose of this volume, it is probably a good policy to make crystal measurements directly on 45° Z-cut plates so as to obtain data intimately related to the manner in which the crystals are used in underwater transducers. If a particular effect cannot be measured with 45° Z-cut plates, then it is of no consequence to underwater transducers.

On the basis of the foregoing, we conclude that at least the first five consecutive resonances of a 45° Z-cut ADP plate correspond to longitudinal modes with lateral Poisson "breathing" coupled into them, provided the width-length ratio is not too large. The frequencies of these resonances are given by

$$\begin{aligned} f_r L &= n(64.7 - 12.9n^2 r_w^2), \\ &= n(64.7) (1 - 0.20n^2 r_w^2). \end{aligned} \quad (62)$$

This result is valid near room temperature, and the temperature correction is so small as to be of negligible practical importance.

As the width-length ratio increases, the lateral motion ultimately becomes so large that the modes became more complicated, as predicted by the theory and as observed experimentally (see Figure 12 of Section 2.5.3). However, it is not worth while to try to treat these more complicated modes theoretically because in practical transducers the width-length ratio should always be kept small enough so that these complicated motions do not occur.

The modes of RS undoubtedly follow a pattern similar to ADP, but to the best of our knowledge have not been studied in detail. One will expect the more complicated type of motion to appear at a lower width-length ratio because of the somewhat larger ϵ_w and the shear of the electrode faces into a parallelogram (see Figures 12 and 14A, 14B, and 14C of Section 2.5.3 and the accompanying discussion where it is shown that the shear Poisson ratio ϵ_s is not zero in RS); therefore, the width-length ratio should be kept lower in RS than in ADP transducers.

Lacking data for detailed verification of the theory for the higher modes, we confine our attention to the first mode. The resonance fre-

quency of the first mode in RS at room temperature, on the basis of UCDWR data, is:

RS, first resonance:

$$\begin{aligned} f_r L &= 46.3 - 11r_w^2, \\ &= (46.3) (1 - 0.24r_w^2). \end{aligned} \quad (63)$$

From the coefficient, 0.24, one finds for the width Poisson ratio,

$$\text{RS: } \epsilon_w = 0.76. \quad (64)$$

Considering the probable error in the coefficient 0.24, this is regarded as excellent agreement with the value of 0.776 calculated⁶ from the crystal constants as determined by Mason.^{1a}

PIEZOELECTRIC COUPLING COEFFICIENT

From equation (38) of Section 3.2.2, the difference between the antiresonance and resonance frequency, for the various modes, is given by

$$\begin{aligned} n(f_a - f_r)L &= \frac{8(F^{+2})_r}{\pi K(z_c^+)_r}, \\ &= \left(\frac{8F^2}{\pi K \rho c} \right) B_n, \end{aligned} \quad (65)$$

$$B_n = 1 + \alpha n^2 r_w^2 + \beta n^2 r_t^2, \quad (66)$$

$$\alpha = \left(\frac{\pi^2}{12} \right) \left[\frac{2Y(\epsilon_w C_{11}^{-1} + \epsilon_s C_{31}^{-1})}{(1 + \epsilon_w)} + \epsilon_w^2 + 2\epsilon_s^2 \right], \quad (67)$$

$$\beta = \left(\frac{\pi^2}{12} \right) \left[\frac{2Y\epsilon_t C_{21}^{-1}}{(1 + \epsilon_w)} + \epsilon_t^2 \right]. \quad (68)$$

Thus, the variational principle predicts that the piezoelectric coupling coefficient will depend upon the width-length and thickness-length ratios, with coefficients that depend upon the modal number. It is readily shown that C_{21}^{-1} and C_{31}^{-1} are negative, whereas C_{11}^{-1} is positive. This means, at least for ADP in which ϵ_s is zero and probably also for RS, that F^{+2} increases with increasing r_w and decreases with increasing r_t . This behavior, for $n = 1$, is qualitatively verified, for ADP at small r_w and r_t , by McSkimin.^{3a} If these data follow equations (65) to (68) closely, then one could determine the values of $F^2/\rho c$, α and β .

Time has not permitted a detailed analysis of these data. Furthermore, it is believed that the analysis should be done by one intimately familiar with the experimental procedures; this is because the impedance of a crystal becomes very large at antiresonance, and any small

shunt, arising from stray capacitance or leakage resistance, although negligible at resonance will cause a serious error at antiresonance.

We therefore adopt values given by Mason^{1b} and Kinsley^{5a} for the electromechanical coupling coefficient, expressed in terms of Mason's D (our F is Mason's $KD/4\pi$),

$$\text{ADP: } D = 12.2 \times 10^4 \text{ dynes/esu charge} \quad (69)$$

$$\text{RS: } D = 11.2 \times 10^4 \text{ dynes/esu charge} \quad (70)$$

These are valid only for the infinitely thin crystal, and, as remarked above, while McSkimin's data agrees qualitatively with the shape corrections predicted by the variational principle, we do not yet know if the theory is correct quantitatively.

From equations (69) and (70) together with the dielectric constants given in the next section, we obtain

$$\text{ADP: } F = 13.8 \times 10^4 \text{ dynes/esu charge} \quad (71)$$

$$\text{RS: } F = 8.9 \times 10^4 \text{ dynes/esu charge} \quad (72)$$

The dimensionless number,

$$\gamma^2 = \frac{4\pi F^2}{K\rho c^2}, \quad (73)$$

characterizes the smallness of the electromechanical coupling. In this formula, γ is the quantity called the electromechanical coupling coefficient by Mason¹ and designated by him as k , except that ρc^2 , the short-circuit Young's modulus, is here used instead of the insulated Young's modulus, the latter being called Y_0 by Mason. The fractional difference between γ and k is of order γ^2 ; the above quantity appears to emerge more directly from the analysis and, in any event, a careful study shows that unless one takes proper account of width corrections for all the parameters, which has not yet been done in numerical detail, fractional differences of this order are of no importance.

The numerical value of γ is about 0.3 for both ADP and RS. This is the basic reason for the narrow band width of crystal transducers, as may be seen by noticing that the product of the

mechanical and electrical Q 's for ADP and RS is

$$Q_M Q_E = \frac{\pi^2}{8\gamma^2} \simeq 14, \quad (74)$$

and that the optimum band width is determined by the two Q 's being approximately equal, so that the optimum effective Q is of order $(14)^{1/2}$ or about 4. This figure refers to a single crystal but in an actual transducer this product, and therefore the optimum effective Q will be larger because shunt capacitance increases Q_E above its single crystal value (also, the effective Q may be larger if Q_M is low because of poor radiation loading). This does not affect the product above, but the two Q 's are then not approximately equal, as they happen to be for full water loading.

DIELECTRIC CONSTANT

From Section 3.2.2, where the low-frequency limit of the equivalent circuit is discussed, one sees that at a frequency well below resonance, the circuit simplifies to two parallel condensers, the blocked electric condenser and the equivalent (low-frequency) mechanical condenser. This equivalent low-frequency mechanical condenser should not be confused with the approximate condenser used with a similar inductance to represent the circuit near resonance.

The ratio of the low-frequency mechanical condenser, in electrical units, to the blocked electric condenser, is γ^2 [see equation (32) of Section 3.2.2]. Therefore, to measure the blocked capacitance one needs only, in principle, to measure the total electric admittance and apply a correction factor,

$$(1 + \gamma^2)^{-1} \simeq 1 - \gamma^2, \quad (75)$$

to eliminate the mechanical condenser.

However, one is measuring a very low capacitance, and strays therefore become very important, so that elaborate precautions³ must be taken to get reliable results. Measurements at this laboratory check those done at other laboratories but have considerable dispersion (about ± 10 per cent) and are therefore regarded as inferior to those obtained elsewhere. We therefore adopt the values given by Mason

for the longitudinally blocked dielectric capacitance of ADP⁵ and RS^{1b}:

$$\text{ADP: } K = 14.2, \tag{76}$$

$$\text{RS: } K = 10.0. \tag{77}$$

The variational principle predicts that this quantity has no appreciable finite width correction (see Section 2.5.3).

SUMMARY OF THE PERTURBED EQUIVALENT CIRCUIT

For convenient reference, the constants and perturbed parameters are summarized in Table 2.

TABLE 2. Constants for infinitely thin rectangular plates of 45° Z-cut ADP and 45° Y-cut RS.

Symbol	Constant	Units	ADP	RS
ρ	Density	g/cm^3	1.80	1.78
Y	Short-circuit Young's modulus	dynes/cm^2	1.95×10^{11}	0.98×10^{11}
c	Phase velocity	cm/sec	3.29×10^5	2.35×10^5
$z_c = \rho c$	Characteristic impedance	$\text{g/cm}^2 \text{ sec}$	5.92×10^5	4.17×10^5
F	Blocked stress per unit field or short circuit charge density per unit strain	dynes/esu charge	13.8×10^4	8.9×10^4
K	Longitudinally clamped dielectric constant	dimensionless	14.2	10.0
ϵ_w	Width Poisson ratio	dimensionless	0.7	.78
ϵ_t	Thickness Poisson ratio	dimensionless	0.2 to 0.3 (?)	(?)
ϵ_s	Shear Poisson ratio	dimensionless	0	(?)
γ	Electromechanical coupling coefficient	dimensionless	0.3	0.3

Some of these values are undoubtedly in error by a few per cent, but until transducer design is greatly refined, they are accurate enough for practical purposes.

The perturbed parameters are given in Section 2.5.3. To use these, they should be evaluated at the resonance near which the transducer is used, which amounts to setting $\theta = kL$ equal to $n\pi/2$ or $n\pi$ for a crystal which is approximately blocked or approximately free-free, with $n = 1, 3, 5$, etc.

The finite width correction to the resonance frequency has been worked out in detail, but that for the piezoelectric constant F^+ has not. The values of the tangential and normal impedances to be used in these formulas are not at present known.

3.2.4

Electrodes

In order to drive all parts of the crystal with an electric field which is approximately uniform, the large faces of the crystal plate are covered with conducting sheets, called the electrodes.

Various types of electrodes have been used by different laboratories. A description of these, together with the techniques involved, is given in Chapter 8. Here we are concerned with the influence of the electrode upon the measurement of crystal constants and the performance of completed transducers.

The electrode believed to most nearly approximate a perfect conducting sheet exerting neg-

ligible influence on the motion of the crystal is a very thin layer of gold applied by an evaporation technique developed at Bell Telephone Laboratories (see Chapter 8). This electrode is therefore used for the evaluation of crystal constants.

The elastic and dissipative effects of other electrodes are greater. However, if the technique of attaching them is good, they all appear to have negligible effect upon the performance of transducers, the slight additional effects being overwhelmed by dissipation of other origin and by radiation resistance. This is readily verified by measuring the shift in frequency and the mechanical Q of a single crystal equipped with various electrodes. These quantities differ from those obtained with the evap-

orated gold electrodes by amounts which are significant with respect to determining crystal constants, but entirely negligible with respect to the performance of an actual transducer. An exception to the above may occur in the case of electrodes which are not cemented to the crystal. In this case, it is believed that castor oil between the crystal face and the electrode may introduce a tangential resistance of practical importance.

Three electrical effects require consideration: (1) the loss arising from the resistance of the electrode, (2) the stray capacitances from the electrodes to each other and to the backing plate and to the case, and (3) the effect of the condensers formed by the cement layers.

The resistance of the electrodes seems to be

the impedance seen looking in at these terminals, thereby increasing the effect of the shunts arising from the stray capacitances to the backing plate and to the case.

To estimate the importance of these cement-layer condensers, suppose the cement layers are identical and have thickness t' and dielectric constant K' . The ratio of the voltage drop in the cement layers to that in the crystal, given approximately by the inverse ratio of the capacitances, is

$$\left(\frac{K}{K'}\right) \left(\frac{2t'}{t}\right). \quad (78)$$

Using rough figures for K' and t' of 2 and 1 mil, respectively, which are extreme examples, this is about 0.05 for a crystal $\frac{1}{4}$ in. thick, and 0.25

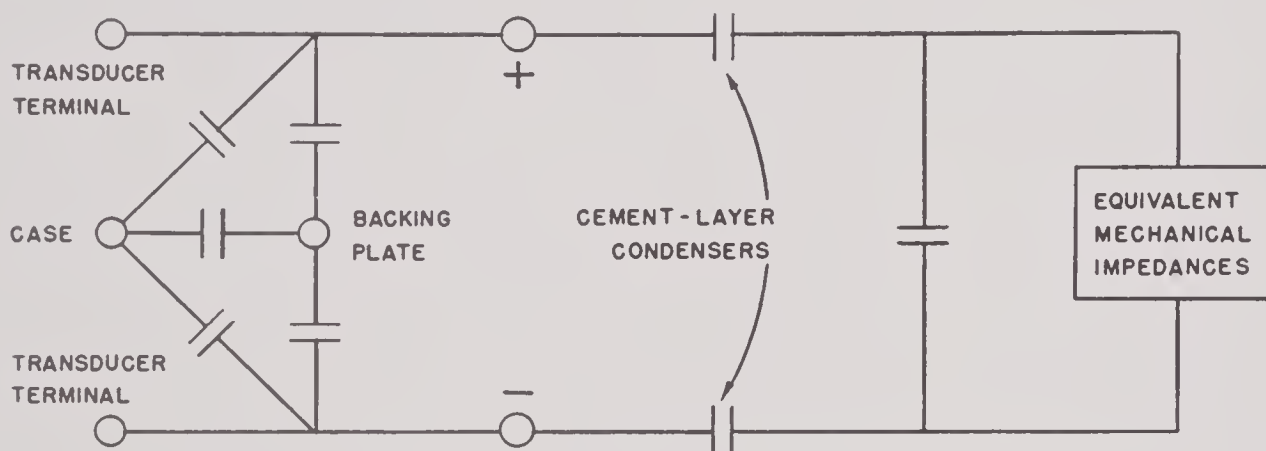


FIGURE 12. Equivalent circuit showing cement-layer condensers.

negligible since the series equivalent resistance of a single crystal working into water is several hundred kilohms.

All the electrodes have stray capacitance to others and to other metal objects in the case. This is a purely electrostatic phenomenon, depending on clearances and the dielectric materials which find themselves in stray fields, and hence will vary with the type of electrode used only in so far as the various techniques lead to different geometry (see Section 4.5 and Chapter 8).

The capacitances corresponding to the cement layers enter the equivalent circuit as shown in Figure 12. These condensers reduce the field in the crystal, and reduce the band width in two distinct ways: (1) they increase the electric Q as seen looking in at the electrode terminals (+ and - in Figure 12), and (2) they increase

for a crystal 0.05 in. thick. If the dielectric constant K' is 5 instead of 2, the effect is only 40 per cent as great; likewise, a cement layer of 0.5 mil will halve the effect again. This indicates that, judging solely from this consideration, it is advantageous to use a cement of high dielectric constant and to make t' as small as possible by using high pressure and a cement which flows easily. This is done in most cases.

We conclude that in most applications, the cement layer is not very important, but that its importance is increased if the crystal is X-cut RS (large K), if the cement has low dielectric constant, or if the crystals are thin. The use of thin crystals appears to be important for high power, and here also any dissipation in the cement layer, while not important from an efficiency viewpoint, may be important in the breakdown mechanism. In this case, the desira-

bility of evaporated gold electrodes should be considered carefully.

3.2.5

Weakened Crystals

Some fragmentary experiments have been done by UCDWR on the weakening of crystals to obtain low resonance frequency without going to undue length.

Various methods of weakening were used, including boring holes normal to the electrode faces and sawing slots in from both secondary radiating faces in planes perpendicular to the longitudinal axis.

In this manner, a $\frac{1}{4} \times 1 \times 1\frac{1}{2}$ in. 45° Y-cut RS plate has been made to have a resonance frequency as low as 2 kc, to be compared with its unweakened value of 27.5 kc. It is, of course, possible to obtain any frequency between these values.

Although the resultant crystals were not as fragile as one might think, they nevertheless could not be trusted without thorough field testing and the pressure of other work during World War II did not permit this. There is still no entirely satisfactory design for crystal transducers to operate below about 10 kc, and hence it might pay to investigate the possibility of building transducers of satisfactory ruggedness with weakened crystals.

3.3

SUBASSEMBLIES

3.3.1

Cement Joints

The satisfactory attachment of crystals to other surfaces is one of the most critical steps in the construction of transducers. The techniques are discussed in Chapter 8, and only the desirable properties of joints and the theory of measuring their impedance are discussed here.

Some of the most direct and useful tests are purely empirical. For example, a cement joint may impose a tangential constraint such that differential expansion will cause the crystals to crack at low temperatures, and only an empirical test can settle this question. Again, a joint may deteriorate if forced to transmit high

acoustic intensity, and the only practical way of detecting such behavior is to measure its impedance preferably while driving (an experimental technique not yet developed) or a very short time before and after such hard driving.

The ideal joint is one which has zero tangential and infinite normal impedance. Failing this, it is believed that the most important single item is that the normal impedance be uniform from joint to joint, since nonuniform joints on a backing plate or bar are believed to excite flexural modes which distort patterns and cause serious losses. Naturally, one would like the resistive parts of both normal and tangential impedance to be small enough to cause negligible losses; however, a tangential reactance, if not too large or variable, is not believed to be serious, since it would merely cause a slight alteration in the resonance frequency by stiffness coupling through the Poisson motion.

The most sensitive means for finding the impedance of a joint consists in cementing a crystal to an approximately quarter-wave backing rod and observing the frequency and the mechanical Q , being careful to exclude all extraneous dissipation. From equation (16) of Section 3.2.2, evaluating the numerator of Z_1^+ at the unperturbed resonance, one has for the impedance of the mechanical arm

$$-iZ_c^+ \cot \theta^+ + \frac{Z_c^{+2}}{Z_1^+}, \quad (79)$$

in which Z_c^+ and θ^+ are real since it has been assumed that precautions have been taken to make internal dissipation negligible. One now regards Z_1^+ as consisting of a reactance X_1 and a resistance R_1 in *parallel*,

$$\frac{1}{Z_1^+} = \frac{1}{R_1} - \frac{i}{X_1}. \quad (80)$$

The deviation of the observed resonance frequency from that calculated from the free-free resonance of the crystal, taking account of the different finite width corrections, gives

$$X_1 = \frac{Z_c^+ \left(\frac{2}{\pi} \right) f_r}{(f - f_r)}, \quad (81)$$

and the resistance is determined from the mechanical Q , or from the absolute admittance (see Chapter 9). The determination of X_1 ad-

mittedly rests upon the small difference between an observed and a calculated frequency. However, if the difference is so small as to cause a large error, then X_1 is, for all practical purposes, infinite.

Many tests of this type were made in this laboratory during the progressive baking of cement joints, and the observed frequency approached a limiting value, as the baking time became long, corresponding to a very high impedance. Simultaneously, Q_M increased, indicating an increase in the parallel resistance. Similar tests were also made to determine the effect of driving the joint very hard (to cavitation for various times), and some types of joints showed progressive deteriorations. This procedure was very helpful in finding a technique which yielded high Q joints that stood up.

3.3.2 Crystal Blocks

Single crystals can be cemented together in a variety of ways, all of which will be referred to as crystal blocks.

cemented into blocks, the polarity being carefully matched. The results are shown in Table 3.

These crystals were taken at random from routine production, and were equipped with 0.001-in. German-silver electrode foils. The small discrepancies in the resonance frequencies of the single crystals are undoubtedly caused by slight nonuniformities in the electrodes. The frequencies of the blocks were calculated as if they were single crystals, and it will be seen that the discrepancies are only a little larger than those for the single crystals. The mechanical Q 's for the blocks were of the order of 500 as compared with 1,000 for the single crystals. The crystal blocks were driven to cavitation for 2 hr and measured again, with the result that neither the resonance frequencies nor the Q 's changed within experimental error.

These results indicate that crystal blocks with good shape factors may be regarded as single crystals for all practical purposes, provided the cementing technique is good. It should be emphasized that the above blocks have width-length ratios appreciably less than 1. Some

TABLE 3. Effect of cementing crystals together on secondary radiating faces, and on their electrode faces.

Dimensions (inches)	Single Crystals		Number of Crystals	Dimensions of block (inches)	Crystal Blocks	
	Resonance frequency (kc) Calculated	Observed			Resonance frequency (kc) Calculated	Observed
A. <i>Secondary radiating faces.</i>						
$\frac{1}{4} \times \frac{1}{2} \times 1''$	61.5	$61.6 \pm .05$	3	$\frac{1}{4} \times 1 \frac{1}{2} \times 1''$	39.1	39.2 ± 0.1
$\frac{1}{4} \times \frac{1}{2} \times 1 \frac{1}{4}''$	50.0	$50.1 \pm .05$	2	$\frac{1}{4} \times 1 \times 1 \frac{1}{4}''$	44.8	44.5 ± 0.1
B. <i>Electrode faces.</i>						
$\frac{1}{4} \times \frac{1}{2} \times 1''$	61.5	$61.6 \pm .05$	2	$\frac{1}{2} \times \frac{1}{2} \times 1''$...	61.25 ± 0.5

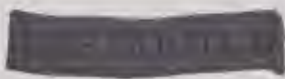
It is sometimes convenient to cement crystals together on their primary radiating faces, to obtain crystals larger than those which can be economically grown (45° plates are cut as shown in Figure 1 of Chapter 1, and the cost of crystal plates therefore increases with the length). It has been demonstrated that such fabricated crystals are in all practical respects the equivalent of a single crystal of the same dimension, provided the cementing technique is good and the proper polarity is observed.

To determine the effect of cementing on the secondary radiating faces and electrode faces, a number of 45° Z-cut ADP crystal plates were

fragmentary results indicate that the motion of blocks (as well as single crystals) becomes quite complicated as the width-length ratio approaches 1. This would be expected theoretically, and is confirmed by the silicon carbide dust pictures, Figure 12 of Section 2.5.3.

The result for cementing on the electrode faces (Table 3) gives 0.2 as a very rough estimate of the thickness Poisson ratio.

On the basis of the foregoing admittedly scant data, it has been the policy of this laboratory to use blocks whenever necessary to get needed resonance frequencies from available crystals or whenever desirable to simplify con-



struction. The satisfactory performance of many transducers using blocks cemented on their electrode faces, and of a few using blocks cemented on other faces, is partial and indirect confirmation of the above results.

3.3.3

Benioff Blocks

An extremely rugged transducer, designed by Dr. Benioff for Submarine Signal Company, employs a structure known as a Benioff block. This consists essentially of a crystal working into a backing and a fronting rod, the two rods being held together by a quite rigid tie rod which opposes the longitudinal vibration of the crystal.

The only feature of this structure that will be discussed here is its band width. The equivalent circuit for the block can be approximately formulated from equivalent circuits for the crystal, the tie rod, and the backing and fronting rods. In the absence of dissipation, Foster's theorem tells us that the slope of the reactance curve for the mechanical arm will be increased at all points, including resonance. Now inserting the radiation resistance, we conclude that the mechanical Q will be greater than for a crystal without constraints imposed by the tie rod. This conclusion is borne out by experiment, the Q obtained from the series resistance curve in water being of order 200 as compared with 3 to 6 for most transducers.

A careful study of the Benioff block has not been made at this laboratory. The foregoing brief discussion gives a qualitative theoretical explanation of its observed sharpness and this indicates that a structure of this type will not be satisfactory for wide-band operation; however, it is possible that it may have practical applications for single-frequency operation.

3.3.4

Unit-Construction

A unique method of mounting crystals has been developed at the Naval Research Laboratory [NRL]. This consists in mounting a small number of crystals on a single cylindrical backing rod with a rectangular plate across the top,

and then isolating the rod by a cylindrical cup attached to the rod near its node by a rubber bond; these cups are attached to the supporting plate. The basic principle is indicated in Figure 13.

Performance data on unit-construction transducers are not available at the time of writing.

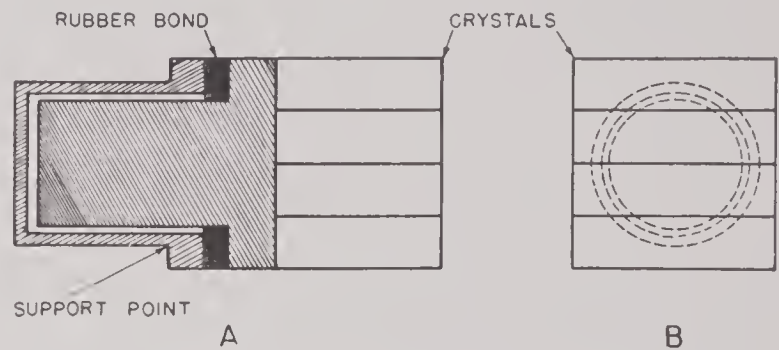


FIGURE 13. Unit-construction (NRL).

However, one would think that this type of construction has much to recommend it.

From the design viewpoint, it would appear to eliminate all troubles arising from flexural modes in a backing plate (see Sections 3.4 and 3.6). A secondary design advantage is that it replaces any loss arising from radiation from the backing rod by a loss in the rubber bond, which is probably much smaller since this bond is so near the node. However, the crystals operate in castor oil, just as in many other transducers, and the motion of their radiating faces is greater than the free end of the backing rod in the inverse ratio of the impedances, about 6 for steel and 2.5 for aluminum; since the loss is proportional to the squares of these amplitudes, we see that the crystal loss is by far the more important, and one does not gain much in reducing the smaller loss by using the cups.

From the production viewpoint, one can foresee a great advantage. Production testing is always a difficult problem, and it is not simple to maintain standards. With this type of construction, much of the critical work would be done on small objects susceptible to rapid and accurate testing. This is an advantage scarcely to be overestimated. It is therefore believed that the possibilities of the unit-construction transducer should be very thoroughly studied and, unless unforeseen difficulties arise, that many types of transducers should use this kind of construction.

3.4 BACKING RODS, BARS, AND PLATES

As the entire surface of an excited crystal is in motion, the problem of supporting it without interfering with the motion is one of importance. A common practice is one of cementing one end of the crystal to a metallic rod or bar, or an array of them to a flat plate. The condition for resonance of a system of a block of crystal cemented to a block of metal, is, as given in Section 7.6

$$-z_c \tan (kL)_c = z_b \tan (kL)_b,$$

where c and b indicate crystal and backing plate, respectively, and z_c is about 5×10^5 and z_b for steel is about 39×10^5 . Thus for a given frequency, the crystal and backing material lengths can be adjusted to any suitable value. This construction allows a much shorter crystal to be used for a given frequency, which is an advantage in saving crystal material. If, for example, using Y-cut RS, it is desired to design a transducer to be resonant at 40 kc and the width and thickness of the units are thin enough to have no effect on the longitudinal velocity, and each crystal is backed by a bar whose dimension ratios have the same property, the following lengths of crystals and backing bars can be used, all of which will resonate at 40 kc.

Bar length (inches)	0.25	0.5	1.0	1.5	2.0
Crystal length (inches)	0.79	1.10	1.30	1.38	1.42

The above formula was developed on the assumption that only the fundamental longitudinal vibrational mode is present in both the crystal and the backing bar, and this assumption necessitates both elements to be long and thin. When the length approaches the thickness in a bar, the frequency of the first mode is lowered, and when the length is small compared to the cross section, this frequency is lowered to less than one-half that of the long bar of the same cross section. A graph of the reduction of frequencies with thickness appears in Chapter 4. Another way of looking at the problem is to consider the velocity of sound in the bar to vary with thickness. The formula $z_c \tan (kl)_c$ is still good if for $k = 2\pi v/c$ the value of c is used that is present in the thick bar.

In an array of crystals, the mechanical cou-

pling between the crystals can be very troublesome, in that it produces uneven end velocities and phases, which in turn make for bad directivity patterns, poor efficiencies, etc. To completely eliminate this coupling, all crystals should be completely isolated from each other, and this has been most nearly done in the case of Cycle-Welded transducers (Chapter 8). However, many transducers have to be built on backing plates, etc., so that the coupling problem must be dealt with. For individual backing of each crystal, the backing bars must be mechanically connected in some way in order to hold the array together. One method is to bolt them all on a thin plate. An example of this construction is the Navy-type QBF transducer, (see Section 3.5). The coupling in this case is reduced to certain frequencies out of the operating band of the transducer. The theory of this isolation is given later in this section.

The most troublesome coupling is in the types where all the crystals are cemented upon the same steel plate or bar. Flexural modes of the plate or bar are very many indeed, they usually lie in the operating-frequency band, and their direction of vibration is that of the crystals.

The natural frequencies of flexure of a rectangular bar of width thickness α and length l , whether bounded or unbounded, are given by

$$V_n = \frac{\pi k}{2l^2} \sqrt{\frac{E}{\rho}} \cdot \beta_n^2; \quad \beta_n = 1.505, 2.50; \quad \beta_n = n + \frac{1}{2}. \quad (82)$$

For steel this reduces to

$$V_n = 2.44 \times 10^5 \frac{\alpha}{l^2} \beta_n^2.$$

The thickness α is determined by the operating frequency of the transducer, the crystal material, etc., and is usually of the order of $1/2$ in. to $1 1/2$ in. It is easily seen that if the first mode is to be around 10^5 c the length must be no greater than about three times the thickness α . This condition restricts the bars to be smaller than is sometimes desirable. Above the first or gravest mode, the higher modes appear in abundance, and in addition the vibration patterns are quite complex due to the superposition of torsional and tangential modes. The modes of a steel bar $9/16$ in. wide, $3/4$ in. thick, and 8 in. long

were studied with the probe technique discussed in Chapter 9, and are reproduced in Figure 14. The calculated flexural frequencies occur at 2.12, 5.80, 11, 20.2, 30.2, 42.0, etc. These frequencies are indicated on the figure. The other modes observed and interspersed among these are torsional, as the phases of their motions shifts 180° as the probe moves across the bar surface perpendicularly to the length.

The calculations of the flexural modes in a backing plate involves a two-dimensional wave equation of fourth order similar to that of the bar, the solution of which is straightforward, but in applying the boundary conditions of no restraint, considerable difficulties arise in the case of the square plate because of the complicated stresses set up close to the free edges.⁸ The case of a circular boundary has been solved⁷ giving the allowed frequencies as

$$f_{mn} = \frac{\pi t}{2a^2} \sqrt{\frac{E}{3\rho(1-s^2)}} \beta_{mn}^2, \quad (83)$$

where

$$\begin{aligned} \beta_{01} &= 1.015 & \beta_{02} &= 2.007 & t &= \text{half-thickness,} \\ & & & & a &= \text{radius,} \\ \beta_{11} &= 1.468 & \beta_{12} &= 2.483 & E &= \text{Young's modulus,} \\ & & & & \rho &= \text{density,} \\ \beta_{21} &= 1.879 & \beta_{22} &= 2.992 & s &= \text{Poisson's constant} \\ & & & & & (\text{about } 0.33). \end{aligned}$$

The gravest mode thus for steel occurs at

$$f_{01} = 4.86 \frac{t}{a^2} \times 10^5.$$

The lowest mode for a steel plate 1 in. thick and 6 in. radius occurs thus around 5 kc. The higher modes are spaced at frequency intervals of only a few kilocycles, and exhibit modal circles and diameters of many patterns.

A collection of modal patterns exhibited by a square plate $1\frac{1}{2}$ in. thick by 4 in. by $4\frac{3}{8}$ in. observed with the probe technique is given in Figure 15. In each case the drive is concentrated at one corner as indicated. These patterns are complicated with superpositions of several modes at once and are practically impossible to calculate. It is significant, however, that the frequency range covers quite thoroughly the entire range from 3 to 100 kc. However, all of them are not necessarily excited in a transducer, because a particular mode is excited only by a particular exciting force. With

a completely uniform drive at a mode frequency, the mode will not be excited, but if the drive is nonuniform (and most of them are nonuniform) some evidence of the flexural mode of the backing plate appears, and may range in importance from negligible to the controlling factor. Two such effects have been noticed, one in probe studies, the other in directivity patterns. Figure 16 shows some probe studies of a motor-crystal face close to the

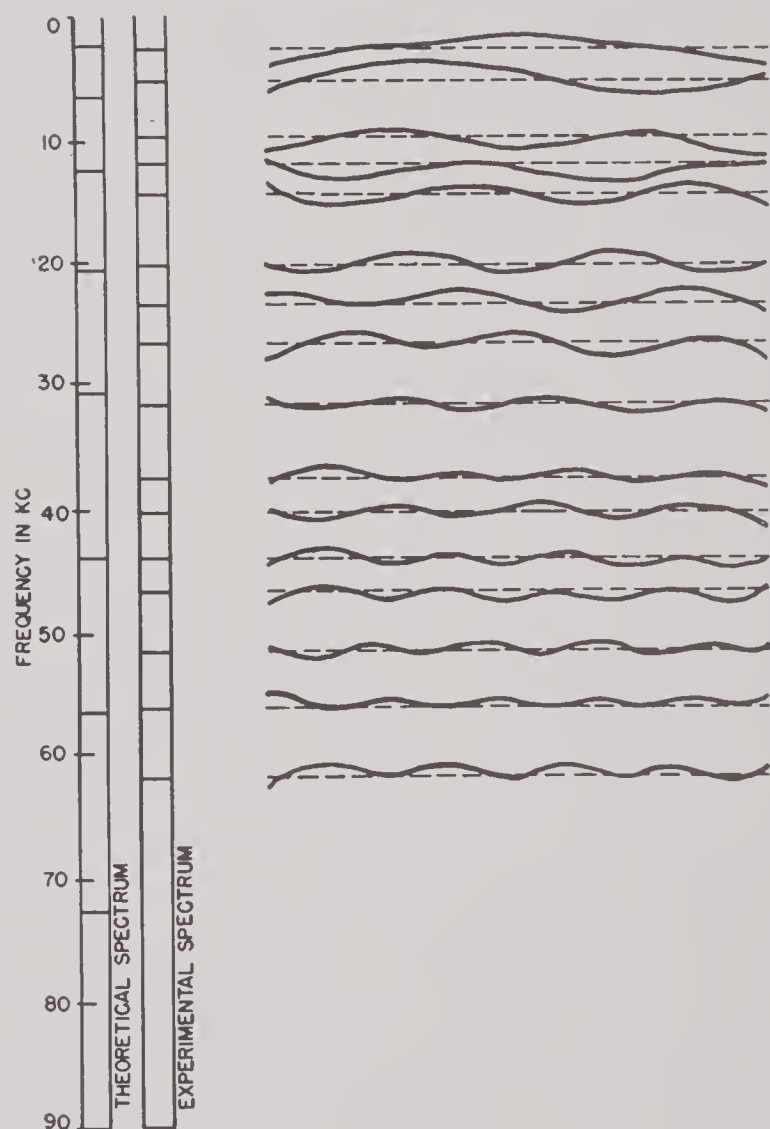


FIGURE 14. Flexural modes of steel bar, $8 \times \frac{3}{4} \times \frac{9}{16}$ in.

frequency of a backing-plate mode. The surface distributions charted there are those of phase, showing that in each case the uniform phase distribution is disturbed by the backing plate at its mode frequency. In directivity-pattern studies there are many examples of erratic behavior in backing-plate transducers at the higher frequencies, while other types (see Section 4.3) usually are not as erratic. At lower frequencies also, whimsical directivities are

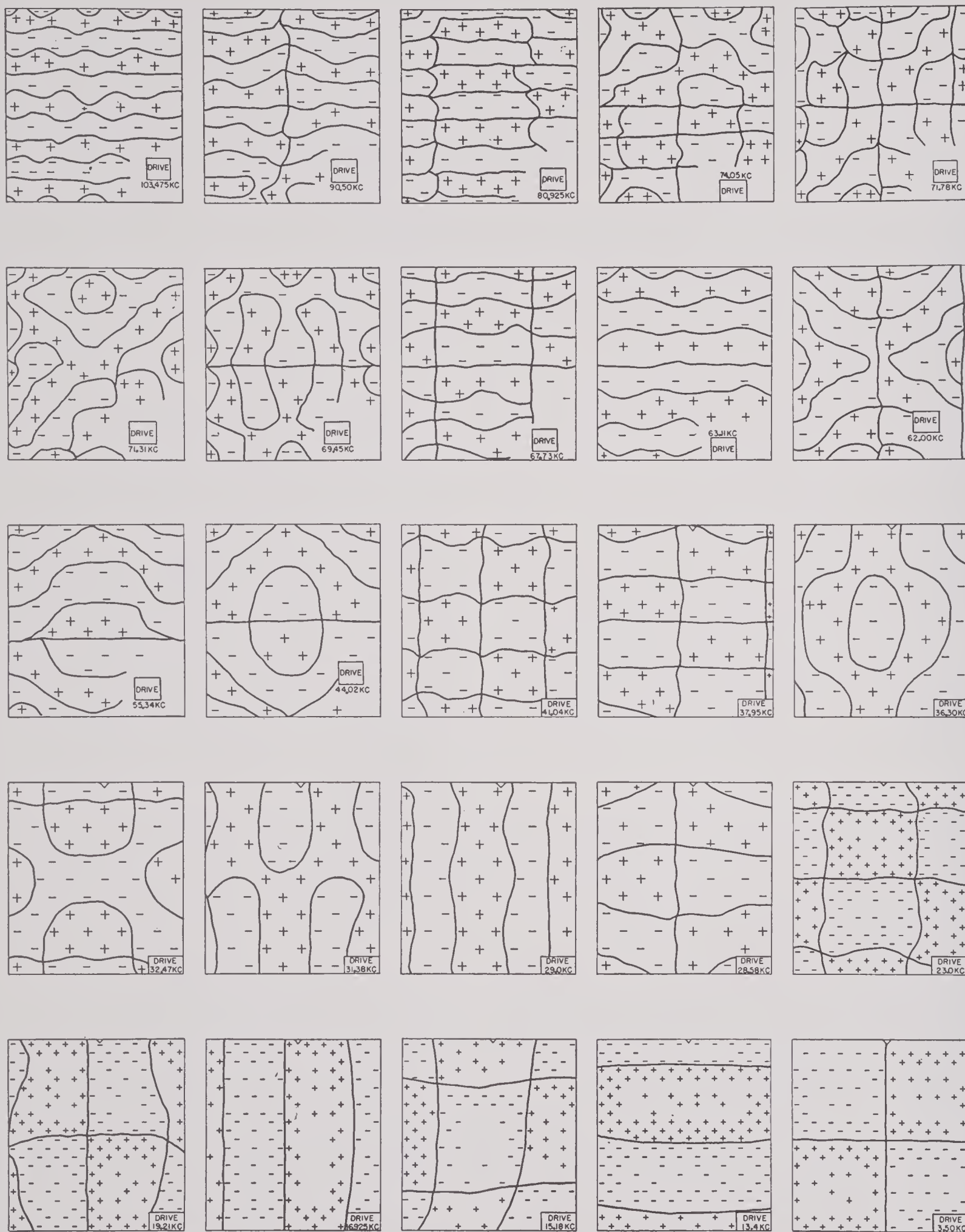


FIGURE 15. Flexural modes of square backing plate $4 \times 4\frac{3}{8} \times \frac{1}{2}$ in.

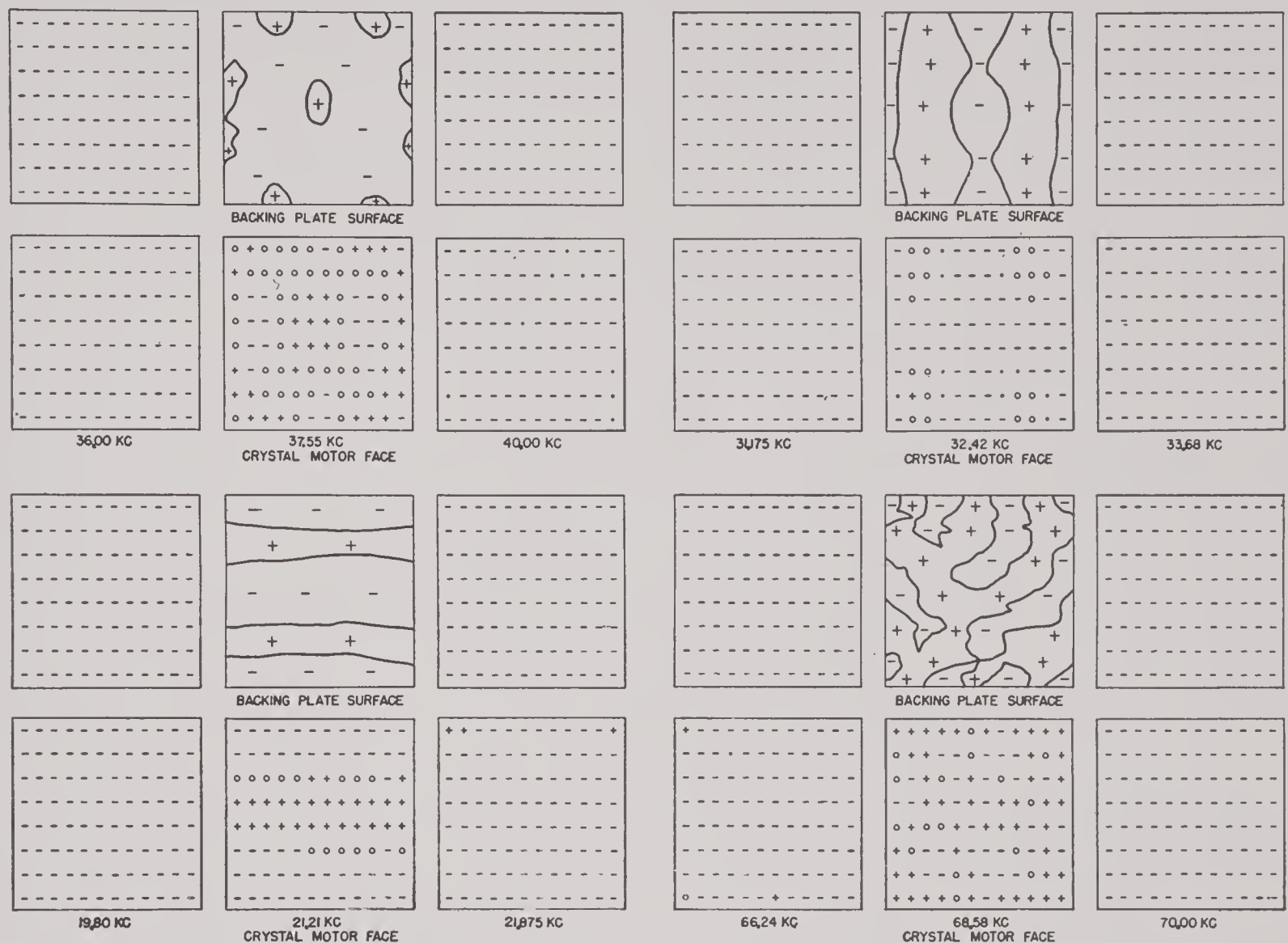


FIGURE 16. Evidence of backing-plate modes on GD28 crystal motor. Phase legend: + indicates 180° phase, 0 indicates 90° phase, — indicates 0° phase.

noticed which in some instances have been traced to irregular surface velocities and phases caused by backing-plate flexural modes.

If deep slots are cut in the back of the plate, flexural modes may be suppressed at least over a frequency band depending on the dimensions of the cuts and their spacings. The theory of this suppression is as follows.

If a rectangular bar is slotted transversely so that the remaining web is a tenth of the bar thickness, and these slots cut out sections of the bar short compared to the wavelength of flexural modes within the bar at a particular frequency, the web can, with good approximation, be thought of as a massless compliance and the remaining block as compliantless mass as shown in Figure A.

Under these assumptions the bar becomes an

acoustic low-pass filter for flexural waves whose electric equivalent is given in the figure. The circuit constants can be calculated by the method illustrated in Figure B. Each mass is joined by a thin web which under transverse vibrations acts as a beam undergoing a strain, the type of which is illustrated in Figure C. The

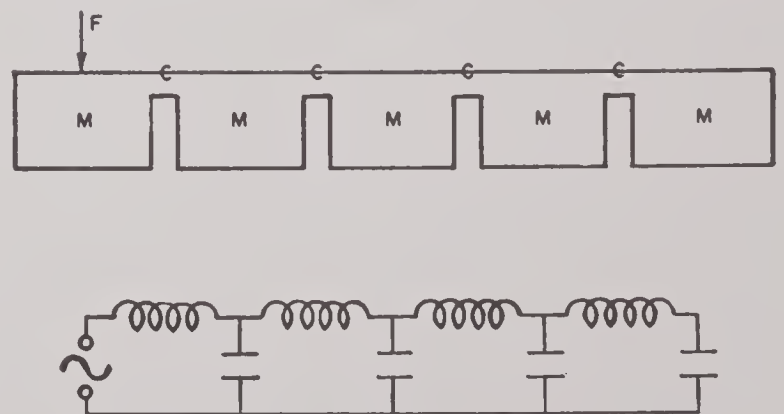


FIGURE A.

vertical compliance of such a beam is calculated to be

$$C_m = \frac{L^3}{12EI},$$

where L is the length of the beam, E is Young's modulus, and I is defined as

$$I = W \int_{-t_0/2}^{+t_0/2} t^2 dt,$$

integrated about the central unstrained horizontal plane in the bar. The cutoff frequency of this filter occurs at

$$f_c = \frac{1}{\pi \sqrt{MC_m}}.$$

Putting in the value of C_m , in which the value of I calculated for a rectangular cross section is substituted, the cutoff frequency becomes

$$f_c = \frac{1}{\pi} \sqrt{\frac{E}{\rho T d} \cdot \frac{t^3}{L^3}}. \quad (84)$$

Substituting in the values of $E = 2 \times 10^{12}$, $\rho = 7.7$, for steel, the cutoff frequency becomes

$$f_c = 64.4 \sqrt{\frac{1}{T d} \frac{t^3}{L^3}},$$

where f_c is in kilocycles, T , d are in inches.

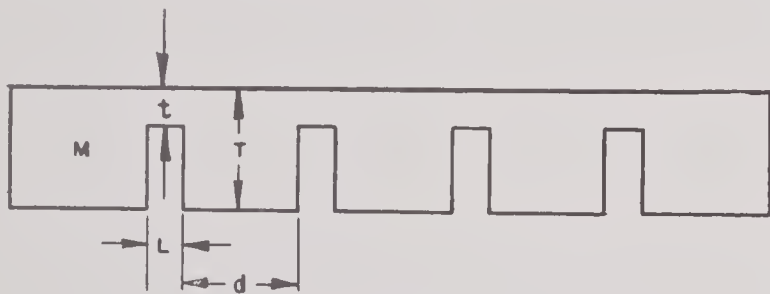


FIGURE B.

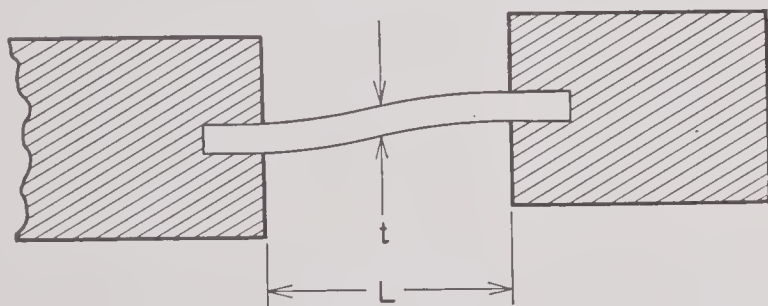


FIGURE C.

SPECIFIC EXAMPLES

QBF-Type Backing System. The backing system of the QBF transducer consists of a $\frac{1}{4}$ in. steel plate to which steel bars $1\frac{1}{8}$ in. square and 2 in. long are bolted and soldered. They are spaced $\frac{3}{8}$ in. from each other on all sides. A

single line of these elements is illustrated in Figure D. The cutoff frequency of this line calculated from the formula developed in the pre-

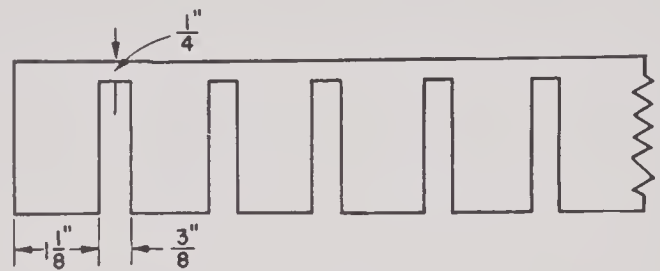


FIGURE D.

ceding section is 22 kc. This is just 2 kc below the frequency at which the unit is designed to operate.

Slotted Square Bar Backing System. This bar (Figure E) showed no eigen modes between a

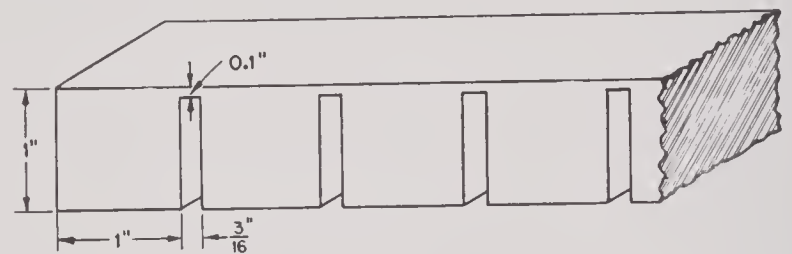


FIGURE E.

band of 30 to about 58 kc. At this upper frequency, the wavelengths are approaching the size of the blocks, so that complicated modes begin to appear. As the frequency is yet raised, the modes get very complicated and very numerous. A spectrum of frequencies of the modes is shown in Figure 17.

The spectrum of another bar similar in every respect except that the connecting webs are twice as thick ($\frac{2}{10}$ in.) is shown in Figure 17. The region of suppressed modes is much narrower in this case, showing that the web is less of a massless compliance than is the thinner web, and emphasizing the necessity of keeping the webs thin. A square plate was slotted in sections of the same dimensions as the first bar above, whose eigen modes appear in Figure 17 as the lower spectra. It is almost impossible to compute the frequencies of these modes, as the calculation involves the problem of the unbounded square plate. However, experiment shows a suppressed region for the plate as for the bars.

In conclusion it can be said that the best way

to get free of flexural modes in the motor is to isolate all crystals with their individual backing terminations from each other. If this is not feasible, flexural modes can be suppressed only within a moderate frequency range.

3.5 MULTIPLE-LAYER BACKING PLATES

Situations occasionally arise in which a backing plate is required, but the thickness or

structure may be described adequately by a transmission-line treatment (which amounts to the assumption of pure plane-wave motion). The internal losses in materials likely to be used in backing plates are so low that the assumption of a dissipationless line is justified; this simplifies the theory somewhat as hyperbolic functions revert to ordinary trigonometric functions.

A single layer of some lossless material may be represented by the equivalent circuit shown

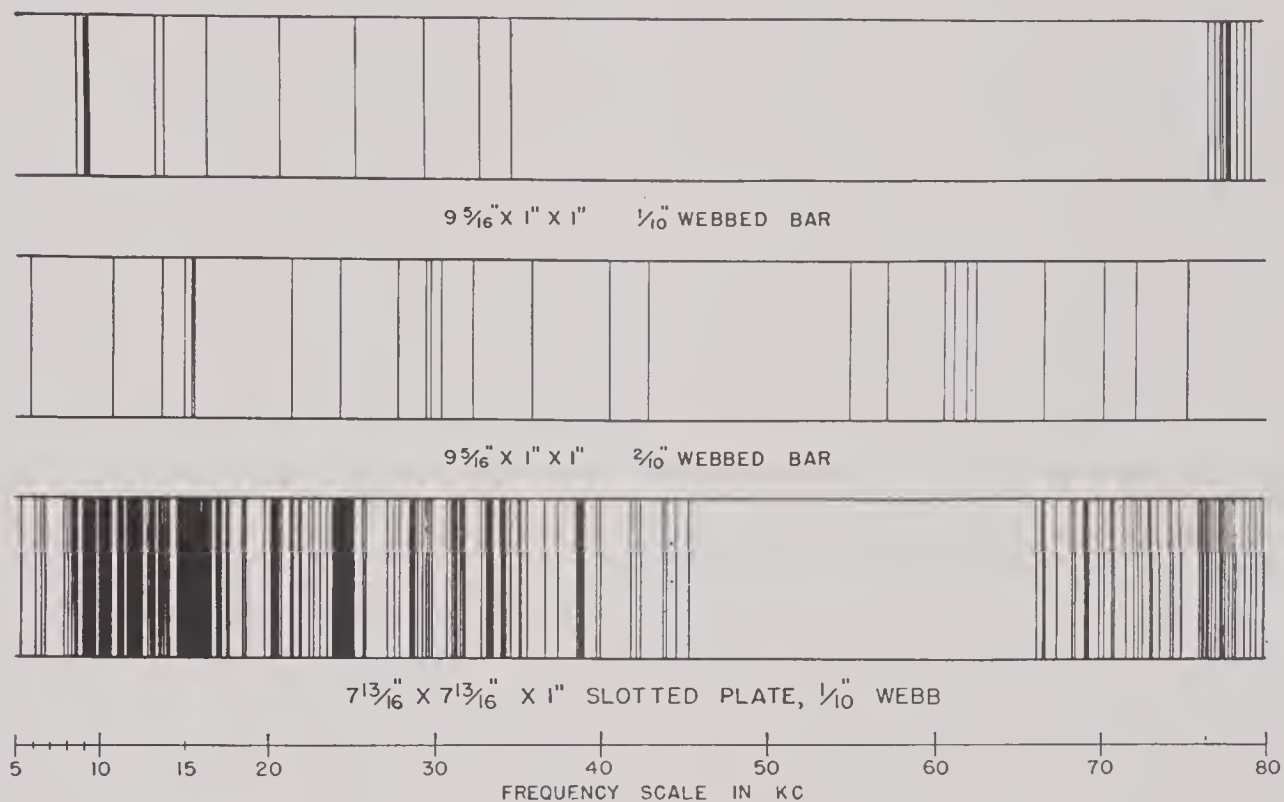


FIGURE 17. Mode spectra of slotted backing bars and plate.

weight of an ordinary plate exceeds allowable limits. Provided restricted band width is acceptable, such a situation may be aided by the use of a multiple-layer backing plate.

Consider first the two-layer system shown in Figure 18. The crystal array is cemented to a plate of thickness L_1 , characteristic impedance Z_1 , in which the velocity of sound is V_1 . This plate is perfectly attached to a second plate of different material whose thickness is L_2 , characteristic impedance Z_2 , and velocity of sound V_2 . This second plate is then terminated by air or other substance whose characteristic impedance may be considered zero.

If the motion of the crystals is simple, uniform, and in phase, and if flexural resonances, etc., in the plates are successfully avoided the

in Figure 19, where Z_0 is the characteristic impedance of the material, and

$$\theta = \frac{\omega L}{V},$$

where L is the thickness of the layer and V is the velocity of sound.

It is easily shown that if an arbitrary complex impedance Z_T is imposed on one end of this line the impedance Z_I seen looking into the other end of the line is

$$Z_I = Z_0 \frac{Z_T \cos \theta + jZ_0 \sin \theta}{Z_0 \cos \theta + jZ_T \sin \theta} \quad (85)$$

Note in passing that if the thickness and fre-

quency are such that the plate is exactly a quarter wave thick then

$$\theta = \frac{\pi}{2},$$

and

$$Z_I Z_T = Z_0^2.$$

In particular, if a lossless quarter-wave line is terminated by zero impedance the input impedance at the other end of the line (other face of the plate) is infinite. This is the basis on which

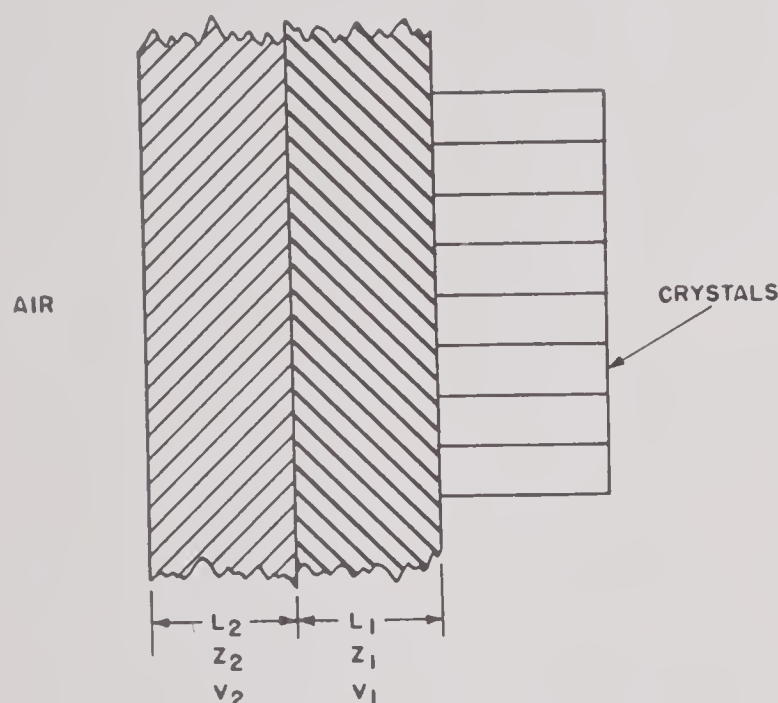


FIGURE 18. Typical two-layer backing plate.

ordinary backing plates are chosen. Note also that if the plate is an eighth wave thick and terminated by air then

$$Z_I = +jZ_0.$$

Since the characteristic impedance (Z_0) of steel is much greater than that of crystals, an eighth-wave plate provides a sufficiently high impedance to nearly clamp the crystals.

Note finally that if the layer is a half wave thick (or any integer multiple of a half wave) then

$$Z_I = +Z_T.$$

This indicates that any integer number of half-wave sections may be "lifted out" of a lossless line without changing the impedances at the ends.

Returning to the problem presented in Figure 18 and using the equation above, one may calculate the impedance seen looking into plate No. 2 from the interface between the plates. The impedance so calculated then becomes the termination impedance imposed on plate No. 1, and the impedance Z_R seen by the crystals looking backward into the plates is readily obtained. The result is:

$$Z_R = jZ_I \frac{Z_2 \tan \theta_2 + Z_I \tan \theta_1}{Z_I - Z_2 \tan \theta_1 \tan \theta_2}. \quad (86)$$

The question now arises: under what conditions is Z_R infinite? Obviously solutions will be obtained when

$$Z_I = Z_2 \tan \theta_1 \tan \theta_2 \quad (87)$$

(with reservations concerning the behavior at the poles which, it will be seen, are of no practical importance).

For any given ω there are an infinite number of L_1, L_2 combinations which satisfy this condition. Obviously the quantity $L_1 + L_2$ (where L_1 and L_2 satisfy the condition) will be some function of L_1 , and the problem is now to select the optimum L_1, L_2 combination.

The problem is solved here on the assumption

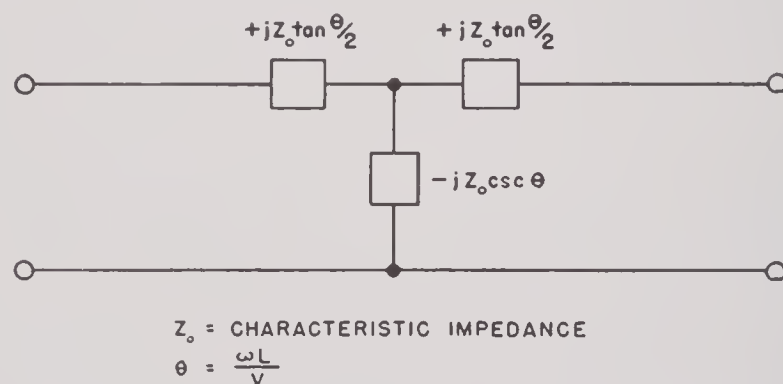


FIGURE 19. Equivalent circuit of a single layer of lossless material.

that the optimum backing plate will be the *thinnest* backing plate obtainable with any particular pair of materials at any specified frequency. One might instead require that the total *mass* be minimized, and different conclusions would be reached by analogous methods.

It is desired to minimize $L_1 + L_2$, subject to equation (87). The method of Lagrange multipliers is used. The theory of this method is

available in standard works on theoretical physics.⁹ We form the function

$$F = L_1 + L_2 + A \left(\tan \theta_1 \tan \theta_2 - \frac{Z_1}{Z_2} \right),$$

where A is an undetermined multiplier.

Partially differentiating:

$$\frac{\partial F}{\partial L_1} = 1 + A \frac{\omega}{V_1} \tan \theta_2 \sec^2 \theta_1,$$

$$\frac{\partial F}{\partial L_2} = 1 + A \frac{\omega}{V_2} \tan \theta_1 \sec^2 \theta_2.$$

Setting these equal to zero, transposing V 's and dividing one equation by the other:

$$\frac{V_1}{V_2} = \frac{\tan \theta_2 \sec^2 \theta_1}{\tan \theta_1 \sec^2 \theta_2}.$$

It is quite convenient that A cancels out, obviating the usual necessity of evaluating the multiplier.

Substituting,

$$\sec^2 \alpha = 1 + \tan^2 \alpha$$

$$\text{and} \quad \tan \theta_2 = \frac{Z_1}{Z_2 \tan \theta_1},$$

we obtain

$$L_1 = \frac{V_1}{\omega} \tan^{-1} \left[\frac{\frac{Z_1}{Z_2} \left(\frac{Z_1}{Z_2} - \frac{V_2}{V_1} \right)}{\frac{Z_1 V_2}{Z_2 V_1} - 1} \right]^{\frac{1}{2}}, \quad (88)$$

$$L_2 = \frac{V_2}{\omega} \tan^{-1} \left[\frac{\frac{Z_1}{Z_2} \left(\frac{Z_1 V_2}{Z_2 V_1} - 1 \right)}{\frac{Z_1}{Z_2} - \frac{V_2}{V_1}} \right]^{\frac{1}{2}}. \quad (89)$$

These expressions serve two useful purposes. Firstly they give a criterion for the *existence* of the minimum, and secondly they give numerical values of L_1 and L_2 to *achieve* the minimum.

To use the functions as criteria, one selects two materials of interest such as lead and steel. The values of characteristic impedance and velocity of sound are inserted in the expressions under the radicals. If the resulting quantity is negative no minimum in $(L_1 + L_2)$ exists, and the minimum thickness is achieved by 100 per cent of whichever material has the lower V . If the quantity is positive a minimum does exist, and minimum total thickness is achieved by using plates whose thicknesses are L_1 and L_2 .

The criterion concerns combinations of two

materials, independent of frequency, and a list is easily composed telling which pairs of materials yield a minimum. In applying the criterion it is immaterial which is considered plate No. 1 and which plate No. 2. Some results of the criterion are:

Steel; lead: no minimum; use 100% lead,

Steel; castor oil: minimum exists,

Steel; aluminum: minimum exists,

Steel; copper: no minimum; use 100% copper,

Steel; tin: minimum exists,

Steel; glass: minimum exists,

Steel; brass: no minimum; use 100% brass,

Aluminum; castor oil: minimum exists,

Aluminum; lead: no minimum; use 100% lead,

Aluminum; glass: minimum exists,

Lead; castor oil: minimum exists,

Lead; copper: no minimum; use 100% lead,

Lead; glass: no minimum; use 100% lead,

Glass; castor oil: minimum exists.

It is interesting to note that in more than half of these randomly chosen examples the minimum does exist. This should encourage a search for other promising pairs, such as glass; silicone fluid.

When applying the criterion the order of the two layers is immaterial. However, it is very important that the layers be ordered correctly if a minimum does exist. In this case two combinations of L_1 , L_2 will result from the two orders in which the materials may be arranged. One of these will be the minimum thickness sought, the other will be *maximum*. This results from the fact that Lagrange's multiplier yields an extreme solution, either maximum or minimum; the ambiguity is easily resolved for any pair of materials by obtaining both solutions.

The \tan^{-1} functions are, of course, multiply periodic. Examination will show that the periodicity corresponds to the addition of increasing numbers of half wavelengths of material. It was shown previously that such a layer contributes nothing, and it is clear that the smallest solution is always to be taken.

It will be made clear by the example below, that if a minimum exists, both L_1 and L_2 will be less than a quarter wave thick. This then

justifies ignoring the poles in the original function.

To illustrate the great economy of space possible by this method, consider the problem of producing a clamping backing plate at 24 kc. The velocity of sound in steel is usually taken as 197×10^3 in. per sec, and a quarter-wave plate at 24 kc is 2.05 in. thick. Compare with this a two-layer plate using steel and castor oil:

Steel

$$Z_2 = 39 \times 10^5$$

$$V_2 = 5 \times 10^5$$

Oil

$$Z_1 = 1.5 \times 10^5$$

$$V_1 = 1.5 \times 10^5$$

(in cgs units)

and at 24 kc: $\omega = 1.51 \times 10^5$.

The order of materials indicated by the subscripts is chosen to yield a minimum. The values of L_1 and L_2 given by the criterion functions equations (88) and (89) are:

$$L_1 \text{ (oil)} = 0.362 \text{ cm} = 0.144 \text{ in.},$$

$$L_2 \text{ (steel)} = 0.334 \text{ cm} = 0.131 \text{ in.}$$

The total thickness ($L_1 + L_2$) is 0.275 in. as compared with 2.05 above: a saving of more than a factor of 7. Notice also that although ($L_1 + L_2$) was minimized, rather than mass, the weight per unit area is reduced by a factor of 13.

If the steel and oil positions were reversed a very thick plate would result. At first sight the design problems of providing the oil layer of controlled thickness between the crystals and the steel seem discouraging. Actually the problem would be relatively simple if the crystals were supported in a jig and the oil layer obtained by shims under the jig. The spacing is not quite as critical as it might seem since the functions are linear in ω . Use of silicone or Univis oil should correct any temperature dependences.

The complexity of the problem increases rapidly as more than two layers are used. For one thing the Lagrange multiplier does not drop out as easily, and the number of simultaneous equations increases. Solutions have been obtained for a three-layer system backed by air, and the equations for L_1 and L_3 are the criterion

functions while L_2 acts as a connection function:

$$L_1 = \frac{V_1}{\omega} \tan^{-1} \left[\frac{Z_1}{Z_2} \left(\frac{\frac{Z_2}{Z_1} - \frac{V_1}{V_2}}{\frac{Z_2 V_1}{Z_1 V_2} - 1} \right) \right]^{\frac{1}{2}}, \quad (90)$$

$$L_2 = \frac{V_2}{\omega} \tan^{-1} \left[\frac{Z_1 Z_2 - Z_2 Z_3 \tan \theta_1 \tan \theta_3}{Z_1 Z_3 \tan \theta_3 + Z_2^2 \tan \theta_1} \right], \quad (91)$$

$$L_3 = \frac{V_3}{\omega} \tan^{-1} \left[\frac{Z_2}{Z_3} \left(\frac{\frac{Z_3}{Z_2} - \frac{V_3}{V_2}}{\frac{Z_3 V_3}{Z_2 V_2} - 1} \right) \right]^{\frac{1}{2}}. \quad (92)$$

For single-frequency operation there appears to be no advantage in more than two layers, and aside from the greater engineering complications the functions seem to be more critically dependent on the layer thicknesses. This is particularly true of L_2 which depends on the tangents of θ_1 and θ_2 . It has not been investigated, but the third layer undoubtedly offers another degree of freedom by which the impedance could be adjusted at two arbitrarily chosen frequencies.

It is apparent that this saving is achieved by using a pole of a function. Plotting Z_R against ω indicates that the high impedance is obtained over a band much narrower than that of a single steel plate. Consequently this method is restricted to applications requiring a somewhat restricted band width. However, the restrictions are not severe, and the possibility of quite practical transducers invites further examination of this method.

A final comment is required concerning the physical interpretation of these theoretical results. Both L_1 and L_2 are much less than $\frac{1}{4}$ wave in the respective media, so the phase change through each plate is small. However, a phase change occurs at the interface, and this quite large change brings the total phase change up to $\pi/2$. This points up sharply a caution not always observed: thin layers of material adjoining layers of very different material may introduce unexpectedly large effects, and a designer can ignore such layers only at the risk of considerable error.

3.6 PROBE EXAMINATION OF MOTORS

It is desirable that a transducer present the same velocity-amplitude and phase over its entire radiating face to the medium. Many factors arise to thwart this ideal, among which are: nonuniformity of crystal drives, backing-plate flexural modes, cavity modes of transducer cases and intercrystal couplings. The effects of all these factors working together are noticed in the erratic directivities, impedances, and sensitivities of the completed transducers. With

shows the effect of gluing the array to a backing plate. This array is made up of carefully selected crystals, and will be described in detail later in this section. Figure 21 shows a contrast of measurements of this motor made both in air and in oil. Phases as well as amplitudes are included in this figure. Figure 22 shows the velocity distribution in air over the face of another motor designed to have two velocity areas for directivity lobe suppression.

These figures show wide variations of both phases and amplitudes in individual crystals.

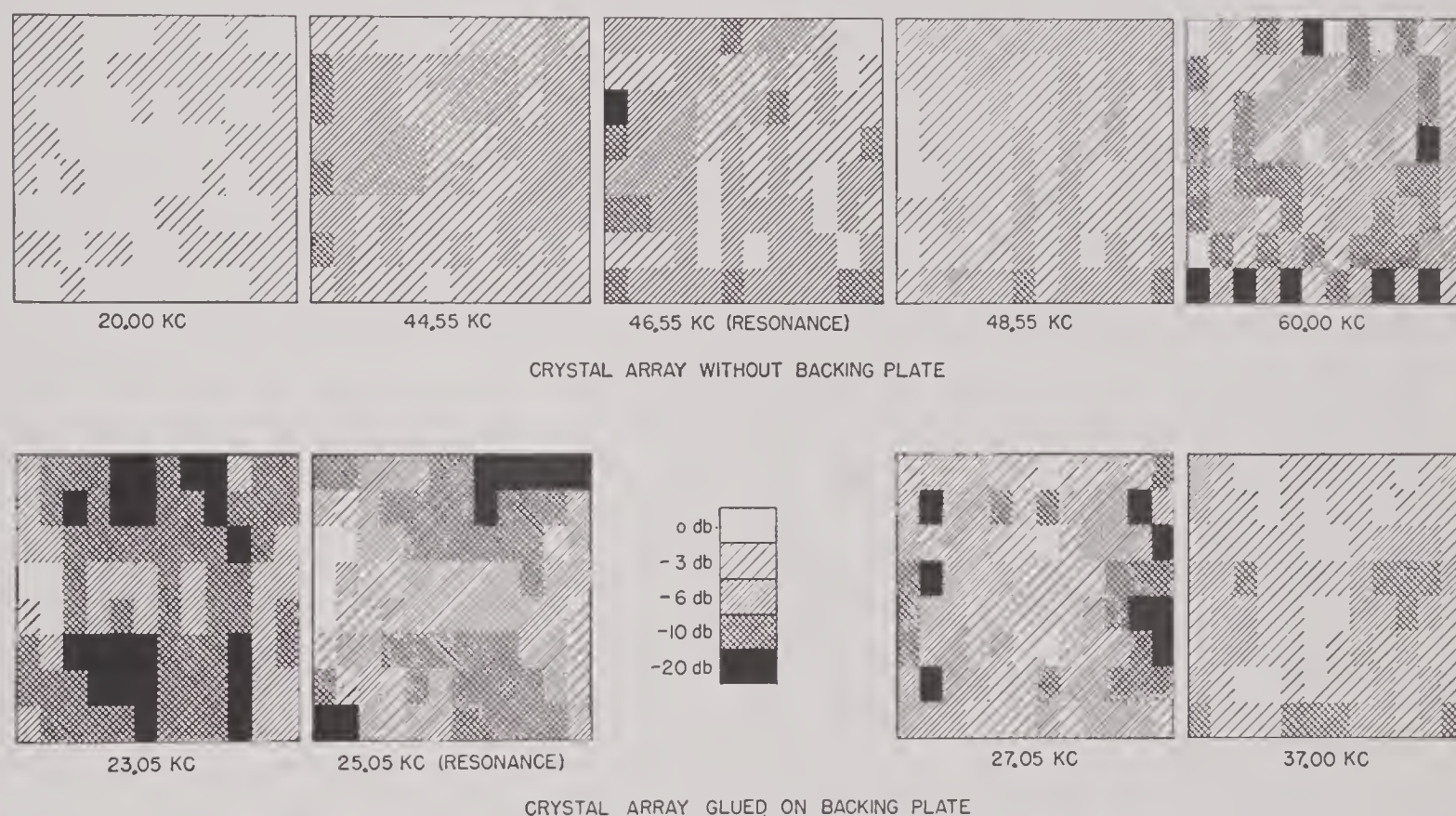


FIGURE 20. Velocity distributions of GD28-1 crystal array with and without backing plate.

probe examination, the individual behavior of each crystal can be studied as to its relative velocity, phase, and frequency response.

The techniques of probe examinations are discussed in Chapter 9. Motors are probed both in air and in oil. Measurements in air are not benefited by the proper impedance loading on the motor, but they are easier to make, and they reveal vibrational modes which undergo no basic change when loaded with liquid. Figure 20 shows velocity distributions of a motor at several frequencies under different conditions. The upper group shows the effect of loading one side of a crystal array, and the lower group

Usually, the variations are less when loaded with an oil medium, but not always. Variations are observed sometimes over the surfaces of individual crystals. At the resonant points of the motor the variations are greatest, probably because the individual crystal resonances have a distribution in frequency. This condition suggests a design that separates the operating and resonance frequencies if uniform velocities are important. Thus it is not surprising that some directivities show erratic behavior, particularly in the side lobes, as this nonuniformity would control them more than the main lobe (see Section 4.3 on directivities).

As an example of the control over construction possible with this technique, the history of the GD28 will be cited. The GD28 is a transducer made up with 96 $\frac{1}{4}$ by $\frac{3}{8}$ by 1.2 in. Y-cut crystals glued on a $\frac{1}{2}$ by $4\frac{1}{2}$ by 4 in. steel backing plate. Every step of the construction was closely controlled, and measurements were made on the unit at each step.

The crystals were first individually measured for activity by the probe and by the position of

in frequency graph, the resonant frequencies appear as shown in Figure 23. The maximum variations in resonant frequencies ranged from 45.4 to 47.9 with a mean at 46.80 kc. The mean deviation was, however, quite small, being 0.42 kc which is about 0.9 per cent. The variations are, however, larger than those of the unassembled crystals. The relative velocities of each crystal at resonance are plotted in a distribution in velocity chart shown in Figure 24. The ve-

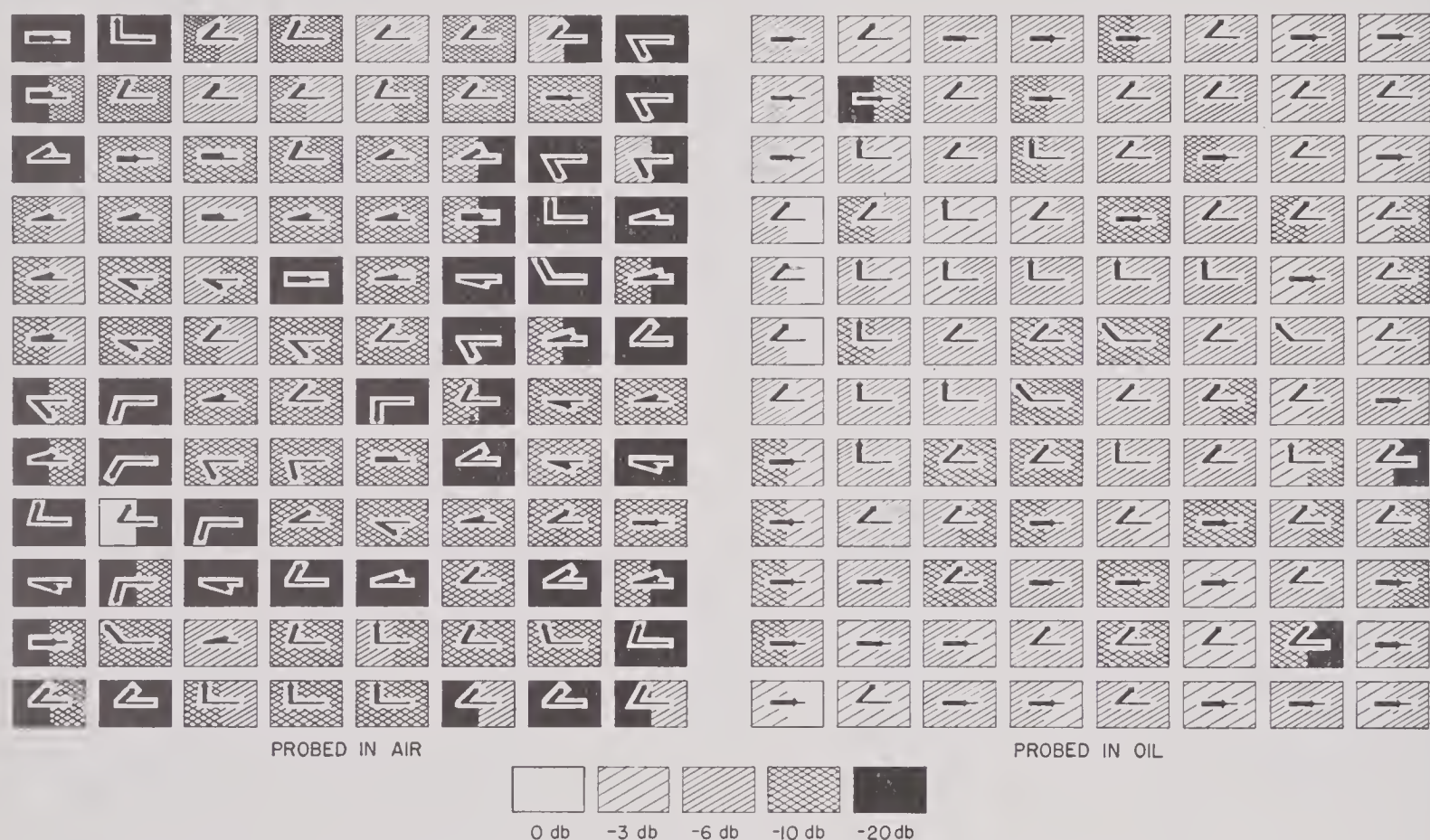


FIGURE 21. Velocity and phase distributions of GD28-1 motor in air and in oil at 25.5 kc.

the discontinuity in the overall impedance curve, and only those that were within a 3-db limit of activity under constant voltage were chosen. The resonances of all crystals were held between 46 and 47 kc. They were then assembled into a matrix 8 by 12 crystals, each crystal separated from its neighbor with $\frac{1}{8}$ -in. sponge rubber. No glue was used in the construction, the matrix being held together loosely with a clamp. The resonant frequency of each crystal was then measured; relative velocity of each crystal at resonance and velocity distributions over the face of this motor were measured at five frequencies. When plotted in a distribution

locities vary over a considerably wider range than 3 db, the initial tolerances. Figure 20 shows the surface-velocity distribution of the motor at other frequencies. The variations at resonances are larger than at other frequencies unless the frequencies are high enough to excite complicated modes. It seems that in this case, at least, the foiling and assembling of 96 crystals into a matrix has contributed to their individual differences in resonant frequencies and sensitivities.

The crystal matrix was then glued on the $\frac{1}{2}$ -in. steel backing plate with the baked bakelite gluing technique developed in this labora-

tory (Chapter 8), and the measurements repeated. The charts of resonant frequencies and velocities at resonance are in Figures 25 and 26, and the velocity surface distributions at four frequencies are shown in Figure 20. The

percentage distribution of 2 per cent on the backing plate is considerably less than 21 per cent off the backing plate. However, the surface-velocity distributions shown on Figure 20 indicate wider limits of variations in the velocities

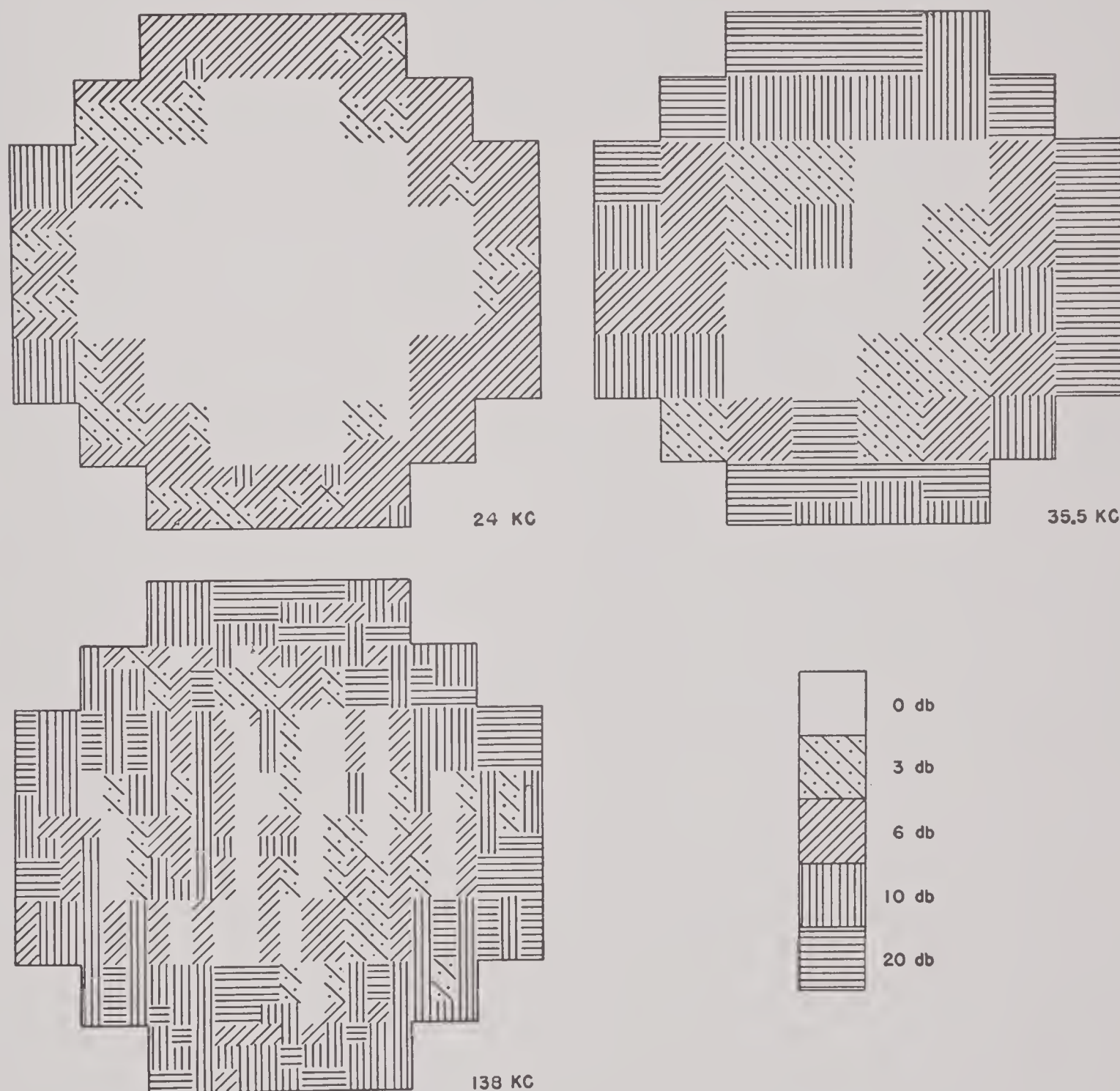


FIGURE 22. Velocity distributions of QBF motor in air.

mean percentage deviations in the resonant frequencies with and without backing plate are about the same showing that the backing plate had little effect in perturbing this distribution. The surface-velocity distributions at resonance are shown on Figure 26. In this case the mean

with the plate than without. These large limits probably are caused by unequal gluing of the crystals.

The effect of the backing-plate modes on the crystal-surface velocities are shown on Figure 14, Section 3.4. The plate modes chosen were re-

moved from the resonance of the crystals far enough to be free of complications of that sort. Figure 14, Section 3.4, shows the modes of the free plate. There are no modes at frequencies *between* the ones shown there. At 21.21, 37.42, 37.55, and 68.58 kc prominent modes were mapped from the back of the backing plate, and

effect of flexural modes upon the overall response of a transducer was encountered in another unit known as the JC2Z1. This unit is 12 in. in diameter designed to operate at 24 kc with a lobe suppression scheme of two velocity zones whose velocity ratios were 3 to 1. The response curve is shown in Figure 27. At 24 kc the re-

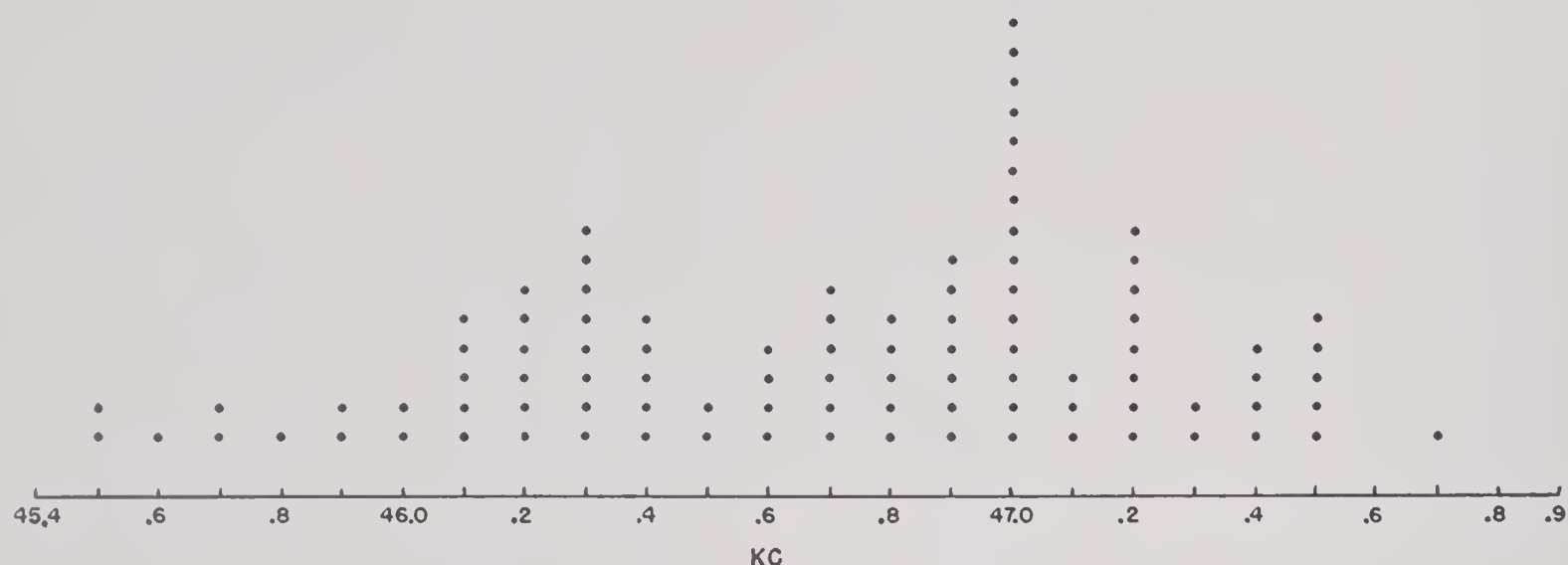


FIGURE 23. Distribution of resonant frequencies of GD28-1 motor without backing plate. Mean: 46.80 kc. Mean deviation: 0.42 kc.

the corresponding phase distributions of the crystal surfaces were mapped. To assure the irregular crystal phases at the mode frequencies being due to these modes, phase distributions at frequencies slightly removed were also mapped and shown in the figure. In every case the fre-

sponse has a 5.5-db dip instead of a peak thus rendering the unit useless for its intended service. Its directivity pattern at 24 kc was badly distorted showing no symmetry or regularity. Probe examinations revealed, at this frequency, a prominent flexural mode in the backing plate

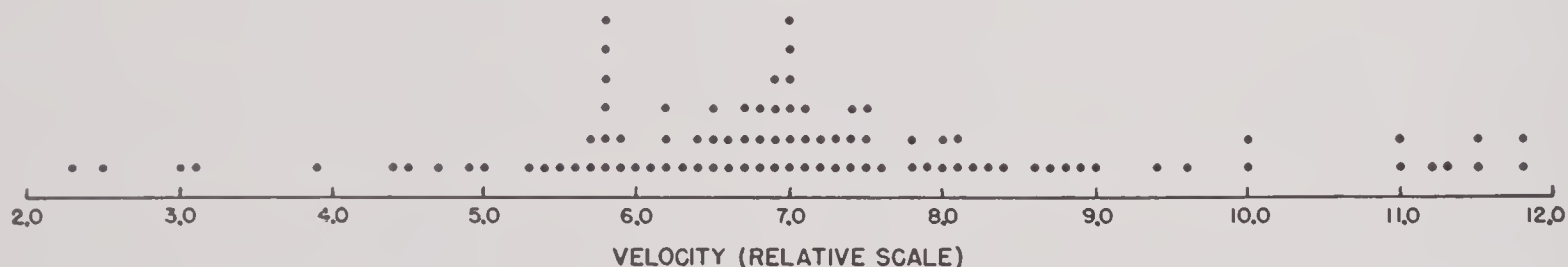


FIGURE 24. Distribution of velocities at resonance in GD28-1 motor without backing plate. Mean: 7.04. Mean deviation: 1.48.

quencies off the modes gave uniform patterns, while the mode frequencies gave irregular phase patterns.

Studies of the GD28 reveal in a general way many interesting things about the combined actions of crystals coupled together through a steel plate, but specifically, the data are not complete enough to warrant many general conclusions about its overall performance. A clear-cut

that had a nodal circle at about the boundary of the two velocity areas. The central part was thus 180° out of phase with the outer ring. Probe examination in air of the velocity amplitude of the inner crystals is shown in Figure 27 showing a large dip in their activity at 24 kc. The crystals of this unit were grouped four to the group, and glued on a backing plate of steel $\frac{3}{4}$ in. thick, backed up with an additional layer

0.638 in. thick of a low-melting metal called Cerrobend. For the purpose of separating the effects of the longitudinal modes from the flexural of this backing system upon the motor face, individual units consisting of four crystals

individual crystals, but the frequencies of the crystal dips vary from crystal to crystal covering a region of 21 to 25 kc, thus softening this general dip for the transducer.

Probing technique has not yet been developed

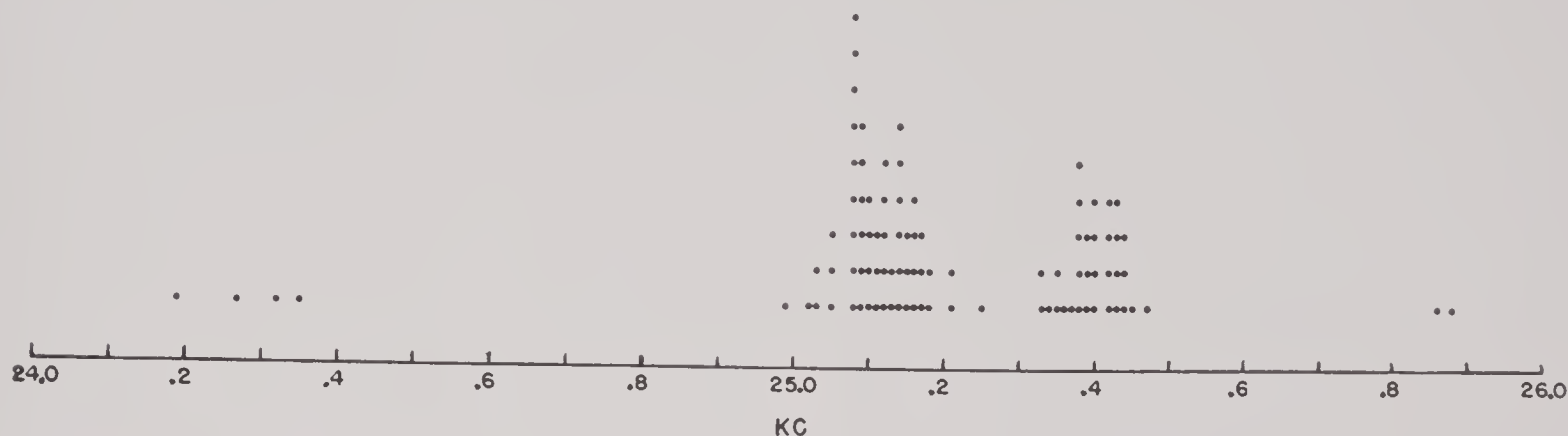


FIGURE 25. Distribution of resonant frequencies of GD28-1 motor with backing plate. Mean: 25.19 kc. Mean deviation: 0.177 kc.

cemented to a 1-in. sq cross section of this backing system were prepared and probed. The general response of such units is shown in Figure 27 by the dashed curve. No sharp dip is

to the point of establishing accurate cause and effect relations between surface velocities and directivities or calibrations, but many valuable uses of it can be made as a tool in controlling

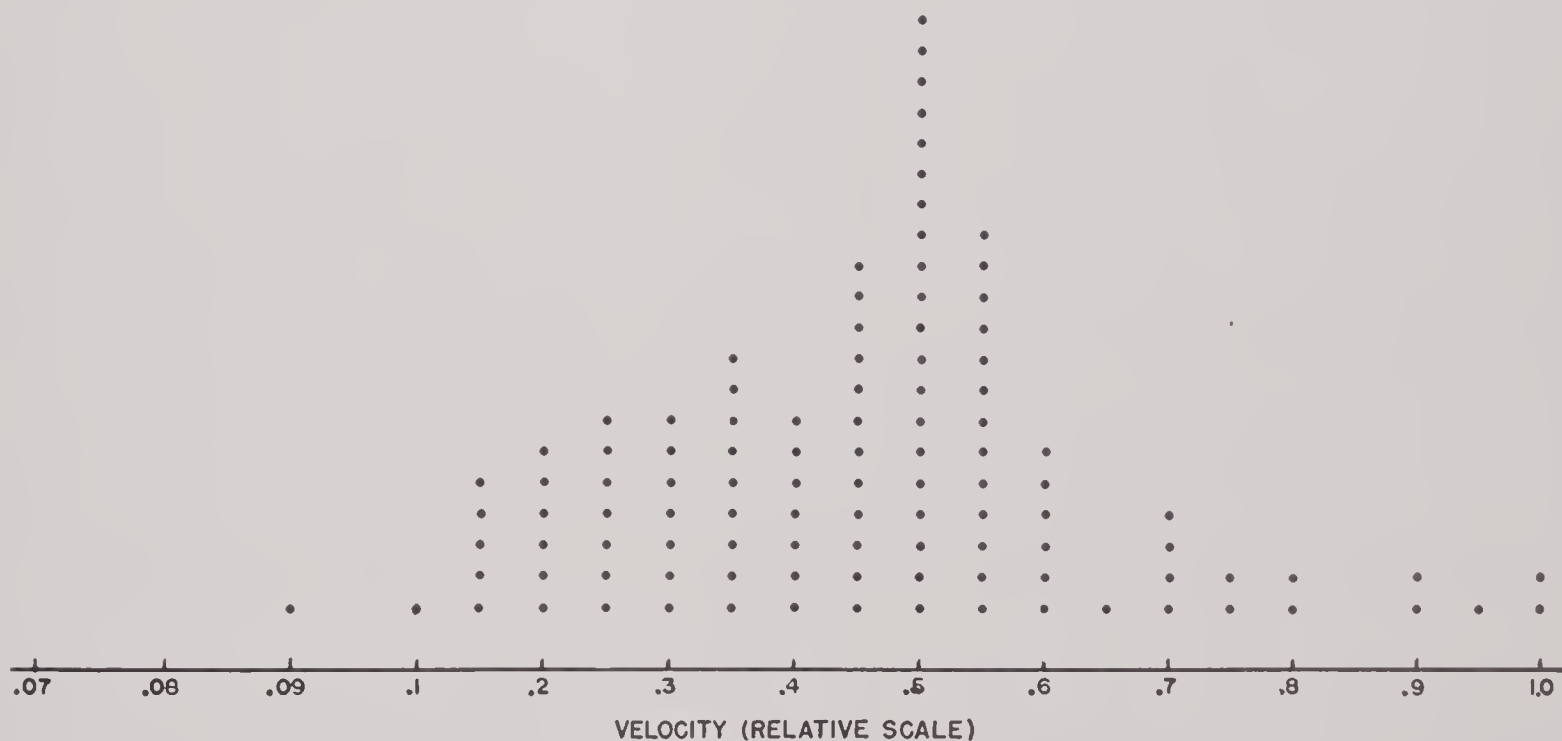


FIGURE 26. Distribution of velocities at resonance in GD28-1 motor with backing plate. Mean: 0.44. Mean deviation: 0.01.

evident, which means that the dip in the motor must be due to flexural modes of the large plate. The response curve of the transducer in water does not have such a sharp dip at 24 kc as do the

the construction of transducers. A few examples of its use have been cited which encourage its development to refinements that will enable it to give more exact information about

the inner workings of transducers. Such information is necessary before accurate design procedures can be established.

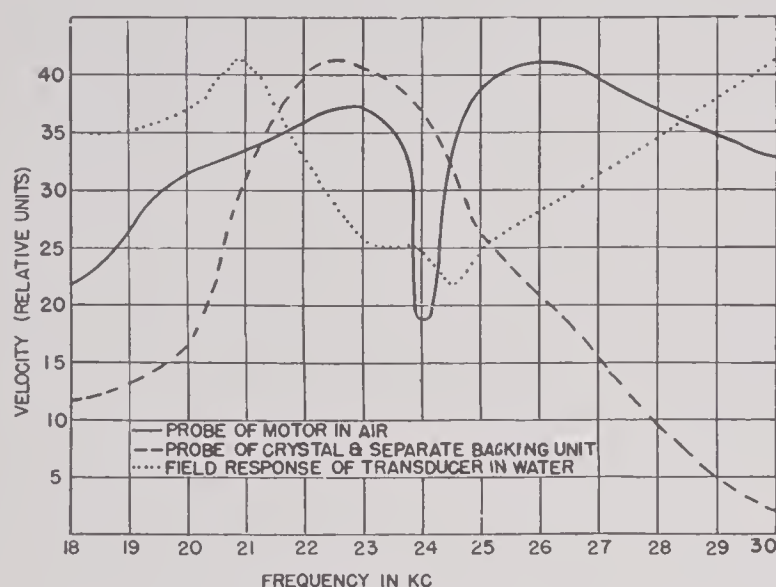


FIGURE 27. Probe studies of the JC2Z-1 transducer.

3.7

PARASITIC MODES

3.7.1

Solid Parts

The transducer case includes all the parts required to hold the active components together and to fulfill the assorted mechanical requirements which may be put on a transducer. Thus, in certain instances, it may be profitable to regard the mounting structure, a streamlined dome, and even the entire hull of a ship as the "case." In general, any part which is not of itself an active part but which is or may be acoustically coupled to active parts should be regarded as part of the transducer case; the degree to which any such passive part affects the transducer behavior depends on the degree to which it is coupled. At the least, the case consists of whatever barrier separates the crystals from the sea water.

Usually the case includes several metal or glass parts: materials of moderately high mechanical Q . Also the frequencies are usually such that the dimensions are "comparable with a wavelength" in these materials. It is to be expected that resonances of the case corresponding to various compressional, flexural, and torsional vibrations will occur in the de-

sired operating frequency band. Except in very rare instances the case structure is so complex that calculation of these resonances is impossible; this very complexity probably increases the number of resonances which may occur in a given frequency band.

These resonances may be divided into two kinds: (1) those in which the vibration leads to radiation into the water or other fairly high resistance; (2) those in which the vibration is only slightly damped. The first kind will have relatively low Q and will exert their influence over a considerable frequency band; the second kind will affect only a very narrow band. The line of demarcation is hypothetical; actually resonances grading from one extreme to the other may be encountered.

Since resonances of the first kind are damped, the impedance into which energy must be put to excite them will be relatively high even at resonance. For this reason, they usually absorb relatively less energy and the effect on the desired frequency-response curve of the transducer is not great. However, these vibrations may radiate significant amounts of energy in directions (and phases) at which the primary radiating face radiates very little, and it is quite likely that the directivity patterns will be distorted by this radiation.

The second kind of resonance radiates no significant energy and can influence directivity patterns only indirectly. For this reason, it is unlikely that such a resonance will affect the directivity patterns. Instead, the low impedance presented at resonance is likely to absorb a large amount of energy which will simply run around in the structure and ultimately be expended in internal losses. The result is usually a rather deep hole in the frequency response of the transducer.

Bearing these properties in mind, one has certain clues to correcting misbehaviors in a transducer. If a sharp hole appears in a frequency-response curve, one is inclined to question the behavior of various internal parts which do not contact the water; if the directivity patterns are distorted, one questions the behavior of the external structure and of the backing plate. Of course, these effects are greatly complicated by cavity modes (see Sec-

tion 3.7.2) and by the various vibrational modes which may occur in the active parts (for example, see Section 3.4) so that a trial and error method is required to find the cause of a given misbehavior.

Since the modes which may occur in a transducer case are beyond calculation, it is best to strive at the outset to avoid exciting any mode. This may be done by designing with three rules in mind: (1) minimize the number of parts; (2) attempt to choose dimensions which are not likely to resonate in the operating frequency band; (3) incorporate as much isolation as is practical so as to decouple the case from the active parts. A more detailed discussion of the methods of accomplishing this is given in the section on design procedures in Chapter 6.

3.7.2

Cavity Modes

The distinction between cavity modes and case modes (Section 3.7.1) is not definite, but a rough distinction is profitable. Frequently a transducer contains castor oil or some similar liquid to couple the crystals to the sea water. In one sense, this liquid is part of the case and the remarks about case modes are pertinent here too. However, there is at least one great difference, and that is that the liquid cannot be wholly decoupled if it is going to fulfill its function. Thus, one is presented with a mass of castor oil, contained in some usually peculiar shape, through which vibrations of a particular kind must be propagated. Even if the walls of the container were perfectly rigid, vibrational modes might exist within this cavity. Since the boundaries are actually case components, there are complicated impedance-boundary conditions imposed which bring in questions of case resonances as well as cavity resonances. In general, we may crudely visualize vibrational modes which are dominated by cavity geometry and call them cavity modes.

Like the case modes, these cavity modes are beyond calculation. If the dimensions of the cavity become comparable with a wavelength in the cavity medium, resonances must be anticipated; and the more complicated the cavity shape, the greater the likelihood of their being

troublesome. Such a cavity mode may have any Q , depending on the boundary impedances, and may or may not radiate into the water. Usually the most noticeable effect is on response curves rather than on directivity patterns, although the latter may be affected.

If trouble is encountered and a cavity mode is suspected, only two courses of action are known: (1) drastically change the cavity geometry in hopes that some change will be effective and no new modes will be formed; (2) decouple as much as possible by putting foam rubber or similar material on the crystals and other parts if necessary. Obviously, the first method is based wholly on wishful thinking unless it is possible to so alter the geometry that no dimension remains comparable with a wavelength. In that event, this first method is preferable; otherwise, the second is more likely to work in a small number of attempts. In fact, this second method has been so successful that it is now common practice to put foam rubber in during initial construction. Actually, when one puts in foam rubber and it works, one wonders forever after what was cured; the cavity modes, case modes, etc., cannot be artificially divorced from each other.

Every transducer presents a new problem. By experience and intuition one may acquire the knack of recognizing which structures are most likely to give trouble, but this skill is very limited and occasional unpleasant surprises will always occur. It is essential that the designer be constantly aware of case and cavity modes as possible explanations of misbehavior, since erroneous diagnosis is very easy.

3.8

WINDOWS

In crystal transducers, the window may serve to separate two liquid media, as sea water and castor oil, or the crystals may be attached directly to one side of the window, the latter not only protecting the crystals from the action of sea water but also serving as their means of support. In either case, an attempt is usually made to match the acoustic resistance of the window with that of the contiguous liquid medium. For a solid window whose shear modu-

lus is negligible, this reduces to a matching of the density ρ and the acoustic velocity C , or of their respective products for the media involved. Treatment of the simple cases of reflection and transmission of sound waves may be found in various texts.¹⁰ The more general case of a solid whose shear mode must be taken into account and where the waves are incident at any angle will be treated in the next paragraph.

Transmission of Plane Waves by a Plane Parallel Solid Window, Neglecting Attenuation Losses. The fraction T of sound energy transmitted by a solid window of density ρ_s immersed in a liquid of density ρ and velocity C is given by the following equation due to Reissner.¹¹

$$T = \frac{4N^2}{(M^2 - N^2 - 1)^2 + 4M^2}, \quad (93)$$

where

$$N = \frac{\rho_s \cos \theta}{\rho C} \left[\frac{V_d \cos^2 2\theta_r}{\cos \theta_d \sin \phi} + \frac{V_r \sin^2 2\theta_r}{\cos \theta_r \sin \gamma} \right], \quad (94)$$

$$M = \frac{\rho_s \cos \theta}{\rho C} \left[\frac{V_d \cos^2 2\theta_r}{\cos \theta_d \tan \phi} + \frac{V_r \sin^2 2\theta_r}{\cos \theta_r \tan \gamma} \right]. \quad (95)$$

The velocity of the shear wave in the solid V_r is equal to $\sqrt{n/\rho_s}$, where n is the shear modulus; the velocity of the longitudinal wave in the solid V_d is equal to $\sqrt{E + \frac{4}{3}n/\rho_s}$, where E is the bulk modulus; θ is the angle of incidence of the wave in the liquid medium, measured from the normal. The angles of refraction of the longitudinal and shear waves in the solid, θ_d and θ_r , respectively, are determined from Snell's law of refraction, hence:

$$\sin \theta_d = \frac{V_d}{C} \sin \theta, \text{ and } \sin \theta_r = \frac{V_r}{C} \sin \theta. \quad (96)$$

The angles ϕ and γ are defined by the relations:

$$\phi = \frac{\omega d}{V_d} \cos \theta_d, \text{ and } \gamma = \frac{\omega d}{V_r} \cos \theta_r, \quad (97)$$

where d is the thickness of the window.

When the angle of incidence exceeds the critical angle for the longitudinal and/or the shear wave, then θ_d and/or θ_r become imaginary so that some of the quantities in the terms for M and N must be replaced by hyperbolic functions. Reference to the original paper of Reissner¹¹ should be made for the modifications required in these critical regions.

An angle of zero transmission always occurs in the neighborhood of a critical angle. By solv-

ing the following equation graphically, one can readily obtain that value of θ which corresponds to the angle of incidence for zero transmission.

$$1 - \left(\frac{V_d}{C} \sin \theta \right)^2 - \frac{V_d^2}{C} \cot^2 2\theta_r \cos \theta_r \sin \left(\frac{\omega d}{V_r} \cos \theta_r \right) = \frac{\omega d}{\omega d} \quad (98)$$

The usefulness of Reissner's equation in predicting the acoustical transmission behavior of solids as a function of the angle of incidence is illustrated in Figure 28 where Mason's¹² calculated and experimental curves for the plastic Lucite may be compared. The agreement is excellent, particularly with respect to the position of the sharp minimum at 44.5° from the normal.

For solids where the shear modulus is negligibly small, as in some types of rubber, equation (93) reduces to:

$$T = \frac{1}{1 + \frac{1}{4} \left[\frac{\rho C}{\rho_s V_d} \frac{\cos \theta_d}{\cos \theta} - \frac{\rho_s V_d \cos \theta}{\rho C \cos \theta_d} \right]^2} \cdot \frac{1}{\sin^2 \left(\frac{\omega d}{V_d} \cos \theta_d \right)}. \quad (99)$$

In Figure 28, this function has been plotted for a sample of rubber together with experimental transmission data, both taken from work by Mason.¹ Again it will be noted that the agreement as a function of the angle of incidence is good.

RUBBER

Rubber has been widely adopted for acoustic windows in transducers, primarily because of the good impedance match obtainable with sea water but in part due to its elastic properties, abrasion resistance, and its electrical resistivity. It will be noted in Table 4 that either ρ and c , or the product ρc , for sea water may be quite closely duplicated in rubber by variations in its composition. Where both ρ and c are matched, it is customary to refer to the rubber as " ρc " rubber. The effective magnitude of the acoustic velocity in a solid body depends on its shape. In a long rod, it is found that the velocity

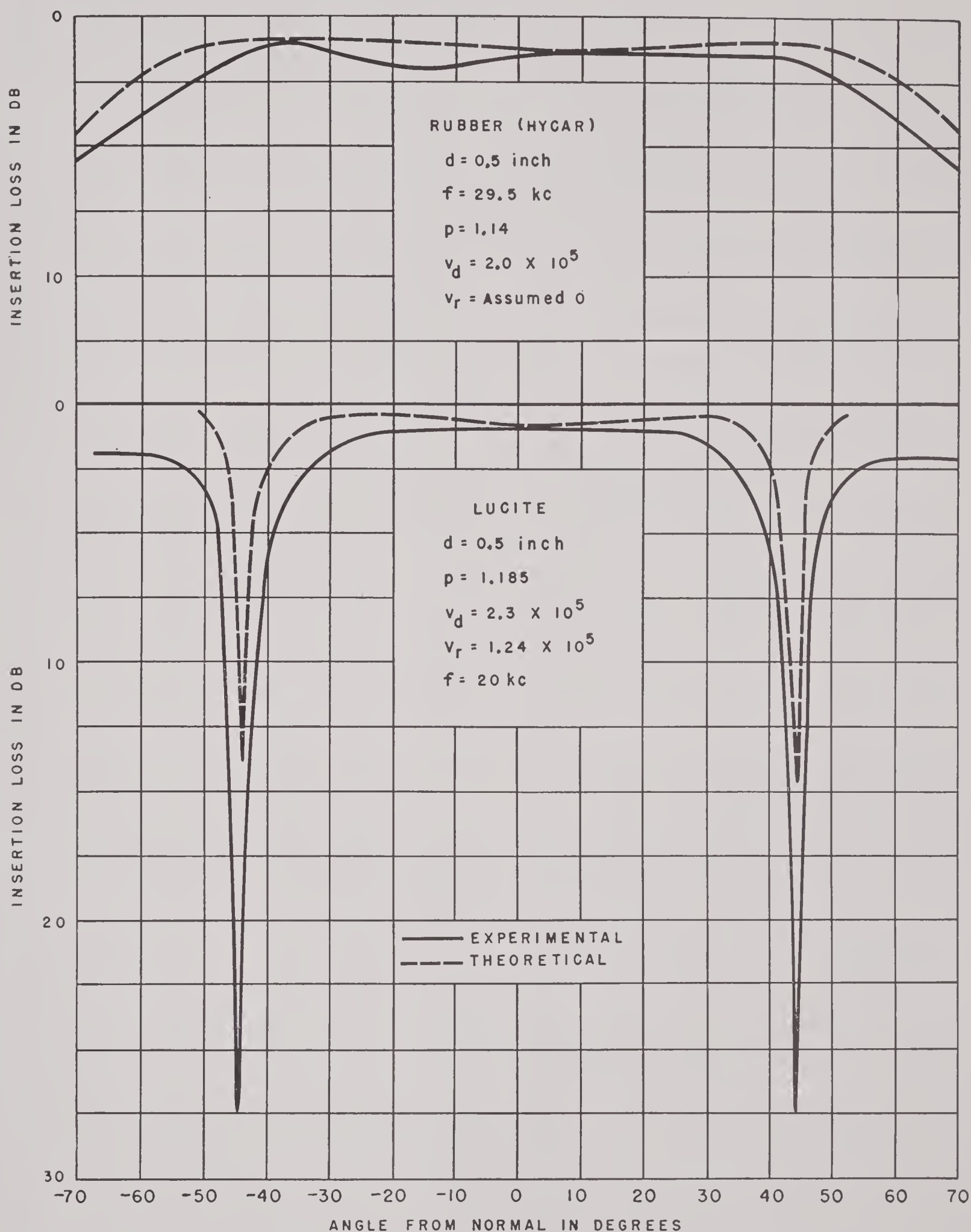


FIGURE 28. Transmission loss as a function of angle of incidence for single rubber and Lucite plates, under stated conditions. (Bell Telephone Laboratories.)

is determined by the value of Young's modulus. For example, most handbook values for the velocity of sound in rubber have been based on measurements of rodlike samples and usually range from 30 to 50 m per sec. For sound windows, the rubber is usually employed in thick sheets rather than as a rod, hence the velocity values in Table 4 are the proper ones to use and range from 1,500 to 1,600 m per sec. These latter values depend on the shear and bulk moduli of the solid. For "sound" rubber,

excellent. A somewhat similar effect was observed with a plano-convex neoprene window where the initially unsatisfactory directivity patterns of the transducer were much improved later by planing off the convex surface of the rubber.

To increase the mechanical strength of rubber windows, they may be reinforced with steel bars, as shown elsewhere in this book for the GD34Z-1 transducer. These bars do not interfere with the radiation in that particular case

TABLE 4. Materials of construction for sound windows and their various constants of acoustic importance.*

Material	Loading factor	Density (ρ) g/cm ³	Velocity (c) m/sec	Acoustic resistance (ρc)	Bulk modulus (E) dynes/cm ²	Shear modulus (μ) dynes/cm ²
Sea water	1.03	1,500	1,545	2.36×10^{10}	0
Castor oil	0.95	1,540	1,460	2.51×10^{10}	0
Steel	7.00	5,000	35,000	179×10^{10}	7.58×10^{11}
Sound rubber	0	1.03	1,530	1,575	2.38×10^{10}	2.76×10^6
Tire-tread rubber	50% C.	1.15	1,600	1,840	2.94×10^{10}	27.6×10^6
Hycar Os-30	0.96	1,560	1,500	2.34×10^{10}	?
Rubber	10:100 ZnO	1.03	1,530	1,580	2.48×10^{10}	?
Perbunan	1.12	1,650	1,850	3.05×10^{10}	?
Butyl rubber	0.97	1,630	1,580	2.58×10^{10}	?
Koroseal	62.5:100 TCP	1.30	2,160	2,810	6.15×10^{10}	?
Neoprene G	1.32	1,500	1,980	2.96×10^{10}	?
Lucite	?	1.185	1,981-2,002	2,360	?	?
Type 8388 (Goodrich)	?	1.15	1,550	17.8	?	?
Type 79-SR-32 (Goodrich)	?	0.99	1,525	15.1	?	?

* Courtesy of Goodrich Rubber Company, Naval Research Laboratories, Bell Telephone Laboratories.

the shear modulus is small and may be neglected; in other types of rubber, it may be important in some cases.

As long as acoustic radiation is incident approximately normally on a rubber window, an accurate match to the ρc of sea water appears quite unnecessary. For large angles of incidence, however, refraction effects have been found troublesome. In the case of a cylindrical rubber sleeve surrounding a square array of crystals, used as a motor, where the rubber stock was neoprene of approximately 40 Shore durometer and may have possessed an appreciable shear modulus, the large variations in the angle of incidence upon the rubber sleeve for the same polar angle subtended at the crystal motor resulted in a very distorted directivity pattern. When sound rubber (ρc) was used with the same crystal motor, the patterns were

since the crystals are attached to the rubber in locations where they may radiate freely between the steel bars. The window for the GD34Z-1 withstood a pressure test of 250 psi.

Where less strengthening is desired, the rubber may be molded over expanded metal screen or reinforced with hardware cloth and still retain its valuable acoustic properties. An important point is to guard against entrapped air during the molding or forming operations. By resorting to "press" curing, air-free stocks can be consistently obtained. The presence of occluded air, of course, would lead to very low transmission.

LUCITE

Data on the acoustic properties of Lucite by Mason¹ indicate that it may be useful over certain frequency ranges, but the variation of its

constants with frequency render it unusable in other frequency ranges. The normal loss through $\frac{3}{8}$ - and $\frac{3}{4}$ -in. Lucite sheets as a function of frequency is shown in Figure 29. The loss is small below 40 kc and in the immediate neighborhood of 60 kc; at 47 and 75 kc there are maxima in the loss curve. The position in the

NYLON

Mason has also measured nylon in the 20- to 30-kc range and found the normal loss to be very low. The angle of zero transmission for nylon is around 62 degrees.

STEEL

The transmission behavior of a $\frac{1}{4}$ -in. steel sheet when used as a window between sea water and a second medium having the same acoustic constants as water has been calculated on the basis of equation (93) for a frequency of 60 kc. The assumed values for the velocity of the

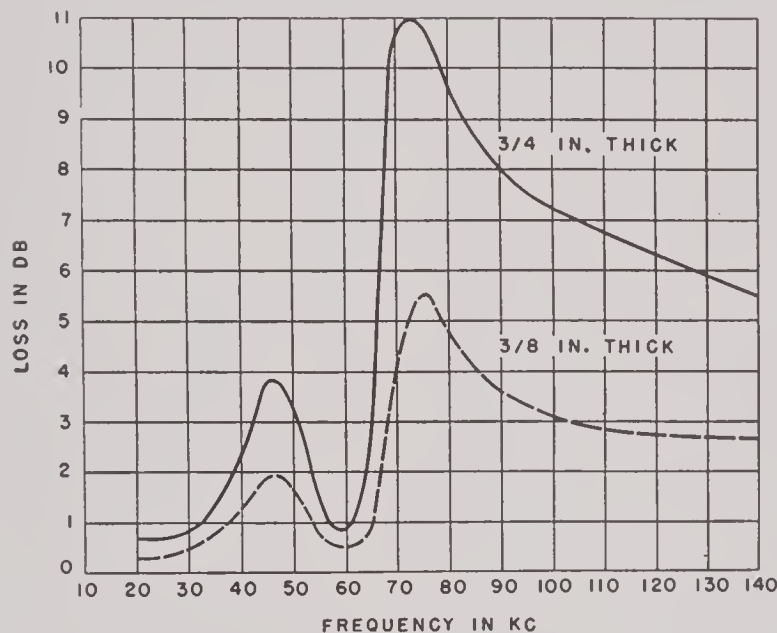


FIGURE 29. Transmission loss at normal incidence as a function of frequency for two Lucite plates, $\frac{3}{8}$ and $\frac{3}{4}$ in. thick. (Bell Telephone Laboratories.)

maxima appear to be independent of the thickness.

The velocity fluctuates between extreme values of 1,981 and 2,002 m per sec in the 20- to 110-kc range, the two maxima appearing at 43 and 71 kc.

TENITE

The cellulose acetate butyrate plastic known as Tenite II has a lower acoustic velocity than Lucite and hence larger angles of incidence for zero transmission. The loss curve at normal incidence for Tenite II-H5 shows a single maximum at 37 kc of 3 db for a $\frac{1}{2}$ -in. sheet; above 50 or below 28 kc, the loss is only 1 db or less. For the range 20 to 30 kc, the best grade appears to be H-4. Mason,¹ from whose work the above information is obtained, states that good transmission is also obtained if Tenite II is molded about an expanded-metal supporting structure.

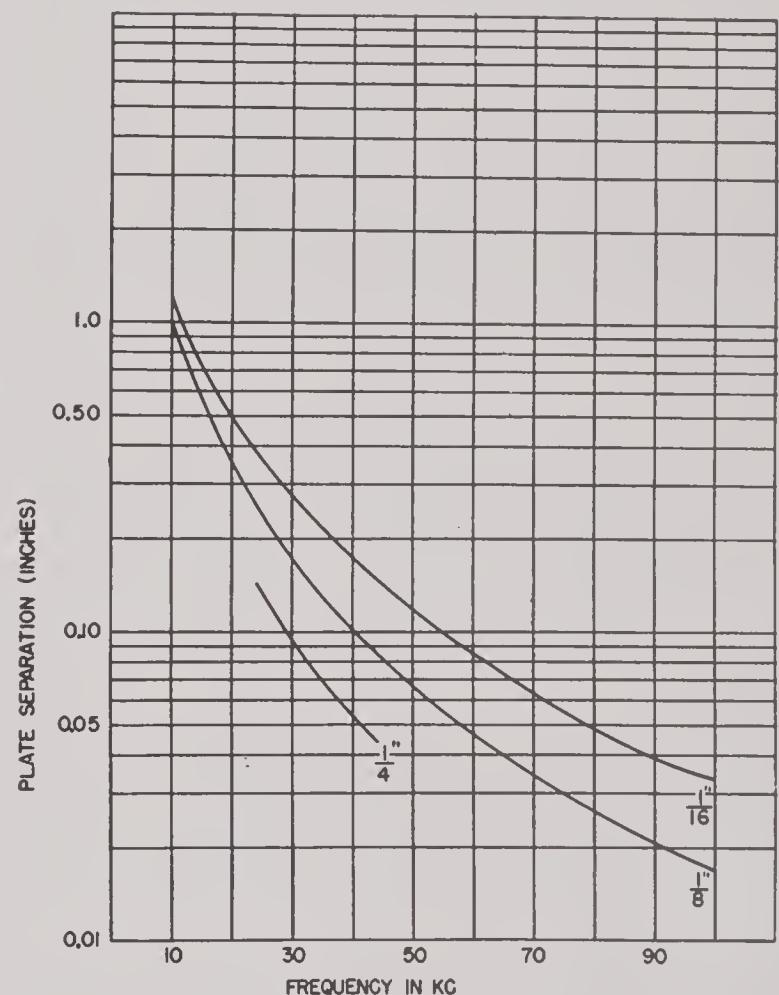


FIGURE 30. Plate separation as a function of frequency for perfect transmission at normal incidence through pairs of steel plates of given thickness.

longitudinal and shear waves were 5.75×10^5 cm per sec and 3.12×10^5 cm per sec, respectively. The transmission is quite uniform for angles of incidence up to 10° from the normal and is approximately 3 per cent. The first angle of incidence for zero transmission occurs near

17°. The transmission behavior in the critical regions is quite irregular.

The transmission loss through a 0.030-in. stainless steel covering on a 54-in. dome has been measured by Dietze.¹³ His experimental values for frequencies of 10, 20, 25, 30, 50, and 60 kc are 0.4, 0.7, 0.3, 0.9, 1.6, and 1.8 db, respectively. In addition to the use of thin stainless steel for the construction of domes, thin tinned-steel coverings have also been used to house transducers. In the "tin-can" transducer case discussed in Chapter 8, the wall thickness is approximately 0.010 in. and hence would have a transmission loss of roughly one-third to one-fourth of the values given above. As the thickness of a steel plate is increased, the transmission loss becomes greater and greater until the plate is no longer of value as a window. However, the transmission does pass through a minimum at some particular thickness and then increases to 100 per cent again when the plate thickness becomes equal to a half wavelength of the radiation being used. Although half-wave plates may find some application as a sort of directional filter, the rapid decrease in transmission as one departs from a normal angle of incidence is too rapid and critical for most uses. Their transmission is also a critical function of frequency.

A better solution to the problem of transmitting acoustic energy through a steel window having considerable strength consists of using two comparatively thin steel plates separated by a layer of material which has the same acoustic impedance as the liquid on the outside of the two steel plates. The theory for the transmission through such a double-layer wall has been developed by McMillan.¹⁴ The theory used in Section 3.5 should also be applicable here. A graph based on the equations of McMillan is given in Figure 30, and shows the plate separation for perfect transmission through a pair of plates as a function of frequency for the case of steel plates having thicknesses of $\frac{1}{16}$, $\frac{1}{8}$, and $\frac{1}{4}$ in. The angular variation in transmission through a pair of $\frac{1}{16}$ -in. steel plates, with separations of 0.064 and 0.072 in. respectively, for a frequency of 70 kc, has been computed by McMillan and is reproduced in Table 5. The results in this table indicate that good transmission at

70 kc can be obtained over a wide angular range through a window having considerable mechanical strength.

TABLE 5. Per cent transmission as a function of angle of incidence through a pair of parallel steel plates, plate thickness $\frac{1}{16}$ in., frequency 70 kc.

Angle of incidence	Per cent transmission	
	0.064-in. plate separation	0.072-in. plate separation
0°	100	82
10°	99	89
20°	86	100
30°	68	83
45°	37	44
60°	33	36

To test the performance of a window possessing this double-layer construction, a number of experiments have been conducted at UCDWR. Tests were made on a pair of $\frac{1}{16}$ -in. thick steel plates separated by distances of 0.044 and 0.143 in., respectively. These pairs of plates were supported immediately in front of appropriate flat-faced transducers and the responses measured as a function of frequency both with and without the various sets of plates. At those frequencies where the theory indicated perfect transmission for the respective double-layer plates, it was found that the measured response through them was equal or slightly greater than without them. These regions of high transmission were quite sharp, but would be suitable for transducers which operate at a single frequency. The transmission behavior at other frequencies was not always completely understood. One would expect difficulties such as flexural modes to occur in these plates as they do elsewhere in steel plates of comparable thickness. The directivity patterns at the frequency of maximum transmission through this type of window were usually as good as, or slightly better than, without them. At frequencies a few kc higher or lower than the frequency of maximum transmission, however, the directivity patterns were often greatly distorted. This would seem to limit the usefulness of this type of construction to transducers operating over a rather narrow frequency range which centered about the frequency of maximum transmission.

The strength obtainable in such a steel sandwich window would suggest its use in sonar domes. Several experiments on cylindrical domes were conducted to test this point, one of them being on a pair of $\frac{1}{4}$ -in. wall concentric cylinders about 10 in. in diameter, another on a pair of concentric cylinders having $\frac{1}{16}$ -in. wall and a diameter of 18 in. In both cases it was found that the directivity patterns were very badly distorted, apparently owing to internal reflections of radiation incident at angles other than normal. Since domes should give little or no interference to the directional characteristics of transducers, the use of a double-layer type of construction is only suggested for this purpose when the radius of curvature can be made quite large. However, it should be pointed out that these experiments were preliminary and exploratory in nature and a more profound investigation might still develop something useful for particular applications.

An ultimate usefulness may develop for this sandwich-type plate in furnishing a strong window for transducers in weapons which are either rocket fired or airplane launched. In this case they would strike the water at very high velocities. Even then they would probably have to be designed to operate at a single frequency or over a very limited range.

3.9 PROPERTIES OF INERT TRANSDUCER MATERIALS

A transducer of any size and complexity usually contains a great many parts besides crystals and backing plates. Usually parts are required to perform such functions as: support the active parts within the case, provide electric connections, support wires, convey wires through watertight bulkheads, provide acoustic isolation, attach various parts to each other, provide a strong container, and provide an acoustically transparent window. At one time or another a great many materials have been used to perform these various functions, and the following is a brief outline of salient properties of the more important substances. The numerical values given are the best available; most of them are taken from the standard ref-

erence literature, but the sources are so diverse that no attempt is made to make proper acknowledgment.

METALS

Aluminum ($\rho = 2.7$; $c = 5.1 \times 10^5$ cgs units). Aluminum has not been used extensively for backing plates because of the relatively great thickness required for a high impedance. The mechanical Q is quite high. Aluminum does not solder or weld easily and is corroded rapidly in sea water. Aluminum alloys might be quite useful for passive internal parts because of light weight.

Brass (various) (67 Cu, 33 Zn) ($\rho = 8.40$; $c = 3.5 \times 10^5$). Brass has not been used for backing plates and there is no apparent advantage thereto. Brass behaves like copper in the presence of castor oil and RS, but small brass parts frequently have been used, generally when cadmium or nickel plated. Brass solders and machines well, and stands up reasonably well in sea water. Some trouble may be encountered from bimetallic corrosion.

Bronze (various) (ρ, c vary but similar to copper). Bronze is used only for cast exterior cases; in this service the bronze may be tin dipped and works very well. However, such a case is quite heavy and expensive. Bronzes generally behave like copper in the presence of castor oil and RS but may be protected by plating. The wide range of commercial bronzes offers many interesting properties. Silicon, phosphorus, and beryllium bronzes have occasional specialized applications such as in springs.

Cadmium. Cadmium is useful only as a plating on other metals. On steel it affords some protection from sea water, but it cannot be relied upon. Usually it will rust through in a week or two. Experience indicates that cadmium affords considerably better protection to steel than do nickel and chromium but not as good as a heavy tin dip or plate. There appears to be no metallic spray, plate, or dip which reliably protects iron from sea water.

Copper ($\rho = 8.5$; $c = 3.56 \times 10^5$). Copper has not been used for backing plates, although it might be useful in particular instances. Copper, RS, and castor oil are reputedly intolerant, al-

though any pair are tolerant. The trouble comes from the formation, over an extended time, of a black conducting sludge in the castor oil associated with corrosion of the copper. The copper may be protected by heavy plating. No data are available on copper, castor oil, and ADP but the combination has been used with no evidence of trouble within one year. Copper may be used for internal electric wiring, but the high crystal impedance usually allows the use of less questionable metals, such as iron; any copper wire so used must be tinned when in the presence of castor oil and RS. The work-hardening of copper during repeated flexure may lead to broken wires if a transducer is subject to vibration. Since any transducer aboard ship may be subject to such vibrations, any wire should be thoroughly secured (with mechanical resistance if possible) to avoid resonant vibrations.

Gold. As an evaporated layer, gold has been used as electrode attached to crystal. In foil, or plated on other foil, it has been used to make connections to crystal electrodes. Evaporated gold electrodes are advantageous for 45° X-cut RS, but this is not required for 45° Y-cut RS or 45° X-cut ADP, except in *very* high-power transducers.

Iron (cast white) ($\rho = 7.6$; $c = 5.1 \times 10^3$). Ordinary cast iron has been used for many transducer parts, particularly exterior cases and backing plates. It is quite brittle and very difficult to solder or weld. One generally has difficulty getting castings which are not porous. There may be advantage in the fact that cast iron is quite stable against cold flow and other inelastic deformation. Cast Meehanite is superior to ordinary cast iron in many ways, chiefly for the chance of getting good castings, and for superior strength. Meehanite is a patented process, licensed to various foundries (information from Meehanite Corp.). Cast steel is probably preferable to either of the above, but has been used very little. Hot- and cold-rolled steel are the most common materials in transducers. Hot and cold forgings are usually more suitable for production quantities than for the small quantities dealt with in initial design. For this reason, the main components of many Submarine Signal Company projectors (to name only one manufacturer)

are forgings. In general, iron and steel are as good a material as any in exposure to sea water, provided wall thicknesses are sufficient to allow some rusting. Nuts and bolts must be protected from rusting on both heads and threads. Nearly all UCDWR backing plates have been cast Meehanite or hot- or cold-rolled steel. When vitreous porcelain enamel is to be applied, the enameling concern should be consulted about impurities which may be harmful to the enamel. There is no reason to think that the black scale occurring on hot rolled and castings is harmful to transducer interiors, provided the scale cannot fall off.

Various surface treatments such as dips and platings can be readily applied to steel but afford only partial corrosion protection, and in some cases are harmful because of bimetallic corrosion. The most common methods of fabrication are soft and hard soldering and welding. The soft solders are suitable only for fairly small parts where strength is not a requirement. The hard solders are suitable only for fairly small parts which can be properly heated and fluxed (unless a furnace is available). Gas and arc welding are most suitable for strength members, and electric arc welding is usually easier to do on very heavy parts. Trouble may be encountered with welds which leak, but a skilled arc welder can reliably make absolutely tight welds. Considerable success has been had with furnace copper brazing (in special ovens with controlled atmosphere), and this method is strongly recommended wherever possible. A copper-brazed joint should probably be protected from sea water because of possible bimetallic corrosion. UCDWR has generally used small (No. 27 AWG) tinned iron wire for electrical hookups within transducers; this wire is soft, cheap, easily soldered, and quite strong. Nuts, bolts, screws, etc., in the interior are usually unplated steel. Very thin-tinned sheet iron such as commonly used in tin cans has been very successfully used in small transducers; it can be used for both the case and the acoustic window. Stainless steel is rather difficult to machine and fabricate, but it can be spot welded, welded, and soldered if the proper methods are used. Besides the obvious corrosion resistance, stainless steel has the advantage that marine

life, such as barnacles, grow on it only slowly if at all. For this reason, also, stainless steel is particularly suited for use in thin sheets (20 gauge or thinner) as the acoustic window.

German Silver. UCDWR has used large quantities of 0.001-in. German silver foil for making connections among crystal electrodes. This foil cuts and solders easily and is quite strong. Its cost is quite high because of the rolling operation, and it probably offers no advantages over silver foil. There are indications that some corrosion process may occur in contact with RS and castor oil (possibly because of the copper content) but UCDWR has not had enough trouble to warrant investigation.

Lead ($\rho = 11.3$; $c = 1.2 \times 10^5$). Lead has been used as the second layer (with steel) in a two-layer backing plate. Because of the low value of c , a clamping lead backing plate at some frequency is both thinner and lighter than a clamping steel plate at that frequency. The mechanical Q of lead is considerably lower than that of steel, but is still so high as to present negligible losses. Lead wool might be used, with castor oil, to form a sound-absorbing medium, but lead wool crumbles and packs so much that its use is of questionable value. Lead is occasionally used as a gasket, but this is only possible when springs, lock washers, etc., are put under the screws to provide constant pressure. If screws alone are used, the lead will cold flow to relieve the pressure, and the gasket may leak.

Magnesium. Magnesium or magnesium alloys might offer possibilities as backing-plate materials or internal passive parts; good castings are relatively easy when the foundry is properly equipped. Extreme corrosion prevents its prolonged use in contact with sea water. Material is now available from Dow Chemical Company by which magnesium is readily soldered.

Silver. Silver wire and silver foil have been widely used in electric connections to crystals. Silver solders easily and is an excellent electric and thermal conductor. The price difference between silver and baser metals is usually trivial. Sometimes silver foil will not solder because of lubricant forced into it in rolling; this difficulty should not arise and is easily corrected.

There is no evidence that silver acts like copper in the presence of castor oil and RS.

Tin. The cost of tin precludes its use except in thin protecting layers on other metals. Experience indicates that where a heavy, well-bonded tin dip or tin plate can be attached to steel it offers the best corrosion protection of any to be had by metallic plating.

Wood's Metal. This alloy and other similar low-melting alloys offer possibilities in making up two-layer backing plates. These alloys wet steel better than pure lead, and the lower melting point is a definite advantage when attaching to the back of a porcelainized steel plate. One of the commercial alloys of this type, Cerrobend ($\rho = 11$; $c = 1.74 \times 10^5$), has been used for this purpose.

Zinc. There is no reason to think that zinc offers any particular advantages in backing plates, although it would probably be satisfactory. Extensive use has been made of high-zinc alloys (particularly the commercial alloy, Zamac) for small castings. These alloys machine easily and cast well, although an excess must be poured because of great shrinkage at the top surface. The outstanding advantage is that these alloys can be handled easily in a small laboratory such as is likely to be interested in transducer development.

PLASTICS

Bakelite. This plastic is commonly used with various fillers, prominent among which are fabric, paper, and minerals. The fabric-base bakelite has been extensively used for various small parts inside transducers. It machines reasonably well and is quite strong. Since it is thermosetting, spontaneous cold flow is not as pronounced as is some thermoplastics. The material has a "grain" and the strength differs markedly with direction. The chief disadvantage is the bad behavior under electric breakdown. In the direction of the grain the dielectric strength is not great, and if a spark jumps, the path is likely to carbonize. For this reason it is customary to impregnate in molten ceresin (until boiling ceases) or Glyptal (preferably in vacuum). Fabric-base bakelite contains a dye which colors castor oil yellow-brown but this is not at all harmful. Paper-base bakelite can

be machined to a better finish than can fabric base, but seems not to be as strong. It, too, shows grain; its dielectric strength is somewhat better. Mineral base is quite hard, and can be machined and lapped to a high finish. Dielectric strength is high, but the material is rather brittle.

Lucite; Plexiglas. Although a difference does exist, no distinction need be made between these plastics. They have fair electrical properties, high dielectric strength, and little or no evidence of "grain." Since they are thermoplastics, they are very likely to undergo spontaneous cold flow to an annoying extent. This makes them particularly unsuited for packing gland parts, etc. When screwed or riveted together, pieces are likely to become loose because of cold flow. Their great usefulness is for high-voltage insulation where power factor and dielectric constant are not important. Lucite ($\frac{1}{4}$ or $\frac{1}{2}$ in. thick) has been used for fronting plates for inertia driven transducers; this seems to work well, but the design was not pursued beyond small units for general laboratory use because of the fragility. The specific acoustic impedance of Lucite is a function of frequency and undoubtedly of temperature; generally, it is quite close to that of water and in some applications makes a good acoustic window. At angles of incidence in the vicinity of 60° , Lucite shows an anomalously high reflection coefficient which must be borne in mind. Like polystyrene and many other plastics, the attenuation (which is a function of frequency) is quite high, and very thick slabs might cause excessive loss on transmission. Lucite and Plexiglas machine well, although they have a tendency to melt, may be given an excellent polish, and cement readily.

Polystyrene. For transducer purposes, polystyrene is superior to Lucite and Plexiglas. Dielectric losses and dielectric constant are exceptionally low.

Polythene (Polyethylene). This plastic became available late in World War II and has found only limited use in transducers. However, its properties are outstanding. Polythene is the only other plastic whose electrical properties compare favorably with polystyrene. The specific gravity is less than unity. Polythene is

rather horny, flexible, and burns slowly. It is thermoplastic, and may be formed readily without elaborate facilities. The only known use in transducers to date is as a molded thin case around a cylindrical low-frequency magnetostrictive transducer developed by UCDWR; this application was highly successful.

Many more plastics with a wide variation of interesting properties are worthy of comment. Among these are Catalin, Lumarith, Laminac, Durez, Tenite, Saran, Viscoloid, Vistanex, Nylon, Celluloid, and Cellophane. It is strongly urged that anyone interested in transducer design investigate thoroughly the various plastics available to him.¹⁵

GLASSES AND CERAMICS

Glass. There are, of course, many kinds of glass with quite different properties. Usually the density varies from 2.4 to 2.8 and the velocity of sound from 5 to 6×10^5 . The mechanical Q is quite high, and glasses are generally well-suited for backing plates (such as Brush C-26). UCDWR has made a few glass fronting plates with indications that this is worth further investigation. Glasses have the distinct advantage that their properties are relatively independent of time and temperature. In cementing it is often advisable to grind a matte surface on the glass to give a "tooth" for the cement.

Porcelain Enamel. UCDWR has made extensive use of porcelain enamel as an insulating layer bonded to a steel backing plate. The exact composition is usually a trade secret of each concern and no attempt has been made to learn it. This is a glasslike substance, usually black or white, moderately homogeneous, and usually applied to bathtubs, stoves, kitchenware, etc. Two general processes are used: the wet and dry processes. UCDWR prefers slightly the dry process in which a dry frit is sprinkled onto red-hot steel and returned to the furnace until melted. The preference may arise from the particular concerns available. Both kinds tend to have internal bubbles when the glaze is ground off; thus Glyptal impregnation is suggested when the porcelain is to be subjected to any considerable voltage. Use of snow-white enamel greatly aids the examination of cement joints.

Porcelain. There are innumerable porcelains

which have possible uses for electrical parts in transducers. One practice worth mention is that of the Bell Telephone Laboratories. At one time they customarily used thin ceramic wafers cemented between the crystals and the backing plate, analogous to the bonded porcelain enamel above. This method seemed satisfactory, but the porcelain has since been replaced by plastic wafers.

Metal-to-Glass and Porcelain-to-Glass Seals. Recently these seals have become available in large quantities from such manufacturers as Stupakoff, Spertie, Westinghouse, and Corning. Within their limitations, these seals are an enormous help in bringing electric leads through bulkheads. Some difficulties which may be encountered are: fragility, inability to stand high pressure (great ocean depth), low electrical resistance caused by occasional poor glass.

RUBBERS

Sound-Water (qc). This rubber, made by B. F. Goodrich Company, was developed specifically for underwater sound transducers. Its specific acoustic impedance is equal to that of water; the composition is not known. This rubber is yellow, resembling pure gum and is soft. It can be bonded to steel and other metals to form acoustic windows, and it is readily available in sheets and hollow cylinders. The rubber seems to contain an oil, and for this reason it is sometimes difficult to cement to it. While it appears to be quite elastic, it is torn rather easily, and is somewhat poor mechanically. It is slightly crazed by prolonged sea water immersion, but stands up very well.

Natural Rubber. Because of World War II, very little natural rubber other than Sound-Water rubber has been used. We are told that natural rubber is damaged by sea water unless first subjected to a deproteinizing process.

Synthetic Rubber. Although there are many other synthetic rubbers UCDWR experience is limited to neoprene. When used in reasonably thin plane windows parallel to plane motors the effects arising from the slight impedance mismatch are not serious. However, thick curved windows may seriously distort directivity patterns and cause marked irregularities in frequency response. For such service qc rubber

appears entirely satisfactory.

The following composition is one often used with success by UCDWR.

Neoprene	38 per cent
Carbon black	40 per cent
Rope seed oil	10 per cent
Zinc oxide	2 per cent
Compounding	10 per cent
Shore hardness	55 to 65: A scale.

Latex and Rubber Suspensions. Several dipping compounds are available by which a thin layer of rubber may be applied to various surfaces. Many of these contain water and are suitable for making streamlined shapes, etc., but may not be put in contact with crystals. These seem to be porous, and the d-c resistance may drop after submersion. There are dipping compounds (whose solvent is carbon bisulphide or other organic liquids) which do very well for applying rubber directly to crystal surfaces. Most of these dipping compounds are air drying and require no further curing; others require subsequent baking at assorted temperatures and times.

CEMENTS

Bakelite Cement BC6052. This cement, a cyclized rubber, is by far the most commonly used cement for attaching crystals to each other and to other surfaces. The technique is not complicated, but is tricky. Results are moderately good, and its use arises from the fact that it is the most practicable cement for RS. It is a common misapprehension that a bakelite-cement joint can be judged by inspection; one of the difficulties of the substance is that good and bad joints look nearly identical. Solvents are, to name a few, carbon tetrachloride, benzene, benzine, acetone, toluene, amyl acetate, ethyl acetate, and ether.

Vulcalock. This is a B. F. Goodrich Company product. It differs from BC6052, if at all, only in having a higher solvent density.

Cycle-Weld. There are several Cycle-Weld cements having various uses. UCDWR has considerable success Cycle-Welding ADP to neoprene and qc rubber. The method consists in the application and curing of a priming coat of 55-6 cement on the rubber and the bonding of the crystals to this by another Cycle-Weld ce-

ment called C-3. Cycle-Weld cement is a patented product of the Chrysler Corporation.

Shellac: Sealing Wax. Since sealing wax is predominantly shellac, it behaves quite similarly; it is a little easier to work and comes in convenient stick form. Sealing wax is quite soft at 100 C and is fluid at a little higher temperature. ADP is not damaged by these temperatures, and may be attached to other surfaces with sealing wax. The simplest technique is to warm the other surface, such as a backing plate and spread over it a uniform layer; the crystals are then set in place and a slight pressure applied to thin the layer of sealing wax between the surfaces. On cooling, a very strong uniform high Q joint is formed, which improves for the next day or two and then remains quite stable. Since shellac polymerizes at elevated temperatures, and even at room temperature, the properties of the shellac may depend upon previous history, times and temperatures during fabrication, and subsequent history. There is some question whether a transducer so constructed might change its properties over a span of years or over the temperature ranges encountered in various seas. Cement joints made this way have quite high Q but are rather brittle and thus have only limited use. Chief suggested use is in research where speed is a convenience. Common solvents are acetone, toluene, benzene, amyl acetate, ethyl acetate, ether, and chloroform.

Beeswax and Rosin. This cement, or one using other waxes such as paraffin, has the virtues that it sticks well to cold surfaces, and its hardness and softening point may be varied by composition. An approximately 50-50 mixture melts at a temperature just slightly above the destruction temperature of RS. The mixture tends to supercool so that it may be used as a cement for RS using a technique similar to that for sealing wax and ADP. The resulting joints are quite good after aging a day or so. It is possible that a microscopic layer of RS is damaged, but this could have no effect except a possible lowering of electrical breakdown voltage. The constitution of a mixture of wax and rosin varies on successive heatings so that occasional checks on melting point are advised. There is no indication that the cement is harmed by castor oil.

Common solvents are acetone, toluene, benzene, amyl acetate, ethyl acetate, ether, and chloroform.

Rochelle Salt. Molten RS has been used as a cement for both RS and ADP crystals. On heating, RS decomposes into potassium tartrate and sodium tartrate (mixture) with the evolution of $\frac{1}{2}$ mole of water. The molten liquid will recrystallize (not as RS), and tends to supercool. The resulting joint undoubtedly contains excess water, the amount depending on its molten history. The most successful joints have been made using salt which has been molten and exposed to air for several hours. There is some indication that electrical breakdown occurs at a noticeably lower voltage through these joints, perhaps because of excess water and perhaps because of the properties of potassium and sodium tartrates. Such joints have very high Q and are somewhat brittle. There is some question whether a joint between crystal and steel, for example, would crack because of differential thermal expansion.

Acryloid, Ferdico Marine, Ferdico Aviation, and Carnauba wax are other cements which have been tested. They all have one or another disadvantage with no particular advantage. Efforts have been made to find a polymerization-type cement suitable for cementing crystals, particularly one which will polymerize in reasonable time at room temperature. To date, this remains a will-o'-the-wisp, although Bell Telephone Laboratories has recently announced a new cement, Butyl C, which may be of this type.

LIQUIDS

Castor Oil. Baker and Company's DB-grade castor oil remains the most universally used liquid in transducers. This oil is rather viscous and the odor is milder than is usually associated with castor oil. This grade is quite pure and is intended for electrical uses. It usually contains large quantities of dissolved air and water which must be removed in vacuum. The viscosity is a marked function of temperature and the coefficient of thermal expansion is rather large. Castor oil becomes turbid at 12 C. The density at room temperature is 0.96 to 0.97; the specific acoustic impedance at room temperature is very close to that of water (the temperature depend-

ence of the specific acoustic impedance of castor oil resembles that of most other liquids; sea water is anomalous and has slope of opposite sign). Castor oil does not harm natural or synthetic rubber, and is probably rather beneficial. The only practical solvent known is benzine (not C_6H_6) and even this is not very good. Castor oil is a definite chemical compound, and is unstable when heated.

Butyl Phthalate. This and similar organic liquids have been used occasionally with evident success for filling transducers. The specific acoustic impedances are usually close to that of sea water, and the viscosities are advantageously lower.

Ethylene Glycol. This is usually used with water, as an antifreeze filling for domes. Rochelle salt is dissolved by ethylene glycol.

Olive Oil; Peanut Oil. These liquids have been proposed as substitutes for castor oil to get lower viscosity. They have not been investigated in detail, but seem promising. There are many other such vegetable oils which also might prove useful.

Silicones. The Dow-Corning Corporation has placed on the market a group of silicone fluids. The viscosities available extend over quite a range, and the temperature coefficient of viscosity is in orders of magnitude less than that of castor oil. By inference, the temperature coefficient of specific acoustic impedance may also be markedly less. These fluids do not harm metals, rubbers, enamels, etc. Present cost forbids general substitution for castor oil, but low melting point, high boiling point, low viscosity (range from which to choose) and low-temperature coefficients suggest that in specific applications these silicones would be preferable to castor oil in transducers.

Acetylated Castor Oil. This liquid is one of the substitutes for castor oil proposed by Bell Telephone Laboratories. Although some advantage may accrue, UCDWR believes that this is overshadowed by the harmful effect on Cell-tite foam rubber. After prolonged immersion the foam rubber swells considerably, appears to soak up the liquid, and certainly loses all of its isolation properties. It may be inferred that the liquid similarly affects solid neoprene and perhaps other rubbers.

Petroleum Oils. These have been proposed as substitutes for castor oil, and one such transducer was successfully built. They have the advantage of low cost, ready availability, wide ranges of properties, and close manufacturing control. They attack natural rubber quickly, but some synthetics (neoprene) are not seriously affected.

DESICCANTS

Calcium Chloride. This common laboratory desiccant is frequently used in cloth sacks in transducers. Because of ions formed, it is not advisable to use it in the castor oil cavity. Its chief use is for drying air-filled cavities where electric connections are made.

Silica Gel. This desiccant is very active and absorbs tremendous quantities of water; it may be used in cloth sacks in the oil cavity if desired and is generally preferable to calcium chloride.

Phosphorous Pentoxide, etc. This and similar desiccants are not suitable for transducer use because of corrosive action.

ISOLATION MATERIAL

Corprene. This is a generic name for various compounds of natural, synthetic, and reclaimed rubbers (or sponges) with ground cork. Corprene is very commonly used to provide acoustic isolation in transducers; the specific acoustic impedance is undoubtedly low compared with water, but its value is unknown. There is reason to believe it to be frequency dependent and perhaps dependent on angle of incidence. At low frequencies it shows marked hysteresis which indicates that a sheet of it will absorb fair quantities of energy. The ideal isolator presents a purely reactive impedance, and this loss is undesirable. Corprene must be sealed over its entire surface (which is not easy) lest it soak up water, castor oil, etc., and change properties in time. Corprene is available in sheets, rolls, rods, and special moldings. It cuts easily with a knife, but accurate dimensions are best shaped on a disk or belt sander. Corprene cements easily to other surfaces, and Corprenes compounded from neoprene are not seriously damaged by petroleum derivatives.

Foamglas. This is a true foam (see foam rubber below) made of glass. The cells are reason-

ably uniform in size, perhaps $\frac{1}{32}$ - to $\frac{1}{16}$ -in. diameter. Foamglas, like glass, is impervious to nearly anything, and absorption is limited to what clings to its surface. Its specific acoustic impedance is quite low and appears to be largely reactive. It is not as good for isolation as Corprene or foam rubber. Foamglas comes in slabs of different sizes and can be cut to fairly accurate shapes with a knife. It can be machined in lathes, milling machines, etc., using a piece of scrap metal as a cutter. Foamglas will support 150 psi when distributed over a few square inches, and will support the hydrostatic pressure of a couple hundred feet submersion in the ocean (exact depth variable and unknown). An outstanding property is the density: 0.17 g per cu cm. Foamglas is manufactured by Pittsburgh-Corning Glass Company.

Cell-tite Foam Neoprene. This material is available in sheets of varying thickness, the large surfaces being smooth. Internally, the sheet is composed of a mass of bubbles whose walls are neoprene. Since each bubble is separated from its neighbors by a neoprene wall, this constitutes a true foam as distinguished from a sponge (such as a natural sponge) in

which the cells are intercommunicating. A true foam will not soak up liquids except by diffusion through the cell walls. The specific acoustic impedance is quite low, probably lower than that of Corprene or Foamglas, and a thin layer seems to act as a remarkably good reflector with little loss. UCDWR tested foam rubber to 250 psi and found that it continues to act predominantly as air (pressure-volume product constant); the tests stopped here, and the upper limit is not known. Being neoprene, foam rubber is not harmed by any common substances in transducers except some organic solvents. There have been indications that under hydrostatic pressure in castor oil foam rubber may lose its gas by diffusion and collapse. Attempts have been made to seal it with coatings but no results are yet available. So far there is no report of a transducer's behavior changing because of this collapse. It is readily cemented using bakelite cement, etc. UCDWR now uses foam rubber for nearly all isolation except where the rigidity of Foamglas or Corprene is required. Cell-tite foam neoprene is manufactured by Sponge Rubber Products Company, Derby, Connecticut.

PROPERTIES OF ASSEMBLED CRYSTAL TRANSDUCERS

By *T. Finley Burke, Glen D. Camp, and Bourne G. Eaton*

4.1 GENERAL CONSIDERATIONS

THE PROPERTIES of the components of crystal transducers have been studied in Chapter 3, in so far as present experimental and theoretical knowledge permits. In this chapter, the properties of complete crystal transducers are studied, to determine to what extent these properties can be deduced from those of the components, and to try to come to a qualitative understanding of the discrepancies.

The dependence of these considerations upon an admittedly incomplete theory should be em-

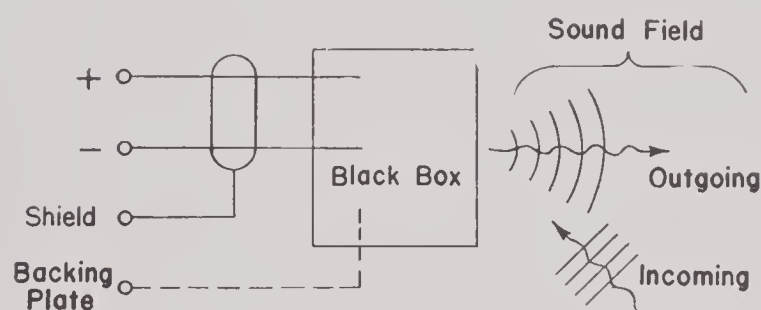


FIGURE 1. A crystal transducer as a "black box." A lead from the backing plate is sometimes brought out for experimental purposes, as indicated by the broken line.

phasized. In the first place, it is important to notice that the study of acoustic vibrations is almost never associated with the direct measurement of acoustic quantities. For example, crystal transducers are calibrated against standards which have themselves been calibrated by reciprocity measurements. At no point in this sequence is a mechanical quantity directly observed, all measurements being electrical and geometrical. Furthermore, granting the theoretical connections which yield acoustic quantities from electrical measurements, one would still be unable to interpret the empirical results in such a way as to motivate design studies, without an approximate theory.

A complete crystal transducer presents itself to us as a "black box," as shown in Figure 1, accessible only through its electric terminals

and the sound field, the latter in the indirect way mentioned above. A calibration group will wish to emphasize this black-box viewpoint, to avoid subtly prejudicing their experimental procedures.

For research and design purposes, one will try to understand the experimental results first as a consequence of the properties of the components and, if this is not possible, in terms of these components together with couplings between them. It turns out that the principal features of a complete transducer are deducible from the properties of the components, but there are usually residual effects of varying magnitude in different units. Some of these residual effects are not understood at all, while others are understood only qualitatively. However, as knowledge and design procedures have improved, the number of transducers having small residual effects has steadily increased. Furthermore, the most satisfactory transducers are those in which these residual effects are negligible, both by empirical results and judged theoretically, the latter because every conceivable additional coupling has a harmful effect. Thus, much of the effort of a designer is directed toward rendering negligible those couplings which he has been able to identify.

4.1.1

Equivalent Circuit

The existence of an equivalent circuit for a linear dissipative crystal transducer has been shown to be a consequence of the general theory (see Section 2.4), and has been verified within experimental error by reciprocity measurements. However, the values of the elements of this equivalent circuit and even the structure of the circuit are largely unknown.

An equivalent circuit for a single crystal has been theoretically deduced in Chapter 3. This circuit includes the effects of finite lateral dimensions and of normal and tangential imped-

ance loads on the radiating and lateral faces to the lowest order. For the present purpose, it is convenient to replace the direct capacitive coupling by an ideal transformer with a 1/1 voltage ratio,^a to avoid confusing electric and mechanical grounds when more than one crystal is involved. The single-crystal circuit, with a transformer replacing the direct condenser coupling, is shown in Figure 2, which should be compared with Figure 5 of Section 3.2.1.

The circuit of a complete transducer, *neglecting all coupling between crystals*, is obtained

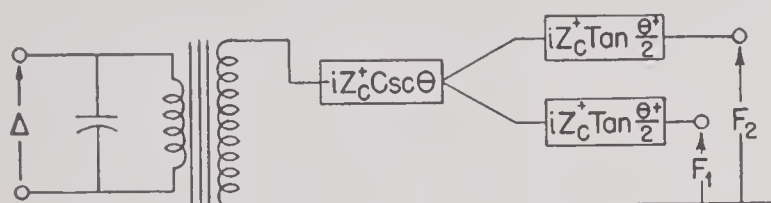


FIGURE 2. Equivalent circuit of rectangular crystal plate including perturbations to the Mason circuit, with ideal transformer instead of capacitive coupling.

from that for a single crystal, Figure 2, by inserting stray capacitances from each electrode to the backing plate (if conducting) and to the case, and then connecting the leads as they are connected in the transducer. This is shown in Figure 3 in which the dotted lines indicate a common type of electric connections, all crystals in parallel and the case grounded, the latter not being shown. This balanced drive is used in an effort to reduce the shunting effect of stray capacitances to the backing plate and case, which reduce the band width; it is found that these strays are very important and also, unless the utmost precautions are taken to keep everything symmetrical, the transducer will have an appreciable unbalance, still further increasing the shunting capacitance (see Section 4.5). The broken leads are to suggest the unknown mechanical couplings here neglected. More than one is drawn from each element to emphasize

^a In this volume, what might be called a completely equivalent electric circuit is used; the transformer converts volts to volts in the ratio 1 to 1, and the velocities and impedances in the mechanical arms are changed from mechanical units to electrical in the ratio 1 to ϕ and 1 to wt/ϕ^2 . Mason¹ leaves the mechanical arms in mechanical units, but uses a transformer that converts volts to force in the ratio 1 to ϕ . Either convention leads to the same results.

that these are the equivalent of a distributed impedance and that additional couplings might occur at any point.

4.1.2

Possible Measurements

The measurements which can be made on a complete transducer with present facilities are conveniently divided into two categories.

1. Those in which only the electric terminals are accessible, the mechanical terminals being terminated in some manner which should be specified as sharply as possible, preferably by being coupled to an effectively infinite medium. These include impedances, both the two-terminal routine measurements and the multi-terminal

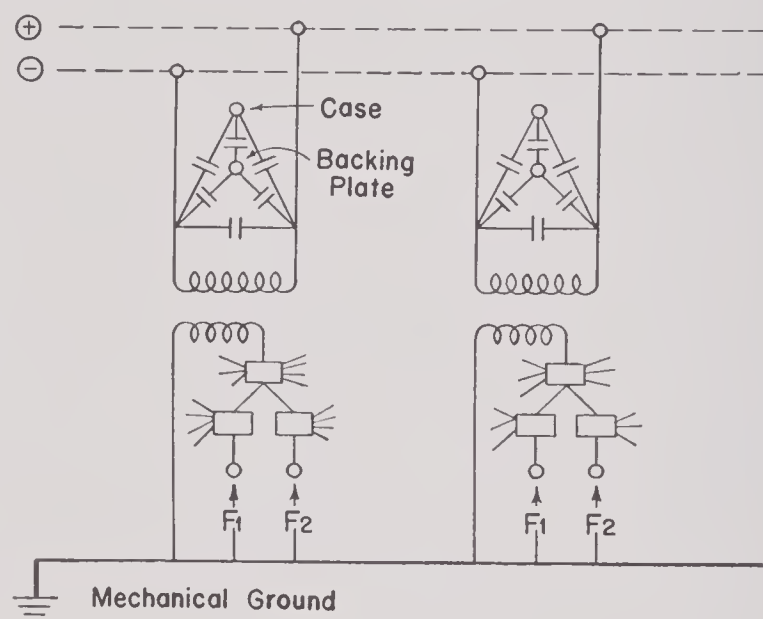


FIGURE 3. Equivalent circuit of a complete transducer, neglecting the coupling between crystals. The broken leads from each lumped impedance are to suggest these neglected couplings.

(usually 4) impedances measured for research purposes; crosstalk between two motors or between two sections of the same motor; internal reverberation, either in steady state or for pulse excitation; and d-c resistance, of primary importance as a production test.

2. Simultaneous electrical and sound-field measurements. These include routine calibration measurements of directivity patterns and various types of responses, and measurements of a similar character but made for research purposes.

In addition to the above, it is believed that valuable information might be gained by

measurements made with the aid of probes at various points inside a transducer. Aside from the possibility of such measurements leading to a better understanding of the internal motion in transducers, probes might also be useful as a means of controlling the gain of a negative feedback amplifier; this might yield much greater band width, determined by the breakdown voltage rather than the mechanical and electrical Q 's. This has never been tried, to our knowledge; there is one possible advantage over a filter-controlled amplifier, in that a crystal inside the transducer is the ideal equalizer for similar crystals (see Chapter 5).

Considerable work has been done with probes at this laboratory (see Sections 3.4, 3.6, and 4.7), but it is believed that further work might be very worth while. It might even be worth while to consider the possibility of building a stroboscopic optical interferometer to serve as a zero-impedance probe.

Most measurements have been made in water, but it is believed that valuable information might be gained by making measurements in air, i.e., with the transducer diaphragm seeing zero impedance. Under these conditions, the crystals do not see zero impedance, since they work into a cavity usually filled with castor oil and bounded by steel, rubber, etc. The results would be difficult to interpret, but might nevertheless be very useful. Two qualitative points are immediately clear: because of the smaller wavelength, directivity patterns are about five times as sharp in air as in water, assuming the same distribution of velocity over the external surface (this is easy to demonstrate qualitatively); and, if the impedance of a transducer is found to be about the same in air as in water, then it must be dissipation controlled and hence be very inefficient. Window-coupled gas-filled transducers, of which this laboratory has built several, would be especially amenable to study in air, since removing the water termination would cause a readily calculable change in the impedance seen by the crystals.

4.2 RADIATION THEORY

The physical system composed of one or more transducers coupled to a real medium (e.g., the

ocean plus a target) is so complicated that its study as a single problem is impractical. It is therefore very fortunate, on the one hand, that the exact nature of the source or receiver is not critical to the study of problems specific to the medium while, on the other hand, only the most primitive properties of the medium are relevant to the design of transducers. Knowing the characteristics of a transducer in an idealized medium and knowing the characteristics of the actual medium, the results to be obtained with the transducer in the actual medium, at least in principle, can be deduced.² For discussing the pure characteristics of transducers, therefore, the medium is idealized to an infinite fluid which is homogeneous, nonrefracting and nonabsorbing. It is therefore completely characterized by its density and phase velocity, ρ and c . Variations of these quantities in the ocean with temperature, pressure, salinity, frequency, and any other variables, important as they are in the study of transmission, reverberation, etc., all have a negligible effect upon the performance of transducers.

4.2.1

The Sound Field

The pressure produced by a given velocity distribution over a closed surface was shown, in Section 2.1.7, to be given by

$$p(2) = -\left(\frac{ik\rho c}{4\pi}\right) \int dS_1 v_n(1) g_r(1,2), \quad (1)$$

in which v_n is the outward normal component of the velocity amplitude at each point on the closed surface and $g_r(1,2)$ is the rigid Green's function.

This Green's function, in an idealized fluid medium, depends upon the shape and size of the transducer surface and upon the wavelength, in addition to the points \mathbf{r}_1 and \mathbf{r}_2 at which it is evaluated. In Section 2.1.7, it was stated without proof that, for a point \mathbf{r}_2 , very far from the transducer and in the critical wavelength region in which most transducers lie, the best known approximation to the rigid Green's function for a point \mathbf{r}_1 on the surface and \mathbf{r}_2 very distant, is

$$g_r(1,2) = (1 + \cos \alpha) g_0(1,2), \quad (2)$$

$$g_0(1,2) = \frac{\exp ik|\mathbf{r}_2 - \mathbf{r}_1|}{|\mathbf{r}_2 - \mathbf{r}_1|}, \quad (3)$$

$$\cos \alpha = \frac{(\mathbf{r}_2 - \mathbf{r}_1) \cdot \mathbf{n}_1}{|\mathbf{r}_2 - \mathbf{r}_1|}, \quad (4)$$

in which \mathbf{n}_1 is the outward normal to the surface at the point \mathbf{r}_1 , and α is the angle at \mathbf{r}_1 between this normal and $(\mathbf{r}_2 - \mathbf{r}_1)$.

The origin may be taken at any fixed point, but for convenience it will always be assumed to be located at some point on or inside the surface of the transducer. Then

$$r_1 \ll r_2, \quad (5)$$

$$\begin{aligned} k|\mathbf{r}_2 - \mathbf{r}_1| &= kr_2 \left[1 - \frac{\mathbf{r}_1 \cdot \mathbf{r}_2}{r_2^2} + O\left(\frac{r_1^2}{r_2^2}\right) \right], \\ &= kr_2 - \frac{k\mathbf{r}_1 \cdot \mathbf{r}_2}{r_2} + O\left(\frac{kr_1^2}{r_2}\right). \end{aligned} \quad (6)$$

Equation (6) gives the phase difference corresponding to the path difference $|\mathbf{r}_2 - \mathbf{r}_1|$. This has a principal term kr_2 corresponding to the path difference from the reference point on or inside the transducer, a term $k\mathbf{r}_1 \cdot \mathbf{r}_2/r_2$ depending upon \mathbf{r}_2 only through its *direction*, and higher-order terms which depend upon the magnitude of \mathbf{r}_2 . The radiation zone is defined as that part of the field beyond which the latter terms are negligible, and the present considerations are confined to this zone. The lowest-order term in equation (6), which depends upon the magnitude of r_2 , is of the order of

$$\frac{\pi r_1^2}{\lambda r_2}, \quad (7)$$

and it turns out that, for moderately directional transducers, the error involved in dropping these higher-order terms in the phase will be negligible if r_2 is about 20 wavelengths or greater. This indicates that in most cases calibrations are done at an adequate distance, but there is no great margin to spare and some calibrations have been performed in the reorganization zone.

Assuming that the phase error roughly given by equation (7) is negligible, the pressure is

$$\begin{aligned} p(2) &\simeq - \left(\frac{ik\rho c}{4\pi} \right) \left(\frac{\exp ikr_2}{r_2} \right) \\ &\int dS_1 v_n(1)(1 + \cos \alpha) \exp \left(\frac{-ik\mathbf{r}_1 \cdot \mathbf{r}_2}{r_2} \right). \end{aligned} \quad (8)$$

It is convenient to separate the dependence on distance and direction into separate factors. One chooses a standard distance r_s , which is usually 1 yd or 1 m. Also, a reference axis is chosen in the direction θ_{ax}, ϕ_{ax} referred to a specified frame of spherical coordinates; for convenience, this is usually chosen as the axis of maximum intensity, or a particular one of these if there are more than one. Then, if $2^{1/2}P$ is the pressure amplitude obtained from equation (8) at $r_s, \theta_{ax}, \phi_{ax}$, one has

$$p = \left(\frac{r_s}{r_2} \right) \exp ik(r_2 - r_s) 2^{1/2}PD(\theta, \phi), \quad (9)$$

$$D(\theta_{ax}, \phi_{ax}) = 1. \quad (10)$$

The factor $2^{1/2}$ is inserted so that P itself will be the rms amplitude.

The factor $D(\theta, \phi)$ is called the amplitude-directivity pattern of the unit as a transmitter. Its angular variation is given by the integral in equation (8),

$$D(\theta, \phi) \sim \int dS_1 v_n(1)(1 + \cos \alpha) \exp \left(\frac{-ik\mathbf{r}_1 \cdot \mathbf{r}_2}{r_2} \right), \quad (11)$$

and it is to be normalized by equation (10). The directivity patterns corresponding to equation (11) for a variety of velocity distributions, together with other relevant matters, are discussed in detail in Section 4.3.

The intensity at any point on a sufficiently distant sphere is, from Section 2.1.7, directed radially outward and has magnitude

$$\frac{|p|^2}{2\rho c} \simeq \left(\frac{r_s}{r_2} \right)^2 \left[\frac{|P|^2}{\rho c} \right] |D(\theta, \phi)|^2. \quad (12)$$

In equation (12), $|P|^2/\rho c$ is the total *response*, for the given surface velocity, and $|D(\theta, \phi)|^2$ is the intensity-directivity pattern. The total response is variously expressed as

$$\frac{|P|^2}{\rho c} = T_E E^2 = T_I I^2, \text{ etc.}, \quad (13)$$

in which T_E , T_I , etc., are the transmitter responses per volt across *specified* terminals or per ampere in these terminals, etc. These specific responses, and the intensity-directivity pattern, are usually expressed in db relative to the appropriate reference level.

The total power radiated is the flux of the intensity across a large sphere,

$$\text{Total power} = 4\pi r_s^2 \frac{|P|^2}{\rho c} \overline{|D(\theta, \phi)|^2}^{\theta, \phi}, \quad (14)$$

$$\overline{|D(\theta, \phi)|^2}^{\theta, \phi} = \left(\frac{1}{4\pi} \right) \int d\omega |D(\theta, \phi)|^2, \quad (15)$$

in which $d\omega$ is an element of solid angle.

The average of the intensity pattern, equation (15), is called the *directivity factor*. The quantity obtained by converting this to decibels,

$10 \log \overline{|D(\theta, \phi)|^2}^{\theta, \phi}$, is called the *directivity*

index; the directivity factor and index of a perfect spherical radiator are 1 and 0 db, respectively, and are less for all other radiators. A rough estimate of the directivity factor of a transducer, suitable for order of magnitude considerations, is obtained by taking the ratio of the solid angle in which the pattern is above -3 db to that of all space, 4π . For example, suppose a pattern has one fairly symmetric main lobe with a 3-db half-breadth of θ_b radians; then the directivity factor is roughly

$$2\pi \frac{(1 - \cos \theta_b)}{4\pi} = \sin^2 \left(\frac{\theta_b}{2} \right). \quad (16)$$

If θ_b is a fraction of a radian, as it will be in many cases, then this is roughly $(\theta_b/2)^2$; thus the directivity factor of a single lobe unit is of the order of one quarter of the square of the (radian) half-breadth.

4.2.2

Radiation Impedance

The calculation of the radiation impedance corresponding to a given surface-velocity distribution is one of the most important and, at the same time, one of the weakest parts of present theory. This complicated matter is discussed in detail in Section 2.1.7, where our ignorance of the rigid Green's function for variously shaped bodies, in the critical wavelength region, is emphasized.

Present knowledge can be summarized roughly as follows.

1. If the radius of curvature of the surface is small compared with the wavelength, and if

the normal velocity is roughly constant in a region with dimensions of the order of 1 wavelength, then the radiation reactance is negligible and the radiation resistance is approximately ρc .

2. If the surface is covered by pistons (crystals) whose distance from center to center is a little less than a wavelength (about 0.8 will do; see Section 4.2.4), then the wave front is "well supported," the reactance is again negligible, and the resistance is ρc times the ratio of the active to the total area.

3. If the wave front is not "well supported," or if there are appreciable variations of the normal velocity in a distance of the order of a wavelength, then the reactance will have a value which is an appreciable fraction of ρc , while the resistance will fall from its full ρc value.

These semiquantitative results are illustrated by the impedance of a circular piston in an infinite baffle,³ but it should be emphasized that the results for a piston in a baffle are not quantitatively applicable to other surfaces.

The physical basis of these results is that a small piston will have particle-velocity streamlines in front of it which diverge, allowing the fluid to escape laterally; however, if the smallest dimension is increased to a wavelength or so, the escape will become small and the piston will begin to behave like an infinite plane.

There is one other attack that gives some information about the resistive part of the radiation impedance, and this may be quite accurate in the case of a normal velocity which is fairly constant over the vibrating diaphragm and zero elsewhere. This arises from the fact that we have a better approximation to the surface-distant than to the surface-surface Green's function. If the normal-velocity amplitude is constant over a surface, then the power radiated is $r_s A |v|^2 / 2$ (the factor $1/2$ enters because v is the peak, rather than the rms, velocity amplitude), in which r is the average specific resistance seen by the piston. Combining this with equation (14) for the total power radiated, one has

$$r \simeq \left(\frac{4\pi r_s^2 |P|^2}{A |v|^2} \right) \overline{|D(\theta, \phi)|^2}^{\theta, \phi}. \quad (17)$$

To use this approximate formula, one calculates

P from equation (8); the constant velocity v will be a factor of P , and hence the $|v|^2$ in the denominator of equation (17) will cancel out; likewise, r_s^2 will drop out. Furthermore, for most units the calculation of P , which amounts to calculating $p(2)$ on the axis, is very much simplified since, for example, a flat unit will have a zero phase shift $kr_1 \cdot r_2/r_2$. The calculated directivity factor should be compared with calibration data, if possible.

It is extremely unfortunate that we are in such a weak position with regard to a quantitative treatment of the radiation impedance problem, because the resistive part of this impedance not only determines the power output but also the band width of a transducer. However, it is important to clearly recognize this weakness.

On the one hand, we have the theoretical difficulties mentioned above while, on the other, the low electromechanical-coupling coefficients of 45° Y-cut Rochelle salt [RS] and 45° Z-cut ammonium dihydrogen phosphate [ADP] make it difficult to deduce the impedance of the mechanical arm from measurements at the electric terminals.

In Section 9.5 it will be pointed out that, since the electromechanical-coupling coefficient of 45° X-cut RS at some temperatures is much greater than for either of the above crystals, the measurement of radiation impedance could be obtained from experimental transducers using X-cut motors, where the mechanical arm is not as badly obscured by the electric condenser, so that present impedance bridges can resolve it. Since the radiation impedance depends only upon the wavelength in water and the geometry of the transducer, the results so obtained would be applicable to any type of crystal.

The precautions of temperature control, etc., necessary to make this method successful, are discussed in Chapter 9.

4.2.3

Reciprocity

In this section, the general reciprocity theorem of Section 2.4 is put into a form suitable for practical application to crystal transducers. The reciprocity relations are the basis of the

absolute calibrations of electroacoustic transducers, that is, their calibration in terms of electrical and length measurements only. It is therefore important to understand the assumptions upon which they are based.

The first assumption is passivity, no sources of energy. This is satisfied in all units except those containing a preamplifier. The second is linearity, both for transducers and medium. We have every reason to believe that this assumption is satisfied far beyond any practical accuracy in the medium and in ADP and Y-cut RS units, the first two probably better than the last because fringing flux involves the nonlinear relation between electric displacement and field in the X-direction of RS. It is definitely not satisfied for X-cut RS, and hence such units should be calibrated by comparison with linear units that have been calibrated by the absolute method. In any event, the two assumptions can be tested by electrical measurements alone.

These two assumptions can be expressed in the form

$$p_f = TI, \quad (18)$$

$$e = Rp_f'. \quad (19)$$

The first asserts that the *free-field* pressure in the medium is proportional to the current inserted into a unit acting as a transmitter; the second that the *open-circuit* voltage produced be a free-field pressure is proportional to that pressure. The quantities T and R depend on distance and direction, properties of the medium and transducer, and frequency, but are independent of level.

The third and last assumption is that any two units, fixed in position in the medium, will behave like a four-terminal electric network. Thus if I inserted into No. 1 produces e in No. 2, it is assumed that the same I inserted into No. 2 will produce the same e in No. 1,

$$e = R_2 T_1 I = R_1 T_2 I. \quad (20)$$

This is a property of a broad class of systems, called linear, passive, and bilateral. It is shown in Section 2.4 that a quite general class of linear-dissipative piezoelectric systems are circuit-like.

From equation (20) we conclude that

$$\frac{R_1}{T_1} = \frac{R_2}{T_2} = \frac{R_3}{T_3}, \text{ etc.} \quad (21)$$

This shows that the directivity pattern of a unit, satisfying the above assumptions, is the same either as a transmitter or a receiver. And more than this, that the ratio of the response as a receiver to that as a transmitter (both in the same direction) is a number which is not only independent of orientation, but *does not depend upon the properties of the unit*. It can therefore depend only upon separation, properties of the medium, and frequency. This quantity, commonly called J , can therefore be evaluated by considering an idealized transducer.

A spherical unit, radius a , is assumed to be so constrained that it can have only uniform

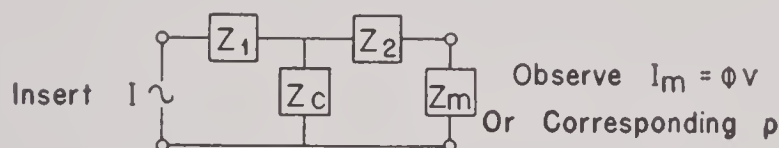


FIGURE 4. Equivalent circuit of a transducer used as a transmitter.

radial motion. Its equivalent circuit as a transmitter is shown in Figure 4, the assumption of this circuit corresponding to the assumptions discussed above. Capital Z , with various subscripts, is here used as the actual or equivalent electric impedance,

The current I produces a current I_m in the impedance Z_m , which represents the medium, and this corresponds to a mechanical velocity v ,

$$I_m = \left(\frac{Z_c}{Z} + Z_m \right) I, \quad (22)$$

$$Z = Z_2 + Z_c, \quad (23)$$

$$v = \phi^{-1} I_m, \quad (24)$$

in which ϕ is the electromechanical-coupling coefficient (whose value need not concern us because it drops out of our final result for J), and Z is the impedance seen looking into the mechanical terminals with Z_m removed and the electric terminals open.

The above velocity is purely radial, and therefore produces a pressure

$$p = \frac{i\rho c v h_0(kr)}{h'_0(ka)}, \quad (25)$$

$$h_0(z) = \frac{e^{iz}}{iz}, \quad (26)$$

$$z_m = \left(\frac{p}{v} \right)_a = \frac{i\rho c h_0(ka)}{h'_0(ka)} = \frac{\phi^2 Z_m}{4\pi a^2}, \quad (27)$$

in which z_m corresponds to Z_m but is specific and measured in mechanical units, and the prime means differentiation with respect to the whole argument ka . Inserting the value of v from equations (22) and (24) into equation (25), we obtain

$$p = TI, \quad (28)$$

$$T = i\rho c \phi^{-1} \left(\frac{Z_c}{Z} + Z_m \right) \frac{h_0(kr)}{h'_0(ka)}. \quad (29)$$

The equivalent circuit as a receiver is shown in Figure 5, in which it is important to notice

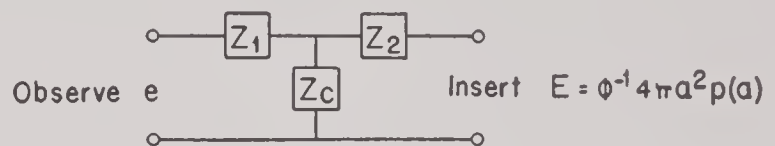


FIGURE 5. Equivalent circuit of a transducer used as a receiver.

that here $p(a)$ is the actual pressure, freefield plus reflected wave, at the spherical surface.

We must now relate the actual pressure to the free field. Let a plane wave $p_f = p_0 \exp(ikz)$, traveling in the positive z direction, fall on the unit acting as a receiver. This plane wave may be regarded as the superposition of incoming and outgoing spherical waves (origin at center of receiver). These will have angular dependence according to the Legendre polynomials $P_n(\cos \theta)$ and since the unit is assumed to have infinite impedance for all of these, except $n = 0$, (uniform radial motion), they will be reflected as if from a rigid sphere and may therefore be ignored. We therefore need consider only the spherically symmetric term, which can be obtained by averaging the pressure over any sphere of radius r ,

$$\begin{aligned} \bar{p}_f &= \left(\frac{p_0}{4\pi} \right) \int \exp(ikr \cos \theta) d\Omega \\ &= p_0 j_0(kr), \\ j_0(kr) &= \frac{\sin kr}{kr}. \end{aligned} \quad (30)$$

To this free-field pressure must be added a

wave which makes the velocity on the surface correct, and which must vary like $h_0(kr)$ since it is outgoing,

$$\bar{p} = p_0 [j_0(kr) + \mu h_0(kr)], \quad (31)$$

$$\bar{p}(a) = p_0(j_0 + \mu h_0) = -zv = \frac{-\phi^2 Z}{4\pi a^2}, \quad (32)$$

$$\left(\frac{d\bar{p}}{dr}\right)_a = kp_0 [j'_0 + \mu h'_0] = i\omega\rho v, \quad (33)$$

in which z corresponds to Z but is specific and in mechanical units, and the argument of j_0 , h_0 , etc., is understood to be ka when not written.

Dividing equation (33) by equation (32), we eliminate v and p_0 and thus find μ ; putting this back into equation (32), the desired relation between $\bar{p}(a)$ and $p_f(a)$ is established, so that we can find v in terms of p_0 ,

$$\bar{p}(a) = \left(\frac{-ip_0}{k^2 a^2}\right) \left(h'_0 + \frac{i\rho ch_0}{z}\right)^{-1} = -zv. \quad (34)$$

This velocity, produced by p_0 , is equivalent to a current ϕv , and the drop across Z_c is therefore

$$e = \phi v Z_c = R p_0, \quad (35)$$

$$R = \phi Z_c \left(\frac{i}{k^2 a^2}\right) (h'_0 z + i\rho ch_0)^{-1}. \quad (36)$$

We thus find for the ratio J ,

$$J = \frac{R}{T} = \phi^2 \frac{(Z + Z_m)}{k^2 a^2 (z + z_m) \rho ch_0 (kr)} = \left(\frac{2r\lambda}{\rho c}\right) i \exp(-ikr), \quad (37)$$

$$|J|^2 = \left(\frac{2r\lambda}{\rho c}\right)^2, \quad (38)$$

and equation (19) becomes

$$e = J T p_f. \quad (39)$$

The absolute evaluation of T , and therefore R , is now seen to be achieved by running three units against one another, at least one being used both as a transmitter and a receiver, according to either of the two schemes:

Transmitter	1	2	3	1	2	1
Receiver	2	3	1	2	3	3

(40)

This gives the three products $T_1 T_2$, $T_2 T_3$, and $T_3 T_1$ in terms of electrical (and distance) measurements only.

In conclusion, we notice that a reciprocity

measurement by itself is not an absolute calibration unless the units and the medium have been shown to satisfy the basic assumptions at the actual operating levels. For example, if one of the transmitters causes cavitation, the whole measurement is invalidated.

The above discussion neglects the effect on the transmitter of the wave scattered by the receiver. This may be important since calibrations are usually done at fairly short range. The usual test is to see if the inverse square law of intensity is satisfied, and this seems to be entirely adequate.

We observe from equation (38) that

$$|T|^2 = \left(\frac{\rho}{2r}\right)^2 f^2 |R|^2. \quad (41)$$

Thus if a correction of 6 db per octave is added to the receiver response (open-circuit voltage per dyne per sq cm, free field), the resultant curve should coincide with the transmitter response (free-field dynes per sq cm per amp) if it is displaced vertically. Furthermore, the necessary vertical displacement of the corrected receiver response should be given by $20 \log(\rho/2r)$. This relation is useful as a check on the consistency of calibration data. One usually finds the above relation to hold within a db or so over a wide frequency range; this not only gives confidence in the accuracy of the calibration data, but also in the validity of the reciprocity assumptions.

A similar relation exists between the short-circuit receiver response (amperes per dyne/per sq cm free field, when receiver terminals are short-circuited), and the constant-voltage transmitter response (free-field dynes per sq cm per v). It is unfortunate that the short-circuit receiver response is not used more widely as a calibration method, since it eliminates errors arising from cable and stray capacitances.

1.2.4

Cylindrical Transducers

Transducers whose active faces form arcs of circular cylinders are of such practical importance as to be worthy of special consideration. The considerations developed in this section

will also have application to other curved-face units.

It is advantageous to first restrict ourselves to a complete cylindrical arc. Neglecting the slight deviation of the flat radiating faces of the crystals from a cylindrical surface, let N equal pistons of height $2h$ be uniformly arrayed so as to form strips on a circular cylinder of radius a , the centers being at $2\pi n/N$ radians ($n = 1$ to N) and the angular width being 2α . We want to know how large N must be to avoid a serious scalloped appearance of the pattern, and how to calculate the impedance and response.

DIRECTIVITY PATTERNS

The pressure at \mathbf{r}_2 , dropping all factors independent of direction, is given by

$$p \sim \int dS_1 v(1) \exp \left(-ik\mathbf{r}_1 \cdot \frac{\mathbf{r}_2}{r_2} \right) \cdot \left(1 + \zeta \mathbf{R}_1 \cdot \frac{\mathbf{r}_2}{R_1 r_2} \right), \quad (42)$$

in which the large R 's are cylindrical, the small r 's spherical, radial coordinates. It is important to include the obliquity factor, last factor in the integrand, in treating cylindrical units to prevent spurious contributions through the cylinder. In this factor, ζ is the impedance of the medium at each point on the surface, in *gc units*. In all that follows, we assume $v(1)$ to be a constant on all pistons and zero between them.

The integration with respect to z_1 gives a factor

$$\frac{\sin(kh \sin \psi_2)}{(kh \sin \psi_2)}, \quad (43)$$

in which $\sin \psi_2 = z_2/r_2$ is the angle from the equatorial plane. This factor is identical with that for a line source.

The obliquity factor can be generated by a differential operator, and the remaining integral therefore becomes

$$\left(1 + \frac{i\zeta d}{dka} \right) \int d\phi_1 \exp [-ika \cos(\phi_2 - \phi_1) \cos \psi_2]. \quad (44)$$

The above integrand can be expanded in a Fourier series⁴ according to

$$\exp iz \sin \phi = \sum_{-\infty}^{\infty} J_m(z) \exp im\phi. \quad (45)$$

The integration extends between $\phi_1 = 2\pi n/N - \alpha$ and $2\pi n/N + \alpha$ for the n th piston and this must then be summed over all pistons. The result is that only those m 's which are integer multiples of N contribute. These give a factor, $\sin \mu N \alpha / \mu N \alpha$.

Dropping further unessential factors, the pressure pattern is

$$p \sim \left(\frac{\sin kh \sin \psi_2}{kh \sin \psi_2} \right) \left(1 + \frac{i\zeta d}{dka} \right) \cdot \sum_{\mu=-\infty}^{\infty} \left(\frac{\sin \mu N \alpha}{\mu N \alpha} \right) \exp i\mu N \left(\phi_2 - \frac{\pi}{2} \right) J_{\mu N}(ka \cos \psi_2). \quad (46)$$

This has a term independent of ϕ_2 , together with terms which give N , $2N$, etc., maxima as ϕ_2 ranges from 0 to 2π . The amplitude of these scalloped petals is determined by the factors $(1 + i\zeta d/dka) \cdot (\sin \mu N \alpha / \mu N \alpha) J_{\mu N}(ka \cos \psi_2)$. If $N\alpha = \pi$, the cylinder is completely filled up, all sine factors (except for $\mu = 0$) vanish and the pattern is uniform. However, it is usually not possible to fill the arc well enough to get much help from the sine factors, and we must therefore look at the Bessel factors. Dropping all but $\mu = -1, 0$, and 1 , and confining ourselves to the equatorial plane where the scalloped effect is worst, we have

$$p \sim (J_0 + iJ'_0) + 2(-i)^N (J_N + iJ'_N) \cdot \left(\frac{\sin N\alpha}{N\alpha} \right) \cos N\phi_2. \quad (47)$$

In most cases of practical interest, the impedance factor ζ will be very close to 1, and to suppress the scallops we must therefore take N large enough that

$$\left| \frac{J_N + iJ'_N}{J_0 + iJ'_0} \right| \ll 1. \quad (48)$$

The Bessel functions, considered as functions of their parameter N for fixed argument ka , oscillate out to $N \simeq ka$ and then fall away exponentially.⁵ This transition from oscillatory to exponential behavior occurs with a change of only 1 in N and we therefore need only choose N a little larger than ka to make the pattern uniform. The amplitude of the scallops in any

particular case is readily calculated from equation (47).

IMPEDANCE

To calculate the impedance of units which are at least a few wavelengths high (the practical case, since any vertical directivity requires this), we can consider the unit to be infinitely long without serious error. A normal-mode expansion is then taken for the pressure, since we need to know it and its radial gradient at the face,

$$p = \left(\frac{i\rho cv N \alpha}{\pi} \right) \sum_{\mu=-\infty}^{\infty} \left(\frac{\sin \mu N \alpha}{\mu N \alpha} \right) \left(\frac{H_{\mu N}(kR)}{H'_{\mu N}(ka)} \right) \exp i\mu N \phi, \quad (49)$$

$$ik\rho cv(a) = \left(\frac{dp}{dR} \right)_a = ik\rho c \left(\frac{N\alpha}{\pi} \right) v \sum_{-\infty}^{\infty} \left(\frac{\sin \mu N \alpha}{\mu N \alpha} \right) \exp i\mu N \phi. \quad (50)$$

It is readily verified that equation (50) gives velocity v on each crystal strip and zero between the strips.

The average pressure acting on a crystal strip is

$$\bar{p} = \left(\frac{1}{2\alpha} \right) \int_{\text{strip}} d\phi p(a), \quad (51)$$

and this just inserts another factor $(\sin \mu N \alpha / \mu N \alpha)$ into equation (49). Now if N has been taken large enough to make the pattern fairly uniform, only the term $\mu = 0$ will contribute appreciably to equation (51), because the factor $H_{\mu N} / H'_{\mu N}$ falls rapidly as N exceeds ka , and we have

$$\bar{p} \simeq \rho cv \left(\frac{2N\alpha}{2\pi} \right) \left(\frac{iH_0(ka)}{H'_0(ka)} \right). \quad (52)$$

This is just $(2N\alpha/2\pi)$ times the pressure produced by a complete arc vibrating radially and we have the physically plausible result that the impedance seen by each crystal is merely that for a completely filled cylinder multiplied by the ratio of the driven area to the total area.

INCOMPLETE ARC

The foregoing refers to a uniform angular distribution of pistons, and we need to know

how our conclusions will be altered if there are only N' pistons with the same center-to-center angle $2\pi/N$.

In this case, values of m other than integer multiples of N make contributions, and equation (46) is replaced by

$$p \sim \left(\frac{\sin kh \sin \psi_2}{kh \sin \psi_2} \right) \left(1 + \frac{i\zeta d}{dka} \right) \sum_{m=-\infty}^{\infty} J_m(ka \cos \psi_2) \exp im \left(\phi_2 - \frac{\pi}{2} \right) \left[\frac{\sin m\alpha}{\pi m/N} \right] \left(\frac{2}{m} \right) \left(\frac{\sin \pi m N'}{N} \right) \exp \left[\frac{-\pi im(N' + 1)}{N} \right]. \quad (53)$$

The physics of this complicated result can be understood well enough for all practical purposes as follows: we restrict our considerations to the equatorial plane, and assume that ka is large enough to make ζ close to 1. Furthermore, we suspect that just as in the case of the complete arc, we will need to take N a little larger than ka to prevent the pattern showing a maximum for each piston.

The factors $J_m + iJ'_m$, obtained by allowing the obliquity operator to act on J_m , will be well represented by their asymptotic expansions out to $|m| \simeq m'$, the integer nearest ka , and will then fall so sharply that we can break the sum there. Since m' is less than N and α is less than π/N , the factor $(\sin m\alpha) / (\pi m/N)$ is approximately $(N\alpha/\pi)$, independent of m . Dropping all factors independent of m and ϕ_2 , the equatorial pattern is therefore approximately

$$p \sim \sum_{m=-m'}^{m'} \exp im\phi_2 \left[\frac{\sin \left(\frac{\pi m N'}{N} \right)}{\left(\frac{\pi m N'}{N} \right)} \right] \exp \left[-\pi im \frac{(N' + 1)}{N} \right], \quad (54)$$

and it is easy to verify that this is exactly the first $2m' + 1$ terms of the Fourier expansion of a function which is constant in front of the active face (including dead strips) and zero elsewhere. Now the effect of the high terms absent in this series is well-known; they are necessary to give sharp corners and complete constancy. We therefore conclude that if ka is large (at least 2 or 3, which is always necessary anyway to get appreciable vertical directivity in a unit of practical size), and if N is a

little greater than ka , then the pattern corresponding to uniform velocity over an incomplete arc is simply a cylindrical wedge in front of that arc, with small deviations from constancy, the corners rounded, and some small spill-over at the edges of the wedge. The angle at which the pattern is down, say, 3 db from the center value, could be calculated by numerical evaluation of equation (53). However, the velocity is never quite constant over the active face, either in magnitude or phase; the effect of obstacles (walls of the case, etc.) have not been considered; etc. For these and other reasons, this computation is not worth making; it is much better to use the foregoing theoretical treatment as a semiquantitative guide to design, build a unit, and see how it works.

We are now in a position to make some further semiquantitative generalizations from the foregoing results, together with similar results for a spherical transducer. The condition that N must be a little larger than ka can be written

$$\frac{2\pi a}{N} < \lambda, \quad (55)$$

and in this form it has a very simple physical interpretation which with an obvious slight alteration is applicable to *noncylindrical* units. The left member is just the arc distance between centers of adjacent pistons and equation (55) therefore asserts that to radiate a good cylindrical wave, that wave must be supported at points less than a wavelength apart. We could have written this down at the outset, but the analysis has revealed one rather surprising quantitative result: the suddenness with which good cylindrical waves set in as N passes the value ka . This is a consequence of the exponential decay of $J_m(ka)$ after m passes ka , and would never have been predicted from qualitative physical arguments alone; one would more likely have expected that the wave would need support at many points within a wavelength whereas, actually, if it is supported an average of 1.2 times in every wavelength, the pattern is excellent. As a practical example of this, we need only examine the patterns of complete arc

units actually built and see how suddenly a breakup occurs from quite a smooth pattern to a scallop with, at first, N petals as the frequency passes through the critical value. Once this breakup occurs, the pattern is controlled by J_N until the frequency is approximately doubled, when J_{2N} suddenly becomes important. For incomplete arcs, the situation is a little more complicated; up to ka a little less than N , the pattern is the rounded wedge previously discussed, but as ka exceeds N everything happens at once. It is of no importance to attempt to calculate these complicated effects; rather, we must merely arrange our designs so as to avoid them and this is very fortunately a much simpler matter. Calculations for flat and spherical units lead to the same conclusions as to the effect of spacing the active elements and we can therefore state a general spacing rule in a form applicable to any transducer, flat or curved: *to generate a wave surface that will not contain a resolution of the active elements, the largest center-to-center distance between active elements must be slightly less than a wavelength (not more than 80 per cent).*

It may at first glance seem curious that the size of the active elements ($2aa$ in the cylindrical case) does not enter into this rule, i.e., that a number of points of negligible size compared to the wavelength, but spaced with a lattice constant of not more than 80 per cent of a wavelength, will give a smooth pattern. The essential point is that interference between the subelements of an element does not become important until the dimensions of the element are nearly a wavelength, and then only at angles considerably removed from the normal. If we keep the center-to-center distance between elements fixed at something less than a wavelength and then allow the elements to grow until they fill the surface completely, the only appreciable effect is therefore a gradual increase in intensity. This result is merely another aspect of the well-known principle in optics that two objects separated by less than a wavelength are not well resolved. While the size of sufficiently close elements has a negligible influence on the pattern, the change in intensity with size changes the impedance seen by each element, as discussed below.

IMPEDANCE OF INCOMPLETE ARCS AND OTHER SURFACES

In order to find the power radiated, we need to know the impedance seen by the active elements. These are assumed to be sufficiently rigid that they move as a unit, so that we need to know the average pressure over their surfaces, as a function of their velocity.

If a single crystal with radiating dimensions small compared to the wavelength pushes into a fluid, the streamlines will tend to slip around to the side and the crystal will see a low radiation resistance. If we support this crystal by neighbors moving in phase, this divergence of the streamlines will be reduced. Now if the distribution of the active elements satisfies the spacing rule for obtaining a good pattern, then the wave surface a wavelength or so in front of the face will have lost most of the spottiness arising from the individual elements, and this rapid transition zone therefore functions essentially as a mechanical transformer. This means that equation (53) is essentially a local relation and we therefore expect the analogous relation to hold on any surface satisfying the spacing rule,

$$\frac{\bar{P}}{v} = \rho c \left(\frac{A_a}{A_t} \right) \frac{iH_0(ka)}{H'_0(ka)} \simeq \rho c \left(\frac{A_a}{A_t} \right), \quad (56)$$

in which A_a and A_t are the active and total areas.

RESPONSE

We are now able to calculate the response, in terms of the response of a related flat unit, of any unit that satisfies the spacing condition, which is of course the only type of unit in which there is much practical interest since one of the specifications is bound to be a pattern that does not resolve the active elements.

Let P be the total power radiated, I_0 the axial intensity, and $D(\theta, \phi)$ the (intensity) directivity pattern, one in the axial direction, so that $I = I_0 D$. Then

$$P = r^2 I_0 \int_{\text{sphere}} D \sin \theta d\theta d\phi = 4\pi r^2 I_0 \bar{D}, \quad (57)$$

in which \bar{D} is the average value of D over a sphere of sufficiently large radius r surround-

ing the unit, and is called the directivity factor. The axial direction is always chosen as the direction of maximum intensity, so that \bar{D} is always less than 1, except for a spherical radiator, for which it is 1.

Now let us build a flat unit, using identical crystals again arranged so as to satisfy the spacing conditions. For example, corresponding to a cylindrical unit of total angle $2\pi N'/N$, radius a , and height $2h$, we build a flat rectangular unit of dimensions $2h$ by $2\pi a N'/N$. The power radiated, etc., from this unit is designated by a prime. P' will differ from P only because of the change in impedance seen by the crystals, caused by a small change in the ratio of active to total area. The ratio P/P' , different from 1 because of this impedance change, will depend upon the drive (e.g., constant current, constant voltage, out of a given amplifier), the matching network used, and the mechanical termination of the crystals (backing plate, inertia drive, etc.). In any event, this ratio is readily calculable from the equivalent circuit of the transducer and the two impedances; usually, P/P' will correspond only to a decibel or two. The axial intensity I'_0 will differ from I_0 because P' differs from P , but more important, because the total power radiated goes into a smaller solid angle, i.e., because \bar{D}' is less than \bar{D} .

We can therefore compare the axial intensity for a curved unit with that of the corresponding flat unit:

$$P = \left(\frac{P}{P'} \right) 4\pi r^2 I'_0 \bar{D}' = 4\pi r^2 I_0 \bar{D}, \quad (58)$$

$$10 \log I_0 = 10 \log I'_0 - 10 \log \left(\frac{\bar{D}}{\bar{D}'} \right) + 10 \log \left(\frac{P}{P'} \right). \quad (59)$$

For a circular arc of total angle ϕ , the change arising from the greater angle into which the energy is radiated is approximately

$$-10 \log \left(\frac{\bar{D}}{\bar{D}'} \right) = -10 \log \phi ka. \quad (60)$$

This can cause a considerable reduction in intensity compared to the corresponding flat unit. For example, our CS-type units operate at $ka \simeq 10$, $\phi = 2\pi$, and equation (60) gives about -18 db; our CQ units operate at a much higher

ka , about 30, but their arc is only 90° , so that equation (60) gives about -17 db for them.

Since the open-circuit response of a unit as a receiver is simply related to its constant-current response,^b we see that the same ratio of directivity factors will enter in the receiver response of a curved-face unit relative to that of a flat unit.

However, in this case the physical interpretation is as follows: a plane wave falling on the unit excites the crystals lying in the first Fresnel zone approximately in one phase, whereas the remaining crystals are excited in all phases about equally so that their resultant is small. For a cylindrical unit, the arc of the first Fresnel zone is approximately $(a\lambda)^{1/2}$, so that a fraction $(a\lambda)^{1/2}/2\pi a$ are excited in the zone. Since the effect of the others is negligible, we can regard them as shunts across those in the first zone and the voltage across any one is therefore only the above fraction of what it would be if they were all excited in phase. On a decibel basis, therefore, we expect the response to be changed on this account by

$$-10 \log \frac{(2\pi a)^2}{a\lambda} = -10 \log 2\pi ka, \quad (61)$$

which is the same as equation (60) for a complete arc.

4.3

DIRECTIVITIES

4.3.1

Theoretical Discussion

The calculations of the directivities of transducers leads at once into the general problem of the determination of a wave motion throughout an unlimited medium caused by an initial disturbance in a small part of the medium. This problem was first solved in general form for periodic waves by Helmholtz.⁶ His solution, in effect, assumes that any wave front can be replaced by a distribution of simple and double sources whose intensities are functions of the velocity potential of the wave being considered

^b See Section 4.2.3 on reciprocity. One subtracts $10 \log (10^7 \text{ gf}/2r)^2$ db from the transmitter response, db above 1 bar/amp, to get the open-circuit response, db above 1 v/bar. In this formula, all quantities are in cgs units.

at the points of the sources, so that the wave motion at any point in space ahead of the wave front can be calculated from surface integrations over these assumed sources.

$$u(x,y,z,t) = \frac{1}{4\pi} \int_s \int \left[\frac{\partial}{\partial n} e^{ik(r_1 - ct)/r_1} - v \frac{\partial}{\partial n} e^{ik(r_1 - ct)/r_1} \right] ds, \quad (62)$$

(v is the velocity potential of the given wave at surface s) where $\partial v/\partial n$ is the normal derivative of the velocity potential at the surfaces s , r_1 is the distance between the surface element ds and point (x,y,z) . The first and second terms in the integral represent the simple and double sources respectively.

There are three cases where the above integral can be handled rather simply, i.e., waves that are plane, cylindrical, and spherical. The velocity potential of these can be written respectively:

$$\begin{aligned} v_p &= Ae^{ik(x - ct)}, \\ v_s &= Ae^{ik(r - ct)}, \\ n_c &= Y_0(kr)e^{-ikct}, \\ Y_0(Kr) &= \frac{2}{\pi} \log \left(\frac{1}{2}kr \right) J_0(kr). \end{aligned}$$

As the spherical wave represents a point source and gives a nondirective field, it is trivial for use in transducer design. The plane and cylindrical cases, however, are useful in that most transducers have either plane or cylindrical radiating faces.

4.3.2

Specific Examples

PLANE RADIATORS

As a large class of transducers have plane radiating surfaces, the case of the plane progressive wave is of great importance. The velocity potential of this wave can be written $u = Ae^{ik(x - ct)}$ in which case the general formula can be written in

$$u(x,y,z,k) = \frac{1}{4\pi} \int_s \int \frac{ik}{r_1} e^{ik(x + r_1 - ct)} \left[1 + \cos \Psi + \frac{1}{r_1} \cos \Psi \right] ds - z, \quad (63)$$

where v_1 is the distance between the area ele-

^c $Y_0(kr)$ is Weber's function.⁷ Any Bessel's function of order zero that has singularity at $r = 0$ can be used.

ment ds and the point (x, y, z) and Ψ is the angle between the x axis and v_1 at the element ds . Two cases arise now, the one for points at large distance from the plane $x = 0$, and the other for points in the neighborhood of $x = 0$. In the first case $k \gg 1/r_1$, and the term $1/r_1 \cos \Psi$ can be dropped. Also as

$$\frac{\partial u}{\partial x} = ik e^{ik(x-ct)},$$

$$\left[\frac{\partial u}{\partial x} \right] = ik e^{ik[x - c(t - r/c)]}$$

the equation becomes:

$$u(x, y, z, t) = \frac{1}{4\pi} \iint_s \left[\frac{\partial u}{\partial x} \right] e^{ikr/r} (1 + \cos \Psi) ds. \quad (64)$$

The effect of the assumed sheet of double sources in the case of a plane wave thus adds the "obliquity" term $\cos \Psi$.

In the second case, where r_1 is not very much larger than a wavelength, the third term must be retained. This problem was first solved rigorously by Sommerfeld⁸ for the case of diffraction of a plane wave around a straight edge. His solution, in effect, describes the physical process as an interference between a plane progressive wave sharply cut off at the geometric shadow and a cylindrical wave generated at the edge of the opaque boundary. The diffraction of a slit would then be described as an interference between three wave systems, two cylindrical with origins at the slit edges, and one plane, whose boundaries are the geometric shadows of the slits. The wave field immediately in front of the slit would then have many maxima and minima depending on the ratio of the slit width to the wavelength, while at great distances the field would display a central maximum with regular lines of maxima and minima on either side. Proceeding from the slit on perpendicular axis, then, there would be alternate maxima and minima out to about 10 slit widths, from which point on out the field would decrease steadily as the inverse square of the distance. The wave field close to the slit has its optical analogy in the Fresnel diffraction, and the field at great distance has its optical analogy in the Fraunhofer diffractions.^d The case of the infinite slit

is not, except for a few cases, directly applicable to diffraction fields in high-frequency sound because no transducers are ever built with infinite lengths and many do not resemble slits, and even to resemble slits or holes, the unit would have to be operated in an infinite baffle; but the general picture is the same for all sources that in size are comparable to the wavelengths they generate. The sound field or any shaped-plane radiator should, close to the surface, exhibit many maxima and minima distributed in space both along the axis perpendicular to the surface and in planes parallel to the surface, and should, at large distances, exhibit a central maxima with side lobes of decreasing amplitude with distance from the central axis. The field at great distances is of course important in sound signaling, and the field close in is important in the coupling between two or more transducers that must be operated close together.

Most of the plane radiators in use are bounded by squares or circles, and the interest is only in the distant part of their sound fields. Under these conditions, the directivities are easily calculated. The case of the circular radiator was first solved by Rayleigh¹⁰ who, neglecting the obliquity factor $\cos \Psi$, evaluated the integral

$$u(x, y, z, t) = -\frac{1}{4\pi} \iint_s \left[\frac{\partial u}{\partial x} \right] \frac{e^{ikr}}{r} ds,$$

where s is a circular area of radius r , $[\partial u / \partial x]$ is constant over this area, and r is the distance from element ds to point (x, y, z) .

As the pressure p is given by $p = -\rho \partial u / \partial t$, the directivity formula for the pressure can be written

$$p(x, y, z) = \frac{\rho c}{4\pi} \left[\frac{\partial u}{\partial x} \right]_{x=0} \iint_s \frac{e^{ikr}}{r} ds.$$

Integrating over the disk of radius r the pressure at point p is

$$p = \frac{\rho c}{4\pi} \left[\frac{\partial u}{\partial x} \right]_0 \frac{2\pi R^2}{r_1} \left| \frac{J_1(x)}{x} \right|,$$

where $x = kr \sin \theta$, θ being the angle between v_1 and the direction of x , $k = 2\pi/\lambda$. Usually only

^d Excellent pictures of the complete sound field are given.⁹

the variation of pressure with angle θ is of interest in which case^e

$$P_d = \left| \frac{J_1(x)}{x} \right| = \frac{1}{2} \Lambda_1(x).$$

The case of the square or rectangular bounded radiator is easier to calculate, the result being

$$P_d = \frac{ab}{v_1} \frac{\sin x}{x},$$

where $x = (ka/2) \sin \theta$ in the plane perpendicular to the side a , or $x = (kb/2) \sin \theta$ in the plane perpendicular to the side b . Again if only the variation with angle θ is needed the first term ab/v_1 may be omitted as $\sin x/x = 1$ for $x = 0$. A graph of the functions $\sin x/x$ and $2J_1(x)/x = \Lambda_1(x)$ is shown in Figures 6 and 7.

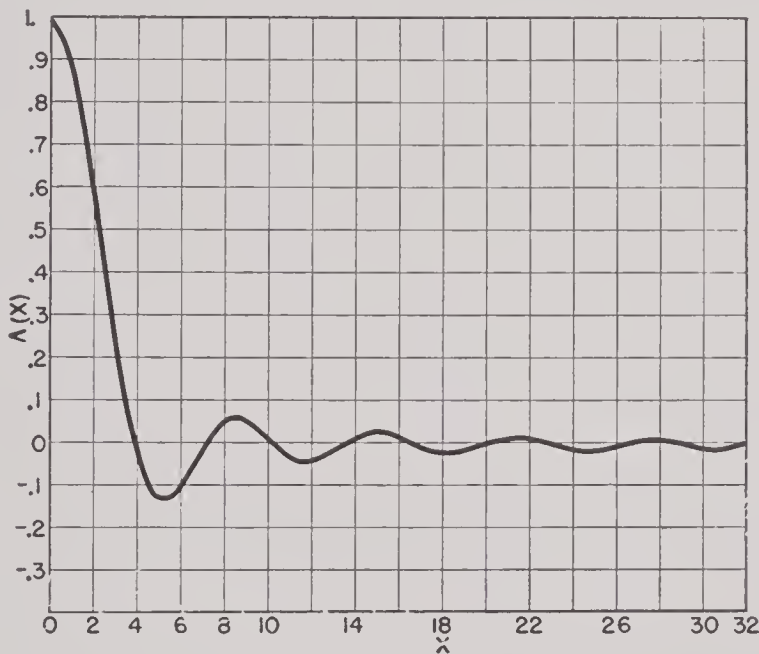


FIGURE 6. $\Lambda_1(x) = \frac{2J_1(x)}{x}$ as a function of x ;
 $x = \frac{2\pi r}{\lambda} \sin \theta$. (Circular-plane radiator.)

The zeros of the $\sin x/x$ function corresponding to the nulls between lobes come at $x = n\pi$, while the maxima occur at the roots of the equation $x = \tan x$. These were calculated first by Schwerd to be $x = 4.49, 7.7, 10.9, 14.1, 17.1, 20.3$.^f

^e For a table of these $\Lambda_1(x)$ functions see Janke and Emde Tables P; also for more details about this integration see reference 11.

^f The zeros of the $\Lambda_1(x)$ functions occur at ($x = 3.8, 7, 10.2, 13.4, 16.4, 19.6, 22 \dots$ and the maxima at ($x = 5.1, 8.4, 11.6, 14.8, 18, 21.2 \dots$).

Other useful facts about these functions are given in Table 1.

TABLE 1

Db down	Formula
<i>Circular</i>	
α = radius	
λ = wavelength	
3	$\theta = \sin^{-1} 0.258 \frac{\lambda}{\alpha}$
6	$\theta = \sin^{-1} 0.350 \frac{\lambda}{\alpha}$
∞	$\theta = \sin^{-1} 0.595 \frac{\lambda}{\alpha}$ 1st zero
17.8	$\theta = \sin^{-1} 0.818 \frac{\lambda}{\alpha}$ max first lobe
∞	$\theta = \sin^{-1} 1.11 \frac{\lambda}{\alpha}$ 2nd zero
23.8	$\theta = \sin^{-1} 1.34 \frac{\lambda}{\alpha}$ max 2nd lobe
∞	$\theta = \sin^{-1} 1.62 \frac{\lambda}{\alpha}$ 3rd zero
<i>Square</i>	
α = side of square	
3	$\theta = \sin^{-1} 0.446 \frac{\lambda}{\alpha}$
6	$\theta = \sin^{-1} 0.605 \frac{\lambda}{\alpha}$
∞	$\theta = \sin^{-1} 1.00 \frac{\lambda}{\alpha}$ 1st zero
13.47	$\theta = \sin^{-1} 1.43 \frac{\lambda}{\alpha}$ max first lobe
∞	$\theta = \sin^{-1} 2.00 \frac{\lambda}{\alpha}$ 2nd zero
18.24	$\theta = \sin^{-1} 2.36 \frac{\lambda}{\alpha}$ max 2nd lobe
∞	$\theta = \sin^{-1} 3.00 \frac{\lambda}{\alpha}$ 3rd zero

The directivity function for a rectangle of sides a and b in the plane containing the diagonal and perpendicular to the face is

$$P_d = \frac{\sin u}{u} \frac{\sin z}{z},$$

where $u = (ka/2) \sin \theta$ and $z = (kb/2) \sin \theta$. In the case of the square this reduced to

$$P_d = \left(\frac{\sin u}{u} \right)^2.$$

It is seen that the side lobes in this plane decrease more rapidly, a fact made use of by mounting square transducers at an angle of 45° to the surface of the water.

For fields close to the transducer, Schwarzschild has attacked the problem in the case of a slit wide compared to the wavelength, and many authors¹²⁻¹⁶ have written on the case of the circular piston. Most of the solutions involved the development of the velocity potential in infinite series that do not converge very rapidly so that large numbers of terms must be considered in the calculations. They have however been able

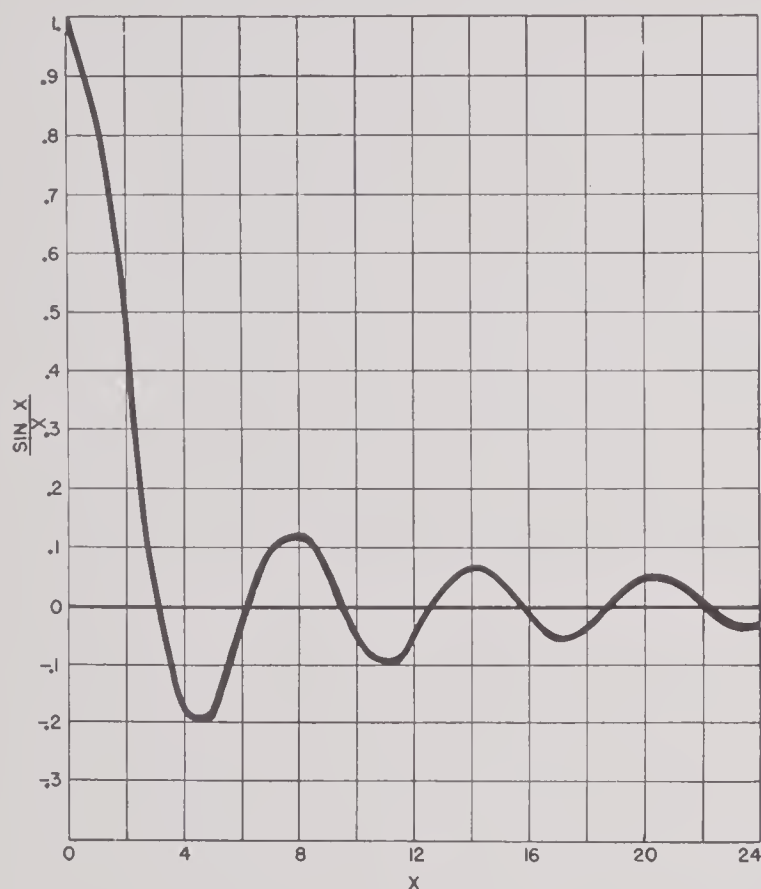


FIGURE 7. $\frac{\sin x}{x}$ as a function of x ; $x = \frac{\pi d}{\lambda} \sin \theta$.
(Square-plane radiator.)

to calculate the field down to distances of the order of the transducer dimensions, and find nulls on the axis close to the transducer in general agreement with the results of the infinite slit.

LOBE SUPPRESSION IN PLANE RADIATORS

The above equations were developed under the mechanism of a plane wave passing through a hole, which necessitates the phase and velocity of the wave to be constant over the integration surface. If the velocity is not constant a different directivity pattern results, and is in some cases an improvement. When the velocity is less around the edges of the transducer than

in the center, the side lobes are always less in magnitude than they are with constant-velocity distribution, but the central lobe is generally broader. Several methods of calculating the sound field from radiators of variable surface velocities and phases have been advanced.¹⁷⁻²⁰ The methods can be generally divided into two classes: those that synthesize a velocity distribution from combinations of simple constant radiators whose directivities are known, and those that use transformations of the type

$$u = \iint v(x, y) \frac{e^{ikr}}{r} ds,$$

that are known or that can be calculated. For practical purposes the first method is the most useful because transducers are not designed with velocities continuously variable but with step variation over their surfaces. However, the second method has given the patterns for a wide variety of distributions which are a valuable guide for design and which also give a perspective to the lobe-suppression art.

Using the second method, Jones¹⁸ has given suppression schemes for nine distributions for the circular transducer, and nine for the square or linear case, which are plotted in Figures 8 and 9. The "efficiency" noted there is the ratio of the average amplitude of vibration to the maximum amplitude. The first or "brute-force" method combines constant-velocity surfaces of different size to synthesize a step formed velocity distribution, and calculate the resulting patterns through combination of the corresponding patterns for each elementary surface. For example two circular transducers of velocities ratio 1 to 2 and size ratio 1 to 0.6 would be combined as is shown in Figure 10, or analytically

$$R = \Lambda_1(kr \sin \theta) + 2 \times (0.6)^2 \Lambda_1(0.6kr \sin \theta).$$

An analogous procedure can be used, of course, in the square case. At first thought it would seem that the maximum-lobe suppression would obtain if the second lobe of one surface were placed on the first lobe of the other, but this is not the case, because other lobes then become important. Several cases using two velocity distributions have been calculated in this manner for both circular and square surfaces,

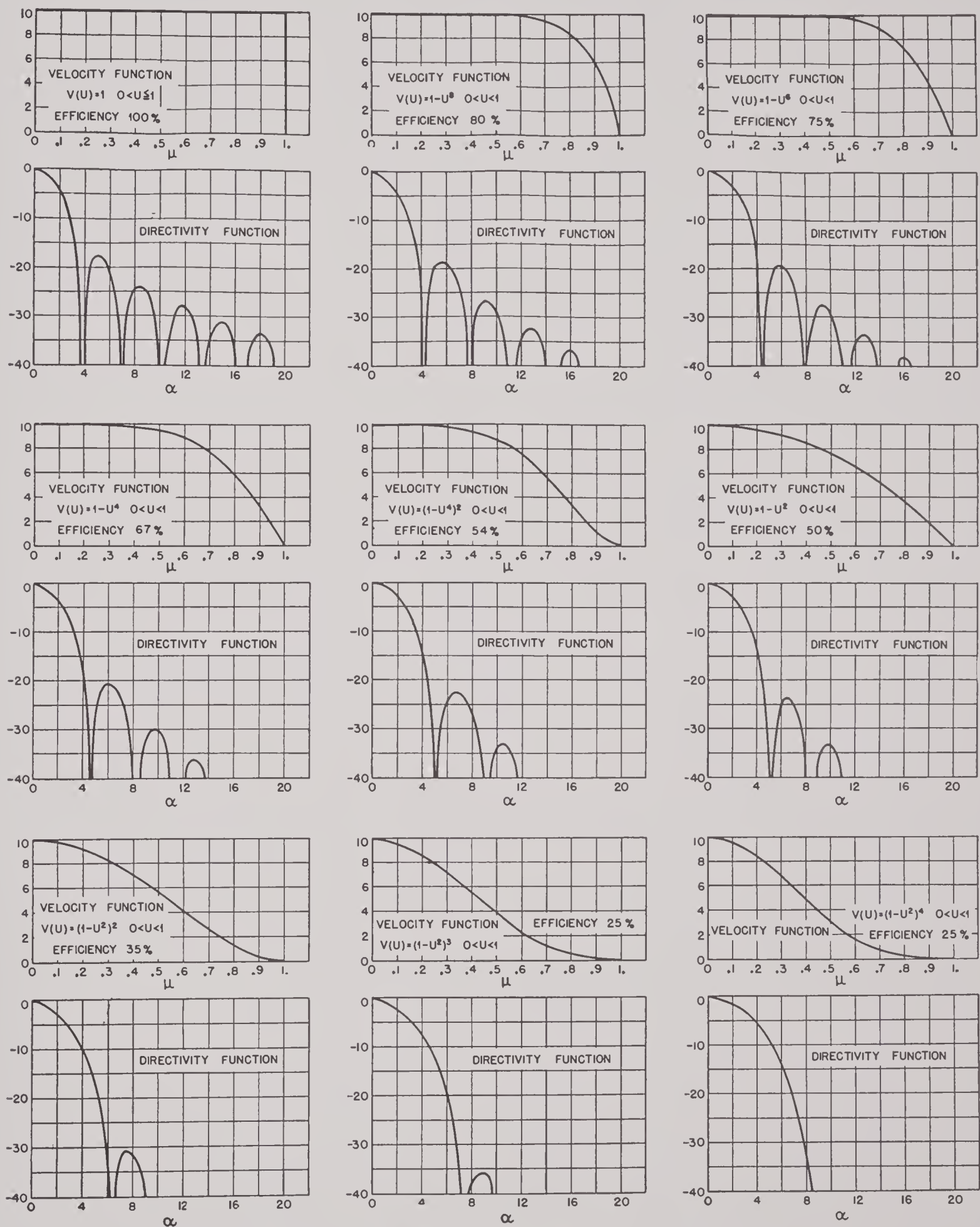
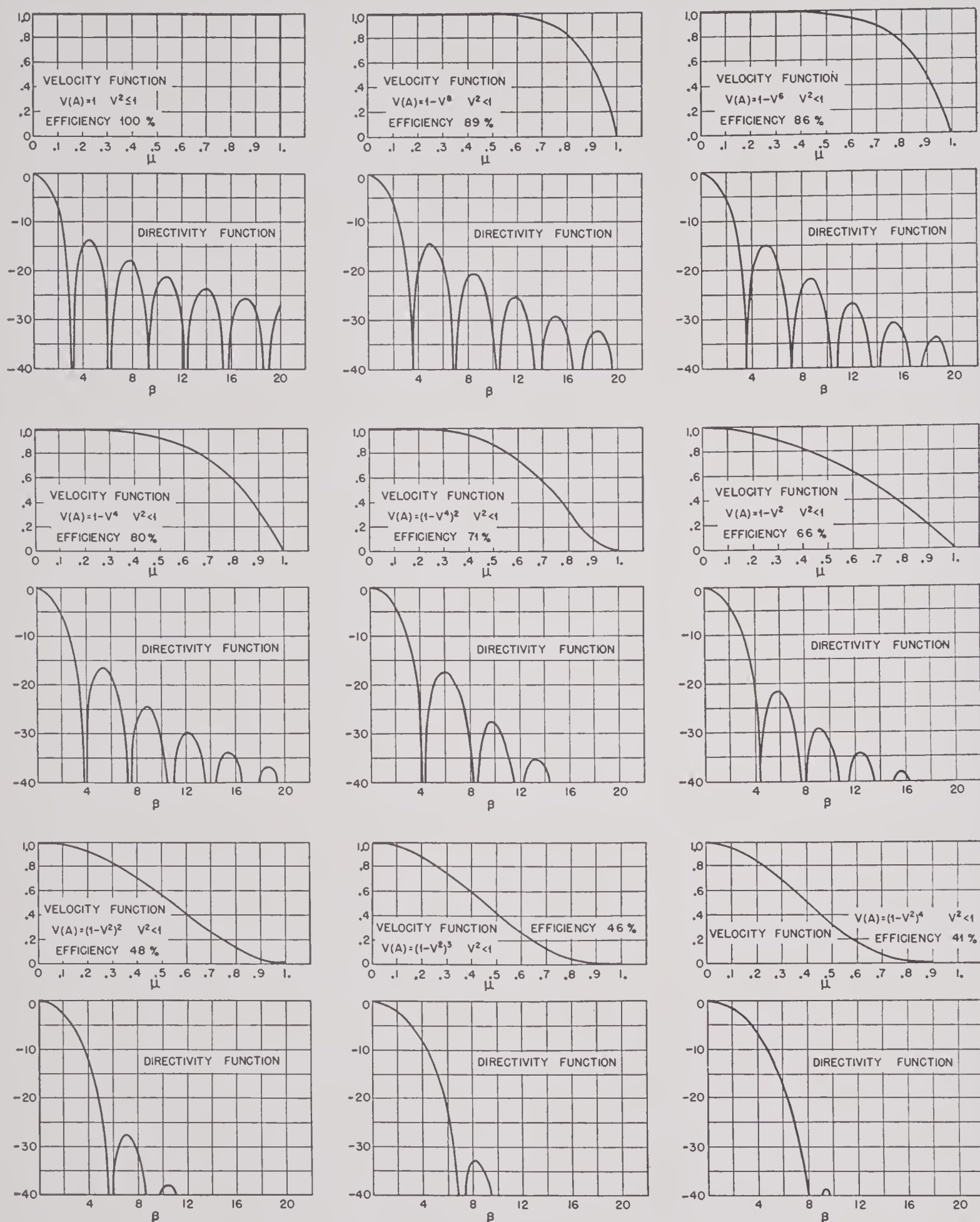


FIGURE 8. Lobe suppression for nine surface velocity functions in the square-plane radiator (Jones¹⁸).

FIGURE 9. Lobe suppression for nine surface velocity functions in the circular-plane radiator (Jones^{1b}).

and appear in Figure 11A and 11B. Experimentally the velocity ratio of 3 to 1 and diameter ratios 0.6 to 1 have given the most suppressed side lobes so far in the circular type as exemplified in Figure 12 patterns of the GA-14Z, which includes theoretical pattern as well.

Lobe suppression can be carried on almost indefinitely using additional steps of velocity until some sort of gaussian exponential velocity distribution is reached. However, the practical difficulties (see below) of constructing a crystal motor so that the amplitudes and phases of each

lying on lines perpendicular to this intersection line will radiate in the same phase as far as the particular directivity plane is concerned.¹

In other words, in any given directivity plane, any plane radiator may be thought of as a line radiator that varies in strength from point to point as the numbers and strengths of the radiators lying in the radiating plane at right angles to the line. With this in mind, lobe suppression may be done by spacing the crystals as well as varying their impressed voltages. Such a scheme is illustrated in Figure 11A

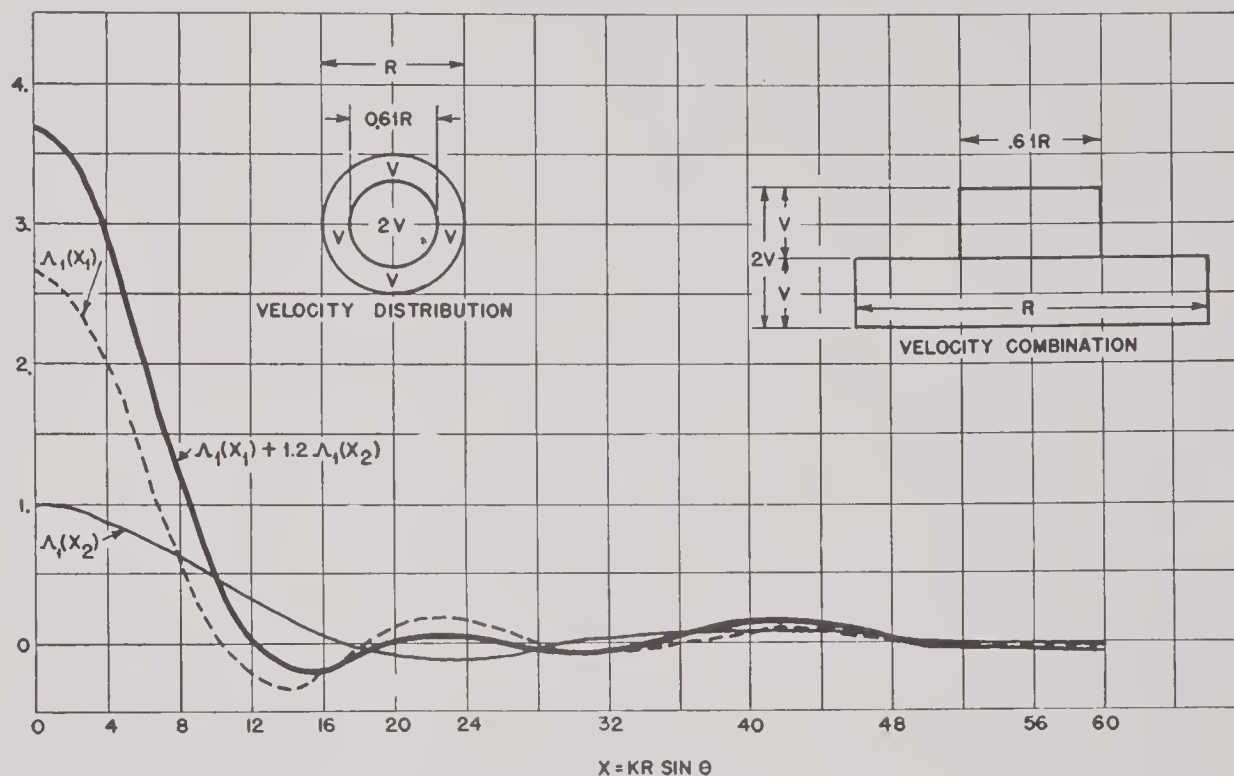


FIGURE 10. Method for calculating lobe suppression by velocity combination with the circular-plane radiator.

crystal actually perform as they are specified make it useless to shade the velocities in any but rather large steps. The relatively small size of the transducer thereby usually limits the number of these steps to two or three at the most. A three-dimensional pattern of a lobe-suppressed square-plane radiator is shown in Figure 13.

LOBE SUPPRESSION BY CRYSTAL SPACING

Directivities are usually calculated in some plane which is normal to the face of the transducer. The intersection of this plane and the transducer face defines a line in which all the radiators in the face may be projected without changing the calculations, as all the radiators

and 11B together with the experimental directivity patterns arising therefrom. This method has the disadvantage however of second-order main lobes as discussed in Section 4.3.5 when the crystal spacing is not small compared to a wavelength. See Figure 19A and 19B.

PHASING

So far the effect of variations in surface velocities only have been discussed. Phase variations also are important, and both phase and velocity variations may be used simultaneously. If the radiating surface is uniform in velocity, the phase in adjacent lobes differs by 180° . By a reciprocal theorem, if the radiator was divided into zones that vibrate in amplitudes decreas-

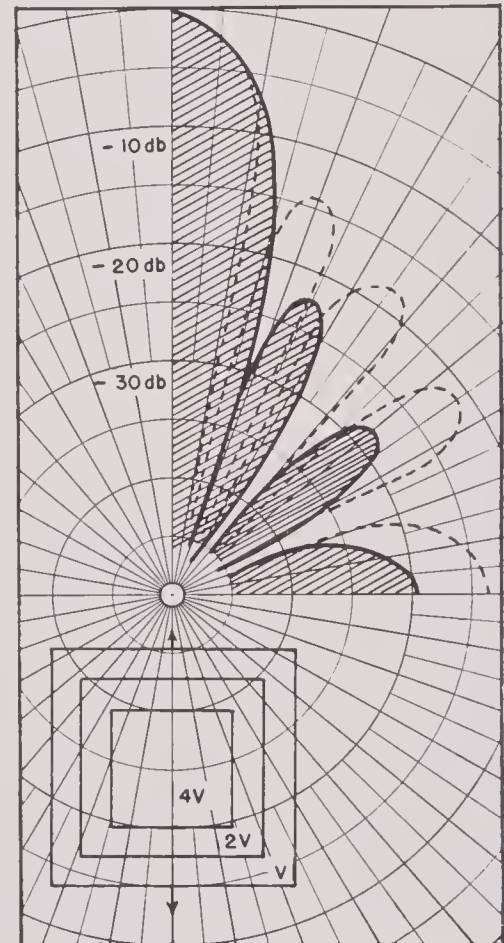
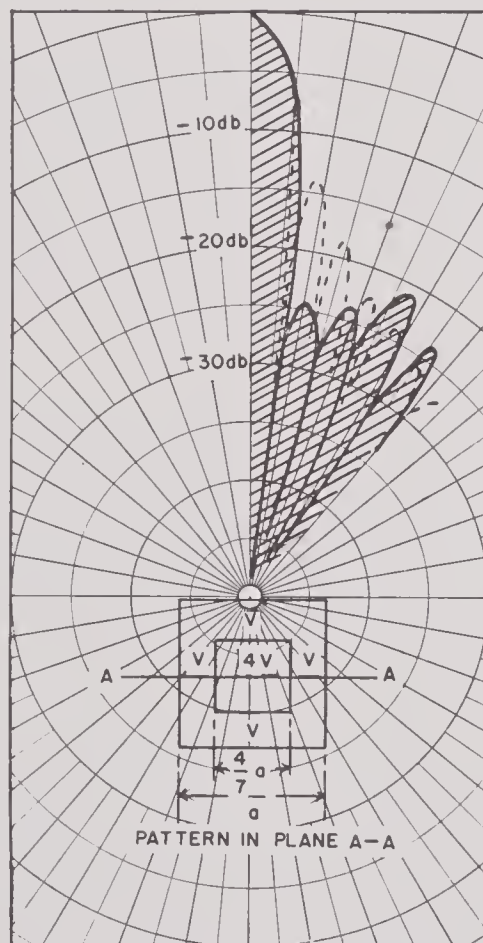
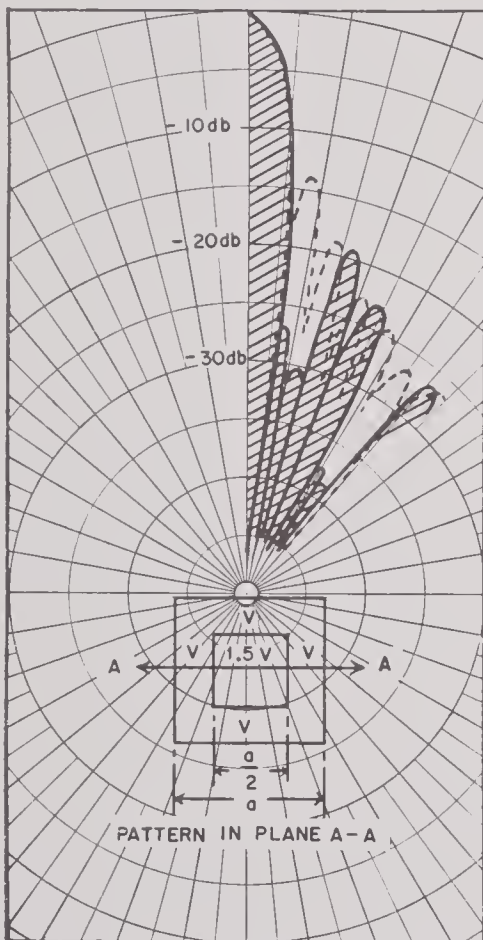
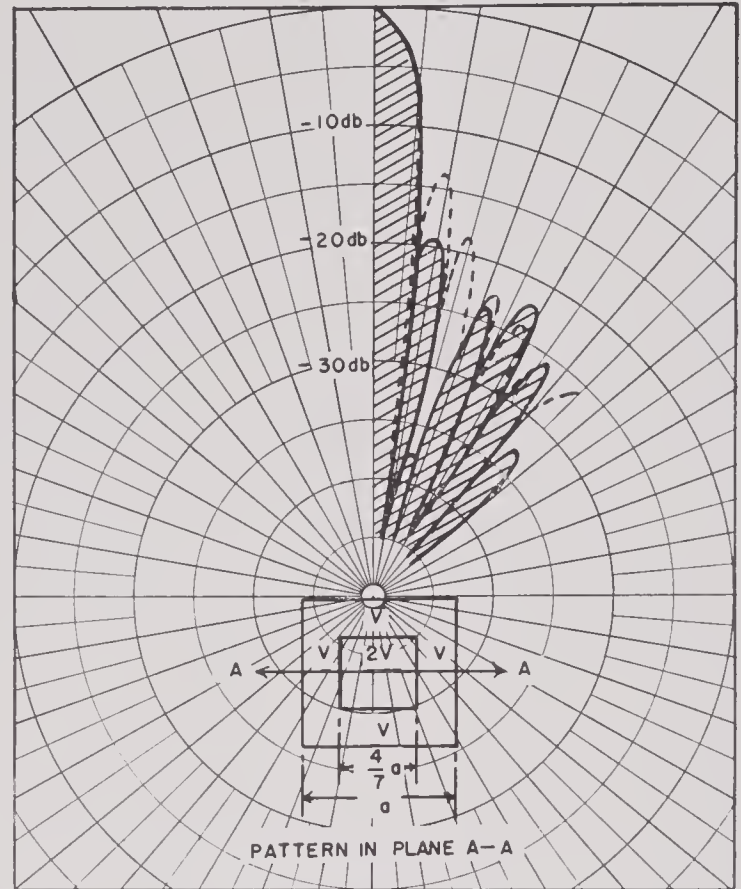
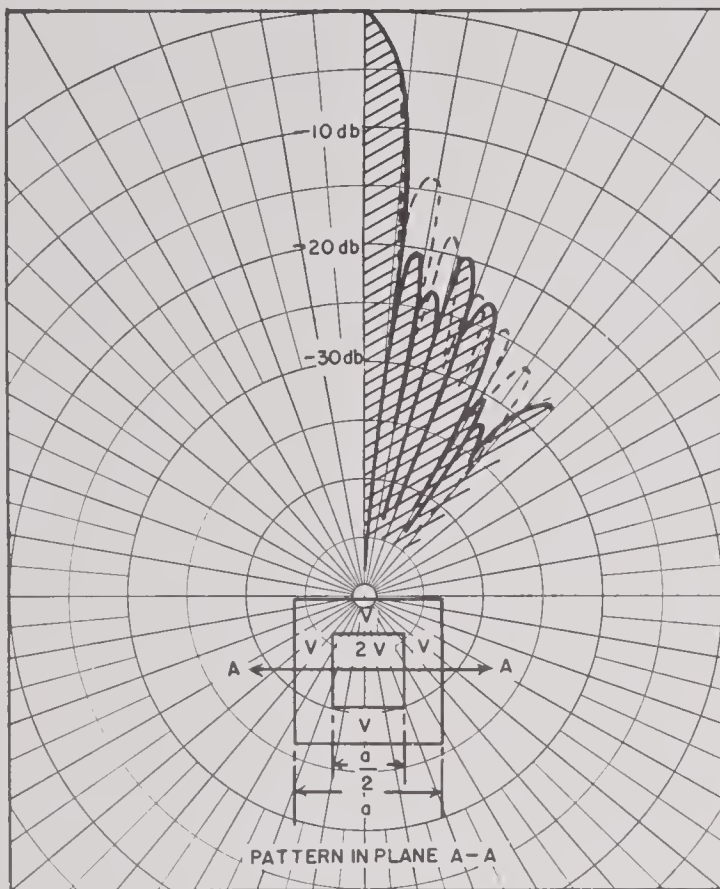


FIGURE 11A. Effect of step velocity distributions and crystal spacing upon the directivity of a plane radiator.

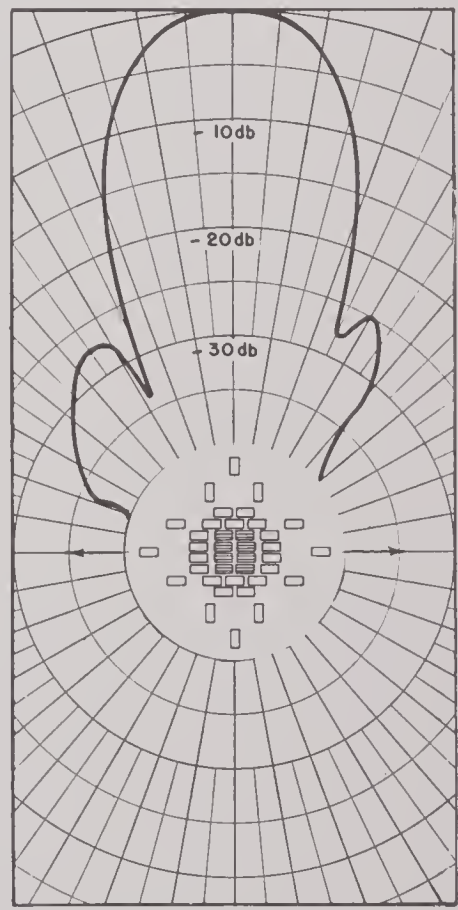
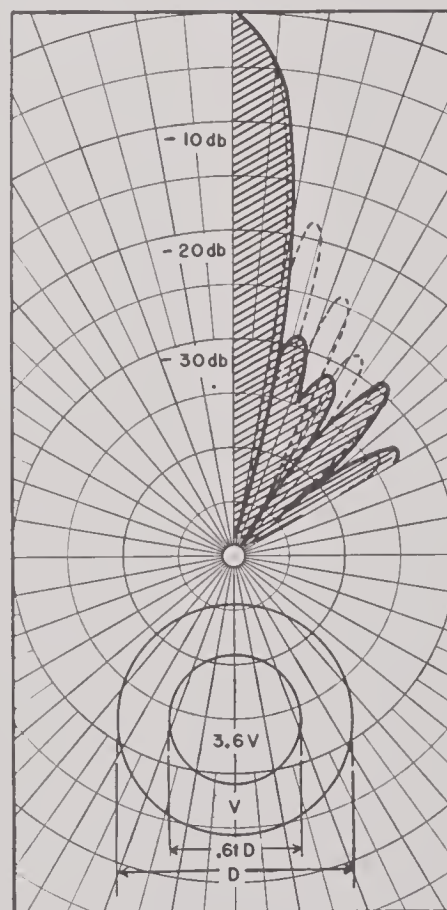
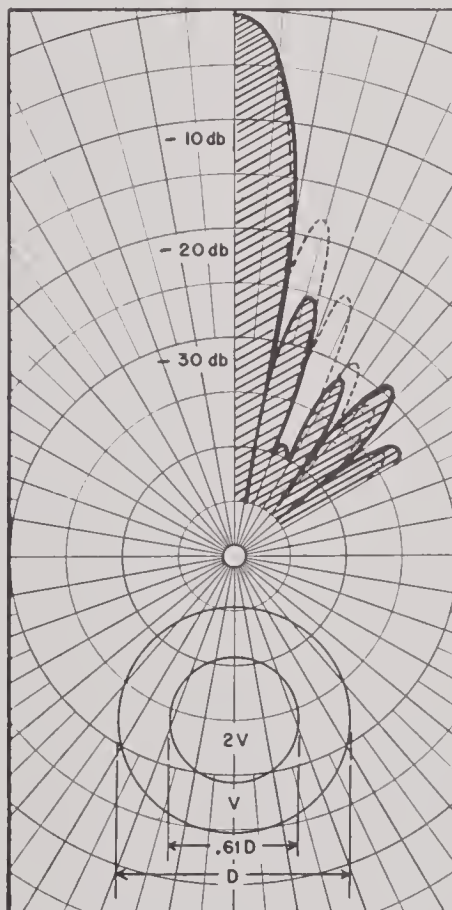
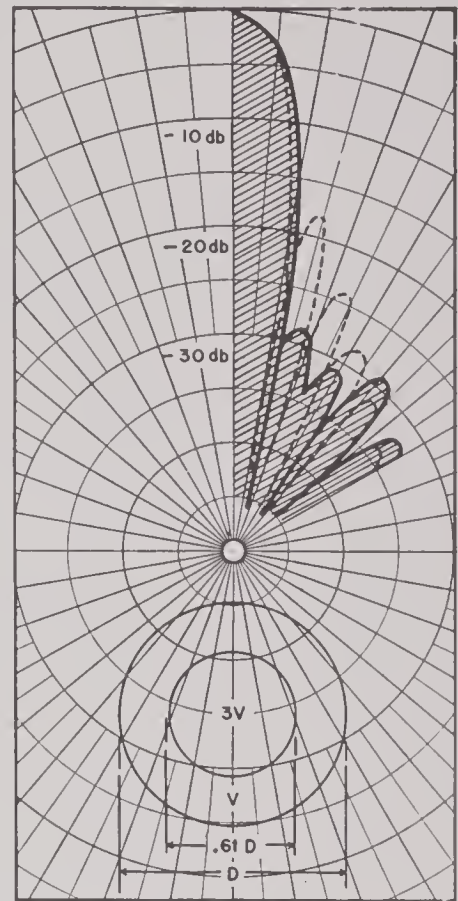
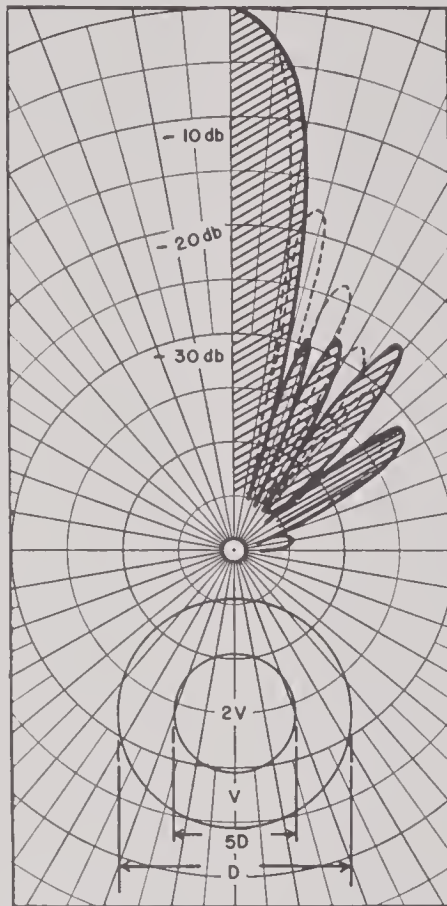
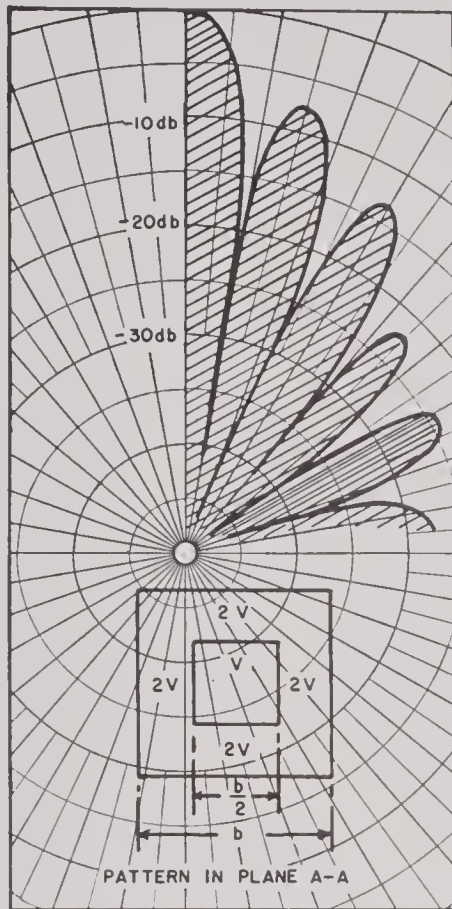


FIGURE 11B. Effect of step velocity distributions and crystal spacing upon the directivity of a plane radiator.

ing in magnitude as the lobes in the pattern of the uniform radiator and alternate 180° in phase, the pattern should be uniform over a certain arc and have no side lobes. This situation is illustrated in Figure 14. Other effects of phase variation can be mentioned. If only two symmetrical zones of phasing are used, the patterns are similar to Figure 15. The most noticeable effect of this type of phasing is in

that would be radiated if it radiated its maximum intensity in all directions. This factor is useful in computing the total acoustic power from an absolute-intensity calibration made upon the principal lobe. It can be computed by the formula

$$\text{Directivity factor} = \frac{\int P^2 d\sigma}{\int P^2_{\text{max}} d\sigma},$$

integrated over a sphere surrounding the transducer. Practically, this is a numerical integration problem and patterns taken in many planes must usually be used. Theoretically computed factors for the case of the line, plane-circular, and plane-square radiators are given in Figure 17. Experimental directivity factors require the use of many curves, as most patterns have little symmetry. An example of a radiator having reasonable symmetry is shown in Figure 18. One showing poor symmetry is shown in Figure 13 (see also Section 4.4.2).

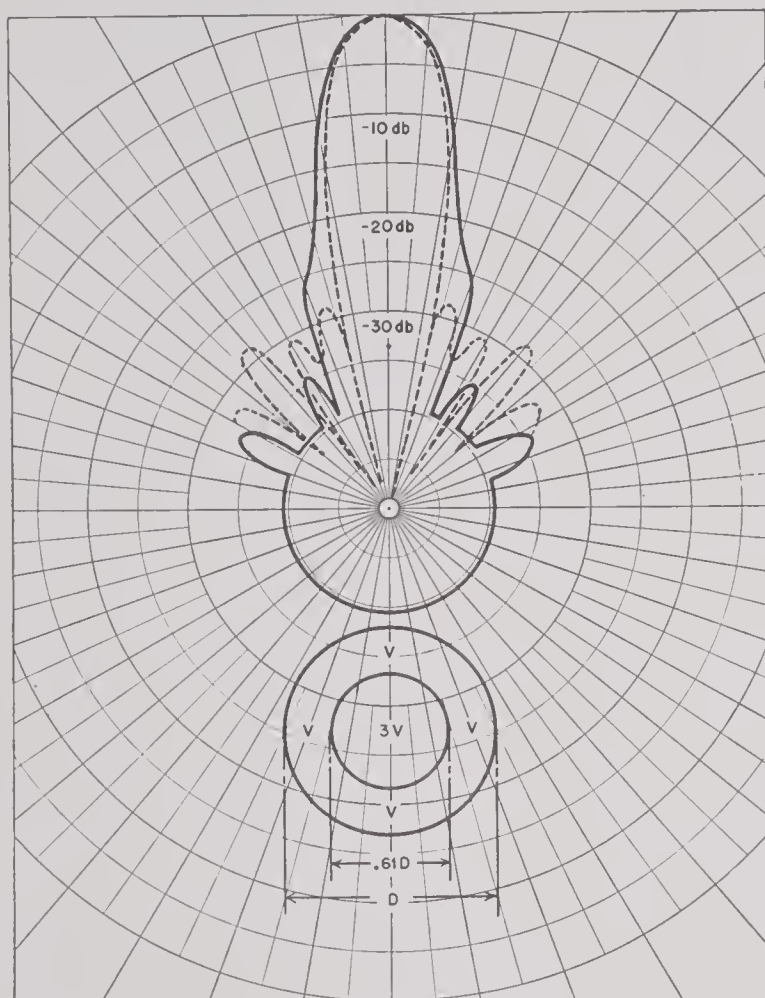


FIGURE 12. Theoretical and experimental directivity patterns of GA-14Z crystal transducer. Solid line: experimental. Broken line: theoretical.

raising the side lobes and eliminating the nulls between lobes. If a linear phase shift across the radiating surface is used, the main lobe is shifted in direction; see Figure 16. Such phasing can be used to train the main lobe electrically while the transducer is fixed.¹⁹

4.3.3

Directivity Factors

The directivity factor is the ratio of the total energy radiated by a transducer to the energy

4.3.4

Experimental Data

From the theoretical consideration given above it is possible in principle to fashion the directivity of a transducer into any desired form. Success in this, however, requires the radiating surfaces to perform according to the prescribed conditions, which leads to one of the most difficult problems in the construction of transducers. In Sections 3.4, 3.5, and 3.7 the nature of this problem was discussed and now a few experimental results of nonuniform radiating surfaces will be discussed. Wide variations in the agreement between theory and experiment are encountered in transducers of different design, and often are encountered in a particular unit at different frequencies. These departures from theory vary in magnitude from negligible to those large enough to render the unit useless for its intended purpose. The analysis of these eccentricities can be divided into two parts, one treating the main or central lobe, and the other treating the side lobes. The most important feature of the main lobe aside from its absolute intensity is its width, which can be defined as the angle subtended by two points on

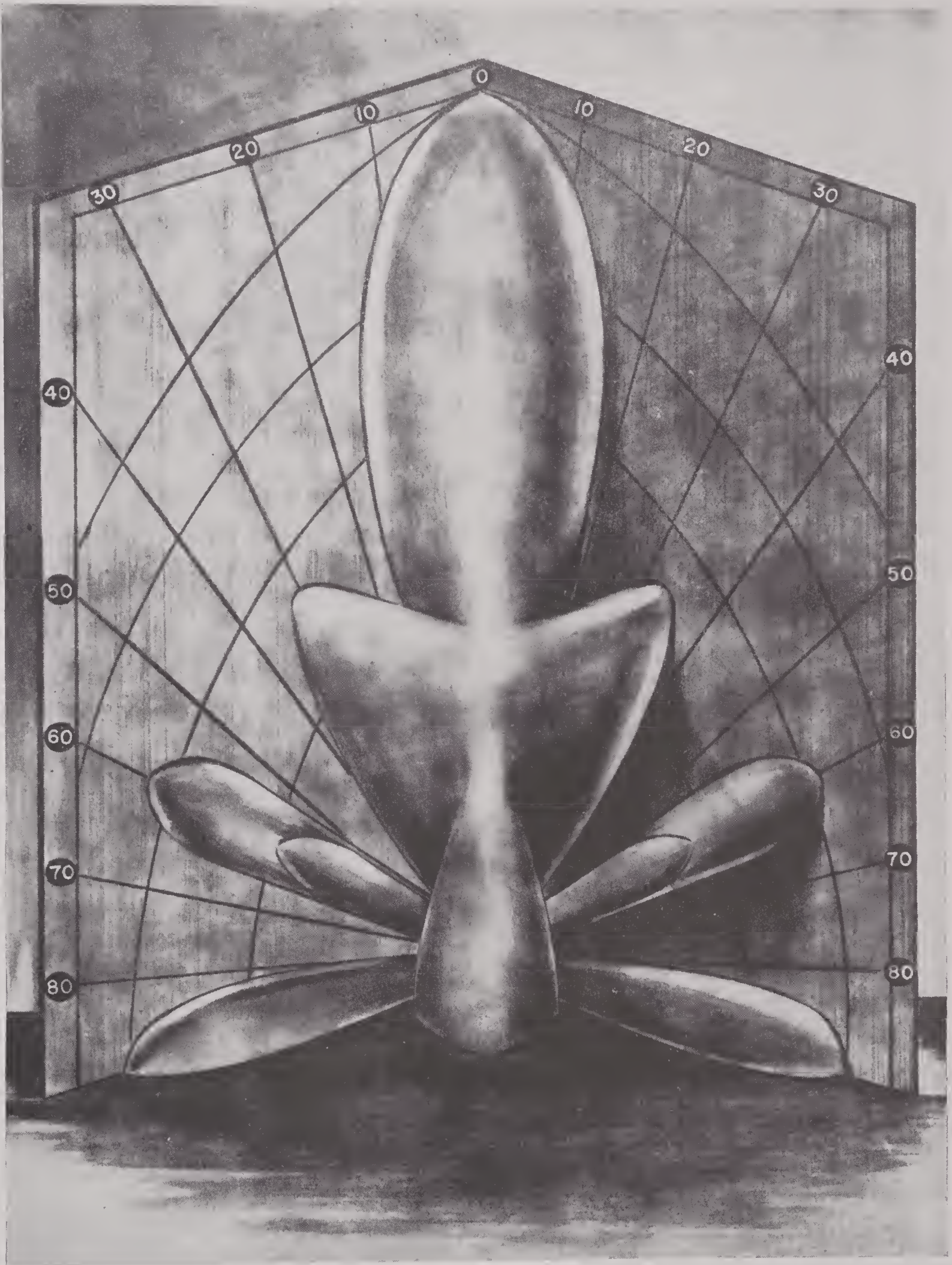


FIGURE 13. Three-dimensional patterns of lobe-suppressed square-plane radiator.

each side of the center that are 6 db down in intensity from the maximum. This theoretical beam width for the square- and circular-plane radiators with this definition are

$$\theta = 2 \sin^{-1} 0.605 \frac{\lambda}{\alpha} \quad (\text{square}),$$

and

$$\theta = 2 \sin^{-1} 0.305 \frac{\lambda}{\alpha} \quad (\text{circular}).$$

See Table 1, Section 4.3. In general the experimental beam widths are in good agreement with

usually with good approximation, be predicted from the overall dimensions of the transducer.

The side lobes, however, being diffraction patterns, are much more sensitive to surface variations in phase and velocity. Agreement with theory in them is rarer than in the central lobe, a situation that is often troublesome in applications. With uniform velocity and phase, theory predicts, for example with the square-plane radiator, that the secondary lobes occur at regular angle intervals with intensities regularly decreasing 13 db, 18 db, 21.5 db, etc. The angle intervals vary regularly with frequency,

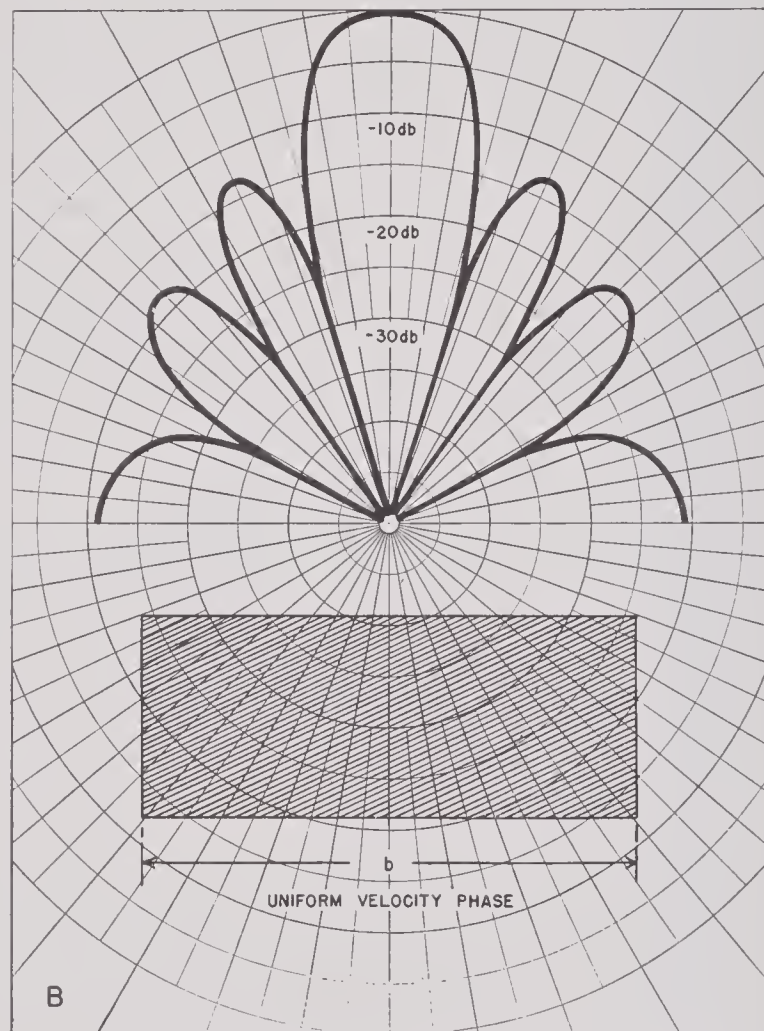
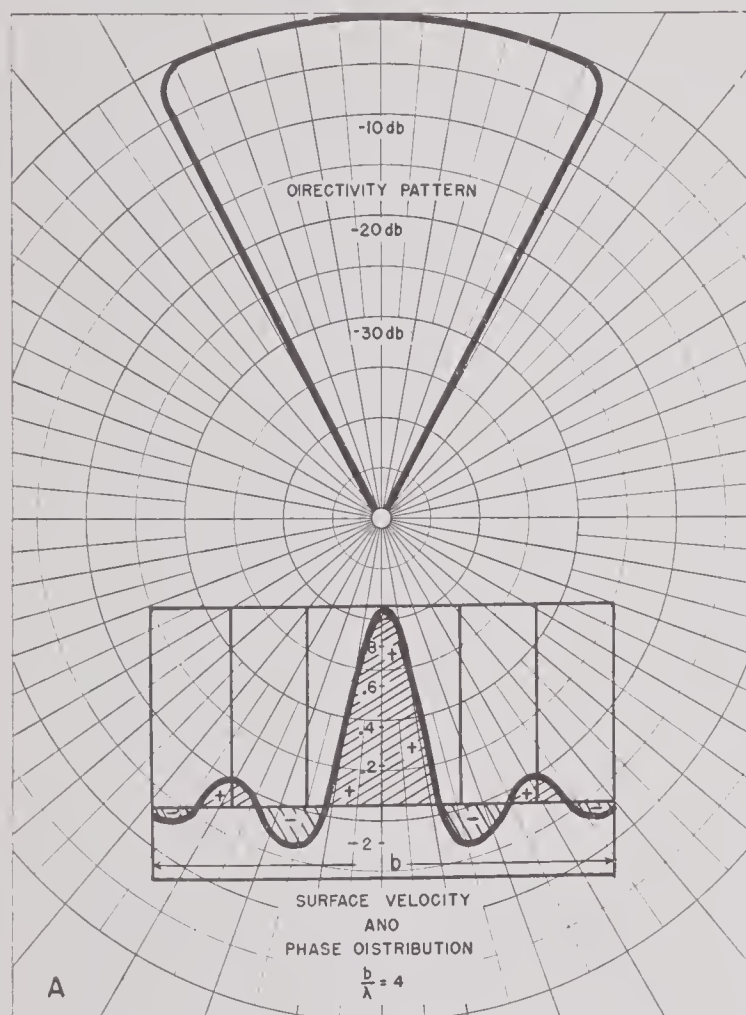


FIGURE 14. The reciprocal relationship between the surface velocity function and the corresponding directivity function in a square-plane radiator.

theory even when the accompanying side lobes are in very poor agreement. Calculations of patterns using more or less heterogeneous surface-velocity distributions show that the main-lobe width is less dependent upon the velocity distributions than are the side lobes. Only with ordered surface-velocity variations is the main lobe affected, and even then not as much as the side lobe. The width of the central lobe can thus,

but the intensity ratios remain the same. Figure 21 shows a set of patterns for such a radiator in which no pattern shows any regular change in secondary-lobe angles, nor do these lobes remain the same in relative intensity. Not much is known about the causes of such erratic patterns, because while a given surface distribution may cause definite patterns, the converse that a given pattern may be caused by one and

only one surface condition is not generally true. A discussion of a few factors known about the effect of surface condition upon directivities can throw a little light upon the situation.

1.3.5 Measurable Cause and Effect Factors

We have seen that a radiator whose center is stronger than its rim will radiate less energy in the side lobes. The pattern of such a radiator

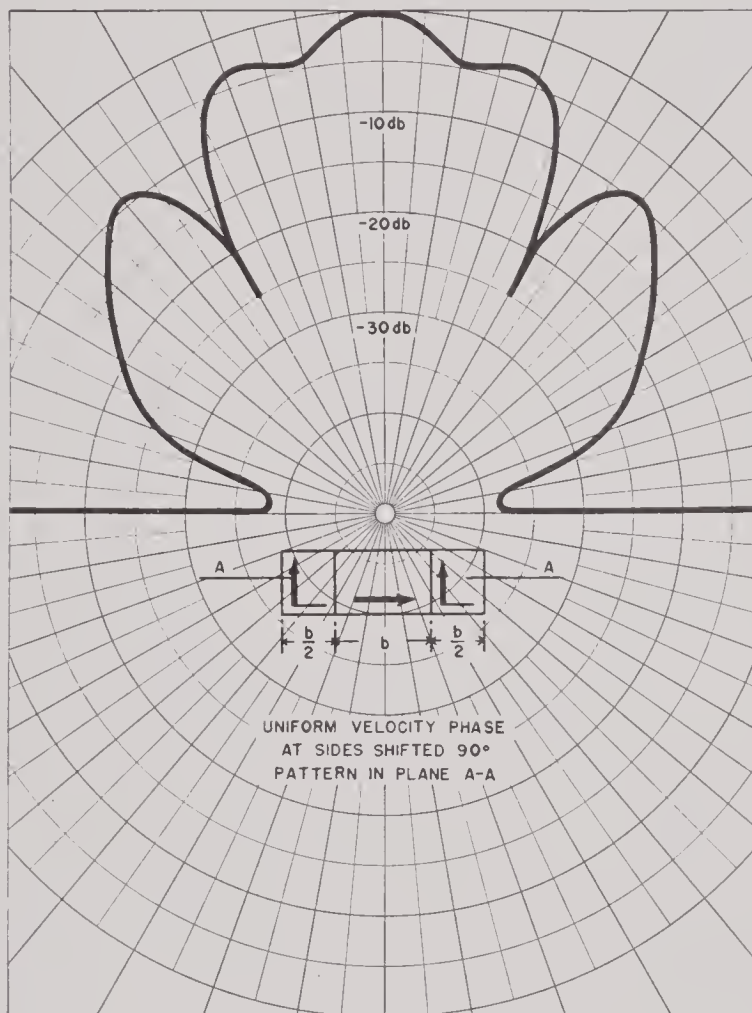


FIGURE 15. Directivity pattern of a line radiator in which the phase of the velocity at the ends is shifted 90° . The absolute magnitude of the velocity is constant throughout.

(the GA-14Z) is shown in Figure 12, both theoretically and experimentally. The side lobes of the experimental pattern are generally much less than those of a uniform radiator, but they are not congruent to the theoretical pattern, nor are they symmetrical. This effect could obtain only from a nonsymmetrical radiator. Conversely, a radiator whose rim is stronger than its center will radiate more energy in the side lobes. See Figures 11A and 11B. Also, a

radiator whose rim is out of phase with its center will radiate more energy in the side lobes. See Figure 15.

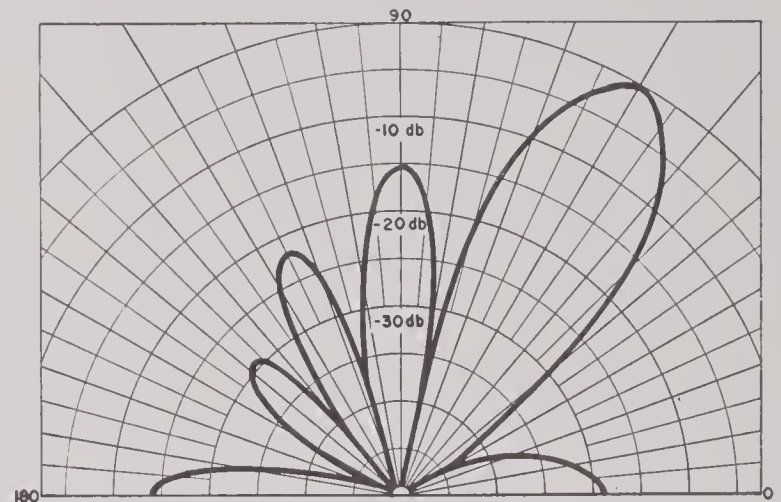


FIGURE 16. Shifting of the main lobe by a linear phase variation over the length of a line of point radiators. Phase shifted 30° per point radiator.

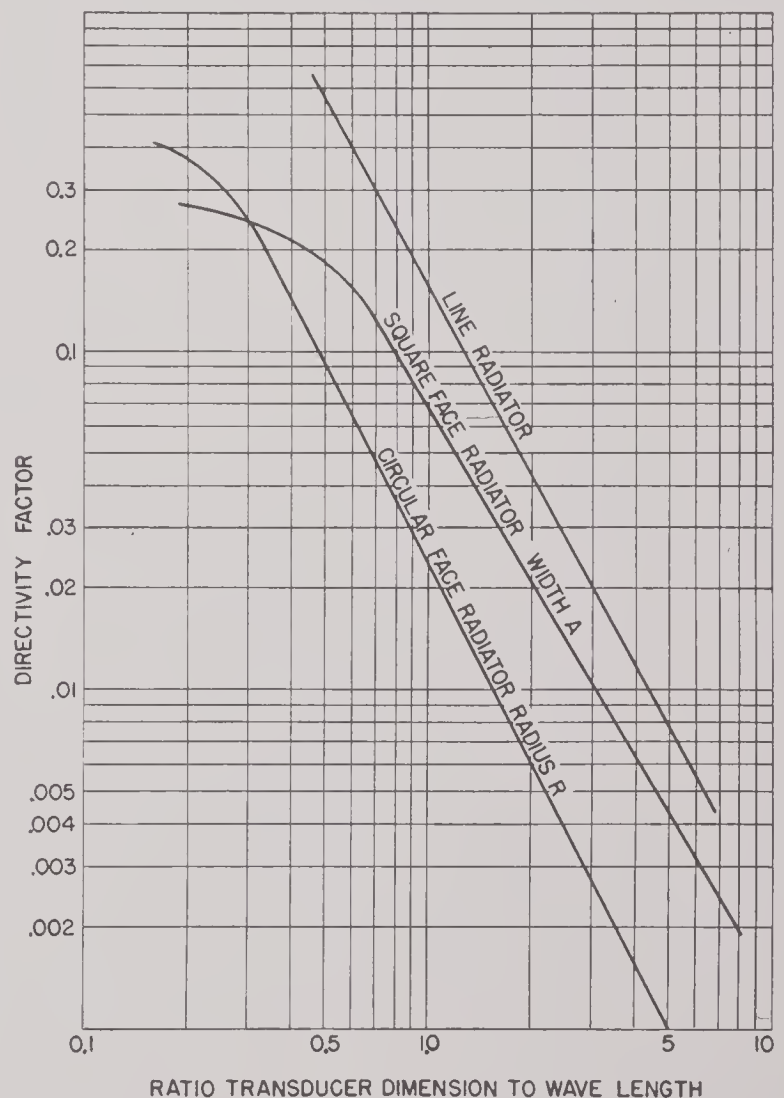


FIGURE 17. Theoretical directivity factors of three types of sound radiators.

Another striking property of this kind of radiator is the disappearance of nulls between

side lobes. Notice that most of the experimental patterns illustrated in this section have many nulls eliminated between side lobes, a fact that indicates nonuniform phasing in most transducers.

Frequently the crystal matrix of a motor is divided into units of two, three, or four crystals forming a block. These blocks are spaced from each other of the order of $\frac{1}{4}$ to $\frac{1}{2}$ in. With the blocks operating under oil, this space may present a radiating element 180° out of phase with the crystal surface because the sides of the crystal blocks are vibrating 180° out of phase with the ends, and this motion is transmitted to the oil cavity between crystal elements. In addition to this effect, there is another one due to the spacing. If n point radiators are put in a line distant from each other by d , the directivity is given by

$$R = \frac{\sin \left(n \frac{\pi}{x} \sin \theta \right)}{n \sin \left(\frac{\pi}{x} d \sin \theta \right)},$$

instead of

$$R = \frac{\sin \left(\frac{n\pi}{\lambda} \sin \theta \right)}{\left(\frac{n\pi}{\lambda} \sin \theta \right)}.$$

As n gets large and d gets correspondingly small, these two formulas approach each other. The first formula will give a second maximum when the $\pi d/\lambda \sin \theta$ reaches π or when $\sin \theta = \lambda/d$. If $d = \lambda$ then there should be a second maximum equaling the central lobe at $\theta = 90^\circ$. Finite spacing between crystals when working under oil should then give two effects, one a smear effect upon the side lobes, the other a second large maximum at high frequencies. An example of each effect is shown in Figures 19 and 20. Figure 19A shows patterns at several frequencies of a transducer in which the crystal spacings are appreciable at different frequencies. At the higher frequencies, the second large maximum is evident. This effect is similar to the second-order spectrum noticed with optical gratings. Another example of this effect can be seen in the GD22 transducer. This transducer is constructed with 24 ADP crystals

Cycle-Welded directly to the rubber window with the technique described in Section 8.5.6. For this discussion it can be considered as a grating-type radiator in which the distances between individual radiators is as large as the radiators themselves. In the center of each diagram of Figure 19B is a chart showing the motor layout. The distances between centers along one axis is twice that along the other axis. Figure 19B illustrates a pattern taken in these two directions. Figure 19B-a is the pattern in the direction of smaller spacing and no large secondary maxima are evident. In Figure 19B-b this second-order effect is just beginning to appear. At higher frequencies the large lobes on the side increase in size and decrease their angle with the zero axis. The widths of the main lobes of both are the same because the motor is square. Figure 19B-c illustrates the effect of the intercrystal spacings in smearing the side lobes. Patterns were taken with the motor air-filled and oil-filled. Figure 19B-c shows immediately the effect of filling the cavity with oil which could be due to intercrystal vibration or to overall cavity modes. That the effect is due to the intercrystal spacings is shown by Figure 19B-d, which is a pattern taken after each crystal had been surrounded with foam rubber (the motor still working in oil). This pattern is nearly as clear as Figure 19B-b.

The transducer case has its effect also upon the directivity. If the window in the case is a poor transmitter, standing waves are set up inside the case which obscure somewhat the connection between the motor and the water. Figure 21 shows a contrast of the patterns of the same motor in two cases, one of which was a simple qc-rubber case. In this comparison, the more transparent case greatly improves the patterns.

4.4 APPLICATIONS OF RECIPROCITY

In this section the reciprocity principle is applied to a generalized transducer, and certain conclusions are drawn concerning the sound field. For this purpose the transducer is assumed to have certain ideal properties such as

uniform phase and amplitude over plane arrays, and the conditions requisite for reciprocity (linear, passive, bilateral). Fortunately the conclusions reached are functions only of the

provided the radiating *surface* fulfills requirements.

As a matter of fact, 45° Y-cut RS and 45° Z-cut ADP obey reciprocity very well. There is

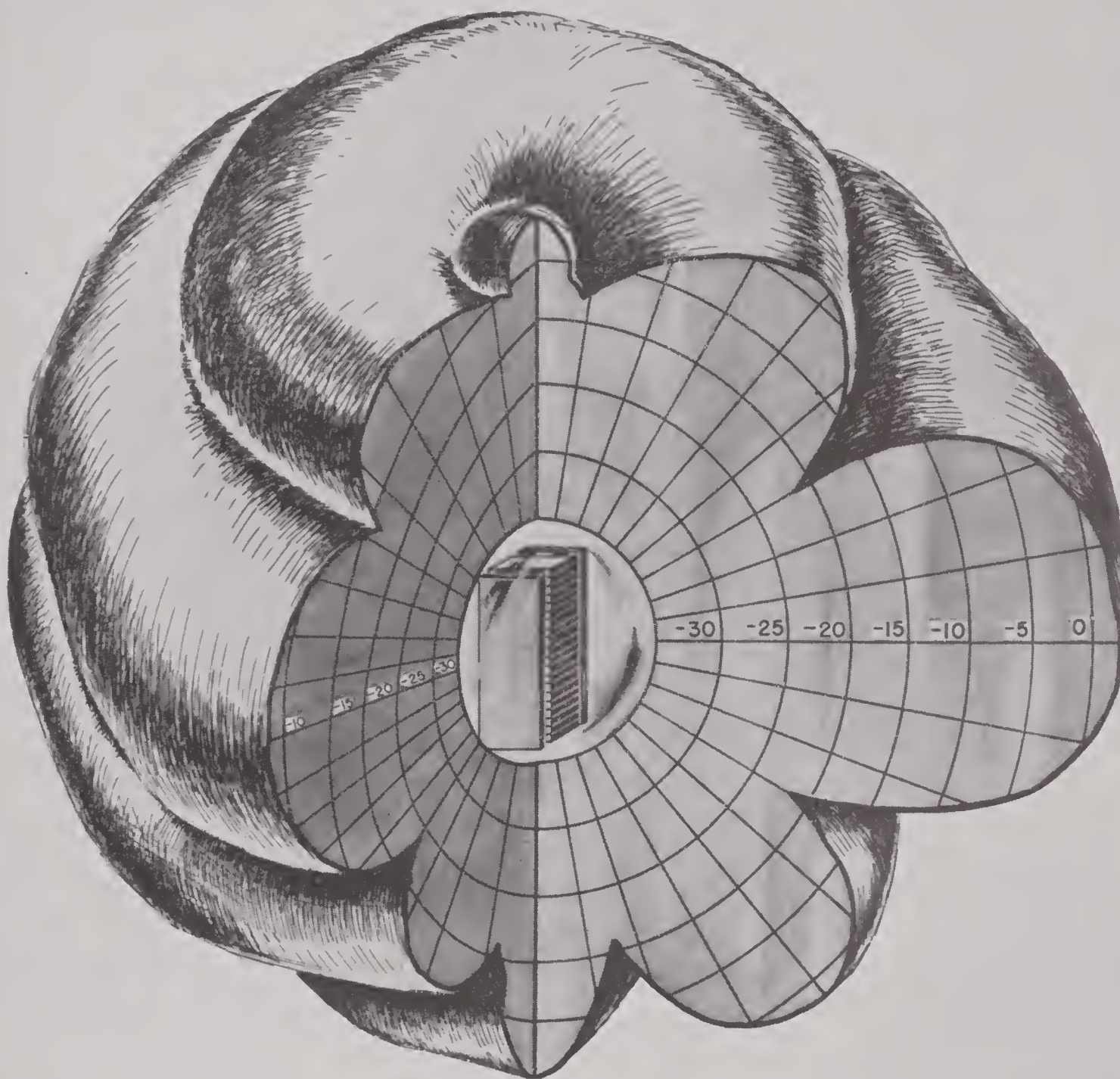


FIGURE 18. Three-dimensional patterns of symmetrically driven double plane radiator.

radiating *surface*, its geometry, amplitude, phase, etc., but *not* of the *nature* of the transducing material (crystal, nickel tubing, etc.). Thus these conclusions apply equally well to transducers which fail to obey reciprocity, pro-

vided the radiating *surface* fulfills requirements. some question of the linearity of glued joints under large stress, and finished transducers may fail to obey reciprocity under very high-power operation. If this does occur it is relatively rare.

4.4.1

Lobe Suppression

When an array is lobe-suppressed it is frequently necessary to drive one portion at greater amplitude than another. If the same

Section 4.8), and it is apparent that the total power radiated by the lobe-suppressed array must be less than that radiated by the uniform array. The quantity of interest in a transmitter is not the total power radiated, but the acoustic

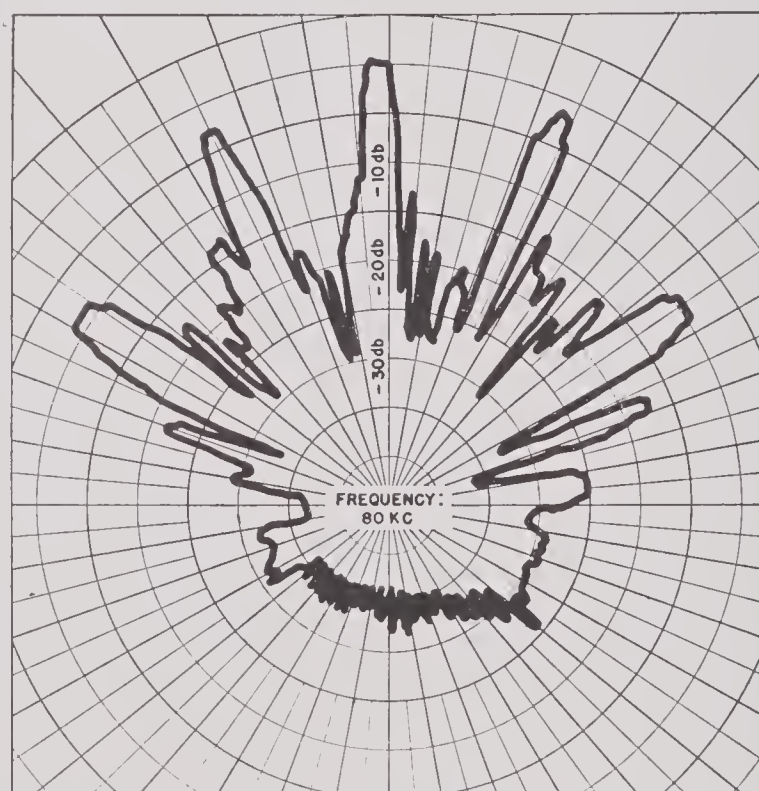
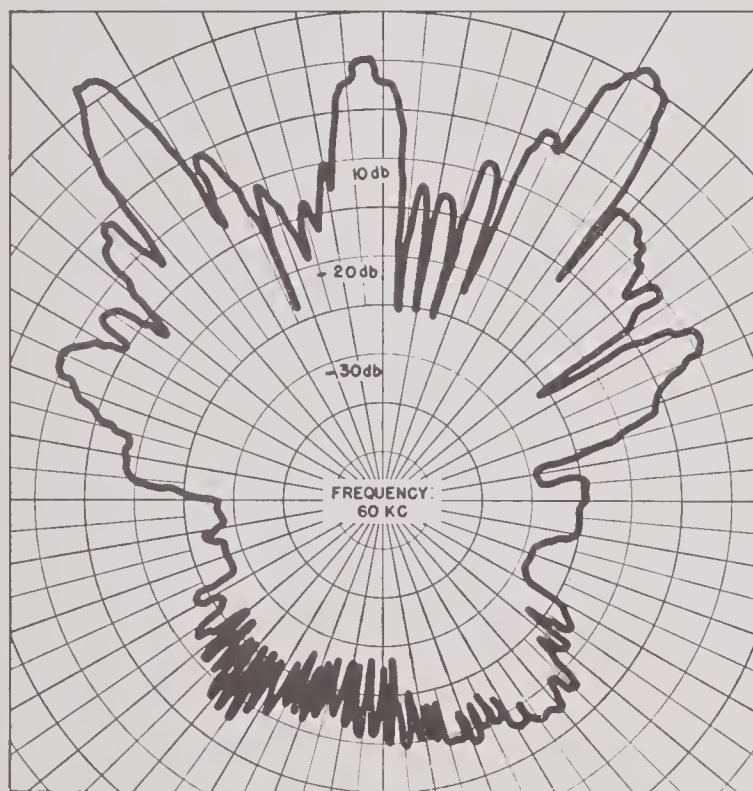
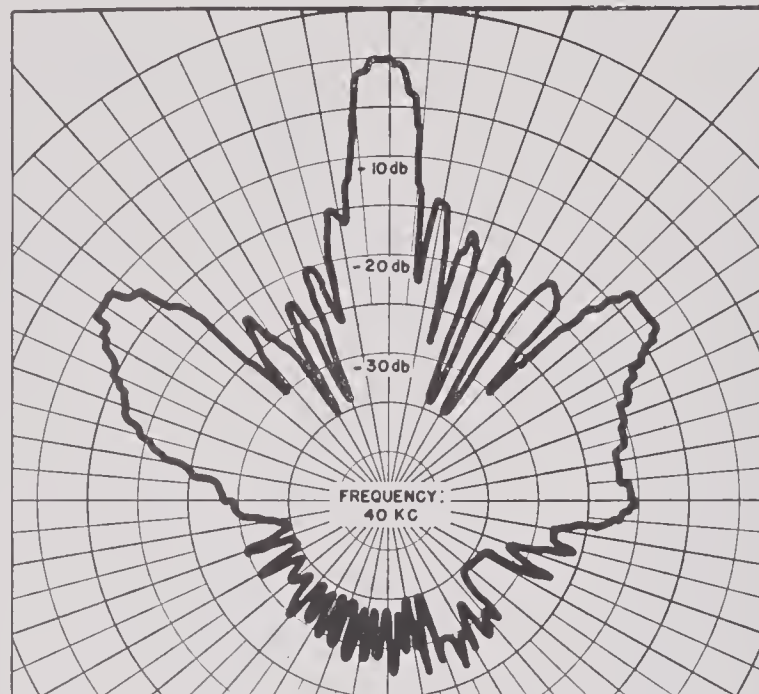
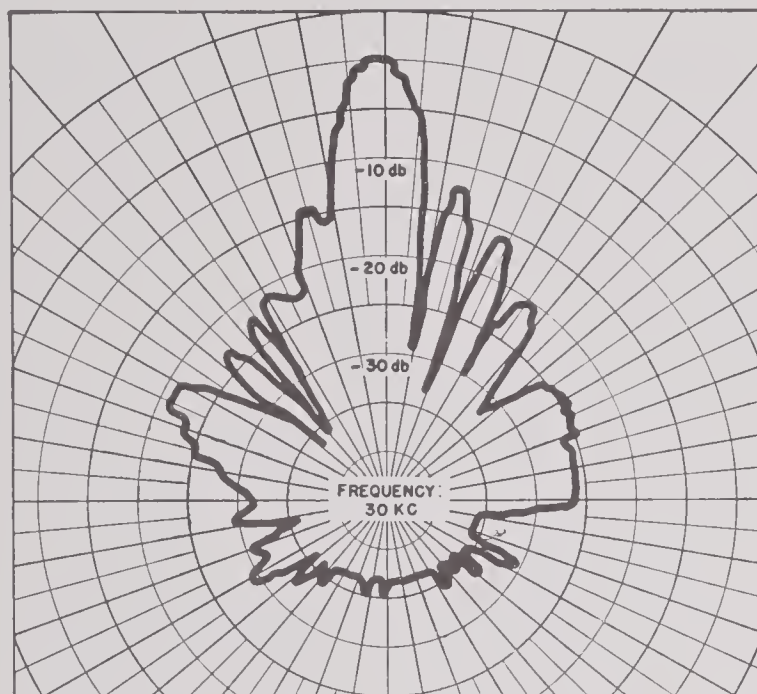


FIGURE 19A. Second-order maxima in the directivity pattern of a transducer in which the crystal spacings are not small compared to the wavelength radiated.

array were not lobe-suppressed all elements could be driven equally. When operating as a transmitter a limitation on output power will be imposed by the hardest driven area (see

pressure produced in some direction (usually the direction of maximum response). By lobe-suppressing, power which was previously radiated into undesired side lobes is directed into

the main lobe; this raises the pressure in that direction and helps to make up for the diminished power output. On the other hand, lobe suppression always causes the main lobe to become a little wider, and this tends to diminish the

number of identical active elements closely and uniformly spaced in a large plane array and all connected in phase. Let any element be represented by a generalized transmission T (see Figure A, page 158).

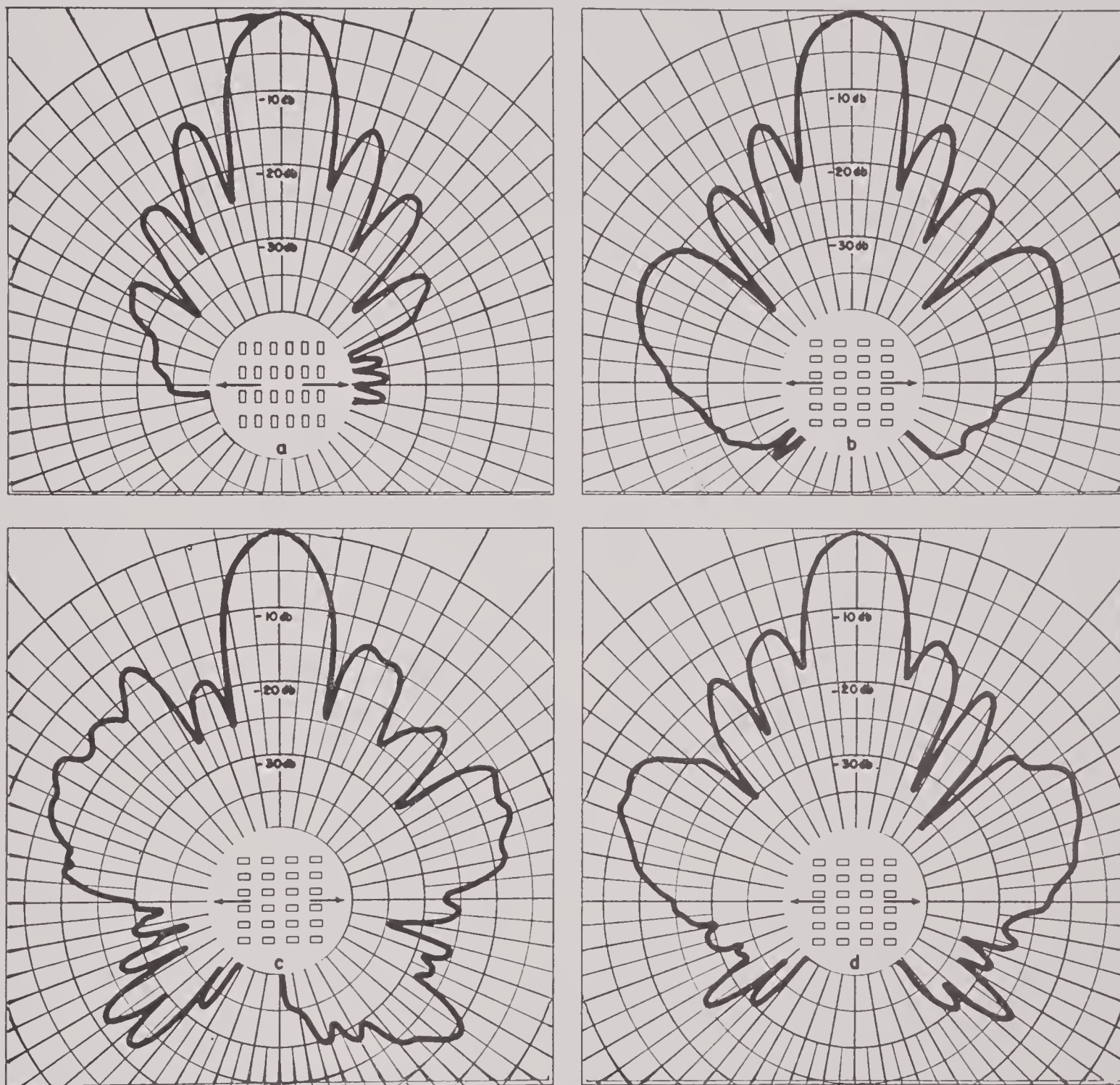


FIGURE 19B. Directivity patterns of the GD22Z transducer, at 60 kc, showing the effects of: crystal spacings, oil versus air inside the transducer case, and foam rubber inserts between the crystals when the case is oil filled.

pressure. It is not possible to weigh the importance of these qualitatively in order to learn the net effect. In this section the result is obtained by use of reciprocity.

Consider a transducer composed of a large

If each element has radiating area a the radiation impedance may be represented by some quantity aZ_R (see Figure B, page 158). Z_R will depend upon the geometry, the nature of the medium, etc., and is not strictly the same

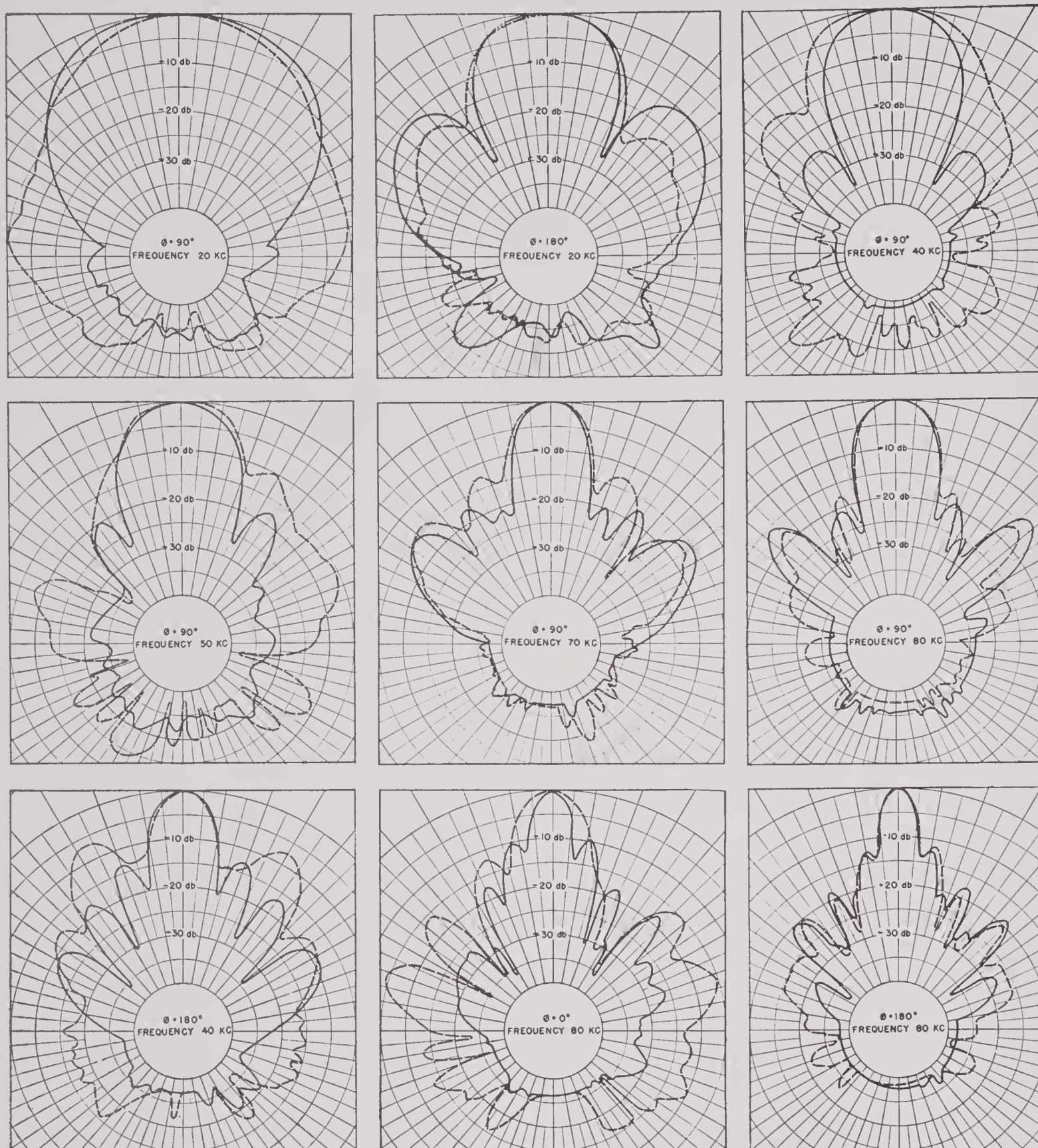


FIGURE 20. Directivity patterns of the FG8Z-3 transducer showing the effect of foam rubber inserts between the crystals in an oil filled transducer at different frequencies. Solid line: with inserts. Broken line: without inserts.

for all the elements. However, it is usual in calculating the radiation field to make certain assumptions tantamount to making Z_R a constant for all elements.

A normally incident sound wave introduces

a voltage in this circuit proportional to the area a . (Refer to Figure C, page 158.)

If, now, the electric terminals are shorted some current I_0 will flow. If the normally incident wave had a free-field pressure of 1 dyne

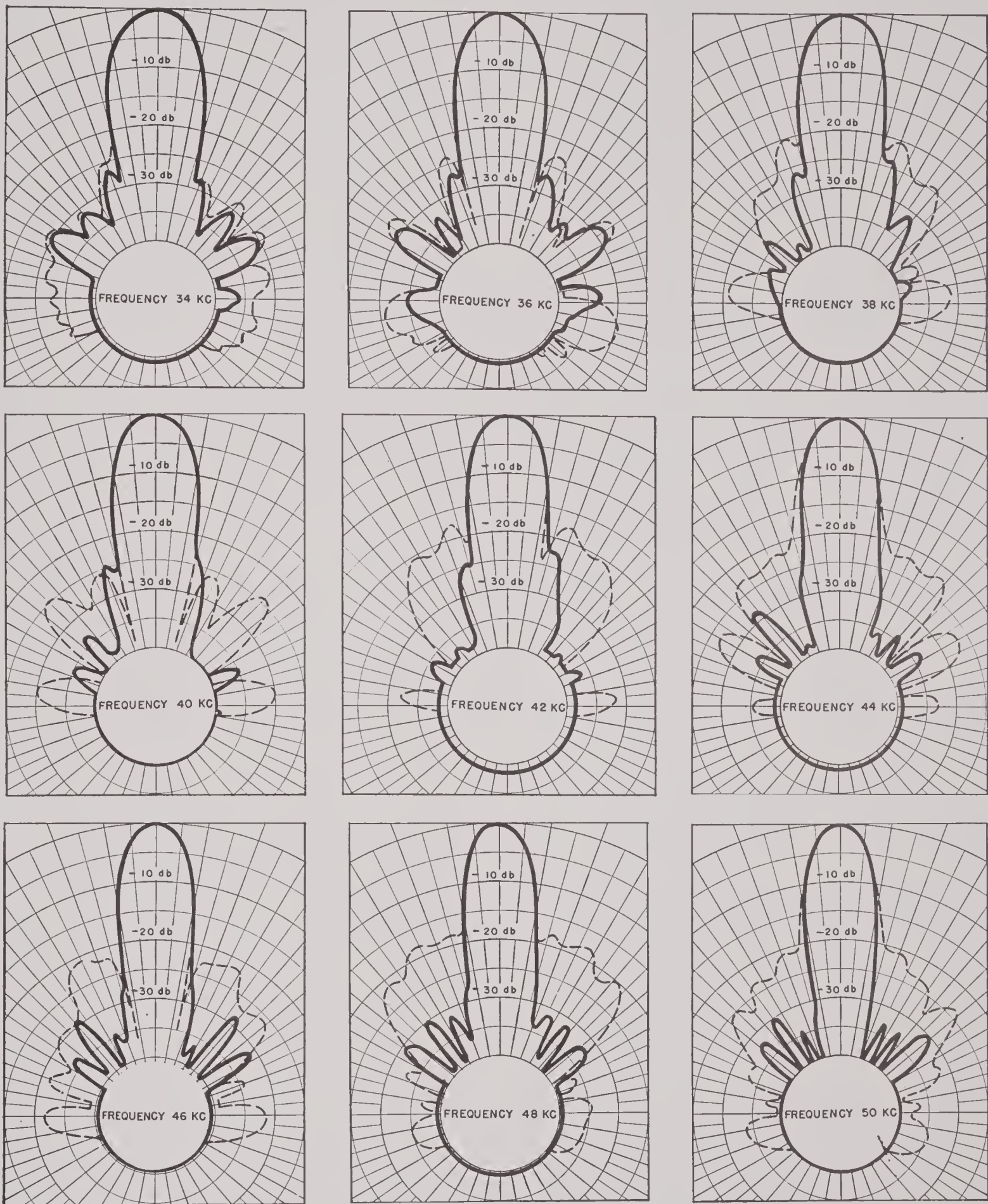


FIGURE 21. Directivity patterns of the CQ6Z6-4 crystal motor showing a contrast between the effects of neoprene and qc-rubber cases filled with oil. Solid line: qc-case. Broken line: neoprene case.

per sq cm, we term I_0 the short-circuit receiver response of the element.

Lobe suppression is achieved by connecting some of these unit elements in series, groups of the series elements then being in parallel

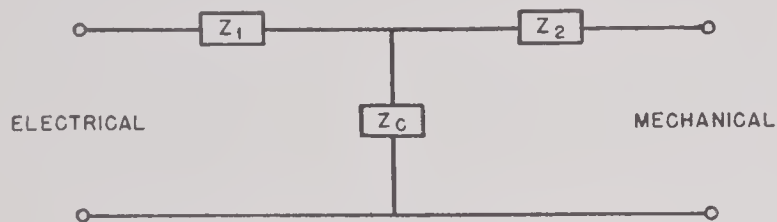


FIGURE A.

with each other and with other individual elements, all in phase. It is easily shown that if any number of these elements are put in series the short-circuit current which flows from the group is the same as the current from a single element.

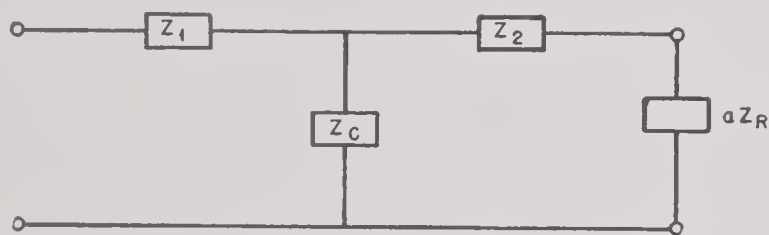


FIGURE B.

Assume that there is, in some plane array, a number N of these elements. If this array were connected all in parallel for no lobe suppression then all N elements would contribute current I_0 , and the short-circuit receiver response of the whole transducer would be NI_0 .

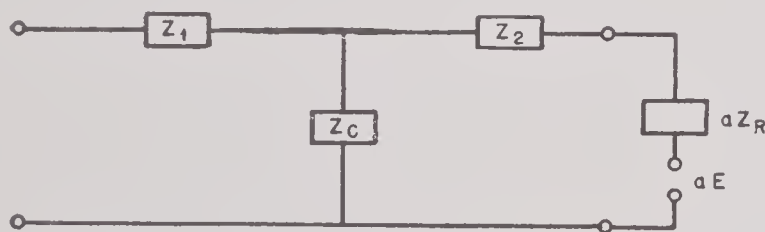


FIGURE C.

Now suppose that the elements in the array were reconnected for lobe suppression. This may involve all kinds of series-parallel arrangements, all in phase, depending upon the lobe-suppression scheme. There may be:

n_1 elements simply in parallel,

n_2 elements paired in series, the pairs in parallel,

n_3 elements in series-triplets, the triplets in parallel, etc., subject to the limitation:

$$n_1 + n_2 + n_3 + \dots = N.$$

However each pair will contribute only I_0 , each triplet I_0 , etc. Consequently a great many crystals might be considered wasted. The total short-circuit receiver response of the newly connected array is only

$$(n_1 + \frac{1}{2}n_2 + \frac{1}{3}n_3 + \dots) I_0,$$

and is always less than NI_0 . Thus the effect of lobe suppression is to reduce the short-circuit receiver response of the transducer by a factor

$$\frac{n_1 + \frac{1}{2}n_2 + \frac{1}{3}n_3 + \dots}{N}.$$

However the reciprocity principle states [Section 4.2.3, equation (21)]:

$$\frac{R_1}{T_1} = \frac{R_2}{T_2} = \text{etc.}$$

Where, if R represents the short-circuit receiver response, T represents the pressure produced in the water at some distance for 1 v applied to the transducer (the so-called constant-voltage transmitter response).

If subscript 1 indicates the original uniformly driven array, and subscript 2 indicates the lobe-suppressed array, then

$$T_2 = T_1 \left(\frac{R_2}{R_1} \right),$$

and it was shown above that this is equal to:

$$T_2 = T_1 \left(\frac{n_1 + \frac{1}{2}n_2 + \frac{1}{3}n_3 + \dots}{N} \right), \quad (65)$$

and we see that T_2 will always be less than T_1 .

This is the expression sought, giving the diminution in intensity radiated caused by lobe suppression. As given here it is for the same voltage applied to the two arrays. It would be a simple matter to compute the impedance change resulting from the lobe suppression, and then express the change in intensity for 1-w input to each array. However the maximum power output at resonance is fixed by cavitation of the single elements, and away from resonance by voltage breakdown of the single elements; this will mean a maximum allowable voltage at any frequency, the same for both

arrays, and the expression above gives the reduction in *maximum possible* intensity resulting from the lobe suppression.

Stated in terms of numbers of elements, this expression is not as might be desired; it can be restated in terms of areas as follows:

The N elements, each of area a , when closely packed, occupy a total area A . The n_1 elements occupy area A_1 , the n_2 elements occupy area A_2 , etc. Thus we may picture the array as a group of zones: one zone of area A_1 is driven at unit amplitude, another of area A_2 is driven at $1/2$ amplitude, etc. Then

$$T_2 = T_1 \left(\frac{A_1 + \frac{1}{2}A_2 + \frac{1}{3}A_3 + \cdots}{A} \right). \quad (66)$$

This form of the expression emphasizes an interesting feature: within our assumption that the radiation impedance is uniform over the array, the reduction is independent of the shapes of the zones and depends only on their *areas*.

It is interesting to evaluate T_2/T_1 for two particularly common lobe-suppression schemes applied to circular arrays:

1. An inner disk, whose diameter is 0.5 of the array diameter, is driven at unit amplitude; the remaining annulus is driven at $1/2$ amplitude. Theoretically the first side lobe is down 22 db.

2. An inner disk, whose diameter is 0.61 of the array diameter, is driven at unit amplitude; the remaining annulus is driven at $1/3$ amplitude. The first side lobe is down 28 db.

The expression for T_2/T_1 gives the reduction for scheme 1 as 4.1 db, a quite sizable reduction. For scheme 2 the reduction is 4.7 db. If one is reconciled to such losses for the sake of lobe suppression, then 4.7 is negligibly worse than 4.1 db, and 2 is the preferable scheme.

4.4.2

Directivity Index

Measurements of directivity index are required in order to obtain the efficiency of a transducer, and it is unfortunate that this is the most difficult and least accurate of all calibration tasks. In the present state of the art very great care is required to obtain an accuracy of

± 1 db, and errors of ± 2 or 3 db are much more usual. For this reason and for obvious theoretical reasons it would be desirable to obtain an expression for the directivity factor and index.

If one is willing to make the usual assumptions of uniform loading, uniform (or at least analytic) phase and amplitude distributions, infinite baffle, etc., one can write an integral expression for the directivity factor. For simple radiators this expression is tedious but may be evaluated. A simple *arithmetic* expression is obtained below, fairly rigorous for any array, and evaluable for any array for which the above assumptions are justified. As in Section 4.4.1 the proof uses the reciprocity principle, but the results depend only on the nature of the radiating surface, and are applicable to transducers which disobey reciprocity.

Consider a radiating surface of arbitrary size and shape driven with reasonably simple phase

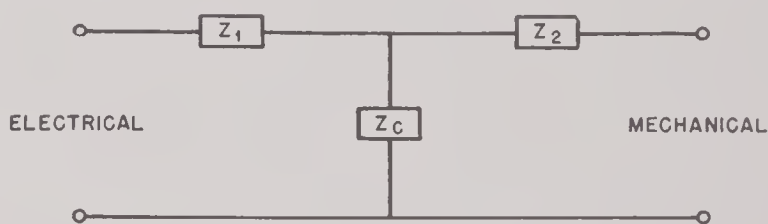


FIGURE D.

and amplitude distributions. (Refer to Figure D.) Such a transducer may be represented by a

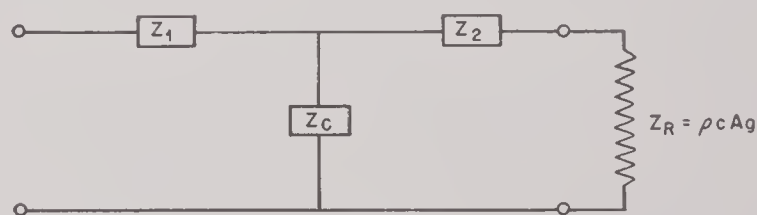


FIGURE E.

generalized transmission T . (All Z 's may be complex.)

If the area of the radiating surface is A and

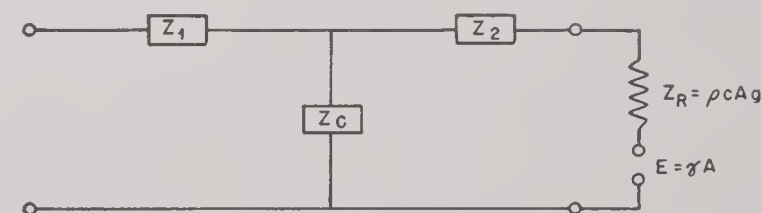


FIGURE F.

the transducer is immersed in a medium of characteristic impedance ρc the radiation impedance may be represented as $Z_R = \rho c A (g +$

jh). The imaginary term is trivial, and since it might be included in Z_2 it is omitted, and the equivalent circuit becomes that shown in Figure E.

Let a plane wave whose free-field pressure is 1 dyne per sq cm be incident from the direction of maximum response. This introduces a voltage proportional to the area shown in Figure F.

Both g and γ are unknown except for certain very simple radiators. Furthermore g and γ will vary from point-to-point over the surface, and the values inserted here are some average over the surface. For simple plane sources containing a small number of zones of constant phase and amplitude, the averaging process would be easy if good approximations were acceptable. For a completely arbitrary phase and amplitude distribution, one might wishfully hope for some average, at least in principle, if the distributions were not too badly nonanalytic.

One may then calculate the current I which would flow if the electric terminals were short-circuited. The current will be proportional to γA , and may be written

$$I = \frac{\gamma A}{Z_T},$$

where Z_T is a transfer impedance, and is a function of Z_1 , Z_2 , and Z_c .

Since we are concerned finally with the *radiating surface* we may assume, without loss of generality, that the T is passive, linear, and bilateral. Then, by invoking the reciprocity of such electric networks, we may write the current I_R which would flow through Z_R if the transducer were driven as a transmitter by 1 v applied to the electric terminals:

$$I_R = \frac{1}{Z_T}.$$

From this we may calculate the electric power expended in the radiation impedance:

$$P_R = |I_R|^2 \rho c A g.$$

Holding this in abeyance, we now invoke the acoustic reciprocity principle; for this we must assume that the medium is also passive, linear, and bilateral; conditions which water satisfies. We obtain the pressure p (dynes per sq cm) in the medium at distance r cm, in the direction

of maximum response for 1 v applied as a transmitter. The reciprocity principle relates this to the short-circuit receiver current I [Section 4.2.3, equation (41)].

$$|p|^2 = \left(\frac{\rho f}{2r} \right)^2 |I|^2,$$

where f is the frequency in cycles.

Now if pressure p were radiated equally in *all* directions the acoustic power output for 1 v applied would be

$$P_1 = \frac{p^2}{\rho c} \cdot 4\pi r^2.$$

Actually p is not radiated in all directions, and we know that the total power input is P_R . Consequently the directivity factor D is given by

$$\begin{aligned} D &= \frac{P_R}{P_1}, \\ &= \frac{\rho c A g}{|Z_T|^2} \cdot \frac{\rho c 4r^2 |Z_T|^2}{\rho^2 f^2 4\pi^2 \gamma^2 A^2}, \\ &= \frac{c^2}{\pi f^2 A} \cdot \left(\frac{g}{\gamma^2} \right), \\ D &= \frac{\lambda^2}{\pi A} \cdot \left(\frac{g}{\gamma^2} \right). \end{aligned} \quad (67)$$

This is the expression for D ; the directivity index is $10 \log D$.

For the vast majority of transducers, g and γ^2 and their ratio are unknown. For an infinite plane, uniformly driven in phase and amplitude, $g = 1$ and $\gamma = 2$. For a point $g = 0$ and $\gamma = 1$; no other surfaces (except perhaps a sphere) are known. It is not surprising that this trick with reciprocity has not introduced anything new to radiation theory. However the function still has great use.

Experience indicates that uniformly driven plane sources have directivity patterns and responses in remarkably good agreement with those predicted by the theory requiring infinite baffle, etc.; this seems to be true even for sources whose dimensions are as small as 1 wavelength. Consequently it is a fair approximation to set $g/\gamma^2 = 1/4$ for such sources. This approximation is exactly equivalent to the simplifying assumptions usually made in computing patterns, etc. Thus the numerical value of D obtained is exactly the same as would be obtained from the

integral evaluation when the integral can be evaluated at all. For all presently practical purposes, then, we may write:

$$D = \frac{\lambda^2}{4\pi A}. \quad (68)$$

In numerous checks this function has been found to agree with integral evaluations and with experimental data well within the experimental error.

Criteria may be established by the accuracy of this function.

1. We know that for large plane A , $g/\gamma^2 = 1/4$. We know also that for very small A , $D = 1$, and consequently $g/\gamma^2 \rightarrow 0$. We know also that the function works fairly well for $A > \lambda^2$. It is likely that the approximation goes bad rapidly for $A < \lambda^2$.

2. If the observed directivity patterns agree with those predicted by the simple theory using infinite baffles, etc., then the approximation $g/\gamma^2 = 1/4$ is justified. If the patterns disagree there is no way of evaluating D theoretically; it can be obtained only by numerical integration of the observed patterns.

In conclusion, note that $g/\gamma^2 = 1/4$ for A infinite and plane, and is equal to 0 for $A = 0$. We may speculate on the behavior elsewhere, and, in particular, wonder if the connection is monotonic with A .

4.5

COMPLEX IMPEDANCE

When electrical measurements are made at the terminals of a single transducer without simultaneous sound-field measurements the only quantity directly observable (except thermal noise) is the complex impedance which may be obtained as a function of frequency, power, etc. Additional information, such as efficiency and response, can be obtained only if the equivalent circuit is known; the accuracy with which such information may be deduced depends upon the completeness and accuracy of the assumed circuit and is always subject to doubt. At best an equivalent circuit is an approximation, and there always remains a considerable burden of proof that the approximation is adequate. In fact University of California Division of War

Research [UCDWR] feels that there has yet to be built the unit whose electroacoustic efficiency can be obtained by electrical measurements.

4.5.1

Motional Impedance

One may measure the complex impedance of a transducer in water (or a motor in air) as a function of frequency. In principle one might measure the complex impedance of the same unit as a function of frequency when mechanical motion was blocked. The vector difference between these is called the motional impedance.²¹ If the real and imaginary parts of the motional impedance are plotted linearly as Cartesian coordinates with the same scales, the resulting locus as a function of frequency is, ideally, a circle passing through the origin. The diameter passing through the origin cuts the circle at the point belonging to the resonant frequency; the diameter at right angles to this one cuts the circle at two points belonging to the frequencies at which the mechanical response is down 3 db (i.e., response for constant-voltage drive in Mason circuit).

While it is possible to determine the blocked impedance of such devices as telephone diaphragms, this is certainly not possible with crystal transducers. The blocked impedance is estimated by interpolating a smooth curve connecting the resistance well above and well below resonance, and the same for the reactance. The difference between the observed resistance and reactance and the interpolated resistance and reactance are assumed to be the components of the motional impedance. Then the efficiency at any frequency is estimated to be the ratio of the motional resistance to the total resistance.

This procedure obviously embodies a great many assumptions. The method of interpolation tacitly assumes that the mechanical branch is singly resonant in the interpolation region; quite frequently this is not true, and the motional-impedance locus is several circles superimposed. For reasons of this kind it is not uncommon to find that several different efficiencies could be obtained.

At best the efficiency so obtained gives the efficiency of conversion of electrical energy to

mechanical. One can imagine situations in which it does not even do that. For example: suppose the equivalent circuit of a transducer were as shown in Figure G. The resistance shunting the mechanical transformer is mechanical, yet it would be lumped with the electric impedance and would not be included in the motional resistance.

The electro-mechanical efficiency of Y-cut RS and Z-cut ADP is very high, so that if reasonable care is taken to reduce electrical losses (e.g., series resistance of wires, dielectric loss) the overall efficiency of conversion to mechanical energy should be very high. It is a poor

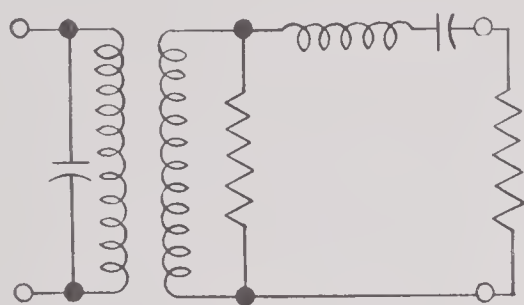


FIGURE G.

transducer which fails in this respect. On the other hand, the largest component of the motional impedance may be internal losses such as occur in glued joints; a high-motional impedance efficiency might be associated with a very low-acoustic efficiency. For this reason motional-impedance efficiency is virtually useless, and is now going out of use with crystal transducers.

4.5.2

Absolute Admittance

By the absolute admittance we mean the length of the admittance vector: the square root of the sum of the squares of the conductance and susceptance.

This quantity is easily obtained with one or two meters and a known resistor, usually by measuring the current into a transducer when driven by a constant-voltage source. The ease of measurement is the chief reason for using the quantity, since it tells one much less than does a complex measurement.

Remote from resonance the admittance of crystals in air behaves like that of a fixed condenser. This contains the admittance of C_0 in the Mason circuit, and also of the mechanical

arm which, remote from resonance, behaves like a condenser. Thus the observed admittance below resonance is greater than that of C_0 alone (by about 9 per cent for Y-cut RS and Z-cut ADP) and this correction must be made when computing the dielectric constant (see Section 3.2.3).

At resonance the admittance of the mechanical arm rises to that of the load impedance; for free crystals in air a Q of 1,000 or more is common, and the admittance at resonance rises many decibels.[§] For high Q , care must be taken to be sure that the series resistor used to determine current is not the limiting resistance in the circuit.

Slightly above resonance, electrical antiresonance occurs; the admittance falls to a very low value determined by the Q of the circuit.

Above electrical antiresonance the mechanical branch is inductive, so the admittance remains less than that of C_0 alone. However at mechanical antiresonance the admittance of the mechanical arm is zero, and the net admittance is that of C_0 alone.

Above mechanical antiresonance the mechanical branch is capacitive and the net admittance is greater than C_0 , rising to the next resonance.

Measurements of absolute admittance of single crystals or groups of crystals are used to determine crystal constants, glue losses, frequency shifts caused by added structure, and so forth. Such data are readily obtained and are one of the best research and design tools. When diagnosing a finished transducer which fails to meet expectations it is very helpful to have available admittance data on the bare dry motor; this helps in deciding whether the trouble is inherent in the motor itself or in the case, cavities, window, etc. It is well for a transducer laboratory to take admittance data on subassemblies as a routine practice.

Little use can be made of the absolute admittance of finished transducers, particularly oil-filled units, either in air or in water. In water the Q 's are so low that the admittance, even that of efficient units, departs little from that of a fixed condenser and all units look pretty

[§] By decibels here is meant $20 \log$ current for constant voltage.

much alike. In air the radiating face sees an impedance very different from that in water; standing waves are set up, with accompanying swings of admittance, which do not exist in water. One usually observes many erratic peaks and dips of admittance which are not meaningful.

1.5.3 Two-Terminal Impedance

A transducer may be regarded as a two-terminal system, electrically, with any shield tied to ground or floating and lead-to-shield effects ignored. Calibration stations usually report complex impedances this way unless more elaborate data are requested. Such data are necessary to an understanding of a transducer's performance and to design of associated electronic equipment. The impedances to be expected of various units are discussed in Section 4.9; here we merely note some general principles and cautions to be observed.

Transducers are usually operated balanced to ground to minimize noise troubles, etc. It is imperative that two-terminal impedances be taken balanced to ground if the unit is to operate balanced. Otherwise the effects of lead-to-shield impedances are improperly portrayed. However the majority of impedance bridges are inherently unbalanced, as are standards for use with bridges. This requires the use of isolation transformers, and great care must be taken to select acceptable transformers.

If, for some reason, a transducer is to be operated unbalanced the impedance should be measured under identical balance conditions, even to the choice of which transducer lead is closer to ground.

Tuning coils are often put between the transducer and its cable. Occasionally the components are such that the net-series inductance of transducer plus coils can parallel-resonate with the shunt capacity of the cable. This causes the impedance seen at the top of the cable to go through gyrations. If the test cable is not identical with the cable to be used on the unit, experimental errors make it impossible to calculate the cable out of the observed impedance. Since this resonance with the cable is never desirable it should be avoided.

No bridge now available is capable of measuring accurately over the range of Q and impedance presented by a wide variety of transducers. Large units, at resonance, may look like perhaps 100 ohms at $Q = 5$; if tuned with coils, $Q = 0$. Small units may look like 100,000 ohms at resonance. Away from resonance Q may be many hundred. To cover all situations a bridge may be called upon to measure Q anywhere from zero to 100, reactances of both algebraic sign, and magnitudes of impedance from a few ohms to a megohm. Since no one bridge can do all this, care must be taken to select a bridge suitable for a given transducer.

The complex impedance of itself does not allow a diagnosis of transducer behavior; together with frequency-response data and directivity patterns it is an important tool. If a transducer misbehaves this is likely to be reflected in the impedance. For example, low efficiency usually results in an abnormally low series resistance, often with no discernible resonance. Spurious vibrations such as harm patterns often show as extra resonant peaks in the series resistance. High Q resonances which cause sharp holes in frequency response usually show as notches in the series resistance.

The reactance is dominated by C_0 and is not as greatly affected by mechanical effects. Usually the reactance is substantially that of C_0 and may not depart noticeably except at places where the series resistance rises to important peaks. Any erratic behavior of reactance not accompanied by understandable resistance changes is most likely an indication of trouble in the measurement setup, but may represent electrical quirks such as saturation of tuning coils.

4.5.4 Three- and Four-Terminal Impedances

Unless one side of a transducer is tied to ground the circuit is actually at least three-terminal. Furthermore the backing plate may not be grounded and may be used as a fourth terminal. Because of capacity coupling there is always some complex impedance between any pair of these terminals. Transducers are always small compared with an electric wavelength so that all impedances, except perhaps

that between the crystal leads, will usually have capacitative reactances; the resistance is usually dominated by dielectric losses rather than by series resistance.

It is exceedingly difficult to determine all six impedances of a four-terminal mesh by measurements on a simple two-terminal bridge. For this the techniques discussed in Section 9.1 are indicated.

Some generalizations may be made on the basis of work done by UCDWR: The most important stray capacities are those from each crystal lead to the backing plate. Usually the clearances from crystals to external case are much greater with consequently lower capacity. Even in transducers whose crystals are separated from a metal backing plate by only $\frac{1}{16}$ -in. porcelain, the stray capacities to the plate change the apparent value of C_0 by perhaps 10 per cent. If the crystals are attached directly to metal these capacities are much greater and such practice should be avoided. Much more extensive investigation is required, but it appears that these strays are one of the many small factors contributing to possible poor behavior; they are not usually in themselves dominating troubles, but efforts should be made to minimize them.

Such measurements as are available indicate that some transducer materials, notably Corprene, have high dielectric losses; if the stray capacities are small these losses are negligible, but care should be taken to minimize electric fields occurring across Corprene and similar dissipative materials.

The most serious effect of the stray capacities is in raising the electrical Q (Q_E) of a transducer and thus narrowing its operating band. It is apparent that if there are stray capacities from each crystal lead to ground the effect on Q_E will be lessened by balanced operation as compared with one side tied to ground.

4.6 STEADY-STATE RESPONSES

Unless otherwise stated, response usually is taken to mean response versus frequency for some constant-drive condition. Steady-state response means that all conditions (both frequency and drive amplitude) are held constant

for sufficient time to insure decay of transient conditions. Under these conditions it is a simple matter to calculate the expected response, at any frequency and level, to the Mason approximation, provided the termination impedances and directivity index are known. This is discussed in Section 4.9. In this section we consider the utility of the various response curves and their general nature.

Responses are usually expressed in terms of constant voltage, constant pressure, constant current, etc. In the course of calibration the voltage, pressure, or current is rarely constant with frequency and is rarely the unit value reported. Corrections to the observed data are applied in order to report *as if* the quantity were unit and constant. In most transducers this is trivial, but some transducers, notably *X-cut RS units*, are nonlinear. In such units the response in service may be different from that indicated. This is particularly true since calibrations are made at low level and most transmitters are operated at high level, perhaps as much as 60 or 80 db higher.

Transmitter responses usually give the pressure at 1 m. The distance may be measured from the center of the acoustic window, the center of the crystal array, or (more usual) the geometric center of the body. In some cases it may be important to state this distance clearly. The responses are nearly always measured at greater separation in order to be in the region where inverse square law is obeyed and to make the units better approximations to dimensionless sources. The data are then calculated back to 1 m by assuming inverse square law. Actually 1 m is too close for most units; it is within the induction field, and the true pressure at that distance may be very different from the reported response.

4.6.1 Constant-Voltage Transmitter Response

This is the response versus frequency for constant voltage applied to the transducer terminals. The voltage is usually reported as 1 v and the response is reported as pressure in decibels above 1 dyne per sq cm at 1-m distance.

This response is one of the most frequently

encountered; it is easily obtained, does not require any corrections for the cable (unless IR drop in the copper is significant), and is particularly useful to designers. Actually no transducer is operated out of a zero impedance source, so that this is not a true picture of the frequency response to be expected when the transducer is put in service. If the transducer is limited by voltage breakdown this curve gives a good picture of the maximum possible output versus frequency.

If no tuning coil is used in the transducer this response always peaks at or very near the transducer's mechanical resonance unless the transducer is so inefficient that no discernible resonance occurs. If a series tuning coil is used the response peaks at the frequency at which the coil cancels the transducer's reactance; if this frequency is not the transducer's own resonance a second, lower, peak or plateau may be observed. When operating with a coil it should be remembered that the voltage across the transducer terminals at the peak response is Q times the cable voltage, this factor may be large, particularly if the reactance is cancelled away from the transducer's resonance, and transducers are often damaged by failure to observe due caution.

Since the presence of C_0 has no effect when constant voltage is applied, the response curve is governed entirely by the behavior of the mechanical branch of the equivalent circuit; near resonance this is symmetric, so the response curve falls symmetrically on either side of resonance.

The maximum value attained depends, among other things, on the thickness of the crystals. A fictitious improvement appears to be obtained if a greater number of thinner crystals is used, but the impedance changes and the increased pressure is obtained by proportionately greater power consumption. This factor must be borne in mind when comparing transducers on the basis of constant-voltage transmitter response.

4.6.2 Constant-Current Transmitter

This is the response versus frequency for constant-current input to the transducer ter-

minals. It is usually reported as pressure in db above 1 dyne per sq cm at 1 m for 1 amp input.

This response is often reported but is more difficult than constant voltage because of the cable. Since cables are changed frequently it is wise to consider them separately and to report the behavior of the transducer proper (as if measured at the terminals to which the cable would be attached) with the cable removed. However, one must have a cable to lead from the underwater transducer to the above-water equipment, so the cable must be calculated out of the data. Usually the current is measured at the top of the cable and the correction for the current which flows in the cable capacity is obtained from impedance data. Some high-impedance transducers may have lower admittance than their cables, and serious errors arise in the cable correction. For such units the constant-voltage transmitter response is more likely to be correct.

This response is not as convenient for designers as the constant voltage because the equivalent-circuit arithmetic is more tedious. Furthermore, stray capacities to ground affect the constant current but not the constant-voltage response. It is easier to learn about the strays from impedance data.

Transducers are often operated out of pentode amplifiers which approximate constant-current sources (within limits) so the constant-current response may closely resemble the response in service for such amplifiers. This similarity must be tempered with many reservations concerning overloading, distortion, etc., and should not be relied upon indiscriminately.

For an efficient transducer the acoustic power radiated at constant-current drive is proportional to the series resistance, peaking near resonance and falling, nearly symmetric, on either side. The response is determined not only by the mechanical branch of the equivalent circuit, but also by C_0 ; both the electrical and the mechanical Q 's enter the calculations. The directivity index changes with frequency, usually between 3 and 6 db per octave, so the response of an efficient unit is just the shape of the series resistance with that slope added. This response is not affected by the presence or absence of series tuning coils.

Like the constant-voltage response, a fictitious improvement is obtained by use of thinner crystals; the series resistances should be considered when comparing transducers on the basis of constant-current response.

4.6.3 Constant-Power Transmitter Response

This is the frequency response, usually expressed as pressure in db above 1 dyne per sq cm at 1 m, for constant power (1 w) expended in the transducer. To obtain this one must have not only constant voltage or constant-current response data but also the complex impedance; cable corrections must be made as for constant-current data, and it may be necessary to correct for the cable dissipation. This involves a fair amount of work, and this response is too rarely reported. Its chief value is to the designer; with it he can learn much about transducer efficiency, and particularly about frequency dependence of efficiency.

For a perfectly efficient transducer the constant-power response is a smooth curve, rising with frequency, following the behavior of the directivity index. Any peak or dip represents some form of anomalous behavior, perhaps distortion of directivity patterns, and perhaps changes of efficiency.

A perfectly efficient point source (i.e., directivity factor equal 1) would produce 70.8 db above 1 dyne per sq cm for 1-w input. If a perfectly efficient transducer has a directivity index of $-D$ db ($D \geq 0$) then, for 1-w input the pressure should be $70.8 + D$ db in the direction of maximum response. If such a transducer had efficiency $-E$ db ($E \geq 0$) the pressure in the direction of maximum response should be $70.8 + D - E$ db. This relationship is a great help in estimating transducer efficiency; D can often be calculated within 1 or 2 db from the expression given in Section 4.4.2, and the efficiency so obtained is likely to be as accurate as can be obtained by present calibration methods.

4.6.4

Constant-Available-Power Transmitter Response

This transmitter response is one frequently encountered. In principle it is the response out

of an idealized amplifier. The idealized amplifier consists of a constant emf in series with a constant resistance. The emf is adjusted to deliver 1 w to a resistive load equal to the amplifier impedance. The resistive load is replaced by the actual transducer, and the response is reported as a function of frequency for constant amplifier emf.

To the extent that this idealized amplifier simulates real amplifiers, the response curve resembles that to be expected in service.

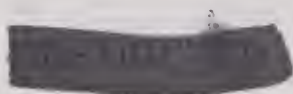
It has been common to report all kinds of transducers out of, say, 135-ohm or 600-ohm idealized amplifiers, regardless of the transducer impedance. The reason for this was that such impedance taps are commonly available, and this reports the behavior to be expected when the transducer is so operated. Of course this is a defeatist attitude, implying that transformers are not to be had, and the apparent merit of a transducer so reported depends entirely on whether or not it happens to match the selected amplifier impedance. In order to judge properly the performance of any transducer it is necessary to match the amplifier to the transducer. Furthermore, transducers should nearly always be tuned, usually with a coil at resonance, so that the ideal amplifier should be a complex-conjugate match to the transducer. Such a curve is then a very useful portrayal of the response to be expected when operated properly.

4.6.5

Open-Circuit Receiver Voltage

This is the open-circuit voltage, usually in db below 1 v, appearing across the transducer terminals, as a function of frequency, when a plane wave whose free-field pressure is 1 dyne per sq cm is incident upon the transducer. It is by far the most common way of reporting receiver response, and is one of the most useful. Like the constant-current transmitter response, cable corrections must be made; these are tedious and for small units may be in serious error. Also, like the constant-current transmitter response, it is independent of any series coils.

Gain is cheap in receiver amplifiers, so that one is inclined to judge transducers on the basis



of open-circuit voltage regardless of impedance. From the standpoint of amplifier design this is nearly always justified, but for purposes of judging transducer performance it is not correct. A fictitious improvement can be obtained by using thicker crystals or by connecting crystals in series, but the impedance changes so as to annul this apparent improvement.

The open-circuit voltage reciprocates with the constant-current transmitter response, and so differs in shape only by a 6-db per octave slope.

If care is taken to consider the shape of the array and the thickness of the crystals, open-circuit voltage offers a useful criterion of transducer efficiency. The maximum value to be expected for plane arrays is easily calculated, and failure to reach this is indicative of a commensurate inefficiency; the method is so useful because no account need be taken of the directivity index if the array is plane.

These maximum values, predicted from Mason theory, for 1/4-in. thick crystals, clamped drive, are:

45° Y-cut RS: 62.4 db below 1 v,

45° Z-cut ADP: 60.7 db below 1 v,

for normally incident plane waves whose free-field pressure is 1 dyne per sq cm.

The maximum occurs close to but not at the resonant frequency; for clamped Y cut it is slightly below resonance, for clamped Z cut slightly above.

1.6.6 Short-Circuit Receiver Current

This response is not common but is coming into use because it does not require cable corrections. It is the current, usually in decibels below 1 amp, which flows in the short-circuited transducer terminals when there are incident upon the transducer plane waves whose free-field pressure is 1 dyne per sq cm.

While advantageous because no cable correction is required, this response is not much use to anyone. Transducer designers are accustomed to using open-circuit voltage and most numerical values are given in those terms. Electronic engineers find the open-circuit voltage more to their liking.

This response reciprocates with the constant-voltage transmitter, and differs in shape only by a 6 db per octave slope. It can, like open-circuit voltage, be used to estimate efficiency. The maximum values predicted by Mason theory are:

45° Y-cut RS: $3.96 \times 10^{-10} n L_{cr}$ amp,

45° Z-cut ADP: $6.11 \times 10^{-10} n L_{cr}$ amp,

where n is the number of crystals all in parallel and all alike, and L_{cr} is the width of a crystal in centimeters. Note that, unlike open-circuit voltage, account must be taken of the *number* of crystals in the array. For this reason this is much less convenient and is not often used to estimate efficiency.

1.6.7 Matched-Receiver Response

This response is not now reported as calibration data. It is the power, in db below 1 w, expended in a complex conjugate load imposed on the transducer terminals when there are incident on the transducer plane waves whose free-field pressure is 1 dyne per sq cm. Since transducers are normally used near resonance, the load impedance should be chosen equal to the complex conjugate of the transducer's impedance at resonance. It is difficult to obtain, and is of interest only to designers, but, like the constant-power transmitter response, is the only receiver response on which transducer performance is properly judged. It should be peaked near the frequency of conjugate match, and should fall more or less symmetrically on either side. It offers a means of judging efficiency and frequency-dependence of efficiency, but is inferior to the constant-power transmitter response in this respect.

1.6.8 System Response

Nearly all transducers are intended for use in a sonar system in which they are driven by real amplifiers, often overloaded and through non-ideal transformers, frequently on long lengths of high-capacity cable, and often with equalization or with filters in the system. We cannot urge too strongly that it become common prac-

tice to obtain transducer response data as operated by the actual system. Many times during World War II it was discovered that experimental systems behaved unexpectedly because of all the new conditions not included in calibration data. When calibrating system responses a person familiar with the electronic equipment should be consulted to be sure that the data truly represent the behavior in service, particularly with regard to power levels.

4.7 TRANSIENT RESPONSES

Many applications of transducers require the transmission of pulses 1 msec or less in time length. In particular are those applications requiring high repetition rates, which rates then are again dependent upon the pulse lengths. The shortest pulse that a transducer will handle is determined by its rise and decay characteristics, which are controlled by many factors, such as electrical Q , mechanical Q , or volume reverberation inside the case and generally are functions of frequency. The prediction of transient behaviors from steady-state calibrations are thereby greatly complicated, and direct measurements of the acoustic pulse transduced are indicated. Using a probe pickup and pulse modulator described in Chapter 9, pulses of 450- μ sec duration coming from a transducer whose resonance is 24.5 kc were recorded and are illustrated in Figure 22. The probe itself has a build-up time of 4 μ sec, which allows it to faithfully follow the pulses of Figure 22.

Referring to the figure, the longest rises and decays appear to occur at the resonant frequencies. The decay tail seems to last about half the time of the pulse itself. At higher frequencies the tail seems to be shorter, but there seems to be a beat frequency between the applied and the resonant frequencies lasting over half the pulse duration. This characteristic appears at most frequencies, and is also found in the pulsing of electrical networks of lumped constants.

There are many other applications of transient testing, because this method facilitates the identification of particular acoustic paths by their lengths. In any underwater acoustic-testing system, unless the medium is infinite in ex-

tent, reverberation due to reflection from the boundaries and other objects in the water are large and usually confuse steady-state measurements. With pulsing, however, effects from different paths can be identified and each one measured separately. The kind of measurements benefited by this technique include crosstalk between two closely spaced units, directivity patterns, free-field responses, etc. Figure 22 illustrates a picture of the signal at the terminals of a receiving transducer whose radiating plane is the same as that of a like transducer being pulsed with 200- μ sec pulses and separated from the receiver by 6 in. The first large pulse is due to a direct path between the two units, and the remaining smaller ones are due to targets in the water 1- to 10-ft distant from the two units. The crosstalk from each path can thus be identified in both distance traveled and magnitude.

4.8 LIMITING FACTORS

In terms of a completed sonar system, the most important limitations of performance are the original specifications on which design was based. If a very small nondirectional unit is specified rather low-acoustic pressure must result; allowing the physical size to increase allows a corresponding increase in output pressure. However, the questions of choice of design to meet specifications are discussed in Chapters 6 and 7. In the present discussion the transducer is regarded as a given thing, its design chosen for some unstated reason, and the inherent limitations are considered.

4.8.1 Steady-State Operation as a Transmitter

Three possible limitations of output power inherent to the transducer come to mind: current, voltage, and power input. Actually, the input current never imposes a limitation of itself, except possibly in series tuning coils which may saturate; such saturation is a trivial problem. If the transducer is operated at or very near resonance the limitation is nearly always caused

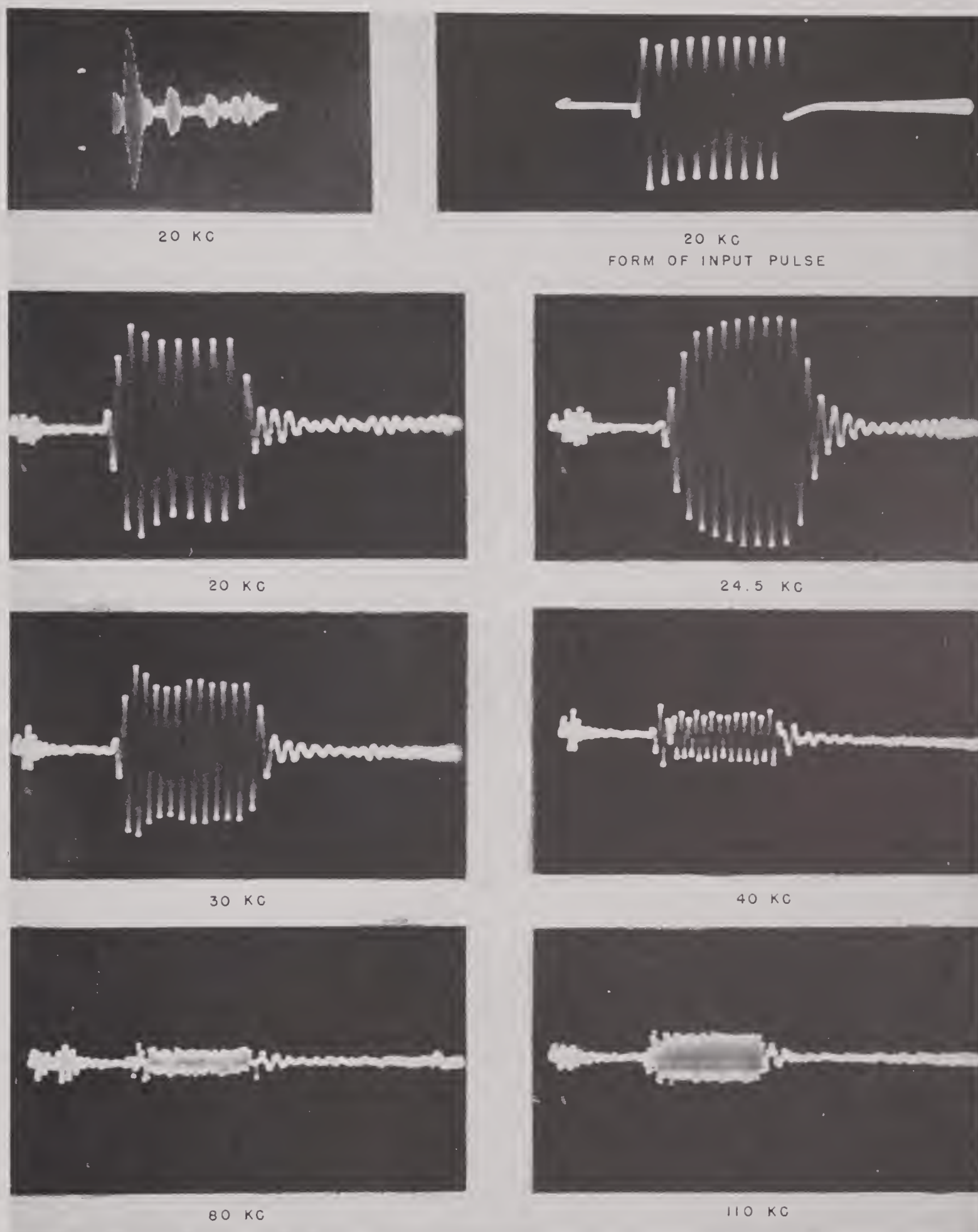


FIGURE 22. Acoustic pulses of 450- μ sec duration transmitted into water by the GD28-1 crystal transducer.

by power; it is relatively easy to drive an efficient transducer to cavitation at resonance. This is discussed in Section 4.8.5.

If the transducer is to operate over any appreciable frequency range, the maximum possible power is likely to be a function of frequency, high near resonance and several db lower at the ends of the band. Near the ends of the band the limitation will be imposed by voltage breakdown, usually across the edges of the crystals, but possibly even through the bodies of the crystals.

The distance from resonance at which the limitation shifts from power to voltage is variable and indefinite. It will depend upon the details of design (particularly on the geometry of the radiating face), upon the crystals used, and, above all, on the cleanliness observed in assembly.

Thoroughly clean new Y-cut RS immersed in dry castor oil withstands up to 20 kv (60 cycle: rms) across $\frac{1}{4}$ -in. thick crystals; at 20 kv nearly all samples break down. The breakdown of Z-cut ADP is not as definite, but under similar conditions occurs at 30 to 40 kv (60 cycle: rms). In each case the breakdown is through the body of the crystal, and tends to initiate at a sharp electrode corner where the field strength is much greater than these numbers indicate. If rounded corners, etc., were used these crystals might stand several times as high voltage.

Finished transducers rarely, if ever, achieve voltage limits as high as the new crystals. During World War II, UCDWR was not able to maintain adequate standards of cleanliness, and the contamination of crystal edges during assembly reduced the voltage limit enormously. Representative UCDWR transducers using $\frac{1}{4}$ -in. thick crystals could not be relied upon above 3,000 v if Y-cut RS, or 5,000 v if Z-cut ADP. The Bell Telephone Laboratories maintained excellent cleanliness standards, and the corresponding limits on their units are much higher. No data are available on units made by Brush Development Company, Submarine Signal Company, or Naval Research Laboratories [NRL], but these may well be higher than UCDWR.

At resonance only about 1,000 v (rms) are needed across $\frac{1}{4}$ -in. Z-cut ADP, or about 1,500

v across Y-cut RS, to produce $\frac{1}{3}$ w per sq cm if the crystal is clamped and fully loaded by the water. However this required voltage rises rapidly as the frequency leaves resonance, and eventually a voltage limitation is met, usually only a small fraction of an octave from resonance.

1.8.2 Short Pings as a Transmitter

Since breakdown by power dissipation undoubtedly involves local heating effects, it is plausible that the power limitation goes up for short pings and a low-duty cycle. If so, then even at resonance the ultimate limitation for sufficiently short pings would be voltage breakdown through the crystal body. Under this condition there is no reason to anticipate input current limitations, particularly if air-core coils are used.

If conditions were such that 20 kv could be put across $\frac{1}{4}$ -in. 45° Y-cut RS, the resulting strain at resonance would be of the same order as the reputed maximum allowable strain for fracture (10^{-4}); the maximum strain predicted by Mason theory for 20 kv is approximately 2.4×10^{-4} . At resonance a maximum strain of 2.4×10^{-4} would radiate roughly 60 w per sq cm, provided water, crystals, etc., remained linear.

If it were possible to put 35 kv across $\frac{1}{4}$ -in. 45° Z-cut ADP crystals at resonance the intensity radiated into water would be roughly 430 w per sq cm; no data are available, but this probably exceeds the maximum allowable strain for fracture.

4.8.3 Partially Loaded Transmitters

In the preceding sections it was assumed that the transducer was fully loaded by the radiation impedance of water. This is substantially true of crystals in a plane array whose dimensions are a couple of wavelengths or more, but it is usually not a good approximation for small radiating faces such as are often used to produce nondirectional patterns. Such faces may be loaded as little as 10 per cent of the full loading.

In such units the strain produced by a given voltage gradient may be many times those mentioned in Section 4.8.2 and allowable strain might possibly impose a limitation before voltage breakdown.

The problem of cavitation (power) limits on such small radiating faces is understood qualitatively, but any exact treatment requires a knowledge of the Green's function from which the point impedance at each point in the radiating surface may be calculated. Qualitatively, it is apparent that the loading will vary with position in the surface, and very probably is greatest at the geometric center. If the average radiation impedance is appreciably lower than the greatest point impedance, the average strain will be unduly great. The crystal face moves approximately as a plane piston, so the intensity radiated at the point of highest loading will be much greater than the average intensity. Thus, if such a poorly loaded face radiated an *average* intensity of only 0.1 w per sq cm it should not be surprising to find cavitation, since the intensity *at some point* might be 10 w per sq cm. This behavior has been observed in several instances, notably UCDWR-type CY4 (see Chapter 6) which shows signs of cavitation on the center line of each radiating face when driven above 1,500 v across 1/4-in. 45° Y-cut RS.

4.8.1

Receivers

Except possibly in extremely quiet water it is not difficult to hear ambient water noise over ordinary transducers. Consequently a transducer's limitations as a transmitter are more important than the limitations as a receiver. However in some units, such as tiny probes, the self-noise inherent in the transducer may obscure ambient sounds.

It is customary to think of the open-circuit voltage of a receiver worked into a grid circuit, without regard to its impedance. This attitude among system engineers is justified so long as the receiver is big. It is apparent that the quantity needed to evaluate correctly the sensitivity of a receiver is the power it will deliver to a per-

fectly matched load impedance for unit incident sound pressure. As the area of the face of a receiver is diminished this delivered power is diminished more or less proportionately, and unless the crystals are thinned the impedance goes up. Consequently a point is reached at which the "resistor noise" corresponding to this impedance obscures the sound coming from the water. As the accepted frequency band is increased this effect is made worse. Small "probe" units are often used as calibration standards, etc., in which service they are expected to be nondirectional at all frequencies and to have reasonably flat response over a wide frequency range. To achieve this the crystal is made very small and the resonance is placed well above the high end of the band. In such units all effects combine to raise the impedance (and inherent resistor noise) and lower the power delivery. If very low frequencies are expected of such very small probes, self-noise may limit performance in quiet water. Except for this rare requirement, no inherent limitation is encountered down to ambient water noise.

4.8.5

Cavitation

The elementary classic theory of cavitation predicts that the liquid will rupture (cavitate) when the negative acoustic pressure equals ambient. In water at zero depth this corresponds to a plane-wave intensity of 1/3 w per sq cm. Extensions of this elementary picture take into account surface tension and vapor pressure of the fluid.

Most observers agree that castor oil and water do not cavitate at intensities a few db above 1/3 w per sq cm. The measurements are difficult and various observers disagree somewhat on the exact intensity. There is good evidence to indicate that the presence of dissolved gas and microscopic bubble-forming nuclei influence the observed cavitation intensity.

The most remarkable feature of cavitation is the apparently random behavior under supposedly controlled conditions. One may set up cavitation in a beaker at controlled temperature (ambient) and after perhaps many minutes the

cavitation may suddenly cease although the applied voltage, etc., remain unchanged. As the voltage on a crystal is raised cavitation usually sets in at a definite voltage. If the voltage is then lowered the cavitation ceases at a lower voltage which appears to be a function of the time spent at cavitation. The voltage at which cavitation starts appears to be a function of the cavitation history of the liquid during several hours preceding. One usually associates with cavitation many different phenomena among which are:

1. Bubble formation; this usually looks like a "smoke" in the liquid, but may contain large bubbles.
2. A "frying noise" alleged to be caused by the collapse of millions of tiny bubbles.
3. Nonlinearity of output acoustic pressure with input voltage.
4. Great wave-form distortion of the sound in the liquid.
5. Considerable temperature rise in the neighborhood.
6. Pitting of the solid surface.

Actually all of these are observed at one time or another, but they need not all occur simultaneously. For example, one may set an ADP crystal cavitating in a beaker of oil, during which time bubbles leave the surface, and the wave form is seriously distorted (destroyed is a better description), yet sometimes no frying noise is heard, no great heating is observed, and no pitting results after many hours. On the other hand, a frying noise may be heard, the temperature may go up, and extensive pitting may occur with no visible bubbles.

It is apparent that cavitation is not a single phenomenon, and one must define exactly the quantity he uses as a criterion for the occurrence of cavitation. This is particularly important when comparing the results of two observers, and some of the differences of opinion may result from use of different criteria.

There is no doubt that the classic theory is inadequate, and much interesting research remains before these phenomena are explained.

For the purposes of this discussion of limitations of performance, the criterion for cavitation is taken as pitting or destruction of crystals after long-time operation. This is certainly the

most fundamental limitation cavitation imposes, although it is possible that wave-form distortion, etc., occurs at lower driving levels. Within this criterion, the following appear to be true:

1. Under otherwise identical conditions ADP can radiate higher intensity than can RS.
2. When fully-loaded plane arrays are used, both crystals can radiate more than $\frac{1}{3}$ w per sq cm at zero submersion.
3. The cavitation intensity rises with increasing depth of submersion. There is disagreement on how fast it rises or on the existence of an upper limit. Probably a designer should not rely on this indefinitely until better data are available, and a 10-db increase is suggested as an upper limit (corresponding to roughly 300-ft depth).

UCDWR has adopted the attitude that cavitation is a statistical affair; the power or voltage limit assigned by a designer is a function of the allowed risk on the particular transducer. If absolutely no risk is allowed the intensity at the crystal face should be held under $\frac{1}{3}$ w per sq cm. If a very good risk is allowed, RS may be worked to $\frac{1}{3}$ or even $\frac{1}{2}$ w per sq cm, depending upon the geometry of the array, and ADP may be worked to 1 w per sq cm. If a definite gamble is desirable one may work RS to 1 w per sq cm and ADP to 3 w per sq cm. If, for some system development, it is desirable to radiate even higher intensities, tests should be conducted on the identical transducers to be used. All these figures are for zero submersion; appropriate increases for depth may be made.

It is commonly assumed that transducers cannot or should not be driven above cavitation because of destruction or because of loss of output power. For RS this is probably true since cavitation heating destroys the crystals very rapidly. However ADP can tolerate very considerable cavitation with minor or no damage. It is by no means certain that the output intensity does not continue to rise for increased electrical input above cavitation (albeit with a lower slope). If possible wave-form distortion may be tolerated to obtain higher intensity at the driving frequency, it might well pay to operate above cavitation on some transducers. Extensive research on this subject is certainly indicated.

4.9 ANALYSIS OF EQUIVALENT CIRCUITS

At first sight the equivalent circuits for various transducers appear quite different both in magnitude and form, and it is not apparent what properties they have in common. Furthermore, numerical calculation of impedance and response for each transducer is exceedingly tedious and to a large extent repetitive. It is the purpose of this section to restate the equivalent circuit in parametric form and to point out the tremendous number of similarities among transducers. From this parametrization expressions are derived which allow the compilation of a set of numerical data applicable to most transducers.

For this purpose the Mason circuit is used without change; although this circuit embodies numerous approximations, no additional approximations are made here. Thus these data present exactly the information given by Mason's circuit. No correction is made for the finite width since actually all these results are width-dependent, but for ordinary purposes the changes are not important to preliminary design, and are outweighed by the more serious couplings encountered in transducers.

The predicted response curves, impedances, etc., are highly idealized. Some excellent transducers depart considerably, but the majority of "ordinary" transducers agree with prediction rather well, provided they are efficient. These curves may be thought of as goals which transducers approach and sometimes exceed. It must be emphasized that despite its limitations the Mason circuit does remarkably well for describing transducer behavior, and in the present state of the art it is adequate for ordinary design purposes.

4.9.1

Mason Circuit

The Mason circuit^h is given in Figure 23. The various quantities are:

ϕ = "turns ratio" of an ideal electromechanical transformer,

^h Some changes are made in the symbols for simplification.^{1a}

V = velocity of sound in the plated crystal in the L_y direction,

Z_0 = characteristic impedance of the plated crystal multiplied by the area $L_w L_t$,

C_0 = static electrical capacity of the crystal as a parallel-plate condenser with dielectric constant K ,

L_y, L_w, L_t = length, width, thickness.

All quantities are given in cgs esu. Some relations among these quantities are:

$$\phi = -\frac{DKL_w}{4\pi}, \quad (69)$$

$$V = \sqrt{\frac{(1 - k^2)Y_0}{\rho}}, \quad (70)$$

$$Z_0 = L_w L_t \sqrt{\rho(1 - k^2)Y_0}, \quad (71)$$

$$k = D \sqrt{\frac{K}{4\pi Y_0}}, \quad (72)$$

$$C_0 = \frac{KL_w L_y}{4\pi L_t}, \quad (73)$$

where D = piezoelectric constant,

K = dielectric constant,

Y_0 = Young's modulus of the unplated crystal in the L_y direction,

k = electromechanical coupling coefficient.

In order to convert mechanical resistance to electric ohms we divide all mechanical impedances by ϕ^2 and remove the transformer (or change its ratio to 1/1). Having done this all impedances are in cgs esu. To convert to practical electrical ohms all impedances are multiplied by 9×10^{11} . All dimensions remain in cgs units.

This circuit, shown in Figure 24, is used for the balance of Section 4.9.

4.9.2

Three Basic Drives

Nearly all crystal transducers may be placed in one of three classes, depending upon the manner in which impedances are imposed on the two ends of the crystal. These are:

1. Clamped drive: the radiation impedance

(water) is on one end of the crystal, the other end is blocked by a backing plate.

2. Symmetric drive: the radiation impedance (water) is on both ends of the crystal.

3. Inertia drive: the radiation impedance (water) is on one end and zero impedance (air) is on the other.

A given crystal operated in symmetric or inertia drive has the same resonant frequency as when free in air; operated in clamped drive the resonance is exactly half the free resonance (Mason approximation).

Actually a backing plate presents an infinite impedance to a crystal at a single frequency (for $1/4$ wave plate) and then only if the plate is lossless, backed by vacuum, and attached by

array so as to be fully loaded. This may not be true of small or curved units, or of arrays in which the crystals are spaced apart (see Section 4.2).

In his book Mason considers only the clamped and inertia drives. For these two circuits he goes on to develop LC approximations to these trigonometric functions. To do this the LC circuit is chosen to resonate at the same frequency as the transcendental function's *first* resonance, and the slopes at resonance are equated. This gives two equations for the two unknowns, L and C . However, the transcendental functions are multiperiodic and the LC circuits are not. Thus the approximation is good only near resonance; it remains good fur-

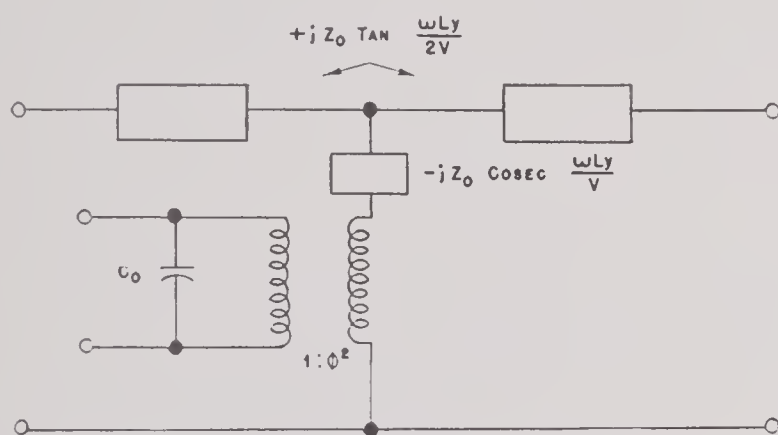


FIGURE 23. Equivalent circuit of a transducer with ideal transformer (Mason).

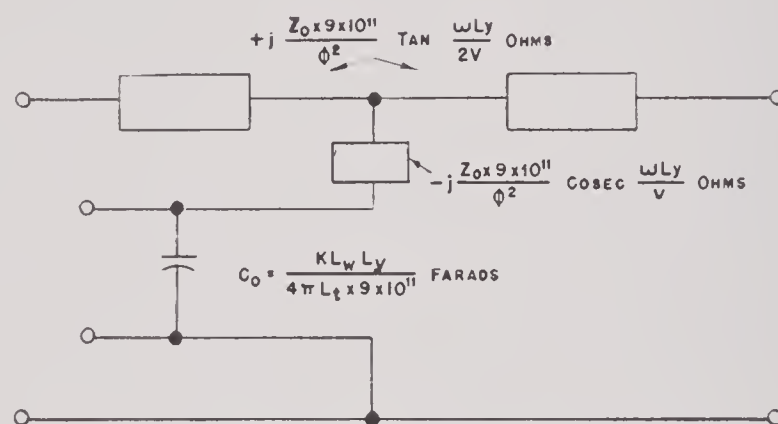


FIGURE 24. Equivalent circuit of a transducer with transformer removed or with an ideal transformer having a 1:1 turns ratio.

a perfect cement joint. However a sufficient approximation for our present purpose is to consider the plate to present infinite impedance at all frequencies.

The three basic circuits then became those shown in Figure 25. Trigonometric identities have been used to combine the cosecant and tangent terms. A transformation attributed to Norton^{1b} has been used to obtain the inertia-drive circuit.

In each case the radiation impedance imposed on a face of dimension $L_w L_t$ is $\rho_1 c_1 L_w L_t$ mechanical ohms. To convert to electrical practical ohms this has been multiplied by 9×10^{11} and divided by the transformer ratio. Here $\rho_1 c_1$ is the specific acoustic impedance of the medium (water); this tacitly assumes that the crystal under discussion is a member of a large plane

ther below resonance than it does above, and is seriously in error at twice the resonant frequency. Mason's results are shown in Figure 26. The quantities shown have been converted to practical electrical units; Mason expresses them in cgs esu.

In all cases these equivalent circuits represent single crystals. If an array contains n crystals all in parallel and all identical, the circuit of the array is obtained from that of the single crystal by *dividing every impedance by n* .

4.9.3

Parametrization

We now define a set of parameters applicable to all the three basic circuits, and restate the three circuits in those terms.

FREQUENCY

In each case the first resonant frequency occurs when the series equivalent reactance of the mechanical branch vanishes. At this frequency

which any other frequency ω is related to the resonant frequency:

$$\omega = \alpha \omega_R.$$

ELECTRICAL Q

In each case, at resonance, the equivalent circuit reduces to C_0 shunted by the radiation resistance. One might think of this as a "low- Q " condenser. Such a use of the symbol Q is common; the Q is defined as the shunt resistance divided by the shunt reactance. In this sense we define Q_E for a transducer: note that it is not to be regarded as a variable with fre-

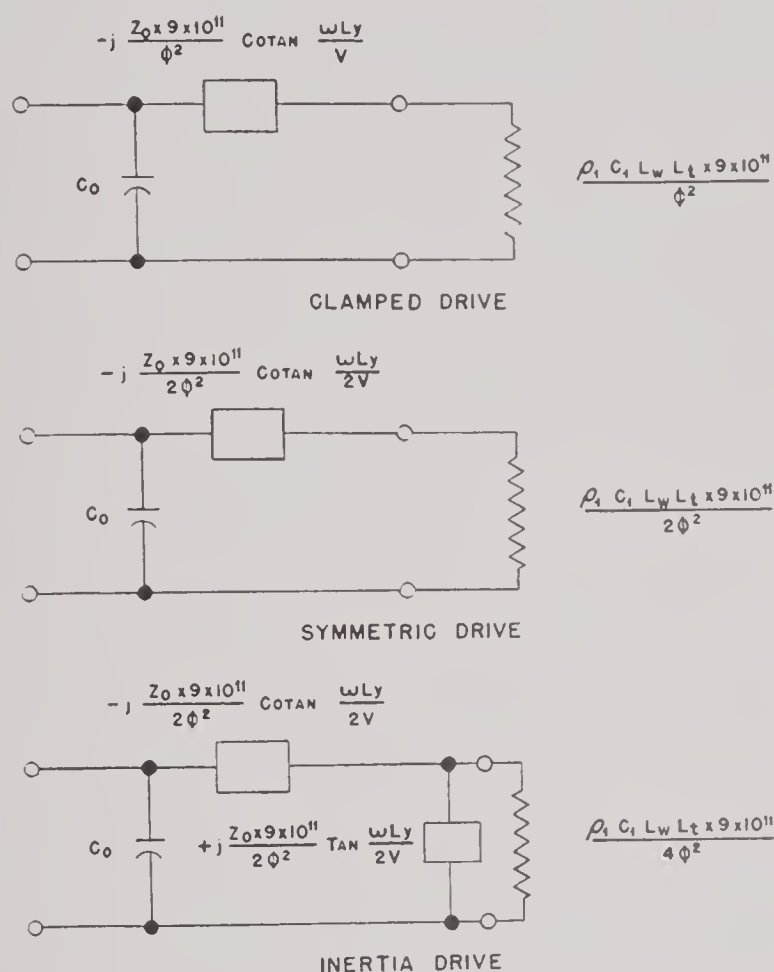


FIGURE 25. Basic equivalent circuits of transducers with transformers removed and with loads included in the circuit.

any voltage applied to the electric terminals is placed across the radiation resistance.

For clamped drive:

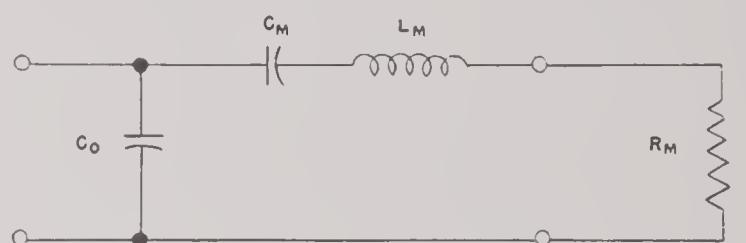
$$\cot \frac{\omega_R L_y}{V} = 0, \quad \omega_R = \frac{\pi V}{2L_y}. \quad (74)$$

For symmetric and inertia drives:

$$\cot \frac{\omega_R L_y}{2V} = 0, \quad \omega_R = \frac{\pi V}{L_y}, \quad (75)$$

where ω_R is the resonant frequency in radians per second.

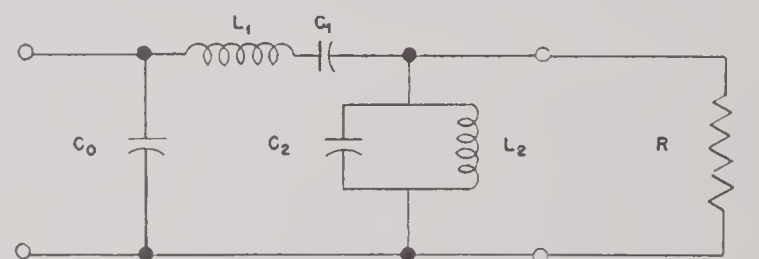
We now define the frequency parameter α by



$$C_0 = \frac{KL_w L_y}{4\pi L_t \times 9 \times 10^{11}} \text{ FARADS}, \quad C_m = \frac{8}{\pi^2} \cdot \left(\frac{k^2}{1-k^2} \right) C_0 \text{ FARADS}$$

$$L_m = \frac{Z_0 L_y}{2V\phi^2} \times 9 \times 10^{11} \text{ HENRIES}, \quad R_m = \frac{\rho_1 C_1 L_w L_t \times 9 \times 10^{11}}{4\phi^2} \text{ OHMS}$$

CLAMPED DRIVE



$$C_0 = \frac{KL_w L_y}{4\pi L_t \times 9 \times 10^{11}} \text{ FARADS}, \quad C_1 = \frac{8}{\pi^2} \cdot \left(\frac{k^2}{1-k^2} \right) C_0 \text{ FARADS}$$

$$L_1 = \frac{Z_0 L_y}{2V\phi^2} \times 9 \times 10^{11} \text{ HENRIES}, \quad R = \frac{\rho_1 C_1 L_w L_t \times 9 \times 10^{11}}{4\phi^2} \text{ OHMS}$$

$$\frac{C_2}{C_1} = \frac{L_1}{L_2} = \left(\frac{\pi}{4} \right)^2$$

INERTIA DRIVE

FIGURE 26. Mason's equivalent circuits for LC approximations to the trigonometric functions and with mechanical units expressed as practical electrical units.

quency, but as a parameter of the circuit, defined only at the resonant frequency. It is customary to ignore the algebraic sign of the reactance, but for our purposes it is necessary

that it be retained; Q_E of any crystal is always a *negative* number.

For clamped drive:

$$Q_E = - \frac{\rho_1 c_1 L_w L_t \times 9 \times 10^{11}}{\phi^2} \cdot \omega_R C_0,$$

substituting for ω_R , ϕ^2 , and C_0 , the values given in Section 4.9.1 and above in Section 4.9.3, this expression reduces to

$$Q_E = - 2\pi^2 \rho_1 c_1 \frac{V}{D^2 K}. \quad (76)$$

For symmetric drive:

$$Q_E = - \frac{\rho_1 c_1 L_w L_t \times 9 \times 10^{11}}{2\phi^2} \cdot \omega_R C_0,$$

which reduces to

$$Q_E = - 2\pi^2 \rho_1 c_1 \frac{V}{D^2 K}. \quad (77)$$

This is identical with clamped drive because, although the resistance is only half as great, the resonant frequency is twice as great and consequently the reactance is only half as great.

For inertia drive:

$$Q_E = - \frac{\rho_1 c_1 L_w L_t \times 9 \times 10^{11}}{4\phi^2} \cdot \omega_R C_0,$$

which reduces to:

$$Q_E = - \pi^2 \rho_1 c_1 \frac{V}{D^2 K}. \quad (78)$$

This is exactly one-half Q_E of clamped and symmetric drive.

Note that the crystal dimensions do not appear in the expression for Q_E ; it is a "crystal constant" whose value depends on the crystal material, the drive, and the water.

MECHANICAL Q

In the clamped and symmetric drives the mechanical branch behaves near resonance like a series LCR circuit as shown in Figure 4. It is customary to speak of the Q of such a circuit. In this usage the phrase has a little different meaning from that used above in the electrical Q . In the series-resonant circuit the Q refers to the resonance and is defined as the inductive reactance at resonance divided by the resistance. However, in this section we do not want the LC

approximation, and must define the mechanical Q_M by an extension of definition as follows.

In a series LCR circuit the Q is defined:

$$Q = \frac{\omega_R L}{R}.$$

The series reactance of this circuit is

$$X = \omega L - \frac{1}{\omega C},$$

and at resonance

$$\omega_R L = \frac{1}{\omega_R C}.$$

Now let us take the slope:

$$\frac{dX}{d\omega} = L + \frac{1}{\omega^2 C},$$

and evaluate it at resonance:

$$\left(\frac{dX}{d\omega} \right)_{\omega=\omega_R} = L + \frac{1}{\omega_R^2 C} = 2L.$$

Substituting this in the expression for Q :

$$Q = \frac{\omega_R}{2R} \left(\frac{dX}{d\omega} \right)_{\omega=\omega_R}. \quad (79)$$

This becomes the definition of Q_M . Like Q_E , it is evaluated at resonance and is a parameter rather than a variable.

For clamped drive the mechanical reactance is

$$- \frac{Z_0 \times 9 \times 10^{11}}{\phi^2} \cot \frac{\omega L_y}{V}.$$

Differentiation by ω generates a $-\csc^2$ which is unity at resonance, so

$$\left(\frac{dX}{d\omega} \right)_{\omega=\omega_R} = \frac{Z_0 \times 9 \times 10^{11}}{\phi^2} \cdot \frac{L_y}{V}.$$

Substituting in the expression for Q :

$$Q_M = \frac{\omega_R \phi^2}{2\rho_1 c_1 L_w L_t \times 9 \times 10^{11}} \cdot \frac{Z_0 \times 9 \times 10^{11} L_y}{\phi^2 V},$$

which may be reduced to

$$Q_M = \frac{\pi}{4} \frac{\rho V}{\rho_1 c_1}. \quad (80)$$

For symmetric drive we go through an analogous process and find that Q_M is identical with that of clamped drive.

Inertia drive presents a more difficult prob-

lem. The presence of the tangent term shunting the radiation resistance complicates the expressions greatly. Upon differentiation one finds that the slope is indeterminate at resonance. Application of L'Hôpital's rule would be tedious and unpromising, so the slope is evaluated at $\omega_R - \epsilon$. The usual approximations are made for small ϵ and then upon passing to the limit one obtains:

$$\left(\frac{dX}{d\omega}\right)_{\omega=\omega_R} = \frac{9 \times 10^{11}}{4\phi^2} \cdot \frac{L_y}{4Z_0V} \left[4Z_0^2 - (\rho_1 c_1 L_w L_t)^2 \right].$$

To evaluate Q_M the series mechanical resistance at resonance is required. The shunting tangent term is therefore infinite so the resistance is just

$$\frac{9 \times 10^{11}}{4\phi^2} \rho_1 c_1 L_w L_t.$$

Substituting in Q_M :

$$\begin{aligned} Q_M &= \frac{\omega_R}{2R} \left(\frac{dX}{d\omega} \right)_{\omega=\omega_R} \\ &= \frac{\pi}{4} \left(\frac{2\rho V}{\rho_1 c_1} - \frac{\rho_1 c_1}{2\rho V} \right). \end{aligned} \quad (81)$$

This expression has an interesting form. The first term is just twice Q_M of clamped or symmetric drive crystals. The second term arises because of the shunting tangent branch; since this branch is infinite at resonance it is not comparable with the radiation resistance (at least for Y-cut RS or Z-cut ADP in water) anywhere near resonance. If one omitted the tangent branch the second term in Q_M would disappear and the value would be exactly twice that of clamped or symmetric. For 45° Y-cut RS or 45° Z-cut ADP the resulting error is negligible (about 3 per cent) but this approximation has not been made in the following sections.

Notice that Q_M , like Q_E is a crystal constant, dependent upon the crystal material, the radiation medium (water), and the type of drive, but not upon dimensions.

Since the behavior with frequency is governed entirely by Q_E and Q_M we see that all transducers containing a given kind of crystal in a given drive condition must be pretty much alike. The resonant frequencies may differ, but in octave measure this difference is removed, and the remaining differences are those of size alone. Of course this is a first approximation;

we may expect various transducers to differ because of second-order effects or because of reduced efficiency. Examination will show that the behavior is a rather slow function of the extent to which the crystals are fully loaded, and not much difference is likely to come from this cause except through consequent changes of efficiency. The reason for this is that the $Q_E Q_M$ product is the dominating term in calculating responses, and this product is independent of $Q_1 c_1$:

$$\begin{aligned} Q_E Q_M &= -\frac{\pi^3}{2} \cdot \frac{\rho V^2}{D^2 K} \\ &= -\frac{\pi^2}{8} \left(\frac{1 - k^2}{k^2} \right). \end{aligned} \quad (82)$$

Note that this product is the same as the ratio of capacities discussed by Mason^{1c} and clearly indicates the fact that the achievable band width for any crystal depends wholly on k . It is remarkable that k for 45° Y-cut RS and 45° Z-cut ADP differ by only a few per cent; these crystals differ negligibly in achievable band width. At present there appears to be no hope for crystal transducers having broader band width except by the discovery of an otherwise suitable crystal having larger k . For example present band widths could be trebled by a material whose k equals 0.5 instead of 0.3.

RESISTANCE

We now define the last parameter R as being equal to the radiation resistance. For generality we use the circuit for n crystals in parallel.

For clamped drive:

$$R = \frac{\rho_1 c_1 L_w L_t \times 9 \times 10^{11}}{n\phi^2}.$$

For symmetric drive:

$$R = \frac{\rho_1 c_1 L_w L_t \times 9 \times 10^{11}}{2n\phi^2}. \quad (83)$$

For inertia drive:

$$R = \frac{\rho_1 c_1 L_w L_t \times 9 \times 10^{11}}{4n\phi^2}. \quad (84)$$

4.9.4

Impedance

In Section 4.9.3 it was shown that the two Q 's are crystal constants; from this we concluded

that transducers containing the same crystals and drive may differ in magnitude, but not in the *shape* of their behavior with frequency. If so, we can obtain the complex impedance in parametric form so that a constant coefficient represents the size dependence and all the frequency dependence is contained in an expression identical for all transducers with the same crystals and drive.

For several reasons R is a suitable quantity to act as the size-dependent coefficient; we seek an expression of the form

$$Z = R(k_1 + jk_2). \quad (85)$$

Here k_1 and k_2 will be functions of Q_E , Q_M , and α , but not of the number or size of the crystals. Then k_1 and k_2 may be calculated as functions of α for each kind of crystal in all three drives and the result allows the determination of the impedance of any transducer by simply evaluating R , a moment's work.

The task is simplified by the fact that Q_E and Q_M are identical for symmetric and clamped drive. Henceforth they are lumped together, and symmetric drive is always represented by

2. For clamped drive,

$$\frac{\omega L_y}{V} = \frac{\alpha\pi}{2},$$

$$\frac{Z_0 \times 9 \times 10^{11}}{n\phi} = \frac{4}{\pi} R Q_M.$$

3. For inertia drive,

$$\frac{\omega L_y}{2V} = \alpha \frac{\pi}{2},$$

$$\frac{Z_0 \times 9 \times 10^{11}}{2n\phi^2} = R \left[\frac{2Q_M}{\pi} + \sqrt{\left(\frac{2Q_M}{\pi} \right)^2 + 1} \right].$$

Upon simplification it is found that R factors out of the expression for Z , leaving a complex number whose two components are the k_1 and k_2 sought. These are:

For clamped drive

$$k_1 = \frac{1}{\alpha^2 Q_E^2 + \left(1 - \frac{4}{\pi} \alpha Q_E Q_M \cot \frac{\alpha\pi}{2} \right)^2}, \quad (86)$$

$$\frac{k_2}{k_1} = \alpha Q_E - \frac{4}{\pi} Q_M \cot \frac{\alpha\pi}{2} \left(1 - \frac{4}{\pi} \alpha Q_E Q_M \cot \frac{\alpha\pi}{2} \right). \quad (87)$$

For inertia drive:¹

$$k_1 = \frac{1}{\alpha^2 Q_E^2} \left[1 + 4M^2 \tan^2 \frac{\alpha\pi}{2} \right] \cdot \left\{ 4M^2 \tan^2 \frac{\alpha\pi}{2} + \left[\frac{\cot \frac{\alpha\pi}{2}}{2\alpha M Q_E} - \frac{2 \cot \frac{\alpha\pi}{2}}{\tan \frac{\alpha\pi}{2}} + \frac{2M \tan \frac{\alpha\pi}{2}}{\alpha Q_E} - 4M^2 \right]^2 \right\}^{-1}, \quad (88)$$

$$\frac{k_2}{k_1} = \frac{4\alpha Q_E \cot^2(\alpha\pi) - \frac{\cot(\alpha\pi)}{M} - 2M \tan\left(\frac{\alpha\pi}{2}\right) + 4\alpha M^2 Q_E}{\tan^2\left(\frac{\alpha\pi}{2}\right)}. \quad (89)$$

clamped drive. In use however, symmetric drive requires its own value of R .

To obtain expressions for k_1 and k_2 requires much algebraic tedium not warranted here. In outline the method is: First obtain the expression for the complex impedance seen looking in at the electric terminals. In this substitute the following expressions derived from the definitions of Q_E and Q_M :

1. Both clamped and inertia drive,

$$-\frac{1}{n\omega C_0} = \frac{R}{\alpha Q_E}.$$

These quantities are among those plotted as functions of α in Section 4.9.8.

4.9.5

Transmitter Responses

Having obtained k_1 and k_2 it is easy to calculate the power expended in the transducer for any selected method of operation. Since the equivalent circuit used assumes the transducer

¹ For simplicity we define $M = \frac{cV}{Q_1 c_1}$. For 45° Y-cut RS, $M = 2.78$. For 45° Z-cut ADP, $M = 3.89$.

to be perfectly efficient this is the power radiated into the water. It is not possible to go on to give the acoustic pressure versus frequency unless the directivity index is known as a function of frequency. This is discussed in earlier sections; here we stop with the power versus frequency, bearing in mind that for ordinary transducers the *shape* of the pressure response versus frequency will differ from the power curve only by a slope of 3 to 6 db per octave.

CONSTANT VOLTAGE WITHOUT COILS

Transmitter calibrations of many transducers are reported as constant-voltage response without tuning coils (see Section 4.6), so that the power expended in the transducer with E volts applied is of interest. This is simply

$$P = \frac{E^2}{R} \left(\frac{k_1}{k_1^2 + k_2^2} \right) \text{ watts.} \quad (90)$$

The factor

$$\frac{k_1}{k_1^2 + k_2^2}$$

is plotted against α in Section 4.9.8.

CONSTANT VOLTAGE WITH COILS

Some transducers have series tuning coils built into them. If coils are chosen to cancel the reactance at any frequency other than resonance the resulting response is so sharp that the transducer is virtually useless. For this reason we assume that the reactance is cancelled at $\alpha = 1$. At $\alpha = 1$ the reactance of the transducer is $(Rk_2)_{\alpha=1}$ so the reactance of the coil must be $-(Rk_2)_{\alpha=1}$. For simplicity we assume the coil to be lossless. Then the impedance of the transducer plus coil is

$$R [k_1 + j(k_2 - \alpha(k_2)_{\alpha=1})].$$

When E volts are applied to the electric terminals the power expended is

$$P = \frac{E^2}{R} \cdot \frac{k_1}{k_1^2 + [k_2 - \alpha(k_2)_{\alpha=1}]^2}. \quad (91)$$

The factor containing k 's is plotted against α in Section 4.9.8.

IDEALIZED AMPLIFIER

The available power response discussed in Section 4.6 has the advantage that it most nearly portrays the response to be expected when the transducer is driven by a real amplifier. The most useful curves are based on an idealized amplifier whose impedance is a conjugate match to the transducer at resonance. In Figure H the minus sign on the coil reactance

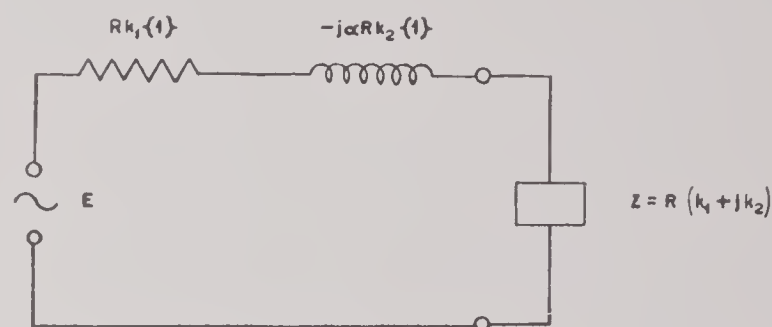


FIGURE H.

is necessary since k_2 is a negative number for any crystal whose reactance is capacitive at resonance.

The power expended in the transducer when driven in this manner is

$$P = \frac{E^2}{R} \cdot \frac{k_1}{[k_1 + (k_1)_{\alpha=1}]^2 + [k_2 - \alpha(k_2)_{\alpha=1}]^2} \quad (92)$$

The factor containing the k 's is plotted in Section 4.9.8.

Note carefully the similarity of this function for both Y-cut RS and Z-cut ADP, operated clamped (symmetric) or inertia. Although the other curves often look very different, this function which portrays the response obtained in service is virtually identical for all six combinations of crystal and drive. This is a consequence of the dependence of the $Q_E Q_M$ product on k alone and of the fact that k is 0.3 for both crystals.

CONSTANT CURRENT

The power expended in the transducer when a constant current of 1 amp is maintained is just Rk_1 . Since k_1 is plotted in Section 4.9.8 for impedance, no constant-current response curve is shown.

4.9.6

Receiver Responses

The short-circuit current receiver response reciprocates with the constant-voltage transmitter response and may be obtained in that way. Similarly the open-circuit receiver voltage reciprocates with the constant-current transmitter response and may be obtained from Rk_1 . Since the reciprocity merely introduces a slope of 6 db per octave, the receiver responses are not plotted in Section 4.9.8.

4.9.7

Miscellaneous

One or two other quantities of interest may be obtained from the equivalent circuit. Although some are best obtained without use of the parameters, they are given here to complete the section.

INTENSITY

Because of the limitations imposed on crystals by cavitation and voltage breakdown (see Section 4.8) it is important to have some estimate of the intensity radiated from the crystal faces at resonance when a given voltage is applied. Unfortunately the highest point intensity depends upon the details of how the radiation load is imposed on each crystal face. However it is useful to have available the intensity which the Mason circuit predicts for crystals fully and uniformly loaded by the medium. For this we return to the equivalent circuits of Figure 3.

In each case, C_0 plays no role. Furthermore, at resonance all the cotangent terms go to zero so the full voltage E is placed across the radiation resistance. If the power expended is divided by the radiating area we obtain the intensity of the radiation leaving the face in watts per sq cm. The results are:

1. Clamped drive,

$$\text{Intensity} = \left(\frac{E}{L_t} \right)^2 \left(\frac{D^2 K^2}{144 \pi^2 \rho_1 c_1 \times 10^{11}} \right). \quad (93)$$

2. Symmetric drive,

$$\text{Intensity} = \left(\frac{E}{L_t} \right)^2 \left(\frac{D^2 K^2}{144 \pi^2 \rho_1 c_1 \times 10^{11}} \right). \quad (94)$$

3. Inertia drive,

$$\text{Intensity} = \left(\frac{E}{L_t} \right)^2 \left(\frac{D^2 K^2}{36 \pi^2 \rho_1 c_1 \times 10^{11}} \right). \quad (95)$$

The values of clamped and symmetric drive are the same because, although symmetric drive radiates twice as much power at a given voltage gradient, it does so from twice as great area (both ends of the crystal). The intensity radiated by inertia drive is four times that of clamped drive and thus offers a distinct advantage in situations where voltage breakdown may impose a limitation.

Obviously the intensity is proportional to the square of the voltage *gradient*, as indicated.

PEAK OPEN-CIRCUIT VOLTAGE

The effect on the equivalent circuit of an incident plane acoustic wave is to insert in series with the radiation resistance a zero-impedance voltage equal to the force exerted on the crystal. If the free-field acoustic pressure is p dynes per sq cm it is not known, in general, what this force is. For an infinite plane array the force would be $2pL_w L_t$ dynes (see Section 4.4.2) and that approximation will be used. In accordance with this we also assume the crystal to be fully loaded by the radiation medium.

In order to express this receiver voltage in practical units it must be multiplied by 300 and divided by ϕ .

At resonance the cotangent terms go to zero and the tangent term to infinity so the equivalent circuits become those shown in Figure 27. Symmetric drive is not included because in no practical case is it known how to treat the pressure imposed on the "back" end of the crystal.

In each case the voltage is divided between C_0 and the radiation resistance, and the observed open-circuit voltage is that which occurs across C_0 .

The algebra is straightforward; the result is:

Peak open-circuit voltage

$$= \left(\frac{2400\pi}{DK \sqrt{Q_E^2 + 1}} \right) p L_t. \quad (96)$$

In obtaining this it was assumed that the maximum occurs at resonance. This is not exactly true; the analysis to determine the frequency at which it does occur is extremely tedious, and the true frequency is quite close to resonance. Furthermore the true peak voltage differs little from that at resonance.

Note that the peak voltage depends only on

the crystal thickness, not on the width, length, number, or arrangement. For this reason this is a very convenient measure of transducer behavior.

PEAK SHORT-CIRCUIT CURRENT

Using the same equivalent circuits (Figure 27) we may calculate the peak short-circuit cur-

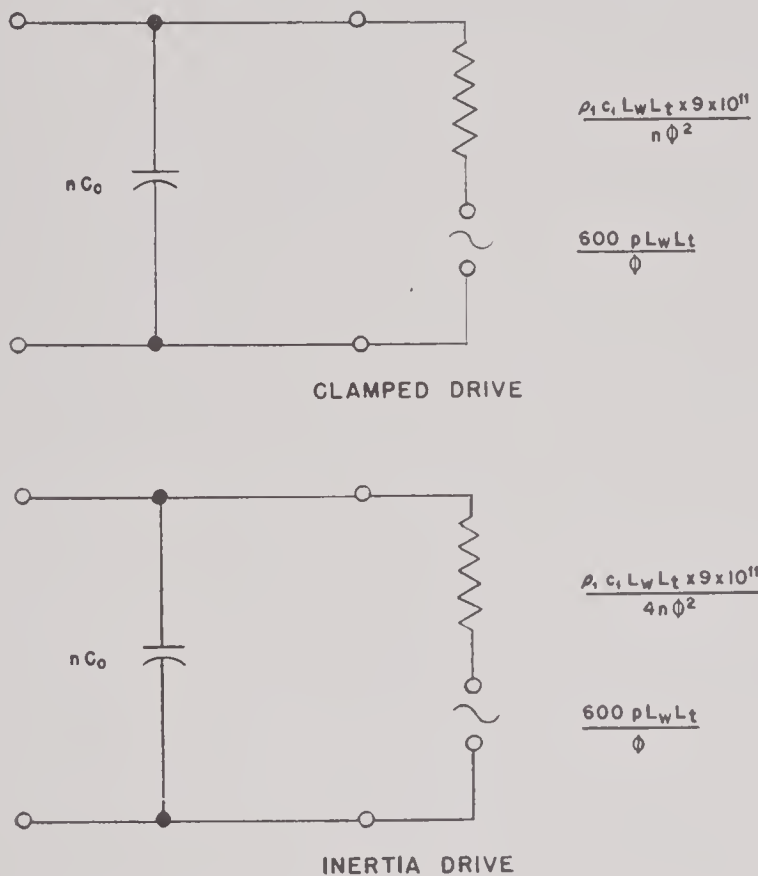


FIGURE 27. Equivalent circuits of transducers operated as receivers at resonance.

rent as a receiver for incident free field pressure p dynes per sq cm.

When the electric terminals are shorted C_0 drops out of the picture; at resonance the series mechanical reactance vanishes, and the shunting reactance of inertia drive is infinite. The radiation resistance alone remains, and the maximum short-circuit current is:

Clamped drive,

$$\left(\frac{DK}{6\pi\rho_1 c_1 \times 10^9} \right) pnL_w \text{ amperes.} \quad (97)$$

Inertia drive,

$$\left(\frac{DK}{1.5\pi\rho_1 c_1 \times 10^9} \right) pnL_w \text{ amperes.} \quad (98)$$

Note that, contrary to open-circuit voltage, the peak short-circuit current is independent of

the thickness of the crystals, and depends on nL_w . For this reason it is not so convenient for comparing transducers.

ABSOLUTE MAGNITUDE OF IMPEDANCE

In matching transducers to amplifiers it is important to have available the theoretical value of the absolute magnitude of the impedance. Since transducers are usually used with series tuning coils which cancel the reactance at the transducer's resonance, such coils will be included in the calculation.

The impedance of the transducer plus coils is

$$Z = R \{ k_1 + j[k_2 - \alpha(k_2)_{\alpha=1}] \},$$

hence,

$$|Z| = R \sqrt{k_1^2 + [k_2 - \alpha(k_2)_{\alpha=1}]^2}. \quad (99)$$

This quantity is plotted as a function of α in Section 4.9.8.

POWER FACTOR

When matching an amplifier to a transducer the power factor is required as well as $|Z|$. As above, we compute the power factor with series tuning coils which cancel the reactance at the transducer's resonance:

$$PF = \cos \phi,$$

$$\phi = \tan^{-1} \left(\frac{k_2 - \alpha(k_2)_{\alpha=1}}{k_1} \right).$$

Thus,

$$PF = \frac{k_1}{\sqrt{k_1^2 + [k_2 - \alpha(k_2)_{\alpha=1}]^2}}. \quad (100)$$

This quantity is plotted as a function of α in Section 4.9.8.

4.9.8

Numerical Values

In this section numerical values of these constants are tabulated for 45° Y-cut RS and 45° Z-cut ADP. Functions of α are plotted in the range $0.6 \leq \alpha \leq 1.6$; the curves may be read to the greatest justifiable accuracy. In all cases the numerical values are obtained from constants given by Mason. In some instances these constants were preliminary values, since

changed by a few per cent, e.g., $(1 - k^2)Y_0$ for Z-cut ADP is now taken to be 19.5×10^{10} , but the curves have not been brought up to date. The constants used in these calculations are:

	45°Y-Cut RS	45°Z-Cut ADP
D	11.2×10^4	12.2×10^4
K	10.0	14.2
Y_0	10.8×10^{10}
$(1 - k^2)Y_0$	18.9×10^{10}
q	1.775	1.80
k	0.305

(The difference in use of k arises from the manner in which these numbers were first reported to UCDWR; there is some doubt of the exact value of k for ADP but it is close to 0.30.)

From these values the following quantities may be calculated, using the definitions given in earlier sections of Section 4.9. Any quantity dependent on q_1c_1 is given for water as the radiation medium ($q_1c_1 = 1.5 \times 10^5$).

	45°Y-Cut RS	45°Z-Cut ADP
V	2.35×10^5	3.24×10^5
Z_0	$4.17 \times 10^5 L_w L_t$	$5.83 \times 10^5 L_w L_t$
ϕ	$-8.91 \times 10^4 L_w$	$-13.8 \times 10^4 L_w$
Q_E clamped	-5.55	-4.54
Q_E symmetric	-5.55	-4.54
Q_E inertia	-2.78	-2.27
Q_M clamped	2.18	3.05
Q_M symmetric	2.18	3.05
Q_M inertia	4.25	6.01
$Q_E Q_M$ clamped	-12.1	-13.8
$Q_E Q_M$ symmetric	-12.1	-13.8
$Q_E Q_M$ inertia	-11.8	-13.6
R clamped	$17.0 \times \frac{10^6 L_t}{n L_w}$	$7.14 \times \frac{10^6 L_t}{n L_w}$
R symmetric	$8.50 \times \frac{10^6 L_t}{n L_w}$	$3.57 \times \frac{10^6 L_t}{n L_w}$
R inertia	$4.25 \times \frac{10^6 L_t}{n L_w}$	$1.79 \times \frac{10^6 L_t}{n L_w}$
Maximum intensity (resonance)		
Clamped	$5.87 \times 10^{-8} \left(\frac{E}{L_t}\right)^2$	$14.0 \times 10^{-8} \left(\frac{E}{L_t}\right)^2$
Symmetric	$5.87 \times 10^{-8} \left(\frac{E}{L_t}\right)^2$	$14.0 \times 10^{-8} \left(\frac{E}{L_t}\right)^2$
Inertia	$23.5 \times 10^{-8} \left(\frac{E}{L_t}\right)^2$	$56.0 \times 10^{-8} \left(\frac{E}{L_t}\right)^2$
Maximum open-circuit voltage (resonance) (rms)		
Clamped	$1.18 \times 10^{-3} p L_t$	$0.938 \times 10^{-3} p L_t$
Inertia	$2.41 \times 10^{-3} p L_t$	$1.90 \times 10^{-3} p L_t$
Maximum short-circuit current (resonance) (rms)		
Clamped	$3.96 \times 10^{-14} p n L_w$	$6.12 \times 10^{-14} p n L_w$
Inertia	$15.8 \times 10^{-14} p n L_w$	$24.5 \times 10^{-14} p n L_w$

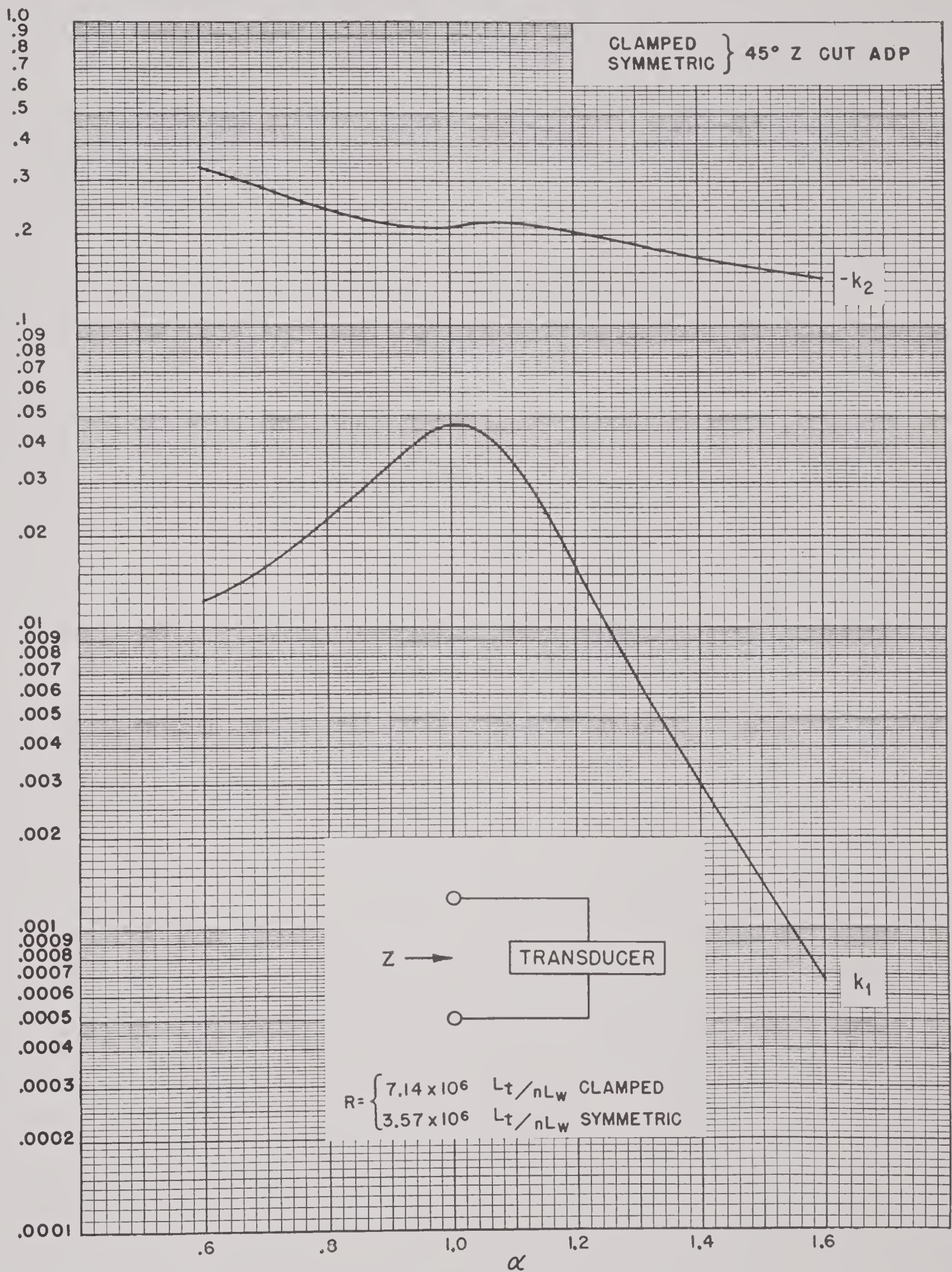


FIGURE 28. k_1 and k_2 as a function of α for clamped or symmetrically driven Z-cut ADP transducers. $Z = R(k_1 + jk_2)$.

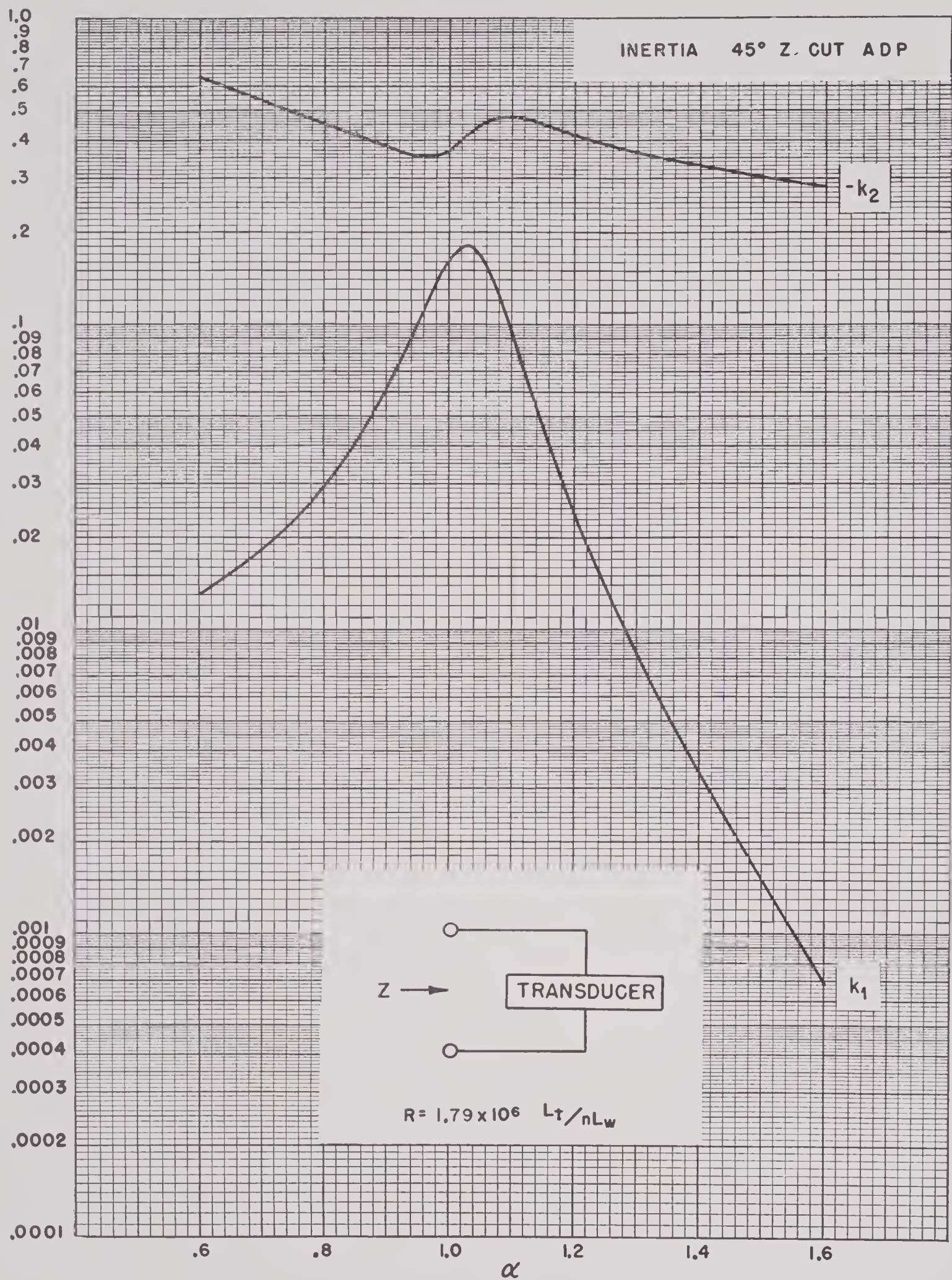


FIGURE 29. k_1 and k_2 as a function of α for inertia driven Z-cut ADP transducers. $Z = R(k_1 + jk_2)$.

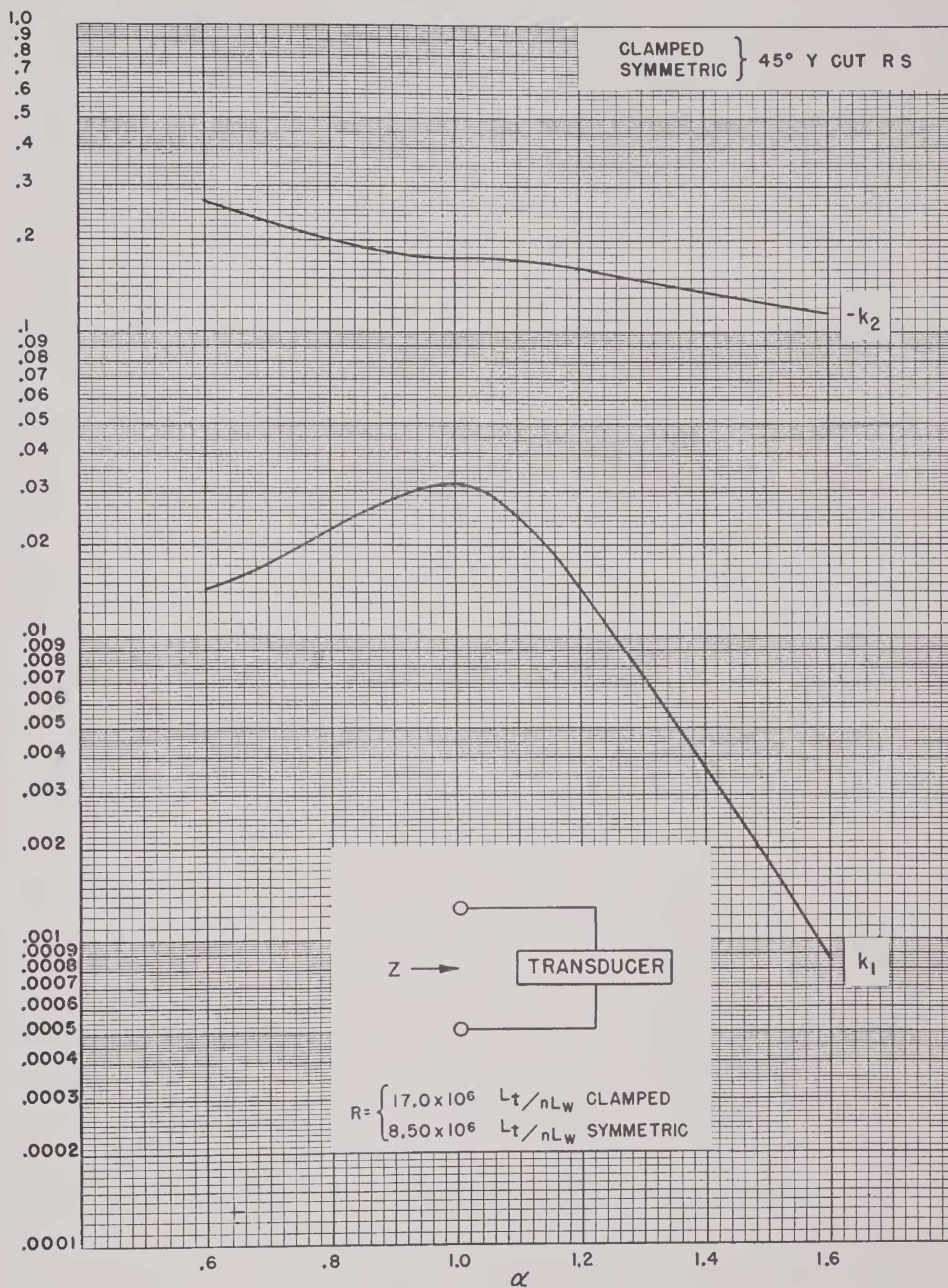


FIGURE 30. k_1 and k_2 as a function of α for clamped or symmetrically driven Y-cut Rochelle salt transducers. $Z = R(k_1 + jk_2)$.

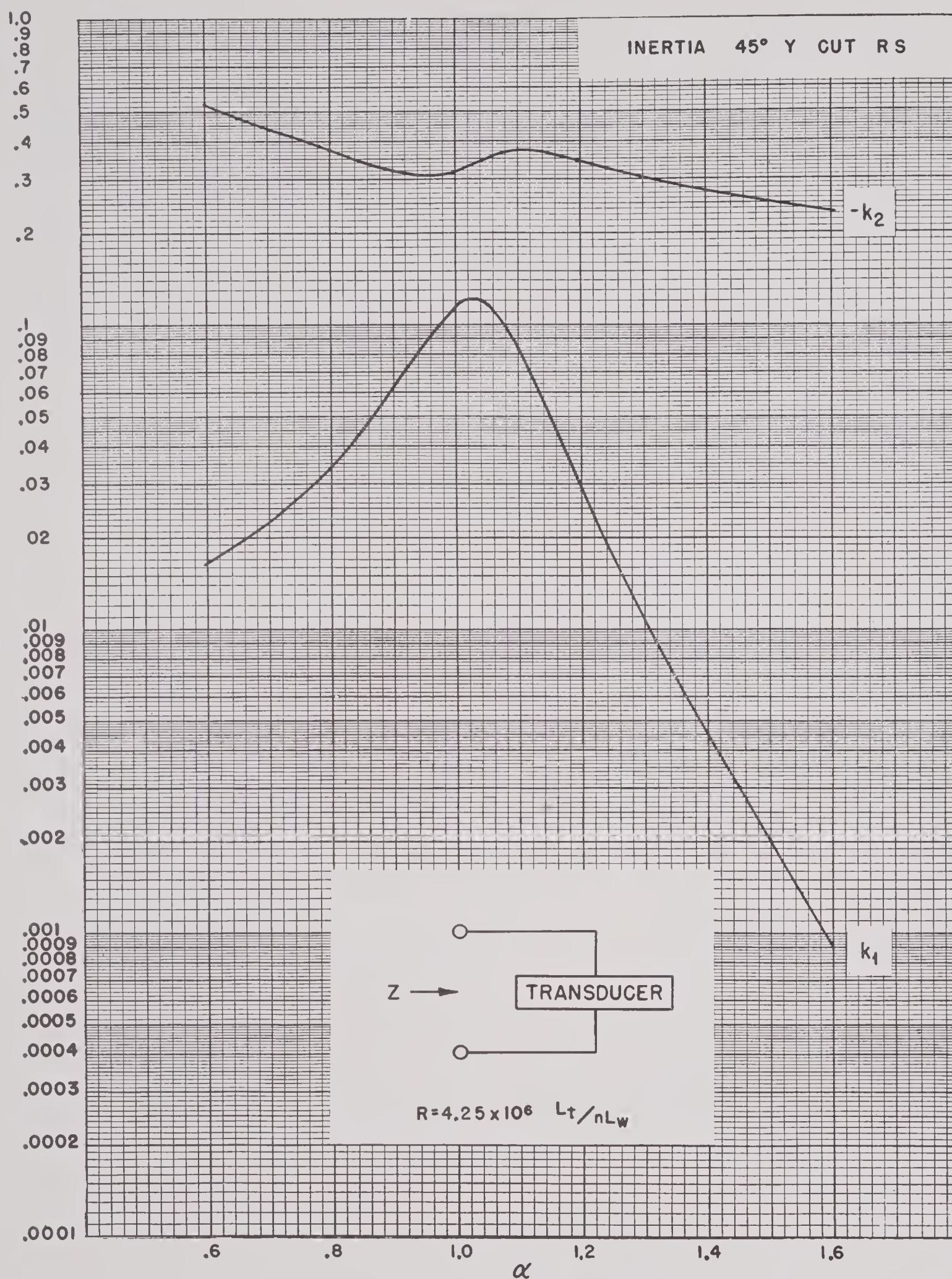


FIGURE 31. k_1 and k_2 as a function of α for inertia driven Y-cut Rochelle salt transducers. $Z = R(k_1 + jk_2)$.

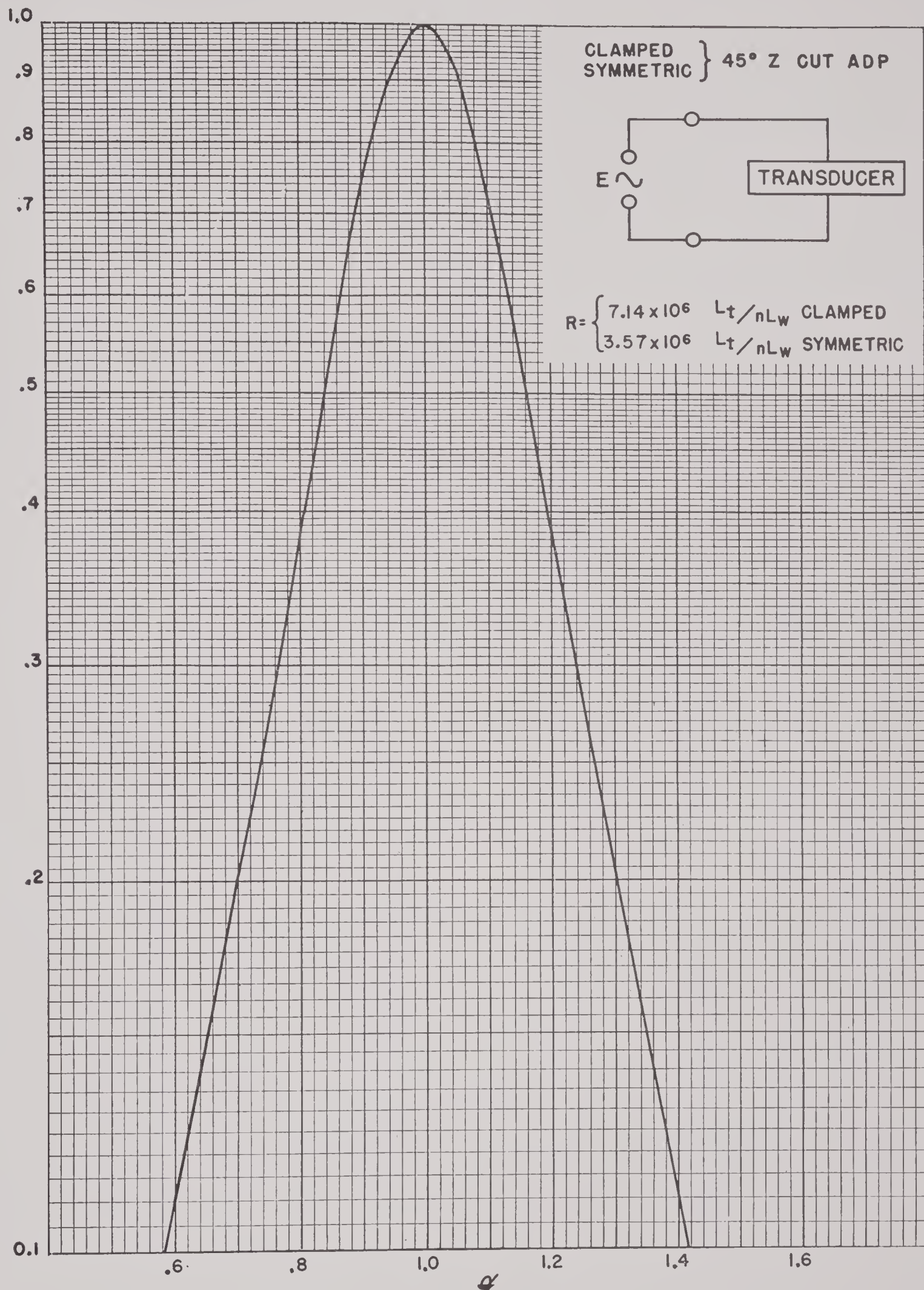


FIGURE 32. The quantity $k_1/k_1^2 + k_2^2$ plotted against α in clamped or symmetrically driven Z-cut ADP transducers with constant voltage applied and without tuning coils. The ordinates of this curve when multiplied by E^2/R give the power expended in the transducer.

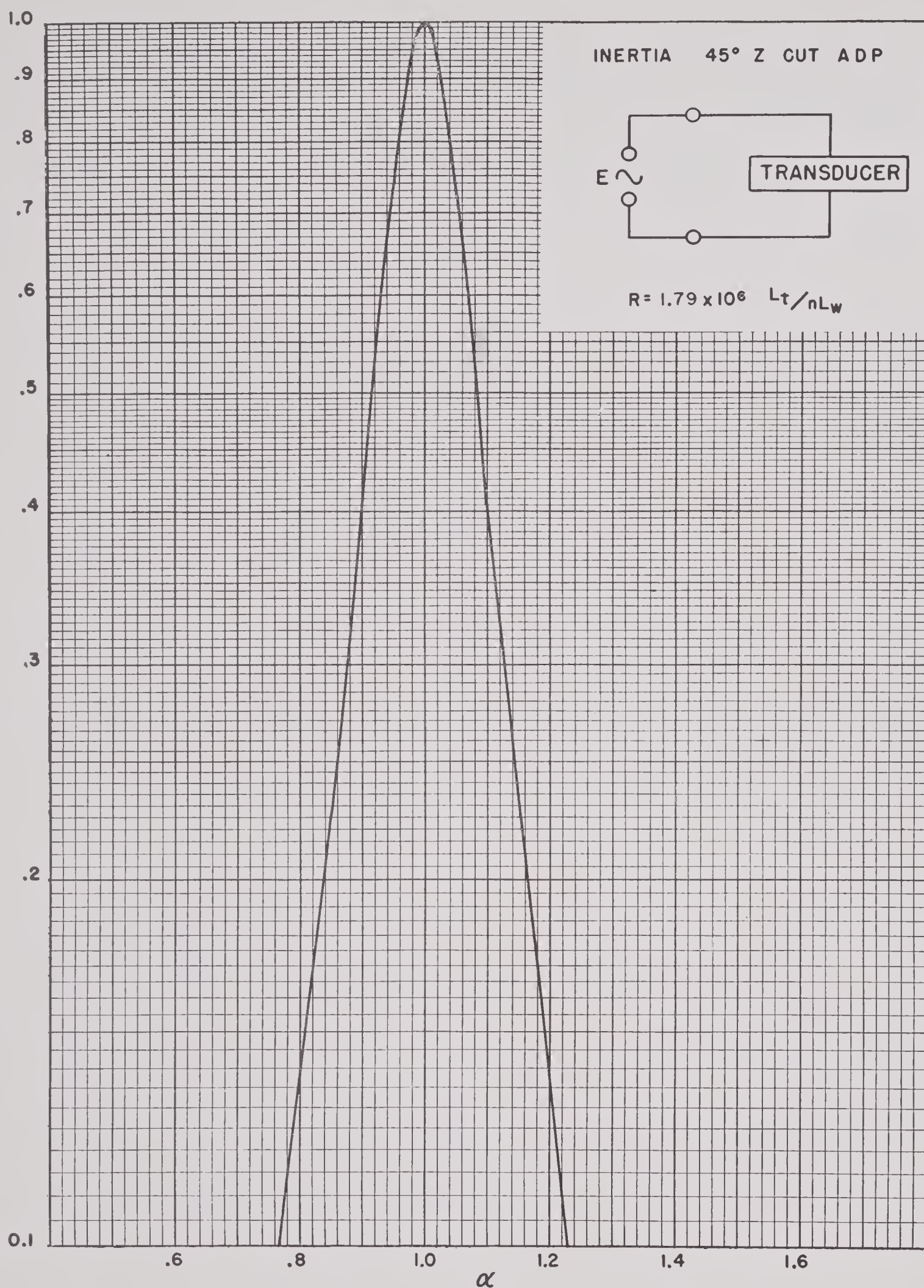


FIGURE 33. The quantity $k_1/k_1^2 + k_2^2$ plotted against α in inertia driven Z-cut ADP transducers with constant voltage applied and without tuning coils. The ordinates of this curve when multiplied by E^2/R give the power expended in the transducer.

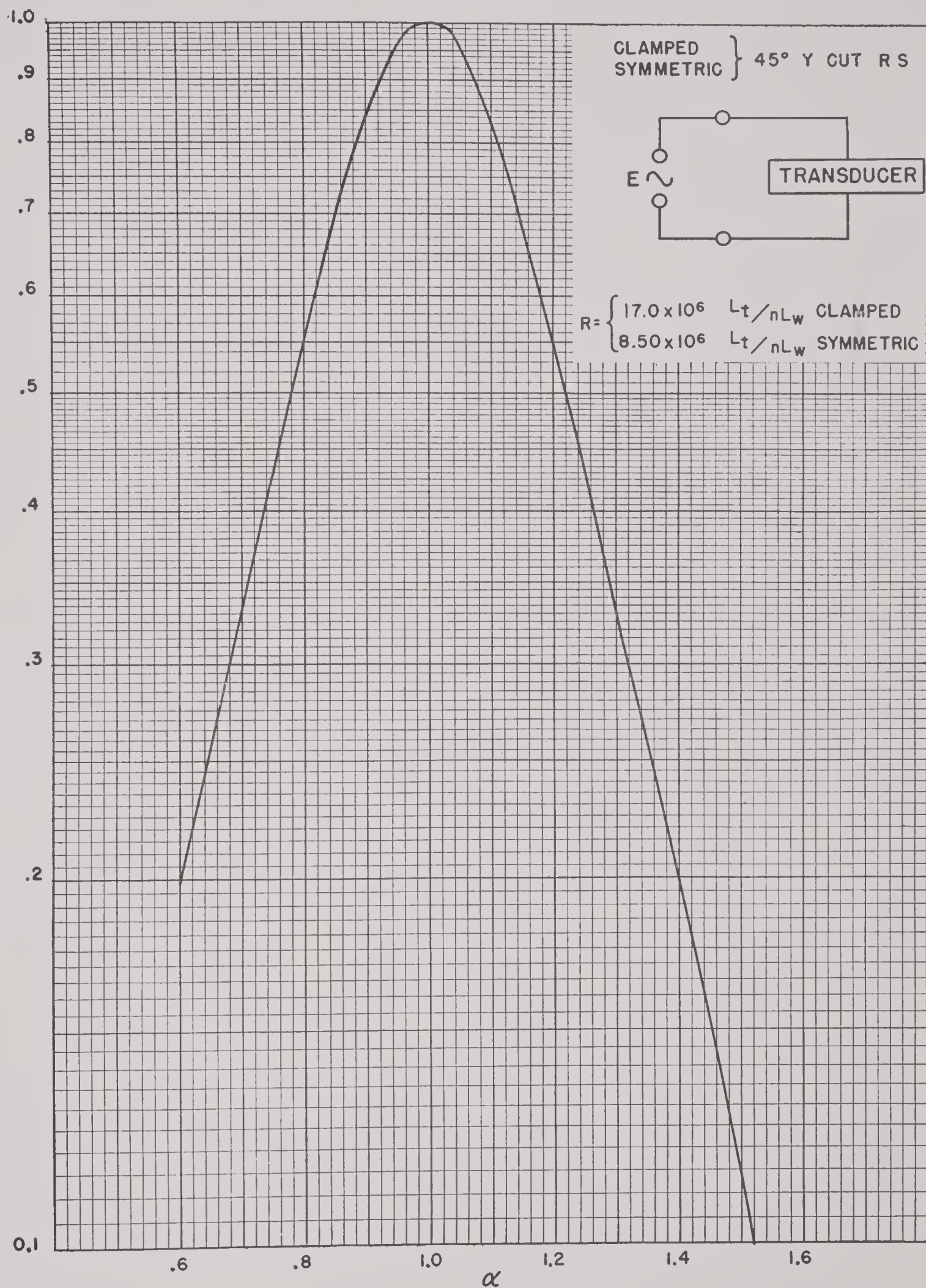


FIGURE 34. The quantity $k_1/k_1^2 + k_2^2$ plotted against α in clamped or symmetrically driven Y-cut Rochelle salt transducers with constant voltage applied and without tuning coils. The ordinates of this curve when multiplied by E^2/R give the power expended in the transducer.

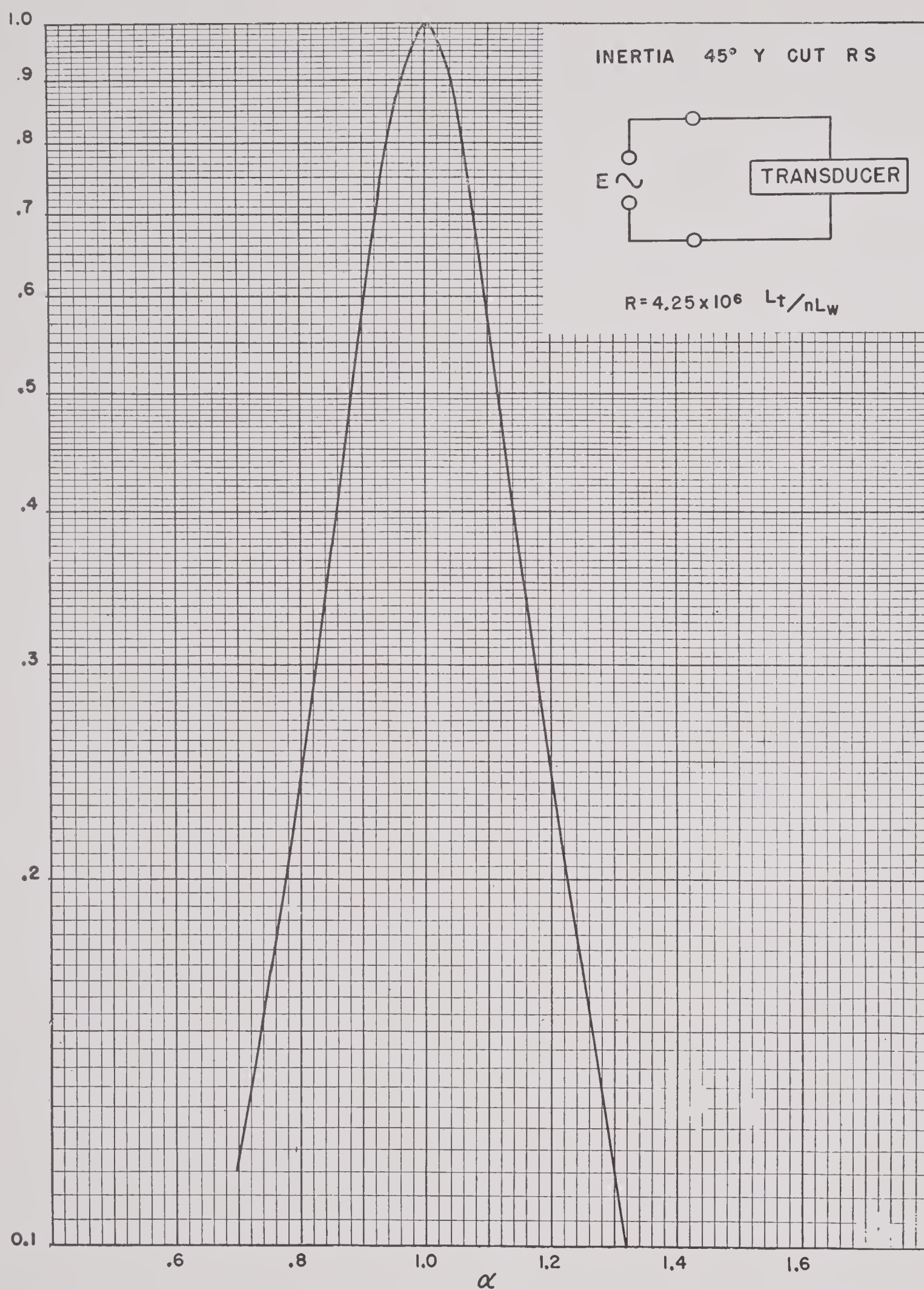


FIGURE 35. The quantity $k_1/k_1^2 + k_2^2$ plotted against α in inertia driven Y-cut Rochelle salt transducers with constant voltage applied and without tuning voils. The ordinates of this curve when multiplied by E^2/R give the power expended in the transducer.

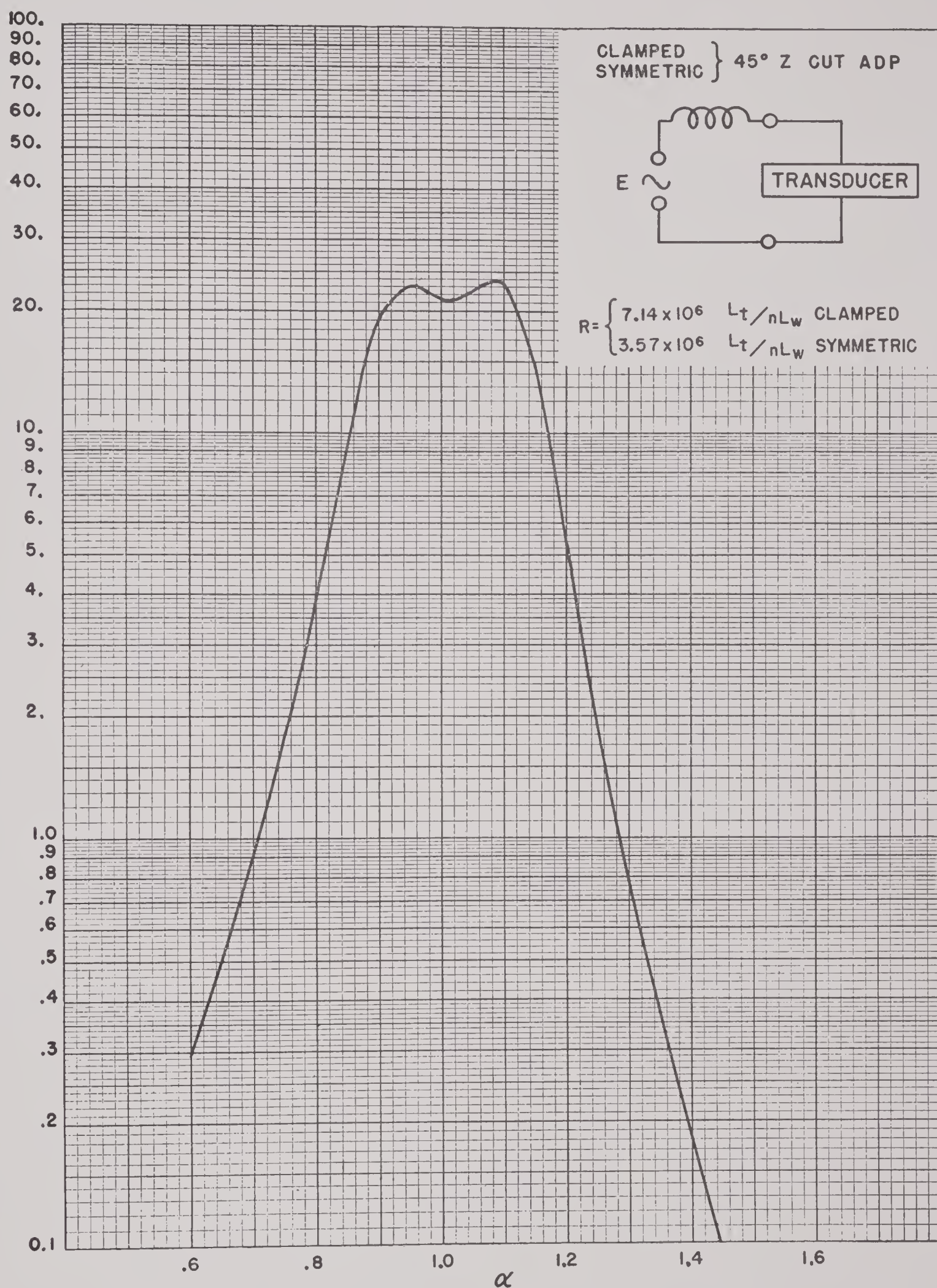


FIGURE 36. The quantity $k_1/k_1^2 + [k_2 - \alpha(k_2)_{\alpha=1}]^2$ plotted against α in clamped or symmetrically driven Z-cut ADP transducers with constant voltage applied and with lossless series tuning coil. The ordinates of this curve when multiplied by E^2/R give the power expended in the transducer.

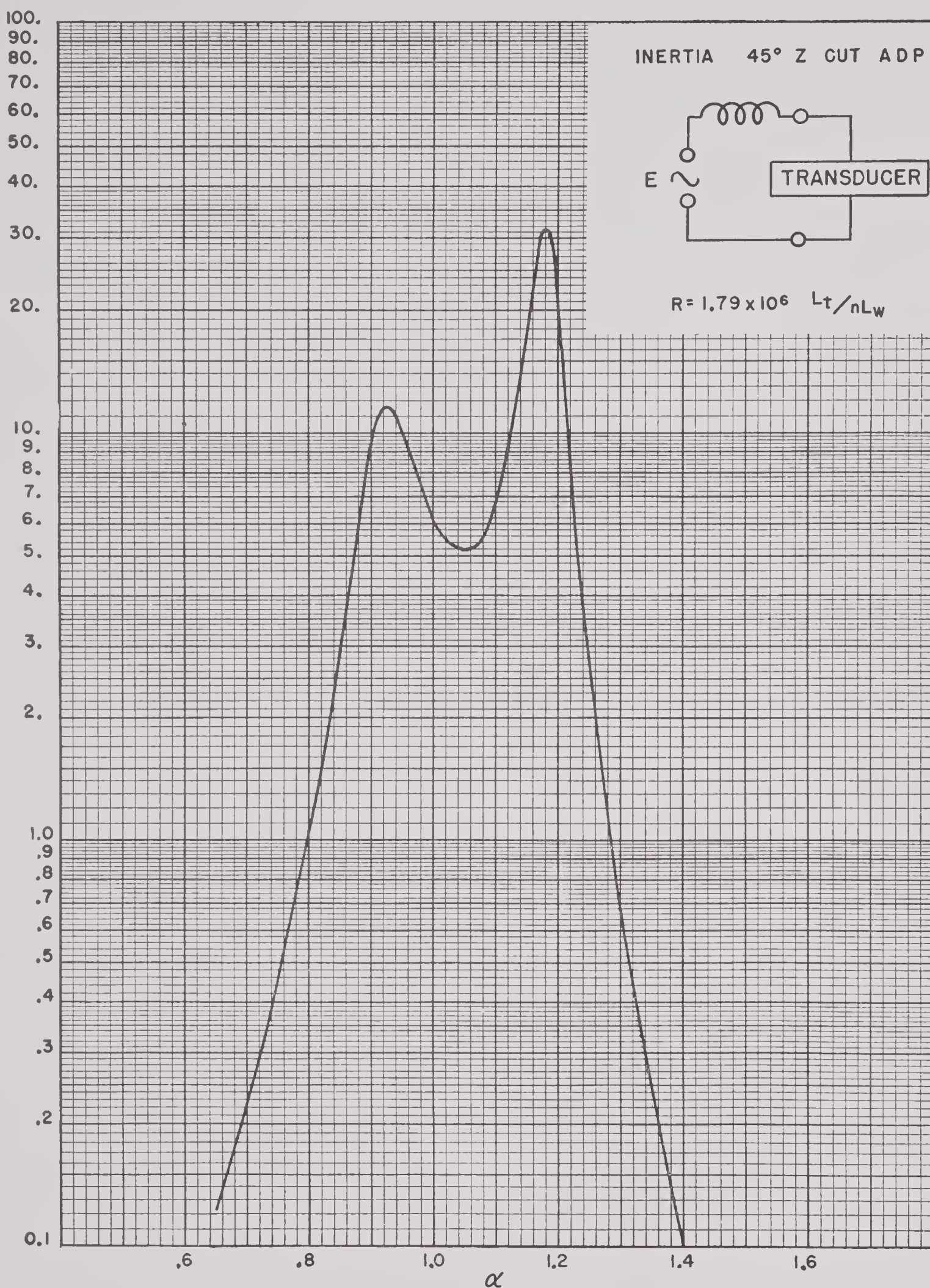


FIGURE 37. The quantity $k_1/k_1^2 + [k_2 - \alpha(k_2)_{\alpha=1}]^2$ plotted against α in inertia driven Z-cut ADP transducers with constant voltage applied and with lossless series tuning coil. The ordinates of this curve when multiplied by E^2/R give the power expended in the transducer.

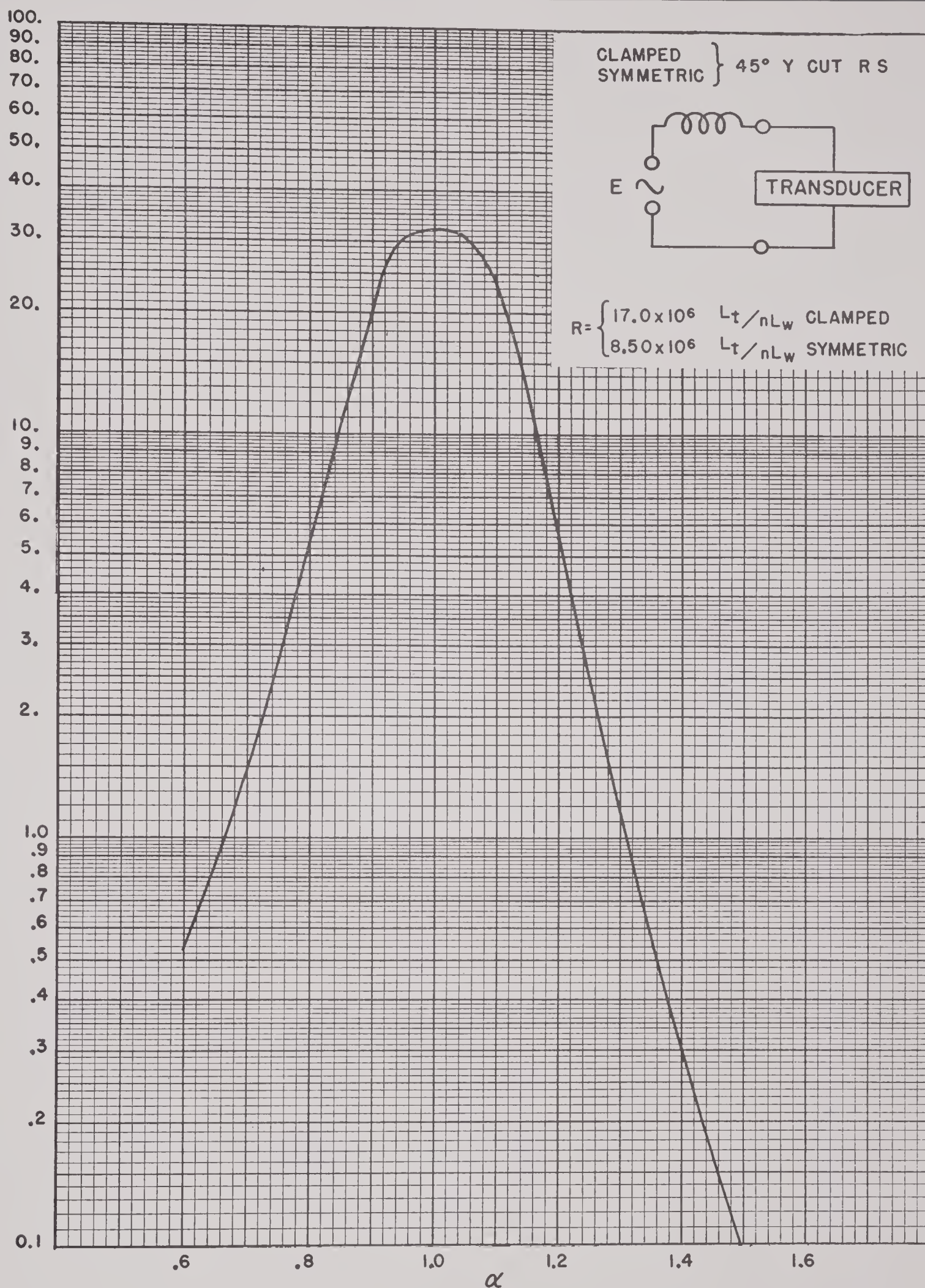


FIGURE 38. The quantity $k_1/k_1^2 + [k_2 - \alpha(k_2)_{\alpha=1}]^2$ plotted against α in clamped or symmetrically driven Y-cut Rochelle salt transducers with constant voltage applied and with lossless series tuning coil. The ordinates of this curve when multiplied by E^2/R give the power expended in the transducer.

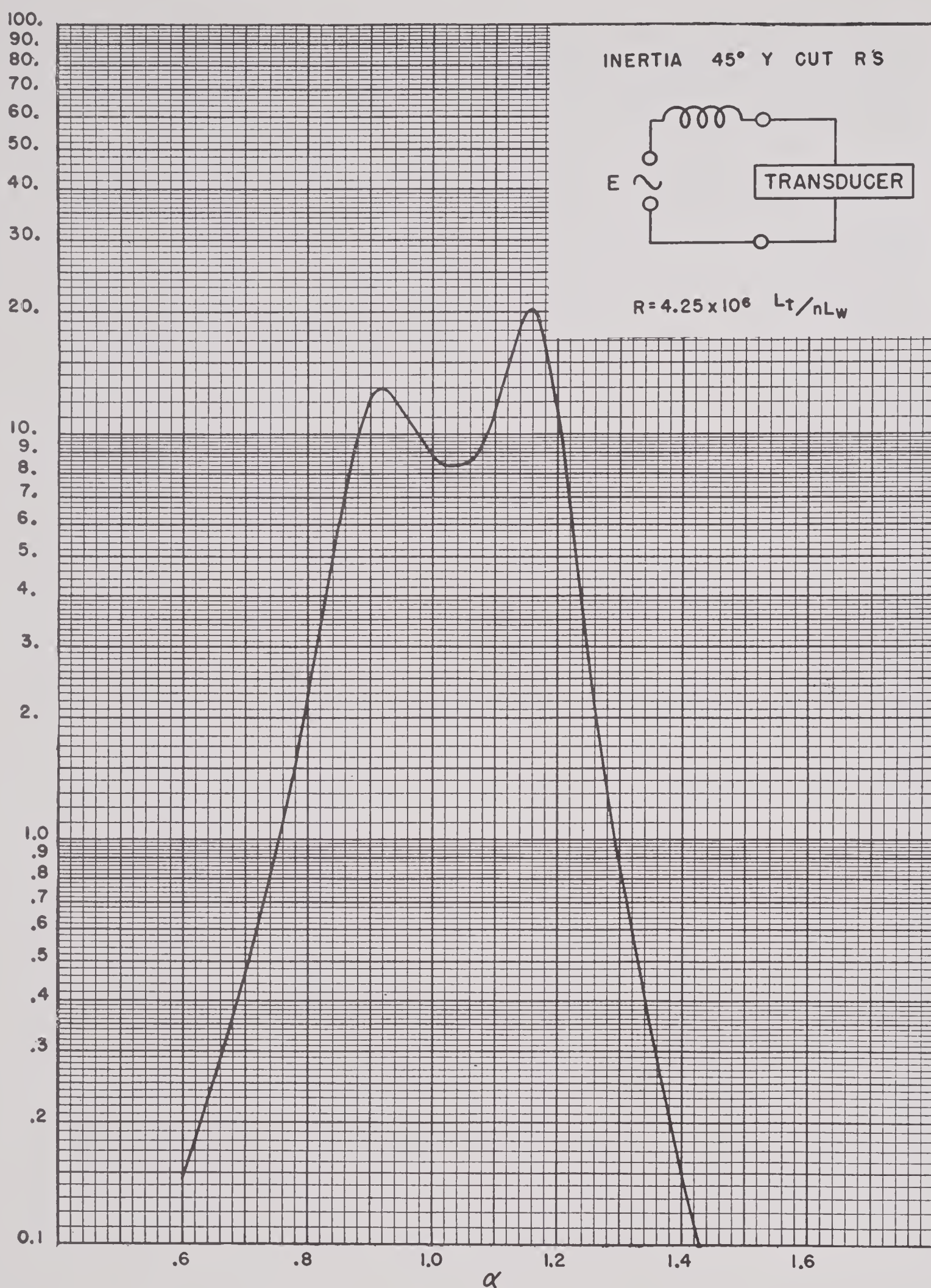


FIGURE 39. The quantity $k_1/k_1^2 + [k_2 - \alpha(k_2)_{\alpha=1}]^2$ plotted against α in inertia driven Y-cut Rochelle salt transducers with constant voltage applied and with lossless series tuning coil. The ordinates of this curve when multiplied by E^2/R give the power expended in the transducer.

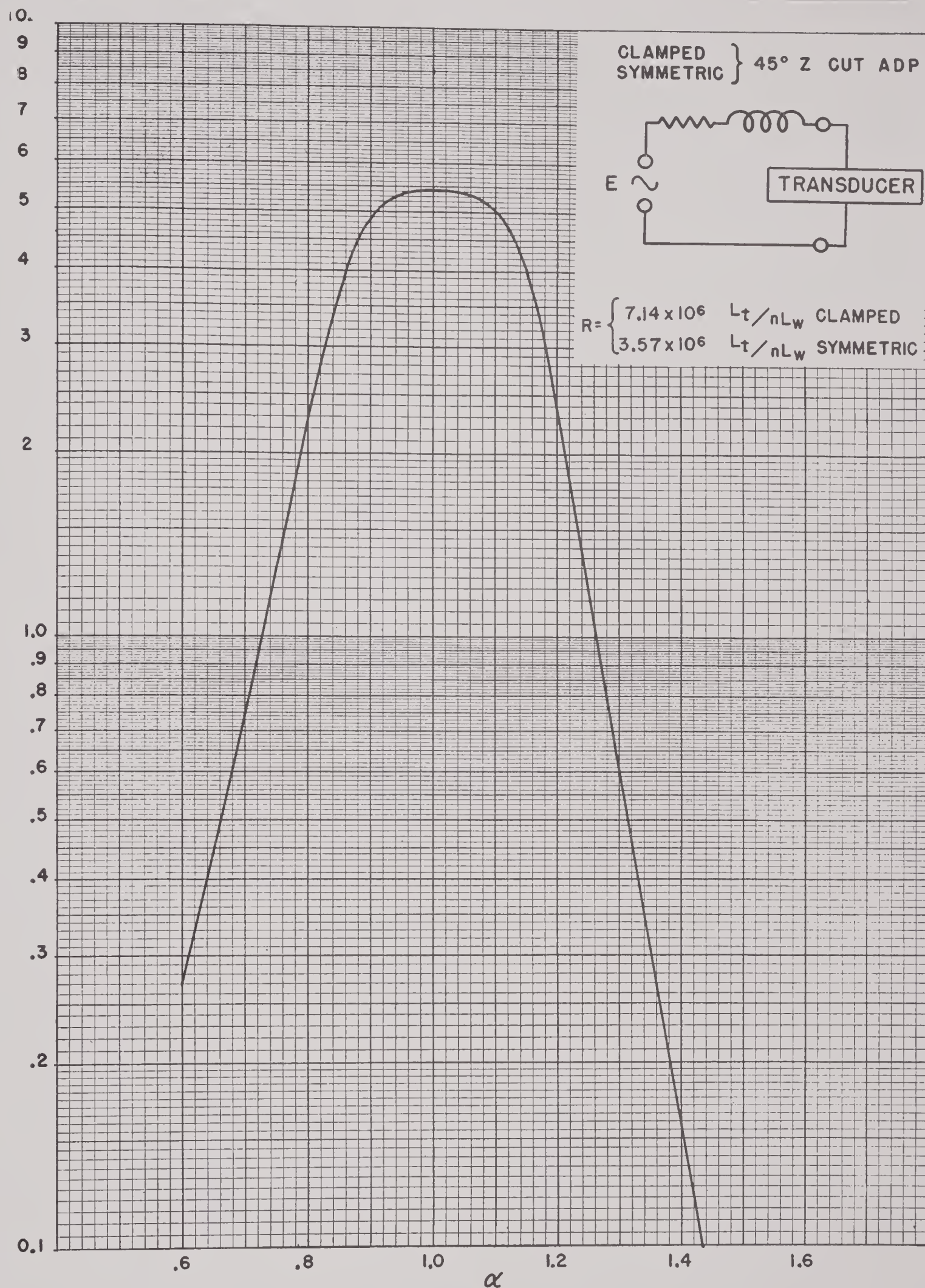


FIGURE 40. The quantity $k_1/[k_1 + (k_1)_{\alpha=1}]^2 + [k_2 - \alpha(k_2)_{\alpha=1}]^2$ plotted against α in clamped or symmetrically driven Z-cut ADP transducers when connected to an idealized amplifier. (See Section 4.9.5.) The ordinates of this curve when multiplied by E^2/R give the power expended in the transducer.

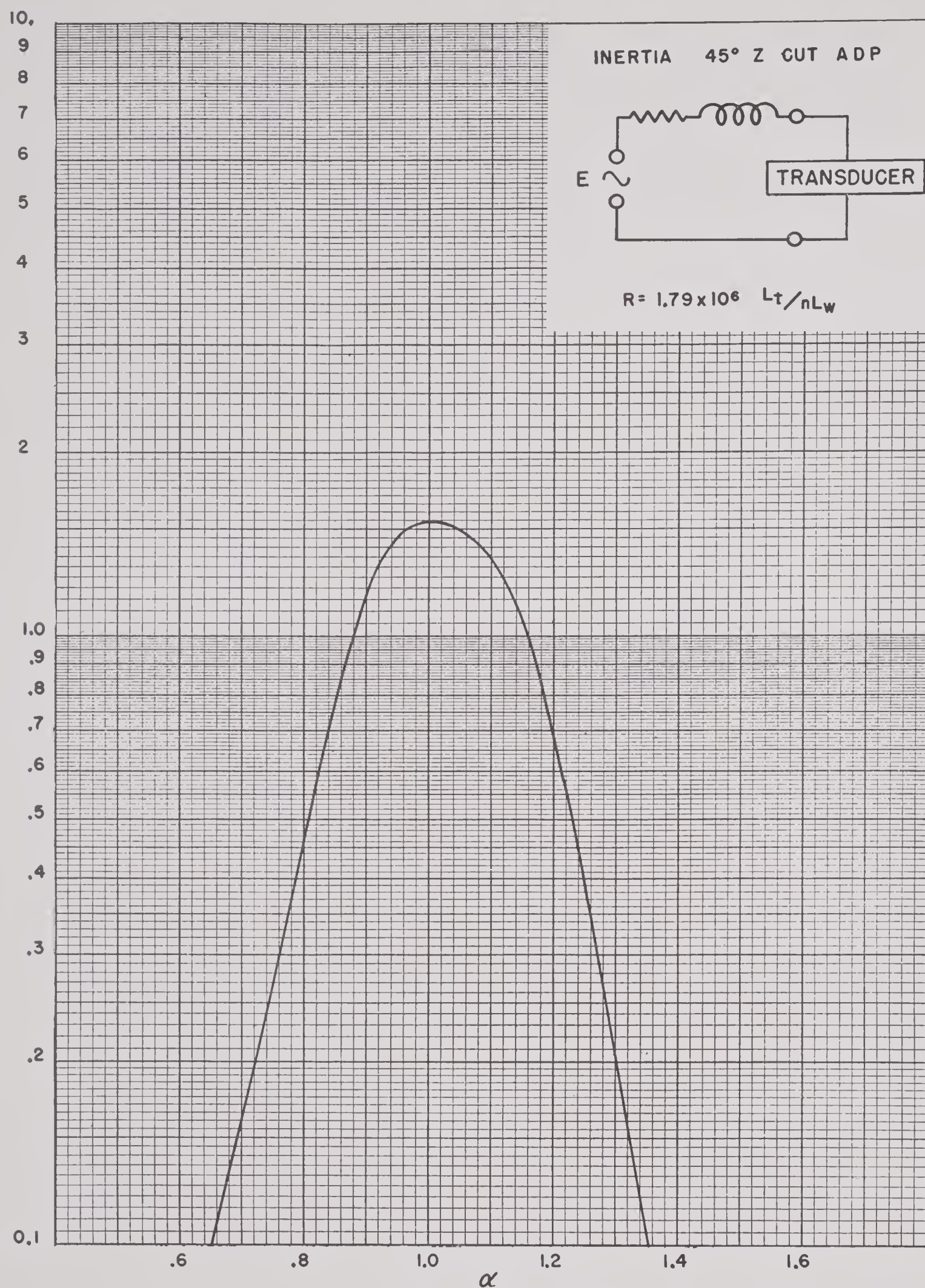


FIGURE 41. The quantity $k_1/[k_1 + (k_1)_{\alpha=1}]^2 + [k_2 - \alpha(k_2)_{\alpha=1}]^2$ plotted against α in inertia driven Z-cut ADP transducers when connected to an idealized amplifier. (See Section 4.9.5.) The ordinates of this curve when multiplied by E^2/R give the power expended in the transducer.

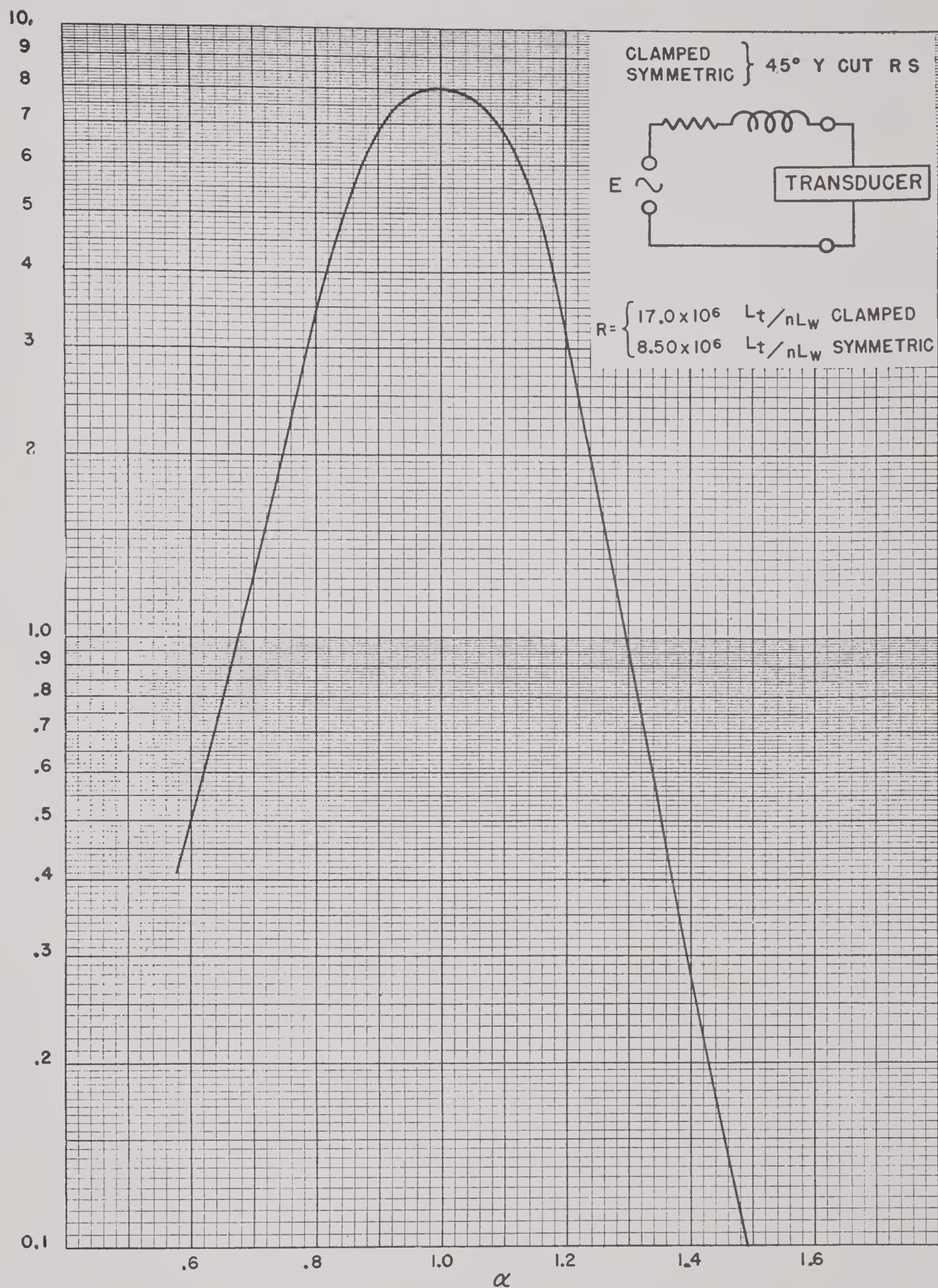


FIGURE 42. The quantity $k_1/[k_1 + (k_1)_{\alpha=1}]^2 + [k_2 - \alpha(k_2)_{\alpha=1}]^2$ plotted against α in clamped or symmetrically driven Y-cut Rochelle salt transducers when connected to an idealized amplifier. (See Section 4.9.5.) The ordinates of this curve when multiplied by E^2/R give the power expended in the transducer.

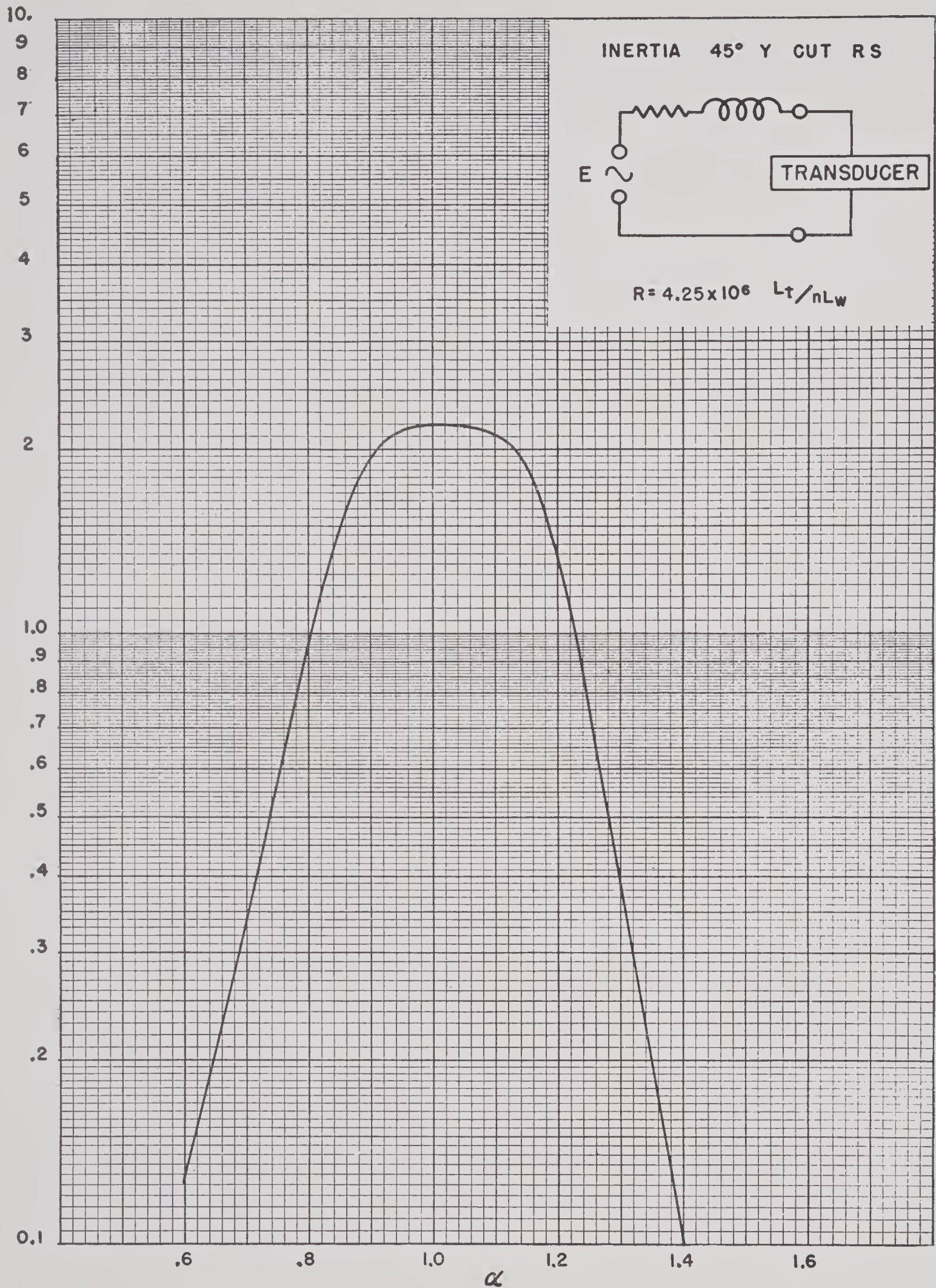


FIGURE 43. The quantity $k_1/[k_1 + (k_1)_{\alpha=1}]^2 + [k_2 - \alpha(k_2)_{\alpha=1}]^2$ plotted against α in inertia driven Y-cut Rochelle salt transducers when connected to an idealized amplifier. (See Section 4.9.5.) The ordinates of this curve when multiplied by E^2/R give the power expended in the transducer.

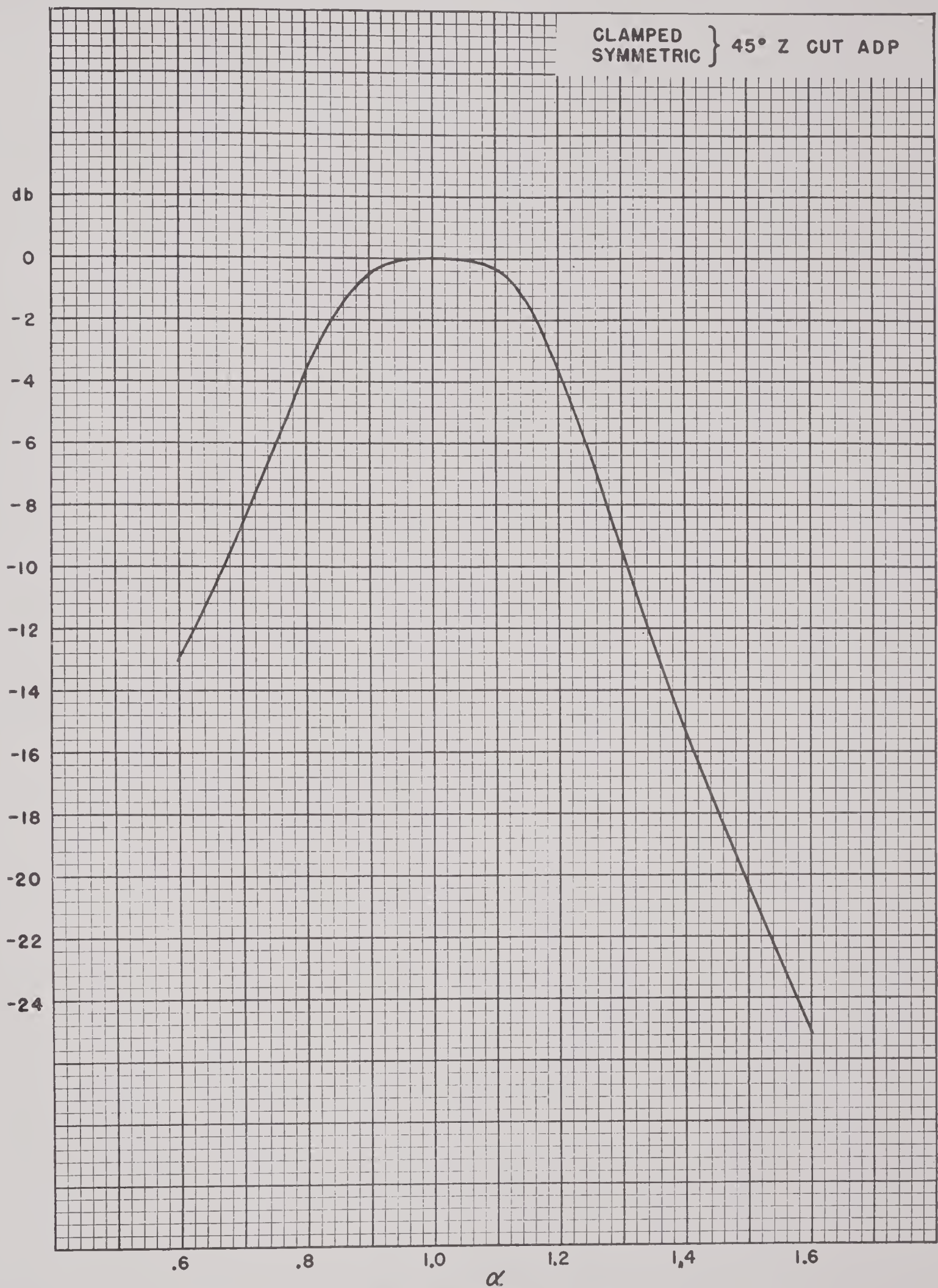


FIGURE 44. The data of Figure 40 plotted in terms of decibels below maximum power.

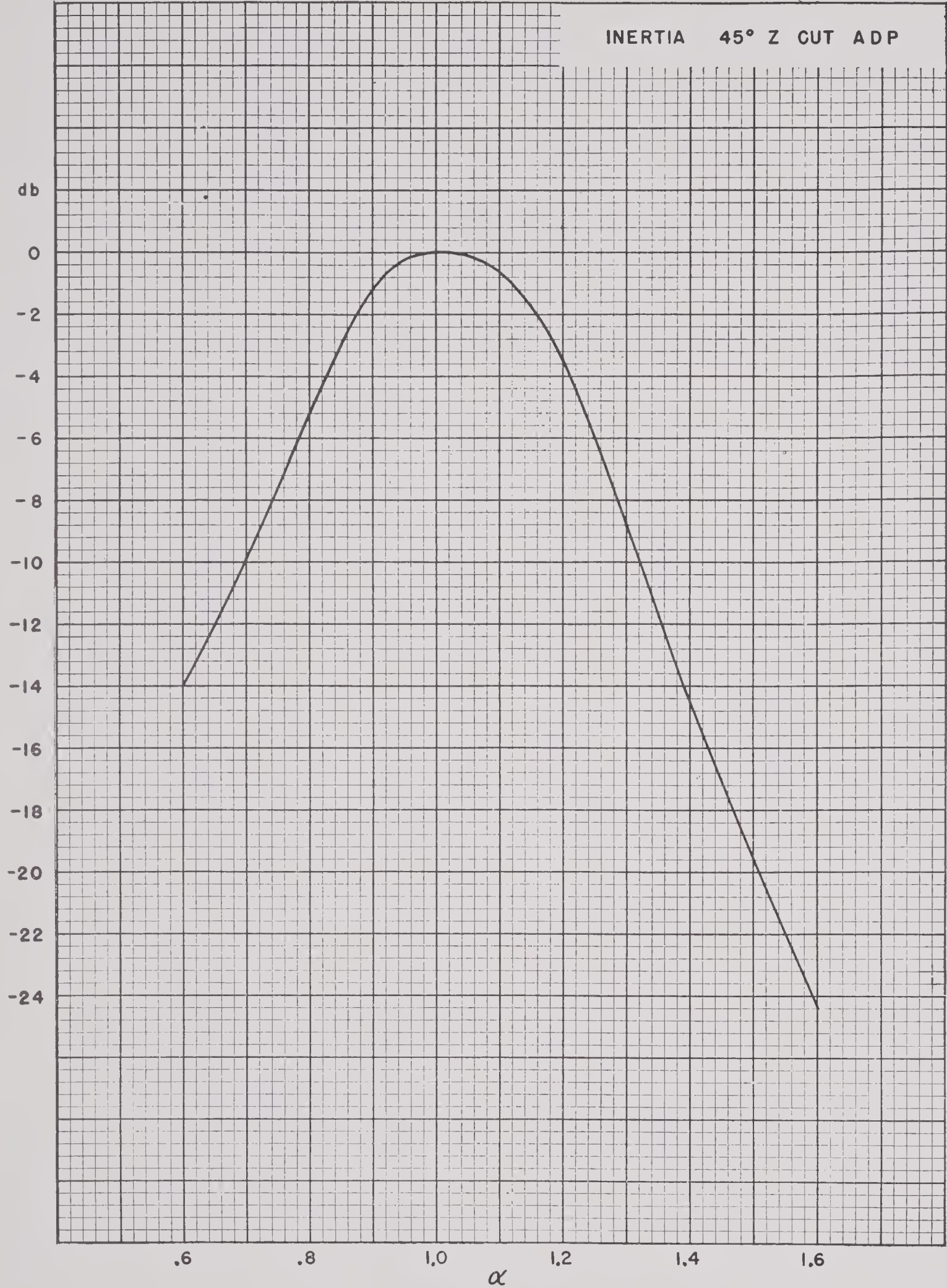


FIGURE 45. The data of Figure 41 plotted in terms of decibels below maximum power.

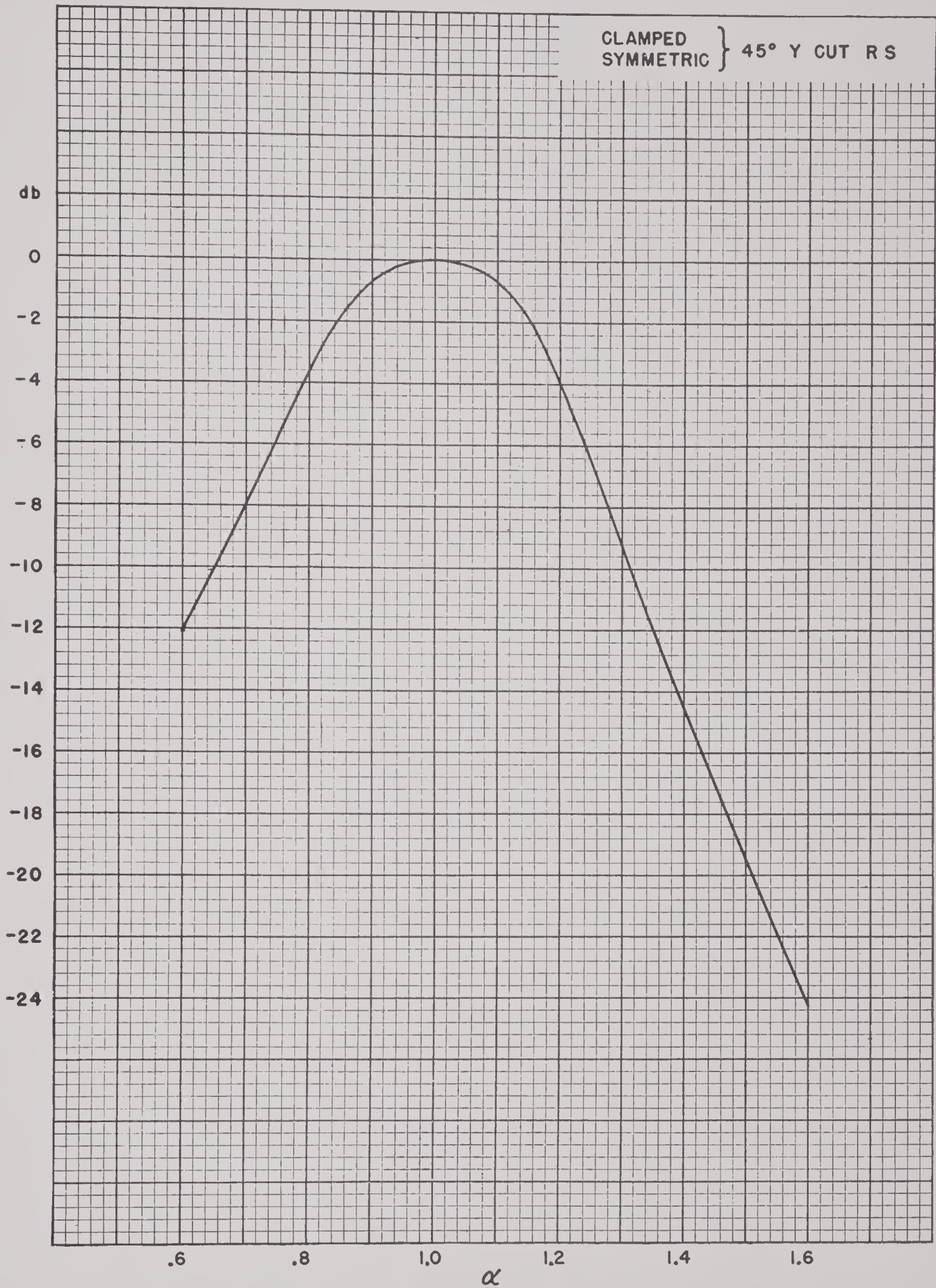


FIGURE 46. The data of Figure 42 plotted in terms of decibels below maximum power.

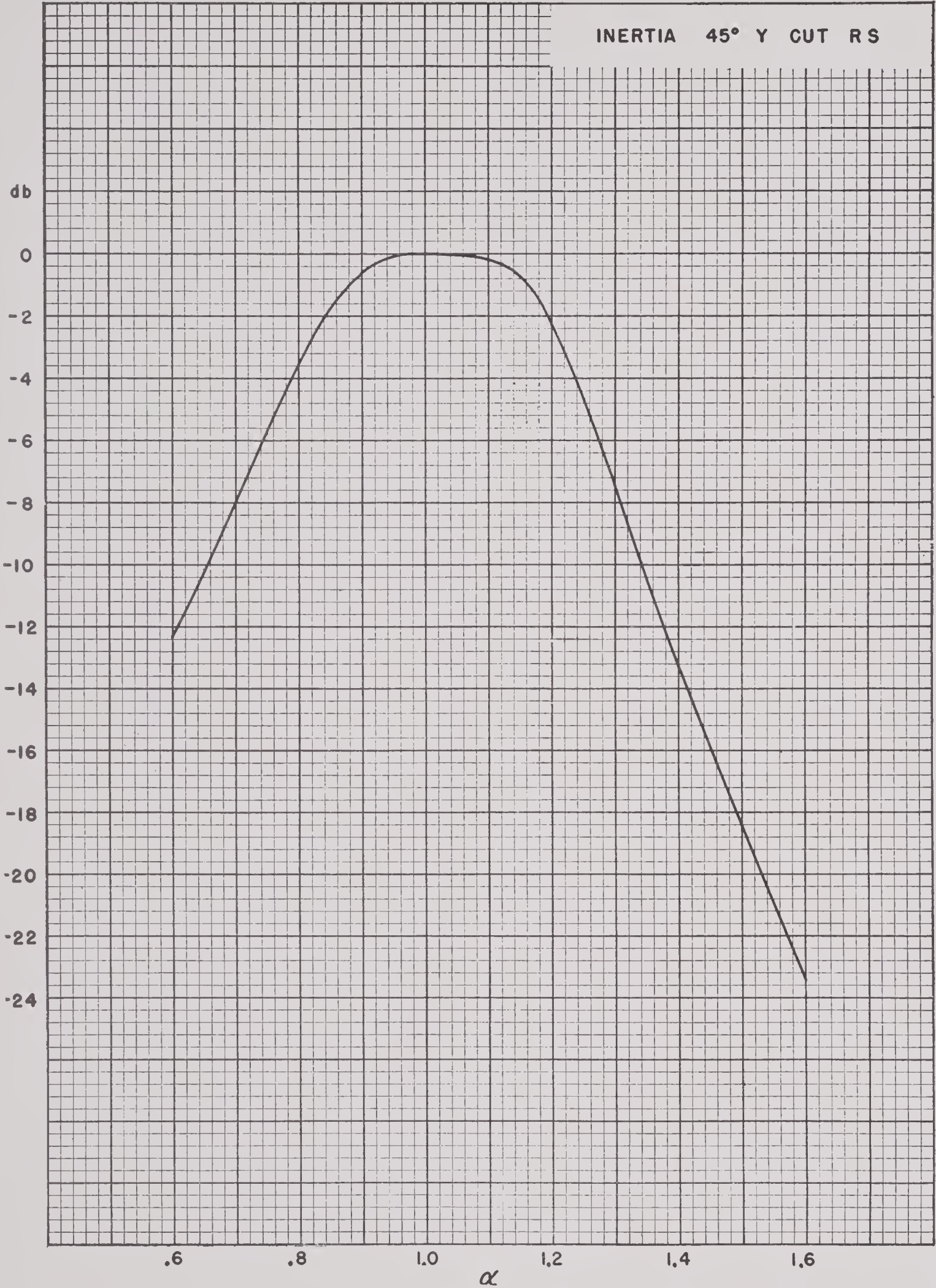


FIGURE 47. The data of Figure 43 plotted in terms of decibels below maximum power.

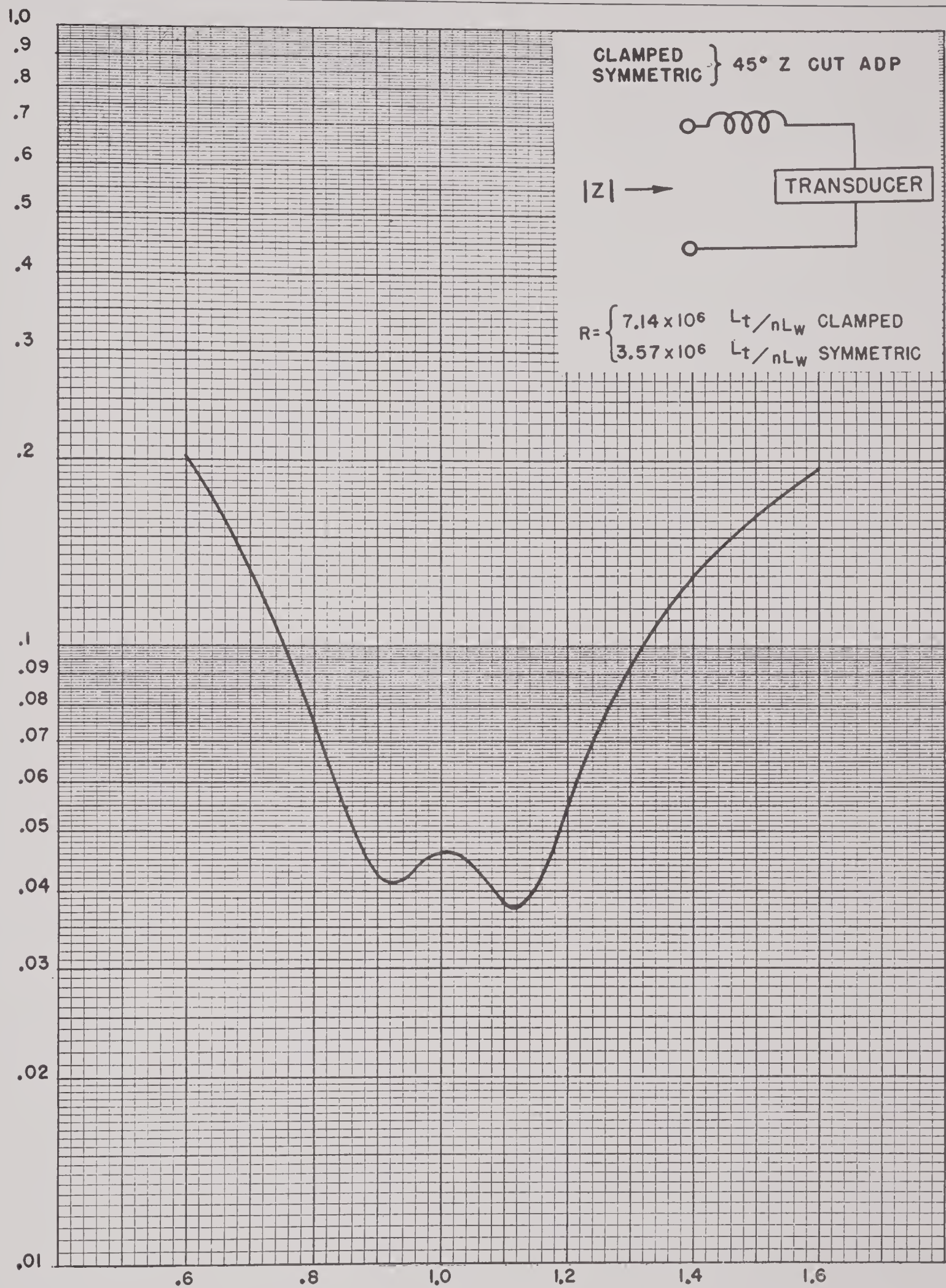


FIGURE 48. Absolute magnitude of total impedance divided by R for a transducer whose reactance is cancelled at resonance by a lossless coil. This curve applies to clamped or symmetrically driven Z-cut ADP.

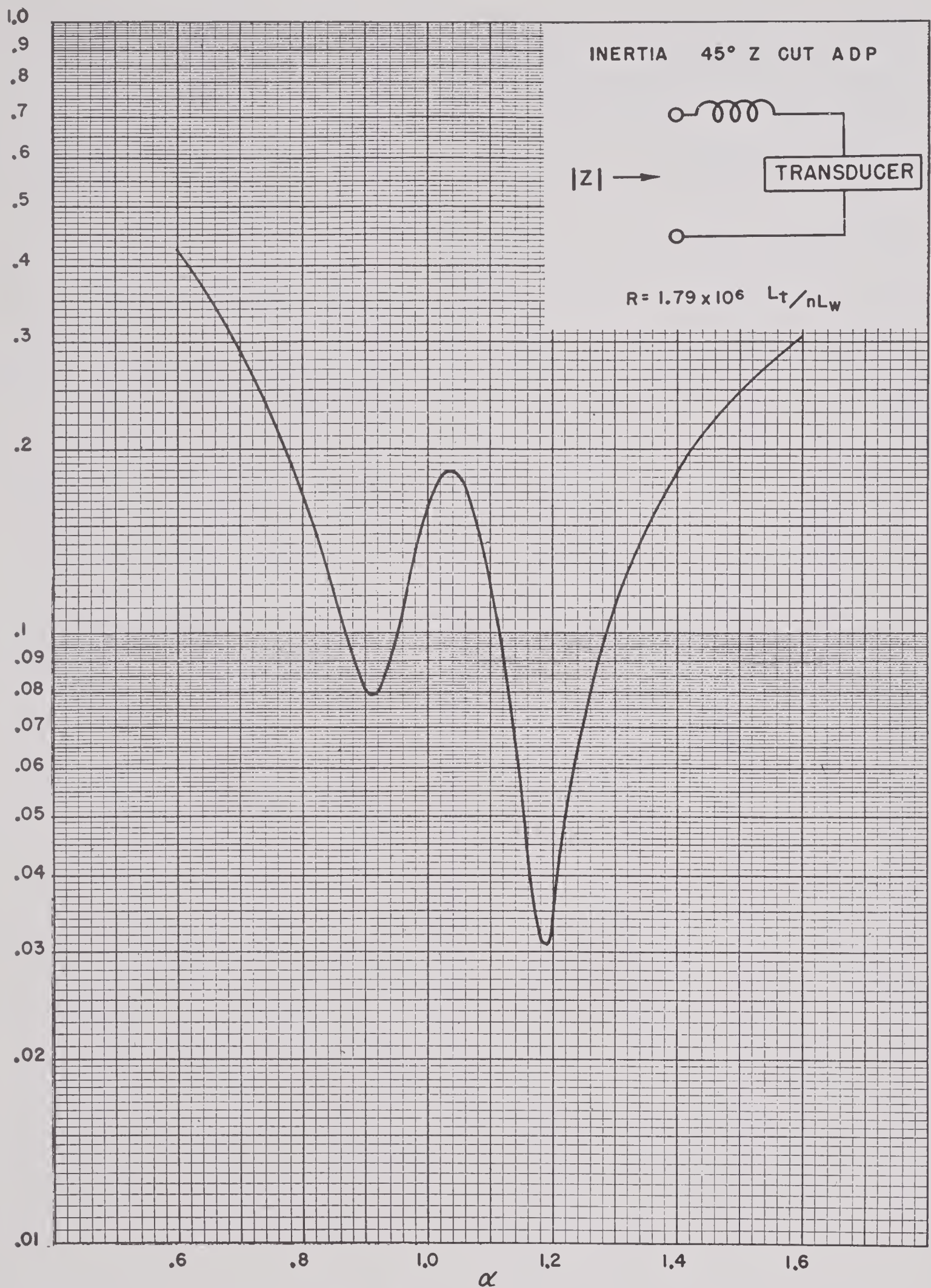


FIGURE 49. Absolute magnitude of total impedance divided by R for a transducer whose reactance is cancelled at resonance by a lossless coil. This curve applies to inertia driven Z-cut ADP.

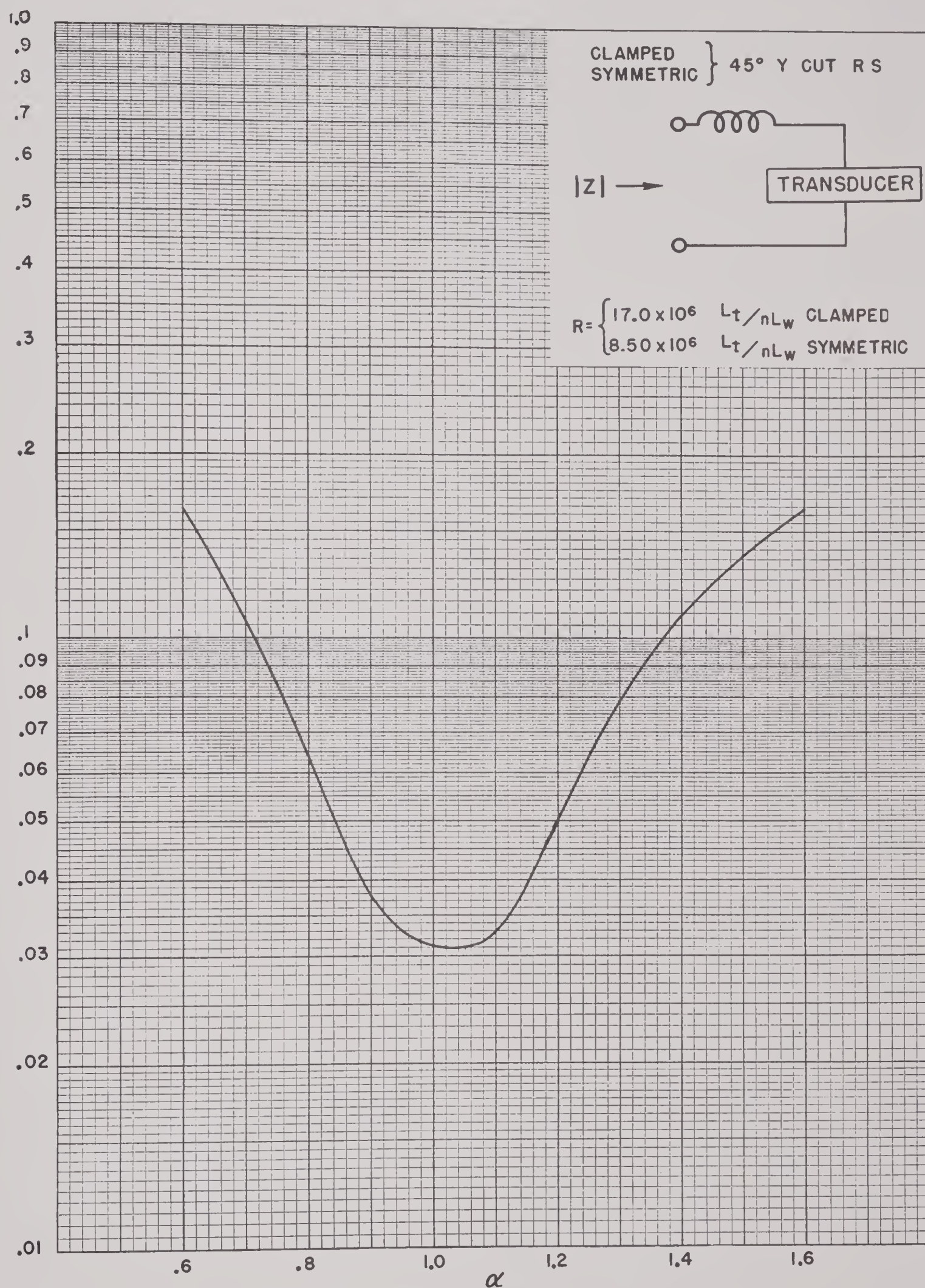


FIGURE 50. Absolute magnitude of total impedance divided by R for a transducer whose reactance is cancelled at resonance by a lossless coil. This curve applies to clamped or symmetrically driven Y-cut Rochelle salt.

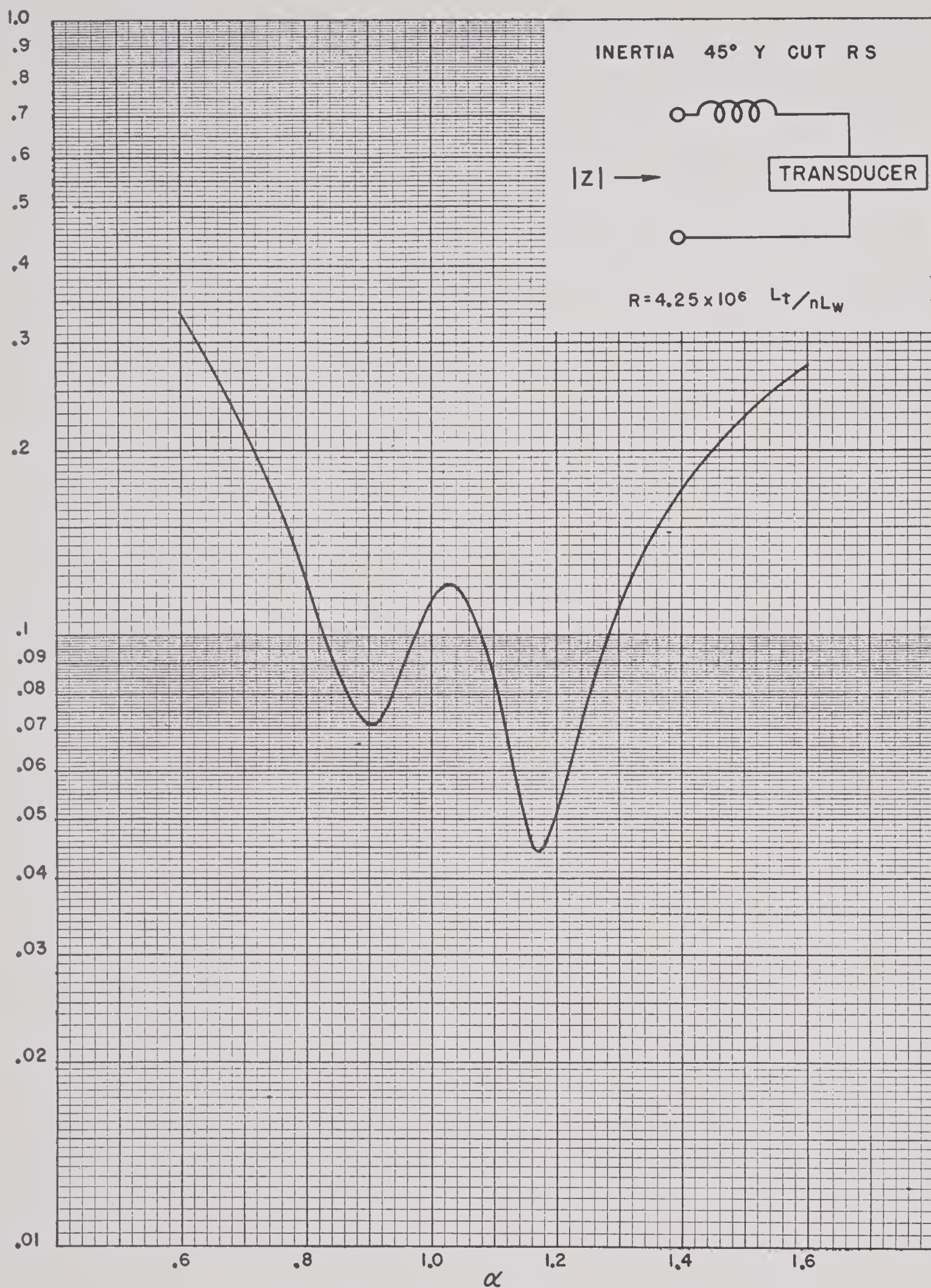


FIGURE 51. Absolute magnitude of total impedance divided by R for a transducer whose reactance is cancelled at resonance by a lossless coil. This curve applies to inertia driven Y-cut Rochelle salt.

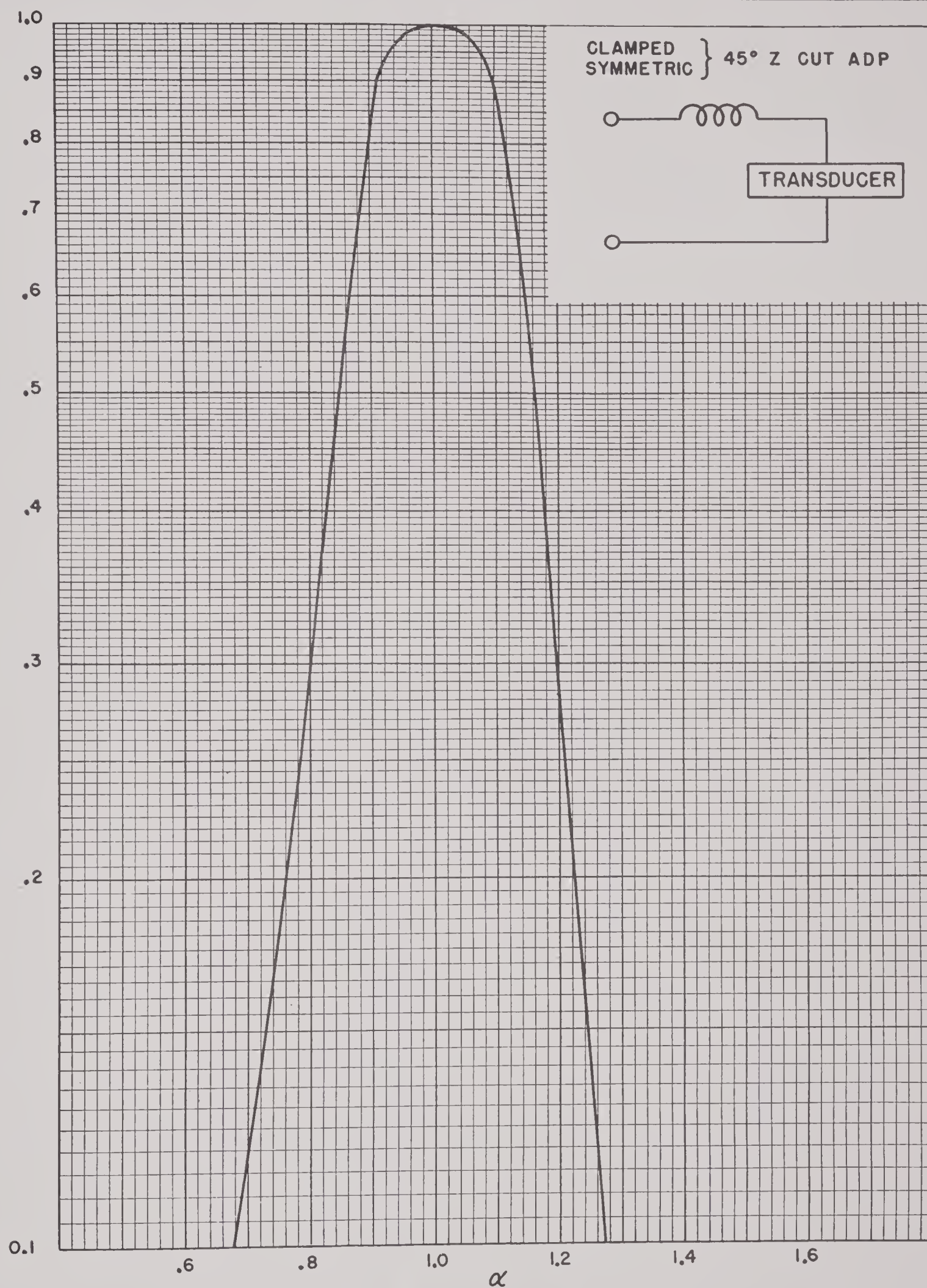


FIGURE 52. Power factor of clamped or symmetrically driven Z-cut ADP transducer with a lossless series coil which cancels the reactance at resonance.

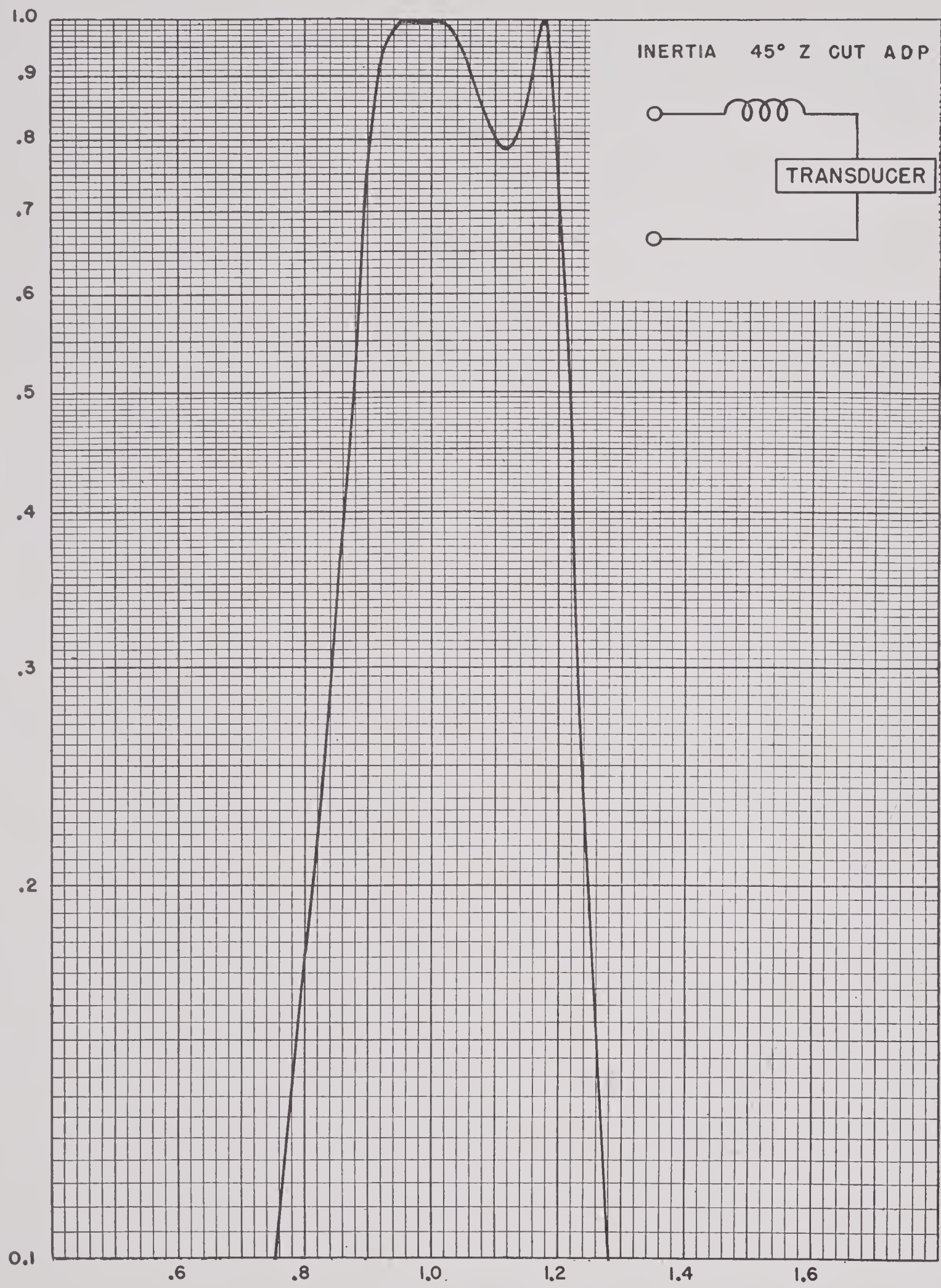


FIGURE 53. Power factor of inertia driven Z-cut ADP transducer with a lossless series coil which cancels the reactance at resonance.

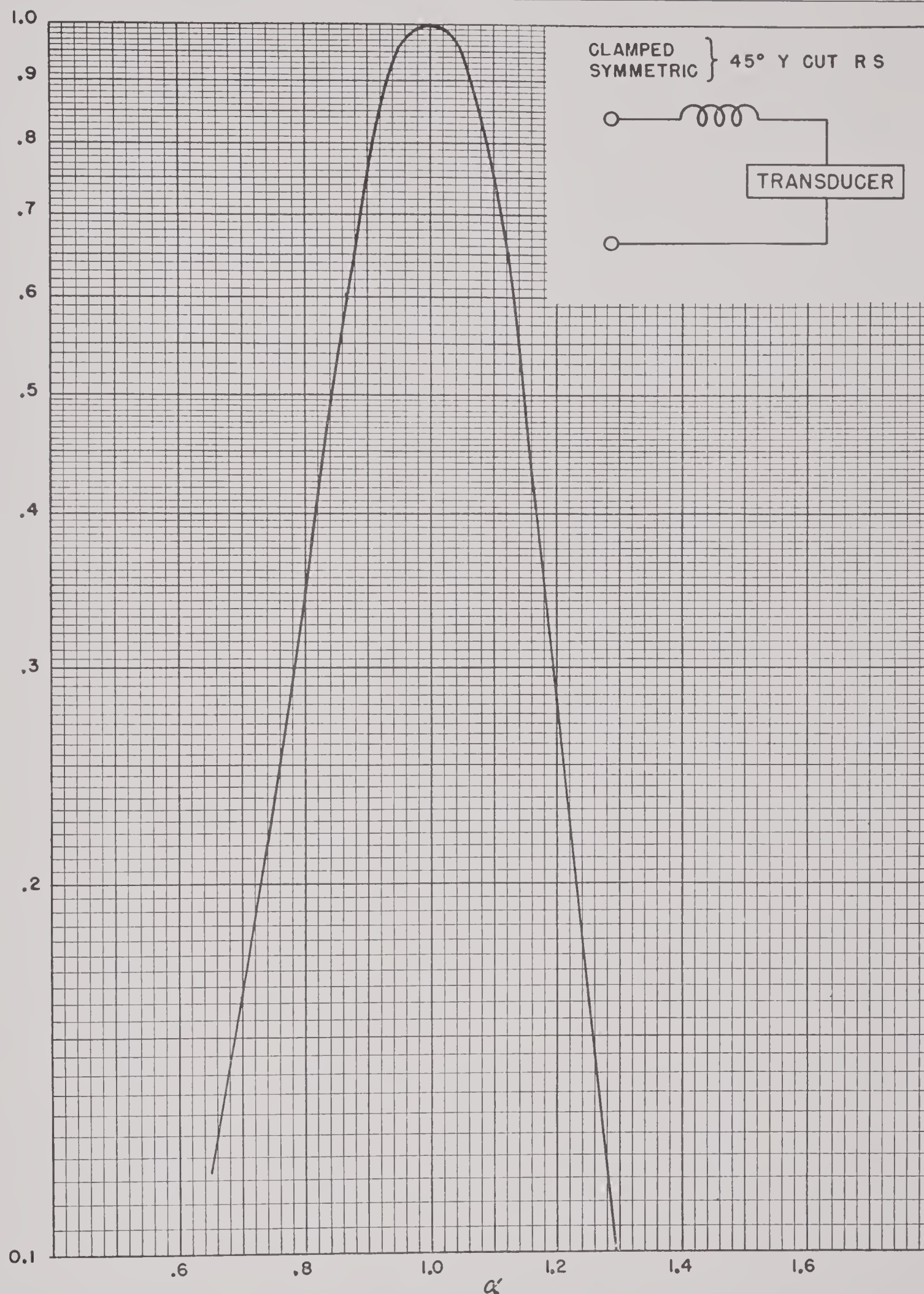


FIGURE 54. Power factor of clamped or symmetrically driven Y-cut Rochelle salt transducer with a lossless series coil which cancels the reactance at resonance.

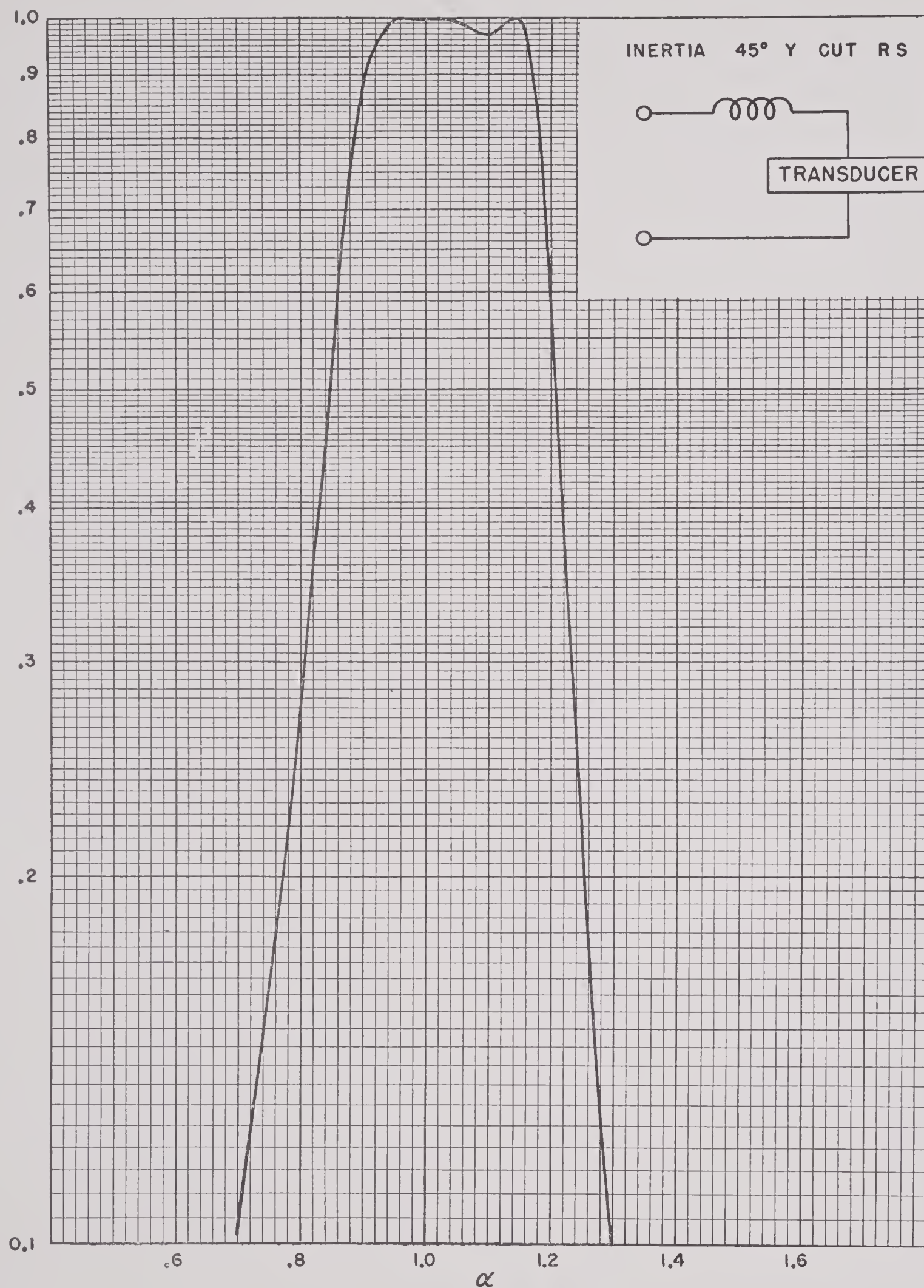


FIGURE 55. Power factor of inertia driven Y-cut Rochelle salt transducer with a lossless series coil which cancels the reactance at resonance.

ELECTRONIC SYSTEMS AND MATCHING NETWORKS

By *Francis X. Byrnes*

IN DESIGNING a crystal transducer the design engineer should at all times keep in mind the fact that the transducer is only one link in a chain that makes up the complete electroacoustic converting system. In any real system, with very few exceptions, the desired end result will be expressed as maximum power output for a given expenditure of weight and space, with the weight and space limitation applying to the system as a whole. With limitations of this type, the transducer designer should not make a change which raises the response of the transducer by 2 db and adds 50 lb to its weight when this 50 lb of weight must be taken from the power amplifier and when the power amplifier in losing this 50 lb also loses 6 db in power output.

Keeping in mind this intimate relationship that exists between the transducer and the other components in the complete electroacoustic converting system, it is obvious that the transducer designer must concern himself with the other elements in the complete system. At the very minimum he must consider the cable used to connect the transducer to its associated electronic equipment. In addition to the cable he must also in the majority of cases concern himself with a matching network to raise the normally low power factor of the transducer. It may also be necessary to change the magnitude of the impedance to a value that will match the associated amplifier. In the case of transmitting transducers in particular, the transducer designer should concern himself with the properties of the associated amplifier. For example, he should take into account the manner in which the maximum power output of the amplifier varies as a function of the magnitude and power factor of the load impedance.

In designing electroacoustic systems incorporating crystal transducers for use over a band of frequencies, too often the entire burden of making the response flat over the band is thrust on the transducer with its associated

coupling network. In many cases, and in particular when the band width approaches an octave or more in width, the best overall efficiency is obtained by incorporating in the amplifier an equalizing network to help flatten the response. This statement will usually apply to the efficiency regardless of definition, i.e., acoustic watts out per electric watts in, watts per dollar cost, watts per pound, or watts per cubic foot of space occupied. The equalizer may be inserted in some portion of the electronic system several stages removed from the transducer terminals.

While the transducer designer may feel that most of the foregoing design problems are more in the realm of the electronic design engineer, he will find that it will pay big dividends in improved performance if he will assume these problems himself, or at least cooperate closely with the electronic engineer in the work on these phases of the system design.

The following sections will discuss these problems and will give suggested design procedures with some practical examples. These procedures have been carefully worked out on paper but in most cases they have not been adequately tested to verify the predicted results. Therefore, they should not be taken as proven methods but should be considered as the best recommendations that the author is able to offer under the present state of transducer development.

5.1 GENERAL PROPERTIES OF TRANSDUCERS

Before going into a discussion of the other elements in the electroacoustic system, a brief summary of the general electrical and acoustical properties of crystal transducers is in order.

Using the simple first-approximation equivalent circuit for a crystal transducer (Figure A),

it can be shown^a that the curve of acoustical output as a function of frequency, of such a transducer for constant voltage or current applied to the electric terminals, will be a maximum at the resonant frequency of the mechanical system and will fall off as the frequency is removed from resonance. The rate at which the response drops off, i.e., the Q or sharpness of the resonance, depends on the Q of the mechanical system which in turn depends on the resistive component of the radiation impedance. This resistance, and therefore the sharpness of the response peak, can be controlled to some extent by various methods such as spacing the crystals in the array or by use of fronting plates. These methods of control are discussed in detail in Section 4.2.

In an actual transducer, of course, there is more than one resonant system and, since most of these systems are made up of distributed rather than lumped elements, there will be many resonances associated with each system. However, in most cases there will be a well-defined resonance at the operating frequency

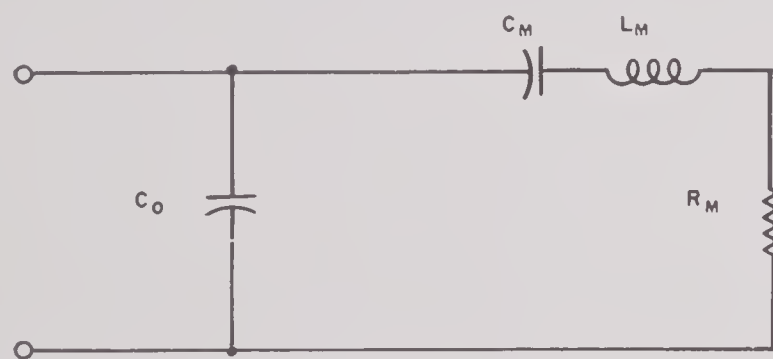


FIGURE A.

or in the operating band, and all other resonances will either be so minor as to cause no trouble or will lie outside the operating band. The two notable exceptions to this general statement are: (1) the case in which a spurious resonance occurs (usually caused by coupling to the housing or to cavities around the crystals), and (2) the case in which the required frequency band is so wide that one or more of the crystal's natural resonances are covered. The first of these exceptions may be remedied

^a For a more detailed discussion of transducer analysis by means of the equivalent circuit see Section 4.9.

by modification of the physical arrangement of the transducer. The second requires revision of the specifications to narrow the frequency band over which the transducer must operate or the inclusion of complicated equalizing networks to compensate for the undulations of the response curve.

A crystal transducer used as a receiver in a uniform sound field will have an output voltage which varies with frequency in the same general manner as does its output when used as a transmitter. This means that the same general problems are involved in equalizing the response of either receiving or transmitting transducers.

Several examples of transmitter and receiver response curves are given in Figure 1, where the transducer output is plotted in decibels below an arbitrary zero reference level against the ratio α of the frequency under consideration to the frequency at which the open-circuit voltage is maximum when the transducer is used as a receiver.^b

From the electrical standpoint a crystal transducer has an impedance essentially the same as a capacitor whose capacitance remains constant as a function of frequency except for variations near resonance which are usually small. The resistive component of this impedance varies considerably with frequency, rising to a peak very close to the resonant frequency and falling off on each side in a manner similar to the frequency-response curves. The relative magnitudes of the resistive and reactive components of the impedance are such as to cause the power-factor curve to have a typical maximum value of from 0.2 to 0.3 at resonance, falling to values as low as 0.02 or 0.01 at frequencies off resonance. In some unusual cases the power factor will rise to values as high as 0.7, and these transducers will show variations in capacitance of almost 3 to 1 when measured at frequencies near resonance.

In designing matching networks for use with the transducer it is sometimes more convenient to refer to the electric Q of the transducer than to its power factor. This Q_e is defined as the ratio of the reactive to the resistive terms in its impedance at any given frequency. This Q_e

^b See Chapter 4, Section 4.9.3.

will range from 1 to 100 to correspond with the power factor range of 0.7 to 0.01 as given.^c

Figure 2 presents several examples of transducer-impedance curves. Examples A, B, and C are curves applying to the same transducers whose response curves are shown in Figure 1.

It should be noted here that transducers using X-cut *Rochelle salt* [RS] crystals will show much greater variations in both the resistive and reactive components of impedance as a

RS and Z-cut *ammonium dihydrogen phosphate* [ADP] crystal transducers.

One other property of a crystal transducer, which must be considered before going into the design of the accompanying electrical system, is its power-handling ability. For high-efficiency transducers used near resonance, which are operated continuously or employed to transmit pulses of more than 10 msec duration, the limitation will be cavitation in the liquid in contact

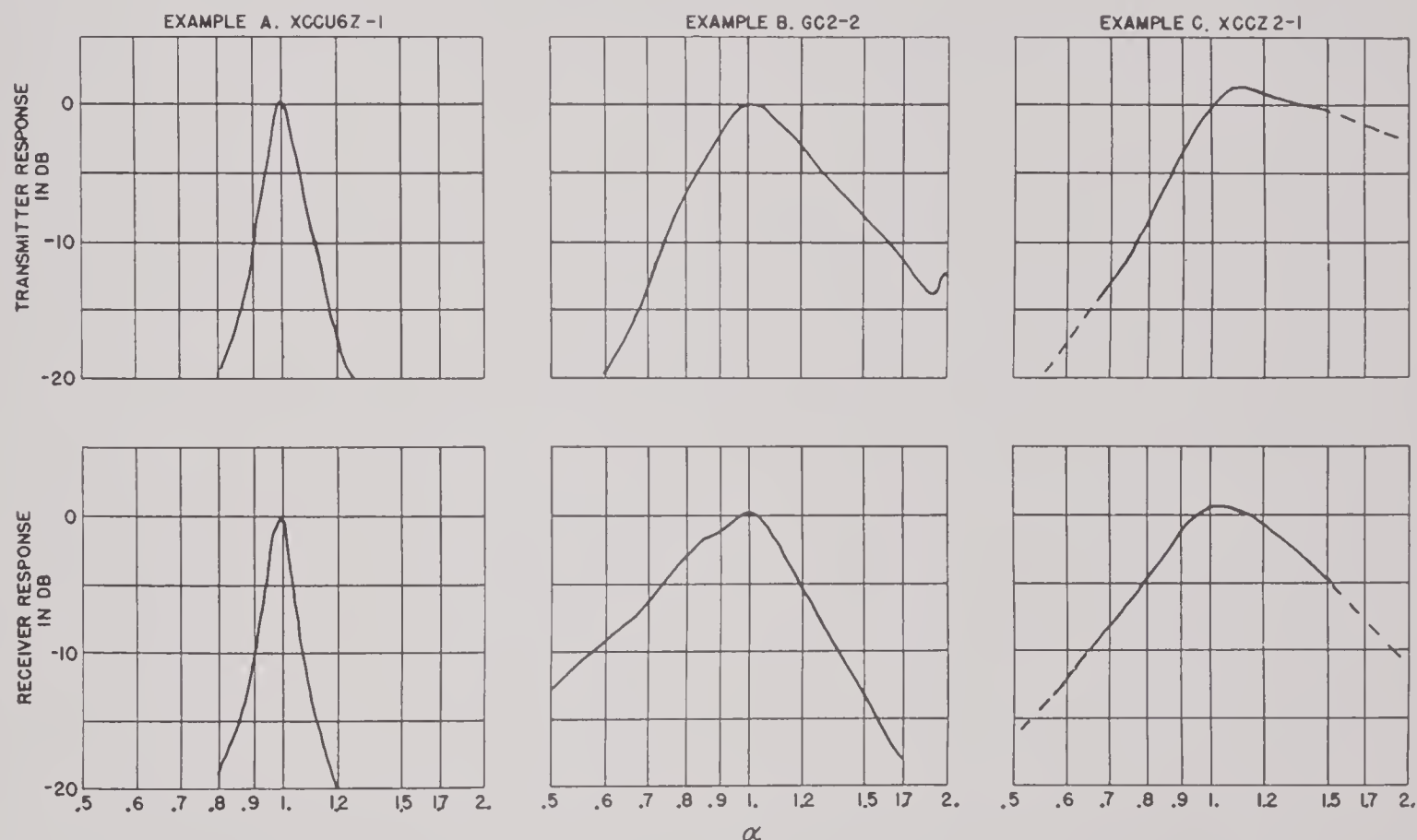


FIGURE 1. Examples of transducer response curves. The transmitter curves are taken with the applied voltage held constant. Those of the receiver represent the open circuit voltage. All the curves have been reduced to zero (0.0) level at $\alpha = 1.0$.

function of frequency. The reactance curve may have regions in which it is inductive and will then pass through two or more points at which it is zero. However, since this impedance, as well as the resonant frequency, is a very marked function of both temperature and the applied field, it is impossible to treat quantitatively an X-cut RS transducer except under very carefully controlled conditions which are never encountered in the field. For this reason the following discussion will consider only Y-cut

^c Note that Q_e is different from Q_E defined in Section 4.9; at resonance, $Q_e = Q_E$.

with the crystal face. The cavitation will damage the face of the crystal motor. If the efficiency of the transducer is low, if it is used far from resonance, or if it is to be used to transmit pulses much shorter than 10 msec the power limitation will usually be that at which voltage breakdown occurs in the crystals.

The nature and power value of the limitation for any particular case cannot be stated accurately because of the many factors entering into the problem. However, the actual value of this limitation can always be stated in terms of a maximum voltage, current, or power, that may

be applied to the terminals of the transducer without damage to that unit. This electrical limitation should then be taken into consideration in the design of the driving amplifier so that its maximum output will not injure the transducer.

A complete discussion of the power limitations of crystal transducers is given in Section 4.8.

5.2

CABLES

In most applications of crystal transducers it will be necessary to use a length of cable

true because of the fact that, if both cables have the same diameter, the capacitance between either conductor and the shield of a two-conductor cable is about the same as the capacitance between the single conductor and the shield in the single-conductor cable. Since the direct capacitance between leads in the two-conductor cable is very small compared to the capacitance to shield, the effective capacitance between conductors can be taken as the two conductor-to-shield capacitances in series. This is approximately one-half the capacitance of either conductor to shield. Thus if the shunt capacitance of a cable poses a problem, a two-

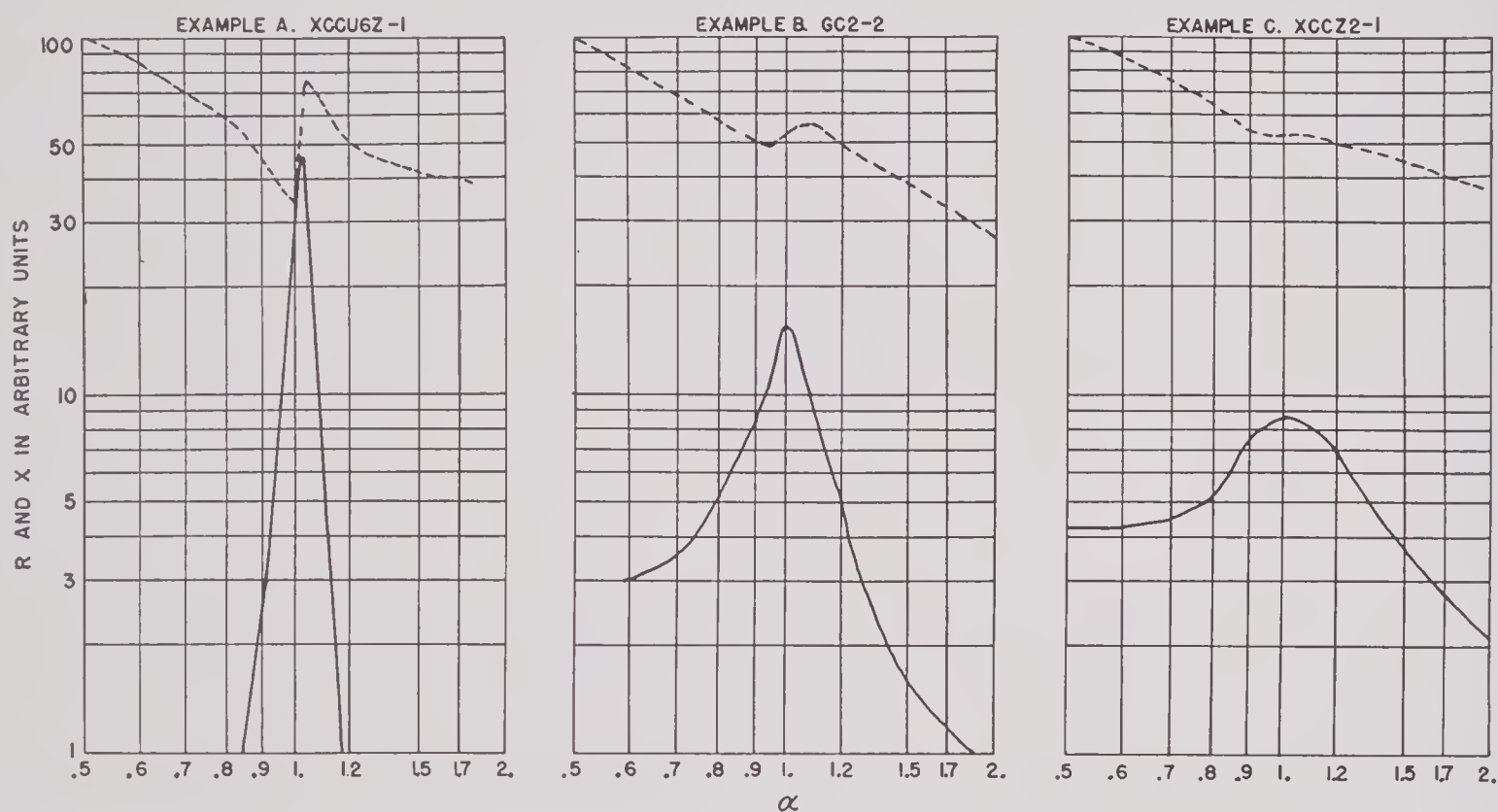


FIGURE 2. Examples of the complex impedance curves of crystal transducers. The solid lines represent the resistance, the broken lines the reactance multiplied by (-1) . All curve values have been multiplied by a factor which brings the reactance to 100 at $\alpha = 0.5$.

connecting the transducer to its associated electric equipment. In many cases the shunt capacitance of the cable will be so high as to exert an appreciable influence on the total impedance of the circuit.

Only shielded cables having two conductors as used in a balanced line will be discussed. Such cables have a shunt capacitance that is approximately one-half that of a single-conductor shielded cable of the same diameter, used in a single-wire line with shield return. This is

wire balanced line will have a 2-to-1 advantage over a single-wire unbalanced line.

Commercially available two-conductor shielded cables for use in balanced lines will have values of effective lead to lead capacitance ranging from about 10 to 100 μf per ft, with power factors ranging from 0.2 to 0.0005 over the frequency range of 1 to 150 kc. Figure 3 is a graph of capacitance and power factor as a function of frequency for a widely used cable which has properties that are quite typical of

the better synthetic rubber dielectric cables. Cables using polyethylene^d as the dielectric have about one-half this capacitance and much lower power factors. The latter may be as low as 0.0005. Cables using vinyl chloride or vinyl chloride acetate copolymers^e as the dielectric will have somewhat higher capacitances than the rubber insulated cables and will have power factors as high as 0.2.

In general, if a fairly good cable is used and it is not so long as to produce resonance effects,

capacitance, will be a negligibly small fraction of the total power.

The effect that the cable will have on the performance of the transducer will depend upon the manner in which its performance is being considered, the actual location of the cable in the system, and the value of the cable impedance relative to the other impedances in the system. The magnitude of the cable's effect may be evaluated in several ways. The transducer's response may be measured with and

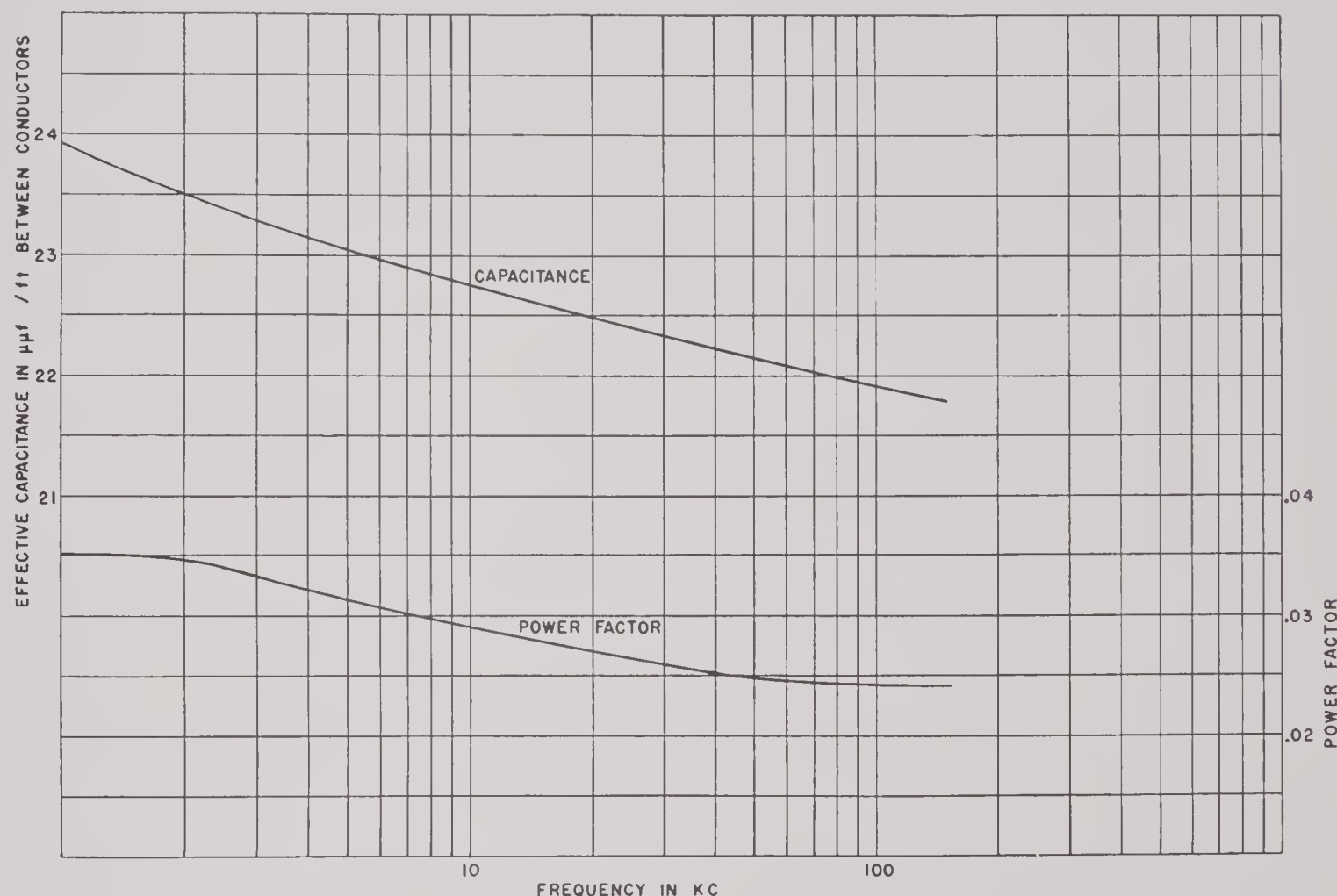


FIGURE 3. Capacity per foot and power factor as a function of frequency for a 35-ft sample of Simplex No. 9061 (modified AA60 or SA60) 2-conductor shielded cable.

the cable can be treated as a lossless capacitor shunted across the line. This treatment is almost always valid because in any well-designed system the current flowing in the shunt capacitance of the cable will be a small fraction of the total current. Thus the power loss, represented by the 0.1 or smaller power factor in this ca-

^d Commercial designations of polyethylene plastics are Polythene and Copolene.

^e Commercial designations of vinyl chloride plastics are Geon and Koroseal; vinyl chloride acetate copolymer is Vinylite.

without the cable; or a standard current of 1.0 amp may be applied through the cable and related to the resulting current in the transducer. If the impedances of all the elements in the circuit are known the effect of the cable upon the transducer may be calculated.

The following statements regarding the effect of the cable may be used as a general design guide. The extent to which the cable influences the response depends upon the ratio of the shunt impedance of the cable to the transducer im-

pedance, and also upon the value of the terminating impedance seen at the input end of the cable. When this impedance is zero (as with a constant-voltage source), the effect of the cable is also zero. In the more common case where a tuning coil is used to cancel the capacitive reactance of the transducer and the cable at some particular frequency, and this system is terminated by the proper impedance to give an efficient transfer of power at this frequency, the principal effect of the cable will be to cause a rapid fall of the response curve as the frequency of the applied voltage varies from the resonant frequency. It should be particularly noted that this sharpening of the electrical resonance curve is minimized if the tuning coil is placed between the cable and the transducer rather than at the amplifier end of the cable. This procedure places the cable in the low-impedance portion of the circuit and minimizes the effect of its shunt impedance. In the case where the transducer is used without a tuning coil the effect of the cable is to reduce the output level of the transducer without any appreciable effect on the shape of the response curve. In general it is seen that the lower the ratio of the cable's shunt impedance to the impedances of the other elements in the circuit the greater will be the effect of the cable on the transducer's performance. In extreme cases where a high-impedance transducer must be used with a long high-capacitance cable with a resulting low-shunt impedance, it may be necessary to use some kind of an impedance-matching transformer between the transducer and the cable. If the transducer is used as a receiver the loss due to the cable may be greatly reduced by the use of a special input amplifier as described in Section 5.4.

One extreme case is sometimes encountered where the required cable length is comparable to a quarter wavelength or more at the operating frequency. For example, a 1,000-ft length of the cable in Figure 3 becomes quarter wave at approximately 125 kc. The apparent discrepancy between this figure and that for a quarter wavelength in air at the same frequency is explained by the reduced velocity through cables of this type. The actual velocity will be that in air multiplied by a factor $1/k$, where k is the

dielectric constant of the cable insulation. In this case the dielectric constant of the rubber insulation was taken as 5.0. When the cable length is significant it can no longer be treated as a simple shunt capacitor. It must be treated as a transmission line with distributed constants and having a characteristic impedance which will be of the order of 100 ohms for all commonly used cables. In order to be used at the end of such a transmission line, a crystal transducer must have its reactance cancelled with a coil and the resulting resistive impedance transformed in magnitude to properly terminate the line, if losses due to reflections are to be avoided. Since a network consisting of a crystal transducer, its tuning coil, and an impedance transformer will in general appear resistive over only a comparatively narrow frequency range, such a system at the end of a long line will have a rather narrow response band.

5.3

MATCHING NETWORKS

Networks used for coupling crystal transducers to electronic amplifiers may be resolved into two general types. The first, and simplest, of these has only to correct the power factor of the transducer. The second type, which is generally more complex, is used to transform its impedance to a higher or lower value.

The design of a simple power factor correcting network is quite straightforward. The circuit consists of an inductor in series or in parallel with the transducer. The reactance of the inductor is made equal to the reactance of the transducer at the frequency of operation. The coil must have a Q high enough to avoid serious power loss and must be insulated to withstand the applied voltage. It must also be capable of carrying the required current and in the case of iron-core coils the hysteresis loss must also be kept low. For the higher supersonic frequencies and for higher power levels it has been found that air-core coils can best meet the above requirements. For lower frequencies and for lower power levels the powdered iron or laminated iron core coils have been found superior. For use in receiving transducers the best

coil is one wound on a powdered iron toroidal form. By a proper choice of the core, very high Q 's may be obtained. The toroidal shape of the coil minimizes pickup due to stray electromagnetic fields.

If a change in the magnitude of the impedance is desired in addition to correction of the power factor of the transducer, it will be necessary to have an impedance-transforming network in addition to the tuning coil. This may be a transformer of the required turns ratio or it may be a simple L - or T -type impedance-transforming network. If in designing the impedance-matching transformer the leakage reactance is deliberately made high and is adjusted to the proper value, it may also serve as the required tuning inductance. Special care must be taken, however, to insure low losses in this leakage inductance. In most cases, an L network consisting of a condenser and a coil can quite satisfactorily carry out the functions of both the tuning coil and an impedance-matching network. Sometimes special circumstances will make it desirable to use other types of networks. An example of this is the case in which it is desirable to obtain a large impedance transformation. A simple shunt coil will in general be better than the alternate L network for the reason that less inductance is required enabling a smaller coil with lower losses. Since the coil is the principal factor determining size, cost, and losses, in a reactive network, the one using the smaller coil will be the best, assuming these three factors alone are considered.

If the system is to be used over a band of frequencies it will be found that the network having the least narrowing effect on the pass band will always be the one employing the least reactive elements, namely, a simple series or sometimes parallel coil whose reactance is equal to the reactance of the transducer at the mid-band frequency. If an impedance transformation must be made in such a band-pass coupling system it can be made with the least effect on the band width by means of a transformer whose response in the pass band is flat. Such a transformer is almost always feasible to build by conventional methods because of the fact that the maximum pass band likely to be encountered in this application is about 1 octave.

5.4

AMPLIFIERS

The most flexible link in the chain that makes up the complete electroacoustic system is the electronic amplifier that either supplies the driving power for the transducer or is driven by the transducer. This great flexibility is due to the fact that all the design factors, including physical shape, output power, input impedance, output impedance, and frequency response are more or less independently variable over a very wide range of values. These same factors which enable flexibility in the design also make it very difficult to establish quantitative design rules. This is particularly true in the case of an output-power amplifier which is operated very near its maximum output. In this case the independence of some of the design factors is to a great extent lost, and the rather high degree of nonlinearity makes necessary the introduction of many higher order terms in any mathematical treatment. The particular load impedance that we are here concerned with, a crystal transducer, adds even more complications because of the wide variation in magnitude of its impedance as a function of frequency and the fact that its power factor will have a low average unless the operating frequency range is restricted to a narrow band near resonance.

For most practical design purposes, however, the following qualitative rules will be found to give satisfactory results.

We will first consider transmitting transducers operating at a single frequency or over a very narrow band of frequencies. The reactance of the transducer plus the connecting cable and any impedance transformer should be cancelled by means of a series tuning coil. The magnitude of the resulting purely resistive load should then be made equal to that value which will permit delivery of maximum power, at the allowable distortion, from the particular tubes being used in the output amplifier. The actual value of this optimum-load impedance may be obtained from examples given in a standard tube handbook or it may be obtained by analytic methods¹ from curves given in the handbook.

The second and most important case to be considered is where the system is to operate

over a fairly wide band; that is from 0.1 to 1 octave in width. The resonant frequency of the transducer should occur at the geometric center (defined as the frequency $\sqrt{f_1 f_2}$) of the band. A tuning coil, that will cancel the reactance of the transducer and its associated coupling network at this frequency, should be used. The impedance of such a combination will show variations in magnitude as large as 10 to 1 and even greater variations in power factor over such band widths. In Figure 4 are shown the

is used, a set of equal power contours plotted on a plane of impedance coordinates can be obtained.² These contour maps can use for impedance coordinates X and R , $|Z|$, and Q_e , or $|Z|$ and *power factor* [PF]. The particular choice will depend on the form in which the impedance data have been presented. All three have been plotted in Figures 5, 6, and 7. The values of X , R , and $|Z|$ are given relative to R_p in the equivalent circuit. This equivalent circuit and the power-impedance contours derived from it

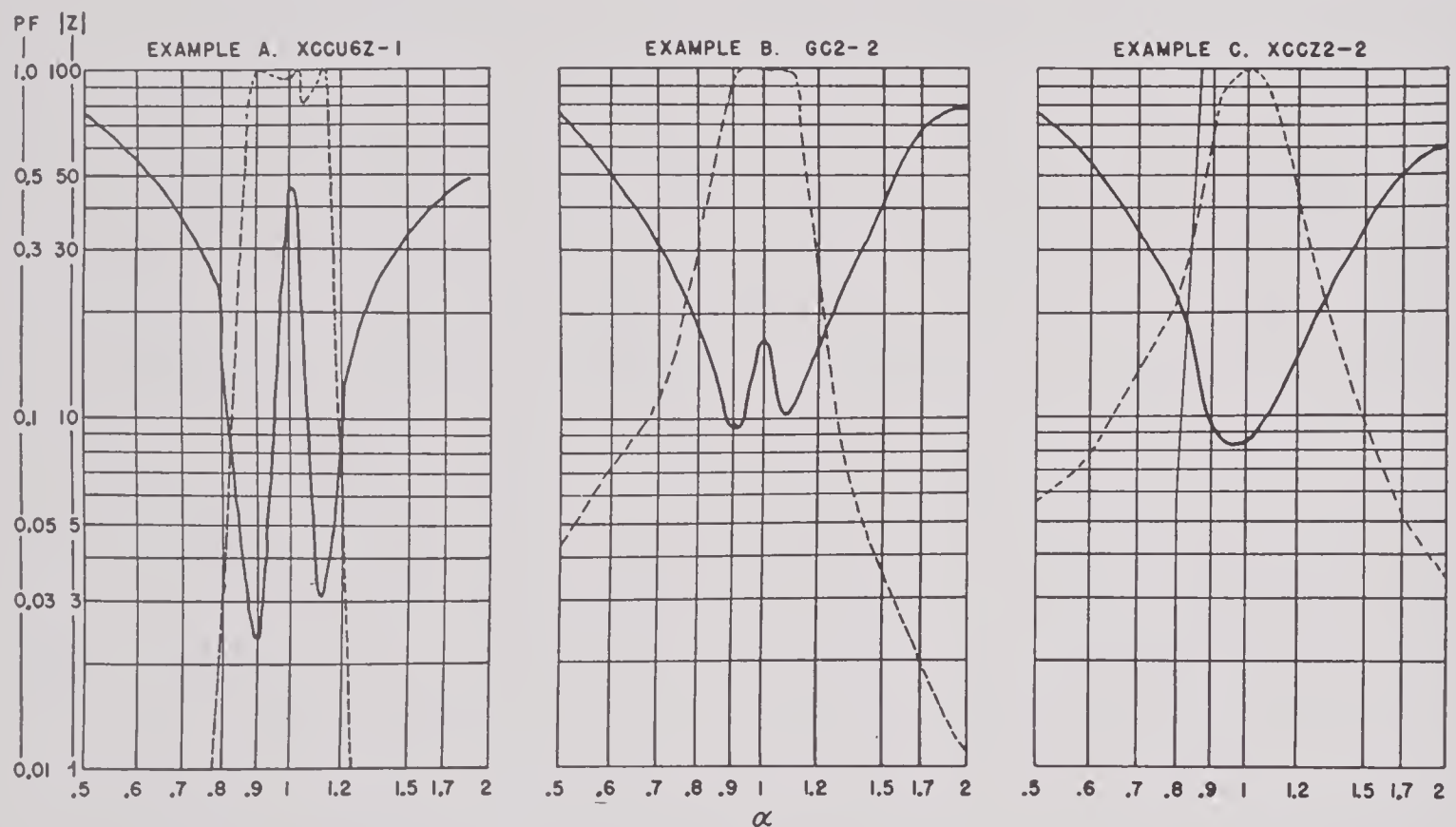


FIGURE 4. Examples of the impedances of transducers which include a lossless series tuning coil such that the combination resonates as $\alpha = 1.0$. Solid line curves are absolute magnitude of impedance, broken line curves are power factor.

impedances of the three transducers given as examples in Section 5.1. They have here been replotted in terms of magnitude of impedance and power factor and include the effect of a series tuning coil resonating at the midband frequency.

In order to decide how the magnitude of such a load should be adjusted relative to the value that the output amplifier would like to see, we will have to take into consideration the effects that varying load magnitude and power factor have on the maximum output capabilities of the amplifier. If the conventional first-approximation equivalent circuit^{1a} for a vacuum tube

will be found to be quite accurate for push-pull class A_1 triodes, using R_p equal to the plate resistance of the tube, if fairly high distortion can be tolerated. (With transducer loads this high distortion is eliminated to a large extent by the filtering action of the transducer and its associated coupling network.) For push-pull class A_1 beam tetrodes, or pentodes, the method will still provide fairly accurate results if a value of R_p is made equal to the optimum value of load, rather than the actual plate resistance. For these tubes the error arising from the use of these curves is much larger if the load is greater in magnitude than it is if the

load is smaller in magnitude than the optimum value. This large error for high-load impedances is not a problem as it will be found that in almost every case wherein the load is a crystal transducer, the amplifier will not be called upon to operate into a load of higher than optimum impedance. The XCCU6Z transducer given as an example above, when matched in a manner

pentode amplifiers if they are not operated too close to the overload point, and if the load-power factor remains sufficiently high. If more accurate performance predictions must be made for these tubes operated under these conditions, a special set of power-impedance contours must be obtained experimentally for the particular circuit being used.

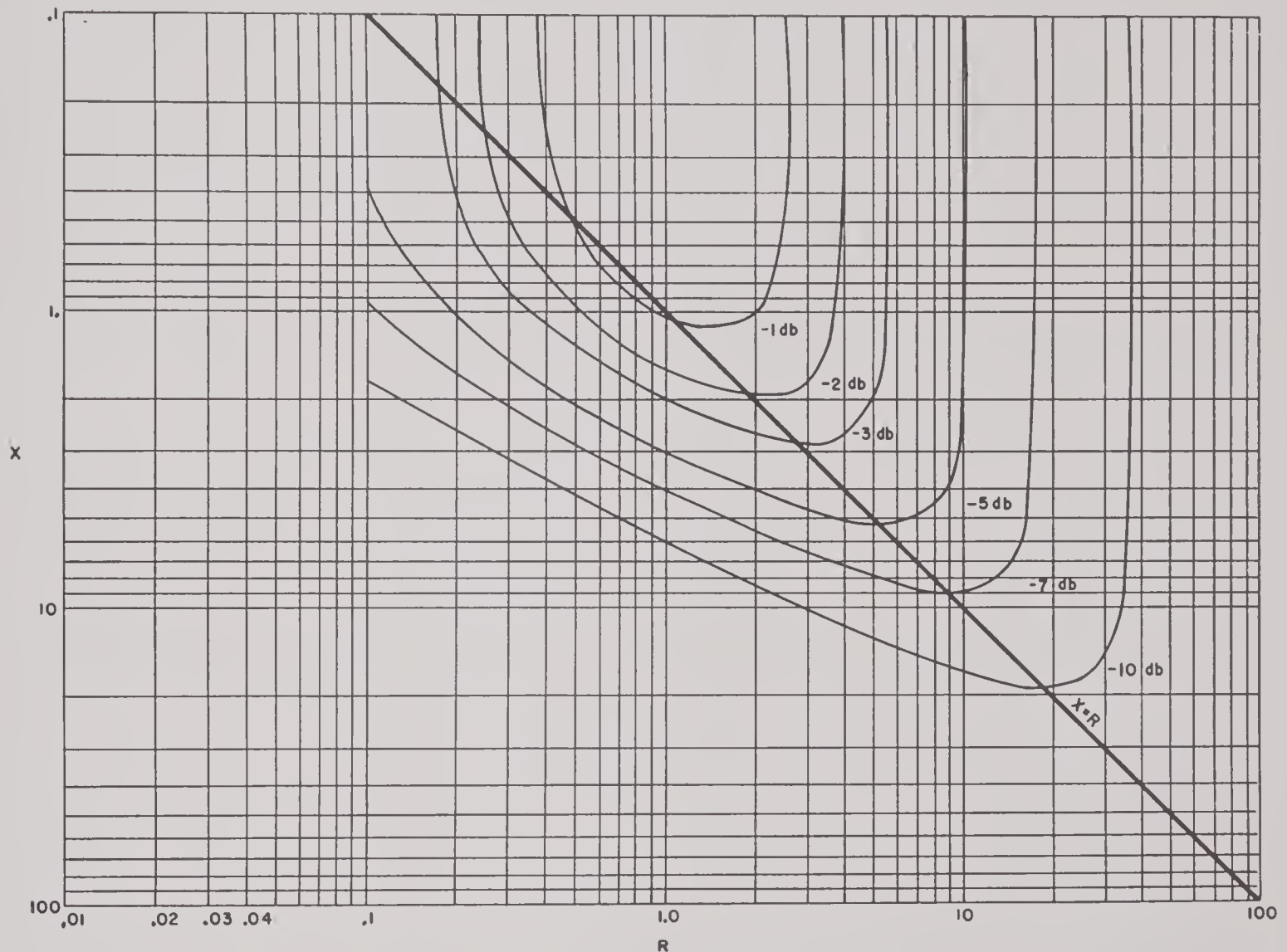


FIGURE 5. Curves showing the effect of varying the load impedance $R \pm jX$ of an ideal amplifier having an internal impedance of $1.0 + j0$ ohms. The power level contours are labeled in decibels below the maximum power capability of the amplifier when operating into a resistive load of 1.0 ohms. The reactive component (X) of the impedance is plotted as the ordinate and the resistive component (R) as the abscissa. The curve $X = R$ is plotted for convenience and its use is described in the text.

to give maximum band width, is an exception to this rule. However, because the power factor is very good and the excitation to the amplifier (if it is properly equalized) will be reduced at the frequencies where the impedance is above the optimum value, the operation will still be satisfactory.

These curves will also apply fairly well for single-ended class A_1 triode, beam tetrode, or

Class AB_1 , AB_2 , and B_2 amplifiers depart even farther from the simple basis from which the above curves were derived. The class AB_2 and B_2 amplifiers are complicated by the fact that the grids will require some driving power from the preceding stage and the amount of power required will depend both on the driving voltage and upon the load in the plate circuit of the driven tubes. When this load varies in the

manner of a crystal transducer it is almost impossible to establish general rules for the results that will be obtained under various conditions. Another factor complicating the class AB_1 , AB_2 , and B_2 amplifier design is that the power drawn from the power supply increases with grid excitation, and if the load has a low power factor, as do transducers in parts of the

pation is not to be exceeded. For the shorter pulses the thermal inertia of the anodes of the tubes can help to reduce the effect of this unusually high anode heat, and this factor will be much less important.

While the power-impedance contours for the class AB_1 , AB_2 , and B_2 amplifiers will have the same general form as those for the ideal ampli-

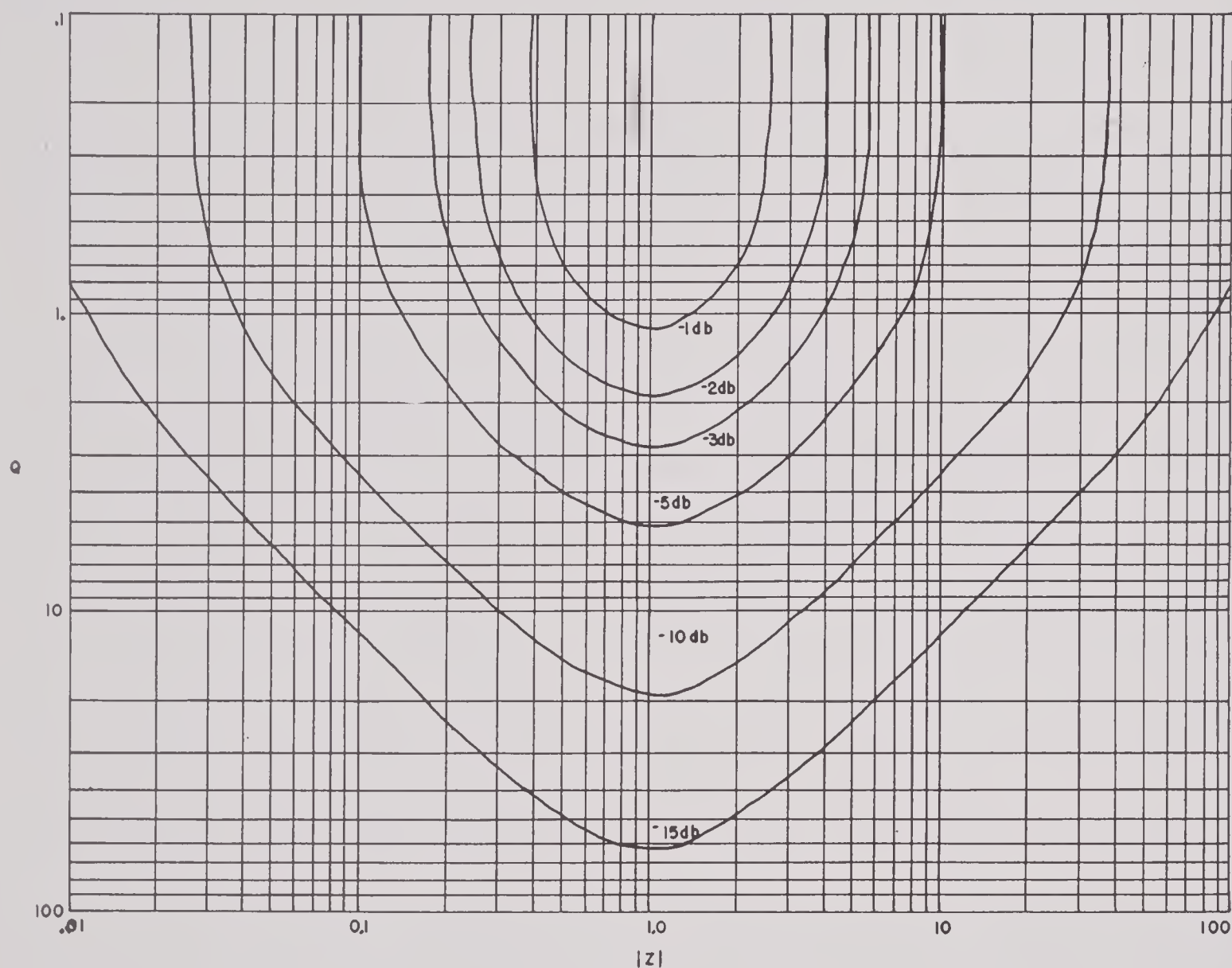


FIGURE 6. Curves showing the effect of varying the load impedance of an ideal amplifier having an internal impedance of $1.0 + j0$ ohms. The power level contours are labeled in decibels below the maximum power capability of the amplifier when operating into a resistive load of 1.0 ohms. The Q of the load impedance is plotted as the ordinate and the absolute magnitude ($|Z|$) of the impedance as the abscissa.

band, it will not absorb much of this increased power input, and the excess will have to be dissipated as heat at the anodes of the tubes. For steady-state conditions, or for comparatively long pulses, this will mean that the maximum power output of the amplifier will have to be reduced if the maximum allowable plate dissipation

is not to be exceeded. For the shorter pulses the thermal inertia of the anodes of the tubes can help to reduce the effect of this unusually high anode heat, and this factor will be much less important.

If impedances of the type given in Figure 4 are plotted on the *same coordinate paper* as Figure 7 (see Figure 8 for example) the re-

sulting plot can be superimposed on Figure 7, and by sliding the two plots relative to each other, keeping the abscissas in alignment, the effect of various impedance-matching ratios can be tried. On the plots using X and R as impedance coordinates the plots should be slid along the diagonal line so that the $X = R$ lines are

width at the 10-db down points at the expense of the midband frequencies then the transducer impedance plot should be slid down until it cuts the $R_p = 1$ line at the -10 -db contour. (See solid curve, Figure 9.) This makes the frequencies of the -10 -db points $\alpha = 0.5$ and $\alpha = 1.7$, and the midband response has been dropped to

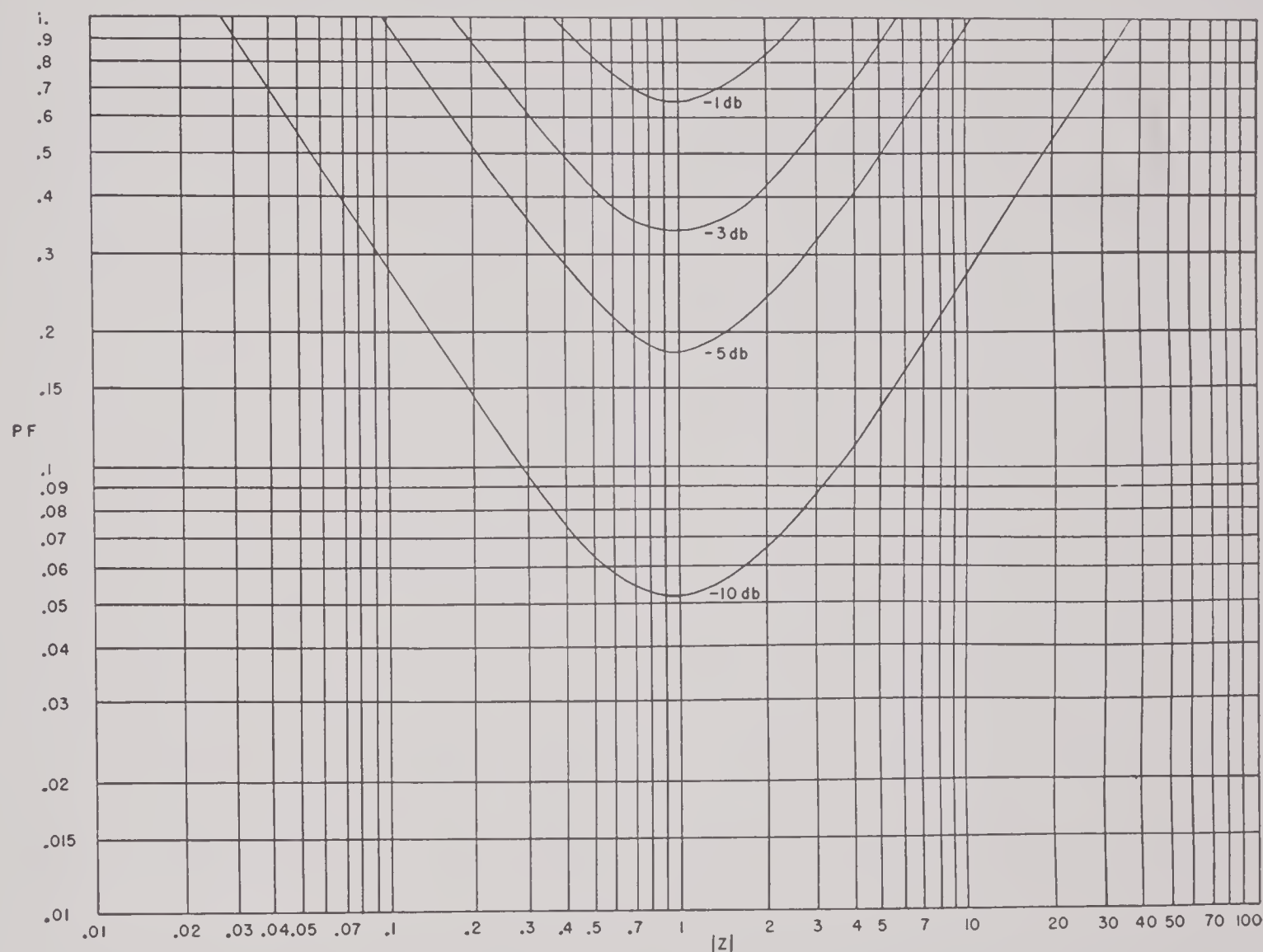


FIGURE 7. Curves showing the effect of varying the load impedance of an ideal amplifier having an internal impedance of $1.0 + j0$ ohms. The power level contours are labeled in decibels below the maximum power capability of the amplifier when operating into a resistive load of 1.0 ohms. The power factor (PF) of the load impedance is plotted as the ordinate and the absolute magnitude ($|Z|$) of the impedance as the abscissa.

kept superimposed. Taking, for example, the XCCZ2-1 and putting its impedance plot on the power-impedance plot in such a position as to make its impedance at midband fall on the $R_p = 1$ line (see broken-line curve on Figure 9), it is seen that the frequencies of the 3-db down points are $\alpha = 0.85$ and $\alpha = 1.2$, and the 10-db down points fall at $\alpha = 0.7$ and $\alpha = 1.5$ approximately. If it is desired to improve the band

nearly -4 db with the former -3 -db frequencies, $\alpha = 0.85$ and $\alpha = 1.2$, being now nearly -5 db in level.

Looking at the solid curve of Figure 9 and noting that the value of transducer impedance where it crosses the $R_p = 1$ line is equal to 58 ohms, it is seen that to achieve the indicated results the amplifier used will have to have a value of R_p equal to 58 ohms or it must be pro-

vided with an output transformer which will transform the actual R_p of the amplifier to this value. An alternative method would be to adjust the thickness of the crystals in the transducer until its impedance was of the proper value to match the particular amplifier.

It should be noted that in achieving the proper match, there are three elements that may be

the cable between the amplifier and the transducer is so short that its shunt impedance is high as compared with the amplifier-output impedance, it is often quite feasible to make the impedance of the transducer match the amplifier directly (perhaps by connecting crystals in series), thus eliminating the output-matching transformer.

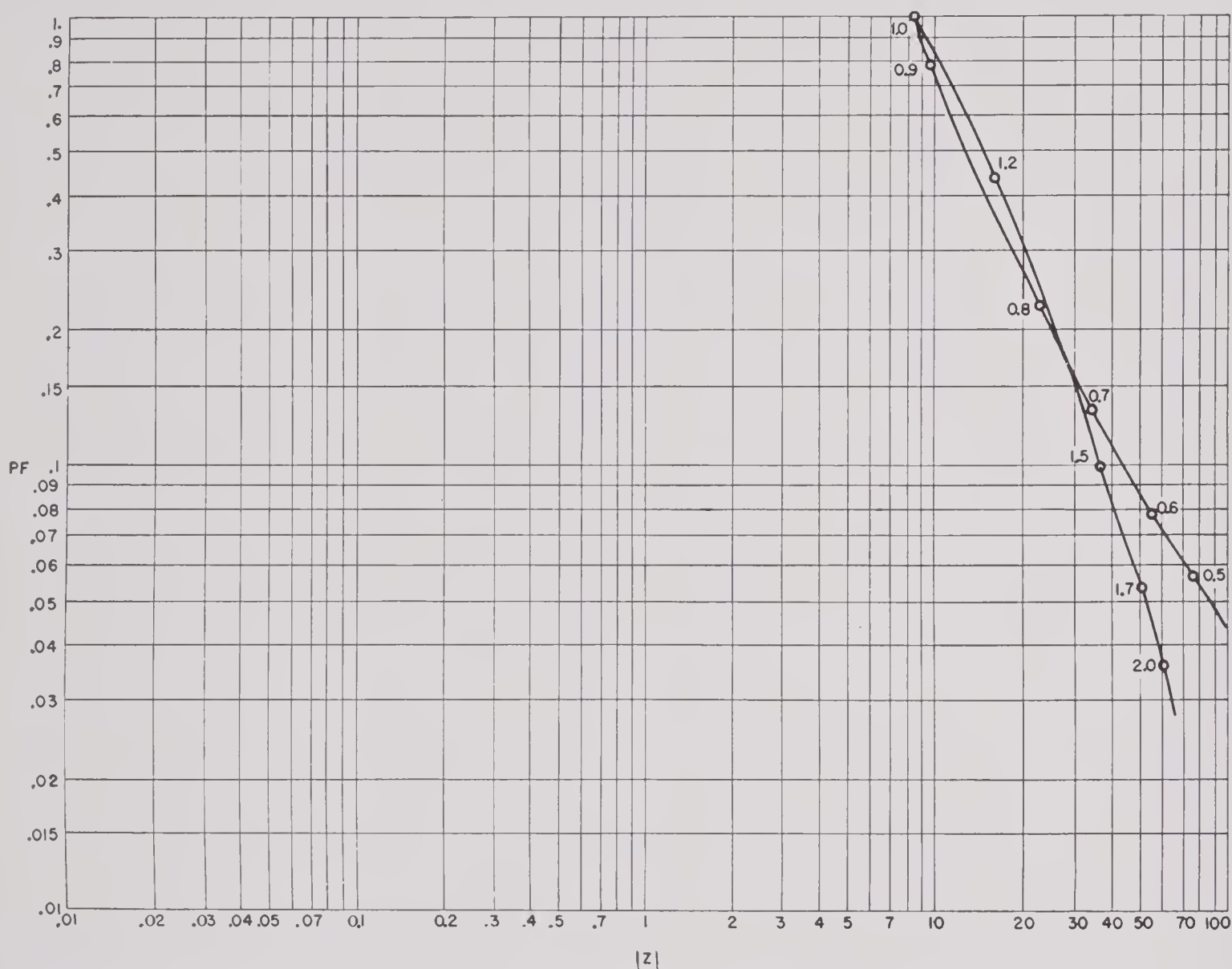


FIGURE 8. Impedance of the XCCZ2-1 crystal transducer plotted on $|Z|$ and PF coordinates. The value of α is shown at points along the curve.

varied if the whole system is being designed as a unit: the impedance of the transducer, the impedance ratio of the matching network, and the output impedance of the amplifier. By keeping this in mind when the system is being designed, it will often be found that a simple modification of one element may result in a major simplification of one of the other elements. For example, if the system is such that

In using these graphs it should be kept in mind that they show only the amount by which the power delivered to the transducer is reduced by mismatching. The actual sound intensity that the transducer delivers in a given direction is also affected by its directivity and efficiency, both of which are functions of frequency. If, for example, the transducer being matched is a highly directional unit and the desired end re-

sult is a flat pressure versus frequency response in the direction of maximum intensity then it will be necessary to compensate for the approximately 6-db per octave rise in output caused by the increase in directivity with frequency. In order to reduce this effect it will usually be found helpful to make the frequency at which the tuning coil and transducer resonate a little

ance contours, and sliding them up and down until the parts of the desired band that are lowest in response have the best possible match.

Even after the impedance match has been adjusted to give the most uniform response curve that is possible it will often be found that the results are not good enough. In this case an equalizer, as discussed in Section 5.5, should be

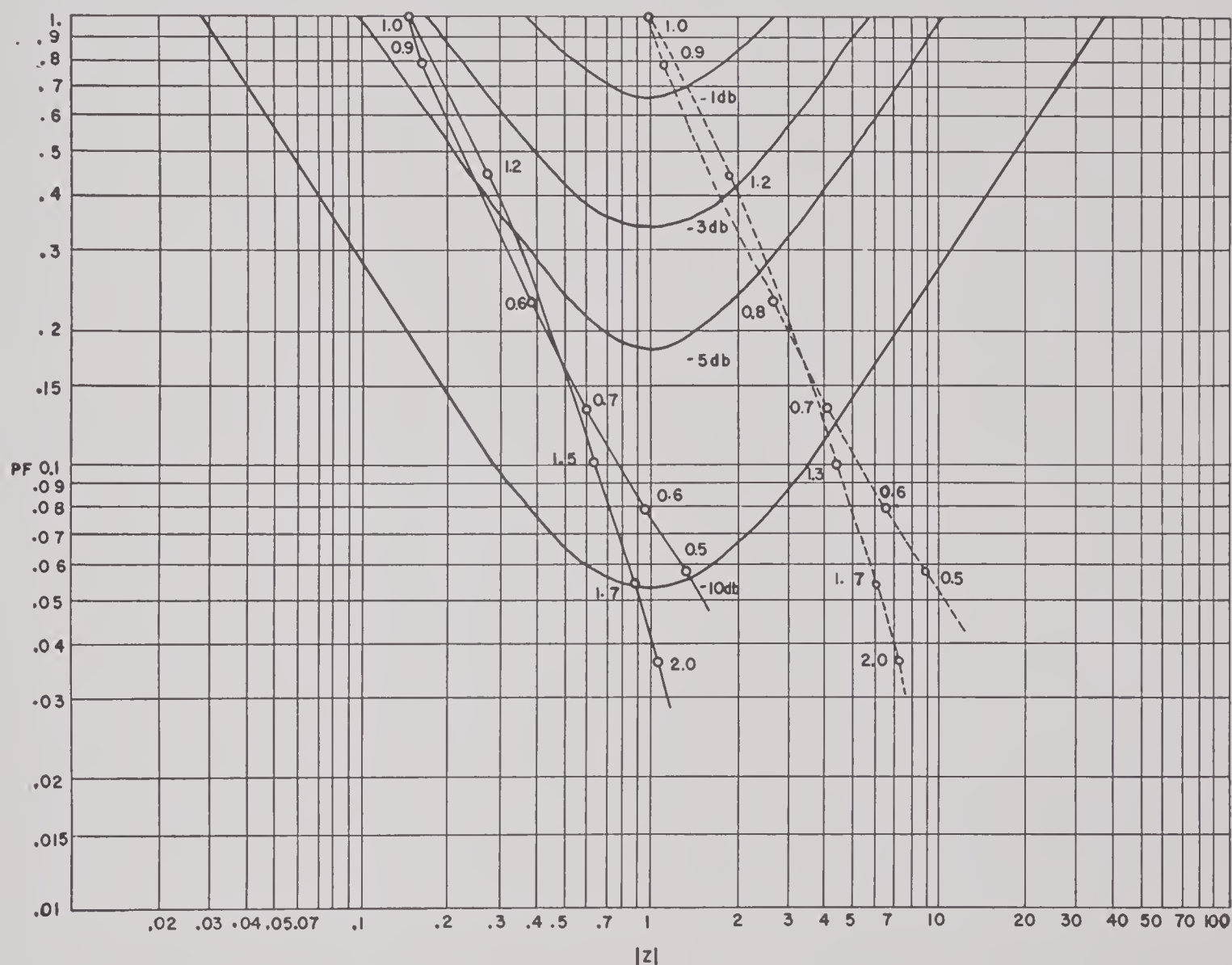


FIGURE 9. Examples of two different conditions of impedance matching for XCCZ2-1 transducer.

lower than the frequency at which the transducer is mechanically resonant. If, on the other hand, there is some source of inefficiency present that increases with frequency it may even be desirable to place this electrical resonance at some frequency higher than that of mechanical resonance. In any case the effect of changing the value of the tuning coil can be observed by plotting the impedance with different coils, superimposing these plots on the power-imped-

used to produce the final flattening of the response curve.

It should be noted that a class C amplifier may also be used resulting in very high efficiency at a single frequency when the electrical Q of the transducer plus its coupling network is high enough to reduce the attendant distortion to a reasonable value. The design of a class C amplifier for this service is quite conventional.^{1b}

It is worthy of note that many applications of crystal transducers use such short pulses that pulsed power amplifiers, as used in radar, may be utilized. The use of such amplifiers will permit smaller tubes for a given output power, or much more power from a given tube. So far as the transducer is concerned, a pulsed power amplifier will act the same as an equivalent class B or C amplifier capable of continuous operation. Since this is true, all the above statements regarding class B and C amplifiers, except those that apply to plate dissipation problems, will also apply to pulsed power amplifiers.

In considering receiving transducers and amplifiers for use with them, the design situation is found to be much simpler than the problems involving transmitting transducers. There are only two conditions that must be satisfied in the receiving system. First, the impedance match should be such that the output power of the transducer is coupled efficiently to the amplifier. Second, the noise voltage in the amplifier should be less than the noise voltage in the transducer output due to acoustic noise in the medium.

This second condition is very easily satisfied under almost all conditions because of the high transducing efficiency of crystal transducers and because of the high ambient-noise level that is encountered under even the quietest conditions of the sea. The one condition under which the amplifier self-noise is likely to be the limiting factor is that in which the pass band is in the extremely low-frequency end of the audio spectrum, and a small low-capacitance hydrophone is being used. Under these conditions the impedance of the hydrophone is very high making it extremely difficult to obtain an efficient transfer of power to the amplifier. This tendency towards lowered output under these special conditions, emphasizes the importance of the best possible impedance match between transducer and amplifier. Special precautions should be taken to keep the amplifier self-noise at a low level.

The first condition is satisfied by a procedure essentially the same as used with transmitting transducers. That is, for single-frequency operation the mechanical resonance of the transducer should be at the frequency of operation and a tuning coil should be used to cancel the

reactance of the transducer at that frequency. The resulting resistive impedance should then be transformed, if necessary, to match the input impedance of the amplifier. For wide band operation the resonance of the transducer should be at the geometric center of the band and a tuning coil should again be used to cancel reactance of the transducer at this frequency.

The power-impedance contours given in Figures 5, 6, and 7 may be used in adjusting the impedance match in exactly the same manner as with transmitting transducers. The value of R_p on the contour will in this case represent the input resistance of the amplifier. Since the power levels in receiving circuits are always quite low, the input resistance of the amplifier will be a constant, and the contours may be used without the reservations necessary in the case of power amplifiers driving transmitting transducers.

Because of the low-power levels encountered in receiving systems there is a special input amplifier that may be used to greatly reduce the effect of cable capacitance shunted across the transducer. In order to use this amplifier the connecting cable must either be a single-wire unbalanced line, or if it is a two-wire balanced line each wire must be in its own separate shield. The shield is then driven with respect to ground by an amplifier which applies to it a voltage which, as nearly as possible, should be the equal in both phase and amplitude of the voltage on the signal wire. This gives an effective guard action which will completely eliminate the effect of the signal lead-to-shield capacitance, provided the applied voltage is exactly equal to the signal voltage. If these voltages are not equal the reduction factor is equal to

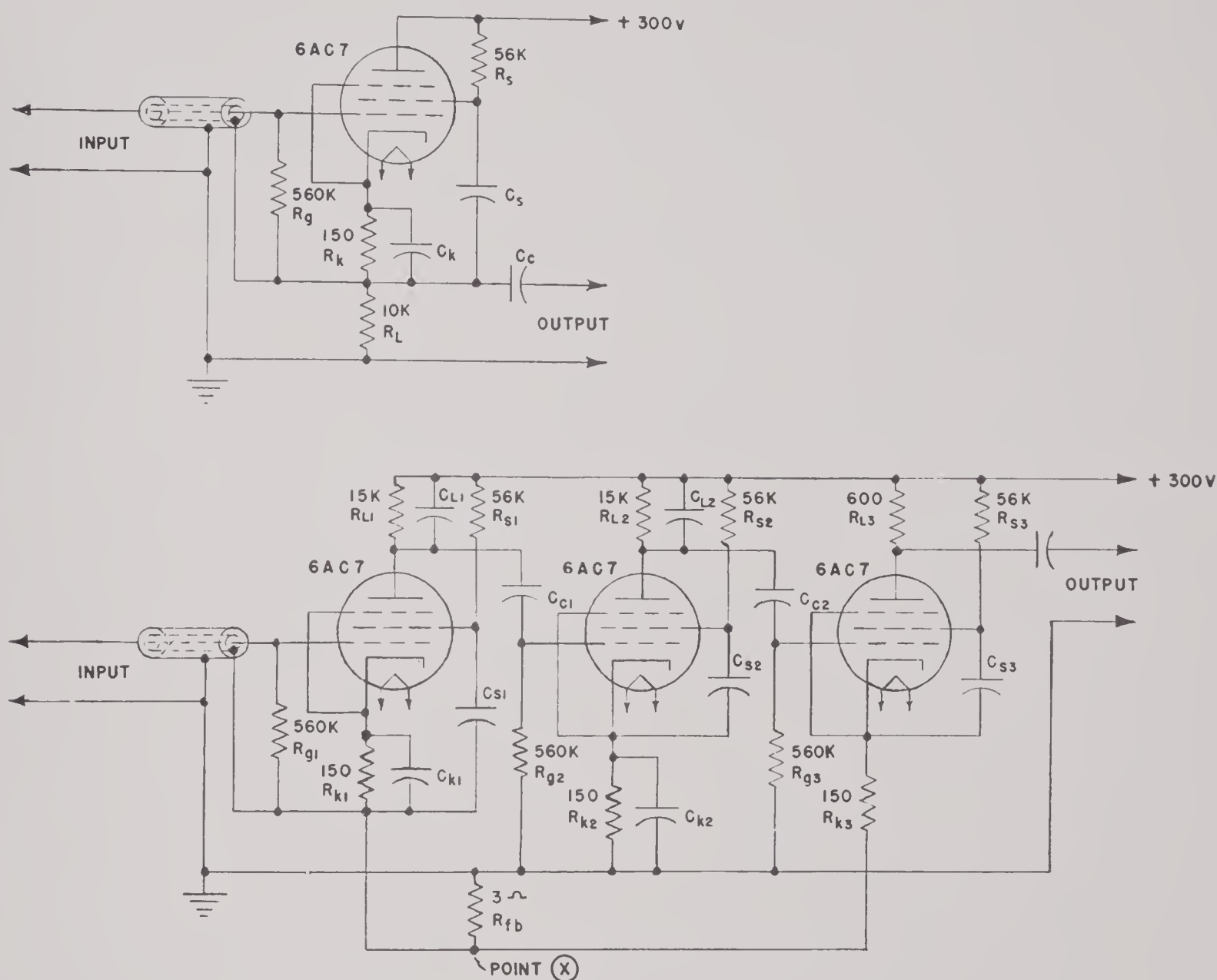
$$\frac{\text{Signal voltage}}{\text{Signal voltage-guard voltage}} \quad \text{or} \quad A + 1,$$

where A is the gain within the feedback loop.

Practical circuits for accomplishing this result are given in Figure 10. The first type of guard amplifier, using only one cathode-loaded stage, will be useful to provide a capacitance reduction factor of the order of 10, with guard-shield-to-ground shunt impedances of the order of 1,000 ohms, if a tube similar to a 6AC7 is

used. The second type of guard amplifier using two amplifier stages plus a coupling stage will give much higher values for the reduction factor and will handle much higher values of guard-shield-to-ground shunt capacitances. The actual values of input-capacitance reduction

shield-to-ground capacitance of 5,000 μmf and a high-frequency cutoff of 200 kc. If the value of the feedback resistor R_{fb} is increased by a factor of 10 the input capacitance-reduction factor will be increased to 1,000 but the maximum value of guard-shield-to-ground capaci-



A = gain measured from the grid of the first tube to point (X) with the negative return of the first stage made to ground rather than to point (X). The values of C_k , C_s and C_c should be chosen to give the required low-frequency response. The value of C_L should be chosen so that its capacitance in parallel with the input and output capacitances of the associated tubes and the stray wiring capacitances will have a shunt reactance equal to R_L at 200 kc. All resistor values are in ohms.

FIGURE 10. Circuits for guard amplifiers.

factors that can be obtained and the actual values of guard-shield-to-ground capacitances that can be tolerated, are dependent on each other and on the high-frequency cutoff of the system. With the circuit constants as given in Figure 10 the input-capacitance reduction factor will be approximately 100 with a guard-

tance that can be tolerated will be only 50 μmf , if the 200 kc high-frequency cutoff is to be retained. If the high-frequency cutoff is lowered by a factor of 10 the tolerable guard-shield-to-ground capacitance is increased by a factor of 10.

In designing a three-stage guard amplifier it

should be kept in mind that it is essentially a three-stage feedback amplifier with a very large amount of feedback. In order to avoid instability the gain and phase-shift characteristics of the amplifier, with the actual input and output loads connected, must be controlled very carefully up to extremely high frequencies. In some cases this control must be exercised to 1,000 times the highest frequency to be amplified. If additional phase-shift and gain-control networks are included in the amplifier, it is possible to obtain results somewhat better than those attributed to the simple amplifier. For example, the amount of guard-shield-to-ground capacitance that can be tolerated may be increased by a factor of about 3.

For design information for feedback amplifiers, and phase-shift and gain-control networks for use with them, refer to the bibliography.^{1c}

In applying these circuits to two-wire lines the required separate shield on each wire necessitates the use of separate guard amplifiers for each wire.

In order to minimize the possibility of stray pickup of interference in the ground system the cable used in this circuit should have an overall shield which is insulated both from the guard shield and from ground, except at one point.

This guard circuit finds particular application in the fairly common case of a small low-capacitance hydrophone to be used at the end of a long cable and at low frequencies. In connection with this application it should be noted that when the a-c return of the input-grid resistor is made to the guard-voltage circuit, as shown in Figure 10, its effective value as seen by the transducer will be increased by the same factor that the cable capacitance is decreased.

The actual voltage gain between input and output terminals of the guard amplifier will be approximately 1 in the case of the single-stage amplifier and 200 in the case of the three-stage amplifier.

5.5

EQUALIZING NETWORKS

In some applications of crystal transducers the flatness of the pass band that can be ob-

tained with the aid of a simple coupling network between the transducer and its associated amplifier is not satisfactory. In this case the frequency response of the amplifier will have to be modified in such a manner as to give the overall response of the amplifier-coupling-network-transducer combination the desired flatness over the required band.

In theory at least, an equalizer may be built to modify the amplifier response in any desired manner. In actual practice it will be found that virtually all good transducers, when coupled through the correct tuning coil to an amplifier having an impedance which gives the most efficient transfer of power over the band, will have a response curve showing a more or less flat-topped peak which will fall off with fair uniformity on both sides of resonance. (Correct tuning coil in this case is the one which cancels the reactance of the transducer at its frequency of mechanical resonance.) Such a response curve may be flattened with an equalizer consisting of a single π or T-section band-pass filter which is terminated by impedances that are higher than the design loads. A band-pass filter used in this manner gives the necessary flat-bottomed valley in the middle of the pass band with the response curve rising to peaks at the edges of the pass band. An actual example of the results obtained by using such a filter to equalize a system consisting of a receiving transducer, amplifier, output tuning coil, and transmitting transducer is shown in Figure 11. The shape of the response curve of this type of equalizer may be varied over a wide range of width of pass band and height and sharpness of the peaks at the edges of the pass band.

A design guide for this type of equalizer with the circuits used and response curves obtained is given at the end of this chapter.

If the response to be equalized is anything other than a simple resonance peak some other type of equalizer must be used. An excellent discussion of equalizers of various shapes is given in reference 3.

EQUALIZER DESIGN GUIDE

The following design procedure for this type of equalizer has been found to be satisfactory

when the usual space limitations are imposed. In the following discussion it will be assumed that the entire filter is to be small enough to fit into a can 4 in. high and 2 in. square.

The first step is to choose the nominal impedance of the filter. This should be as high as possible so as to realize the maximum possible gain from the amplifier stage which uses the filter as its plate load. In practice it will be found that the highest impedance value that can be

and 40 kc the coil that will best meet these requirements is a toroid with a powdered Permalloy ore. At higher frequencies a solenoid-type coil with a powdered iron core will be best.

The tuning capacitor C used in the π -type filter should be chosen so as to resonate with the coil L at the upper edge of the pass band, and it should resonate at the lower edge of the pass band in the case of the T -type filter. The coupling capacitor C_c should then be adjusted

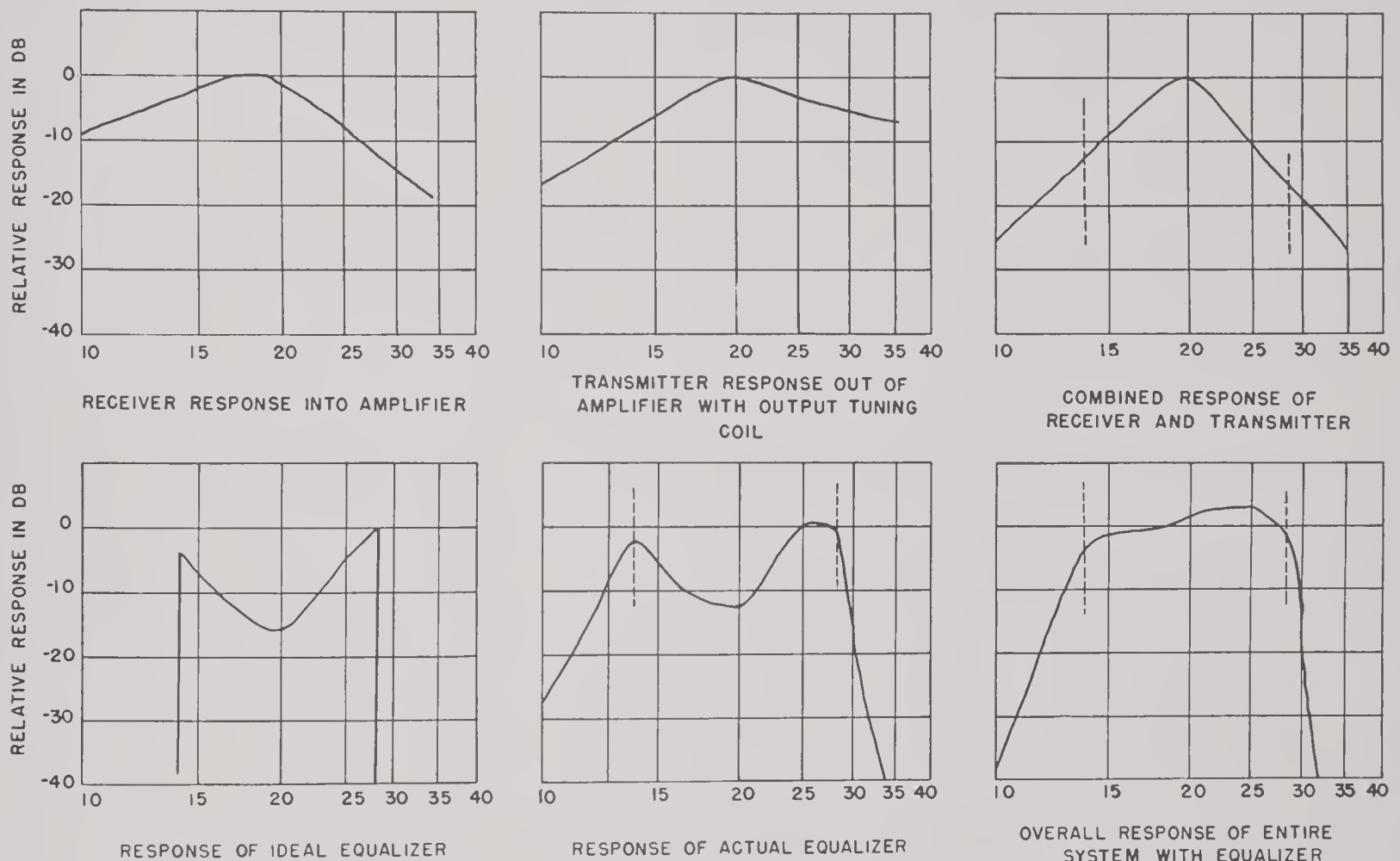


FIGURE 11. Example of results obtained by equalizing a system consisting of a receiving transducer, amplifiers, output tuning coil, and transmitting transducer over the band of 14 to 28 kilocycles. Frequency in kilocycles is plotted in the abscissa.

obtained will be about 10,000 ohms and that the limiting factor will be the coils. The procedure then, is to find the highest inductance coil that will fit into the available space and will meet the electrical requirements. The Q must be greater than 10 and the natural resonance of the coil must be at least one octave higher than the upper cutoff frequency of the filter. It will be found that at frequencies lying between 1

to locate properly the lower edge of the pass band, in the case of the π -type filter, or the upper edge of the pass band, in the case of the T -type filter. This last adjustment should be made with the R_p 's having a value of at least 100,000 ohms and with R_s shorted out.

The value of the R_p 's and R_s should then be adjusted to give the desired shape of response using Figures 12D, E, and F as a guide. It

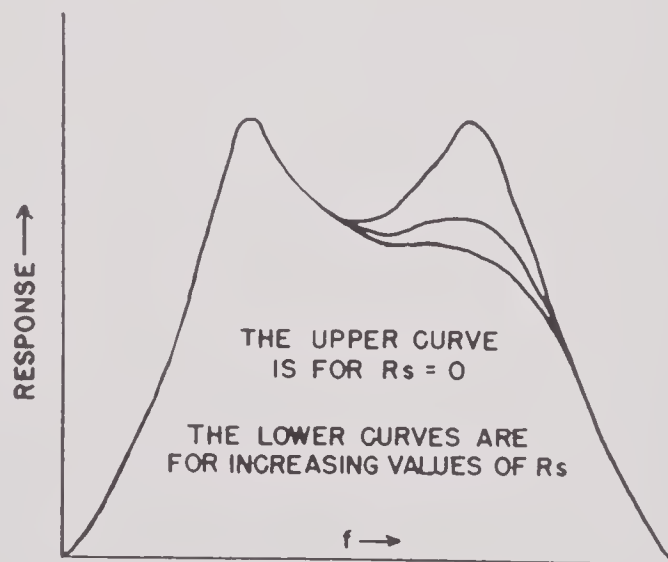
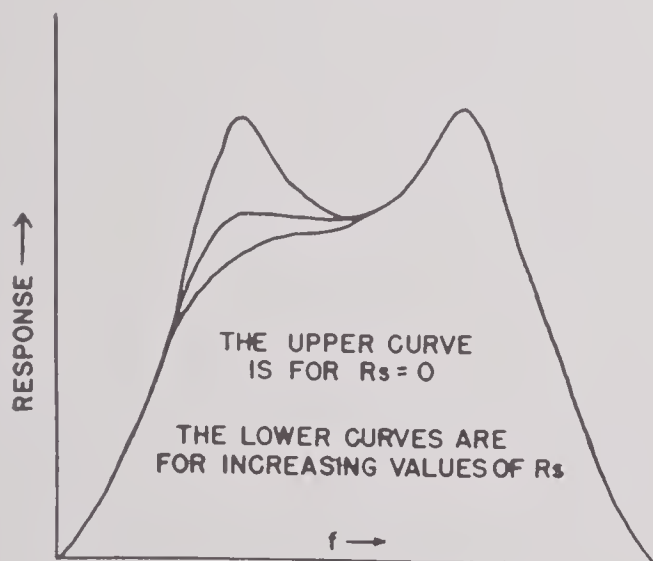
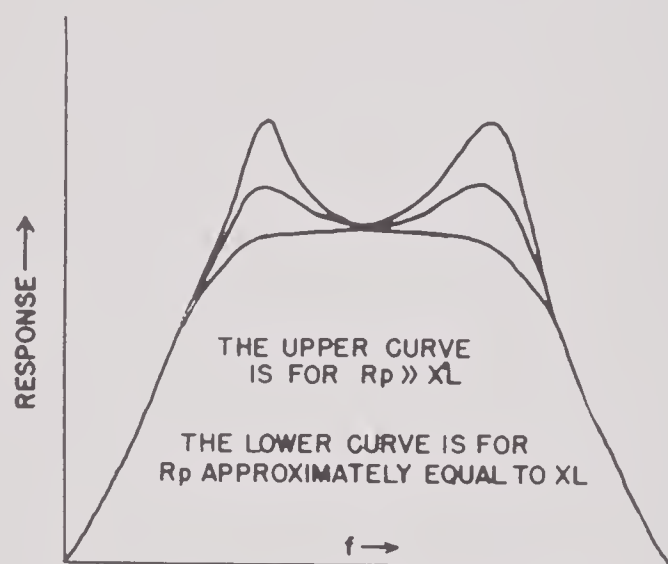
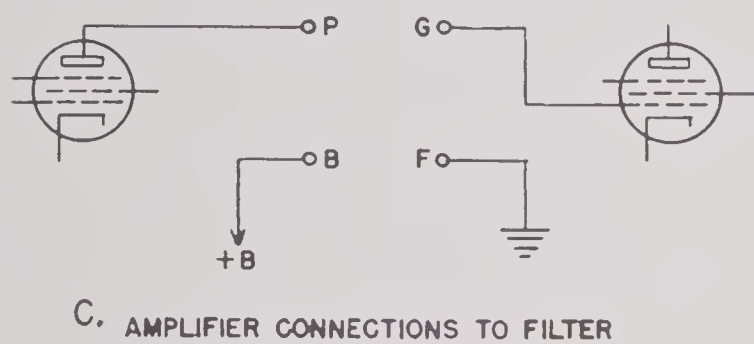
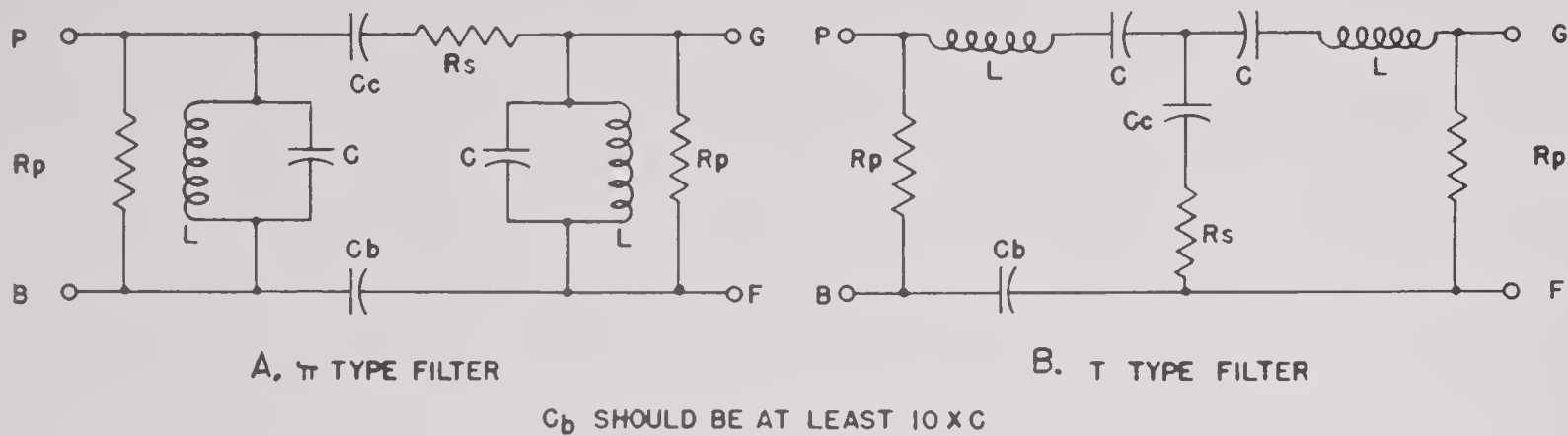


FIGURE 12. Equalizer design guide.

should be noted that if it is desired to have the response higher at the high-frequency end of the band, the π -type filter will have to be used, while if the low-frequency end is to be higher the T -type filter must be used. It should be kept

in mind when adjusting the R 's, that the R_p 's affect the height of the peaks on both ends of the band, while R_s affects the height of the lower peak only in the case of the π -type filter, and the upper peak only in the case of the T -type filter.

Chapter 6

DESIGN PROCEDURES

By *T. Finley Burke*

THIS CHAPTER is concerned with the elementary procedures involved in designing a transducer to meet given specifications. Our attitude is optimistic; the Mason circuit and its simple consequences are used, little attempt being made to anticipate the innumerable ways in which a transducer may misbehave. The design selected on this basis is by no means complete, requiring the modifications discussed in Chapter 7. However, all the major features are usually settled by this simple approach, and the preliminary design will look and act much like the final unit if design is properly carried out.

6.1 SPECIFICATIONS

The need of a complete set of performance specifications before design can start is obvious. These should result from a conference between the consumer and the designer. Specifications drawn up without such a conference are likely to request impossibilities or else to request less than optimum performance. In drafting the specifications the transducer should be regarded as one component of an integrated system, and consideration should be given whether a particular feature (e.g., flat frequency response) is best accomplished in the transducer or elsewhere in the system. Furthermore, some estimate should be made of the volume of future production in order to weigh the advantages of novel or expensive materials.

The following list of items which may require specification is more detailed than is usually required in any one instance. It is intended as a check list for suggestions.

1. Tactical use of the complete system including mode of operation.
2. Transducer to be used as transmitter, receiver or both.
3. Frequency response.
 - a. Number of db down from maximum at stated frequencies.

- b. Allowable local variations in frequency response.
 - c. Overall flatness required; allowable slope.
 - d. These properties to obtain when driven from or working into specified amplifier in specified manner.
4. Directivity patterns at specified frequencies.
 - a. Width of main lobe in horizontal and vertical planes.
 - b. Lobe suppression in horizontal and vertical planes.
 - c. Axial or other symmetry required.
 - d. Directivity index.
 - e. Extent of suppression of backward radiation.
 - f. Permissible departures from ideal.
 - g. Special features, such as *bearing deviation indicator* [BDI].
5. Power levels at frequency and direction of maximum response.
 - a. Pressure in the water at stated distance from transmitter.
 - b. Ping length and duty cycle of transmitter.
 - c. Voltage to be delivered across specified impedance by receiver for unit incident sound pressure.
 - d. Required minimum efficiency.
6. Complex impedance as a function of frequency.
 - a. Approximate magnitude required.
 - b. Tuning coils or other matching networks.
 - c. Ratio of series reactance to series resistance:
 - (1) Frequency of minimum ratio.
 - (2) Required minimum, allowed maximum.
 - (3) Specified frequency dependence.
 - d. Nature of amplifier to be used.
 - e. Length and nature of electric cables, voltage restrictions.

- f. Other electrical components.
7. Special features required.
 - a. Horizontal or vertical BDI.
 - b. *Maintenance of close contact* [MCC].
 - c. Phase steering of directivity patterns.
 - d. Low crosstalk between transmitter and adjacent receiver.^a
 - e. Other special features such as intention to operate simultaneously at two frequencies.
8. Service conditions.
 - a. Maximum and minimum ocean depth to which transducer will be subjected.
 - b. Maximum speed at which transducer will be moved through water.
 - c. Whether transducer will be rotated; streamlining to be provided.
 - d. Maximum accelerations to be encountered; dropping, depth charge, gun blast.
 - e. Temperature conditions to be encountered.
 - (1) In shipment and storage.
 - (2) In operation.
 - f. Any especially rough handling anticipated.
 - g. Weight, size, shape, and density requirements.
 - h. Corrosion problem to be expected.
 - (1) Frequency of inspection, painting, and repair.
 - i. Any special provisions for repair in the field.
 - j. Service life, whether or not expendable after single use.
- k. Other components of the system, such as a dome, which directly influence design.
- l. Mounting position on ship or other body; possible interferences from ship's hull, shroud lines, cavitation bubbles from other structures, ship's wake, etc.
- m. Required mounting holes or studs, gaskets, packing glands, terminal strips, access holes, nameplates, camouflage paint.
9. Manufacturing requirements.
 - a. Allowable cost.
 - b. Expected volume of production.
 - (1) Immediate.
 - (2) Pilot models.
 - (3) Large production.
 - c. Time allowed.
 - d. Any special manufacturing facilities available.
 - e. Should manufacturer's tests be devised?
 - (1) On components and subassemblies.
 - (2) Bench tests on full assembly.
 - (3) Water tests.
 - f. Any considerations of packaging for shipment and storage.
 - g. Any requirements for operating and service manuals to be prepared.

^a Crosstalk is best specified at a particular frequency as follows. Let the transmitter be driven in some constant (unspecified) manner so as to produce an acoustic pressure P at unit distance in the direction of maximum intensity. When the transmitter is driven in this manner, the crosstalk causes an electric signal in the receiver. If this signal in the receiver were caused by a normally incident plane acoustic wave, the pressure P_R of this hypothetical wave could be determined from the frequency response calibration of the receiver. Then the crosstalk is defined:

$$\text{Crosstalk (in db)} = 10 \log \left(\frac{P_T}{P_R} \right)^2.$$

This definition is concerned with an operationally useful quantity; it avoids distinctions between electric and acoustical couplings, difficulties in the method of measurement, and the particular character of the associated electric circuits.

6.2 CHOICE OF CRYSTAL MATERIAL

To all intents this book is limited to 45° Y-cut *Rochelle salt* [RS] and 45° Z-cut *ammonium dihydrogen phosphate* [ADP]; little is given here or anywhere else concerning 45° X-cut RS and its design parameters. In certain applications, notably in small probe units (e.g., Brush Development Company Model C-11), X-cut RS has the advantage of low impedance without serious limitations caused by temperature and field dependence. In those applications, operating far below resonance, the information given by Mason in his book¹ is adequate for design. The X-cut RS near its resonance is properly the subject of another book the size of this one, but it is the consensus that it offers no advantages to outweigh the temperature and field dependence.

In choosing between 45° Y-cut RS and 45°

Z-cut ADP the designer must have in mind all the different factors discussed in this and the next chapter. However, some generalizations may be made.

On the whole Z-cut ADP is preferable to Y-cut RS because of the greater range of temperature over which it is safe and because of the lack of water of crystallization. Probably as a consequence of the foregoing advantages, Z-cut ADP can radiate significantly higher intensity without cavitation damage (see Section 4.8). Because of the higher temperatures allowed, better cement joints can be made to Z-cut ADP; in particular, the Cycle-Weld technique for attaching crystals to rubber windows requires ADP (see Section 8.5.6).

It will be seen from Section 4.9.8 that although the constant-current and constant-voltage response curves differ, there is little to choose between when driven out of an amplifier. ADP leads to lower-impedance transducers for a given resonant frequency, a small advantage in its favor. However crystals about $1\frac{1}{2}$ times as long for a given frequency are required if Z-cut ADP is used instead of Y-cut RS; at low frequency such long crystals may not be available. Also, ADP has much lower volume resistivity than does RS, and in transducers to be operated far below resonance this might limit performance. Lastly, the "vertical-stack" design embodied in University of California Division of War Research [UCDWR] Model CY4 (see Section 6.8) is very useful for certain applications, but to date no method has been found for using this design with Z-cut ADP.

The choice is summed up by saying that Z-cut ADP is preferable unless some particular reason (such as low frequency, or vertical-stack design) indicates otherwise.

6.3 CHOICE OF BASIC DESIGN

Having chosen the crystal material, the designer must next select the basic design: clamped, symmetric, or inertia drive (see Section 4.9).

If symmetric drive is desired it is probably for a more or less nondirectional vertical stack, and Y-cut RS is required. The only other com-

mon use of symmetric drive is in small probe units (e.g., Brush Development Company C-11) in which symmetric drive is easiest and most natural in order to produce the nondirectional pattern usually required.

Because the uses to which symmetric drive is put are so specialized, no competition exists between it and the other two designs. Where symmetric drive is good it is so much better, and where it is poor it is so much worse, that the choice is clearly marked.

Symmetric drive is unexcelled for line sources (vertical stack) which are to have moderate directivity in one plane and to be more or less nondirectional at right angles. However such vertical stacks have an inherent power limitation dependent upon the radiating area; if the area is insufficient there is nothing to be done but abandon the design in favor of a cylindrical unit using inertia or clamped drive.

In almost every case inertia and clamped drives compete. The selection depends upon the details of the problem and upon personal opinion. The pros and cons may be summarized.

1. Clamped drive advantages:
 - a. Oldest style; best understood.
 - b. Inherently rugged.
 - c. Naval Research Laboratory [NRL] unit construction eliminates many troubles from backing-plate vibrations.
 - d. Relatively high radiation impedance in equivalent circuit diminishes effect of a given loss resistance.
 - e. Oil allows high voltages.
2. Clamped drive disadvantages:
 - a. Usually efficiency is at least 2 or 3 db below 100 per cent. Probably viscous losses in oil and cement cause this.
 - b. Heavy.
 - c. Relatively higher voltage required for given power output.
 - d. If large backing plates or oil cavities are used, spurious vibrations may harm patterns or response.
3. Gas-filled inertia drive advantages:
 - a. Glued joints are not at point of high stress, thus give less trouble.
 - b. Patterns usually excellent.
 - c. No oil to give viscous losses.

- d. Efficiency usually very high.
- e. Performance highly predictable.
- f. Relatively lower voltage for given power output.
- 4. Gas-filled inertia drive disadvantages:
 - a. Difficult to strengthen window in large units.
 - b. Relatively new; Cycle-Weld cement not tested over many years.
 - c. Relatively low radiation resistance in equivalent circuit makes a given loss more important.
 - d. Special filling with Freon (or similar) gas required to allow high voltage.

Oil-filled inertia drive is subject to the worst troubles with clamped drive. These are viscous losses, spurious modes, etc. On the other hand it has few of the advantages of gas-filled inertia drive.

The curves showing response when driven by an ideal amplifier (see Section 4.9.8) indicate that there is little reason to choose one design over the other on the basis of Mason theory; the choice must be based on the features inherent in the present methods of construction, and is subject to change as improved designs appear and as more is learned of present design.

that frequency; this may then be corrected for the radiation reactance expected.

If a crystal is to be mounted on a clamping backing plate (i.e., $\frac{1}{4}$ wave thick at resonance), the backing plate should be regarded as a mirror in which the crystal sees its own image. The resonant frequency is then that predicted by equation (62) of Section 3.2.3 for a crystal as big as the clamped crystal *plus its image*. For infinitely slender crystals the clamped frequency would be exactly one-half the free-free frequency. However for a crystal having finite width, only the length is doubled by the mirror; the width-length ratio is lessened, and the clamped frequency is somewhat higher than one-half of the free-free frequency. The limitations on choice of shape are the same as for inertia-drive crystals.

The suggested upper limits on the width-length and thickness-width ratios are approximate; the chief reason for the limitation is to diminish the fluxing of the electric field. The dielectric constant in the X and Y directions in ADP is about 56, but the piezoelectric constant is very small. Thus the dielectric constant encourages fluxing but no serious mechanical effects result so that the effect results only in an increase of Q_E with consequent narrowing of band width.

The dielectric constant of Y-cut RS is 10.0, whereas that in the X direction may be hundreds or even thousands depending on field and temperature. Thus lines of electric flux may bend into the X axis only too easily. In the X direction D is nearly as great as in the Y, so this fluxing couples in very important unwanted properties of X-cut RS. For this reason it is more important to keep good shape factors in Y-cut RS than it is in Z-cut ADP.

A second reason for minimizing the shape factors is to diminish the losses in glued joints. The cemented face of a crystal is subject not only to normal forces but also to tangential, coupled in both directions by Poisson's ratio, and in the width by piezoelectric coupling. This results in a tangential motion of the cemented face, of amplitude proportional to the distance from center. This tangential motion puts the glued joint in shear, a force leading to large viscous losses. Obviously these losses are mini-

The next design step is the selection of the size of crystal. This is rather simple. It is always desirable to place the resonance of the transducer at the geometric center of the specified operating band of frequencies. If the crystal is to be used in an inertia drive the dimensions are obtained from equation (62), Section 3.2.3. The only limitation is that it is well to keep the width-length ratio less than $1/2$ and the thickness-width ratio less than $1/2$.

The only uses to which symmetric drive is put are such that the radiation reactance lowers the resonance significantly; for example, in UCDWR Model CY4 the observed resonance is $22\frac{1}{2}$ kc in water although the resonance in air is 27.6 kc. The uncorrected size for a given frequency is the same as the inertia-drive size for



mized by keeping the $L_w L_t$ face area, particularly the width, as small as possible.

There is undoubtedly a dependence of the electromechanical-coupling coefficient k on shape factor, and a maximum may occur for some shape. However the effect seems to be small, and the above considerations of fluxing and viscous loss overshadow it.

6.5

DESIGN OF ARRAY

Having selected the crystals and the basic design, the next step is to lay out an array. This really involves two steps: choice of the array for directivity pattern purposes and then for power handling capacity.

For the purposes of meeting pattern specifications one may forget about crystals. The transducer is thought of as an array of radiating surfaces undergoing normal motion. Within any one zone the amplitude and phase is usually considered uniform; various zones are usually driven at the same phase, but perhaps at amplitudes in integral-number ratios of some one zonal amplitude. The problem then is to so adjust the shapes and relative amplitudes as to produce the desired pattern. In doing this one makes use of theory which embodies many simplifying assumptions (e.g., for plane arrays: an infinite baffle); it is very fortunate that the majority of transducers do not misbehave seriously, and agree rather well with this theory. The directivity pattern functions for line sources, arcs of circles, squares, circles, etc., are available in the literature² and are discussed in this book (Chapter 4). From these an array is selected.

The second aspect of design of the array is the problem of distributing crystals in such manner as to produce a radiating surface which approximates that selected. Crystals are most easily handled if all alike, and it is easiest to produce variations of velocity amplitude by connecting pairs, triplets, etc., in series, paralleling the groups in phase. For this reason the array selected should have integral amplitude ratios and the number of different zones should be a minimum. In fact adequate lobe suppression can almost always be achieved by just two zones of different amplitude.

Having decided to connect crystals in series in certain zones if needed, the crystals are laid out in such manner as to facilitate the attachment of foils for electric connection. This layout requires patience, ingenuity, and some practice to prevent large voltage drops across small spaces, etc. In making up the layout the following rules are followed.

1. There should be sufficient crystal area to radiate the required power (see Sections 4.4 and 4.8).
2. The available area should be only about 60 to 80 per cent filled by crystals (see Chapter 7).
3. The crystals should be arranged in groups (see Chapter 7).
4. The center-to-center distance between adjacent groups should not exceed 0.8 wavelength (see Section 4.2.4); for safety 0.5 wavelength is preferable.

Crystals are rectangular, and are most naturally composed into plane rectangular arrays. If a long rectangle is desired, this is very convenient. However, if a circularly (axially) symmetric pattern is desired this is a temptation to use a square array; circular arrays have much more desirable patterns than do squares. The task of approximating a circle with a number of rectangular crystals is unpleasant but justified by superior patterns and lobe suppression.

A typical plane circular array is shown (one quadrant) in Figure 10.

6.6

EXTERIOR CASE

Most commonly the exterior case of a transducer is steel with a rubber window. If the steel is sufficiently thick, corrosion is not a great problem. Occasionally bronze cases are used to retard corrosion, but if real corrosion resistance is required, Monel metal, *passive* 18-8 stainless steel (Type 304 or 316), or *passive* Inconel must be used. Metallic platings such as galvanize, cadmium, or nickel actually *accelerate* corrosion by electrolysis.

For small volume production cast cases are most convenient, but in large quantity forgings are likely to be superior.

Only Monel or passive stainless-steel screws should be used, and it is advisable to protect

them by tar. Socket-head screws are preferable to slotted-head.

Where possible, furnace copper brazing is an excellent means of fabricating steel parts; very strong watertight joints are easily obtained, and a joint may be inspected visually. Such bonds must be protected from electrolytic corrosion by tar or by a good paint such as Amercoat (see Section 8.7.5).

Sound-water [qc] rubber is superior to any other for acoustic windows, but a neoprene tire stock (40 per cent carbon black) has been used successfully in relatively thin flat windows before plane parallel arrays.

If gas-filled inertia drive is used it may be necessary to stiffen the window. This may be done by molding steel bars of appropriate shape into the rubber (see Figure 7). Since an array should contain crystals grouped together with spaces between groups, the steel bars can be arranged to occupy these spaces. Usually the resulting directivity patterns are not disturbed.

For symmetric drive units ordinary tin-can metal has been used. This use has been limited to expendable units in which corrosion is no problem, and has been at relatively low frequency (25 kc). Even at this frequency the performance is handicapped a little, and such material probably cannot be used much above 50 kc without noticeable effect on the transducer.

In some units a small cylindrical rubber sleeve has been used as outer case and window. To stiffen the sleeve a perforated metal cylinder was forced inside the rubber. This provided considerable strength, but at the expense of poorer performance. If such a perforated metal cylinder is put *outside* the rubber, care must be taken to prevent entrainment of air bubbles; a screen of bubbles on the face of a transducer virtually prevents radiation of sound.

The problems of design of the exterior case for strength, streamlining, assembly, cost, weight, are engineering problems of no great complexity and are not rightly part of this book.

6.7

RESPONSES

Having selected the kind, size, number, and array of crystals, the predicted performance

(Mason theory) is obtained from the data in Section 4.9.8.

The first step is to evaluate the constant R appropriate to the transducer. From this the complex impedance without coils is obtained. If desired a series tuning coil may be readily calculated in.

Using R , the power radiated by constant voltage, with or without coils, and the power radiated when driven by an ideal amplifier are easily obtained from the curves in Section 4.9.8.

If the array is plane the directivity index may be estimated from Section 4.4. This will allow the calculation of acoustic pressure from the radiated power obtained above. Receiver responses may be obtained from the transmitter responses by reciprocity (Section 4.2.3).

If the predicted response curve does not have the desired shape with frequency an equalizing network of some kind is required. Preliminary estimates of this network may be made, sufficient to allow for design of a container if it is necessary. For this the power factor and $|Z|$ are helpful, and may be obtained from Section 4.9.8. Final design of such a network (see Chapter 5) should await the calibration of the completed transducer.

If the response is flattened by an equalizer it is likely that the maximum power output is limited by voltage breakdown at the ends of the frequency band (see Section 4.8). If this voltage is known the maximum possible acoustic pressure is easily calculated. However this voltage is so dependent upon the care exercised during assembly that no estimate can be made here.

It must be emphasized that the response curves predicted in Section 4.9.8 assume the transducer to be perfectly efficient. Inefficiency will lower the level and often narrows the band width, and perhaps introduces extra peaks and dips in the curves.

6.8

EXAMPLES OF VARIOUS STYLES

It may be helpful to the reader to examine examples of transducer design. The accompanying photographs, Figures 1 through 7, together with others in this book, show many of the features discussed. No claim is made that these



units are outstanding, but neither are they poor. In all instances they are models designed by UCDWR.

SYMMETRIC DRIVE: CY4, KC2

Both contain 45° Y-cut RS arranged in a single vertical stack; filled with castor oil and contained in a tin can. Both operate in the vicinity of 20 kc. See Figure 22.

CLAMPED DRIVE: GA14Z, JB4Z, CP10Z, CQ4Z, CQ8Z, FG8Z

In every example the transducer contains 45° Z-cut ADP crystals cemented to a porcelainized-steel backing plate. The motor is contained in a heavy steel exterior case with a rubber window.

Resonant frequencies range from 24 to 60 kc in these examples. It will be noted that the two CQ models are dual transducers containing a GA14Z and a CP10Z motor.

INERTIA DRIVE: FE2Z, GD34Z

Both units contain 45° Z-cut ADP crystals attached to a neoprene window by Cycle-Weld cement. The FE2Z was designed to have a broad pattern in one direction and a very sharp pattern in the other with excellent lobe suppression. This was achieved, and the efficiency is good. GD34Z was designed as a test of the feasibility of strengthening rubber windows by steel bars. The results were entirely satisfactory, the efficiency high, and the patterns good.



FIGURE 1A. Interior of the KC2 transducer.



FIGURE 1B. Exterior of the KC2 transducer.

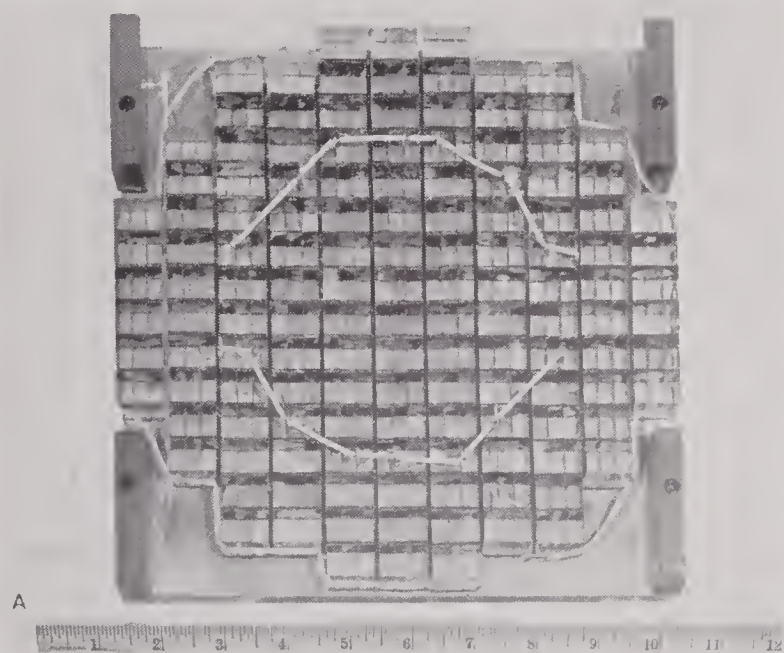


FIGURE 2A. Interior of the GA14Z transducer.

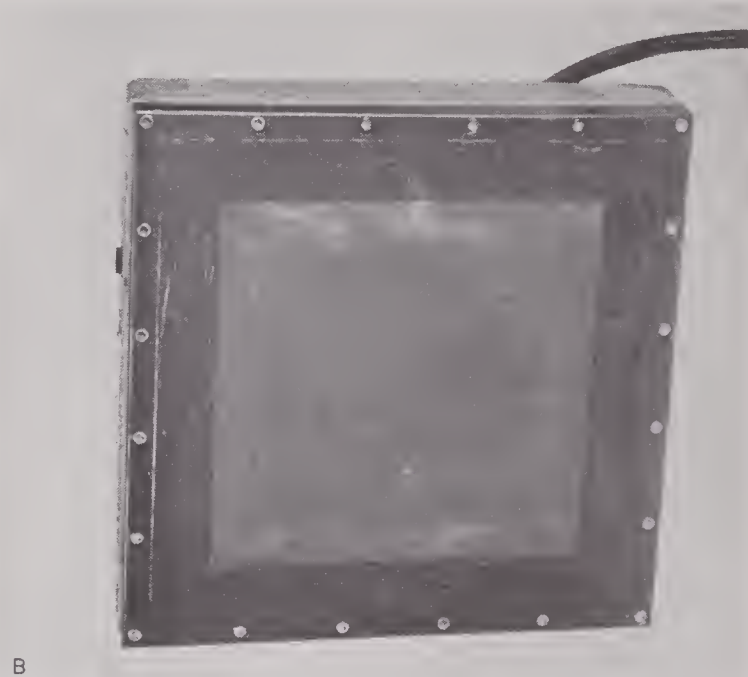


FIGURE 2B. Exterior of the GA14Z transducer.

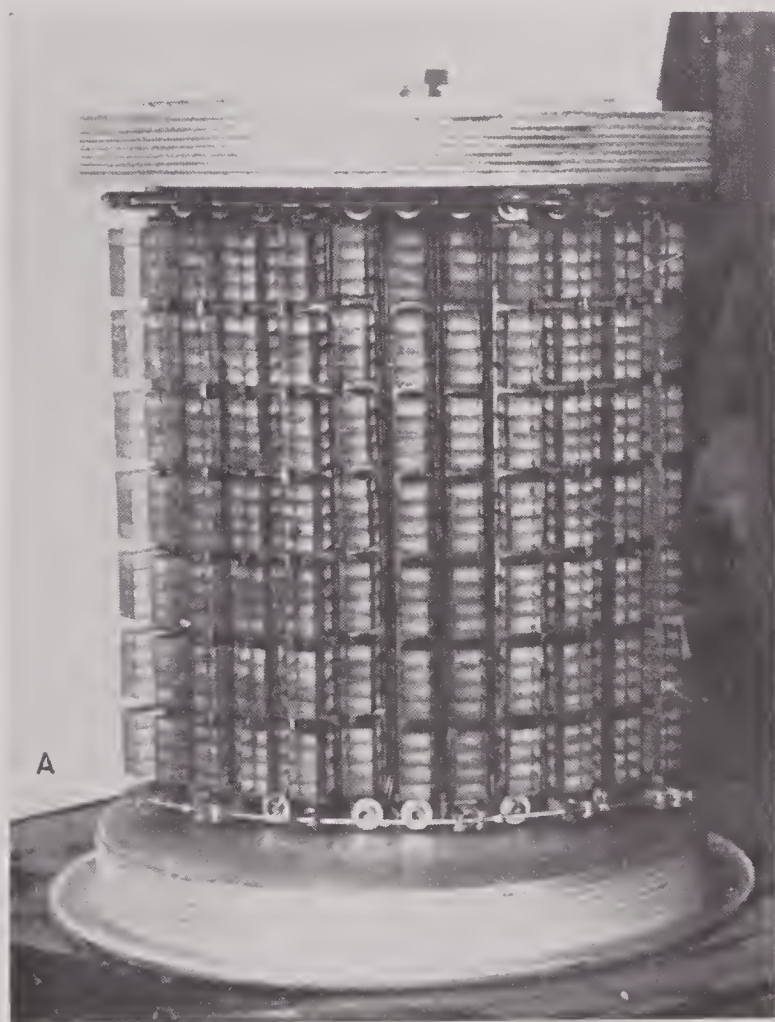


FIGURE 3A. Interior of the CP10Z transducer.



FIGURE 3B. Exterior of the CP10Z transducer.

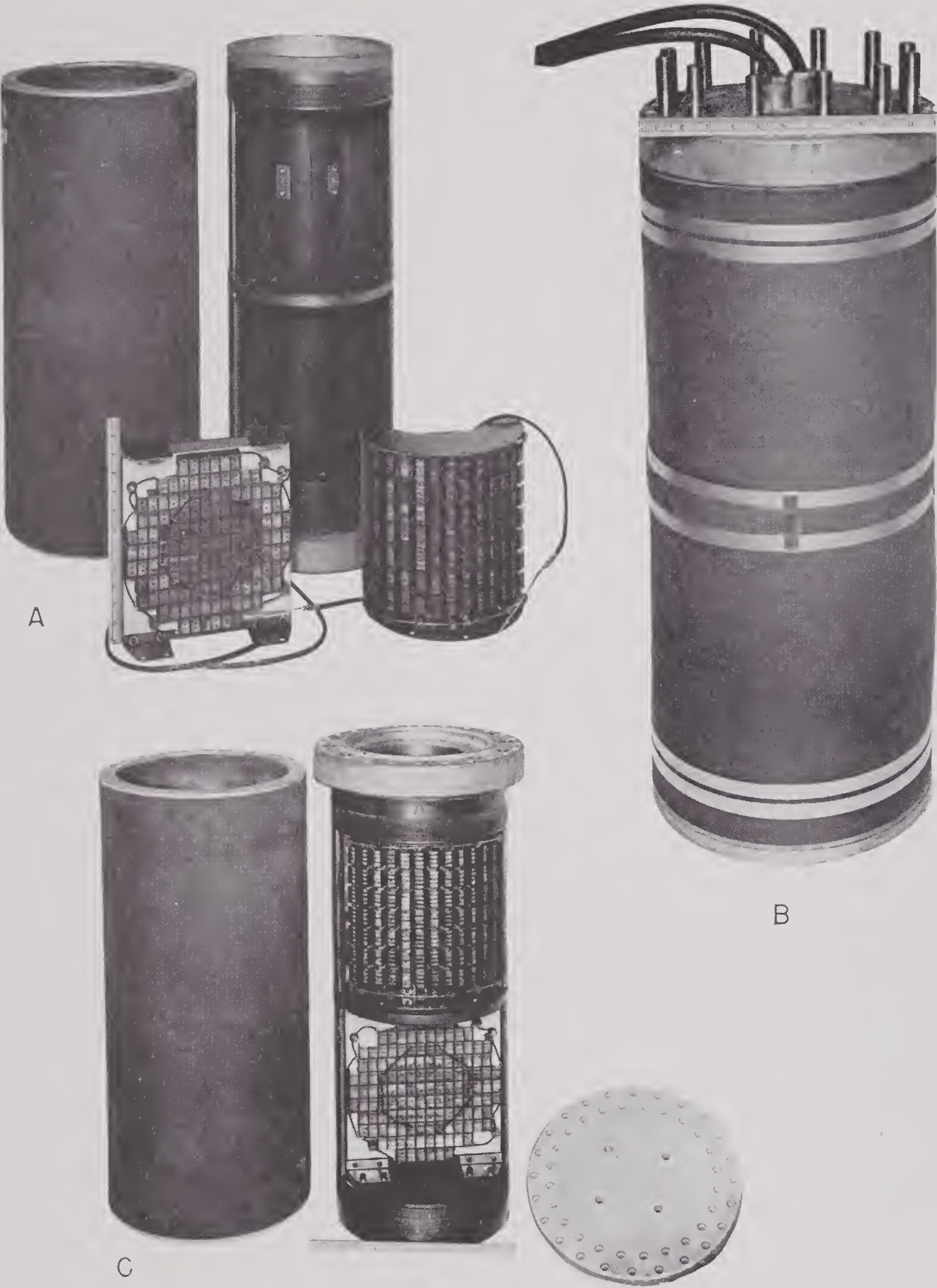


FIGURE 4. Interior, exterior, and assembly of the CQ4Z transducer.

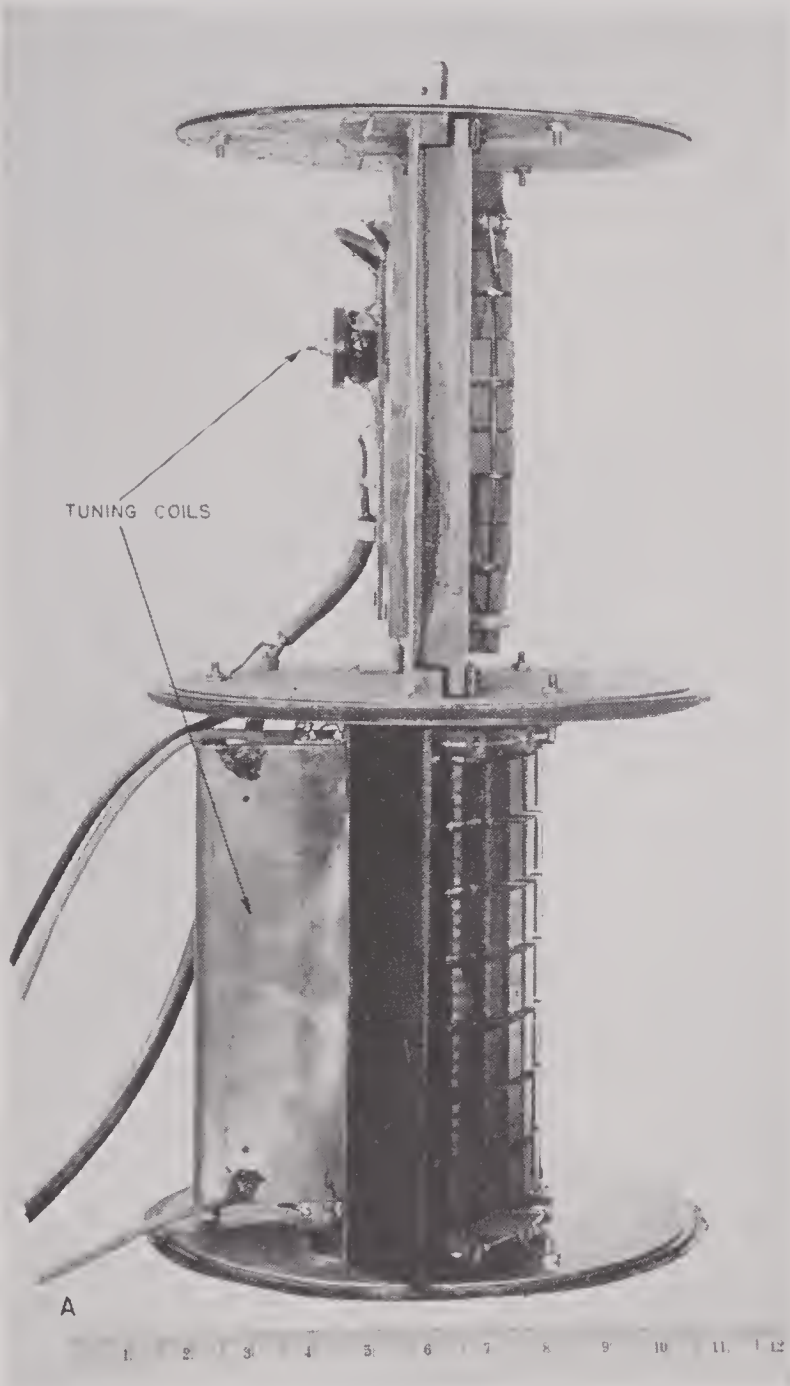


FIGURE 5A. Interior of the CQ8Z transducer.



FIGURE 5B. Exterior of the CQ8Z transducer.



FIGURE 5C. Assembly of the CQ8Z transducer.

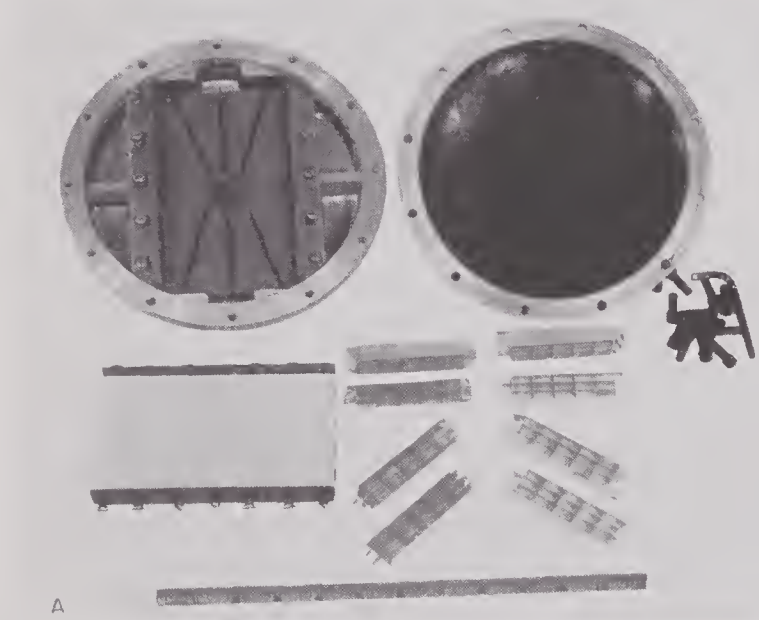


FIGURE 6A. Assembly of the FG8Z transducer.

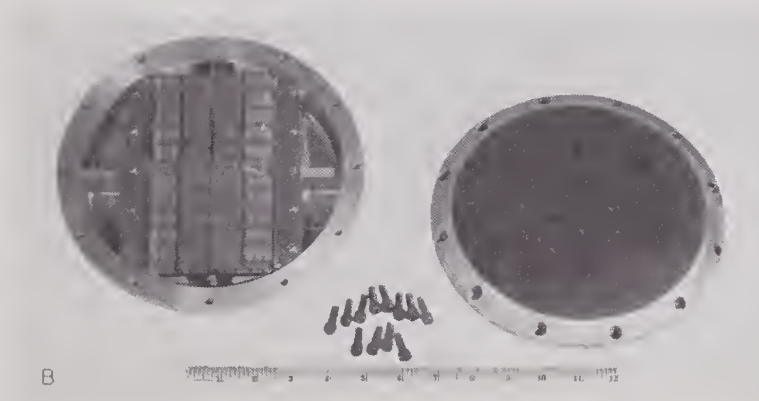


FIGURE 6B. Assembly of the FG8Z transducer.

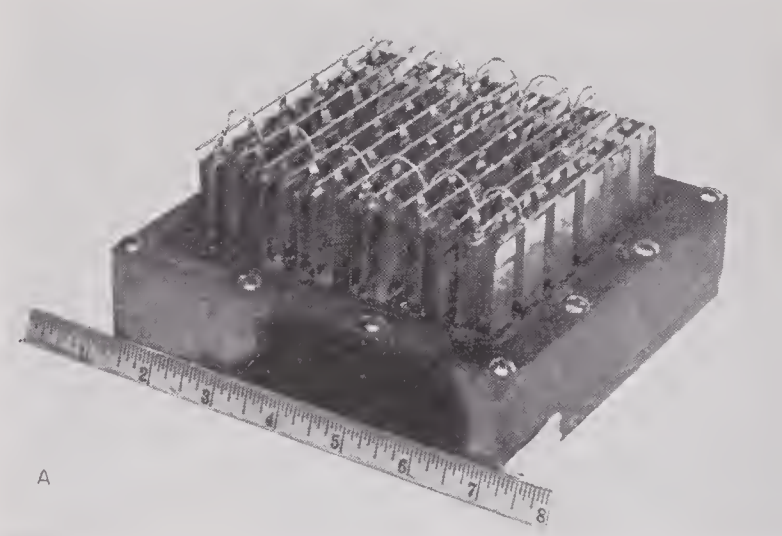


FIGURE 7A. Interior of the GD34Z transducer.

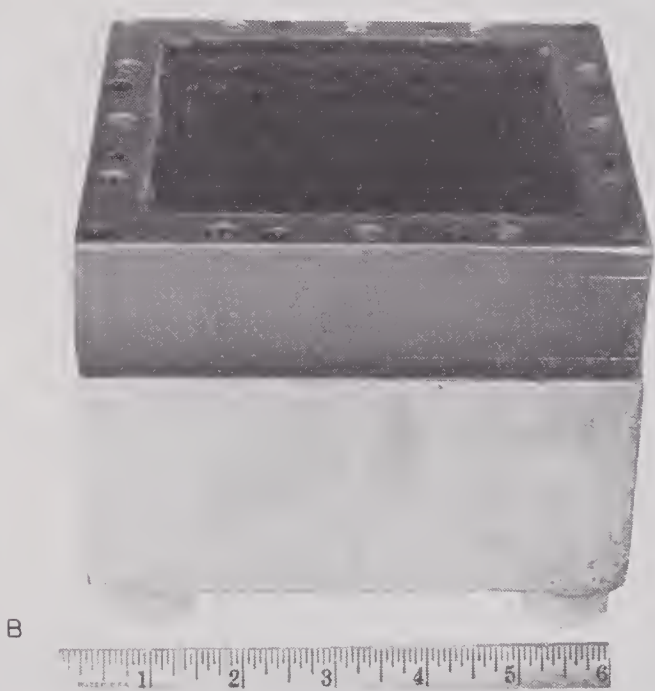


FIGURE 7B. Exterior of the GD34Z transducer.

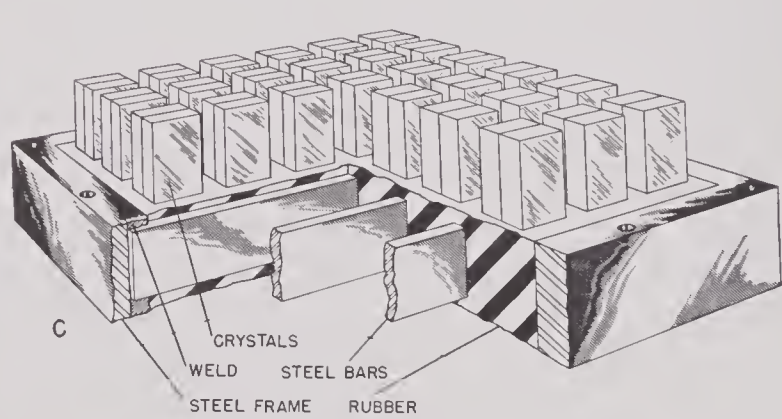


FIGURE 7C. Cutaway of the GD34Z transducer.

6.9 ANALYSIS OF THREE DESIGNS

In this section we review the design procedures which led to three transducers constructed by UCDWR, and we compare the predicted behavior with observation. It must be remembered that one phase of design is the process of recalling things which happened long ago; this backlog of experience is a prime attribute of any successful designer. It must also be borne in mind that these units contain such things as foam rubber, the reasons for which are discussed in the next chapter.

6.9.1 Clamped Drive: JB4Z

SPECIFICATIONS

This transducer was requested by a UCDWR group for use with an experimental echo-ranging sonar system. At first only one unit was to be built with a remote possibility of large-scale production. To date only one or two more have been built.

It was requested that the array be flat and circular roughly 15 in. in diameter so as to resemble the JK transducer built by Submarine Signal Company. The system was to operate over a ± 3 -kc band width centered at 24 kc, and was to radiate very short pings of high intensity. Ping power of 1 kw was contemplated as a working hypothesis. No lobe suppression was requested and the exterior did not have to be streamlined, at least in early models.

In the first design conference it was evident that this would fit naturally into the J-style exterior case designed by UCDWR but resembling very closely the spherical JK housing. Some of these parts, including the backing plates and molded neoprene windows were on hand.

In this same conference it was agreed that series coils tuning at the transducer's resonance would be advantageous, provided resonance was fairly well-centered in the band. Series coils were to be mounted inside the transducer but would be selected after calibration of the transducer to determine its impedance and frequency response.

It was suggested that at a later date horizontal or vertical BDI might be useful, so it was

decided to wire the four quadrants independently and make all eight terminals available.

CHOICE OF CRYSTALS

The request for very high voltages and acoustic intensities clearly indicated the choice of ADP.

CHOICE OF BASIC DESIGN

The J-style case mentioned above was a convenient starting point since the parts were on hand. This is designed as a backing-plate device, and, while possible, it would be tedious to convert this to inertia drive. In retrospect it appears that the JB4Z which resulted was quite successful; an inertia-driven device would undoubtedly have been equally successful.

CHOICE OF CRYSTAL SIZE AND SHAPE

Among the parts on hand were steel backing plates $\frac{3}{4}$ in. thick ready for use. If possible, crystals should be chosen to use these plates.

In Chapter 7 it is stated that resonance will occur when a crystal and backing plate satisfy:

$$Z_c \tan \theta = -Z_B \tan \phi. \quad (1)$$

In this instance:

$$\begin{aligned} Z_c &= 5.83 \times 10^5, \\ Z_B &= 39 \times 10^5, \\ \phi &= 0.381 \times 10^{-5} \omega. \end{aligned}$$

There were on hand Z-cut ADP crystals $1\frac{1}{2} \times \frac{1}{2} \times \frac{1}{4}$ in. Ignoring the finite width correction for the moment, for these crystals

$$\theta = 1.176 \times 10^{-5} \omega.$$

Thus the resonant frequency for a $1\frac{1}{2}$ -in. long ADP crystal cemented to a $\frac{3}{4}$ -in. thick steel plate would be the *smallest* value of ω which satisfies

$$\tan (1.176 \times 10^{-5} \omega) = -6.7 \tan (0.381 \times 10^{-5} \omega).$$

The solution is

$$\omega = 1.525 \times 10^5,$$

or

$$\begin{aligned} f &= \frac{\omega}{2\pi}, \\ f &= 24.3 \text{ kc.} \end{aligned}$$

Examination of the finite-width correction [see equation (62), Section 3.2.3] indicates that for a $1\frac{1}{2} \times \frac{1}{2}$ -in. crystal on a *clamping* ($\frac{1}{4}$ -

wave) backing plate the finite width lowers the resonance roughly $\frac{1}{2}$ per cent. One might expect a similar lowering here, since the $\frac{3}{4}$ -in. thick steel plate clamps the crystal fairly well. Reducing 24.3 kc by $\frac{1}{2}$ per cent, it was predicted that this system would resonate at approximately 24.2 kc.

DESIGN DETAILS

The parts available allowed an array 14 in. in diameter without crowding, and this was acceptable. The area of the array could thus be as great as 750 sq cm, even allowing for wasted space. Such an area would easily be capable of

quadrants and carried through the backing plate by backing glands.

The backing plate was coated with porcelain enamel $\frac{1}{16}$ in. thick which was tested for voltage breakdown after grinding. The array was assembled in a jig and cemented with bakelite cement, being baked under pressure.

For voltage protection, the silver foils used to connect to the crystals were kept $\frac{1}{8}$ in. away from the porcelain. Similar precautions were observed throughout. For reasons discussed in Chapter 7, foam rubber was placed wherever required to cover the $1\frac{1}{2} \times \frac{1}{4}$ -in. crystal faces.

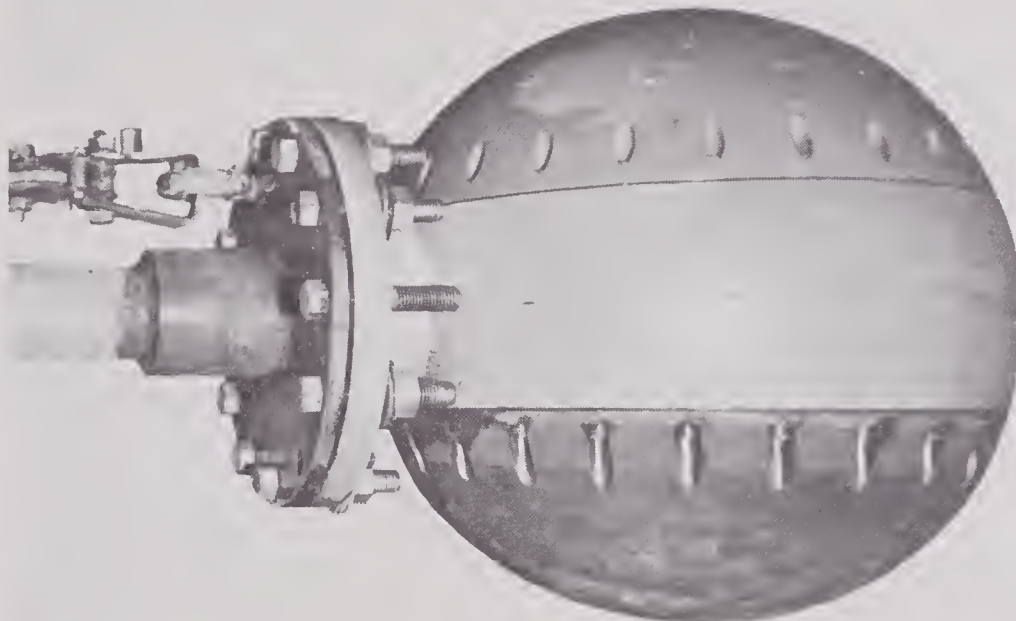


FIGURE 8. Exterior of the JB4Z transducer.

1 kw of continuous radiation, since the crystals were ADP. It was decided that the crystals could be spaced apart. An array was chosen which involved 728 crystals, a radiating area of 587 sq cm.

In the chosen array the crystals were cemented together in blocks of three, in phase, with intervening foils; each block was thus $1\frac{1}{2} \times \frac{1}{2}$ in. These blocks were then spaced $\frac{3}{32}$ in. from each other to fill the 14-in. circle. All crystals were in parallel in phase, but leads were brought out separately from the four

The cavity bounded by the backing plate (and crystals) and rubber window was filled with castor oil. The space behind the backing plate was an air cavity which provided the necessary low impedance behind the backing plate, and also made room for electric connections and tuning coils.

The exterior case itself was cast Meehanite. The completed unit formed a 19-in. diameter sphere weighing roughly 500 lb, with mounting flange to fit a standard Navy column. See Figures 8 through 10.

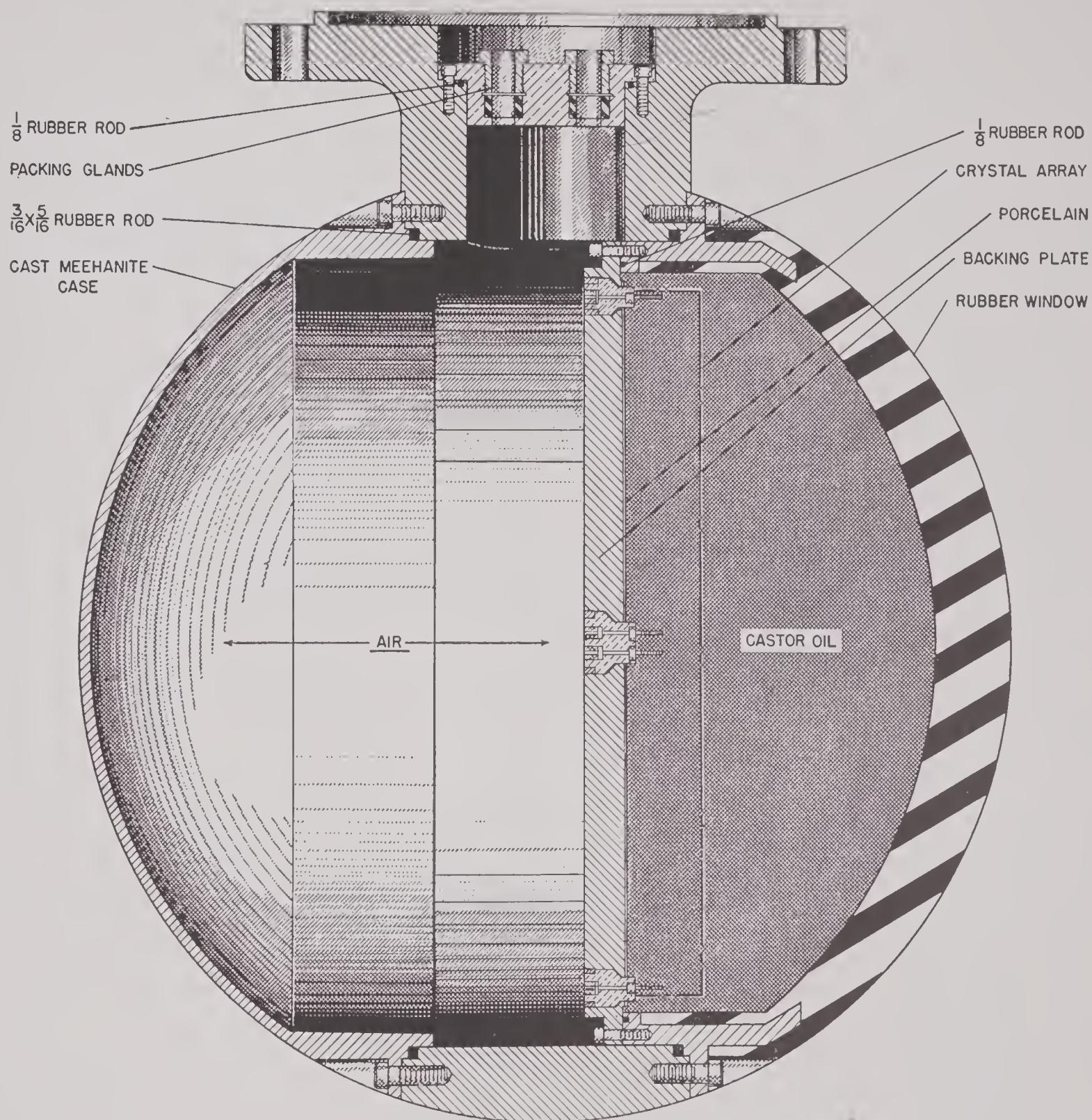


FIGURE 9. Cutaway of the interior of a J-style transducer.

RESPONSE

This unit used essentially clamped ADP crystals so (from Section 4.9.8):

$$R = 7.14 \times 10^6 \frac{L_t}{nL_w}, \quad (2)$$

where, $L_t = \frac{1}{4}$ in.,
 $L_w = \frac{1}{2}$ in.,
 $n = 728$,

hence, $R = 4.9 \times 10^3$.

Using this value of R the predicted complex

impedance was obtained from the graph in Section 4.9.8. Since the available calibration data report the transducer in series with a series coil, such a coil has been calculated into the prediction. This theoretical coil was chosen to cancel the reactance at 24.2 kc and was assumed lossless. The predicted impedance (dotted) is compared with the observed impedance (solid) in Figure 11. It can be seen that the actual transducer resonated a little below

24.2 kc, and the coil used cancelled the reactance at 23.3 kc. The observed resistance is higher than prediction, partly because the coil used did

The array is of 14-in. diameter so that $A = 154$ sq in. At 24 kc the index is -24.9 db. From this we conclude that the transducer should produce

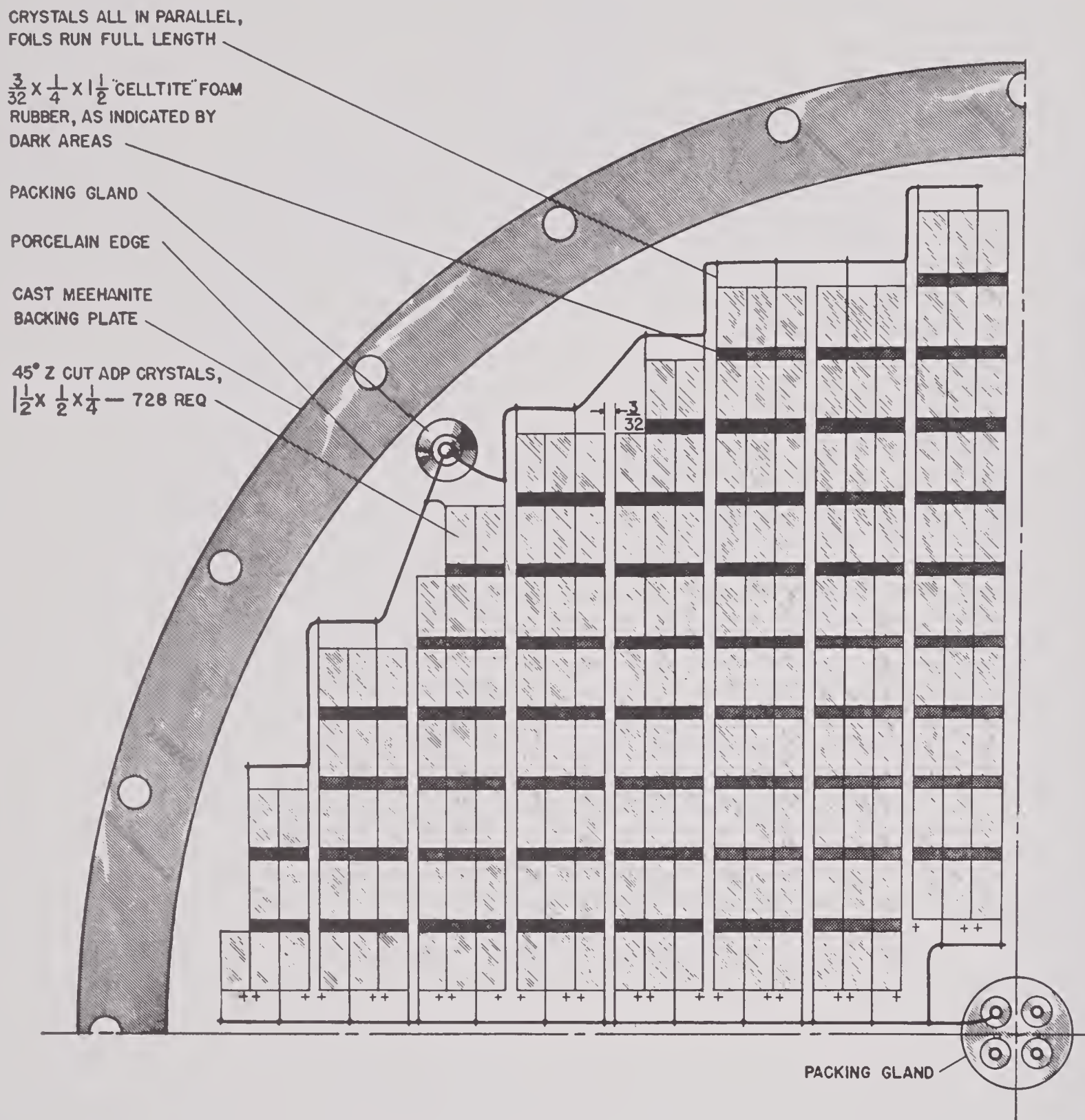


FIGURE 10. One quadrant of the crystal array of the JB4Z transducer.

not have infinite Q . On the whole the agreement of prediction and observation is good.

From Section 4.4.2 we obtain the expression for the directivity index.

$$10 \log \frac{\lambda^2}{4\pi A}$$

$70.8 + D = 95.7$ db above 1 dyne per sq cm at 1 m for 1-w input if it is perfectly efficient (see Section 4.6.3). Section 4.9.8 tells us the power input for 1 v applied with a series tuning coil. From this the constant-voltage transmitter response can be predicted (in computing this it

is necessary to add $20 \log \alpha$ db for the frequency dependence of the directivity index). The predicted curve (dotted) is compared with the observed (solid) in Figure 12.

Note first that there is a small unexplained frequency shift, undoubtedly arising from the

direction, but the cure is in lobe-pattern improvement.

2. Since the actual tuning coil used tuned at

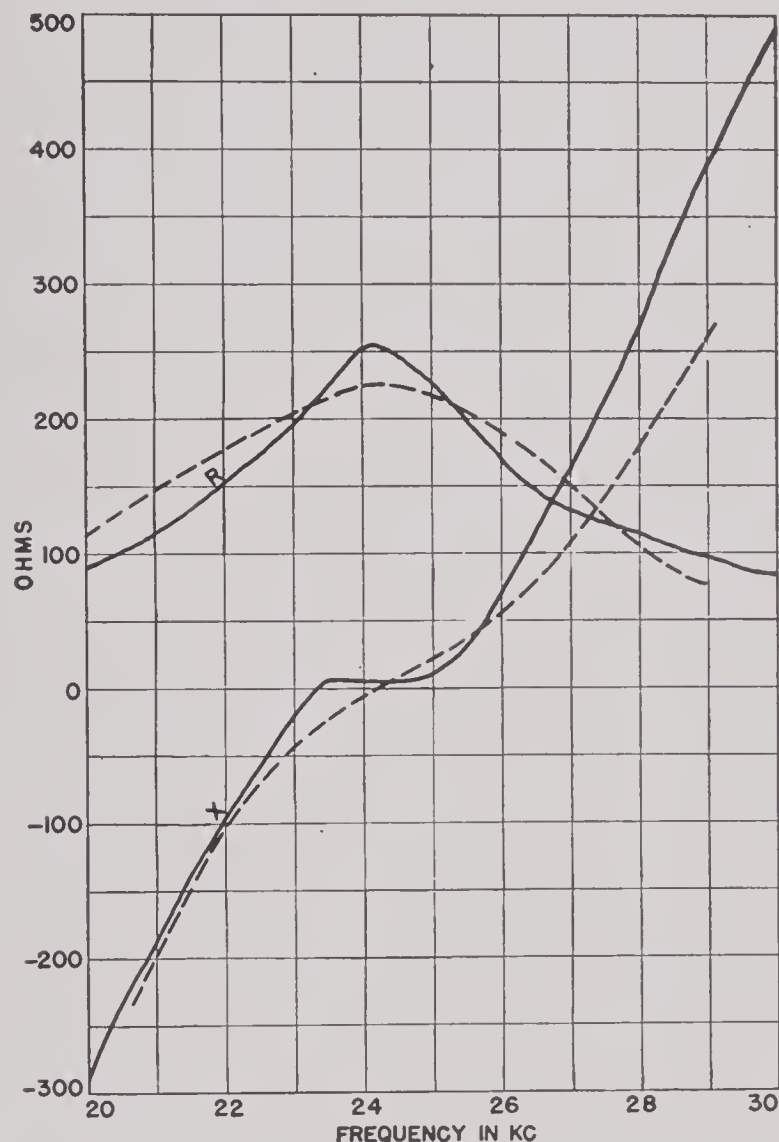


FIGURE 11. Complex impedance of the JB4Z transducer (solid line) compared with theory (dotted line).

numerous approximations in the theory. Second, the efficiency appears to be very low. It is not, however, as bad as it appears for these reasons.

1. The typical pattern shown in Figure 14, shows that the side lobes are higher than they should be. This makes the transducer less directional. It is estimated that the directivity index is approximately -23 db instead of -24.9 at 24 kc; this lowers the predicted curve 2 db. It is true that this is energy going off in an unwanted

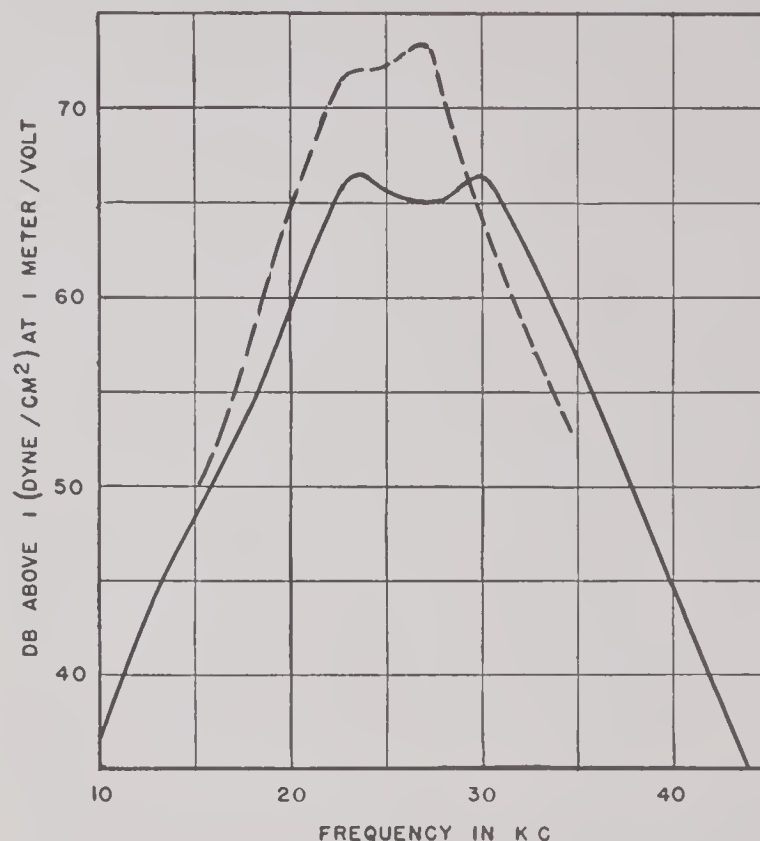


FIGURE 12. Transmitter response of the JB4Z transducer with constant voltage applied (solid line) compared with theory (dotted line).

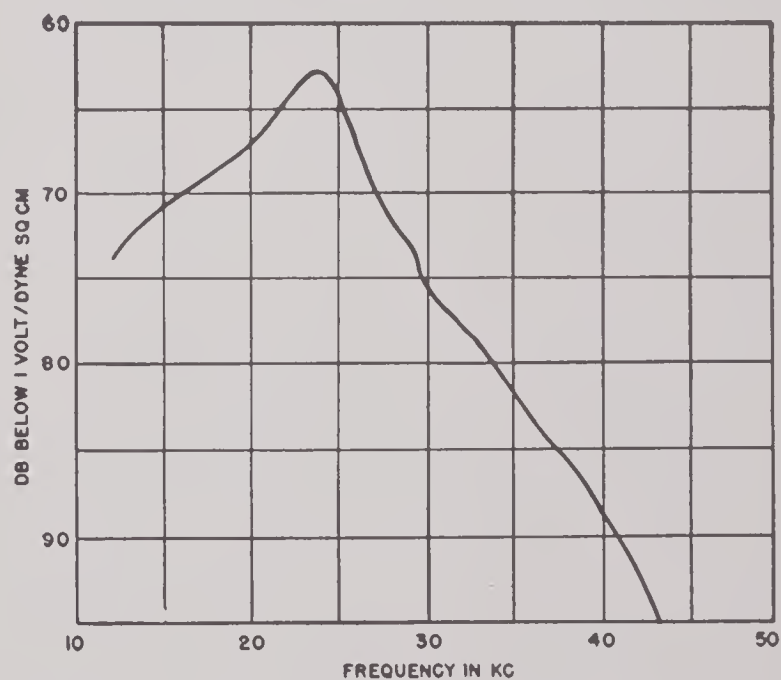


FIGURE 13. Open-circuit voltage response of the JB4Z transducer as a receiver measured at the end of a 63-ft cable with a 3-mh coil in series with each leg.

23.3 kc, the frequencies below resonance were favored a little at the expense of the response at resonance. This is probably sufficient to ex-

plain why the two peaks in the observed curve are of equal height.

Applying these corrections to the comparison of prediction with observation, it appears that the transducer efficiency is -3 db (50 per cent), a very reasonable estimate. The maximum open-circuit voltage is a couple of db low, confirming the estimate of -3 db efficiency.

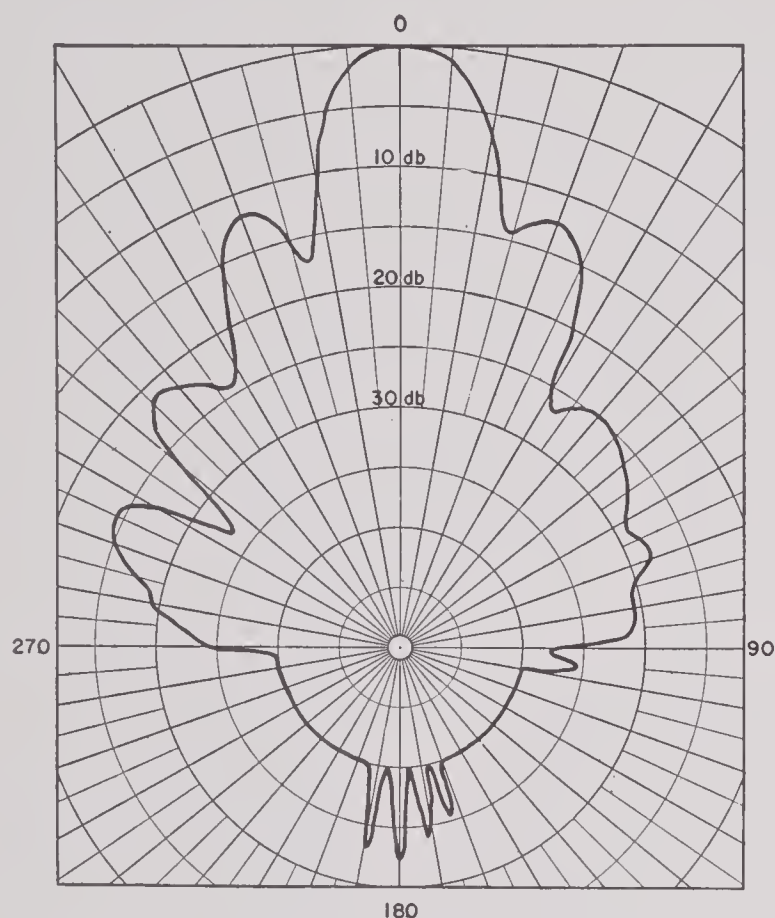


FIGURE 14. Directivity pattern of the JB4Z transducer at 24 kc.

In all respects this is a typical clamped-drive unit as constructed by UCDWR; the efficiency is only 50 per cent, and the patterns are not quite so good as theory. This transducer has been operated for over a year in very high-power service with complete satisfaction.

6.9.2

Inertia Drive: FE2Z

This transducer was designed and built for research by the UCDWR Transducer Laboratory, but it has since been used for sonar system research.

The original aim was to test the then new technique of Cycle-Welding crystals to rubber

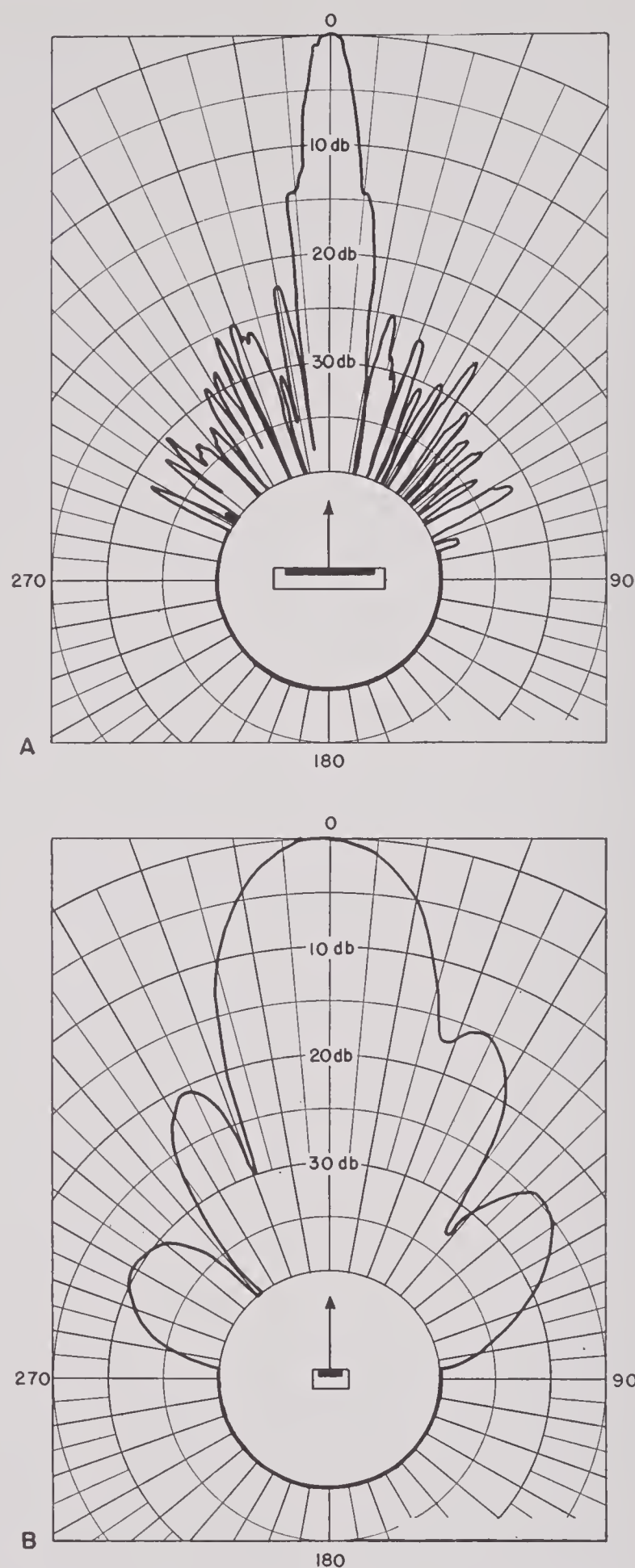


FIGURE 15. Directivity patterns of the FE2Z transducer at 90 kc.

windows. As a goal at which to aim, it was decided to attempt to improve the lobe patterns of

a similar production-type transducer. Figure 15 indicates the success of this venture.

CHOICE OF CRYSTALS

To minimize the size and number of required crystals it was decided to build a high-frequency

rubber would shift the resonant frequency if the crystals were too close together. Spacing the crystals a little nearly eliminated this. Since this shift might introduce some unwanted effect, it was decided to space these crystals $\frac{1}{16}$ in. apart. Equation (62) of Section 3.2.3 pre-

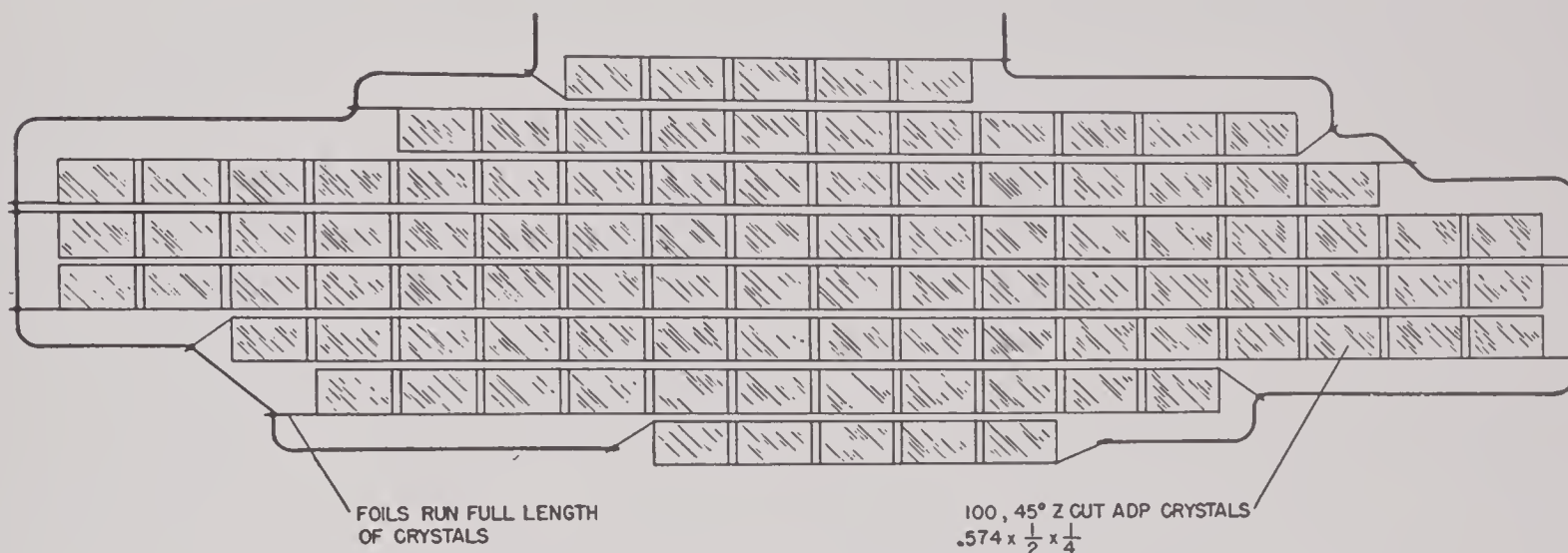


FIGURE 16. Crystal array of the FE2Z transducer.

transducer; if successful it would be simple to design a larger unit to operate at a lower frequency. Some ADP crystals $0.574 \times \frac{1}{2} \times \frac{1}{4}$ in.

dicts that these crystals should resonate at 95 kc. However the bench tests indicated a frequency nearer 90 kc when the crystals were mounted on the rubber in air, so this was taken as the predicted frequency.

CHOICE OF ARRAY

The production-type transducer was tall and slender, having a pattern shaped like a slice of pie, a broad wedge in the horizontal plane, but very narrow in the vertical plane. Unfortunately the side lobes were high, and it was this drawback which was to be improved in the new unit. (See Figure 15.)

Some old parts for an exterior case were available; these would allow an array approximately $21\frac{1}{2}$ by 10 in. There was no particular specification on the width of the horizontal pattern. An array $21\frac{1}{2}$ in. wide at 90 kc should produce a pattern 15 or 20° wide, depending on the lobe suppression, so that this was selected.

At the operating frequency the main lobe was to be $\pm 2^\circ$ wide in the vertical plane at the -3-db points. This called for an array 11 in. long, but 10 in. was considered to be close enough.

The array shown in Figure 16 was carefully chosen to produce good lobe suppression in the

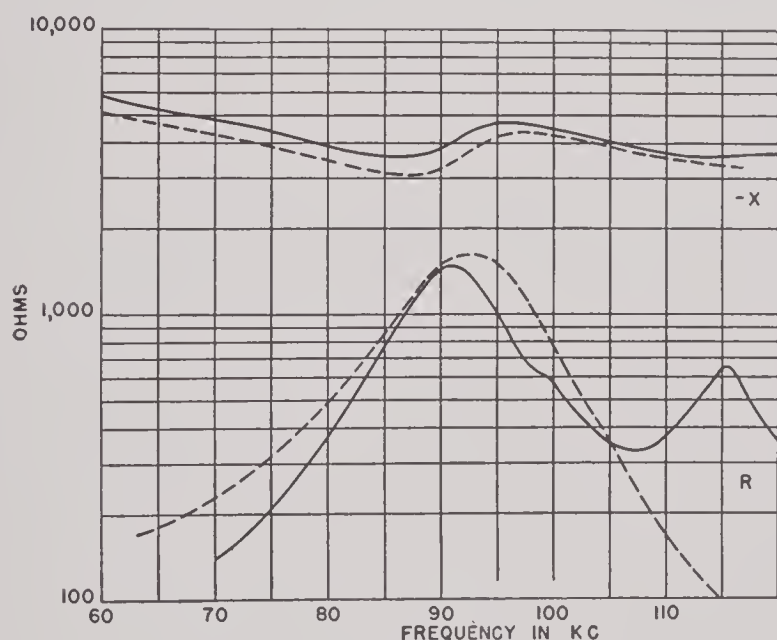


FIGURE 17. Complex impedance of the FE2Z transducer (solid line) compared with theory (dotted line).

were in stock and these were used. There was no compulsion to resonate at some specified frequency.

Earlier bench tests had indicated that the

vertical direction. The ideal velocity distribution is gaussian, and it was attempted to approximate this curve in a large number of small increments. The lobe suppression is accomplished geometrically rather than by putting

more recent developments it is clear that an equally successful unit could be produced using thicker rubber. The window used was neoprene tire stock; excellent Cycle-Weld cement joints to this rubber are easily made, whereas the tech-

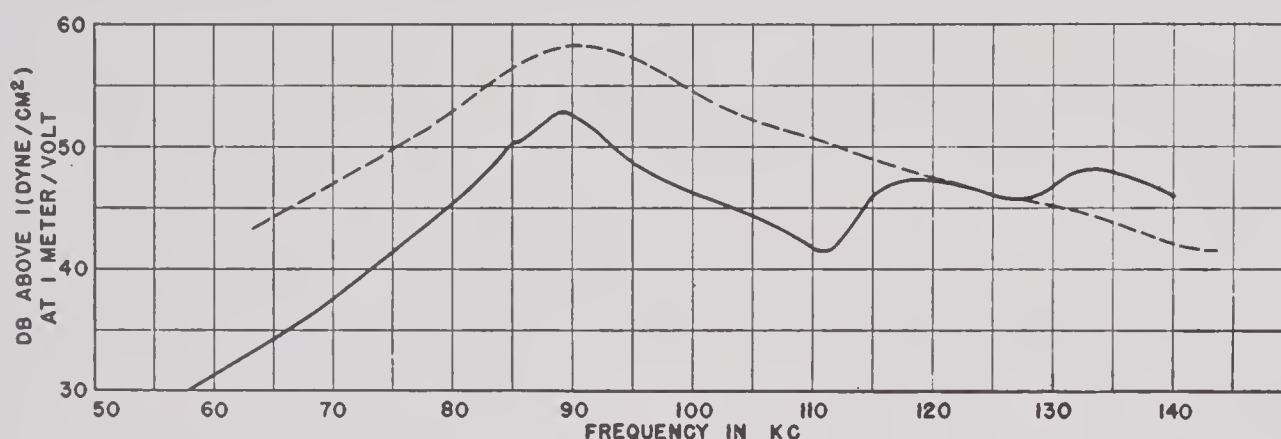


FIGURE 18. Transmitter response of the FE2Z transducer with constant voltage applied (solid line) compared with theory (dotted line).

crystals in series. The array is not symmetric about the center line, in order to increase the number of increments; this should skew the patterns negligibly.

DESIGN DETAILS

In order to assure uniformity, the crystals were tested individually and selected. This step

niques for qc rubber had not been completely worked out at this time.

The crystals were cemented to the window and electrical connections made. Space was provided for a matching network, and the array was bolted into the case. The interior was pumped out and filled with Freon gas since this has higher dielectric strength than air; Freon

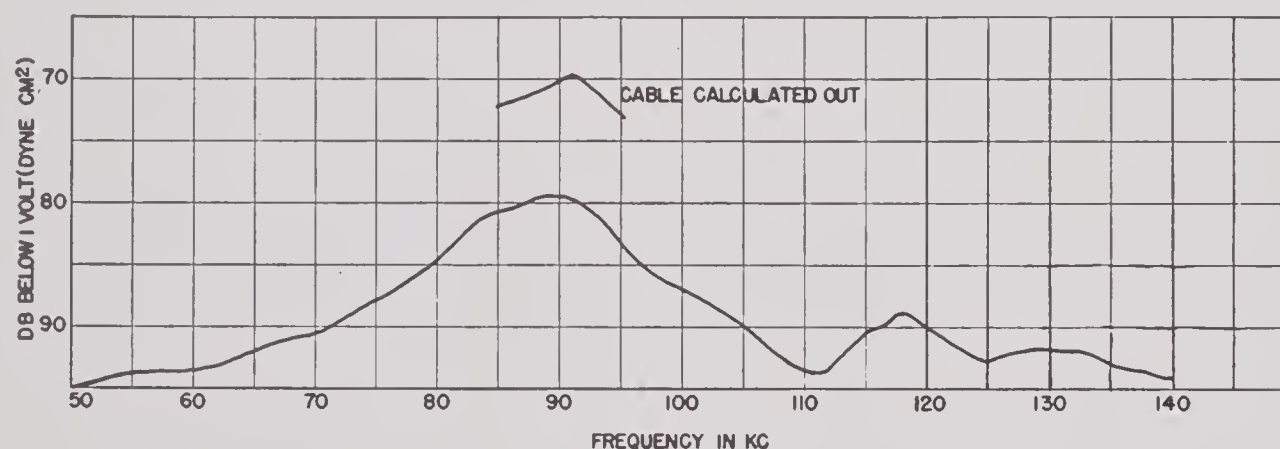


FIGURE 19. Open-circuit voltage of the FE2Z transducer as a receiver measured at the end of a 35-ft cable.

is an elaboration which is probably not essential to production.

The exterior case selected was simply a rectangular metal box, with packing glands, to which a rubber window could be bolted. The window was originally $\frac{1}{2}$ in. thick but was ground down to $\frac{1}{8}$ in. for this unit. In view of

increases the power-handling capacity but has no other effect on the performance.

RESPONSE

For inertia drive ADP (see Section 4.9.8)

$$R = 1.79 \times 10^6 \frac{L_t}{nL_w}, \quad (3)$$



and in this unit $L_t = \frac{1}{4}$ in.,
 $L_w = \frac{1}{2}$ in.,
 $n = 100$,
 so that $R = 8.95 \times 10^3$.

Using this value of R and assuming the resonance would occur at 90 kc, the predicted impedance was obtained from Section 4.9.8; it is

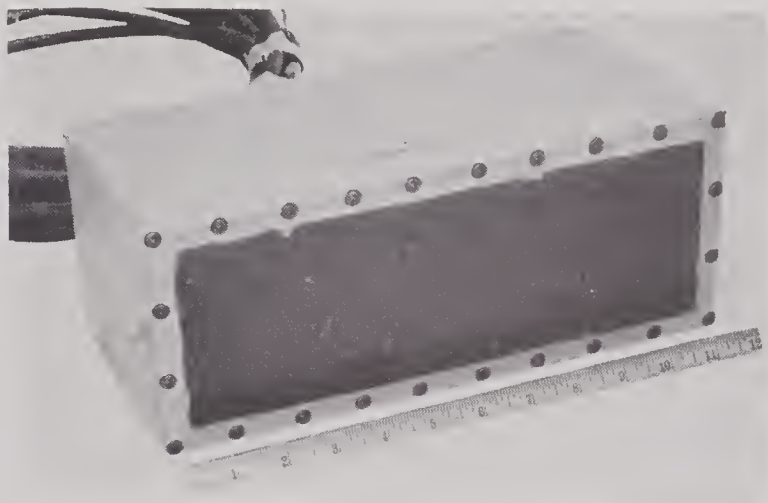


FIGURE 20. Exterior of the FE2Z transducer.

compared (dotted) with the observed impedance (solid) in Figure 17. The agreement is, on the whole, very good; if anything, resonance occurred even lower than 90 kc.

Using the above value of R and the graph in Section 4.9.8, the constant-voltage transmitter

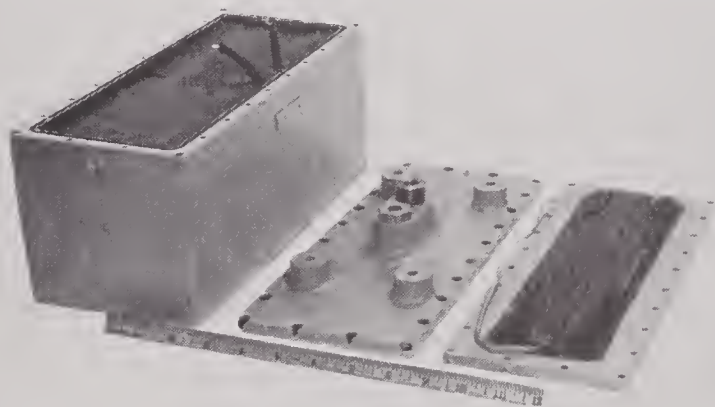


FIGURE 21. Assembly of the FE2Z transducer.

response was obtained. This required some rash assumptions to obtain the directivity index. The expression derived in Section 4.4.2 is usable only if the array may be considered an infinite plane, a poor approximation for this unit. In order to calculate A easily it was assumed that an area $\frac{5}{16}$ by $\frac{9}{16}$ in. belonged to each crystal; for 100 crystals, A equals 17.6 sq in. At 90 kc

the wavelength is $\frac{2}{3}$ in., so that at that frequency the directivity index was assumed to be -27.0 db. A correction $10 \log \alpha^2$ was applied for the frequency dependence of the directivity index. The response shown (dotted) in Figure 18 is compared with observation (solid).

This too indicates that resonance actually occurred a little below 90 kc. Since the theory used to obtain the directivity index is inadequate, there might be a 1- or 2-db error. Including this in our estimate, it appears that the efficiency was between -3 and -7 db (not so good as gas-filled inertia drive goes.)

The apparently poor efficiency is explained by the construction. In order to prevent excessive deflection of the thin-rubber window from hydrostatic pressure, a sheet of foam rubber was placed between the back ends of the crystals and the back of the exterior case, in this position the crystals were pressed into the Air-foam rubber. There may be serious tangential loss in the rubber when used this way, and the poor efficiency is not surprising. Very probably the efficiency would have been 3 db higher had the crystals not been standing in foam rubber.

6.9.3

Symmetric Drive: CY4

SPECIFICATIONS

This transducer was to be expendable with a service life of roughly $\frac{1}{2}$ hr. Previous to use it was to be stored aboard ship in an air-tight strong container. It was to be immersed with reasonable care and was to operate at approximately 50-ft depth, although it might occasionally go several hundred feet deep.

It was to be used only as a projector over as wide a frequency band as possible in the vicinity of 20 kc. The response was to be as flat as possible; equalization could be introduced in the electric circuit. See Section 5.5.

The directivity pattern was to be approximately circular in a horizontal plane, and in the vertical plane the main lobe was to be at least $\pm 12^\circ$ to 3-db down points at 20 kc (no requirements on side lobes).

The amplifier was to be located nearby and be rated at 10 w. Maximum possible acoustic output was requested. Operation was to be sub-

stantially continuous although switching transients might occur causing momentary high voltage.

Since no cable was needed to reach the amplifier, high impedance was allowed; a few thousand ohms would match the amplifier output stage.

It was essential that the transducer be as small as possible. Minimum density was requested.



FIGURE 22. Interior and exterior of the CY4 transducer.

Mounting facilities were to be worked out as design progressed. Immediate large-scale production by an inexperienced manufacturer was contemplated, and minimum cost was greatly desired.

The entire project was of extreme urgency.

CHOICE OF CRYSTAL

Urgency left no choice of crystal. It was evident that pattern and density requirements ruled out backing plates. The ADP crystals resonant free-free at this frequency were not available in quantity. The required efficiency ruled out X-cut RS. The crystals had to be Y-cut RS, and preferably in a readily available size.

CHOICE OF BASIC DESIGN

The nondirectional horizontal pattern invites symmetric drive, although it was not immediately clear that all specifications would be met.

At this time inertia drive was unproved, and symmetric drive was chosen. Similar units using X-cut RS had been built previously and met the directivity specifications.

In retrospect it appears that the symmetric CY4 is so successful that inertia drive would offer no improvement.

CRYSTAL SIZE AND SHAPE

The largest Y-cut RS then stocked in quantity by the design group were $1\frac{1}{2} \times 1 \times \frac{1}{4}$ in. These crystals resonate at 27.6 kc [equation (63), Section 3.2.3] which was too high. However the design contemplated had small radiating faces (compared with a wavelength) and an appreciable radiation inductance was expected. This inductance would lower the resonance an unknown amount, perhaps enough. Longer crystals might be preferable, but they were not available.

DIRECTIVITY PATTERN

The horizontal pattern of the contemplated array cannot be calculated by any available theory. However, previous experience indicated that a pair of radiating faces 1 in. wide, facing in opposite directions in phase, $1\frac{1}{2}$ in. apart, would meet the requirements. Such a pattern is quite sensitive to the $1\frac{1}{2}$ -in. dimension and it was not known if greater separation would do. This reinforced the decision to use crystals $1\frac{1}{2}$ in. long.

Thus it was decided to use a single vertical stack of crystals $1\frac{1}{2} \times 1$ in. of undetermined height. Radiation was to be taken from the $1 \times \frac{1}{4}$ -in. crystal faces, and the $1\frac{1}{2} \times \frac{1}{4}$ -in. faces were to be covered to prevent out-of-phase radiation; Corprene or foam neoprene would be used for this. For convenience, electric connections would be made underneath this covering.

The height required to produce a vertical pattern $\pm 12^\circ$ wide to 3-db down points at 20 kc is approximately 6 in. This would necessitate an outer case $6\frac{1}{2}$ or 7 in. high. It was decided to shorten the stack to 5 in. or a little more. A line source $5\frac{1}{8}$ in. high will produce, at 20 kc, a pattern $\pm 15^\circ$ wide to the 3-db down point.^b A

^b Compare Figure 45, Chapter 1; the patterns of the finished transducers are 15 or 16° wide.



stack of 20 crystals, each $\frac{1}{4}$ in. thick, would be the right height so this was tentatively selected, final decision depending on the resulting impedance.

MECHANICAL DETAILS

The mechanical design chosen is quite novel. It had never been tried before, and there were serious doubts about it, but it turned out well and has since been used in several other designs with equal success.

The exterior case and acoustic window are identical, and consist of a standard olive can. This had the advantage that closure is simply effected with an ordinary can-sealing device. The castor oil is introduced later through a soldered bushing, and the hole is closed by a pipe plug seated on wet Glyptal.^c Electric leads are brought out by a pair of metal-to-glass seals soldered into the lid before closure. The entire transducer is attached to the rest of the device by a crimped seal over a gasket catching the rolled edge on the end of the tin can.

The can material is approximately 0.010 in. thick and is reasonably transparent to sound at 20 kc. There is some evidence that the transducer would behave a little better in a *gc*-rubber sleeve.

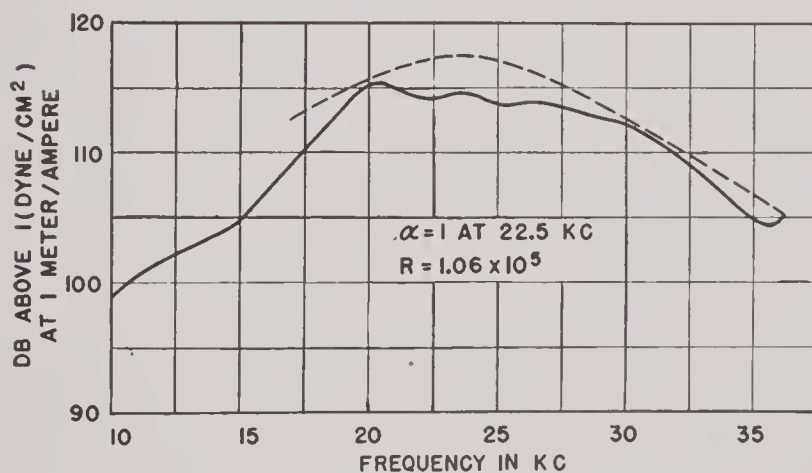


FIGURE 23A. Average transmitter response of five CY4 transducers (solid line) compared with theory (dotted line).

The tin can is soft and easily dented, but must be smashed considerably before the crystals are damaged. There is some compressible material inside (Corprene) and the can tends to collapse if submerged deeply, but no damage is done.

^c Glyptal insulating varnish supplied by General Electric Company.

The tin can would soon rust through and is not suitable for prolonged service, but is ideal for an expendable device. Corrosion before use is prevented by the air-tight packaging.

When turned over to a manufacturer no great difficulty was encountered, and several thousand units were made.

RESPONSE

From Section 4.9.8 we have

$$R = 8.50 \times 10^6 \frac{L_t}{nL_w} \quad (4)$$

For this unit $L_t = \frac{1}{4}$ in.,
 $L_w = 1$ in.,
 $n = 2,$

so that $R = 1.06 \times 10^5.$

Using this value of R we could obtain a predicted impedance. However the resonant frequency predicted by Mason theory with the width correction is 27.6 kc, whereas the actual resonance in the water is lowered to $22\frac{1}{2}$ kc by the radiation reactance. Such a comparison would be useless. Instead let us use some hindsight, and admit that the frequency is lowered this much. If we then compute the predicted

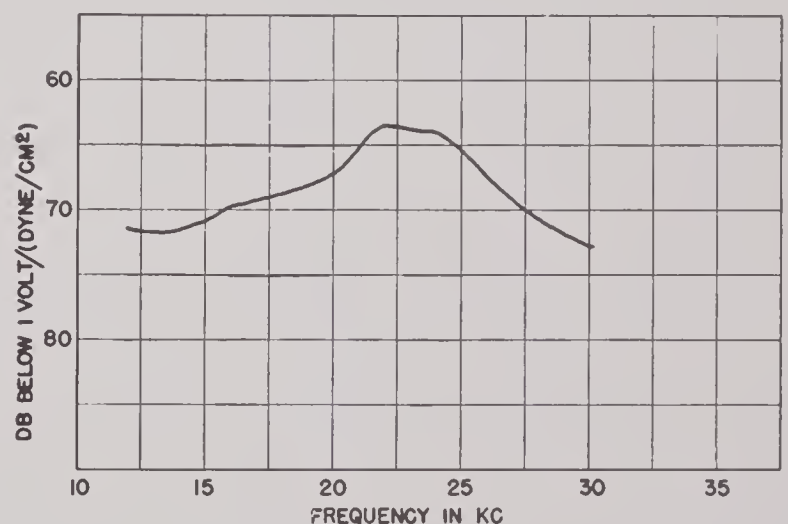
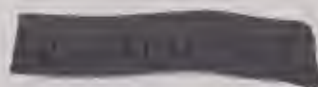


FIGURE 23B. Receiver response of the CY4 transducer.

impedance from Section 4.9.8 we obtain the dotted curves in Figure 23A, B, C, D. We see that there is considerable discrepancy which would be removed by raising both resistance and reactance by a factor of, say, 1.4.

Examine the consequences of the rather arbitrary frequency shift from 27.6 to $22\frac{1}{2}$ kc. The



assumption has been made that the crystal remains fully loaded by the radiation impedance of water, so that $R = 1.06 \times 10^5$. Of course the capacity of C_0 in the equivalent circuit remains unchanged, but the reactance of C_0 at $22\frac{1}{2}$ kc is greater at the lower frequency. Furthermore, in deriving the expressions in Section 4.9 no

circuit with an added mechanical inductance (assumed constant) sufficient to lower the resonant frequency to $22\frac{1}{2}$ kc.

The directivity index function derived in Section 4.4.2 is not alleged to be usable for an array of this kind. However, it is interesting to compare the index it predicts with the index ob-

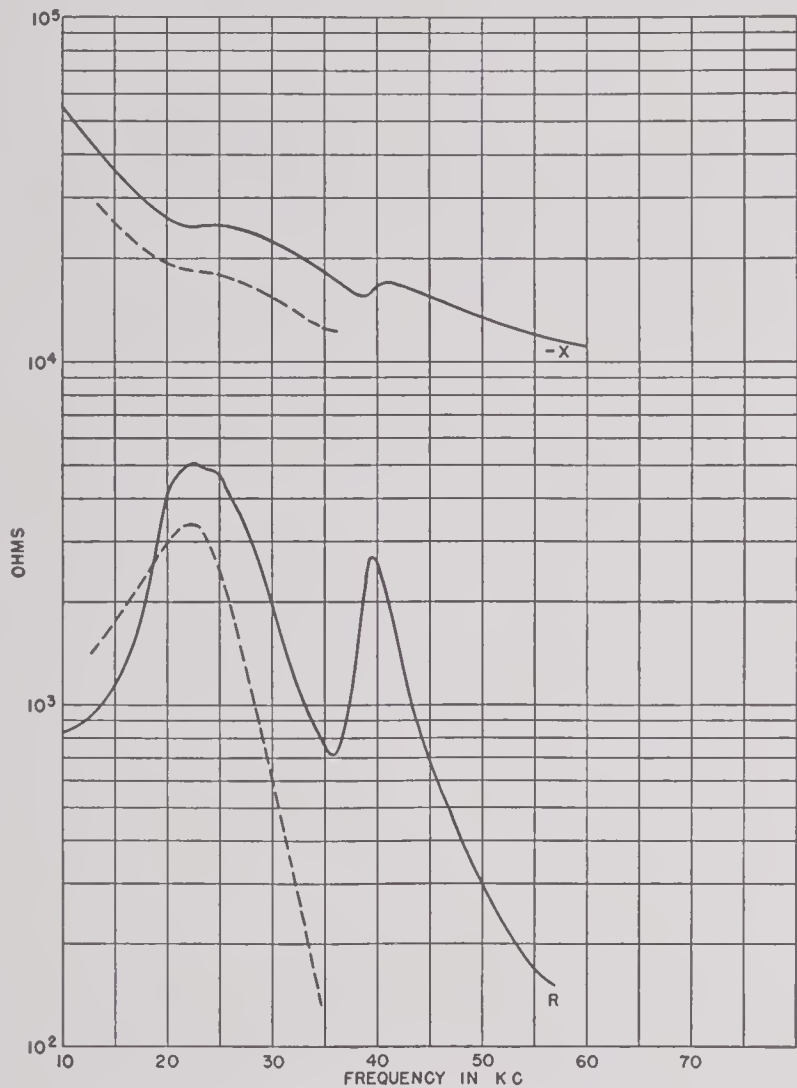


FIGURE 23C. Complex impedance of the CY4 transducer (solid line) compared with theory (dotted line).

width correction was included. As far as Mason theory is concerned the resonance should occur at 30.9 kc. It is at 30.9 kc that Q_E equals -5.55 ; at $22\frac{1}{2}$ kc Q_E should be less by a factor of 1.37. Yet we have required it to be -5.55 in computing this theoretical curve. Thus we see that much of the discrepancy results from misuse of the theory, and the transducer is not as anomalous as it would appear.

This situation is not rare, and this example serves to illustrate the limitations of the curves in Section 4.9.8. A better prediction is obtained by calculating directly from the equivalent cir-

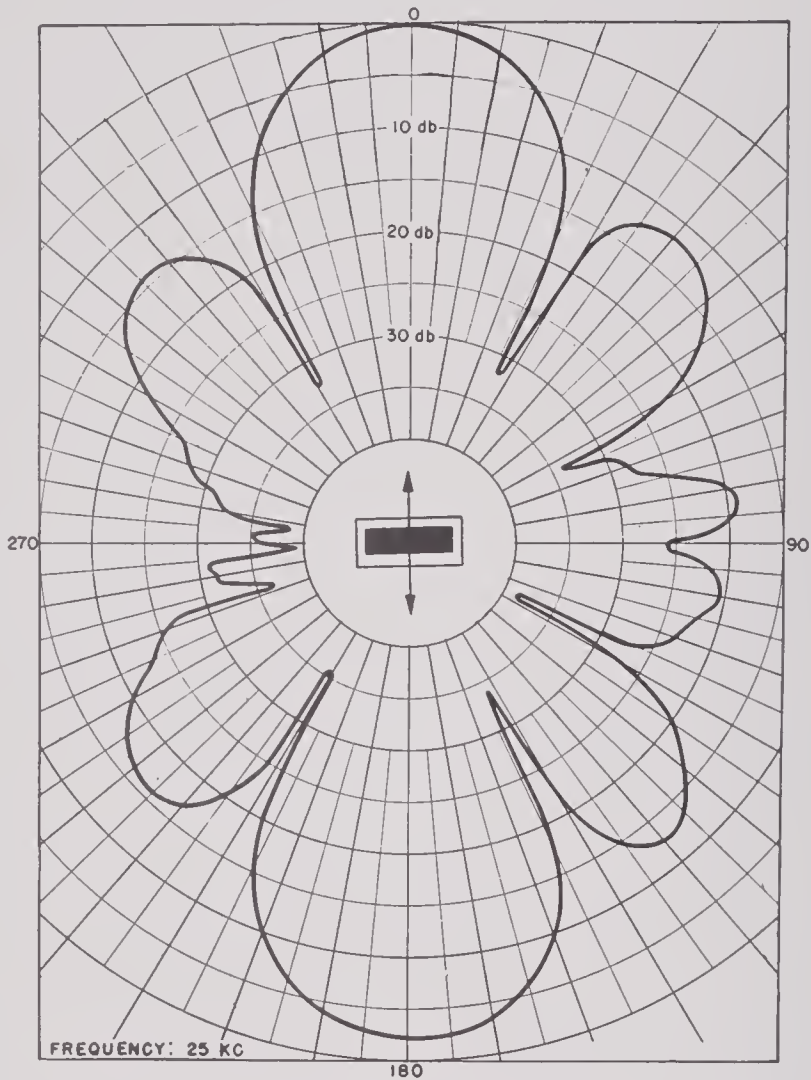


FIGURE 23D. Directivity pattern of the CY4 transducer in the vertical plane.

tained by numerical integration of observed patterns:

Frequency (kc)	Observed (db)	Predicted (db)
15	— 9.20	— 8.96
20	— 9.08	—11.46
25	—10.15	—13.40

If we ignore this error, we may proceed to calculate a response curve from the theoretical index and the data in Section 4.9.8. It happens that constant-current transmitter responses are available for this transducer so that response

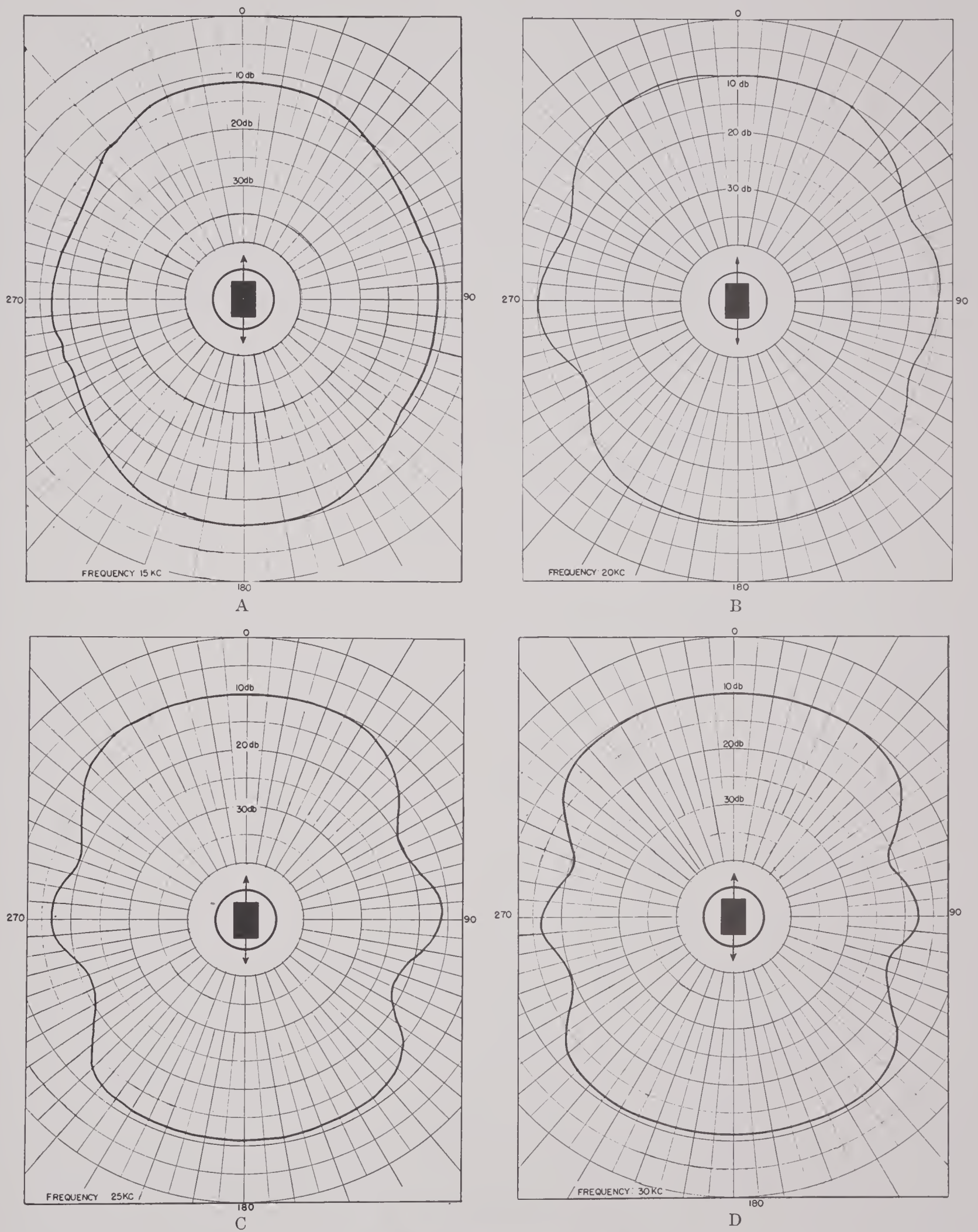


FIGURE 24. Directivity patterns of the CY4 transducer.

is computed. See Figure 24A, B, C, D. The equation used is:

$$\text{db above 1 (dyne/cm}^2\text{) at 1 m/amp} = 70.8 + 10 \log \left(\frac{\lambda^2}{4\pi A} \right) + 10 \log \alpha^2 + 10 \log Rk_1, (5)$$

where 70.8 is the pressure from a 1-w spherical source, the directivity index is computed at α equals 1 (22½ kc), the α^2 term is necessary to take care of the frequency dependence of λ^2 , Rk_1 is the power expended when 1 amp flows through the unit, and k_1 is the curve in Section

4.9.8 appropriate to clamped (symmetric) Y-cut RS with $R = 1.06 \times 10^5$.

This curve is dotted in Figure 23. The goodness of prediction is entirely fortuitous, and should not be regarded as a justification of the many poor approximations inherent in this method. The directivity patterns of a unit such as this are fast functions of the dimensions of the crystal, and no available theory allows correction for this in the computations. Furthermore the radiation impedance is complex, and changing rapidly with frequency at 20 kc. As yet we have no data on the radiation impedance (see Section 9.4).

Chapter 7

DESIGN ADJUSTMENT

By *T. Finley Burke*

IN THE PRECEDING CHAPTER the steps were outlined by which a designer arrives at the principal features of a design to meet certain specifications. If the Mason circuit were always obeyed this would be sufficient. However, there remain many features not yet considered which influence the behavior, and which must be accounted for if the unit is to be successful. In this chapter the aim is to discuss means of minimizing the deleterious effects so as to finally produce a unit as good as that predicted in Chapter 6. Notice that the aim is not to obtain better performance, but simply to keep it as good. At the present time there is not available sufficient information to allow the use of second-order effects in such way as to obtain behavior superior to that predicted by Mason theory; it is to be hoped that extensive research will, in time, discover means of accomplishing this.

The points to be discussed are understood only qualitatively. No adequate theory exists, and all that can be done is to point out the effects, cite examples, and expect the reader to acquire sufficient experience to weigh the merits of each new problem. Since every decision is a compromise of some kind, and since each transducer is a new mystery, the acquisition of good judgment is an expensive and lengthy process; the novice finds the conflicting effects confusing, but should not be discouraged by poor results. Nearly every good transducer in service was preceded by a family of failures which, at times, did not appear to be a convergent sequence of improvements.

7.1 SINGLE CRYSTALS

In selecting the size and shape of the individual crystals to be used, the first step is to adjust the resonant frequency (Section 6.4). While sufficient for preliminary designs, this may not be the final choice. The remaining problems are different for the three basic drives.

7.1.1

Clamped Drive

The glued surface of a clamped crystal undergoes tangential motion which results in viscous losses in the glue. The amplitude in each direction is proportional to the crystal dimension. Consequently one can expect the efficiency of a single crystal to improve as L_w and L_t are diminished. Since the efficiency of the whole transducer is the average of the efficiency of each crystal, it is desirable to minimize L_t and L_w .

On the other hand, if L_w and L_t are diminished the total area of L_w and L_y and $L_t L_y$ faces must increase since more crystals are required. These faces also undergo tangential and normal motions, and expend energy in losses. The energy so wasted increases with the area of these faces, and is thus reduced by increasing L_w and L_t .

The two effects conflict, and some compromise must be reached. Among the transducers made by the various suppliers (such as Bell Telephone Laboratories, Brush Development Company, Submarine Signal Company, and University of California Division of War Research [UCDWR]) there is a complete gamut of compromise, but the preference seems to be $L_y > L_w > L_t$. Any possible advantages obtained from $L_w > L_y$ appear to be overshadowed by the losses. A convenient shape results and good efficiency is obtainable, if the designer attempts to keep $L_w \leq \frac{1}{2}L_y$. However $L_w \leq 0.1L_y$ seems to be too small; the glued joints to a great many small surfaces are too difficult.

Since the tangential motion in the L_t direction is less than that in L_w , the viscous loss is not as severe, and greater L_t could be tolerated. However it is important to keep the crystal a good parallel-plate condenser, and for this one should probably have $L_t \leq \frac{1}{2}L_w$. Quite good transducers have been built with $L_t = 0.1L_w$, but this is extreme, and the transducer begins to contain too much glue.

7.1.2

Inertia Drive

For gas-filled inertia drive the reasoning is quite different. If adjacent crystals are not cemented together (see Section 7.2) negligible losses occur on the $L_w L_y$ and $L_t L_y$ faces, so that minimum L_t and L_w is indicated. However the parallel-plate condenser restriction still holds: $L_t \leq \frac{1}{2} L_w$. Slender crystals, not cemented to each other, are too loosely attached to the window if L_w and L_t are too small; the crystals can lean over irregularly and are too easily damaged. The designer must judge for himself how rigid and strong the array must be.

7.1.3

Symmetric Drive

Symmetric drive, at least in vertical-stack units such as UCDWR Model CY4 (see Figure 22 of Section 6.9), offers much less freedom of choice. In such units a certain directivity pattern is expected at the resonant frequency. The pattern is a sensitive function of the crystal shape, and allows very small range of selection. For example, to produce the CY4 pattern at 20 kc the crystals must be $1\frac{1}{2} \times 1$ in. (so far as is now known); it is fortunate that such Y-cut Rochelle salt [RS] crystals resonate at $22\frac{1}{2}$ kc. To produce an analogous Z-cut ADP stack resonant at $22\frac{1}{2}$ kc would require crystals perhaps $2\frac{1}{2} \times 1$ in.; the patterns would be very different and probably not acceptable. Not much has yet been done on the dependence of these patterns on crystal size and shape except to establish the extreme sensitivity. It is certain that no present theory allows their calculation, and much more experimental investigation is indicated.

In any event, the selection of shape for vertical-stack design is controlled by pattern requirements, independent of the shape dependence of the losses. There is no particular reason to avoid $L_w > L_y$, but $L_t \leq \frac{1}{2} L_w$ and $L_t \leq \frac{1}{2} L_y$ is indicated.

7.1.4

Weakened Crystals

Sometimes it is necessary to produce a resonant frequency lower than can be reached by

any available crystal. In some instances this may be done by weakening the crystal. For example, consider 45° Y-cut RS crystals $1\frac{1}{2} \times 1 \times \frac{1}{4}$ in. to be used in a vertical stack. In air these crystals resonate at 27.6 kc; in a finished CY4 in water, they resonate at $22\frac{1}{2}$ kc. The radiation is taken from the 1-in. edges. If slots are cut into the crystal toward the center from the centers of the two $1\frac{1}{2}$ -in. edges, the free-free resonance is lowered (see Figure 1).

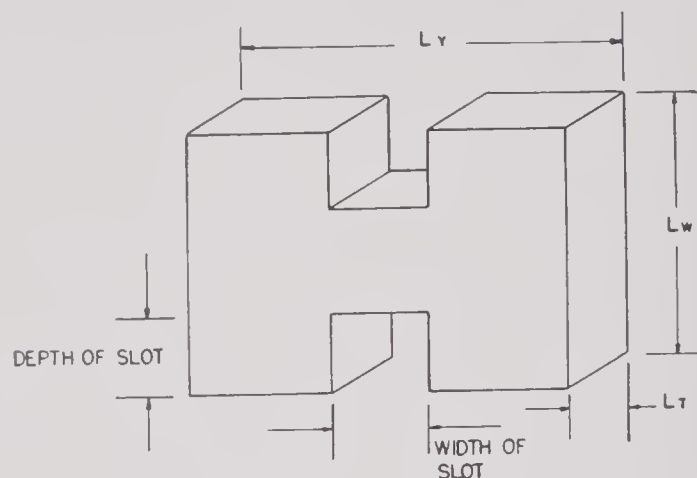


FIGURE 1. Crystal weakened to lower its resonant frequency.

Only shallow slots are required to lower the resonance to 22 kc in air, and the resulting crystal is quite strong and capable of driving to cavitation. At this lowered frequency the radiation reactance is not as effective in lowering the resonance in water, so that a finished CY4-style unit in water, using these weakened crystals, resonates at 18 or 19 kc. This is a rather mild example; by extensive slotting and considerable weakening the resonant frequency of a $1\frac{1}{2} \times 1 \times \frac{1}{4}$ in. Y-cut RS crystal was lowered to 3 kc.

If the depth of the cut is held constant and the slot is widened the frequency varies peculiarly. If the slots were made as wide as L_y itself a slice would have been taken off the sides, reducing the width-length ratio, and the resonant frequency would be *higher* than that of the original crystal. Thus one expects the slot to lower the resonance, and then as the slot is widened the frequency should rise, finally, to a higher value. Actually the frequency is constant over a considerable range of slot widths, the rise coming suddenly just as the slot width becomes equal to L_y . The reason for this is that the slot

leaves a mass of crystal projecting from each of the four corners. Because of "whipping," these masses introduce considerable inertial reactance and hold the frequency down.

If slotted crystals are used in a liquid such as castor oil, peculiar effects should arise from the oil in the slot. These may be worth investigation, but it appears likely that the chief effect is to restore some of the stiffness removed by the slot. To avoid this the slot should be filled with an isolation material such as Airfoam rubber.

7.2 GROUPS OF CRYSTALS

Instead of spacing every crystal away from its neighbors or packing all the crystals together in a block, it is customary to group them in small blocks which blocks are then spaced apart from their neighbors. The reasons for selecting various block arrangements are different for the different drives.

7.2.1 Clamped Drive

Two major effects occur when crystals stand near or against each other on a backing plate and oil or glue is placed between the crystals: (1) viscous losses occur because of the lateral and tangential motions, and (2) bending forces are exerted on the backing plate.

Considering the first of these, cementing crystals together or coupling them by thin oil layers is quite similar to having selected bigger crystals, and the viscous losses at the backing plate encouraged by large L_w and L_t are increased (see Section 7.1.1). Furthermore, there appear to be losses on the $L_w L_y$ and $L_t L_y$ faces, even when the crystals are not yet attached to the backing plate. These losses are not at all understood, but probably arise from the fact that no crystal face remains perfectly plane as the crystal distorts; glued joints between, say, the electrode faces ($L_w L_y$) are subjected to extension in some places and compression in others resulting in viscous loss.

Considering the second effect above, the bending of the backing plate, as a group of crystals

expands laterally the crystals tend to push each other apart. In so doing they bend the backing plate convex outward. This is reversed at the next half-cycle, and the result is that the flexural modes of the backing plate are strongly driven. In fact even a single crystal expanding and contracting tangentially at the plate does this too; it is apparent that if a flexural normal mode of the backing plate occurs anywhere near the driving frequency it is inevitably excited.

Both of these effects would be minimized by spacing each crystal from its neighbor and putting Airfoam rubber between the crystals; the effects would be made more troublesome as crystals were crowded together. Unfortunately it is not always good to space the crystals apart. For one thing, it greatly complicates the assembly of a motor having hundreds of crystals. Shims must be put in the spaces, and later removed at the crystals' jeopardy. Also, only perhaps half of the available area can be covered by crystal so that the radiation resistance is unduly low [see equation (56), Section 4.2.4].

A compromise is effected by grouping into blocks containing a small number of crystals. In any one block the crystals are glued together with the best possible joint. If this joint is poor the efficiency is lowered badly. These blocks are then lapped flat and cemented to the backing plate with intervening spaces. These spaces may later be filled with isolation material (see Section 7.5.5).

No fixed rules exist for the choice of crystal blocks. It is uncommon to have as many as ten crystals in a block; four is perhaps an average number. Usually the block is square, and the length of the crystals should exceed the other dimensions, preferably by as much as a factor of 2. If this factor gets too big the crystals are long slender fingers, easily knocked off of the plate, so that some judgment is needed.

7.2.2 Inertia Drive

If gas-filled inertia drive is used there is negligible lateral coupling, even between "touching" crystals. Furthermore flexural modes of a rubber window give little or no trouble, so that the problems are greatly simplified. If the crystals

are spaced apart the radiation resistance is lowered and this may be disadvantageous. It is probably preferable to bunch the crystals close to each other but leave them not cemented. If they were cemented the losses occurring at the $L_x L_y$ faces would be encouraged to no advantage.

7.2.3

Symmetric Drive

To date the only symmetric drive units containing more than a couple of crystals have been the UCDWR vertical-stack designs. In them there has been no occasion to space the crystals in blocks. The procedure has been to pile crystals one on top of the other (on the electrode faces) with interposed 0.001-in. foil for electric connection. The crystals were not cemented to each other, and in at least two models the foils were wrinkled. The efficiency has always been high.

In an experimental unit flat foils were used and the entire pile of crystals was glued together. The resulting unit had poor efficiency. This is not explained, but it is apparently another manifestation of the losses occurring when $L_x L_y$ faces are glued together.

7.2.4

Foiling

Often blocks of crystals are arranged in which the number of crystals per block is equal to the ratio of the amplitudes in two lobe-suppression zones. For example, in using a 3/1 velocity ratio it is natural to make up blocks of triplets. In the low-amplitude zone all three crystals are in series in phase and only the extreme foils are driven electrically. One must then decide whether or not to place electric conductors at the internal "electrode" faces even though they are not connected to anything.

Two things may be said in favor of having these internal electrodes. First, they establish equipotential planes and diminish the fluxing of the electric field. This is just the matter of keeping $L_z < \frac{1}{2}L_x$ in order to keep a good con-

denser. Second, these internal electrodes could be interconnected among the blocks to help maintain uniformity over the array.

There is an important disadvantage to these internal electrodes; the number of individual glued joints is doubled. Since losses at these joints do occur it might be expected that the losses would be increased by the extra joints. This has in fact been observed, and it looks as if this disadvantage is more serious than the advantages above, so that the internal foils are not generally recommended. Some thought should be given for each new transducer and simple tests should be run to determine the Q of each style of block in air.

7.2.5

Directivity Patterns

In selecting the size of a group of crystals to form a block the rule given in Section 4.2.4 must be observed. There it is stated that the center-to-center distance between adjacent blocks should not exceed 0.8 wavelength. This is a fast function, and one does not have to stay much inside 0.8 to be safe. However if possible it is preferable to try to limit this to 0.5 wavelength. In a plane array, if this rule is violated the system acts like a diffraction grating. The directivity patterns resemble those of an optical grating, showing first order, second order, etc. In transducer nomenclature these higher orders constitute side lobes not many db down, and the patterns are useless.

7.2.6

Example

A typical clamped-drive transducer using crystals arranged in blocks is UCDWR Model JB4Z in which the crystals are each $1\frac{1}{2} \times \frac{1}{2} \times \frac{1}{4}$ in. They are grouped in triplets to form blocks $1\frac{1}{2} \times \frac{1}{2} \times \frac{3}{4}$ in. In this unit there is no lobe suppression, so that there is a foil between each pair of crystals in each block, and all crystals are in parallel. The blocks are spaced $\frac{3}{32}$ in. from each other and the spaces are filled with Airfoam rubber. This unit operates at 24 kc at



which frequency the wavelength is $2\frac{1}{2}$ in.; the greatest center-to-center distance is $\frac{1}{3}$ wavelength. No diffraction-grating behavior is observed near resonance, although it might be expected near 75 kc.

7.3

ARRAYS

In making up crystal arrangements to produce desired directivity patterns, several sources of trouble may arise. By no means are all of these yet discovered but some are discussed below.

7.3.1

Cylinders

Sometimes it is required to produce a non-directional directivity pattern in one plane and to radiate considerable power. A line source, such as a vertical stack, would not be capable of radiating the power, and a cylindrical source is required. This subject is discussed in Section 4.2.4, from which we note two things.

A cylinder can be driven by crystals only at a finite number of points N around the circle. The resulting directivity pattern will have "scallop" corresponding to the N driven points unless $N > ka$. As is noted in Section 4.2.4, the patterns become smooth circles very soon as N exceeds ka , so that $N = ka + 2$ or 3 yields fairly smooth circles.

When N crystals are arranged in a circle to drive a cylindrical source, the total fraction of the area driven is $NL/2\pi a$ where L is the width of the chord formed by the radiating edge of one crystal (usually L_t). Then the radiation resistance to be inserted in the equivalent circuit for a crystal face $L_w L_t$ is

$$\rho_1 c_1 L_w L_t \left(\frac{NL}{2\pi a} \right) \text{ mechanical ohms.}$$

The factor $NL/2\pi a$ is a particular value of the quantity g used in Section 4.4.2. Note the rule $N > ka$ above, and that the quantity $NL/2\pi a$ may be written

$$\left(\frac{N}{ka} \right) \left(\frac{L}{\lambda} \right).$$

For small cylinders N/ka is likely to be close to

unity, and L/λ is likely to be quite small. Thus the radiation impedance may be very low for such a unit, and even small losses may seriously lower the efficiency.

7.3.2

Lobe Suppression

Any number of lobe-suppression schemes may be invented for a particular shape such as a plane circle. The merits of complicated schemes must be weighed against ease of construction. It is difficult to lay out arrangements for electric foils if the crystals are not all the same size or integral multiples of the same size. Since variations of velocity are most easily accomplished by connecting varying numbers of crystals in series, lobe-suppression schemes should be limited to those having integral-number amplitude factors.

In Section 4.4.1 it is shown that the maximum radiated pressure is diminished by lobe suppression; this diminution resulting from a given scheme must be weighed against the lobe-suppression. The 3/1 scheme for circles (diameter ratio 0.61) gives -28 db lobe suppression. Actually to achieve this requires very nice control over the phase and amplitude distributions, and it is doubtful if much better suppression could actually be obtained with any scheme. In any event, -28 db is adequate for all ordinary purposes, and there appears to be little need of schemes involving more than two zones. Although transducers have been built using as many as five zones they were not better suppressed than two-zone units.

7.3.3

Multiple Motors

Very often the desired band width is greater than present crystals allow and multiple motors are indicated. There are two ways in which the motors might be arranged: (1) several separate motors near each other, or (2) motors interleaved with each other. Both have drawbacks.

If separate adjacent motors are used the undesired mechanical couplings can be eliminated

by suitable baffles. However, the apparent source of sound moves around from one motor to another as the frequency is changed; in units for use as calibration standards this is very troublesome. A more important drawback is the behavior at the crossover frequencies. If a pair of motors for use in frequency bands have acceptable patterns when operated alone in their respective bands, then if both were to be driven at the crossover frequency the pattern of combination would be very poor, particularly if there were much phase difference between the motors. It is unpleasant to disconnect one unit and connect the other at crossover, but there appears to be no way of avoiding it; the band over which crossover troubles occur might be made indefinitely narrow by filters, but could not be entirely eliminated.

This crossover difficulty might be overcome by interleaving the crystals of the two motors so that they occupy the same area. Provided phase differences could be fixed up and the 0.8-wavelength rule were not violated, this should be successful. However this is likely to result in serious losses resulting from adjacent crystals moving with different velocity. Also much difficulty must be expected from the mechanical couplings of the crystals of one motor to those of the other. At best the design of such a multiple unit would be very involved.

If multiple motors are to be used with crossover networks instead of switches, there are several ways of connecting them electrically. They might be all connected in parallel and then tuned with a single coil. However at the frequency at which one motor is resonant the others would be shunting capacities, the effective Q_E of the resonant motor would be raised, and the band width narrowed.

A better procedure would be to series-tune each motor separately and then parallel the units. If the problem is treated by filter theory, crossover networks might be designed using the inactive elements as filter sections for the active motor. This is a very involved problem.

No matter what crossover network is used, the relative phases must be picked correctly to give the best patterns at crossover; for this it must be remembered that the phase changes by π crossing each resonance.

7.4

TANGENTIAL MOTION

When a surface vibrates tangentially in a viscous fluid, shear waves are propagated outward. The attenuation is much greater than that of longitudinal waves, and in castor oil at frequencies from 10 kc to 100 the $1/\epsilon$ distance is measured in tenths of millimeters. Crystals move tangentially and thus radiate such shear waves, and this outgoing energy is a loss which reduces the efficiency.

If a crystal is separated from other surfaces by several times the $1/\epsilon$ distance it behaves as if it were immersed in an infinite ocean of the fluid. For this reason crystals only $1/8$ in. apart in castor oil are tangentially independent of each other. Under this condition the shear waves cause a noticeable but not serious loss and acceptably high efficiency is achievable. If, however, a tangentially vibrating surface is placed closer than a shear wavelength to another surface undergoing different motion (or stationary) the shear losses are greatly increased, apparently going up like the reciprocal of the separation. Thus crystals close to each other in castor oil are likely to compose a very inefficient array, and crystals not actually cemented together should be spaced apart a millimeter or more. If crystals are placed close to each other they should be glued, and the glue should be thoroughly baked to raise its Q .

Usually it is difficult to sort out the effects of viscous loss in order to demonstrate them, but in one instance there is a fairly clear-cut example.

The directivity patterns of a CY4 transducer near resonance are acceptable for the original purpose, but are by no means circular. In an effort to improve the patterns of the CY4, it was suggested that more nearly circular patterns would result if every alternate crystal were rotated 90° in a CY4 so as to make a four-faced vertical stack. Of course the $1\frac{1}{2} \times \frac{1}{4}$ -in. faces of each crystal would have to be covered with Corprene to prevent out-of-phase radiation.

This experimental transducer (XCY8-1) was built and tested. The patterns were much improved and were quite usable, being rather square but essentially circular instead of re-

sembling figure eight. However the efficiency was obviously very poor whereas that of CY4 is quite good (see Figure 2 in which CY4 is shown solid and XCY8-1 dotted). The symptoms exhibited by XCY8-1 are typically those of a unit of negligible efficiency: open-circuit voltage more or less flat in frequency, irregular, no marked resonance, and level more than 20 db below theoretical.

It was finally realized that the alternate crystals rotated 90° with respect to each other had their electrode faces separated only a few thou-

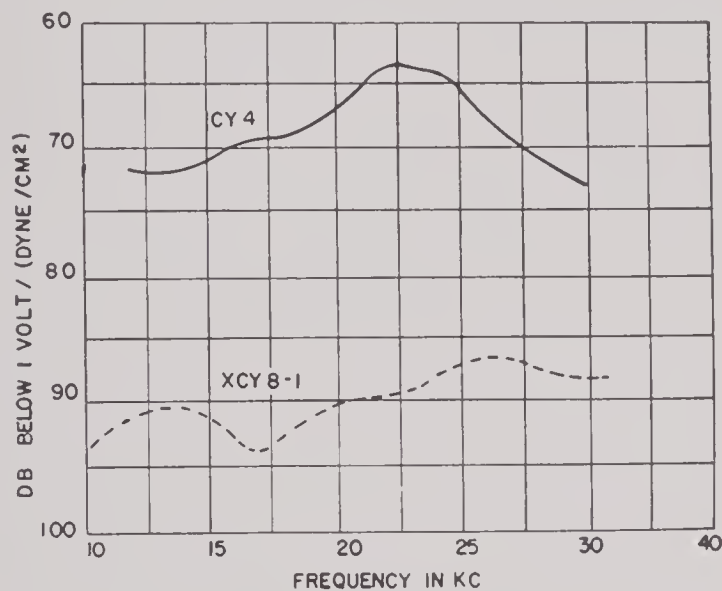


FIGURE 2. The receiver response of the CY4 transducer as compared with that of the XCY8-1 showing the low efficiency of the latter.

sandths of an inch, causing serious viscous losses. It would, of course, do no good to interpose rigid separators between crystals since the losses would then occur between electrode faces and separators. What was required was a means of separating the crystals by small beads placed at the geometric center of each crystal where the tangential motion is a minimum. To do this disks of solid rubber $\frac{5}{16}$ -in. diameter and $\frac{1}{32}$ -in. thickness were used. To make room for these, two crystals were left out, leaving 18. No other changes were made and the new unit was designated XCY8-2. Figure 3 shows the improvement over XCY8-1. There appears to be no doubt that the loss in XCY8-1 was caused by shear waves in castor oil.

7.5

ISOLATION MATERIAL

7.5.1

Materials

In any number of places isolation material is needed to control the sound. The ideal substance, acoustically, is vacuum, but to contain the vacuum requires a stiff wall whose characteristic impedance is too high. Thus the next best material is a mass of bubbles contained in some thin soft-walled substance. To prevent soaking up liquids the structure must be a foam

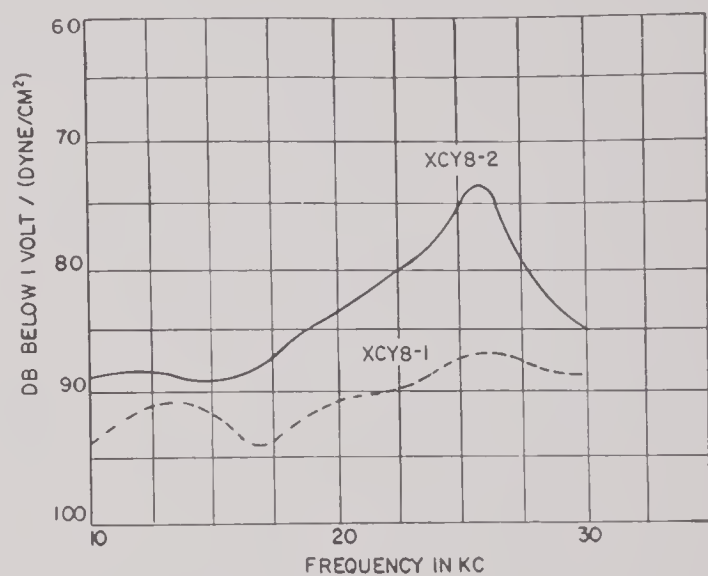


FIGURE 3. The receiver response of the XCY8-1 transducer as compared with that of the XCY8-2 showing the improved efficiency of the latter.

rather than a sponge. Even if the input impedance is not zero (vacuum) it must be quite low compared with that of water, and should be largely reactive to prevent dissipation. In many respects this is a description of foam rubber whose bubbles contain some gas. Cork is a sponge rather than a foam and is prone to slow saturation with the liquid unless the surface is sealed. To a lesser extent this is also true of Corprene.

The input impedance of Cell-tite rubber seems to be quite low (not known exactly) and at least the normal component is not too resistive. However there appear to be large variations among samples and some lose the gas by diffusion through the walls. This trouble is

likely to be met in any thin-walled substance, but might be less for butyl rubber.

Queer effects are sometimes observed with foam rubber which would be explained by assuming a fairly large and perhaps resistive tangential impedance. For example, when a sheet of Airfoam rubber is cemented to a large flat sheet of 20-gauge steel and the reflectivity to normally incident plane waves is measured, it is found that higher reflectivity is seen looking into the steel with Airfoam on back than looking into Airfoam with steel on back. This is so generally true that Airfoam is best put on a rigid surface *through* which the sound is incident.

The Bell Telephone Laboratories have recently used Airfoam rubber jacketed by a fairly heavy layer of rubber. For use in sheets as a reflector this should be excellent, but the tangential impedance must be larger. For this reason this jacketed material would not do well between crystals in an array.

Corprene is, in many respects, inferior to Airfoam rubber. There is some reason to think its input impedance is higher and its Q lower, thus inviting losses in oil. Certainly it exhibits marked mechanical hysteresis at very low frequencies. However it is stiffer and more easily cut, so that it has its uses in such places as holding together the vertical-stack transducers.

Foamglas is a foam whose walls are glass. Its density is very low, and it is quite stiff. However its input impedance is probably much higher than that of foam rubber or Corprene, and it does not do as well for isolation. The chief use is in places where the isolation must support its own weight.

7.5.2 Backing-Plate Termination

It is usually assumed that a backing plate is terminated by zero impedance. If air is used this assumption is justified since the characteristic impedance of air is only 43 ohms. In many transducers the region behind the backing plate is filled with castor oil and some low-impedance layer is required. Both foam rubber and Corprene have been used for this, but foam rubber is generally preferred. In this use the jacketed

foam rubber developed by Bell Telephone Laboratories should be excellent.

7.5.3

Case Lining

Some sound usually leaks out of an oil-filled unit in unwanted directions through the metal case. To prevent this it is helpful to line the entire interior with Airfoam rubber or Corprene cemented to the case. In this use there is little preference of one over the other.

7.5.4

Gas-Filled Inertia Drive

The window of a gas-filled inertia-drive unit may be large and thin: if subjected to hydrostatic pressure the face would bend inwards causing various damage. The best way to prevent this is to stiffen the window with steel rods molded in the rubber. Occasionally a rigid surface is provided close behind the crystals to prevent their moving backward. Because the crystals pushing against a hard surface might break, and an unknown reactive impedance might be imposed on them, Airfoam rubber is put between the crystals and the rigid surface. In every instance the efficiency is lowered: the crystals push rather deeply into the rubber, and it seems likely that tangential losses result from the crystals rubbing against the Airfoam. This practice is not recommended.

7.5.5

Liquid-Filled Inertia Drive

In principle inertia drive results if one end of the crystal is terminated by a low impedance: it is not necessary that the interior be gas-filled. Several UCDWR oil-filled transducers have been built in which inertia drive was attempted by terminating the crystals in Airfoam rubber. In view of Section 7.5.4, the crystals should not merely rest on the Airfoam: however, one cannot Cycle-Weld successfully to Airfoam rubber. Instead the crystals were Cycle-Welded to a thin strip of solid neoprene and this was in turn backed by the Airfoam. No adequate explanation has been proposed, but in every instance

the efficiency has been very poor. Very probably some tangential loss is involved; in any event much research would be required to make this method successful.

7.5.6 Spaces between Groups of Crystals

In Section 7.2.1, reasons were given for grouping crystals in blocks which were then separated from each other; it was remarked that Airfoam rubber may be put in the spaces.

No rules can be given for when to put Airfoam rubber in these spaces. If the transducer has acceptable patterns and good efficiency, the Airfoam should be left out since it is certain to introduce some tangential losses between itself and the crystal surfaces. On the other hand, several units whose patterns and efficiency were bad were cured by the Airfoam. To date the procedure is cut-and-try.

If Airfoam is used it is not necessary to fill the gap completely; apparently the mere provision of a pressure-release surface is sufficient. By half filling the gap all the good will be obtained and a little less new loss is introduced.

For several years UCDWR customarily put Corprene between crystals, and even went so far as to embed crystals in Corprene on five sides. Out of all the units so built only one, GC2, was acceptably efficient, and it remains a mystery. There is little doubt that serious tangential losses occur if Corprene is very near or against crystals.

7.6 BACKING PLATES

Throughout the better part of this book a backing plate is treated as a simple structure in order to facilitate theoretical work. Usually it is taken to be a uniform lossless layer backed by zero impedance so that its input impedance is just $+jZ_p \tan \phi$. In Section 4.9 it is even regarded as infinite at all frequencies. While these may be first- or zero-order approximations, a much more rigorous treatment is required to explain transducers fully. The Naval Research Laboratory [NRL] has published a very detailed analysis of certain backing-plate struc-

tures¹ which certainly deserves much study, but even there many approximations had to be made.

7.6.1 Spurious Vibrations

The most common approximation is the assumption of plane waves; any backing plate is irregularly excited because the crystals do not cover it completely and their surfaces do not move as planes. This results in the excitation of (probably) every normal mode of the plate, and if some normal modes happen to be close to the driven frequency they will be strongly excited. Except for the limited control over these modes described in Section 3.4, nothing can be done but cut-and-try if troublesome resonances are encountered. As a general rule it is well to cut a plate up into pieces small compared with a wavelength (in the plate), but this is not always possible. Some improvement may be obtained by damping the plate, but this cannot lead to high efficiency. Of all the backing-plate schemes proposed the NRL unit-construction seems to offer the greatest promise (see Section 3.3.4).

7.6.2 Multiple Layers

The multiple-layer backing plate described in Section 3.5 has been tried in a few cases. Further investigation of its capabilities seems indicated, but it is probably useful only in very special problems where space and weight specifications justify its use.

7.6.3 Glass

Most backing plates are solid steel, although some glass plates have been used (e.g., Brush Development Company Model C-26). Glass has much to offer: it is quite strong, has negligible dissipation, and is a nonconductor. This last property greatly simplifies the problems of reducing stray capacity and handling high voltage. No analysis has been carried out, but the band width of a glass-backed unit should not be much less than that of a steel backed unit. The

lower coefficient of thermal expansion should allow high- Q glued joints, and any loss of band width might be recovered.

7.6.4

Insulation

If a metal backing plate is used some insulator should be put between the crystals and the metal to reduce the stray capacities and to allow high voltages. For this purpose Submarine Signal Company, has used empire cloth. Bell Telephone Laboratories has used ceramic wafers and mineralized plastic wafers cut in individual squares to go under each crystal block. This is quite good if high-quality glued joints are used. UCDWR has used porcelain enamel applied in a furnace. This is likely to contain pits which must be filled to obtain high voltages, the surface must be lapped, and there is some question of whether differential thermal expansion might cause exfoliation (to date UCDWR has observed none). To offset these disadvantages, one glued joint is eliminated.

7.6.5

Thin Plates

If a high-impedance material such as steel (39×10^5) is used for a backing plate it is not necessary to use a quarter-wave plate in order virtually to clamp the crystal. Plates as thin as an eighth wave do quite well. However the resonant frequency is not quite as low as that of a completely clamped crystal. If one ignores the finite width correction of the crystal (adding it later on) the resonant frequency is at least close to that which satisfies

$$Z_c \tan \theta = -Z_B \tan \phi, \quad (1)$$

where Z_c = characteristic impedance of crystal,

Z_B = characteristic impedance of backing plate,

$$\theta = \frac{\omega L_y}{V} \text{ in crystal,}$$

$$\phi = \frac{\omega L_B}{V_B} \text{ in backing plate.}$$

In deriving this it is assumed that the radiation resistance is zero; it enters slowly for $Z_B \ll Z_c$ and the error is not great.

A graph of this function reveals that ω is a fast function of L_B when L_B is less than an eighth wavelength. This means that for small L_B the resonant frequency may vary from crystal to crystal in an array because of small departures from uniformity. For this reason very thin plates should not be used.

An eighth-wave plate reduces the frequency almost to that of a quarter-wave plate for $Z_B \gg Z_c$. For plates thicker than quarter wave the resonance moves down very slowly and the Q of the resonance rises rapidly. Such very thick plates are not recommended. Fry, Taylor, and Henvis discuss this subject more thoroughly.¹

7.7

WINDOWS

The ideal acoustic window for transducers does not exist; it would be identical with sea water in all respects except to be an electric insulator and a solid. Unfortunately all real windows differ significantly from water. For one thing the slope of the characteristic impedance of water versus temperature is anomalous and has opposite sign from most substances. Thus any window can be expected to match water only at one temperature. Fortunately it is not necessary to match perfectly for most uses, and in fact a decided mismatch is often tolerable.

7.7.1

Sound-Water (qc) Rubber

For several years a rubber developed at NRL and available from B. F. Goodrich Company has been used for windows. It is commonly called qc rubber, and until recently that title was a unique description. Recently Bell Telephone Laboratories [BTL] has developed their own qc rubber and the term is often used indiscriminately. Acoustically there is little difference between the two. The BTL rubber appears to be a little stronger and harder, but no important differences are claimed.

In both rubbers it has been attempted to match the q and c of water separately as well as the qc product. The success is remarkable, and there is no doubt that these rubbers are the best



window material available; quite thick curved sections may be used with negligible effect on patterns or response.

Both rubbers bond to metal and in this way make strong (but flexible) windows.

7.7.2

Neoprene

During World War II UCDWR used neoprene for windows to facilitate procurement; tests were run which indicated negligible harmful effect in ordinary circumstances, and the neoprene windows were adopted to the exclusion of qc rubber. However difficulty was encountered in a unit having a cylindrical rubber window 10½ in. inside by 1-in. wall thickness at 42 kc. When qc rubber was substituted the troubles disappeared. For thin (say ½-in.) windows in flat sheets before plane arrays, neoprene is acoustically satisfactory and mechanically superior to qc rubber, provided effects of the order of 1 db are ignored, but in thick sections and particularly in curved thick sections neoprene is unsatisfactory.

7.7.3

Other Materials

Many other materials are usable for windows in special applications. Some of these are discussed in Section 3.7 and in Chapter 8.

7.7.4

Size of Window

Ideally a window should probably extend all the way around a transducer in order not to disturb the directivity patterns. Bell Telephone Laboratories particularly tend to extend their qc-rubber windows about $\pm 90^\circ$ from the forward direction. However most other manufacturers usually use a window which is just a little bigger than the crystal motor and not too far away. Probably some shadowing results but it does not appear to alter the directivity patterns appreciably. By restricting the size of the

window greater strength is obtained; an important consideration in many units.

7.8

CROSSTALK

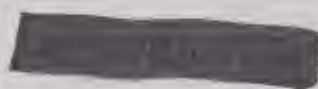
In some very special applications it is necessary to operate a transmitter and a receiver near each other, simultaneously, at the same frequency. Such a system is troubled by crosstalk, the signal which passes from projector to receiver through close-in or internal paths.

To reduce crosstalk it is necessary, of course, to keep the receiver out of the main lobes of the transmitter directivity pattern. However this is usually not enough since the two motors are mounted in a common structure. It has been found that sound will run through a metallic structure just like an electric current. If a metallic path exists by which sound may get from one motor to the other it will do so, no matter how unbelievably devious the path. It is usual that the most important crosstalk paths run through washers to bolts, from bolts to angle iron, and from the angle iron to a casting, and so on, perhaps through a dozen compartments.

It is necessary to open these paths by inserting isolation material such as Corprene. When isolating a bolt it is necessary to provide not only Corprene washers under the head and under the nut, but also a Corprene bushing between the bolt and the drilled hole. Foam rubber is not recommended for this use because it takes a permanent set too easily under static load. Corprene is stiffer but also will take a set, so that very large areas should be used to distribute the load.

In tightening isolated bolts, lock nuts should be used so that the nut can be left loose; too much compression of Corprene restores a significant amount of crosstalk. Isolation blocks should be provided immediately adjacent to both the receiver and the transmitter. It is helpful also to support the crystal motors within the cases on isolation material.

If the two motors are mounted in a common exterior case it is necessary to so design the interior that any oil paths involve devious routes. It is helpful to connect the two chambers



only by tubes or holes whose diameters are small compared to a wavelength.

If, in the common case, the two motors share a large acoustic window it is found that the window material can act as a wave guide, piping significant amounts of energy from one unit to the other. This happens even for *qc* rubber windows because, while close, this material is not *identical* with water. If this coupling exists it is necessary to insert a large impedance mismatch in the window material between the two motors. In rubber this is best accomplished by molding in a Corprene layer, or by molding in a quarter-wave steel layer.

If two motors occupy a common exterior case

it may be important to use a *qc*-rubber window on the transmitter. While the transmission through other windows might be as high as 99 per cent, a little of the transmitted energy fails to escape and returns to the interior. This represents a negligible loss as far as transmission is concerned, but the returned energy may increase the internal energy density greatly, thus raising the crosstalk level by internal paths a great deal.

If every precaution is taken to reduce crosstalk, it is usually possible to reduce the level below that determined by long-range scattering (reverberation). This is, of course, a lower limit beyond which there is no point in striving.

Chapter 8

CONSTRUCTION TECHNIQUES AND EQUIPMENT

By *Fred M. Uber*

8.1

INTRODUCTION

THE NUMEROUS EXPERIMENTAL and production techniques involved in the construction of transducers have resulted from the efforts of many different individuals working in various laboratories. In order to present the best methods there has been no attempt to limit the subject material to the practices of any one individual laboratory. In particular, it has been felt that a limitation of this chapter to a discussion of the techniques in use at University of California Division of War Research [UCDWR] would not be considered in the best interest of the transducer art. Consequently, the writer has made a special effort to visit the several laboratories engaged in research and development on synthetic crystal transducers in order to be able to evaluate critically or at least describe the various techniques in current use.

Although it is obviously impossible in a chapter of this kind always to give proper credit to the originators of various techniques and items of equipment, an effort will be made to do so, at least in so far as credit is due the various laboratories. Where photographs have been reproduced, by-lines indicating their source will occur in the titles to the figures. Besides UCDWR, information has been obtained principally from the Brush Development Company, the Bell Telephone Laboratories [BTL], and the Naval Research Laboratory [NRL].

PRECAUTIONS WHEN HANDLING CRYSTALS

The need for exercising care in the handling of piezoelectric crystals should be apparent to those familiar with their function. If not, the discussion on properties of crystals, which follows in the next several sections of this chapter, should make it clear. The electrical characteristics of crystals in particular can be adversely affected if the crystals are improperly handled.

Of all the variables and unknown quantities

that are encountered in the construction of synthetic crystal transducers perhaps the most annoying one is associated with the irresistible urge of individuals to handle the crystals with their bare hands. To one accustomed to dealing with inanimate objects this may not appear off-hand as an insurmountable difficulty, but in actual practice in the laboratory or in small-scale production it becomes almost impossible to control. From the time work is begun on an original mother crystal until a transducer is completed, numerous operations must be performed, including final surfacing operations, application of electrodes, polarizing, cementing to supporting structures, wiring, and final testing. This entire process may require for its completion periods of time varying from a few days to a few weeks and perhaps as many as a dozen individuals may have taken part. When the transducer has been finally assembled it is difficult, if not impossible, to be certain that one or more of perhaps a few hundred crystals have not been touched by someone's fingers.

The actual chemical and/or physical changes that are brought about on the surface of a crystal due to human contact can readily be imagined although they may defy detailed scientific description. Both *Rockelle salt* [RS] and *ammonium dihydrogen phosphate* [ADP] are water soluble so that any contact with moisture would certainly produce a deleterious effect on the surface conductivity. It is quite possible that materials which may be deposited on the crystal surface are more hygroscopic in nature than either ADP or RS. Substances present on the skin may also react chemically with the crystalline materials. There is apparently no point in trying to pursue these suppositions in detail, particularly since there seems to be but one solution to the entire problem. This solution is simply to refrain from touching crystals with the bare hands.

Various laboratories have furnished protective coverings, either for particular fingers or

for all of the fingers on both hands. At the Brush Development Company, where numerous production workers are engaged in the manufacture of bimorph crystals, a relatively high degree of success has been attained by requiring that rubber finger cots be worn. In their experience it was not sufficient to have these cots worn on the thumb and index finger, which alone are normally used in handling crystals. When this was done, some individuals would resort to using the unprotected fingers. Hence, their current practice is to require that these cots be worn on all fingers of both hands. Even this does not constitute a sufficient solution unless the rubber cots are constantly maintained in an immaculate condition. Just how difficult this can be will be realized when one recalls how frequently the fingers may be allowed to come in contact with other parts of the body. Objections to the use of rubber coverings on the fingers arise as a result of the enhanced perspiration beneath them. An attempt to overcome this objection has led to a trial of fairly thick rubber finger protectors containing perforations but they are not a satisfactory solution. Cotton gloves, such as are used by film cutters in the motion-picture industry, have also been tried.

In the last analysis it would appear that the eternal vigilance requisite for the successful production of high-power crystal transducers is probably to be expected only of that relatively small number of individuals who are fully cognizant of the factors involved and who are capable of painstaking work. However, there are many auxiliary aids which may prove efficacious in stimulating satisfactory performance of tedious work. For one thing, great importance must be assigned to psychological factors. One scheme, so advantageously exploited among nurses and workers generally having to do with public health, is the suggestive use of white to promote cleanliness. Another psychological stimulus could be furnished by providing each operator with an air-conditioned booth or small room in which to work.

The effect of adverse humidity conditions on both RS and ADP crystals makes it appear advisable to have a special air-conditioned room in which the crystal processing and the assem-

bly of crystals into transducers can take place. Equipment should be provided which filters the air in addition to controlling the humidity and temperature conditions. Related to this problem of air conditioning is the further problem of providing for the disposal of the dust which arises during dry-grinding and milling operations. This is discussed further in Section 8.4.2. The use of adhesives which contain volatile organic solvents may also make provision for an adequate chemical hood advisable for spraying operations.

8.2 CHARACTERISTICS OF CRYSTALS

8.2.1 Chemical Properties of RS

Chemically, RS is a double tartrate of potassium and sodium having the formula: $\text{KNaC}_4\text{H}_4\text{O}_6 \cdot 4\text{H}_2\text{O}$. Rochelle salt crystals have

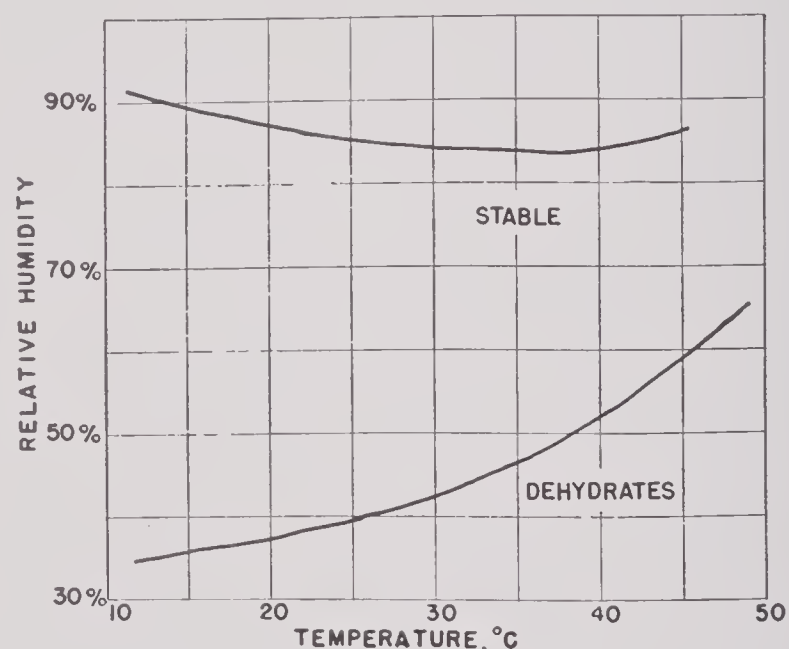


FIGURE 1. Stability limits of Rochelle salt as a function of temperature and relative humidity.

been known for nearly three centuries, having been produced from the dextro form of tartaric acid which was abundantly available commercially from the wine industry. The fact that RS contains four molecules of water of crystallization has an important bearing upon its general behavior. At 55.6 C two molecules of RS transform into one molecule of sodium tartrate and one of potassium tartrate with the evolution of one molecule of water. Complete liquefaction

results when the temperature reaches 58 C. The behavior at temperatures below 50 C can be seen by an inspection of the curves in Figure 1. At relative humidities higher than the upper limit shown in this curve, moisture will collect on the surface of the crystal, while at relative humidities below the lower limit given in the curve, the crystals dehydrate. The maintenance of proper storage conditions for RS crystals is discussed at some length in Section 8.2.9.

The solubility of RS in water at 0 C is 420 g per l and at 30 C it is 1,390 g per l. This high solubility is an important consideration in controlling the rate of crystallization of RS from saturated solutions by decreasing the temperature. Rochelle salt is only slightly soluble in ethyl alcohol so that absolute alcohol may be used to remove surface moisture from crystals. However, dehydration would result if absolute alcohol were used too generously or remained in contact over too long a period. Rochelle salt is soluble in ethylene glycol, but not in benzene, carbon tetrachloride, and in numerous other organic solvents.

The density of RS at 25 C is 1.775 ± 0.003 g per cu cm.

8.2.2

Crystallizing RS Bars

Considerable information exists in technical literature on the growth of crystals from aqueous solutions, both on a laboratory and on a production scale. Successful crystallization of large bars depends on several factors.

1. There must be a carefully controlled degree of supersaturation of the solution in order to provide the highest rate of deposition of crystalline material without the formation of flaws or irregular growth. This control of the supersaturation may be brought about in any one of three ways. The first one is essentially of laboratory importance only and consists of controlling the rate of evaporation while maintaining a constant temperature. The rate of flow of water vapor from the solution into a condensation trap can be regulated by varying the air pressure in the system. The second method^{1, 2} controls the saturation by a variation in the temperature and has been employed on

a large scale in the commercial production of RS. With this method, it is customary to start with a high initial temperature and allow the solution to cool at a carefully controlled rate for a period of 3 to 6 weeks. The initial temperature must not be above 40 C or sodium tartrate will be deposited. It is convenient if the temperature finally reached is approximately that of a normal working room so that the crystals do not crack upon being brought out of the growing room. The third method³ of controlling the concentration depends on circulation of the solution between a stock of finely divided crystal material and the growing bars. In this case a temperature differential is maintained to promote the dissolution of the finely divided crystals and the subsequent deposition on the growing bars.

2. Seeds of proper shape and orientation must be provided. In the case of RS, these seed bars may have a square cross section $\frac{3}{8}$ to $\frac{1}{2}$ in. on a side and may be as much as 20 in. long. They are placed in slots on the bottom of the rocking tank which contains the solution. The orientation of the seed bar in the slot depends on whether X-cut or Y-cut crystals are to be processed from the final mother bar. In Figure 7 the original seed bar is shown being milled off the mother crystal in order to provide a reference surface.

3. It is important to provide for a continual circulation of the solution over the entire surface of the growing bar. Both the rapidity of the circulation and its direction of motion are fairly critical. In the absence of satisfactory circulation conditions, the rate of crystal growth is not uniform over the surface of the bar so that vacant or flawed regions known as veils occur. Other factors, such as the hydrogen-ion concentration of the solution, also have an important bearing on the rate and quality of crystal growth.

Synthetic RS crystals have been produced in this country in commercial quantities for many years by the facilities of the Brush Development Company and the crystals employed at UCDWR during World War II were made available by them. The writer of this chapter has had no direct experience in the growing of RS crystals, but has had the privilege of visiting the plant

of the Brush Development Company and observing the growing and processing techniques.

8.2.3

Thermal Behavior of RS

The thermal-expansion coefficients of RS have been reported by Vigness⁴ to have the following values parallel to the direction of the axes. From the standpoint of construction technique, the thermal-expansion coefficients are of interest only as they affect the differential expansion between a crystal and the base to which it is cemented.

Axis	Temperature range in degrees C	Coefficient per degree C
X	12-35	58.3×10^{-6}
Y	12-24	35.5×10^{-6}
	24-35	39.7×10^{-6}
Z	14-24	42.1×10^{-6}
	24-35	34.6×10^{-6}

The variation with temperature of some other physical properties of RS will be found discussed elsewhere in this volume. Its electrical resistance as a function of temperature is treated in Section 8.2.4.

8.2.4

Electrical Properties of RS

The characteristic curve of leakage resistance as a function of temperature for an RS crystal is shown in Figure 2. The measurements for this graph were obtained by McSkimin⁵ and were taken on a crystal 1.6 cm long, 1.0 cm wide, and 0.4 cm thick with tin foil electrodes being placed on the largest surface. Hence, the resultant interelectrode distance was 0.4 cm. It will be noted that the leakage resistance decreases very rapidly with increase in temperature above 43 C. In obtaining these data the relative humidity was maintained at the equilibrium point for the dehydrated salt, that is, at that value of the relative humidity where dehydration just begins. The entire crystal was immersed in oil. At a temperature of 51 C the leakage resistance has decreased to 500,000 ohms. A further increase in temperature results

in still further leakage, until at a temperature above 55 C the crystal is rendered useless because of melting.

If the temperature of an RS crystal is either lowered or raised rapidly, leakage resistance curves differing widely from the characteristic curve of Figure 2 may be obtained. As an example of this behavior, a crystal coated lightly with Vulcalock cement was placed inside a can, together with a small quantity of crushed hydrated RS. It was found by McSkimin⁵ that raising the temperature of such a crystal only 1 degree caused the leakage resistance to drop very rapidly from over 100 megohms to several megohms as shown in Figure 3. At 35 C the crystal had less than 100,000 ohms resistance. The only satisfactory explanation of this behavior appears to be that RS adsorbs water on its surfaces. The amount of water adsorbed is a function of both pressure and temperature: the higher the temperature the less the adsorption, the higher the pressure the greater the adsorption. On this theory the behavior of the Vulcalock-coated crystal can be explained by assuming that a small quantity of adsorbed water was trapped beneath the cement on the crystal surface. Raising the temperature only slightly could result in driving off a small amount of this water into the very limited space between the cement coating and the crystal surface with a resultant rapid increase in the relative humidity. The high relative humidity resulted in the excessive leakage measured.

By removing any adsorbed water from the crystal before putting on the surface coating, it should be possible to approach quite closely the characteristic curve of Figure 2. This procedure was followed to obtain the second curve shown at the right in Figure 3. The tremendous improvement is very marked. In numerous tests it was found by McSkimin⁵ that the removal of adsorbed water minimized leakage in all cases.

For transducer applications where it is necessary to apply high voltages to the crystal electrodes, the presence of moisture on the interelectrode surfaces of RS crystals will cause arcing. Arcing between electrodes will occur at some critical voltage, the failure taking place quite rapidly. This voltage breakdown may be caused to occur at much higher potentials by

using care in the removal of adsorbed water. McSkimin⁵ has reported that a crystal having several hundred megohms leakage resistance may nevertheless have a small amount of adsorbed water on its interelectrode surface. If the crystal is immersed in oil or if the surface is cemented over and perhaps attached to other materials, this trapped water cannot be dispersed readily in the case of a sudden increase

importance to keep electrical leakage at a minimum is where it is desired to use RS in transducers operating at frequencies of only a few cycles per second. The performance of a transducer at low frequencies is limited seriously by a low-leakage resistance so that unusual precautions must be taken in such equipment to obtain the highest possible values of electrical resistance.

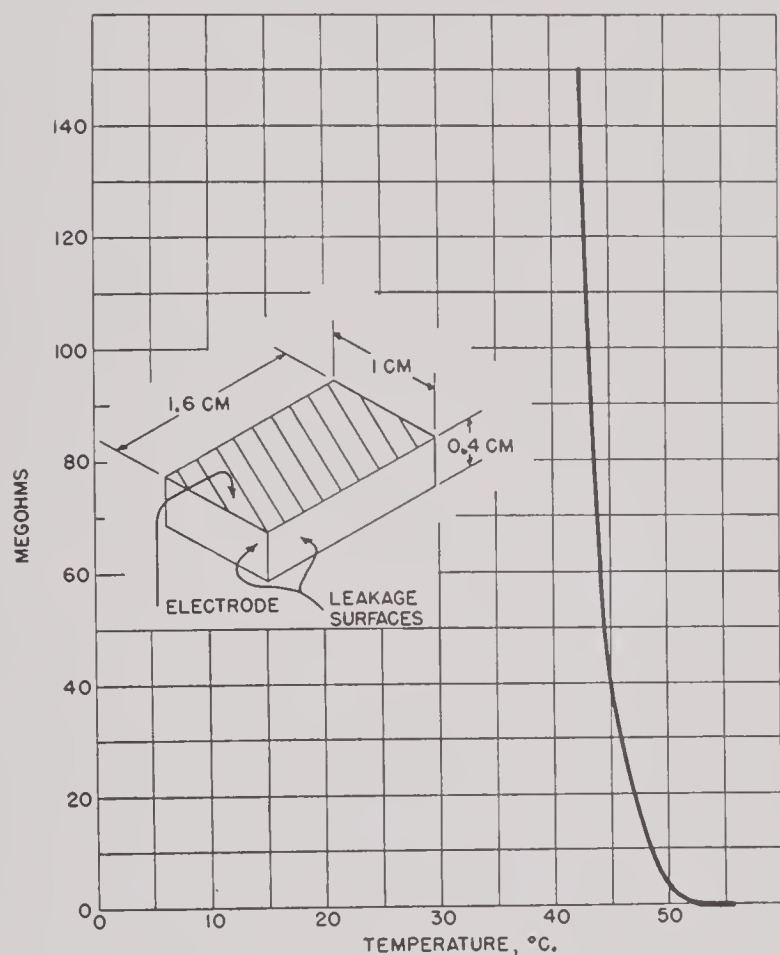


FIGURE 2. Characteristic leakage resistance of Rochelle salt crystals.

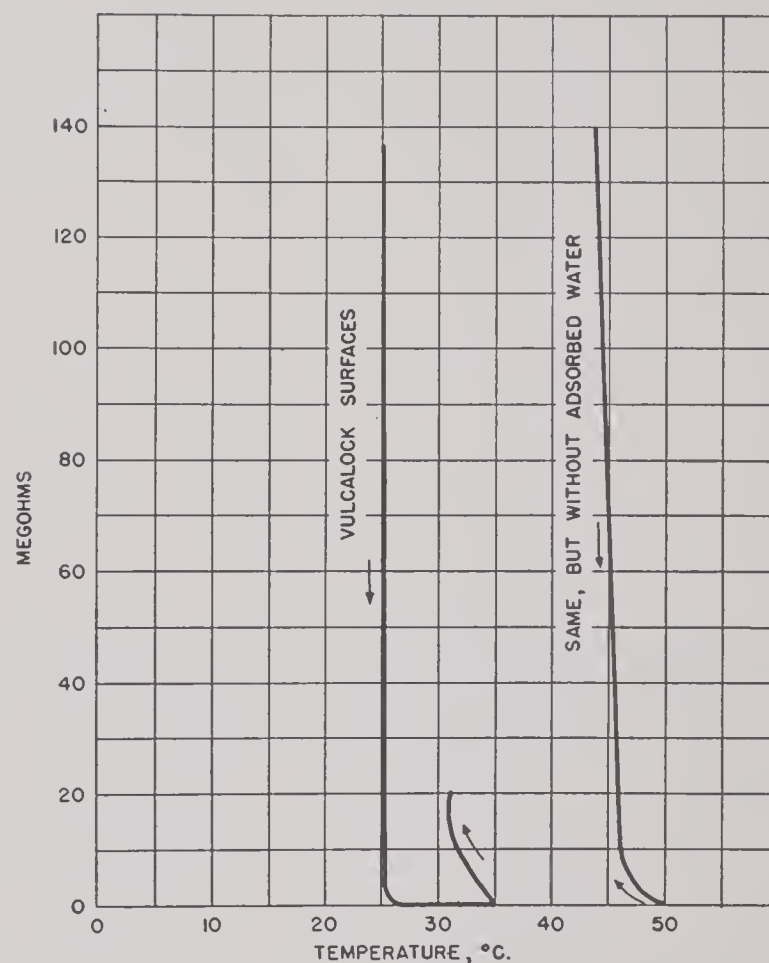


FIGURE 3. Leakage resistance of a Rochelle salt crystal coated with Vulcalock cement, with and without adsorbed water.

in temperature. Owing to the power dissipation by even a high leakage resistance, the temperature at the surface of the crystal will be increased slightly. As has already been pointed out in discussing the curves of Figure 3, a temperature increase of only a degree or so may be necessary to cause a rapid decrease in resistance. Since the power dissipation increases rapidly with a decrease in resistance, the effect is seen to be regenerative and voltage breakdown happens abruptly. The importance of removing all adsorbed water is evident.

Another application in which it is of extreme

8.2.5

Chemical Properties of ADP

Piezoelectric ADP crystals are composed of ammonium dihydrogen phosphate, $\text{NH}_4\text{H}_2\text{PO}_4$, also called primary ammonium phosphate. In literature⁶ of the Brush Development Company, these crystals are referred to as PN crystals. ADP crystals are thus seen to be without any water of crystallization and are therefore stable in vacuum, in air up to 93 per cent relative humidity, and in the presence of strong desiccants. The density of ADP is 1.803 g per cu cm.

ADP crystals are readily soluble in water.

The number of grams of ADP per 1,000 g of saturated solution at any temperature T in degrees centigrade, can be calculated from the following expression: $171 + 4.70 \cdot T$. A large number of organic solvents are without noticeable effect on ADP, including carbon tetrachloride, the lower ketones and esters, and benzene. It is not soluble in castor oil.

At temperatures higher than 125 C, an ADP crystal will lose ammonia from its surface unless kept in an atmosphere containing ammonia vapor. At 125 C the dissociation pressure is 0.05 mm Hg; at 150 C it is still below 1 mm of Hg pressure. Continued loss of ammonia results eventually in a coating of phosphoric acid on the crystal surfaces.

8.2.6

Crystallizing ADP Bars

The production of synthetic ADP bars has been carried out on either a pilot plant or commercial scale during World War II by four different laboratories. Pilot plants were in op-



FIGURE 4. Large ADP crystal grown in reciprocating radial crystallizer. (Bell Telephone Laboratories.)

eration at NRL and at BTL. Commercial growing plants, financed by the government, were built and operated by the Brush Development Company at Cleveland and by the Western Electric Company at its Hawthorne Plant. No ADP bars have been crystallized at UCDWR and no direct experience with growing processes, other than brief observation, has been had by the writer. Consequently, the intention here is not to enter into a detailed discussion on the growth

of ADP bars but rather to outline the general steps in the process and to indicate where further information may be found. The most detailed report available on the crystallization of ADP bars is contained in a confidential publication of BTL.⁷ This report covers the laboratory work which was done at BTL in connection with the design and operation of the growing plant operated by the Western Electric Company. It will be assumed here that anyone interested in growing ADP bars will become familiar with the contents of this report.

The flat seed plates for growing ADP crystals are square and have about the same area of cross section as the fully grown mother bar. The seed plate can be seen in the central section of the mother crystal photographed in Figure 4. A seed plate, fully capped, is also shown schematically in the drawing of Figure 9. These seed plates are obtained by slicing the full grown bars. Since the growth of ADP crystals is primarily in the longitudinal direction, it is difficult initially to obtain seed plates of large area. In fact, the greatest deterrent to the rapid inauguration of a growing plant is the time-consuming task of producing the initial supply of seed plates with large cross sections.

Two types of equipment have been used for growing ADP bars. One contains horizontal trays which are subjected to a rocking motion. The rocking-type crystallizer had previously rendered excellent service in the synthesis of RS bars; most of the ADP bars produced to date have come also from the rocking type of equipment. The second type of apparatus, so far confined largely to pilot-plant operations, provides circulation by having the seed bars undergo a reciprocating rotary motion inside a cylindrical solution tank. The latter type plant seems to possess some superior advantages for growing ADP bars.

The supersaturation of the ADP solution may be maintained either by gradually decreasing the temperature of the solution or by the continual addition of salt to a constant temperature bath. The initial temperature of the saturated solution at the Hawthorne Plant was 41 C for the seed-capping operation and 46 C for the subsequent growth of the seed caps to mature bars. The final solution temperature should be

that of the processing room in order to avoid fracture of the crystals by introducing thermal strains upon their removal from the growing tanks. Other things being equal, the crystals should preferably be grown by means of a constant-temperature process, but operating controls seem to be somewhat more difficult. If technical difficulties could be satisfactorily overcome, the ideal method would be a continuous constant-temperature operation in which the crystal bar would be withdrawn from the saturated solution at exactly the same rate as formed.

The production rate and the quality of the ADP bars depends markedly upon the purity of the solution and difficulty has been experienced in getting sufficiently pure materials. The impurity that causes the greatest concern is the sulphate ion and one must go to great lengths to reduce its concentration to an optimum value. Its bad effect on the electrical resistivity of the bars will be discussed in Sections 8.2.8 and 8.5.7. On the other hand, the rate of growth of ADP bars is very materially improved by the presence of the sulphate ion. Particularly in the capping of flat seed plates, advantage has been taken of this fact to hasten the capping process. After complete caps have been formed, the seed crystals should be transferred to a solution relatively free from sulphate, the exact sulphate concentration depending on the electrical resistivity desired in the final product. Of the metallic impurities, barium ions may give some trouble. For details, refer to the original report.⁷

8.2.7 Thermal Behavior of ADP

The melting point of ADP crystals is 190 C. There is no transformation point, Curie point, or other thermal irregularity between the melting point and -100 C. Decomposition with loss of ammonia may occur below the melting point and is discussed in Section 8.2.5.

The thermal coefficients of expansion for ADP have been determined and are $(33 \pm 3) \times 10^{-6}$ per degree C, perpendicular to the Z axis, and $(5 \pm 3) \times 10^{-6}$ per degree C, parallel to the Z (optic-) axis. Sudden cooling of ADP crystals results in fracturing. Cracking of crystals

cemented to a support owing to differential thermal expansion will be discussed in Sections 8.6.4 and 8.6.5.

8.2.8 Electrical Properties of ADP

The electrical characteristics of particular concern to this chapter are the volume resistivity and the surface resistivity. Of the two, the volume resistivity overshadows the latter in importance since the surface resistance of ADP is about fifteen times as great as its volume resistance. The surface resistance does not seem to be materially affected by humidity unless the latter attains a very high value. However, in handling ADP crystals, the surface conductivity must be considered, especially from the standpoint of any increase owing to contamination. The remarks in the introduction of this chapter on handling precautions are applicable in this connection.

The volume-resistivity characteristic of ADP is quite sensitive to the existence of impurities in the growing solution, the most important impurity being sulphate. The resistivity of ADP as a function of the sulphate content of the saturated solution in which the mother crystal is grown has been determined at BTL⁷ and is shown by a graph in Figure 5. In the specifications outlined in Section 8.5.7, it will be noted that ADP crystals are graded on the basis of their volume resistivity.

The volume resistivity for a Z-cut ADP crystal as a function of temperature, as measured by Johnson and Briggs,⁸ is reproduced in Figure 6. Similar data have been obtained by other workers. Typical resistance values between the electrode faces of a clean ADP crystal 1 cm square in area and 2 mm thick, in dry air, as given by the Brush Development Company⁶ are:

Temperature in degrees C	Resistance in megohms
25	1,500
35	1,000
46	500
75	100
100	17

The leakage conduction in ADP crystals is therefore found to be quite different from that

in RS. In an RS crystal the conductivity is primarily a surface phenomenon and depends on the relative humidity of its environment. Even when immersed in a water-free liquid, RS will furnish its own moisture from its water of crystallization to bring about lower surface resistance and perhaps, under operating conditions, eventual electrical breakdown. Since ADP crystals contain no water of crystallization to escape, their surface resistance remains high

tion of the surface insulation in ADP must be well above 100 C. Even storage at 100 C for 6 months does not produce any permanently adverse effect on surface leakage.⁶

8.2.9 Storage Conditions for Crystals

In the use of RS, it is necessary to control the humidity for best results. Only by so doing

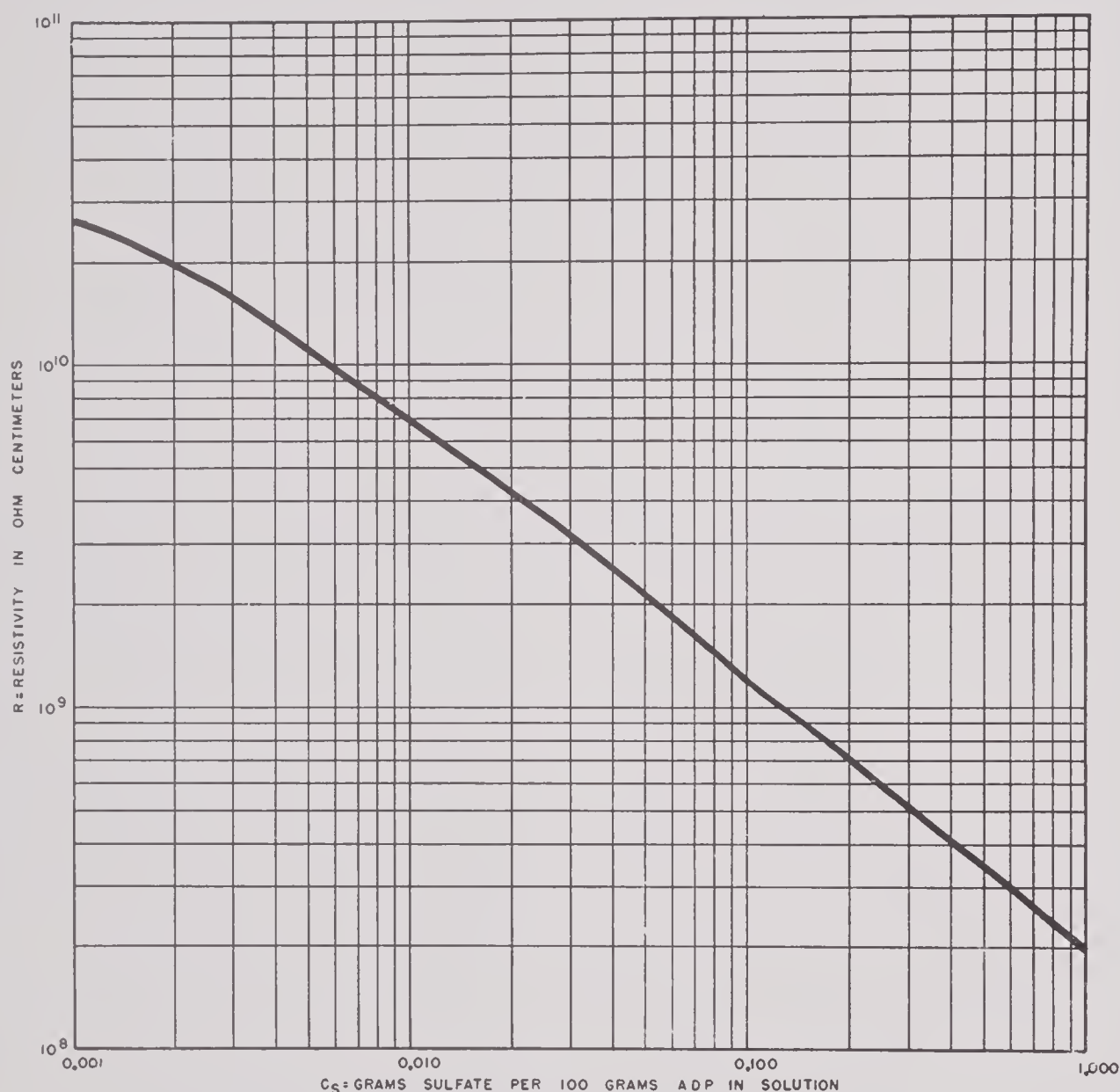


FIGURE 5. The electrical resistivity of ADP crystals as a function of the sulphate content of the growing solution.

even while immersed in oil at high temperatures. With ADP, however, high temperatures may produce a loss of ammonia from the surface and thereby result in a surface coating of phosphoric acid. This acid coating would naturally result in high electrical leakage. The temperatures necessary for permanent deteriora-

is it possible to attain minimum electrical leakage and minimum transient effects. It is also important to avoid dehydration of the crystal surface since this could lead to a high-voltage drop in the dehydrated layer. At a relative humidity below about 35 per cent, RS crystals lose moisture and dehydrate, while above 85 per

cent relative humidity, moisture collects on the surfaces and the crystals dissolve. The safe upper and lower limits of relative humidity as

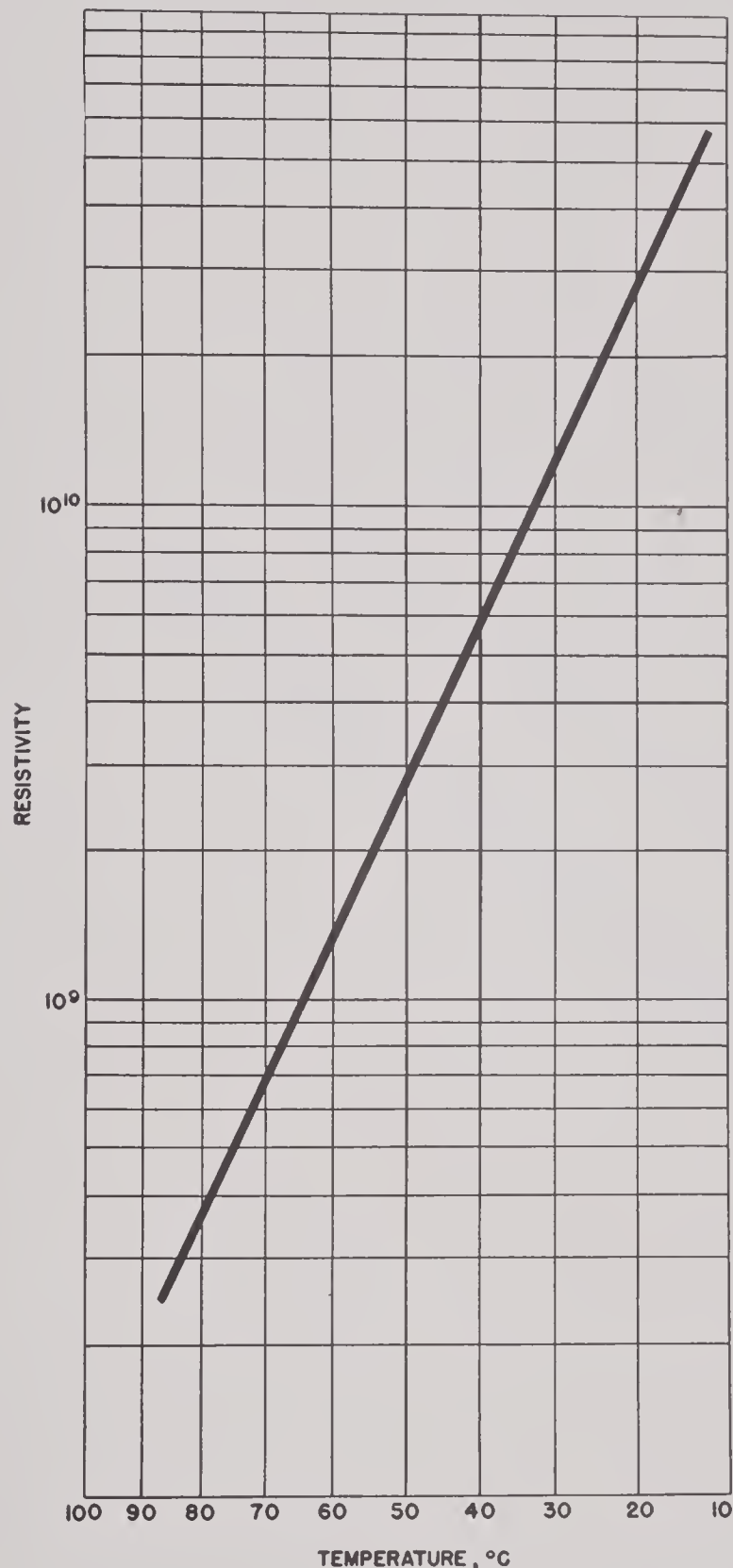


FIGURE 6. Electrical resistivity of ADP crystals as a function of temperature.

a function of temperature for the proper storage of RS crystals are shown graphically in Figure 1. In general, it is better to keep the relative humidity for crystals stored in air near

the lower limit shown on the graph. This can be done at all temperatures by enclosing the crystals in a hermetically sealed box, together with a mixture of hydrated and dehydrated RS in powdered form. If sufficient care is exercised to remove adsorbed water from all the hydrated salt concerned, then dehydrated salt need not be mixed with the hydrated RS for control purposes. It is usually desirable, however, to use a small quantity of dehydrated salt to insure the removal of excess moisture. In regard to the amount of RS required, the following rule may be used: allow 1 per cent of the enclosed volume to be control salt. This allows a very high factor of safety.

If RS crystals are to be surrounded by oil, any moisture on them should be removed by placing them in a vacuum chamber for perhaps 5 or 10 minutes. The length of time in which RS may be evacuated without serious dehydration is markedly dependent on its surface texture. Likewise, the moisture and air should be removed from the oil before immersion of the crystals. This point is treated at some length, and complete equipment for dehydration is discussed, in Section 8.8.9. The remarks in this paragraph are also applicable to ADP crystals.

As regards a safe upper temperature limit for the storage of RS crystals, the value of 50 C or 122 F is suggested.

The storage of ADP crystals does not present any special problems. The relative humidity should not exceed 90 per cent, however, nor should the temperature be appreciably over 100 C. At temperatures higher than 100 C, it would probably be desirable or even necessary to have an atmosphere of ammonia vapor to prevent decomposition of the crystal-surface layers if storage were contemplated for an appreciable length of time.

8.3 PREPARATION OF INDIVIDUAL CRYSTALS

8.3.1 Orientation of RS Bars

The appearance of a synthetically grown RS bar intended for X-cut crystals is shown diagrammatically in Figure 8. The location of



X-cut and Y-cut shapes is also shown in relation to the principal surfaces of the mother crystal. In order to obtain crystals of the desired orientation, it is necessary to start with accurate reference planes on the mother bar. It has been found that the two larger sloping surfaces of an RS bar do constitute satisfactory reference planes. A practical procedure is to design and build a jig on which these two reference planes

8.3.2 Rough-Cutting Crystals from RS Bars

An RS bar intended for the production of X-cut crystals is shown diagrammatically in Figure 8. A schedule of the necessary steps for roughing out either X-cut or Y-cut crystals as desired, can easily be prepared from an inspection of this diagram. For the production of X-cut crystals the base reference surface of the

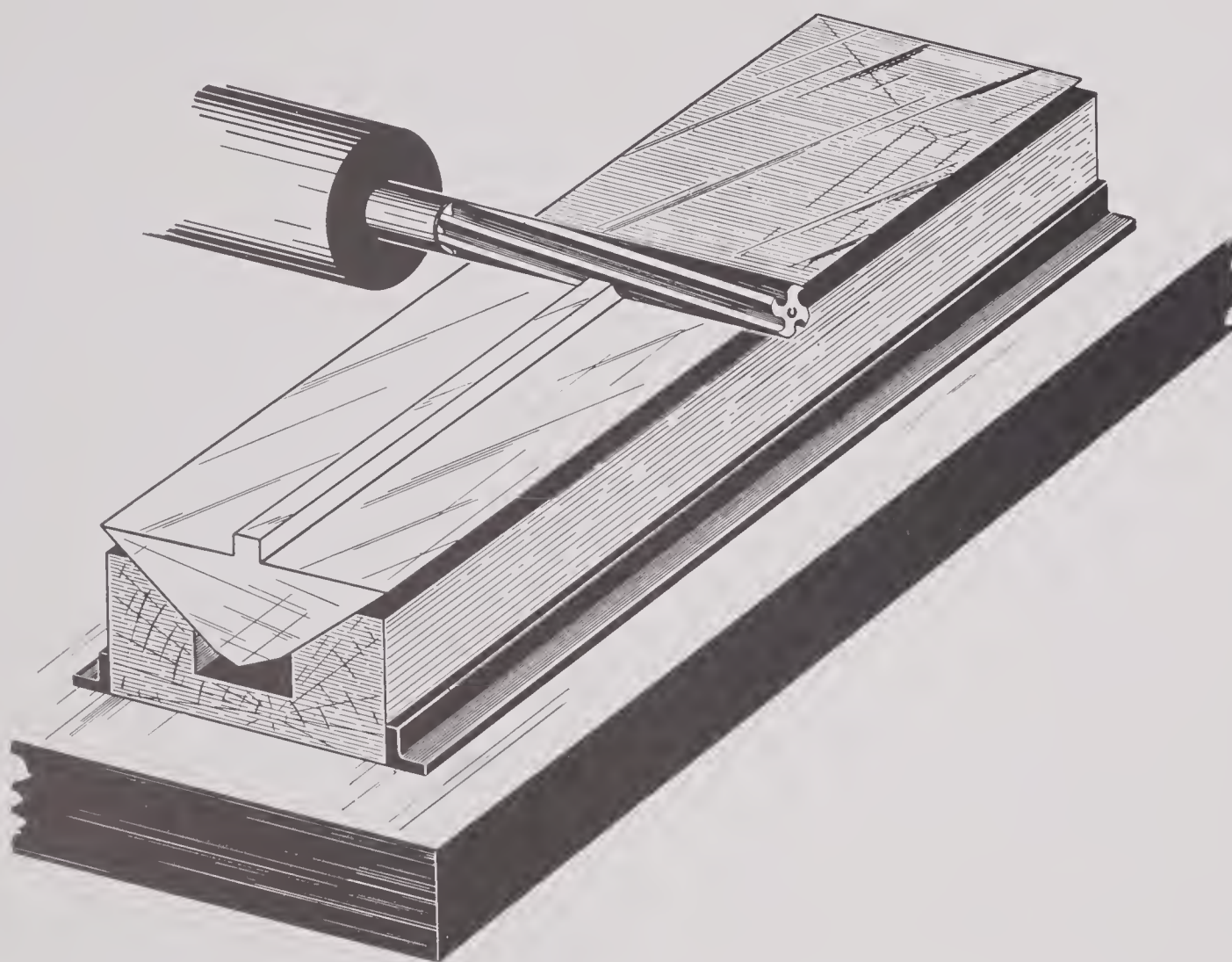


FIGURE 7. A Rochelle salt mother crystal whose seed bar is being milled off to form a reference surface.

may rest in the correct position while the large base of the crystal which contains the seed bar is surfaced by means of a milling cutter. Figure 7 illustrates the position of a mother crystal of RS on such a fixture during this particular surfacing operation. In addition to the large base surface thus obtained, a second reference plane is desirable which will be perpendicular to the base plane and parallel to the long dimension of the bar. This may be produced by a second milling operation while the bar is still in the same jig.

bar is held in a vertical position against a guide and thin slabs are obtained by cutting with a band saw, as discussed in Section 8.4. In this manner, the entire bar is sliced into several large thin slabs which are then ready for further subdivision into individual rough crystal shapes.

The slabs are next sawed obliquely into strips with the aid of a 45-degree guide. The same type band saw may be used as for the above slab cuts.

The strips may now be sawed into rough-cut crystal shapes by again using a band saw and

the necessary guides. In every case it is desirable to have the rough-cut crystals oversize by about 0.040 in. in all three dimensions to allow for later finishing operations.

If Y-cut crystals are desired, the slabbing of the bar shown in Figure 8 would be done by making longitudinal cuts along a plane perpendicular to the large reference surface. The further processing of the slab into rough-cut crystal shapes would be done in a manner analogous to that already outlined for X-cut

be adequate. For production work, milling equipment involving rotary tables of the type illustrated in Figure 26 will probably be much more economical. With four milling heads around a turntable the cutters may be adjusted so that both a coarse and a fine-finish cut will be taken during each half revolution.

Dry-grinding processes have not proved satisfactory for finishing RS crystals.

8.3.4

Orientation of ADP Bars

A photograph of an almost perfect ADP mother bar is reproduced in Figure 4. Its size can be appreciated by comparing it with the woman's hand which rests upon it. This particular bar was grown in a reciprocating radial crystallizer. The clear flat seed plate is plainly

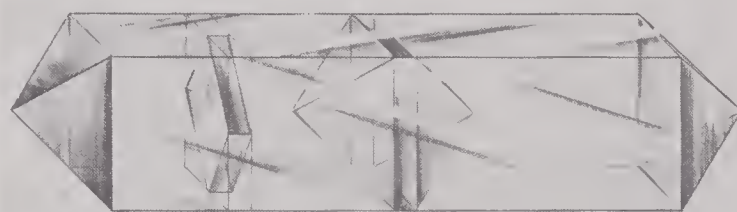


FIGURE 9. Sketch indicating the location of a 45° Z-cut plate and a capped seed plate within the mother ADP crystal.

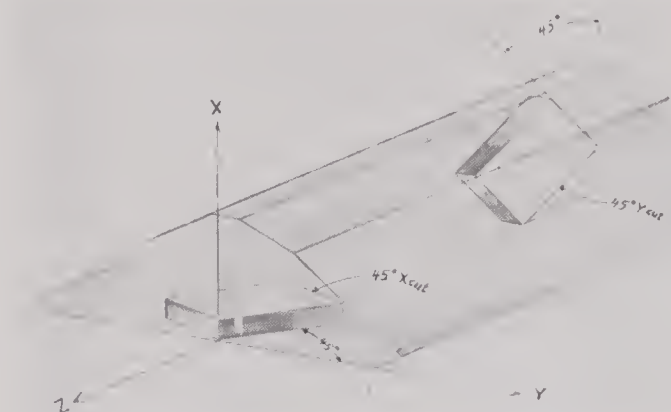


FIGURE 8. Diagram of the position of 45° X-cut and 45° Y-cut Rochelle salt crystals in the mother bar.

crystals. For the economical production of Y cuts it would be preferable to grow the mother bar originally from a seed bar so oriented that the Y cut could be obtained by exactly the same steps as have been outlined above in detail for X cuts.

8.3.3 Surface Finishing RS Crystals

The Brush Development Company has had very extensive experience over a period of many years in the processing of RS crystals. In their current production work on surface-finishing RS crystals they rely exclusively on milling processes. The actual description of their milling equipment will be presented in Section 8.4.5. The milling equipment discussed in Section 8.4.6 for ADP crystals is also applicable to RS.

The final choice of equipment for milling RS will depend on the volume of work to be done. Where relatively few crystals are being processed, as in an experimental laboratory, the apparatus described in Section 8.4.6 will probably

be adequate. For production work, milling equipment involving rotary tables of the type illustrated in Figure 26 will probably be much more economical. With four milling heads around a turntable the cutters may be adjusted so that both a coarse and a fine-finish cut will be taken during each half revolution.

visible at the central section of the bar and on either side of it are the two white, pyramidal seed caps. The composition of the solution into which the seed plate is first introduced is such as to force these caps to form very rapidly. The rapid initial growth, though economical, is responsible for the lack of clarity in this region of the bar. The usable portion of the bar is the clear area lying between the extreme tips of these seed caps and the pyramidal faces at either end.

The location within the mother bar of the 45-degree Z-cut ADP plates, the only type cut used in transducers, is indicated in Figure 9. In order to obtain these crystals in rough form from the original bar, one must first establish reference planes. The long prism faces of the bar are not satisfactory for this purpose since they have an appreciable taper which is unavoidably incurred during growth. The pyramidal end faces of the crystal, however, are sufficiently flat and

the pyramidal angles are quite constant. The pyramidal faces each make an angle of $44^\circ 50'$ with the longitudinal optic axis of the bar.

In processing a bar the central seed plate region is first removed by means of the abrasive cutoff wheel described in Section 8.4.3,



FIGURE 10. Orientation of the pyramidal end of an ADP mother crystal in a special jig for grinding reference surface. (Naval Research Laboratory.)

leaving the two clear end portions. Reference surfaces are established on these two end portions by either one of two procedures. The method currently used at NRL employs a special jig in which the pyramidal end of the bar may rest, as illustrated in Figure 10. While being held firmly by hand in a vertical position in this jig, one corner of the bar is ground off with a vertical belt sander at an angle of 45° to a depth sufficient for a reference plane. If desired the other three corners of the bar may be ground off similarly so that a square bar results. This square bar is then sliced directly into 45° -degree Z-cut plates with an abrasive cutoff wheel as described in Section 8.4.3.

An optical method of providing proper orientation of the original bar has been used at BTL. This method of orientation will be made clear by careful examination of the instrument shown in Figure 11, and referred to as a "reflectoriascope." An automobile headlight lamp at the left supplies light which is collimated in the direction of the longitudinal axis by means of a lens. This parallel beam falls on two adjacent pyramid faces which then reflect separate portions of the beam through each of two lenses so that images of the lamp filament are focused on two white screens at right angles to each other. If the crystal is turned slightly these images move on their screens. By adjusting the crystal properly both images can be caused to center on cross lines ruled on the screen. When these images are so centered the crystallo-

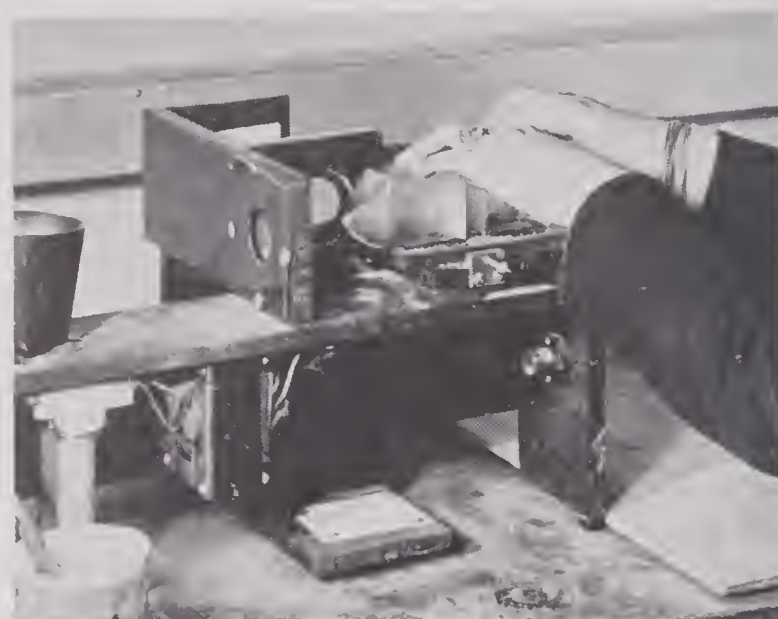


FIGURE 11. Reflectoriascope for orienting ADP mother crystals, preparatory to grinding reference surfaces for locating 45° Z-cut plates. (Bell Telephone Laboratories.)

graphic axes are parallel with the edges of a mounting board which is under the crystal. If the crystal is secured in this position it can be accurately cut while using the mounting-board surfaces as planes of reference. The mother bar is attached to the bakelite plate by means of a thermosetting plastic cement which sets at room temperature. This Norace cement, when first mixed, has the consistency of putty so that the position of the crystal can be readily adjusted when on the reflectoriascope and yet retain its correct position by subsequently taking

a permanent set. For further directions on the use of this cement see Section 8.6.8.

The bakelite plate containing the properly mounted ADP bar ends is now held against a 45-degree angle block on the guide table of a belt sander. The reference surface is ground as illustrated in the photograph in Figure 20. The photograph shows the left half of the crystal being sanded, the right half already having been ground down. When the crystal block is later sliced into Z-cut plates of the desired thickness, each slice will contain a portion of this reference surface.

Where the half-bar is held vertically on a special jig which fits the pyramidal end faces, while the reference surfaces are ground by a vertical belt sander, the maintenance of correct orientation of the ADP bars depends largely on the skill of the operator. This procedure, which has been used and recommended at NRL, apparently works out very well for the currently available sizes of ADP mother bars. It appears that the usable part of an ADP bar could become so long that difficulty would be experienced in obtaining a correctly oriented and satisfactorily flat reference surface by this method. The optical orientation method employed at the BTL would seem to be preferable from the standpoint of maintaining accuracy of the reference plane, particularly for grinding the usable end portions of longer ADP bars. However, the optical method involves a cementing operation which requires setting time and is undoubtedly much slower. The additional accuracy would not justify the increased cost in many cases.

While the dry-grinding method of producing reference surfaces is rapid and apparently quite satisfactory, it is also possible to use a liquid cooled abrasive cutoff wheel for this purpose. Such wheels are regularly used for the subsequent slicing of ADP bars, as discussed in Section 8.4.3, and would therefore be generally available.

8.3.5 Rough-Cutting Crystals from ADP Bars

Following orientation and the grinding of reference surfaces on ADP bars, as just out-

lined in Section 8.3.4, the bars are best cut into slices by means of wet abrasive cutoff wheels. This type of equipment is illustrated in Figure



FIGURE 12. Laying out crystals before finish cutting to correct length and width. (Bell Telephone Laboratories.)

25 and its use is discussed in some detail in Section 8.4.4. It will have been made clear from an inspection of the diagram of Figure 9 that 45-



FIGURE 13. Grinding crystals to length and width dimensions on belt grinder. A fine grit belt is used for the finishing cut. (Bell Telephone Laboratories.)

degree Z cuts are obtained by slicing the bar at right angles to its long axis. The thickness of the slices should be about 0.040 in. oversize in

order to allow for later finishing cuts. To insure that these slices have parallel surfaces, they may be held next on a special vacuum chuck arranged parallel to the belt, and therefore oriented at right angles to the bed, of a belt sander shown in Figure 13. Then both electrode faces of the crystal plate are ground down to about 0.017 in. oversize and made parallel with each other.

Where all four corners of the mother bar are ground to produce reference surfaces, so that a square cross section results, merely sawing these bars into slices yields rough 45-degree Z-cut crystal shapes. If only one side of the bar has been given a reference surface it may be desirable to lay out a cross section of the crystal shape desired by means of a parallelogram arrangement such as illustrated in Figure 12. This procedure permits an inspection of the crystal plate and enables the rough shape to be laid out so that faulty spots on the slice are avoided. The desired crystal shape may then be roughed out by placing the crystal slice on an appropriate jig and grinding it to the proper oversize dimensions with a belt sander. The illustration in Figure 13 will make this procedure clear.

Abrasive cutoff wheels furnish an alternative method of obtaining rough crystal shapes from the original slices. Preference here seems to lie with the individual and to depend also on the availability of equipment. Liquid coolants are always employed with these wheels when cutting ADP crystals. For some crystal sizes, economy considerations alone would necessitate the use of a sawing procedure. Since the use of band saws with ADP is not feasible, recourse is had to cutoff wheels of the abrasive type or to diamond wheels.

8.3.6 Surface Finishing ADP Crystals

Surface finishing of ADP crystals may be accomplished satisfactorily by any one of several techniques. A dry-grinding process has been developed and used rather extensively at NRL, at BTL, and at the Hawthorne crystal-growing plant of the Western Electric Company. Milling processes which had been developed and used by

the Brush Development Company over a period of many years for RS have also been applied to ADP. The Brush Development Company continues to use milling equipment for this purpose and UCDWR has also employed a modified milling technique. Wet-grinding equipment has been adapted to finishing ADP surfaces at NRL, where use has been made of thin abrasive cutoff wheels bonded to steel disks for this purpose.

To obtain correct length and width dimensions by means of a dry sander, a 120-grit belt is used and the chuck is arranged to employ stops as shown in Figure 13. A dry disk sander could be used but is probably not quite as desirable. In order to finish to the correct thickness the crystals are then transferred to a belt surface grinder such as illustrated in Figure 22 and described in greater detail in Section 8.4.2. In this device, which was used at BTL,⁷ a number of crystals are held on the vacuum chuck at one time and are passed under a pulley carrying a fine abrasive belt. Equipment of this type is suitable for laboratory use or for small-scale production. For large-scale production, surface finishing may be done more economically with the type of equipment shown in Figure 26.

At UCDWR the finishing of ADP crystals has consisted primarily in altering the dimensions of crystals which were previously furnished in a finished condition but whose dimensions were not appropriate for the application at hand. The type of milling equipment employed is illustrated in Figure 27 and has been discussed in detail in Section 8.4.6. Its principal advantage lies in the ease with which its simple sweep-cutting tool can be reconditioned. The larger and more expensive cutters, such as the spiral-end mills used by the Brush Development Company, are more difficult to resharpen. In general, it may be said that milling operations on ADP place greater demands on the cutting tools and hence are less satisfactory and more difficult than in the case of RS. Since this is largely a matter of securing satisfactory cutting tools, more favorable alloys for this purpose may be eventually developed. If so, a milling process might still become the most satisfactory technique for finishing ADP crystals.

Since abrasive cutoff wheels employing a liquid coolant have proved entirely satisfactory



for slicing ADP, they would seem to be adaptable also for the finer finishing operations. Actually this is the case and NRL has used the identical type of abrasive cutoff wheels for this purpose by bonding them to metal disks. A photograph of their equipment is shown in Figure 23 and a detailed discussion will be found in Section 8.4.2. Accurate duplication of crystal dimensions is facilitated by a micrometer adjustment and the use of a hydraulic-feed mechanism.

Since any of the techniques mentioned above succeed in producing entirely acceptable results on ADP crystals, the choice between them has usually rested on individual preferences and on the availability of equipment at the several laboratories. Sometimes a choice can be made on the basis of the quantity of crystals being processed. For example, the sweep-type milling cutter used at UCDWR is not well suited to mass production although it possesses many advantages for the experimental laboratory. Wet-grinding equipment as developed up to the present time is likewise not well suited to mass production. On balance, it would seem that the dry-grinding equipment is most economical where great numbers of crystals are involved.

8.3.7

Spliced Crystals

For low-frequency applications, it may be difficult or impossible to secure single crystals of sufficient length to have a resonance in the desired region. However, it has been found that a sufficiently long crystal may be obtained by bonding together two or more smaller crystals. This bonding operation may be performed before the original bars are cut into individual crystals. These spliced crystals can readily be detected visually and it is important to distinguish them from those grown originally as single crystals.

In fabricating RS crystals, melted RS may be used as a cement according to the directions in Section 8.6.9. Thus, the bonding layer has properties almost identical to that of the crystal itself. No special precaution is necessary when bonding spliced RS crystals to supporting structures by the application of the regular ce-

menting techniques outlined later in Section 8.6.

In commercially available Y-cut RS crystals the splice has appeared at an angle of 45 degrees when viewed on the electrode face as illustrated in Figure 14. By looking at the location of Y-cut crystals in the mother bar it will be seen that there is an economical advantage in bonding these crystals at the 45-degree angle. Voltage

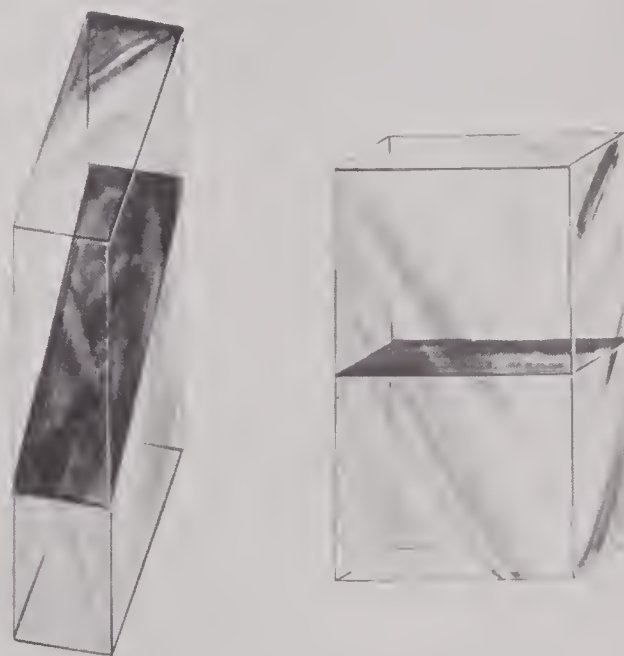


FIGURE 14. Spliced crystals. Left, a 45° bond; right, a 90° bond.

tests have been made at UCDWR on several hundred such crystals having dimensions $3 \times 1 \times \frac{1}{4}$ in. It was found that only about 1 per cent resulted in voltage breakdown within the cemented joint when tested at 6,000 v. It seems, therefore, that spliced RS crystals are about as dependable from a voltage standpoint as those cut in a single piece from the mother bar.

Large ADP crystals can also be formed by bonding two smaller crystals together, but with a thermoplastic cement such as Vinylseal. Defects at the bond are readily detected visually, owing to the increased reflectivity in areas where the bond has failed. Since the cement softens at higher temperatures there may be applications where such crystals cannot be used. Specifically, the Cycle-Welding technique for bonding ADP crystals to rubber, described in Section 8.6.6, involves temperatures which are excessive for this type of fabricated crystal. The spliced ADP crystals which have been available

commercially have had the splice through the center of the crystal and perpendicular to the long dimension as in Figure 14. Since these are 45-degree Z cuts, it would seem that some economical advantage could also be gained by having the splice at an angle of 45 degrees.

8.3.8

Electrodes

Electrodes may be applied to crystals in any one of several ways. Each laboratory which makes use of piezoelectric crystals apparently

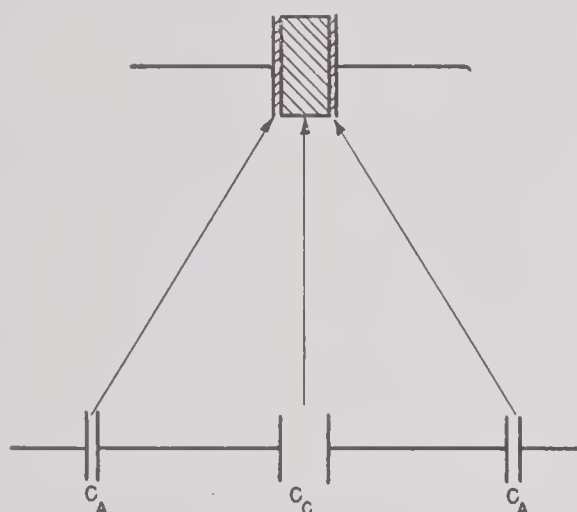


FIGURE 15. Equivalent circuit of crystal and its electrodes when a dielectric cement layer intervenes.

prefers its own adopted method to the exclusion of all others. This would seem to indicate that any one of several procedures may be entirely satisfactory. According to the Navy specifications⁹ for ADP crystal plates, metal electrodes may be applied by any method, such as plating, foiling, sputtering, or depositing by evaporation, provided such electrodes pass certain electrical and mechanical tests enumerated in the specifications. These tests follow:

5-2 The metal electrode shall be substantially uniform in thickness over the entire electroded surface, and shall adhere to the crystal surface sufficiently well to meet the following adherence requirements: (a) After a crystal is passed once a distance of approximately 6 inches over a cloth or felt surface saturated with carbon tetrachloride or other suitable solvent and uniformly exerting a force on the electrode surface of the crystal of 12 to 16 ounces, the electrode shall appear to be of uniform thickness over the entire surface as

gauged by eye, and shall meet the electrical resistance requirement of paragraph 5-3.

5-3 Electrical uniformity of the crystals shall be determined by measuring the d-c resistance between both sets of diagonal corners of the electrode surface by means of blunt gold-plated contact probes. The resistance measured in this manner shall not exceed 20 ohms in either diagonal for the crystal sizes listed in paragraph 4-1. The term "corner" is taken to mean a point approximately $\frac{1}{8}$ " in from either of the two edges of the crystal forming the corner.

The largest electrode surface listed in paragraph 4-1 referred to above is 1x1.1 in.

When a metal foil is used as an electrode, a thin layer of adhesive intervenes between the foil and the crystal. This means that the electrode is electrically coupled to the crystal through a capacitance C_A . This capacitance is in series with the crystal capacitance C_C , and it is apparent that C_A must be large (i.e., the cement layer must be thin) compared to C_C or an appreciable fraction of the available voltage drop may occur in the adhesive layer. The equivalent circuit is drawn in Figure 15. Assuming the dielectric constant of the adhesive to be about 3 or 4, the problem is not serious with Y-cut RS or Z-cut ADP where the dielectric constant of the crystalline material is about 10 or 14. With X-cut RS, which may have a dielectric constant of several hundred, however, it may be difficult to make the adhesive layer thin enough, especially when very thin crystals are used as in bimorphs. A solution to this problem is the application of a conducting layer directly on the crystal by evaporating metal or by spraying a conducting solution. Marked increase in voltage sensitivity is claimed to result in the case of X-cut bimorphs with electrodes of this type.

EVAPORATED ELECTRODES

In order to achieve intimate contact with the crystal surface it has become the practice in a number of laboratories to evaporate metallic substances onto the electrode faces of the crystals. Owing to its general chemical inertness and the high quality of the low-resistance electrical contact readily obtainable by pressure, pure gold has been most widely chosen for this application. The gold may be applied either by evaporation or by cathode sputtering. The sput-

tering process is probably undesirable because of the high temperatures developed at the crystal surface unless extreme precautions are taken, and the greater difficulties involved in controlling the gas pressure and the thickness of the film.

Gold may be readily evaporated by hanging small hairpin loops of 0.020-in. gold wire, spaced

The practical application of evaporated gold to crystals presents primarily an engineering problem. The vacuum equipment should have sufficient capacity to attain a pressure of approximately 10^{-5} mm of mercury in a very short time. Large valves in the vacuum line should enable the diffusion pump to be connected or disconnected at any time without waiting for

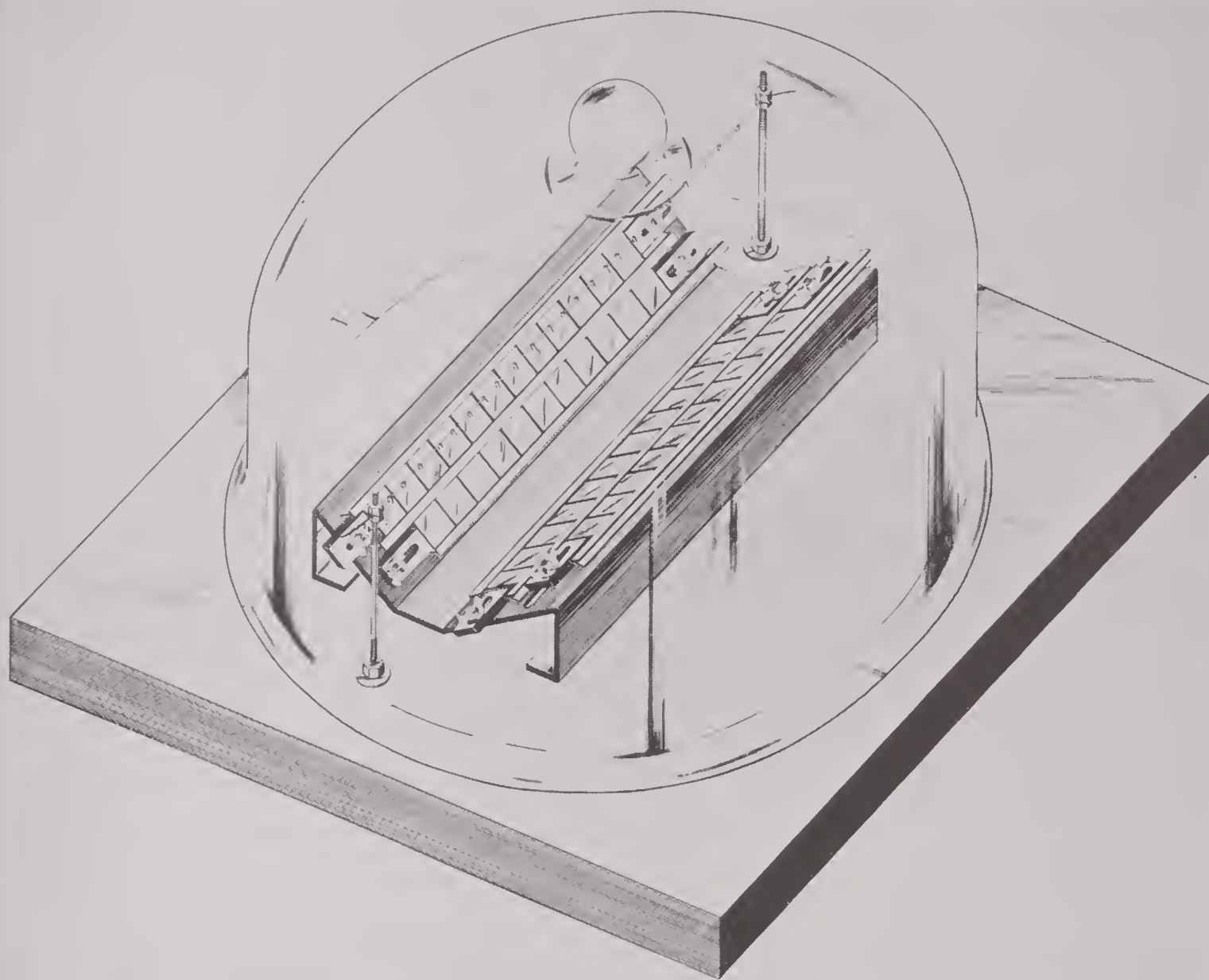


FIGURE 16. Apparatus for the evaporation of gold electrodes.

at regular intervals, on a straight 0.040-in. tungsten wire and heating the latter to incandescence. A schematic arrangement for this process is shown in Figure 16. With the tungsten wire at a distance of 3 or 4 in. from the crystals, a practical evaporation equipment should permit the electroding of 100 or more crystals in one operation.

it to warm up in advance or to cool off before opening the system. These valves should be such as to give long periods of carefree operation. To prevent the crystals from cracking due to uneven heating, it is important that the gold be evaporated within a matter of seconds. Actually, it amounts to a flashing process. The thickness of the foil can be controlled most readily by

measuring the amount of gold which is suspended on the tungsten wire, assuming that the temperature is raised to the point where all the gold evaporates from the tungsten for each operation. A similar process has been used even for RS crystals by BTL, but it is clear that they may be subjected to a vacuum for a very limited time only without dehydration and that any de-



FIGURE 17. Arrangement for sandblasting crystal surfaces. (Naval Research Laboratory.)

terioration which could result from exposure to high temperatures must be avoided.

The cleaning of crystals prior to evaporation of the metal should be such as to leave them completely free from fat soluble substances. Carbon tetrachloride is an excellent solvent for this purpose. The crystals may be washed in carbon tetrachloride, or perhaps still better, a continuous degreasing apparatus may be set up in which carbon tetrachloride vapor condenses on the crystals. In some laboratories it is felt that better adhesion of the metal to ADP is obtained if the crystal surface is lightly sanded before being subjected to the evaporation process. The sandblasting equipment used for this purpose at NRL is shown in Figure 17. As a test

for the satisfactory adhesion of gold to crystals, one should wipe the electrode with a cloth wet with carbon tetrachloride, as stated in the Navy specification quoted in Section 8.3.8. This test is based on the fact that unsatisfactory electrodes usually result from the presence of fatty material on the crystal surface and hence gold deposited on top of fatty substances would be wiped off by rubbing with a cloth wet with a fat solvent.

It will be found necessary to protect the edges of crystals during evaporation in order to maintain their high d-c resistance. This may be achieved by covering the edges of all crystals with a metallic baffle during the evaporation process. An alternative procedure might consist of placing rubber spacers between each crystal and maintaining a slight compression so that it is impossible for the gold to penetrate to the edge faces of the crystals. These two suggestions for baffles are depicted in the drawing of Figure 16. At least one laboratory finds that more satisfactory adhesion of gold may be obtained by first evaporating a film of aluminum on the crystals. The aluminum gives a hard coating which is very difficult to remove, while the gold serves as an inert protective covering for the aluminum. This double evaporated layer can be applied conveniently in the apparatus of Figure 16 because the aluminum evaporates first upon heating the tungsten element and is followed later by the gold.

SPRAYED ELECTRODES

A second method of electroding crystals, which has found rather wide application, consists of spraying a conducting suspension or a molten metal on the crystals. At least three different materials have been used for this purpose, namely, molten tin, metallic silver in suspension, and graphite in suspension.

The silver suspension which has been used satisfactorily for some time at NRL for ADP crystals is made up according to the following formula:

Powdered silver, DuPont V-9	250 g,
MM cement, EC678	100 cc,
MM cement, EC658	10 cc,
Ethylene dichloride ($C_2H_2Cl_2$)	300 cc,

where MM represents a product of the Minnesota Mining and Manufacturing Company. The powdered silver is added to the solvent and shaken vigorously for 10 minutes. The two MM cements are then added and mixed thoroughly. The silver suspension should be strained through cheesecloth to remove all large particles. The silver preparation is best applied to the crystals by spraying; with a little experience, it is not difficult to obtain a uniform layer. The proper thickness is gauged by the desired electric resistance of the electrode. This preparation deteriorates with time so that it is necessary to make up new batches about every 10 days. It was found that the resistance of the electrode obtained increased with the age of the silver suspension. For a crystal 1 in. square, the d-c resistance measured across the diagonal of one electrode surface normally lies within the range 1 to 4 ohms. The Navy specifications quoted in Section 8.3.8 set up a maximum of 20 ohms.

For RS crystals NRL has made use of electrodes obtained by spraying molten tin. A spray gun which has proved satisfactory for this purpose is obtainable from the Alloy-Sprayer Company of Detroit, Michigan.

Graphite electrodes have been used for many years in the manufacture of X-cut RS bimorphs for air microphones and phonograph pickups. These electrodes seem to be quite satisfactory for such applications although they are not recommended for high-power devices. This power limitation may result from faulty adhesion to the crystal and a subsequent deterioration in the electrode, perhaps caused by localized overheating. It is suggested that the aqueous graphite suspension (Acheson 1008) be sprayed on the crystal with a type WO de Vilbiss spray gun at 50 psi pressure. It is customary to apply two coats with a 10- to 15-sec drying period between them. The thickness of the graphite layer on the crystal should be such that few or no pin holes will be observed when examination is made by looking through the surface toward a strong light. In any event, it will be found necessary to protect an electrode of this type. One method of so doing is to attach an additional tin foil over the graphite electrode by a cementing process as discussed in a later

section. Another method consists of attaching a narrow strip of foil to serve as an electric lead, and then to cover the entire crystal with a waterproofing compound.

FOIL ELECTRODES

Thin metal foils may be obtained in any one of a wide variety of elements and their alloys. The selection of the most desirable material for use as an electrode depends primarily on corrosion resistance and softness. The foils most frequently used have been pure silver, nickel silver or German silver, and pure tin.

When pure silver foil is used, it is customary to anneal it so that it will adhere well to the crystals. The annealing is done in the temperature range 1000 to 1100 F, preferably in an electric oven, while keeping each sheet separate in order to prevent sticking. Coin or sterling silver does not soften under this annealing treatment and therefore has been found unsatisfactory as a foil. Pure silver that has not been annealed may break at points of flexing. This is particularly the case where narrow tabs may be subjected to a sharp bending action a few times.

A pure silver foil 0.0017 in. thick seems to offer the best mechanical advantages as regards ease of handling and of soldering. Any slight irregularity or waviness in the annealed silver foil may be removed by stroking the foil with a 1/4-in. round steel rod while the foil is held against a flat glass plate. The principal advantage in using this heavier type of foil for an electrode is that it serves both as an electrode and as the foil wiring strip which is so often required with other types of electrode. The increased stiffness of the foil permits soldering directly to it and for this purpose an extension of the foil is always provided for use as a wiring tab. This type of foil electrode can be conveniently used for either single crystals, in which each crystal has its own soldering tab, or it can be used in long strips to which perhaps a dozen crystals or more are cemented, the entire strip possessing a single tab for soldering. Illustrations of various type tabs are shown in the figures accompanying several sections under Section 8.7.

Where long strip foils are desired, they may be cut by hand or preferably with a shear of the

Diacro type, which have been made available by the O'Neil-Irwin Manufacturing Company, Minneapolis. Foils intended for individual crystals are best cut by means of a special die for each size. Standard dies are normally too expensive where only limited quantities of a given size of electrode are needed. To take care of the latter case, advantage has been taken of the

ture of 110 F and at 60 per cent relative humidity for a period of 12 hours or longer in the case of RS crystals; for ADP crystals curing at a much higher temperature is permissible. At UCDWR, an 80-C oven was used for ADP crystals.

Tin foil has been used extensively for crystal electrodes at UCDWR. This material has the

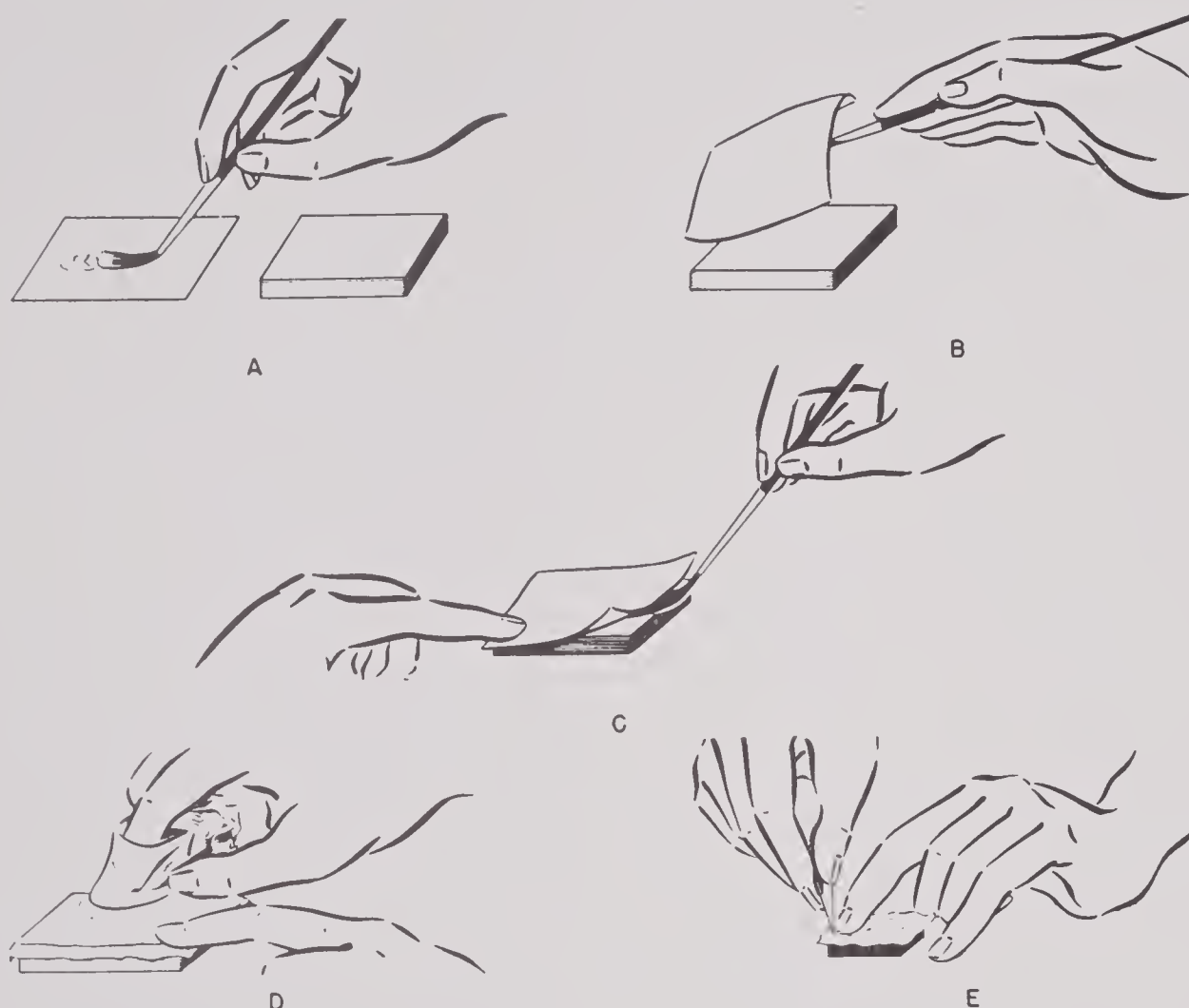


FIGURE 18. Stages in the application of tin foil electrodes: A. Picking up foil with camel's-hair brush dipped in Acryloid cement. B. Inverting foil over crystal. C. Removal of the brush. D. Rubbing foil to remove excess cement and to insure close contact with crystal. E. Trimming off excess foil with razor blade.

rather novel means of punching thin foil which is discussed in detail in Section 8.4.7.

It has been the custom at UCDWR to attach silver foils to ADP crystals with bakelite BC-6052 cement or with Vulcalock cement. These cements may be either brushed or sprayed, but the most uniform results are doubtless to be obtained by spraying. After the foils are attached to the crystals and are firmly pressed by a rubbing operation, they are placed in a pneumatic press and subjected to a pressure of 25 to 40 psi. While in the press they are cured at a tempera-

thickness of 0.000275 in. and is apparently pure tin. This foil is malleable and is so thin that the vapor from the solvent in the adhesive is able to escape through the foil. The fairly rapid escape of the solvent is an important consideration since it prevents the electrode from becoming too readily damaged during assembly operations. For electrodes which have been attached sufficiently ruggedly for use in transducers, practically all solvent must have evaporated.

The technique of attaching tin-foil electrodes is shown in a series of illustrations in Figure

U.S. GOVERNMENT PRINTING OFFICE

18A, B, C, D, E. The foils should be cut over-size so that they will extend about $\frac{1}{8}$ in. beyond the edge of the crystal surface on all sides. These foils are conveniently picked up with a camel's-hair brush containing a small quantity of adhesive as shown in Figure 18A. While the foil adheres to the brush, it is turned over and laid on the crystal. The brush is then withdrawn from beneath the foil, taking care to hold the foil on the crystal with a finger, as illustrated in Figure 18C. Inasmuch as an extremely thin layer of adhesive is desired between the foil and the crystal, it is necessary to massage the foil with a piece of soft cloth covering a finger, as shown in Figure 18D. Stroking and rubbing the foil rather briskly in all directions should result in an extremely close attachment. The cloth will take on a black discoloration in the process. After these foils have been applied to both sides of a crystal, the excess foil around the periphery may be trimmed off with a razor blade in the manner illustrated in Figure 18E. It will be noted that a fingernail is used as guide in cutting off the excess foil. The excess cement around the edge of the crystal should now be removed by means of a cloth dampened in a suitable solvent, such as methyl ethyl ketone.

A satisfactory adhesive for attaching tin foils to crystals is Acryloid B-7. The original cement, as it comes from the manufacturer, should be diluted in the ratio 1 part Acryloid to 4 parts ethyl acetate. Further details are given in Section 8.6.9 covering the use of this adhesive.

It will be observed that the appearance of the two sides of commercial tin foil are unlike, one being dull and the other polished. It has been customary to attach the dull side of the foil to the crystal in order to obtain a better bond.

Where crystals with tin-foil electrodes are used as part of an array, electric connections must be made by cementing to them more substantial strip foils, as discussed more fully in Section 8.7.4 on wiring.

8.3.9

Polarizing Crystals

TECHNIQUE

The method of polarizing crystals used at UCDWR is clearly indicated in Figure 19. Other

laboratories use similar devices. The crystals are placed individually in the holder illustrated and a slight horizontal force is exerted to insure good electrical contact. It is not necessary that the crystals themselves possess electrodes provided the crystal holder has electrode surfaces sufficiently large to cover an appreciable area of the crystal surface. With the crystal in the position shown in the figure, a sudden downward thrust is exerted on the top of the crystal by means of some blunt object. The eraser end of a pencil has proved entirely satisfactory. At the moment of application of the force, the needle of the indicating instrument will give a rapid deflection followed an instant later by a sharp kick of the needle in the opposite direction as the force is released. According to the direction of the deflection, an appropriate mark is then placed on one side or edge of the crystal to indicate its polarity. The definition which established which side of the crystal receives the polarity mark is quite arbitrary so that it is quite possible that the same crystal could be marked in different ways at various laboratories. The definition stated in the Bureau of Ships specifications is given in the following section.

The extent of the deflection depends on both the actual force applied to the crystal and the suddenness with which the force is applied. It also depends on the sensitivity of the polarizing equipment, a discussion of which will be found in Section 8.4.8. Although a mere flicker of the needle is sufficient to establish the polarity, it is convenient to have a somewhat larger deflection. With a sensitive instrument one can readily distinguish between X-cut RS, Y-cut RS, and ADP crystals by the amount of the deflection. The deflection obtained from crystals of each of these materials decreases in the order named.

It might be thought that the deflection obtained in the polarization process might furnish a reliable indication of the piezoelectric activity of the crystal, provided that an arrangement could be devised whereby each crystal tested could be subjected to the same impulse. Some preliminary trials in this direction were made at UCDWR and several hundred crystals were subjected to activity tests. Although a number



of inactive crystals were discovered, this type of test was discontinued, partly because the apparatus had not undergone sufficient development, but largely because the measurements have no particular meaning. The conditions under which crystals are ultimately used were not closely duplicated in the test equipment. To be reliable the measurements would have to be standardized and humidity and temperature

arrow-shaped mark on the radiating face of each crystal. This method is convenient in that it permits visible inspection of crystal orientation during assembly operations and in the completed transducer. It is essential that the ink used for marking shall be nonconductive. To date a commercial preparation with the trade name Dykem has been used. A color code, with green for ADP, red for Y-cut RS, and blue for X-cut RS has also proved to be a laboratory convenience.

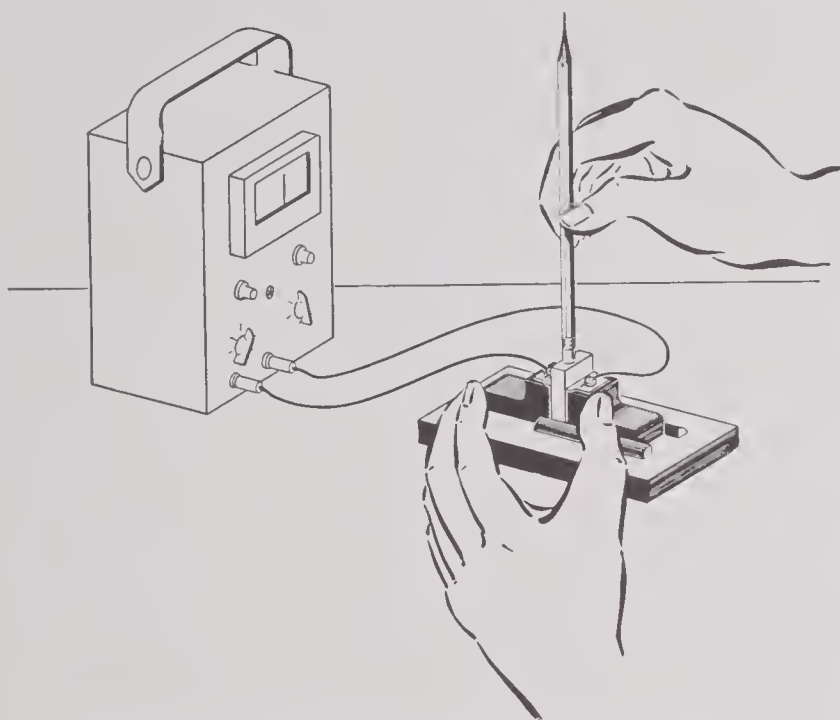


FIGURE 19. Diagram of polarity indicating equipment used at UCDWR.

conditions brought under control. As far as the detection of an occasional inactive crystal is concerned, these may be spotted during the polarizing process just described.

MARKING

The following statement on marking the polarity of crystals is taken from the specifications of the Bureau of Ships⁹ [BuShips], to which reference has already been made.

The polarity of each crystal plate shall be clearly designated by a mark on that electrode surface which becomes positive when pressure is applied in the direction of the longest dimension of the crystal plate. The mark shall be placed at the upper right-hand corner of the face as it appears when the long dimension of the crystal is vertical. This shall not adversely affect the crystal plate characteristics, and shall be of a permanent nature.

It has been the practice at UCDWR to indicate the polarity of crystals by placing an

8.4

PROCESSING EQUIPMENT

Even though it is possible to purchase crystals to the exact specifications required for a given application, it is not always feasible to do so for an experimental laboratory. This is particularly true for the physical dimensions of a crystal which control its frequency and its capacitance. Accordingly, it is a great convenience to be able to vary these dimensions at will without experiencing the delays so often involved in obtaining delivery on special sizes. In fact, it has been the standard practice at UCDWR to maintain a fairly large inventory of crystals in a relatively small number of standard sizes and to modify these to the exact dimensions required for any particular transducer under construction. It is therefore felt that the processing equipment and operations discussed in this chapter may find rather wide use for modifying the dimensions of crystals which were originally purchased in finished stock sizes.

The viewpoint adopted in this section has been to present the various types of equipment currently in use for processing crystals at the various laboratories engaged in the construction of transducers. Where possible, definite recommendations are made as to the type of equipment best suited for specific operations.

8.4.1

Grinding RS

Grinding processes are not currently employed in large-scale production for finishing RS crystals and consequently no equipment for

this purpose will be discussed. Neither is a grinding method used in the production of reference surfaces on the mother bar.

For the final polishing of occasional crystals to be used in precise measurements, recourse may be had to very slow speed grinding or lapping processes, either wet or dry. The main point is to avoid overheating of the crystal. Detailed references to articles on polishing of research specimens are given by Cady.¹⁰

8.4.2

Grinding ADP

It has already been indicated in an earlier section that the reference surfaces on ADP bars may be provided quite readily by a grinding op-



FIGURE 20. Grinding reference surface on an ADP crystal block with a vertical belt sander. (Bell Telephone Laboratories.)

eration such as illustrated in Figure 20. Unlike RS, ADP crystals can be ground very rapidly and satisfactorily with dry abrasive belts. Noth-

ing elaborate in the way of special equipment is required for this operation, ordinary commercial belt sanders being quite acceptable. A vertical-type sander is convenient for this purpose. Best results appear to be obtained with a fairly coarse grit, one laboratory suggesting No. 40, another preferring No. 60. The joint which occurs where the two ends of the belt are cemented together should be inspected to make



FIGURE 21. A dry disk sander in the process of grinding an ADP crystal. (Naval Research Laboratory.)

sure that it is thinner than the remainder of the belt. Since there is no abrasive at the joint heat is liable to be generated by it if too thick with a consequent cracking of crystals. It has been reported⁷ that the 45-degree plane of the ADP bar, which is ground down in order to form a reference surface, can be ground easier than the prism faces. This favorable circumstance lessens the probability of cracking the crystal bar while grinding the 45-degree reference plane. Belt speed is not a critical factor.

For rough-cutting ADP crystal shapes, the same sander is useful. This has been pointed out in Section 8.3.5 and the process of obtaining correct length and width dimensions is illustrated in Figure 13. In addition, it may be necessary to rough-grind the thickness dimension, particularly if the crystal plate as sliced by the abrasive cutoff wheel does not possess parallel

electrode faces. If so, provision for a satisfactory chuck must be made. At BTL,⁷ a vacuum chuck with a vertical surface was used to hold the crystals while they were ground against a vertical belt sander. The crystals should still be oversize to permit a finish cut to be taken, 15 to 17 thousandths of an inch being sufficient.

It is also possible to use a dry disk sander, either for grinding reference surfaces on ADP or for the rough shaping of crystal plates. The

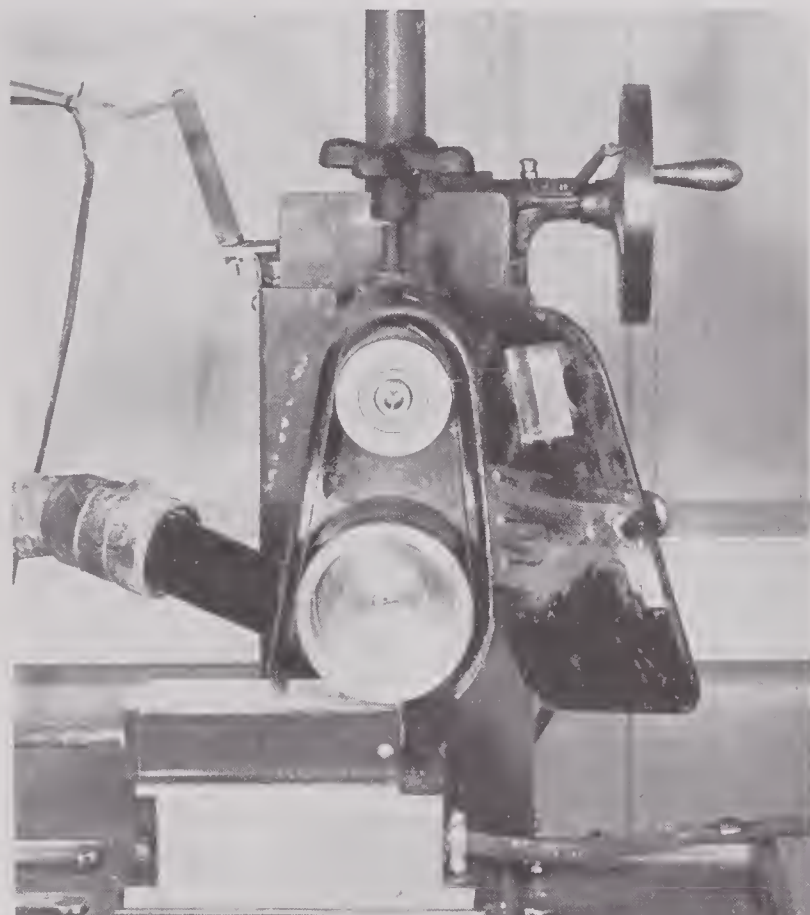


FIGURE 22. Surface grinder with abrasive belt for grinding crystal plates to size. (Bell Telephone Laboratories.)

operation of a disk sander at NRL for grinding a reference surface is shown in Figure 21.

Rough cut ADP crystals, about 0.017 in. thicker than that finally required, may be ground to their final thickness dimension with a belt sander. This grinding method for the finish cut was used successfully at the Hawthorne Plant of the Western Electric Company during World War II. One type of belt sander adopted for this operation is shown in Figure 22. The crystals are held on a vacuum chuck which in turn rests on a traveling horizontal bed. This enables the crystals to be moved underneath the

pulley which carries an abrasive belt. A machine of this type may readily be improvised by altering small surface grinders so that a pulley replaces the ordinary abrasive wheel. The provision of an idler pulley which is adjustable in angle insures the retention of the abrasive belt on the pulleys. In the grinder shown in the illustration, the hand wheel at the upper right, which raises and lowers the sanding mechanism, is graduated to 0.005 in. The vacuum chuck must have a very flat surface to avoid breakage of thin crystal plates and it has been found convenient to surface it with the same belt used for grinding the crystals. A fine belt, 120 grit, is used for the finish cut.

For production surfacing of crystals a double-head grinding unit such as illustrated in Figure 26 is very useful. Two Sanford grinding columns are shown mounted over a turntable of the vacuum chuck type. Vacuum connections are made through blocks to only those regions of the table which are passing under the sanding-belt pulleys. Therefore, the crystals may be readily adjusted in position or removed from the table at any time except when the crystals are actually under the sanding belt. Two operators are required, one to feed each side of the turntable. This machine was used at the Western Electric Hawthorne works⁷ and was capable of surfacing two sides of about 3,000 crystal plates 1 in. square in an 8-hr period. A somewhat larger diameter table would permit a total of four belt sanders about its periphery, thus enabling a coarse and a fine finish cut to be taken on one side of each crystal during a half revolution. With an operator to turn the crystal over, the other surface is finished on the second half of the revolution.

Since some hazard, as well as annoyance, is caused by the ADP dust liberated while sanding, it is necessary to install a dust collector on dry-sanding equipment. One convenient way of doing this is to attach a commercial dust collecting unit to each dry sander. In the method used at NRL, the dust is drawn into the top of a large tank in which the coarse granules may settle and be salvaged; the finer particles are drawn through a water spray in the exhaust system.

The final lapping of rough-cut ADP crystals may also be done on a wet sander. To date, only

disk sanders have been employed for this purpose. The NRL equipment is photographically illustrated in Figure 23. A 120-grit silicon carbide disk, 0.060 in. thick, has been recommended by NRL. The thin silicon carbide disk has been attached to the steel backing plate of the sander with Vulcalock cement, then cured for 3 hr at 300 F in a press.



FIGURE 23. A wet disk sander for the fine finishing of ADP crystals. (Naval Research Laboratory.)

In this operation it is desirable to have the cooling liquid strike against the center of the disk from beneath the work table. Water and propylene glycol in equal parts have been suggested at NRL as a satisfactory solution for cooling. The solution is recirculated in the equipment continuously during operation and need be changed but once a month. Ethylene glycol would also be satisfactory were it not for its toxicity. Some laboratories⁷ have found that a saturated aqueous solution of ADP is preferable to either of the above glycols. After grinding, the coolant solution may be removed from the crystals by immersing them in carbon tetrachloride.

8.4.3

Sawing RS

All the rough cutting of RS bars into crystal plates may be done with band saws. This in-

cludes the cutting of the mother bar into long thin slabs, the slabs into strips, and the strips into the final rough crystal shapes, all as outlined in Section 8.3.2. A linear cutting speed of approximately 3,600 fpm has been found to be satisfactory, but it is not a critical figure. Nickel-steel blades have been found to give good service. Saw blades in use currently at UCDWR have ten teeth to the inch and were originally designed for wood cutting. New blades as purchased were usually found unsatisfactory for sawing crystals. Besides being insufficiently sharp, the rake and clearance angles and the set of the teeth did not have optimum values for this application.

A relatively thin saw, about 0.02 in. or slightly less, is perhaps the best. The set of the teeth should result in an overall thickness about twice that of the blade material. All points on

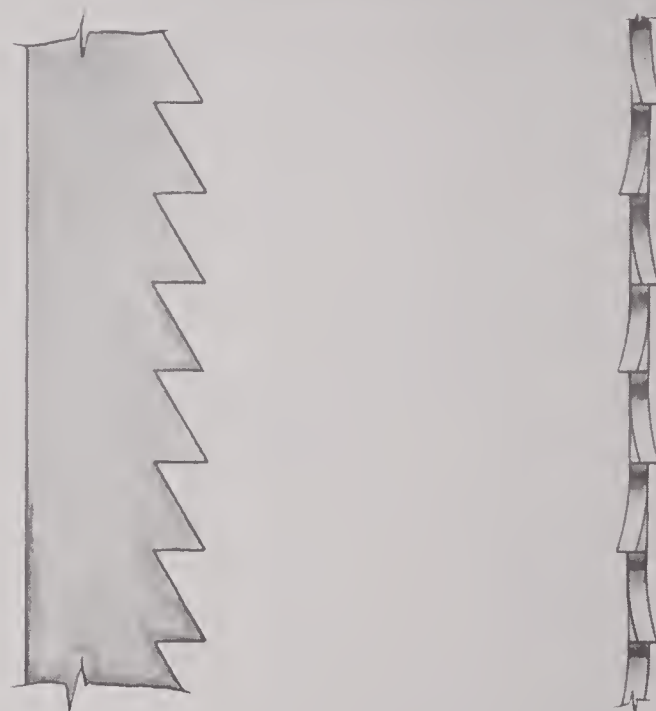


FIGURE 24. Band saw. Left: Face view showing the zero rake angle and the 30° clearance angle. Right: Edge view showing the set and the angle of filing the teeth.

the saw should be set, with alternate points being set in opposite directions. Satisfactory shape and set of the saw teeth are illustrated in Figure 24. A zero rake angle appears to be desirable but not essential in the case of RS. Al-

though the clearance angle is not critical, a 30-degree angle has been chosen at UCDWR, primarily for convenience in sharpening the teeth with a three-cornered file. A very fine file is recommended. Assuming that the saw is clamped horizontally, the correct file stroke for sharpening is to have the cutting edge of the file vertical and at right angles to the plane of the blade for all teeth. The sharpness of each tooth at the cutting point is of paramount importance.

The Brush Development Company, which has processed RS crystals for many years, has spent a great deal of time in developing sawing techniques.¹¹ Their methods differ somewhat from the above, but mostly in detail only. Inasmuch as they regard their exact techniques as trade secrets, it is not possible to report in greater detail on their current methods.

In rough-cutting RS, it is recommended that the crystals be made about 0.030-in. oversize in all dimensions in order to allow for finishing operations. To avoid chipping, it is extremely important to have the saw very sharp at all times. Chips are most likely to occur at that edge where the saw teeth leave the crystal. When sawing thin slabs or strips into individual crystals, it has been found at UCDWR that chipping of the bottom crystal face can be avoided to some extent by a preliminary scoring. This scoring is brought about by a backward rotation of the sample through 90 degrees, sawing a shallow groove in the bottom face, then turning the crystal back to its original position and completing the cut by sawing through the groove.

8.4.4

Sawing ADP

It is so much more difficult to saw ADP crystals than RS crystals that an ordinary band saw has been found unsatisfactory in general. However, some use has been made of a band saw at UCDWR for cutting previously finished crystal plates in half, and with fair success. For sawing ADP, it is strongly recommended that the blades have the appearance of the illustrations in Figure 24. Frequent filing of the blades will be found essential. The remarks on chip-

ping which appear in Section 8.4.3 are particularly applicable when sawing ADP plates. It is standard practice to saw ADP with a thin silicon carbide wheel although diamond cutoff wheels have also been used. A satisfactory size and grade of silicon carbide disk according to experience at NRL is a 12-in. disk, 0.060 in. thick, with 120 grit. With the 12-in. silicon carbide disk, a speed of 3,400 rpm was reported to be satisfactory.

The equipment used at NRL is illustrated in the photograph of Figure 25, in the process of

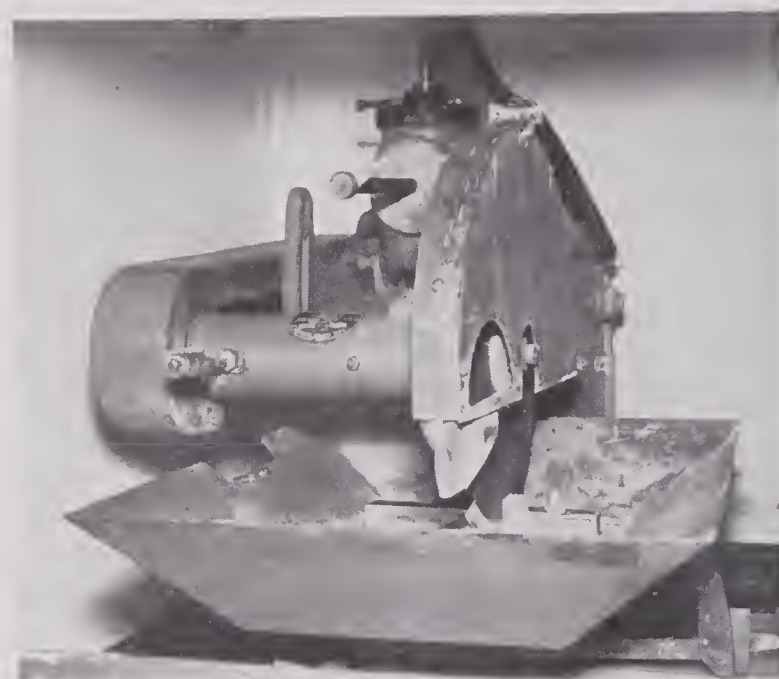


FIGURE 25. A wet abrasive cutoff wheel in the process of slicing an ADP crystal. (Naval Research Laboratory.)

slicing an ADP bar. This apparatus is a Felker Model 120. An important feature for this type of work is the hydraulic-feed mechanism which furnishes a readily adjustable and uniform cutting pressure. The liquid coolant strikes across the radius of the disk on both sides. NRL suggests a cooling solution made up of 3 parts water and 1 part propylene glycol for this sawing operation. After cutting, the crystals are placed in trays containing carbon tetrachloride in order to remove the cooling liquid.

In sawing through thick bars, it is essential that the cutting disk run true. Consequently, most disks will need to be trued following installation. It is also essential that the disk have some taper from the edge inward toward the center to avoid binding. If disks are not avail-



able in this form, it will be found necessary to provide taper, especially for deep cuts.

The experience of BTL on sawing ADP crystals is quoted from their report⁷ as follows:

The saws are abrasive cutoff wheels such as are used on metal. We have not found the grit size to be critical but prefer grits between 60 and 100. Silicon carbide or aluminum oxide seem to be equally satisfactory, the binder has not been found to be critical.

Our work has shown that relatively slow wheel speeds are preferable to fast, partly because the machines in

tremely little cross motion. Saw blades that have been used for a considerable time tend to become thinner near the edge than near the center. This causes a wedging action that not only makes the saw turn hard but also cracks thin slices. It can be eliminated by undercutting the saw faces with a diamond in a lathe. It has been found to be good practice to undercut 8" saws of $\frac{1}{16}$ " thickness by about .007" on each side from a point $\frac{1}{2}$ " inside the periphery right to the pressure plates.

A continuous stream of cooling fluid must flow to each side of the saw. At first small gear pumps were

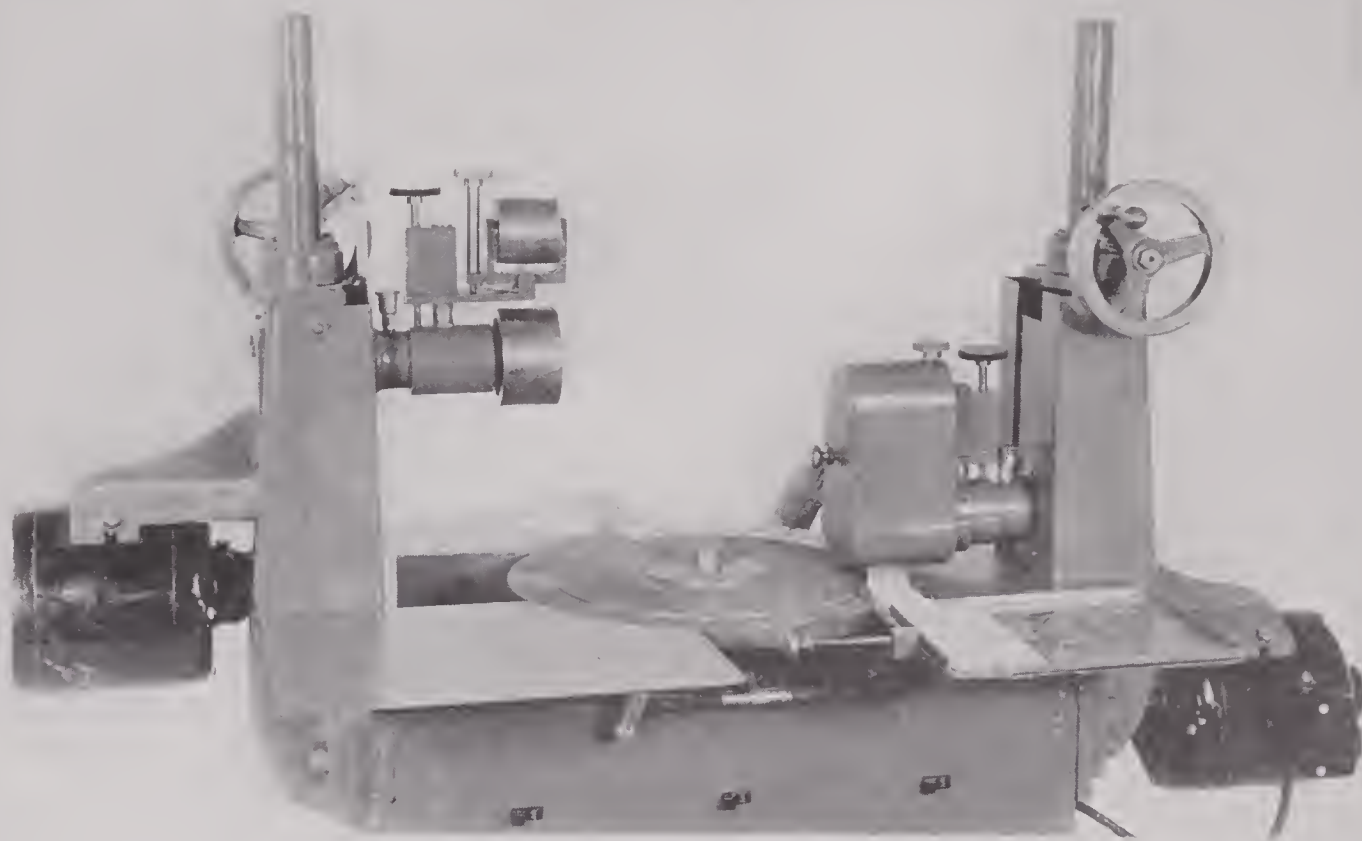


FIGURE 26. Production surfacing machine for crystal plates. For Rochelle salt, spiral milling cutters may be used; for ADP, sanding belts are used.

which the saws are used are prone to build up vibrations at higher speeds. The machines were Felker Di-met models No. 11B and No. 80, as used in quartz cutting. They were operated at about 1600 rpm with 8 inch saws although occasionally a 12" or 16" saw was used at the same speed for exceptionally large crystals.

The saw blades were trued and the surface roughened simultaneously by using a straight knurl as a dressing tool, turning the saw slowly by hand so that the knurl crumbled the saw edge, leaving a fine roughness. Saws so treated cut several times as fast as those that were trued with a diamond. Sawing machines must be very carefully lined up so that as the saw moves through the crystal it moves quite accurately in a plane with ex-

used for this purpose, but later they were replaced by centrifugal pumps which dipped in the solution. This obviates the priming problem. The centrifugal pump has no packing glands and no bearings that contact the fluid, the motor being high above the fluid.

Besides saturated ADP solution, which has been found to be the most satisfactory saw coolant, mixtures of propylene glycol and saturated ADP solution have also been used. Light oils like kerosene have also been tried but in every case the straight saturated ADP solution is preferred.

In sawing large crystals it is very important to have the sawing fluid at the same temperature as the crystal, within about 2°C. The best arrangement is to maintain

the whole cutting shop at a constant temperature 24 hours of the day, and to cut no crystal until it has been in this room for several hours. This is particularly true in the winter when the day to night temperature varies widely if the plant runs only one shift per day. For a while all crystals were stored in an oven thermostatically controlled at 30°C. The saw coolant was also controlled at 30°C.

8.4.5

Milling RS

The final surfacing operations on RS crystals have been done with milling cutters. These cutters may be either spiral face milling cutters or spiral end mills. Spiral end mills with four flutes, a diameter of $\frac{5}{8}$ in., and an operating speed of 5,000 rpm or more are suggested for this purpose. Sharp cutting edges are essential and a rather large clearance angle is recommended.

Any one of several arrangements for milling should give equally acceptable results. Much depends on the actual quantity of the material being processed. For an experimental laboratory an ordinary plain milling machine would be sufficient, but for production work it is advantageous to install more elaborate equipment. The photograph in Figure 26 shows a type of small production machine with interesting possibilities in this direction. This particular machine is equipped with belt sanders but it is a simple matter to design milling heads for this type of equipment, as has been done by the Brush Development Company. The rotary table turns continuously at a speed which enables crystals to be placed on the table by one operator and removed from it by another operator following the milling cut. By having two cutters in tandem, both a coarse and finish cut may be taken in sequence in the same operation. In fact, the process may be speeded up still further by having four milling cutters work on the same operating table. In this way one side of a crystal may be given a coarse and a finish cut while the table rotates 180 degrees, after which an operator turns the crystal over so that the second surface is finished during the second 180 degrees rotation. The crystals are held tightly on this rotating table by a vacuum chuck arrangement. To facilitate addition and removal of the

crystals, only that part of the table in the immediate vicinity of the milling cutters is connected to the vacuum line.

The milling equipment used at UCDWR for ADP, which employs a simple sweep cutting tool, functions just as satisfactorily for RS. A complete description occurs in Section 8.4.6.

8.4.6

Milling ADP

The milling of ADP crystals is a much more difficult task than the milling of RS. As a consequence, the milling cutters quickly become dull

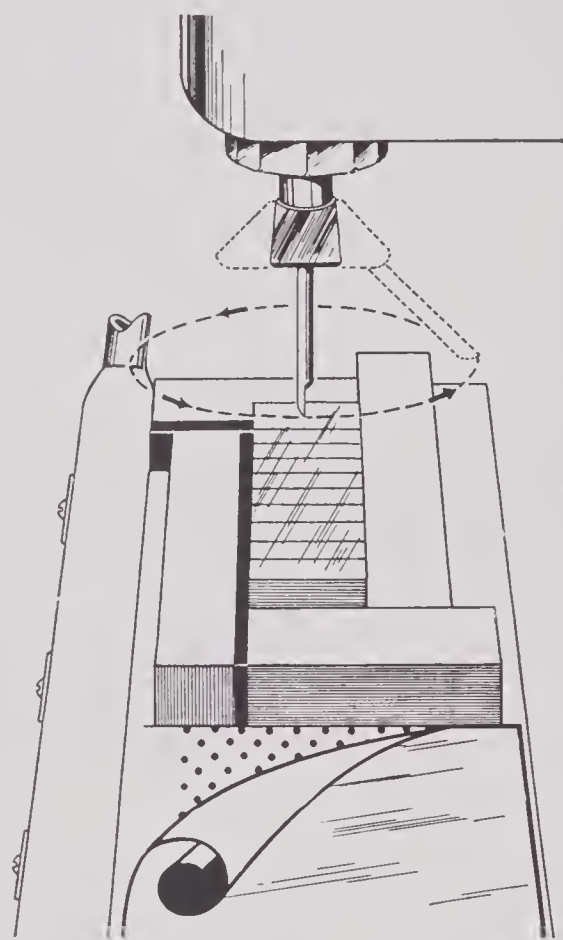


FIGURE 27. Vertical milling machine or jig borer as used at UCDWR for finishing either ADP or Rochelle salt crystals. Note the support at the edges and sides of the crystals, also the use of a vacuum chuck.

and frequent attention is required to maintain them in a sharp condition. Some of the harder cutting alloys are valuable for this application, but the ideal solution is yet to be found. To the writer's knowledge, the Brush Development Company continues to surface ADP crystals with spiral milling cutters of the type discussed

in Section 8.4.5. Their successful work with milling cutters on RS probably accounts for their adaptation of the same method to ADP.

The task of maintaining sharp milling cutters for ADP crystals can be simplified if one adopts a vertical milling machine, commonly referred

tals are placed on a traveling milling machine bed and held fast by means of a vacuum chuck. Rectangular bars of steel, also held on the table by means of the vacuum, are used to give support to the crystals in the direction of motion of the cutter. The actual angular position of the cutter can be observed from the two drawings in Figure 28 which show vertical cross sections. The bottom illustration indicates that the clearance angle should be about 55 degrees and the angle of rake should be zero. The top illustration of Figure 28 shows that the cutting edge should make an angle of approximately 10 degrees with respect to the top surface of the crystals being cut. A satisfactory speed is approximately 4,200 rpm. It will be found necessary to resharpen these cutters at fairly frequent intervals, but owing to their simplicity this is a very easy operation. The sharpening may be done on a disk sander having a very fine grade of Carborundum paper, grit No. 320A being satisfactory. The particular stellite bits used had a diameter of $\frac{3}{16}$ in. and a length of about 2 in. Care must be exercised to avoid checking of stellite by heating during sharpening.

With the sweep cutting tool just described, a rough cut of 15 to 20 thousandths of an inch could be taken from an ADP crystal each time the cutter traversed the block of crystals. For finishing cuts, 1 or 2 thousandths of an inch was satisfactory. To avoid chipping, the tool had to be sharp.

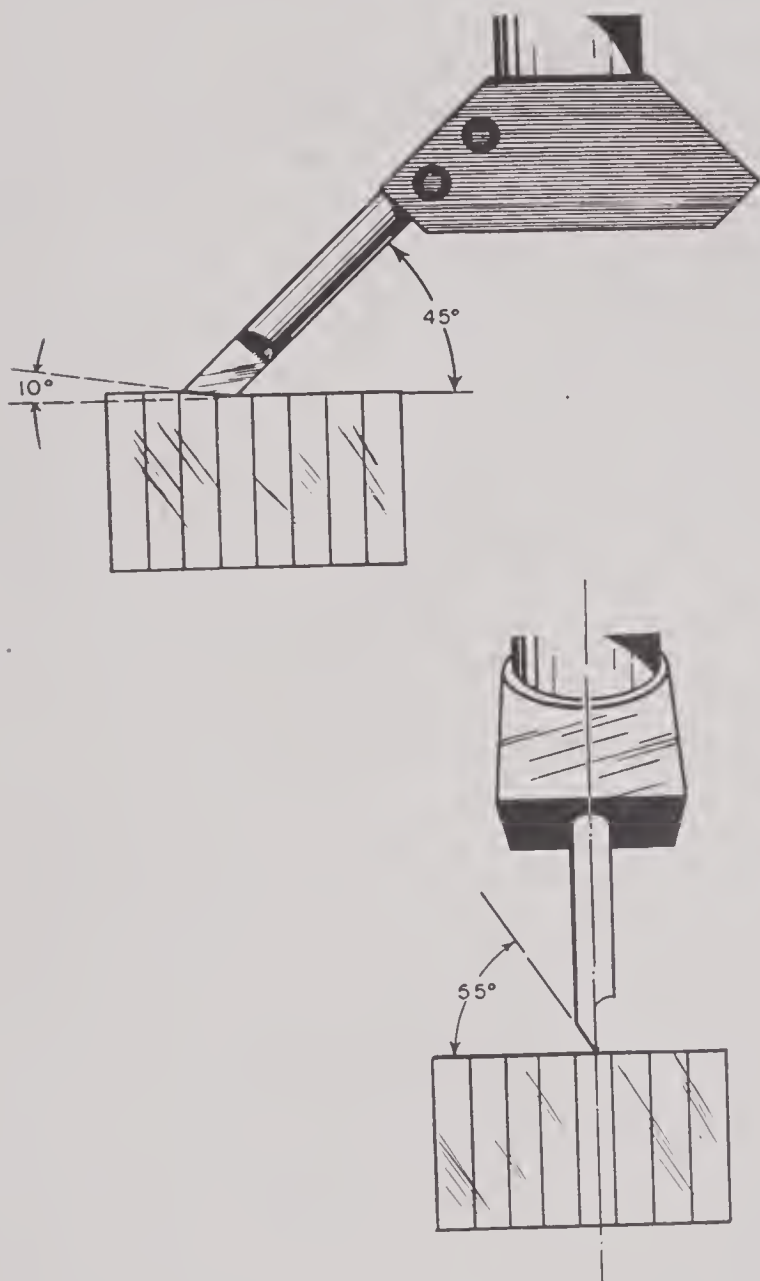


FIGURE 28. Position of stellite tool in vertical milling head. Above: Side view showing angle made by tool shank with respect to the horizontal plane and also the cutting angle with respect to the horizontal crystal surface. Below: Edge view showing the zero rake angle and the 55° clearance angle of the stellite cutter.

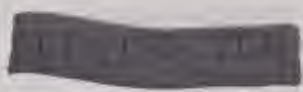
to as a jig borer, since it uses only a single-sweep cutting bit. Such a milling machine has been in use for some time at UCDWR. This type of equipment is shown in Figure 27. It will be noted that the stellite bit is inserted in the tool holder at an angle of 45 degrees. The crys-

8.1.7

Die Cutting of Foils

Where foil stampings are required in large numbers, it would probably be most economical to produce them by means of a standard-type die in a power press. In an experimental laboratory, however, there are occasions where only a few or perhaps a few hundred foils of a given size are needed. A simplified die-cutting process which is well adapted to small production has been used at UCDWR for some time and will now be described.

An exact profile of the desired shape and size of the foil is marked off on a piece of thin steel stock and then machined or ground accurately to dimensions. This thin piece of steel is then



soldered to a large supporting plate as shown in Figure 29 and constitutes the male part of the die. The thickness of the steel stock is indicated in the figure as 0.05 in., but this dimension is not critical and could be as thin as $\frac{1}{32}$ in. When machining grades of steel are used, the die should be hardened. It has been found, how-

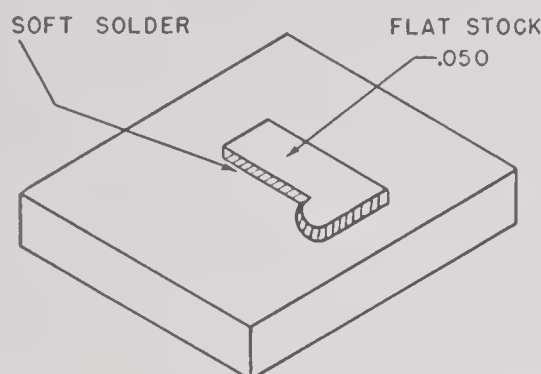


FIGURE 29. The die used for blanking thin foil electrodes.

ever, that dies of this type may be conveniently ground from a very heavy grade of hacksaw blade. The base to which the thin steel die is soldered should have an area five or six times greater than the die. It is important that the edges of the die be perpendicular to its face and that the corners be very sharp.

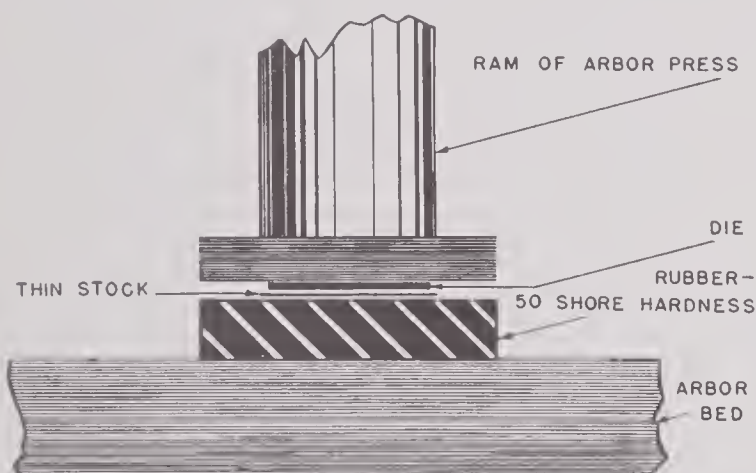


FIGURE 30. Blanking electrodes from silver foil with die shown in Figure 29.

In stamping out silver foil with this die a simple arbor press may be employed. The die is held on the ram of the press and the silver-foil stock is placed on top of a thick sheet of rubber which rests on the bed of the press. The sheet of silver foil used should always have margins $\frac{1}{8}$ to $\frac{1}{4}$ in. larger than the blanking die. The rubber should be $\frac{1}{2}$ to 1 in. thick and should

have a Shore durometer hardness test of 50 to 70. Trials using different hardnesses of rubber should be helpful. When the ram of the arbor press is brought down, as depicted in Figure 30, the die is forced through the silver foil into the rubber. In this manner a very clean-cut replica of the original die may be cut from the foil.

These dies should be capable of cutting several hundred blanks without resharpening. The blanking die may be sharpened by grinding down about 0.002 in. on its flat surface, care being taken to see that the corners are left as sharp as possible.

This method of blanking thin sheets of any of the softer metals may find a wide variety of applications in an experimental laboratory. While production is not particularly rapid when a hand-operated arbor press is used, there is no reason why the process could not be made at least semiautomatic in a power-operated press, perhaps of the pneumatic type.

8.1.3

Polarizing Crystals

The technique for polarizing and marking piezoelectric crystals has been discussed in Section 8.3.9. The actual indicating equipment would be expected to vary in detail from one laboratory to another. Since only a qualitative indication of polarity is sought and not a quantitative deflection, no great demand is placed upon the instrument. However, the deflections should be great enough to avoid undue inconvenience in reading them and to give unmistakable indications.

The electric circuit diagram for the equipment used at UCDWR is shown in Figure 31. It operates from a 110-v a-c line and gives very satisfactory deflections for the crystal sizes used in underwater sound transducers. Since the circuit elements are shown sufficiently clearly in the figure to permit the instrument to be built, further comment is not required, except that the meter *M* has 100-0-100 μ a movement.

An indicator with simpler circuit elements has been used successfully at NRL. The circuit diagram for their instrument is reproduced in

Figure 32. The circuit is novel in that the low B potential is placed on the control grids. The voltage generated by pressing on the crystal is placed upon the two screen grids. Better stability than that obtained from the usual tube

from making whatever tests may be required to establish acceptability. Hence, the selection of crystals for transducers from the standpoint of discarding any substandard ones will be discussed at some length.

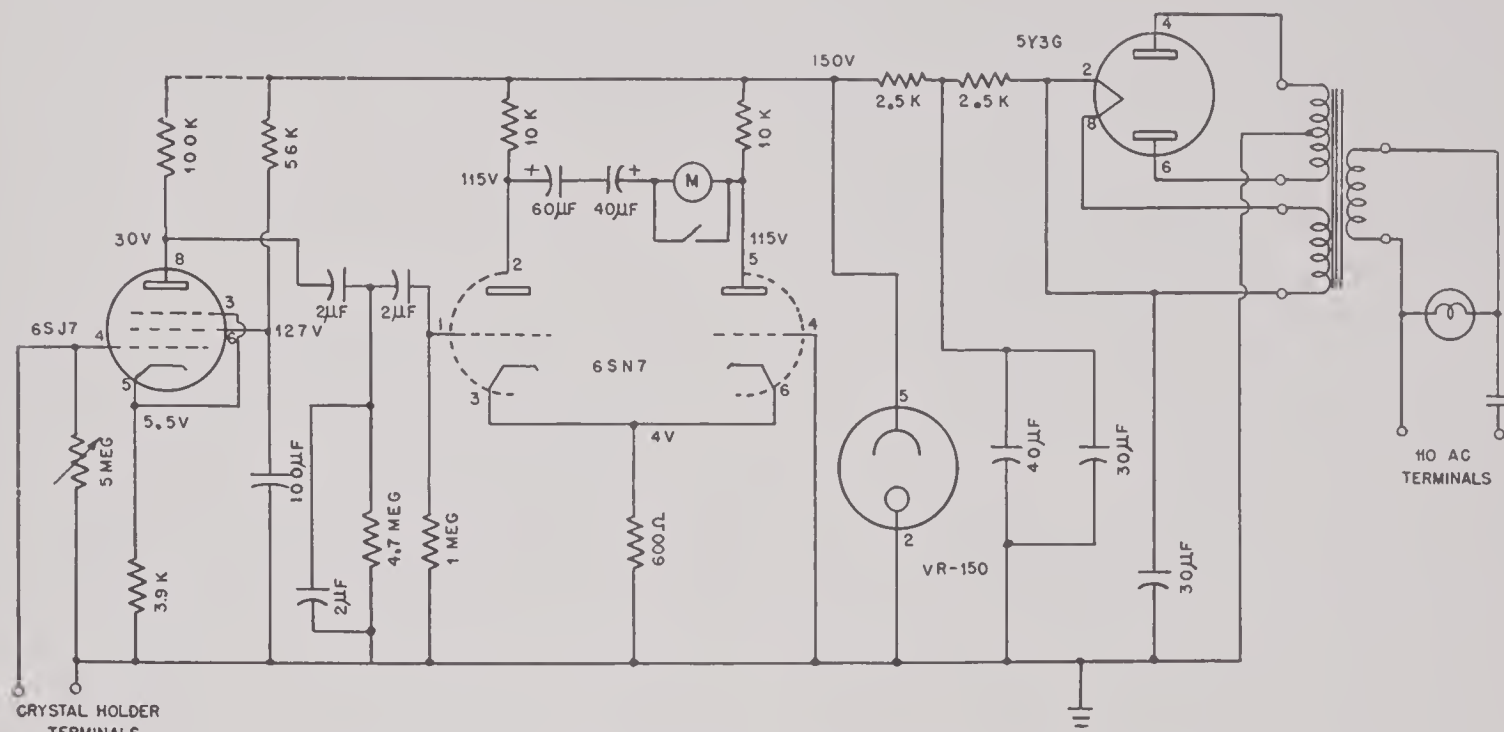


FIGURE 31. Circuit diagram of the UCDWR polarity indicator.

connections is claimed. Since the writer has neither built nor had experience with this equipment, no critical comment can be added.

8.5 SPECIFICATIONS FOR SINGLE CRYSTALS

Official specifications for piezoelectric crystals are not in a satisfactory state at the present time. In fact, as far as the writer is aware, such specifications do not even exist in the case of RS. In the discussion of various properties amenable to quantitative specification in the sections to follow, an attempt will be made to point out reasonable expectations for the several characteristics and to indicate the nature of inspection tests to be performed.

The UCDWR Laboratory has purchased all of its crystals from outside sources. However, this dependence on a commercial source of crystalline material, even though the quality of the piezoelectric crystals so obtained may be consistently good, does not free a laboratory

8.5.1

Visible Defects

Visible defects in crystals are of two sorts, veils and chips. Veils occur within the body of crystals and are caused by unfavorable saturation conditions in the solution during the

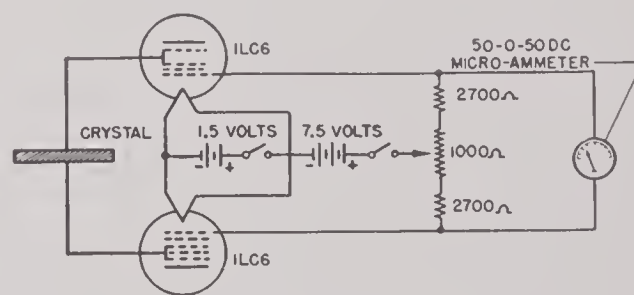


FIGURE 32. Circuit diagram for NRL polarity indicator.

growth of the mother bar. Improper saturation conditions may be caused by either an incorrect temperature or inadequate circulation. These veils are of two distinct types, the one being associated with a supersaturation condition and the other with an unsaturated condition. In cutting 45 degree Z-cut ADP plates from the

mother bar, it is especially important to exclude the seed-cap region with its usually prevalent veils.

It is not uncommon for veils to contain small quantities of the original saturated salt solution. Their presence leads to voltage breakdown and crystals containing them must be discarded. According to the Navy specification for ADP⁹ all crystals having appreciable veils as gauged by eye shall be rejected unless they pass successfully a voltage-breakdown test. This test is detailed in Section 8.5.8. Where crystals are to be used in transducers at operating voltages in excess of those specified in the Navy voltage test, it is clear that they should be tested at the higher operating voltage in question.

With respect to crystals which possess minor flaws, such as chipped corners or slight surface imperfections, the question as to whether they shall be used is more difficult to decide. According to the Navy specification⁹ mentioned, finished crystal plates with minor flaws and imperfections shall be acceptable provided they meet certain standards of appearance and also meet the electrical and mechanical performance requirements enumerated in a later section. The Navy appearance standard consists of photographic views of chipped crystals, the chips being of various sizes. Crystals with very small chips were considered acceptable, those with larger chips were labeled "no go." The size of the chips for acceptable crystals seemed to be about $\frac{1}{16}$ or $\frac{3}{32}$ in. in diameter and considerably less in depth. The crystals in the category labeled "no go" had larger and deeper chips, or perhaps a whole corner would be chipped off across the entire thickness dimension.

Much difference of opinion exists on the question as to when a crystal is or is not acceptable owing to the presence of chipped regions. From the standpoint of their performance in a transducer, the existence of chipped corners may not be serious. According to the observations of W. P. Mason, communicated in conversation, the location of voltage breakdown points in defective transducers were not correlated with the presence of chips or minor surface flaws in individual crystals. Inasmuch as a high percentage of the crystals obtained from a mother bar suffer from visible flaws incurred during

processing, greater attention should be given to setting up definitive standards based on actual performance data.

In an experimental laboratory, where crystals are constantly being cut to particular size specifications, any relatively large crystal containing chipped edges may be salvaged and recut for use in another transducer employing a higher resonant frequency.

8.5.2

Geometric Tolerances

In the case of ADP crystals, certain standard dimensions were designated during World War II by BuShips. With respect to length, the crystals were either 1.10 or 1.25 in.; with respect to width, either $\frac{1}{2}$ or 1 in.; and with respect to thickness, either $\frac{1}{8}$, $\frac{1}{4}$, or $\frac{1}{2}$ in. Tolerances in either length, width, or thickness were specified as ± 0.005 in. This tolerance specification is regarded as a liberal one. A tolerance as low as ± 0.001 in. still would be considered reasonable although it might involve a slight extra charge.

Angular tolerances were not explicitly stated in the specifications⁹ set up by BuShips. However, they were implied when limiting values were placed upon electrical characteristics, a discussion of which is contained in sections to follow. Crystal tolerances with regard to squareness of cut might reasonably be held to ± 1 degree, but the tolerance of the orientation angle cannot readily be held to such a low value. However, a tolerance in orientation of ± 2 degrees is a reasonable one.

Angular orientation errors do not offer any particular difficulty in the case of ADP crystals since the rate of change of the dielectric constant with respect to angle is a slowly varying function. In the case of X-cut and Y-cut RS, however, there is a very large difference in the dielectric constant between the X and Y axes. Particularly in Y-cut crystals, slight deviations from the correct angle of orientation can produce a marked difference in the capacity of the crystal and a routine inspection of all Y-cut crystals may be necessary. The best test is probably a capacity check as discussed in Section 8.5.4.

8.5.3 Polarized Light and X-Ray Diffraction

The fact that piezoelectric crystals are birefringent has led individuals to make use of polarized light in an effort to determine axes of orientation. The optic axes of both RS and ADP lie in the longitudinal dimension of the mother bars. In the case of 45-degree Z-cut ADP crystals the electric field is applied in the same direction as the optic axis.

The simplest type of polarized light observation may be made with some such equipment

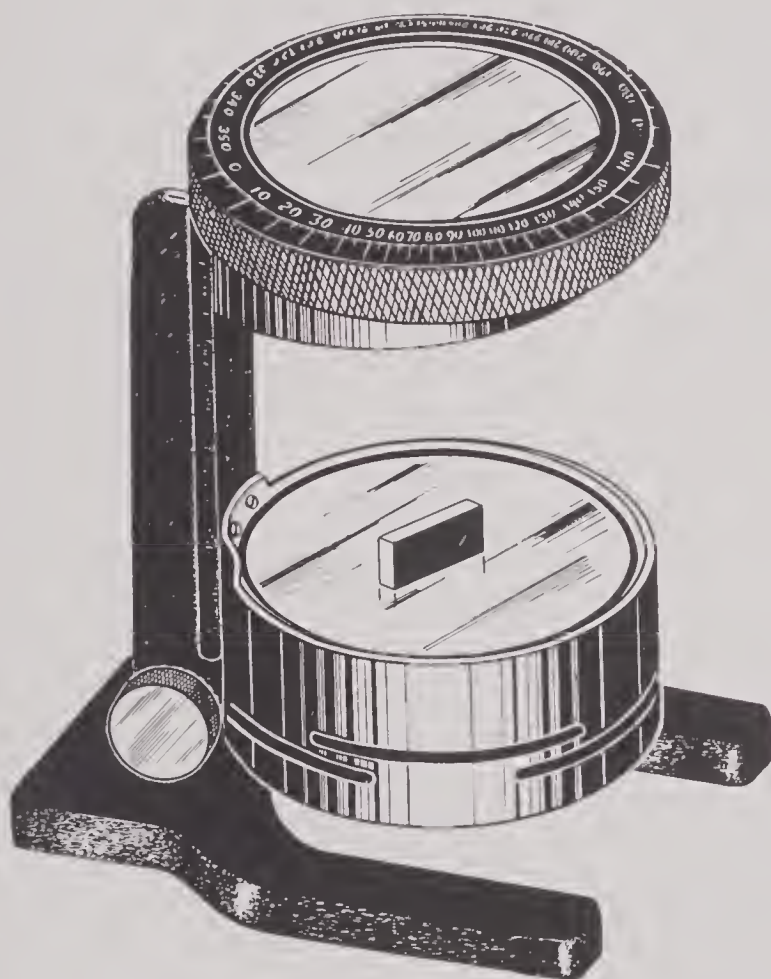


FIGURE 33. Instrument for observing crystals in plain parallel polarized light.

as is illustrated in Figure 33. This piece of apparatus consists of a polarizer and an analyzer, each made up of a large sheet of polaroid. It is customary to rotate the analyzer until the field is dark. If a 45-degree Z-cut ADP crystal is laid with its electrode face on the polarizer, an observer would be looking in the direction of its optic axis. Consequently, the field would remain dark even though the crystal were rotated 360 degrees about its optic axis. If the

crystal were laid on its long edge or on its end, an observer would see alternating periods of light and darkness during a 360-degree rotation. Hence, this simple observation with rudimentary equipment could reveal whether crystals were cut an entire quadrant off from the correct orientation.

In the case of 45-degree X-cut and 45-degree Y-cut RS crystals, the orientation does not permit observation along the optic axes when the crystals are simply laid on the polarizing plate. Therefore, alternating periods of darkness and light will be observed on the analyzer when rotation occurs about any of the three axes of either type of crystal. Consequently, it would be necessary to resort to more complicated arrangements to secure any precise data on the orientation. In view of the fact that all these crystals may readily be cut to an accuracy of 2 or 3 degrees, it would not seem particularly useful to proceed to more refined polarized light

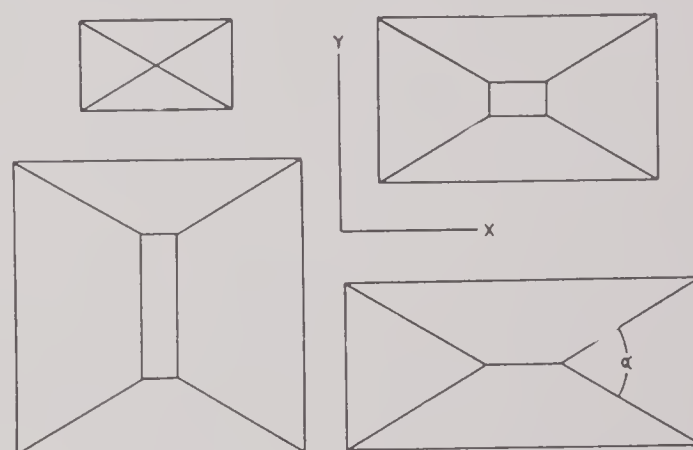


FIGURE 34. Etch figures on a Rochelle salt surface normal to the Z axis. In each case, the X axis is horizontal, the Y axis is vertical.

methods of observation. On the other hand, observation of RS crystals in convergent polarized light might be desirable in that unsymmetrical patterns would appear if the angle of cut were incorrect by a small amount.

For an accurate check on the correctness of angular cut for any of the crystals under discussion, access should be had to X-ray diffraction equipment. While the X-ray examination of each crystal which enters into the construction of a transducer is normally not justified, occasion may arise when it would be desirable

to test sample crystals by this method. The NRL has installed X-ray diffraction equipment for this purpose but such facilities have not been available at UCDWR.

The following account of etching tests made by Cady¹⁰ may be helpful in distinguishing the axial directions in RS plates. Very characteristic figures are easily produced by lightly moistening a polished crystal surface. After drying, a face normal to the X axis is found to be covered with fine striations parallel to the Z axis. On faces normal to the Z axis, minute rectangular pyramids ("etch hills"), sometimes truncated, extend upward from the surface. Some characteristic forms for the X - Y plane are shown in Figure 34 as viewed from above. The X axis bisects the projection on the X - Y

in the crystal. Any of several well-known methods may be employed for accurately measuring these small values of capacitance to the desirable tolerance of $\pm 0.1 \mu\text{mf}$ in the capacitance range of 5 to 30 μmf .

Inspection of the equivalent electric circuit of a crystal, shown in Figure 37, indicates that the proper place to measure C_0 might be at a point considerably above the resonant frequency of the crystal, since at that point the impedance of the series LCR branch would be so high that the impedance of the whole crystal unit would be effectively that of C_0 alone. Difficulties arise, however, owing to the fact that a crystal is not singly resonant over a wide range of frequencies, e.g., at certain frequencies, modes of vibration other than the longi-

TABLE 1. Navy specifications⁹ for some electrical characteristics for ADP crystals.

Dimensions (in.)	Resonant frequency (kc)	Capacity at 1,000 cycles (μmf)	Capacity ratio	Difference between antiresonant and resonant frequencies (kc)
$1.10 \times 1.00 \times 0.250$	48.4 ± 0.5	15.7 ± 1.0	15.2 ± 1	1.57 ± 0.1
$1.10 \times 1.00 \times 0.500$	48.4 ± 0.5	7.8 ± 0.5	15.0 ± 1	1.58 ± 0.1
$1.25 \times 0.5 \times 0.125$	50.3 ± 0.5	17.8 ± 1.0	14.1 ± 1	1.75 ± 0.1
$1.25 \times 0.5 \times 0.250$	50.2 ± 0.5	8.9 ± 0.5	14.1 ± 1	1.75 ± 0.1
$1.25 \times 0.5 \times 0.500$	50.0 ± 0.5	4.5 ± 0.5	14.3 ± 1	1.72 ± 0.1

plane of the acute angle alpha, which has a value of roughly 60 degrees. On a face normal to the Y axis, the pyramids are of the same general nature as illustrated in Figure 34, the longer dimensions of the base being in most cases parallel to the Z axis. Owing to the strong polarity in the X direction, one might expect marked differences in the etch figures on opposite sides of an X -cut plate. On the contrary, the striations look just alike.

8.5.4

Capacitance

An important electrical property of a piezoelectric crystal is its static capacitance C_0 , which represents the capacitor formed by the dielectric of crystalline material between the two electrodes. Some of the factors which affect the measured value of C_0 are: angular orientation, linear dimensions, temperature, crystal holder, and irregularities such as chips or flaws

tudinal mode will be excited as well as higher-order harmonics of any of the possible modes. Therefore measurements of C_0 obtained near any of the higher response frequencies would be in error. This difficulty of avoiding higher-order resonances at frequencies above the fundamental longitudinal resonance, has led to the practice of measuring the capacitance at low frequencies, usually at 1,000 c. Since the reactance L is negligible at this low frequency, instead of C_0 , the capacitance measured will be C_T , where C_T is equal to $C_0 + C$.

For 45-degree Y -cut RS and 45-degree Z -cut ADP, C_T has a value about 9 per cent higher than C_0 alone. The Navy specifications⁹ for ADP include the value of C_T at 1,000 c and allow a tolerance of from 5 to 10 per cent depending upon the size of the crystal. Table 1 gives the Navy specifications for the capacitance at 1,000 c for five common sizes of ADP crystals. In addition, it also gives values for the resonant frequency, the capacity ratio, and for the dif-

100-150000

ference between the antiresonant and resonant frequencies. The meaning of these latter quantities will be discussed further in subsequent sections. It has been found by McSkimin¹² that reasonable values for the capacitance of ADP crystals at 1,000 c are given by the following equation:

$$C_T = \frac{1.38lw}{t} \mu\mu f \quad (\text{dimensions in cm}) \quad (1)$$

where l , w , and t , represent the length, width and thickness of the crystal, respectively, in centimeters.

For 45-degree Y-cut RS crystals, the capacitance may be calculated to a fair approximation

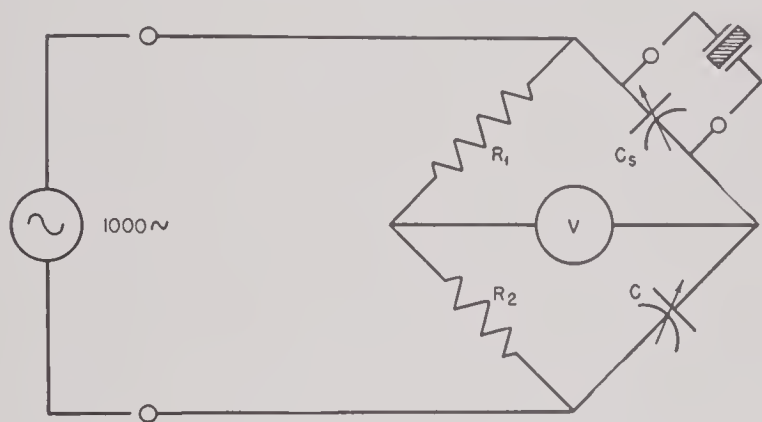


FIGURE 35. Capacitance bridge for measuring C_0 .

by substituting the constant 0.87 for the 1.38 of equation (1). Since the effective dielectric constant of Y-cut RS varies markedly with angular orientation, the capacitance measurement serves as a valuable check on the correctness of the cut. Some published tabular data¹³ on the capacitance of about 600 commercial Y-cut crystals indicate that fluctuations of as much as ± 7 per cent from the average value given by the above equation may be expected.

For 45-degree X-cut RS, such simple calculations of capacitance are impossible. The dielectric constant varies markedly, not only with temperature but also with the applied field strength, and in neither case in a monotonic fashion. Reference is made to a paper by Froman¹⁴ for graphical data on X-cut RS.

A simple bridge circuit readily adapted to this type of testing appears in Figure 35. Capacitance measurements of sufficient accuracy are obtained by incorporating a substitution

method into the bridge. The resistance arms R_1 and R_2 are equal and C can be any high quality capacitor (variable or fixed) capable of balancing the other bridge arm containing a calibrated standard C_s . The high-impedance voltmeter V should have sufficient sensitivity to give sharp indication of balance. In operation the crystal, supported in a suitable holder, is shunted across C_s . A balance is obtained by varying either C_s or C . Then the crystal is removed and the bridge rebalanced by varying C_s . The value of C_T is the difference between the two settings of C_s .

Another satisfactory method of determining C_T is to employ the admittance measuring circuit shown in Figure 38 of Section 8.5.5. In this

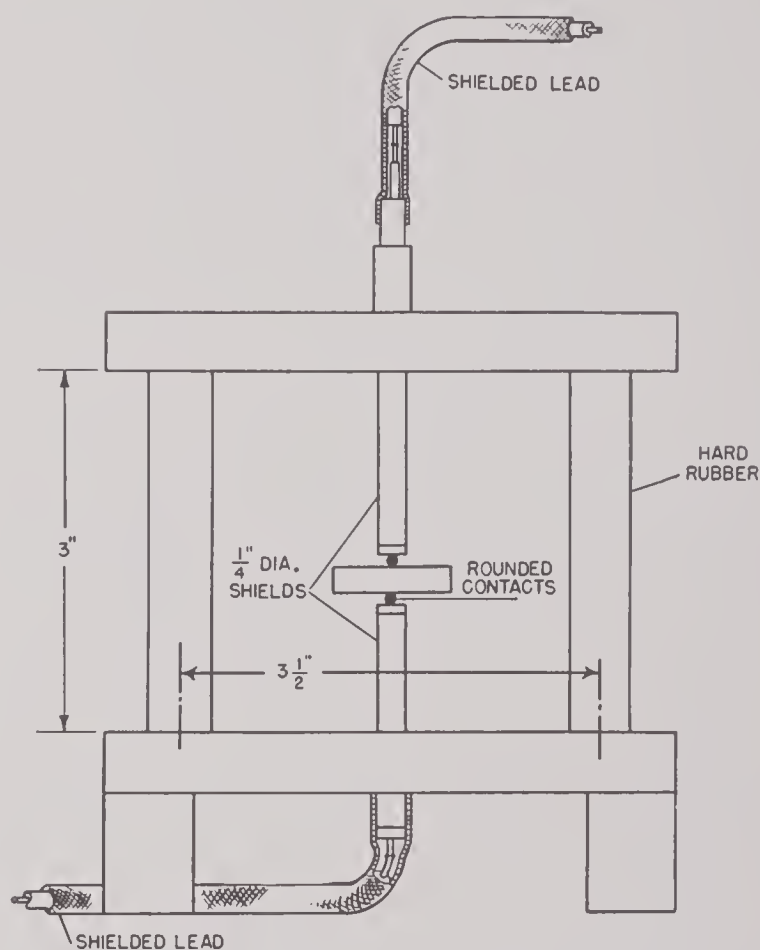


FIGURE 36. Special crystal holder for reducing stray capacitance. (Bell Telephone Laboratories.)

circuit the magnitude of crystal admittance may be computed, and hence C_T , since the voltage across the crystal, the current through the crystal, and the applied frequency are known. Observations made between 1 kc and one-half the resonant frequency f_r will show that within the

limits of measurement the crystal behaves as a capacitor having an admittance of $\omega(C_0 + C)$.

Where a high degree of accuracy is necessary, reliable shielding and grounding techniques must be used throughout the test circuit and for the crystal holder. Not only errors in absolute values but also relative errors owing to temperature variations may be minimized by reducing stray capacitance and grounding effects of the crystal holder, and by careful choice of the materials used in constructing the holder. The effect of the stray capacitance is to cause an apparent increase in C_T . The effect of ground proximity is to disturb the fringing flux distribution around the crystal and therefore to lower the measured value of C_T . In general, errors due to ground proximity are greater for crystals of larger thicknesses and for the smaller widths. A special crystal holder designed by McSkimin¹² is illustrated in Figure 36. The grounding effect is controlled and stray capacitance is reduced to about 0.01 μmf by making the electrical connections through shielded cables to a carefully isolated crystal.

8.5.5

Admittance and Q

An inspection of the simple equivalent circuit for a piezoelectric crystal, shown in Figure 37, indicates the existence of a critical frequency



FIGURE 37. Representation of a crystal and its equivalent circuit.

f_m at which the mechanical LCR arm of the network will exhibit a maximum admittance. At frequencies increasingly higher than f_m , the admittance rapidly decreases until a minimum value is reached at the frequency f_n . The absolute value of the admittance at f_n is usually so small and the minimum so flat for the fundamental longitudinal response of a crystal that

a precise determination of f_n is difficult. As the frequency increases above f_n , the admittance increases until it approaches the value of ωC_0 , i.e., the crystal appears as a capacitor with the capacitance C_0 . It was shown in Section 8.5.4 that at frequencies considerably below f_m , the crystal appeared as a capacitor with the capacitance $C_t (= C_0 + C)$.

The salient features of an admittance-versus-frequency curve are shown in Figure 39 for an ADP crystal with the dimensions $1\frac{1}{2} \times 1 \times \frac{1}{4}$ in. The first maximum occurring at 39.2 kc represents resonance for the fundamental longitudinal vibration of the crystal, its accompanying antiresonance appearing at 40.6 kc. A number

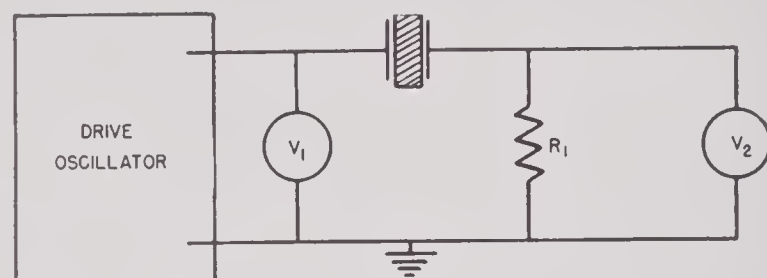


FIGURE 38. Admittance circuit: two voltmeter method.

of maxima and minima corresponding to higher-order resonances and antiresonances are also shown. At frequencies well below f_m , the admittance is primarily a function of the capacitive reactance and therefore increases 6 db per octave. The dashed line corresponds to the admittance for the true static capacitance C_0 . An experimental approximation to the mechanical Q of a crystal Q_m is obtained by dividing f_m by the difference in the frequency settings required in order to reduce the admittance 3 db on either side of f_m .

The circuit employed at UCDWR for admittance measurements is reproduced in Figure 38. A constant voltage V_1 is applied to the crystal and then, as the frequency of the generator is varied, the current through the crystal is observed in terms of the voltage drop V_2 developed across a relatively small resistor R_1 in series with the crystal. Some error will be introduced by using the same value of R_1 throughout an admittance test but for the sake of the general picture this may usually be neglected. A more detailed discussion of the absolute ad-

mittance measurement is given in Section 9.1.1, but it will be noted here that the variable-frequency generator must meet several definite requirements. Briefly, it should operate from 1 to 150 kc with a stability of ± 20 c at all frequencies, be capable of adjustment in increments of 1 or 2 c, have a low output impedance, and have an extremely low harmonic content. The construction of the crystal holder must be such as always to enable the crystal to be sup-

Typical values of Q_m for actual transducers range from perhaps 10 down to 2.

8.5.6

Resonant Frequencies

The two resonant frequencies of major interest may be termed "series resonance" f_r , and "antiresonance" f_a . Series resonance or simply "resonance" is defined as the frequency at which the series LCR branch of the equivalent circuit

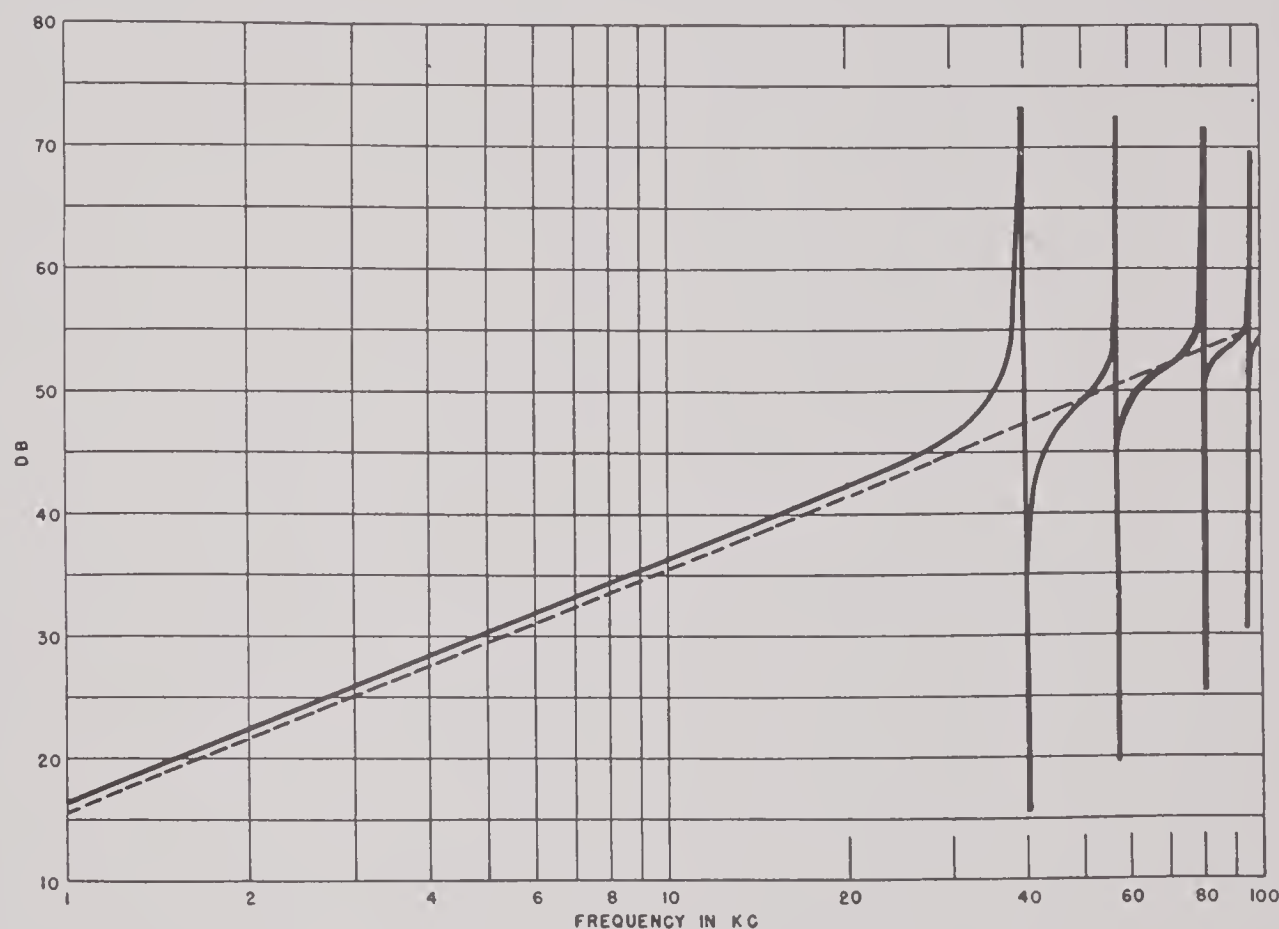


FIGURE 39. Typical admittance curve for single crystal.

ported in exactly the same manner if reproducible measurements are to be obtained.

No specifications have been set up for ADP or RS crystals in terms of their admittance characteristics. Since the values are obtained from air measurements they probably have little bearing on the behavior of loaded crystals operating under water. In the latter case, for example, Q_m is quite small compared to the high values characteristic of crystals freely vibrating in air. In reported measurements¹³ on a total of several hundred 45-degree Y-cut RS crystals, divided into ten groups on the basis of their dimensions, average values for Q_m of the various groups ranged from 3,990 to 6,950.

(see Figure 37) appears as a pure resistance, i.e., the net series reactance is equal to zero. Antiresonance occurs at a slightly higher frequency when the series LCR branch exhibits a net inductive reactance and is defined as the frequency at which the susceptances are equal and opposite in the two parallel branches of the equivalent circuit.

The frequencies f_r and f_a are related to the frequencies f_m and f_n corresponding to maximum and minimum admittance as follows:

$$f_r - f_m = \frac{R^2 C_0}{L} \text{ and } f_a - f_n = \frac{R^2}{2L} (2C_0 - C).$$

In the practical case where crystals are meas-

ured in air, the terms in R^2 are negligible so that $f_r = f_m$ and $f_a = f_n$. Thus, within the limits of experimental measurement, series resonance is indistinguishable from the point of maximum admittance and antiresonance is indistinguishable from the minimum admittance frequency.

In the Navy specifications⁹ for certain standard sizes of ADP crystal plates, the following statement occurs:

The oscillatory characteristics of the various crystal plates shall be determined by means of their respective resonant and antiresonant frequencies. The values of resonant frequency, capacity at 1000 cycles per second, and capacity ratio shall be within the limits given in Table 1. The values of capacity at 1000 cycles are for direct crystal capacity and are exclusive of capacities to ground of either electrode. The values of capacity ratio are determined from the resonant and antiresonant frequency measurements by the formula:

$$\text{Capacity ratio} = \frac{C_0}{C} = \frac{f_r^2}{f_a^2 - f_r^2} = \frac{1}{(f_a^2/f_r^2) - 1}.$$

It will be observed that Table 1 lists tolerances for f_r of ± 0.5 kc and for the ratio of capacities, C_0/C , of ± 1 . As an alternative specification to the capacity ratio given in Table 1, the crystals may meet a specification for the difference between the antiresonant and resonant frequencies with a tolerance limit of ± 0.1 kc.

Although no specifications on RS crystal plates with regard to resonant frequency are known to the writer, available measurements¹³ on several hundred 45-degree Y-cut plates give an indication of the tolerances to be expected in commercial lots. It appears from these data that a tolerance of ± 1 per cent on resonant frequency would be quite reasonable, especially for crystals resonating at 55 kc or less. In fact, for the latter group, ± 0.5 per cent could be met. In this same report,¹³ values of R at resonance are also stated for 45-degree Y-cut RS. In general there seems to be no point in measuring R , unless perhaps in the case of spliced crystals.

With slight modifications the circuit used for measuring admittance (Figure 38) may be used for determining f_r , f_a , and R . In the circuit of Figure 40, R_1 and R_2 have values between 10 and 100 ohms. The detector is a sensitive, high-impedance device, and the variable frequency oscillator meets the requirements outlined in Section 8.5.5 for stability, etc.

In the measurement of f_r and f_a , a constant-amplitude low voltage is applied across R_1 from the oscillator. Then as the frequency of the driving voltage is varied, the frequencies corresponding to the points of maximum and minimum current through the crystal are observed. Unless absolute values of voltage or

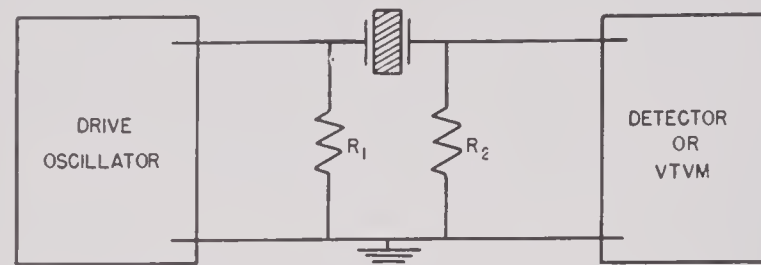


FIGURE 40. Useful circuit for determining f_r , f_a , and R .

admittance are required an uncalibrated detector is all that is needed in measuring f_r and f_a . These two important frequencies should be measured to as high an accuracy as the frequency stability of the oscillator and the sensitivity of the detector will allow, preferably to one part in fifty thousand or better.

The resistance of the series LCR branch of the crystal equivalent circuit may be readily measured also with the test circuit of Figure 40 by the substitution method. The procedure is as follows: With the test crystal in position, the frequency of the driving oscillator is carefully adjusted to the series resonant frequency of the crystal and the exact reading of the indicator on the detector noted. The crystal is now removed from its holder and a variable resistor substituted in its place. While holding the oscillator frequency at f_r , adjust the value of the variable resistor until the reading of the detector is identically the same as before. Since the impedance of the crystal reduces to R at f_r , the value of R is equal to the value of the substituted resistor. Either a calibrated detector or a vacuum-tube voltmeter is desirable, but not necessary, in measuring R . Since the substitute resistor should be noninductive, a more practical solution may be to use a series of accurately known fixed resistors of which noninductive types are available. The substitution method of determining R permits greater accuracy in practical test circuits than a maximum- and minimum-admittance method.

A direct instrumental method for measuring the capacitance ratio C_0/C has been developed at the BTL and is discussed in their report on ADP.⁷

8.5.7

D-C Resistance

According to Navy specifications⁹ for ADP crystal plates, "the D.C. volume resistivity between the electroded faces of the crystal plate shall be not less than the following for the grades specified": [quotation includes following table]

Grade	Resistivity at 25 C ohm-centimeter
AAA	1.0×10^{10}
AA	0.9×10^9
A	2.5×10^8

Since the volume resistivity of ADP depends primarily on the purity of the supersaturated solution in which the crystals are grown, it is necessary to test only a few representative samples from each batch and not to make resistance tests on every finished crystal plate.

A more detailed discussion of both RS and ADP with respect to electric resistivity occurs in Sections 8.2.4 and 8.2.8, respectively.

8.5.8

High Voltage

According to Navy specifications⁹ for ADP plates, "Crystals of grades AA and AAA shall be capable of withstanding voltage gradients of 20,000 volts per inch of thickness at a frequency approximately one-half the resonant frequency given in Table I [Table 1 of this chapter] for the size of crystal being tested. For this test, the crystal should be submerged in a suitable fluid (carbon tetrachloride is one such fluid), and the voltage shall be maintained for a period of at least 30 seconds." The plates will be considered as having met this requirement if a suitable sampling does so.

Since clean ADP crystals $\frac{1}{4}$ in. thick will usually withstand 20,000 v rms at 60 c, the above specification is not a stringent one. Rochelle salt crystals would also readily pass this specification. Should a particular application

require crystals to be driven at a voltage higher than the Navy specifications given above, then each crystal should be tested well in excess of the actual operating voltage.

Although no design of high-voltage test equipment is given here, reference is made to special equipment designed for this purpose at BTL.⁷ Its main feature was a resonant high-voltage circuit involving the capacitance of the crystal under test; in case of crystal breakdown, the circuit characteristic changed in such a manner as to reduce the applied voltage.

8.6

CEMENTS

The quality of the cement joint with which piezoelectric crystals are attached to supporting structures is one of the most important considerations in the construction of transducers, yet there is practically no agreement as to the best technique. Much of the discussion on cementing procedures must be written in the subjunctive mood. Even the choice of a cement cannot be made on a conclusive basis and some workers in the field go so far as to say that almost any cement will be satisfactory if the proper technique for its application is once developed.

Extreme pessimism on the subject of cements is probably not justified, although at best it is admittedly difficult to standardize techniques. In the absence of unanimity among the various laboratories engaged in this type of work, it seems best to describe in some detail some of the more customary methods in use at the present time. In addition, the special requirements peculiar to this problem will be outlined and discussed.

8.6.1

Specifications

Several of the specific requirements which must be met by any cement intended for attaching crystals to supporting structures will be enumerated and briefly discussed.

1. The cement must not interact with the crystalline material. This requirement precludes the use of a water soluble cement for either ADP or RS. With RS it is also necessary to avoid dehydration. For the most part, the numerous plastic cements which require an accel-

erator are likewise excluded from consideration, since practically all of them contain either an acid or an alkaline catalyst. Preliminary trials at UCDWR with several plastic cements containing catalysts were unsuccessful.

2. The cement must have a low electrical conductance.

3. The cement must be capable of being cured within certain critical temperature ranges. In the case of RS the upper temperature limit is 50 C, so that most thermosetting and thermoplastic cements cannot be used. With ADP crystals the upper temperature limit is in the neighborhood of 135 to 140 C. This limit is not particularly restrictive and does permit the use of both thermoplastic and thermosetting cements.

4. The cement must produce a joint in which only a small loss of mechanical energy can occur while the crystal is being driven. This energy loss should not increase greatly when high strains exist in the cement layer. This requirement is very important but fortunately it is subject to scientific measurement.¹⁵

5. The cement must be capable of taking care of the differential coefficient of expansion existing between the crystals and their supporting structure. The severity of this requirement depends on the actual specifications which are imposed for a given application. As the tendency is to set increasingly wider limits upon temperature performance, especially by extending the low temperature end, it has become more difficult to find an adequate cement.

Although there are literally thousands of cement compositions available commercially, most of these consist of modifications of perhaps a dozen basic types. It is highly probable that the best cement composition for crystal applications has not yet been developed. Furthermore, it is clear that not one, but several cements will be found exceedingly useful for the various combinations of crystalline materials and supporting structures encountered.

8.6.2

Application Conditions

Following the selection of a cement which possesses the best combination of desirable properties for a given application, it will be

discovered that only the first of a long series of difficulties has been met. The quality of a cement joint has been found to depend on numerous variables.¹⁵ Several of the factors involved will be discussed in this section, others in Section 8.6.3.

The Method of Applying the Cement. The possibilities that exist are spraying, brushing, dipping, and roller coating. A choice between these methods may depend in part on the amount of work to be done, but more important is the quality of the joint produced and, in the interest of uniformity, the ease of duplicating performance from day to day. It has been found in practice that some cements are best adapted to a given method of application; for others, the method may be immaterial.

The Amount of Cement. Quantity is a critical factor. Generally speaking, the cement layer should be thin, but if too thin there may not be sufficient accommodation for differential thermal expansion and cracking of the crystal results. If too thick, the loss of mechanical energy in the cement layer becomes excessive. Standardization of cement layers to a given thickness is most difficult because it depends on the method of application, on the judgment and operating skill of the technician, on the temperature and pressure and duration of the curing process, and on the maintenance of a given consistency in the original cement. These individual factors will be discussed later in some detail.

The Condition of the Cemented Surfaces. With regard to the condition of the crystal surface, two factors need be mentioned. With some types of cement it is entirely satisfactory to have a smooth surface on the crystal. This is particularly true for thermoplastic and thermosetting cements in which the solvent is permitted to escape before the surfaces are joined. Although there is a question of individual preference between smooth versus sanded surfaces, it would seem that a roughened surface should give a better bond as a general rule. The surface of the supporting structure will vary with the type of material. Metallic surfaces, in general, will be smooth. Where insulating wafers are used between crystals and backing plates it is desirable to provide a path for the solvent in

the cement to escape. This can result from the use of either porous wafers or insulating wafers containing specialized channels for this purpose. It is obvious that surfaces should be thoroughly cleaned before the application of an adhesive, either by a light sanding operation as shown in Figure 17 or by wiping with a suitable organic solvent.

Humidity. Humidity is a factor, especially in the case of RS. A humidity-temperature curve which gives the upper and lower limits of stability for RS is reproduced in Figure 1. It is essential to work slightly below the lower limit curve shown on this graph so that the crystal surface will not adsorb any appreciable moisture at any time during the cementing and curing process. Unless all surface moisture is removed from RS crystals before cement is applied, the resulting bond will be very poor. It is also important to avoid dehydration of the salt. This means humidity control in accordance with the data recorded on the humidity-temperature graph.

8.6.3

Curing

Some type of controlled curing oven is essential. With ADP, only temperature need be regulated and the highest temperature needed is not in excess of 150 C. With RS, it is necessary to control the relative humidity as well. Since commercial equipment entirely suited to both temperature and humidity control is available, detailed information on suitable laboratory apparatus of this kind is omitted from the present discussion.

With regard to the conditions which must exist during the curing process, the discussion may be confined to two main headings.

1. The pressure on the cemented surface must be controlled in order that a proper thickness of cement layer will result. Pressures as high as 200 psi may be in order, especially for large arrays. The actual pressures applied in a particular case must be correlated with temperature. At high temperatures, too high a pressure will result in most of the cement being squeezed out. Thus it will be seen that a fairly critical control of the pressure is demanded. Additional

remarks on this topic will accompany the detailed directions for the use of individual types of cement.

2. The temperature and duration of the curing process must be adapted to the particular type of cement being employed. With some types of cement, curing consists essentially of a drying process during which the solvent escapes. The rate of escape of the solvent depends on temperature, time, the area involved, the nature of the solvent and the porosity of the surfaces. It is usually recommended that an appreciable amount of the solvent be evaporated before the two surfaces come together. This results in a tacky condition of the surface and hastens the subsequent drying process. The most satisfactory temperature-time relationship for securing a satisfactory tacky condition can be determined experimentally by trying different combinations and then testing the quality of the bonds obtained.

In thermoplastic or thermosetting bonds it is customary to permit all the solvent to escape before the surfaces are in contact. In this case the application of heating either results in a sufficient softening of a thermoplastic cement or in a proper degree of polymerization of the thermosetting cement. Data covering the proper temperature and pressure in these cases can usually be obtained from detailed instructions furnished by the manufacturer. Accordingly, they are much more amenable to control.

8.6.4

Vulcalock and Bakelite Cements

In the construction of transducers the two adhesives most commonly used have been Vulcalock and bakelite cement. At UCDWR the bakelite cement used had the number BC-6052. In an early report¹⁵ from BTL bakelite cement BC-8723 was recommended. Vulcalock and bakelite BC-6052 cement seem to be very similar with possibly some difference in the composition of the solvent. Both seem to be based on a natural-rubber component and both yield sufficiently to prevent the cracking of crystals when subjected to low temperatures, except in extreme cases.

In the application of either of these cements



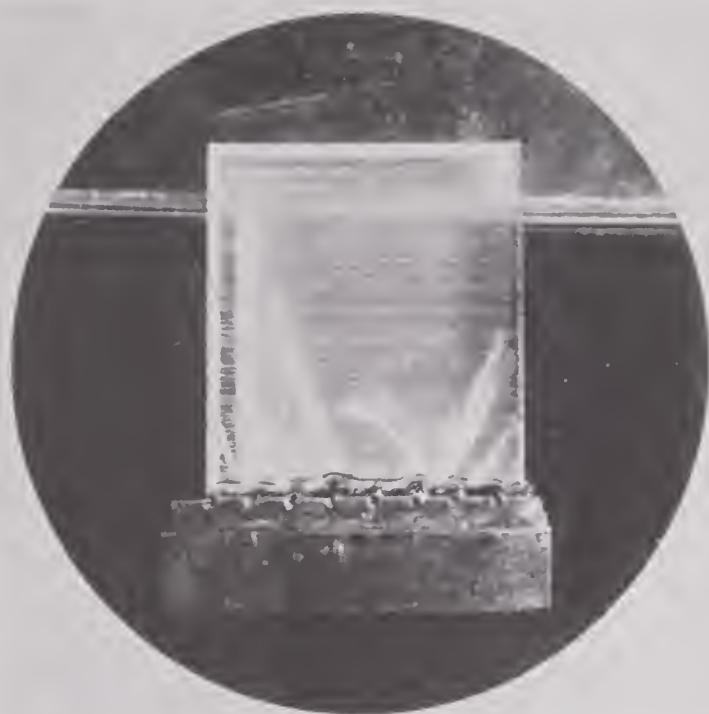


FIGURE 41.



FIGURE 42.



FIGURE 43.

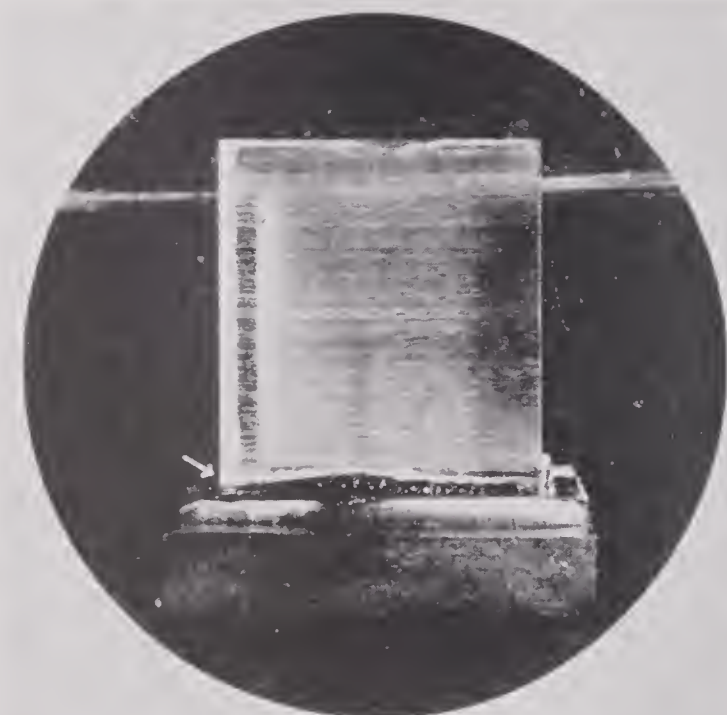


FIGURE 44.

Contrasting effects of -40°C temperature of Vulcalock (Figures 41, 42) and Butyl-C (Figures 43, 44) cement joints between ADP crystals and insulating wafers of either Durez plastic (Figures 41, 43) or porous ceramic (Figures 42, 44). The other side of each wafer was bonded to a steel plate with XCU 16257 urea formaldehyde cement. Following their preparation, all specimens were subjected to a vacuum and aged in castor oil for seven days at 60°C . Cooling to -40°C took place in either 3 hours from 30°C (Figures 41, 43) or 3 hours 20 minutes from 28°C (Figures 42, 44). With Vulcalock bonds, first cracks appeared at either 10°C (Figure 41) or 13°C (Figure 42); with Butyl-C bond, a tiny crack appeared in one crystal at -39°C (see arrow in Figure 44), the other remained intact (Figure 43). (Bell Telephone Laboratories.)

the best method¹⁵ seems to be to apply a thin uniform layer of cement on both surfaces and allow it to air dry for a definite length of time. The cement should always possess the same consistency initially and drying should take place at a prescribed temperature and for a definite length of time, since the thickness or tackiness of the cement is a controllable function of the drying time. A cement of satisfactory consistency, at the time of pressing the specimens together, has a composition of about 60 per cent of solid matter by weight. A pressure as high as 200 psi can be maintained for a few minutes without forcing out too much of the cement and results in a good bond. The pressure should then be reduced to 30 psi and the specimens placed in a drying oven. This reduction of pressure is necessary to prevent further loss of cement when the increased temperature of the oven causes it to become more fluid. However, it is definitely beneficial to compress the cement as it contracts from loss of solvent. Therefore, the pressure should not be reduced too much. The length of time for curing either bakelite or Vulcalock cement should be at least 24 hr and even longer times are beneficial. The temperature in the case of RS may be 40 C with the relative humidity 50 per cent. For ADP the temperature may be higher, even 80 C, and the drying time need not be as long.

The unsatisfactory use of Vulcalock for cementing ADP crystals to supporting structures in transducers which must operate at extremely low temperatures is photographically depicted in Figures 41 and 42. In Figure 41 an ADP crystal has been bonded with Vulcalock cement to a Durez wafer and in Figure 42 to a porous-ceramic wafer. In both cases the wafers were, in turn, bonded to steel plates with the catalyzed urea formaldehyde cement XCU 16257. The use of the latter cement is discussed in some detail in Section 8.6.8. The ADP crystals in these two illustrations were treated in essentially the same manner, having been subjected first to a vacuum and then aged in castor oil at 60 C for 7 days. At the end of this period the crystals were cooled from around 30 C down to -40 C in approximately 3 hr. In Figure 41 the first cracks in the crystal appeared at 10 C and in Figure 42 at 13 C. This behavior of crystals bonded with

Vulcalock cement may be contrasted with that of crystals bonded with Butyl-C cement, discussed at length in Section 8.6.5, by a direct comparison of Figure 41 with Figure 43 and of Figure 42 with Figure 44.

In connection with the use of Vulcalock cement it will be of interest also to read the comments in Section 8.2.4 concerning the trapping of moisture beneath cement layers. The effect on the leakage resistance of RS crystals coated with Vulcalock cement is brought out graphically in Figure 3. This graph emphasizes the necessity for the complete removal of all adsorbed water before the application of the cement. This is probably best accomplished by subjecting the crystals to a vacuum for a few minutes just previous to the application of the cement.

The question of the compatibility between the cement and the transducer liquid in which crystals will be immersed must also be considered. Both Vulcalock and bakelite cements may be used with DB grade castor oil. In other liquids, for example, mixtures of castor oil with some organic solvent such as xylene hexafluoride or diethylbenzene, it cannot be assumed that the bonds will remain unaffected by the immersion liquid. In fact, it has been reported¹⁶ that Vulcalock bonds are unsatisfactory in a liquid containing 85 per cent DB castor oil and 15 per cent diethylbenzene.

8.6.5

Butyl-C Cement

Most cements that have been investigated do not permit a transducer to be operated at very low temperatures owing to the difference in the coefficient of thermal expansion between the crystals and the rigid base to which they are customarily cemented. This usually results in fracturing the crystals long before a temperature of -40 C is reached. Since there is a tendency to extend transducer specifications to include -40 C as the lower operating limit of temperature, an effort has been made to secure a satisfactory cement for this purpose. As the result of an extensive investigation at BTL,¹⁶ Butyl-C cement has been found to fulfill this specification. The photograph in Figure 43



shows an ADP crystal cemented to a Durez wafer with Butyl-C cement, and the Durez wafer in turn cemented to a steel block with XCU 16257 urea formaldehyde cement. It will be noted that no fractures have appeared in this crystal, even though it has been cooled down to -40°C in a fairly short time interval. The same is essentially true of another ADP crystal, illustrated in Figure 44, which has been attached to a porous ceramic wafer with Butyl-C cement, the other conditions being practically identical. It was found in this case that a very small crack appeared at -39°C . For comparison, reference should be made to Figures 41 and 42 where ADP crystals have been bonded with Vulcalock cement and subjected to the same treatment as just described. The superiority of Butyl-C cement for low-temperature applications will be immediately evident.

In concluding their report, Frosch and Williams¹⁶ recommended the use of Butyl-C cement for both ADP and RS where there was danger of cracking at low temperatures. They found that it was necessary to employ porous-ceramic insulators rather than Durez where high Q values and high power were required. A rigid bond between these ceramic wafers and steel resonators was also necessary. Butyl-C cement can be used safely in contact with DB castor oil although other immersion liquids cannot be recommended without further tests.

It is regretted that more definite information on the composition of Butyl-C cement is not at hand. The principal ingredient is a polymer which is composed of a curing synthetic rubber modified with an aliphatic thermoplastic resin. In manufacturing this cement it is originally prepared in two parts, A and B, according to the following directions.¹⁷

Part A

- 100 parts by weight polymer
- 5 parts by weight zinc oxide
- 3 parts by weight stearic acid
- $\frac{1}{2}$ part by weight sulphur
- 2 parts by weight GMF

The above constituents, with the exception of the GMF, are thoroughly mixed on cold differential mixing rolls. After complete mixing is obtained, the GMF is added and mixing continued for as short a time as possible. We have found that the material should not be allowed to heat appreciably during the mixing as

the molecular weight of the polymer is reduced or the GMF causes gelation at elevated temperatures.

Part B

- 100 parts by weight polymer
- 5 parts by weight zinc oxide
- 3 parts by weight stearic acid
- $1\frac{1}{2}$ parts by weight sulphur
- 4 parts by weight lead peroxide (PbO_2)

These components are mixed thoroughly on cold differential mixing rolls.

Both Part A and Part B are made up into a 30 per cent solution in benzene. To each 700 cc of mixed cement is added 21 cc of isopropyl alcohol.

Butyl-C cement is ready for use when equal parts by volume of components A and B are thoroughly mixed. The mixture has a useful life of about 2 hr. When cementing metal foils to crystals the Butyl-C mixture is further diluted with an equal volume of benzene. In using Butyl-C cement a thin brush coat is applied to the required areas and the cement is allowed to dry until its surface becomes dull in appearance. The surfaces which are to be cemented together are then assembled in an appropriate jig with a pressure of 6 to 7 psi. The jig is placed in an oven at 60°C and the assembly allowed to cure for 24 hr.

Butyl-C cement was developed originally by the plastics group of the Chemical Department of BTL at Murray Hill, New Jersey. Some difficulty has been experienced in obtaining a prepared cement from commercial sources which would duplicate the original material satisfactorily. It is regretted that the exact composition of the polymer entering into the manufacture of Butyl-C cement is not available to the writer for inclusion in this volume. Further information regarding it can be obtained from BTL.

8.6.6 Bonding ADP Crystals to Rubber

The bonding of piezoelectric crystals to rubber has proved to be a valuable technique. It has given rise to the development of one type of inertia drive transducer at UCDWR in which the radiating face of the crystal is bonded directly to the rubber window of the case. In another type, the nonradiating end of the crystal is bonded to a thin supporting strip of rubber which is later backed by a pressure release



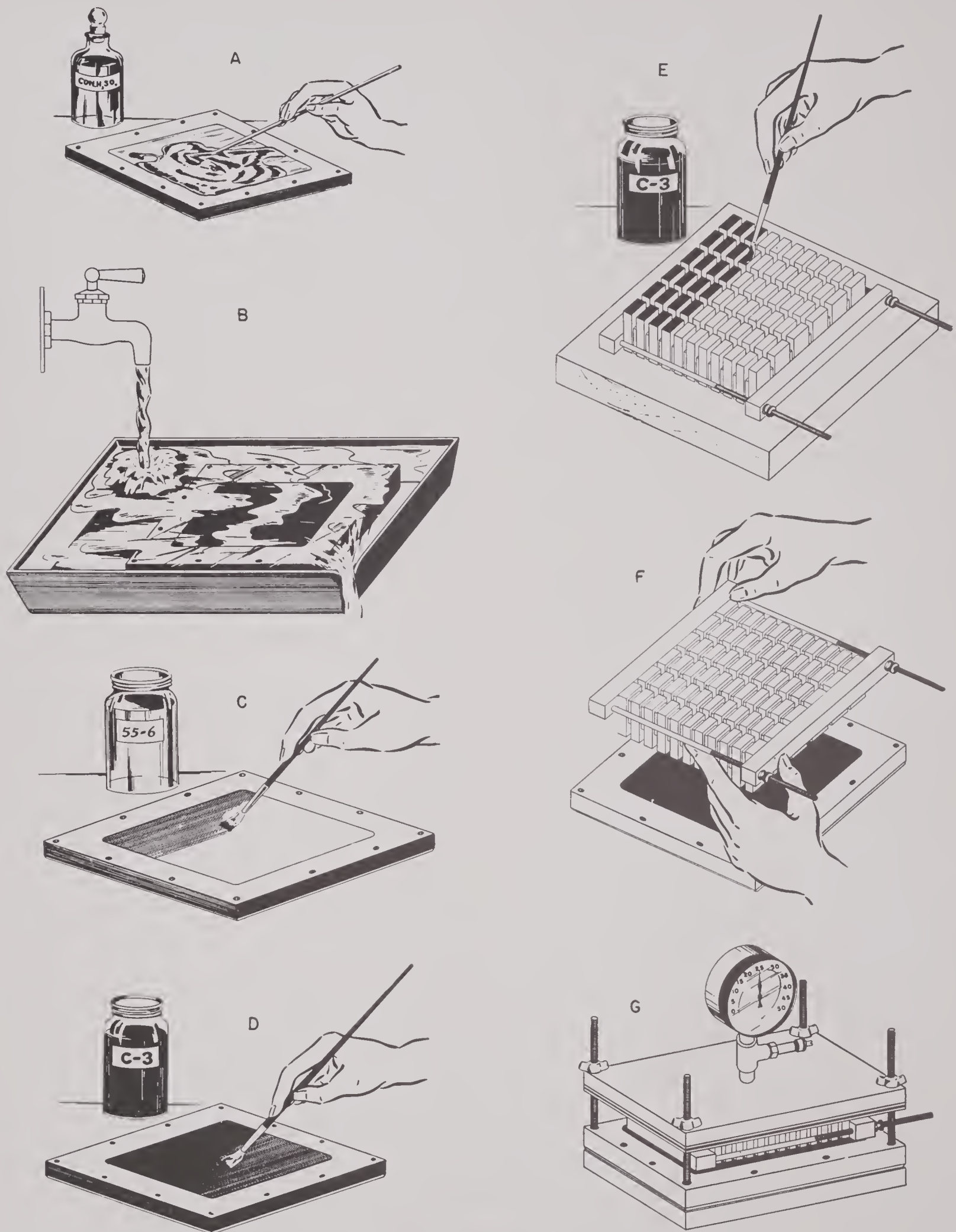


FIGURE 45. Steps in the bonding of ADP crystals to rubber by the Cycle-Weld process.

of cellular rubber as illustrated in Figures 57 and 58. Crystal arrays bonded to strips of rubber in this manner are readily formed into various configurations as discussed in Section 8.7.3.

A standard procedure in bonding many materials to rubber is to make direct use of Type 55-6 Cycle-Weld cement, a trademarked product of the Chrysler Corporation, Cycle-Weld Division, Detroit, but this method is not applicable with ADP crystals inasmuch as Type 55-6 cement does not bond well to ADP. The technique that has been developed at UCDWR consists in the application and curing of a priming coat of Type 55-6 cement on the rubber, the crystals being bonded later to this priming coat with Type C-3 Cycle-Weld cement. The steps involved in this process are portrayed in Figure 45 and a sample of the processing record sheet found convenient at UCDWR is reproduced in Figure 46.

Rubber or neoprene is first cleaned thoroughly to remove talc and any other contaminating substance; sanding may be necessary with some samples of sheet material. The surface to be bonded is then cyclized by covering it with, or immersing it in, concentrated sulfuric acid for from 3 to 15 min (Figure 45A). Too long a period results in a brittle surface layer of appreciable thickness so it is better to try first the lower time limit stated above on any given type of material. For neoprene, 3 to 5 min has been satisfactory; for ρc rubber, 3 min or less. After washing off the excess acid with a generous amount of water, place the rubber in a tray with running water for perhaps an hour in order to insure the removal of the acid (Figure 45B). Then wipe the rubber dry with clean toweling and warm gently to insure that the surface is moisture free. It is very important that the sulfuric acid be thoroughly removed since its hygroscopic nature would result in a water layer being formed on the surface of the rubber. This would be detrimental to the bond as well as to the electrical resistance of the crystal.

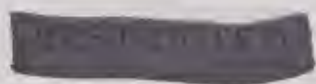
The Type 55-6 Cycle-Weld cement is applied to the prepared rubber surface with a fine camel's hair brush (Figure 45C). It should be brushed as quickly and evenly as possible over the surface. It is difficult to do this without

leaving brush marks owing to the rapid evaporation of the solvent (methyl ethyl ketone). If the thickness of the priming coat permits, the ridges which result from uneven brushing may be sanded off following the curing process. Spraying of the Type 55-6 cement has not been satisfactory and is not recommended. The priming coat is allowed to dry at least 30 min at room temperature and then 10 min at 80 C. The object of these two steps is the slow removal of the solvent; an alternative procedure is to hold the samples at room temperature for 4 to 48 hr. To bring about the thermosetting of the Type 55-6 cement, it should be cured for a period of at least 60 min at 125 C. At 150 C, 15 min should be sufficient.

Type C-3 is a thermosetting adhesive for bonding metals, wood, glass, and plastic materials. It adheres well to ADP but not to rubber. However, it makes an excellent bond to the previously cured priming coat of Type 55-6 cement. After cleaning the crystal surface by wiping with cheesecloth moistened with methyl ethyl ketone or other suitable solvent, the C-3 cement is applied with a camel's hair brush, Figure 45E, or a drop is added with a small wood stick and then spread evenly over the area. To secure a layer of cement 0.0015 to 0.002 in. thick, one must make a liberal application of the liquid and spread it out very quickly. If an attempt is made to brush it thinly over the surface of a crystal, it is very likely to streak. Any further application of cement will redissolve the original layer thus giving a streaked or spotty film of variable thickness. A little practice will soon teach one an acceptable technique. The manufacturer recommends spraying and supplies for this purpose a special spray cement, but thinning the brush-type cement with methyl ethyl ketone is also satisfactory. Extensive "cobwebbing" is encountered with too thick cement. In production work, an effort should certainly be made to master a satisfactory spray procedure.

In the same manner (Figure 45D), Type C-3 cement is brushed or sprayed over the Type 55-6 priming coat which has been cured previously on the rubber.

The C-3 cement applied to the crystals and to the rubber is now allowed to dry at room tem-



CYCLE-WELD PROCESSING RECORD

Technician _____ Date _____
 Type of Rubber _____ Material _____ Transducer No. _____

A. Apply concentrated sulfuric acid to rubber surface for 3 min.

Time in _____ : _____ Time out _____ : _____ Elapsed time = _____ :

B. Wash rubber surface for 30 min. in running water, then rinse in distilled water, air-dry thoroughly and then oven-dry at 150°F for 10 minutes.

Time in _____ : _____ Time out _____ : _____ Elapsed time = _____ :

C. Brush 55-6 cement on rubber, then dry and cure as follows:

Room temperature (30 min.); from _____ : _____ to _____ : _____ = _____ min.

180°F oven (10 "); " _____ : _____ to _____ : _____ = _____ min.

270°F " (60 "); " _____ : _____ to _____ : _____ = _____ min.

D. Brush C-3 cement on rubber (apply over the cured 55-6 cement).

Room temperature (30 min.); from _____ : _____ to _____ : _____ = _____ min.

180°F oven (25 "); " _____ : _____ to _____ : _____ = _____ min.

E. Brush C-3 on ADP crystals (cleaned previously with methyl ethyl ketone) and dry at:

Room temperature (30 min.); from _____ : _____ to _____ : _____ = _____ min.

180°F (25 "); " _____ : _____ to _____ : _____ = _____ min.

F. Assemble in press, apply 15-25 lbs/in² pressure and cure at 270°F for 90 minutes at glue line.

Time in _____ : _____ Time out _____ : _____ = _____ min.

REMARKS: (Write below any unusual behavior or any irregularities in processing.)

FIGURE 46. Cycle-Weld processing record used at UCDWR.

perature for at least 30 min in order to permit an initially low rate of escape for the solvent. Then it may be heated 25 min at 80 C to remove the solvent completely. An alternative procedure consists in drying at room temperature only, but for a period of 2 to 48 hr.

The surfaces to be bonded are assembled in their final position (Figure 45F), and a pressure of 25 to 60 psi is applied. The exact pressure used depends on the area involved and on the hardness of the rubber; this value can be estimated visually, using as a criterion the absence of any marked distortion of the rubber. To insure a uniform pressure, a pneumatic press, such as illustrated in Figure 45G, is recommended.

To cure the C-3 thermosetting cement, the assembly is heated to 125 C in an oven and maintained with this temperature *at the glue line* for at least an hour. Although the timing is not very critical, with a longer period probably being beneficial, the damaging of the ADP crystal surfaces by prolonged exposure to heat constitutes the limiting factor. Too long exposures of ADP to temperatures of 125 C, and especially to 150 C, causes a surface breakdown of the ADP with the emission of ammonia vapor and the appearance of a phosphoric acid layer on the crystal.

ADP crystals must be allowed to cool slowly down to at least 80 C to avoid fracture from thermal strains. In the laboratory, it is often convenient to turn off the power and allow them to cool overnight without removal from the oven; in production, an annealing oven would be used.

If the outlined procedure is correctly followed, the resultant bond should be stronger than either the rubber or the crystal. Tests of these bonds usually ruptured the rubber; only occasionally did a crystal break. For maximum bond strength, the rubber used should have high tensile strength, low free sulphur content, low percentage of mineral filler, a hardness of 40-70 Shore durometer, and should be resistant to the curing temperature.

High humidity is detrimental to this type of bond, apparently by its effect on the C-3 cement layer. Provision should be made for the inclusion of a drying agent, such as silica gel, in any

transducers employing this ADP-rubber construction. Extended field trials have not yet been made. Reference may be made elsewhere in this volume for a discussion of transducers which have been designed to take advantage of this technique.

8.6.7

Thermoplastic Cements

Although little use has been made of thermoplastic cements in the construction of crystal transducers, they would seem to offer good possibilities in this direction. This is particularly the case for ADP crystals since they are quite capable of withstanding the required high temperature. The only thermoplastic cement employed to date with ADP crystals has been a modified polyvinyl acetate which has been used in the manufacture of spliced crystals as pointed out in Section 8.3.7.

From experience of a preliminary sort at UCDWR, Butacite VF-7100 cement, an unplasticized polyvinyl butyral produced by Du Pont, appears to have much promise for crystal applications. In bonding ADP crystals to each other and to steel very high Q joints were obtained with it. The tests were not carried out over a sufficiently long period to test their endurance under various conditions so that no specific recommendation can be made. In the opinion of the writer further investigations should be conducted with this cement.

It is recognized that almost every manufacturer of plastics produces one or more types of adhesive in the thermoplastic category. There is neither intention nor sufficient basis to indicate the superiority of any particular type or brand for crystal applications at this juncture but merely to point out that in the limited experience at UCDWR one or two types have been tried and found promising. Since the bonding of crystals to supporting structures is a very specialized application, it is perhaps not to be expected that existing compositions of thermoplastic cements will be entirely suitable. It is more realistic to assume that variations in composition must be systematically investigated with a view to obtaining the necessary and desirable qualities for each specific type of bond-

ing operation. The qualities that must be considered have been discussed explicitly in Section 8.6.1 and implicitly in Section 8.6.2 and succeeding sections.

8.6.8 Cements Containing Catalysts

UREA FORMALDEHYDE

In conducting tests on ADP crystals bonded to wafers and then to steel plates, BTL has made use of a catalyzed urea formaldehyde adhesive.¹⁶ These tests have been referred to in Sections 8.6.4 and 8.6.5. The particular adhesive employed was a product of the Bakelite Corporation and consisted of a liquid, XCU 16257, and a solid catalyst, XK 16229. These two materials were mixed thoroughly just before using and in the ratio of 10 g of the liquid to 0.8 g of the catalyst. This mixture has a usable cementing life of approximately 2 hr.

For the tests mentioned, a thin brush coat of the cement mixture was applied to the steel and to the insulators, and the parts allowed to cure unassembled overnight at room temperature. After rough lapping the cement surface of both the steel and the insulators, a second coat of cement was applied. The insulators were then assembled onto the steel plates and sufficient pressure was applied to hold the parts in place. The assemblies were cured for 24 hr at room temperature.

NORACE CEMENT

Norace cement, a product of the Norton Company, Worcester, Massachusetts, is a thermosetting plastic which sets at room temperature. It has been used for cementing ADP bars to supporting plates by BTL, as discussed in Section 8.3.4. For this application the method of preparation of the cement has been described as follows.⁷ Ten cubic centimeters of the powder was measured out and emptied into a wax-paper cone. This cone was made by folding the paper as in a chemical filter and was then held in a 60-degree conical depression in a lead block. A stirring rod was used to make a depression in the powder and 3 cc of acidified solvent were added and quickly stirred to form the cement of mud-like consistency. The paper cone was then removed from the lead block so that most of the

material could be scraped from it and transferred to the mounting block. The acidified solvent was prepared by adding 5 per cent of glacial acetic acid to the number 1 solvent furnished with the cement.

8.6.9 Miscellaneous Adhesives

MOLTEN ROCHELLE SALT

In an early study¹⁵ on glued joints and the acoustic losses which occur in them, it was found that fused RS was one of the four most promising cements investigated. In fact, fused RS resulted in the hardest and most loss-free bond. This cement is rather difficult to use and, if the crystal is cemented to a support having a different coefficient of expansion, it is liable to crack when used over an extended temperature range. Perhaps its most satisfactory application is in bonding RS to RS. Two very common cases arise which call for a RS to RS bond. One is the production of spliced crystals, already discussed at some length in Section 8.3.7, and the other is in the production of bimorphs.

Clear fragments of RS may be fused by placing them in a clean utensil (stainless steel is quite satisfactory) and heating slowly to a temperature of 93 C. It may be advantageous to use a water bath or double-boiler arrangement. It is important that everything be kept meticulously clean and that not over a few hours supply of material be made up at one time. While awaiting use, the fused RS should be maintained at 93 C in a melting pot and dipped out in small quantities from time to time. At the Brush Development Company, where this cement is used in the commercial production of bimorphs, the fused RS is ladled onto stainless steel slabs 5x8x1/8 in. thick in order to permit some precooling before applying the cement to the crystals. After skimming the surface of the cement pool on the slab with a wooden stick, the face of the crystal to be cemented is dipped into the pool of fused RS and then placed on the other half of the bimorph with a gentle sliding pressure.

ACRYLOID B7

The second promising cement referred to in the discussion in Section 8.6.9 is Acryloid B7,

a product of Röhm and Haas. According to the study¹⁵ mentioned, it appears to give a better bond to a smooth surface, such as steel, than some other cements. One disadvantage of Acryloid B7 is that its drying time is somewhat longer than for Vulcalock or bakelite cement. However, this defect might be improved by the use of a different solvent.

The use of Acryloid B7 at UCDWR has been limited almost exclusively to the cementing of tin-foil electrodes to crystals, according to the steps outlined in Section 8.3.8.

8.7 PREPARATION OF ARRAYS

8.7.1 Layout and Assembly

Crystal arrays for transducers are designed with so many variations that it is extremely difficult to describe satisfactory methods of assembly that would be generally applicable. It should be pointed out that perhaps too much stress cannot be placed on the necessity for appropriate jigs and auxiliary devices. Not only will time and effort be saved in the final assembly operations, but the results achieved will be much more uniform. The designing of special jigs is a problem that must depend for its solution on the ingenuity of the shop foreman or of the transducer designer. How elaborate a particular jig should be will probably depend on whether it is made for production work or merely for a few transducers of a given design.

In this section it will be the intention to indicate how various simple crystal arrays may be assembled by means of satisfactory jigs and how these assembled arrays may be mounted on permanent supports. With one or two exceptions, subject material and illustrations for this section have been based on experience at the UCDWR Transducer Laboratory.

SIMPLE FLAT ARRAYS

Full-scale drawings of the crystal array are usually made available to the construction foreman by the designer. The crystals, when furnished previously with electrodes, may be arranged on a glass plate according to the design drawing. It is necessary to pay attention at this

point to the polarity marks in order to make sure that all the crystals are properly oriented. For a simple array where the crystals are all driven at a single velocity, the polarity arrangement is usually as shown in Figure 56.

Where individual crystals have previously been furnished with electrodes which do not permit a direct soldering of wires to them, it will often be found convenient to assemble the crystals into linear strips or bars. This type of assembly is illustrated in Figure 47 where a row of crystals that has been cemented to a

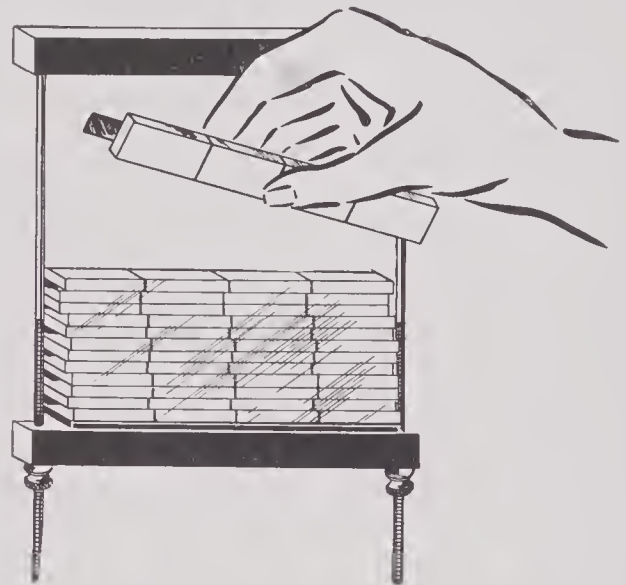


FIGURE 47. A strip of crystals, which have been bonded previously to a foil, is being placed in position in a simple jig as one step in the assembly of an array.

narrow strip of silver foil is shown being placed in position in a simple jig. In order to insure correct alignment of the crystals while cementing them to the foil in such a row, the edge of each crystal was allowed to rest against a guide. The separation distance between adjacent crystals along the strip is adjusted with a spacer each time an additional crystal is added. As each strip of crystals is placed in the jig, care must be taken to observe polarity requirements. In an array of this type, the individual rows of crystals may or may not be bonded to each other. As illustrated in Figure 47 the rows are not bonded together. After all the strips are assembled in the jig, a thin layer of compliant material should be placed as a facing against both of the metal bars which act as clamps. The metal bars are then pulled together by tighten-

ing the nuts on the threaded rods. Before a final tightening, the assembly of crystals may be adjusted for correct alignment by the use of a common carpenter's square. When a small unit has been completely assembled and tightened, the entire jig may be lifted without the crystals being displaced. Planeness of the array is obtained by having all of the crystals lying on a piece of plate glass or on a surface plate before clamping. Owing to irregularities in the crystals, the surface of the array may still not be sufficiently flat so that a subsequent grinding operation may be required. This is particularly true when the array is to be attached to flat or rigid plates and will be discussed further in Section 8.7.2.

In arrays where the electrodes consist of heavy foil which is sufficiently thick to permit



FIGURE 48. A flat crystal array clamped in position in a simple jig, ready to be attached to a backing plate.

wires to be soldered directly to them, the crystals may be bonded to long strips of foil which cover the entire electrode area of each crystal face. Such an array is shown in Figure 48 and it will be noted that the foils extend an appreciable distance beyond the end of the crystals. Any excess length of foil may be trimmed off after the foils are wired as discussed in Section 8.7.4 and illustrated in Figure 61. It will also be observed that foils of alternate polarity extend on opposite sides of the array. The polarity arrangement is as shown for the array of Figure 56.

In simple arrays where the crystals are not intended to be in contact with each other but are spaced individually as in Figure 57, or in groups of a few crystals each as in Figure 49, provision must be made for maintaining the spacings while the crystals are being bonded to supporting structures. Bakelite or micarta separators have been found convenient for the main-

tenance of such spatial arrangements (see Figure 55). To insure that the plastic strips may be readily removed following the final cementing operation, it is advisable to cover each individual strip with a layer of plain paper. After the crystals have been bonded permanently to their support, the paper-covered separators may be readily removed from between the crystals.

LOBE-SUPPRESSED FLAT ARRAYS

The layout and assembly of flat arrays involving some scheme of lobe suppression usually presents more difficulties than an array driven at a single voltage. A common type of lobe suppression array is shown in the retouched photo-

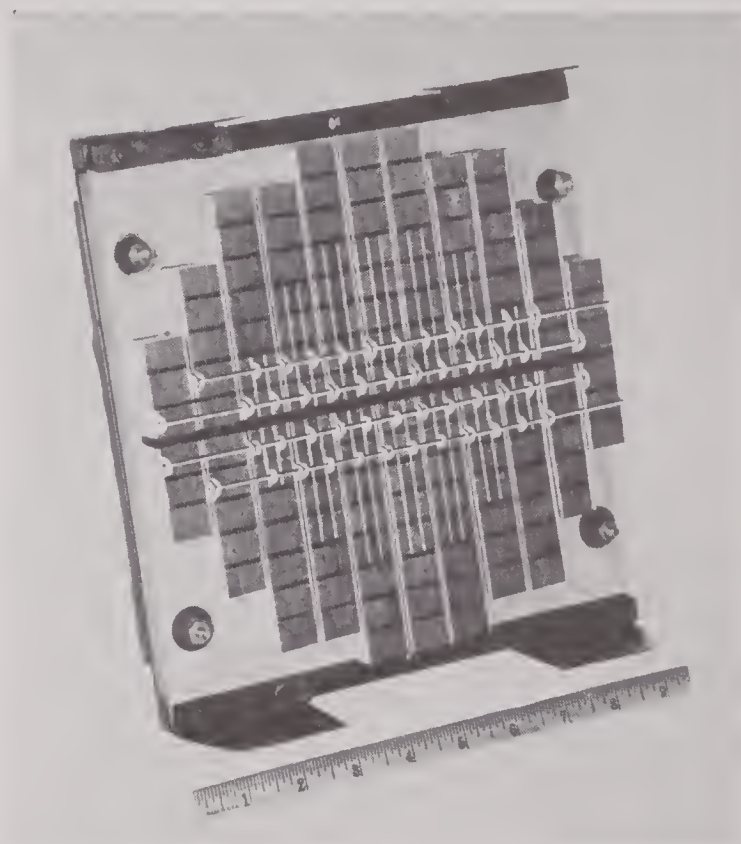


FIGURE 49. Photograph of a UCDWR split array which has been retouched to exaggerate the foiling arrangement for a 3 to 1 scheme of lobe suppression. The crystals in the central region operate at full amplitude; in the peripheral region, at $\frac{1}{3}$ amplitude. The two halves of the array may be operated either in phase or out of phase.

graph of Figure 49 for a transducer where it is intended that the two halves of the crystal motor may be operated either in phase or out of phase. The crystals in the central part of this array are driven at three times the velocity of the crystals in the peripheral region. This ratio

of driving voltage is provided by having all of the crystals in the central region in parallel, while in the outer zone, the same driving voltage is applied to each group of three crystals connected in series. The simplicity of wiring arrangements for this 3 to 1 ratio will be apparent after studying Figure 49 in which the ap-

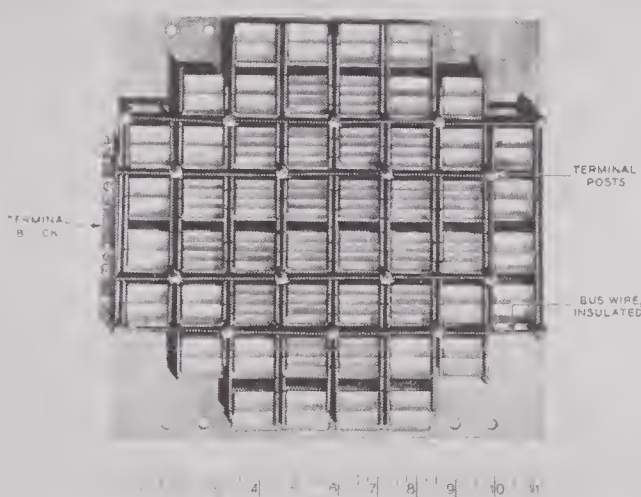


FIGURE 50. The lobe-suppressed crystal motor of the QBF echo-ranging projector. The central zone consists of 24 full amplitude blocks of 4 crystals each; the outer zone 28 half amplitude blocks of 2 crystals each. (Bell Telephone Laboratories.)

pearance of the foils has been exaggerated for emphasis. It will be noted that every third foil is continuous past the crystals of both the inner and outer zones. The triplet crystal groups in the outer zone may, of course, be replaced by single crystals having the same total thickness. Some gain in uniformity of the electrical field in these crystal groups could be obtained by furnishing intermediate electrodes between the individual crystals of each group. In general, however, this procedure has not been followed at UCDWR.

In constructing the array of Figure 49 the triplet groups were first bonded together with bakelite cement. Complete half rows were next assembled by starting with a long silver foil of the correct width and successively cementing crystals, triplet blocks, and foil strips to it, with the proper spacing and polarity orientation, until the 11 pairs of semirows were prepared. These assembled rows were then placed in a pneumatic press and cured according to the

schedule for bakelite cement given in Section 8.6.4. After curing the cement bonds in this manner, the rows of crystals were assembled in a jig with the proper spacers to give the configuration shown in the figure. The array was then mounted on its backing plate as directed in Section 8.7.2.

A transducer employing a 2-to-1 type of lobe suppression is shown in Figure 50. This type of crystal motor is used with the QBF echo-ranging system projector and was designed by BTL. The same driving voltage is applied to each and every crystal in this array but owing to the fact that the crystals in the central zone are just half as thick as the crystals in the peripheral zone, the crystals in the central zone are driven with twice the velocity. In other words, we have what is known as a 2-to-1 scheme of lobe suppression. It will be noted that the crystals are bonded together in groups, each group having a radiating face one inch on a side. In the central zone four crystals comprise a group; in the outer zone, two crystals. In this transducer the wiring connections to the evaporated gold electrodes are made with strips of gold-plated nickel silver foil 0.001 in. thick. A close inspection of the photograph in Figure 50 will reveal dark areas where these foils come in contact with the interconnecting wires. The spacing between the crystal groups is $\frac{3}{8}$ in. in both directions.

CYLINDRICAL AND CURVED ARRAYS

Several possibilities exist for the mode of assembly of cylindrical or curved arrays. One type occurs in the crystal motor which is used as the sound source in the UCDWR-type CQ transducer and is illustrated in the photograph of Figure 33 of Chapter 1. In this case, quartets of crystals are bonded together and seven of the quartet groups are attached to each backing bar, the bars themselves being so arranged as to constitute part of a cylindrical surface. In a second type, illustrated photographically in Figure 40 of Chapter 1, the crystals are bonded directly to the interior of a rubber cylinder. A jig for the assembly of the crystals for this type transducer is shown in Figure 51. The crystals are foiled on both sides in linear strips of four crystals each. The foils, of 0.0015-in. silver sheet, extend past each group of crystals at one

end or the other in order to provide soldering lugs. These crystal strips are prepared and cured in advance of the final assembly operation, at which time they are inserted in the radial slots of the jig illustrated in Figure 51. When all of the strips of crystals are in place, the jig is then lowered into a reinforced rubber cylinder, shown in Figure 68. When finally adjusted to their correct position, so that the crystals are located midway between the steel rods in each case, the rubber tube within the jig is

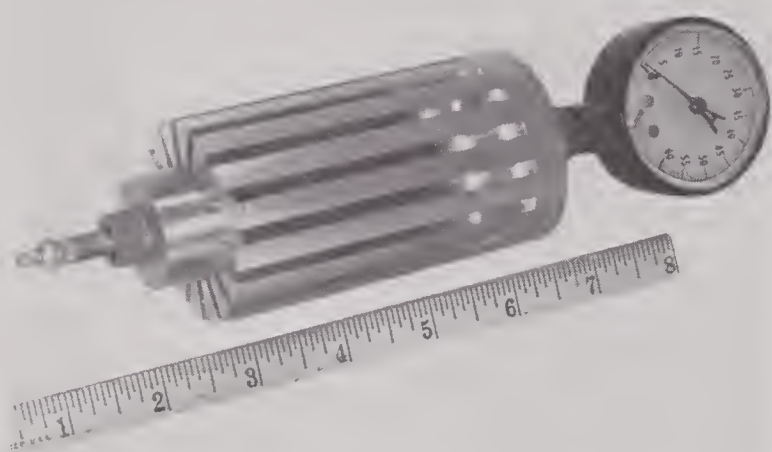


FIGURE 51. A special jig used at UCDWR for assembling the cylindrical inertia-drive transducer shown in Figure 40 of Chapter 1. By inflating the rubber core of the jig the radiating faces of the crystals are pressed firmly against the interior surface of a reinforced rubber cylinder (see Figure 68) during the bonding operation.

inflated, thus forcing the radiating face of each crystal out against the interior wall of the rubber cylinder. The bonding to the rubber is done by means of the technique described in Section 8.6.6.

Another method for the production of cylindrical arrays will be made clear by an inspection of Figures 57, 58, and 62. The crystals in this case possess independent silver foils with soldering lugs and are bonded to a thin flat sheet of rubber. Following the bonding process, according to the procedure outlined in Section 8.6.6, the crystal assembly is coiled about a circular support such as illustrated in Figure 58 or 62. They are held in place by a combination of wrapping with nylon thread and cementing to a central core.

In assembling cylindrical arrays, it is very important to observe the polarity marks on the crystals. If alternate pairs of foils are to be positive and negative respectively, an even number of crystals or crystal groups must be used around the circumference of the cylinder.

STACKED ARRAYS

Perhaps the least troublesome type of array to assemble is that of a simple stack. Each individual crystal is first furnished with electrodes. Where the electrodes are of a type that do not possess lugs for soldering, narrow foil strips are cemented lightly to each crystal and brought out either at the ends or sides of the crystals as shown in the illustrations in Figure 59 and Figure 60. Where the electrodes do possess soldering lugs, a single-foil electrode may be used between each pair of crystals. Whether the entire stack of crystals should be bonded into a single block is questionable from the standpoint of efficiency. Jigs for maintaining the correct alignment in such a crystal stack can obviously be of a very simple type and no illustrations of jigs are included here.

The stacks may be arranged in various ways to meet design specifications. The crystals may radiate either off their end faces or off their side faces. They may be arranged spirally as in Figure 38 of Chapter 1, or make various angles with each other. Most of the stack-type transducers made at UCDWR have been assembled from RS crystals and resemble Figure 59. Non-radiating faces were blanked off with one of the isolating materials discussed in Section 8.7.5.

8.7.2

Backing Plates

STEEL BACKING PLATES

Steel has been used more frequently than any other material as a backing plate for crystal arrays. The choice of steel has been based in part on its mechanical strength and on its machinability as well as on its acoustical behavior. In using a conducting backing plate, provision must be made at the outset for sufficient electrical insulation to withstand the voltages employed. This insulation may be provided in a variety of ways, all of which may be entirely satisfactory.



The customary method at UCDWR has been to apply a thick coating of porcelain enamel directly to the steel. The porcelain enamel base used for this purpose consists of a low melting point glass frit and is applied to the steel by the so-called dry process. In this dry process the backing plate is first heated in a furnace to a cherry-red color and the frit is sprinkled on the surface by means of a dusting screen. The frit thus deposited immediately melts and so forms a glazed surface. This layer should be smooth and free from bubbles if properly applied. However, a few small bubbles usually exist in such porcelain layers and may later give rise to electrical breakdown. A method for treating the porcelain in order to prevent voltage breakdown will be discussed in a later paragraph.

The surface of these porcelain coatings is never sufficiently flat for attaching large crystal arrays. In addition to slight irregularities on the surface, there is also a rounded edge or a meniscus at the border between the porcelain and the steel. Grinding or lapping of the surface is therefore necessary. This surfacing may be accomplished by first grinding with coarse silicon carbide and then finishing with a finer grade of silicon carbide. Suitable grades for this purpose are No. 60 and No. 80. A standard lapping technique is to use a large brass platen or grinding flat with the backing plate itself constituting a tool. The flatness of the resulting surface obviously depends on the skill of the operator, but there should be little difficulty in attaining a surface which is flat within ± 0.003 in.

In cases where holes must be drilled through the backing plate, the drilling should be done before the porcelain coating is applied, otherwise there is danger of cracking the porcelain. Should it prove necessary to provide holes through the porcelain layer, it can be done by grinding with a tool designed for this purpose while employing wet silicon carbide as an abrasive. Wood dowels make satisfactory tools. In some instances it has proved desirable to divide the surface of a backing plate into two or more areas in order to minimize vibration or to segregate regions of a plate underlying crystal groups driven at different velocities for purposes of lobe suppression. In such cases it is

likewise essential to wet-grind the porcelain with specially designed tools employing silicon carbide.

After the glazed coating of the porcelain has been removed by grinding, a fine porosity will be evident together with perhaps a few larger holes which are plainly visible. If these holes which have resulted from grinding into fairly large bubbles originally present in the porcelain remain, voltage breakdown may occur at perhaps 1,000 v or less. By using a leak tester, such as employed for detecting leaks in glass vacuum systems, all defective spots should be located and marked.

In order to improve the breakdown voltage of porcelain-coated vacuum plates, the following procedure is currently employed at UCDWR. The porcelain is first cleaned with benzine and then scrubbed thoroughly with Glyptal thinner No. 1500. The backing plate is then warmed to about 120 F and a thin layer of clear Glyptal is brushed over the porcelain surface. The plate is now placed in a vacuum chamber where a low pressure is established and then broken two or three times. Finally, the plate should be left in the evacuated chamber for a period of time sufficiently long to enable the plate to cool to room temperature. This may require 2 or 3 hr. Upon removal of the plate from the vacuum chamber, the excess Glyptal should be scraped off with a razor blade. After allowing the plate to set for an additional 2 hr it is sanded freely with a fine grade of silicon carbide paper (Carborundum 220A-320A). After allowing the plate to set again for an hour or more, the porcelain surface should be washed with a cheesecloth dampened with benzene. The porcelain should be voltage checked again with the leak tester. If satisfactory, it is ready for use; if not, it must be treated again in a similar fashion in order to fill up all defective cavities with Glyptal.

A second method of providing insulation in metal backing plates consists in cementing insulating wafers between the crystals and the backing plate. The Bell Telephone Laboratories have favored this method, having used originally a ceramic wafer approximately $\frac{1}{16}$ in. thick. These wafers contained narrow flutes or channels every $\frac{1}{8}$ in. to permit the escape of



excess cement and solvent vapor. Later, preference was given to a plastic wafer made of a Durez resin. These wafers were cemented to the steel with a very hard cement in which the acoustic losses were reduced to a very low value (see Figures 41 to 44).

The Naval Research Laboratory has made use of a $\frac{1}{64}$ -in. bakelite material as an insulator. This product was similar to micarta but contained a cloth insert.

GLASS AND PLASTIC PLATES

By resorting to glass backing plates, one avoids completely the intermediate insulating materials required for any electrically conducting backing plate. This appears to be a real advantage in that it avoids some energy loss which takes place in the additional cement layer. It also reduces stray electrical capacitance to the backing plate. A ground surface on the glass is probably advisable in order to obtain improved adhesion to the crystals. This ground surface may be made by using 80-grit silicon carbide as an abrasive.

Care should be taken to see that all glass used for backing plates is well annealed and without strain. Strains can be readily detected with polarized light by means of the device shown in Figure 33. Mounting of glass backing plates offers somewhat more of a problem than metal, especially where holes are to be provided. Although holes may be readily drilled in glass plates, they do reduce the strength at that point and increase the likelihood of breakage. A more desirable method for mounting is to bevel the edges of the plate in such a manner that suitable wedges may be used to hold the backing plate in position, preferably in a shock-absorbent mounting.

MISCELLANEOUS PLATES

Metal backing plates other than steel have been found useful, particularly for low-frequency applications where the thickness of a steel backing plate becomes excessive. Lead has found the most extensive use. Since the velocity of sound in lead is about one-fourth that of steel or glass, lead backing plates are thinner by a ratio of approximately 4 to 1. Consequently, there is a large resultant saving in both space

and weight. Lead is most conveniently used as a backing plate by adding it to a rather thin steel plate which has already been porcelain coated. Since the melting point of lead is 328 C, difficulty may be experienced in coating the steel with lead without cracking the porcelain.

Where other types of insulation are employed, namely, ceramic or porcelain wafers or

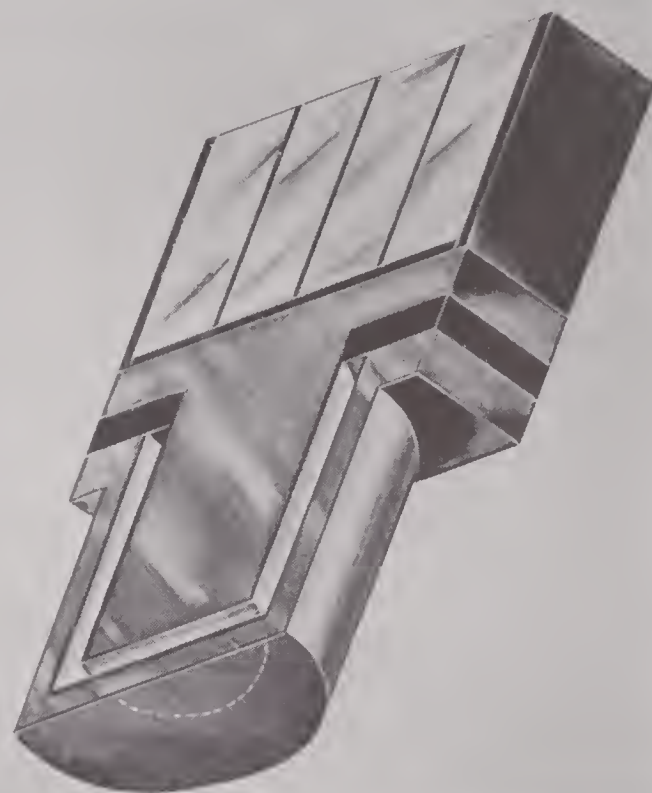


FIGURE 52. A unit type of backing-plate construction developed at the Naval Research Laboratory. The thick black rubber washer forms an air seal for the metal cap and provides a shock mounting for the backing plate.

thin bakelite sheets, there would seem to be no objection to attaching these directly to a lead plate, providing the lead plate is capable of supporting itself against mechanical deformation.

The low melting point alloy called Cerrobend may prove useful in place of lead for backing plates. A porcelainized steel plate of sufficient thickness is first tinned properly and then the Cerrobend is poured on the tinned surface until the retaining mold is filled to the desired depth. Since Cerrobend melts at a temperature below the boiling point of water, the operation may be carried out safely without cracking the porcelainized surface. The final operation is to chuck the backing plate in a lathe and turn off the ex-

cess metal. Any holes for the accommodation of electric leads or for oil filling may be provided at the time of casting the Cerrobend by inserting suitable cores at the desired locations.

Duralumin has been used in the unit-type backing-plate construction originating at NRL. This construction is shown in Figure 52 where it will be noted that the backing plate consists

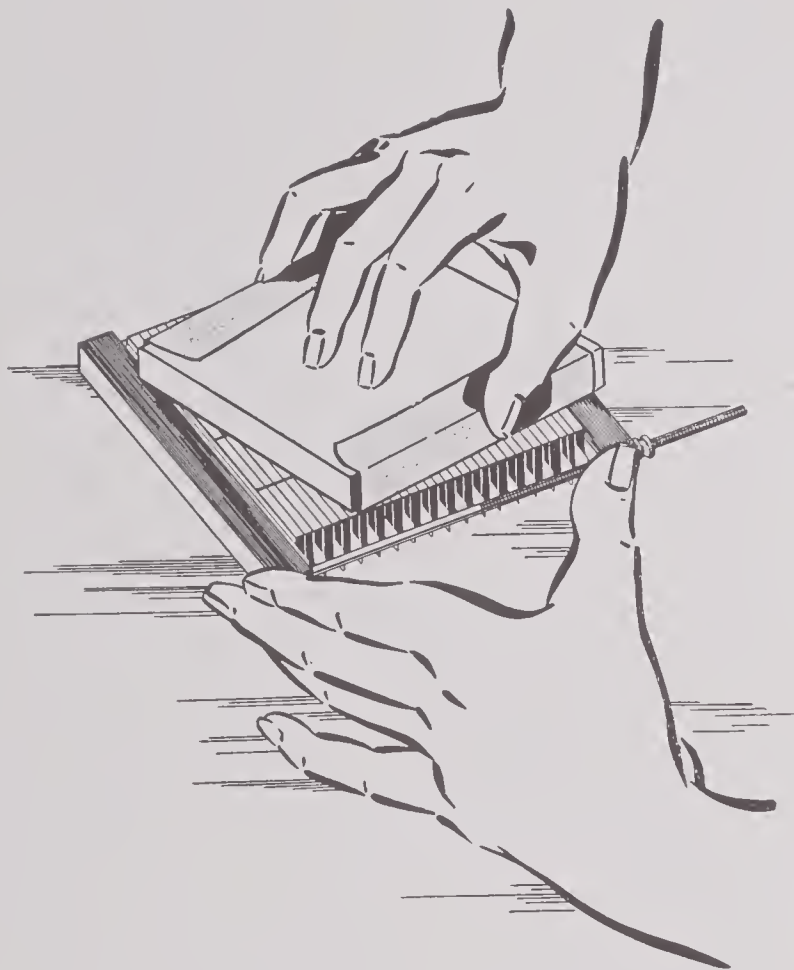


FIGURE 53. Lapping of a crystal array in preparation for mounting it on a porcelain-coated steel backing plate.

of a square cross section immediately beneath the block of crystals and then reduces to a circular cross section for the part which extends into the metal-air cell. A transducer employing such units has been illustrated in Figures 29 to 32 of Chapter 1. The advantage of Duralumin is primarily one of reducing the weight since it has an acoustic velocity approximating that of steel. The air space between the backing plate and the metal cap is sealed by means of cement and a thick rubber washer. The insulating layer between the crystals and the metal backing plate consists of a thin sheet of bakelite impregnated fabric. The thickness is approximately $\frac{1}{64}$ in.

The crystal block is also surrounded on all four sides by the same type of bakelite material.

MOUNTING TECHNIQUE

In cementing flat arrays of crystals to backing plates, it is essential that both the backing plate and the face of the crystal array be plane

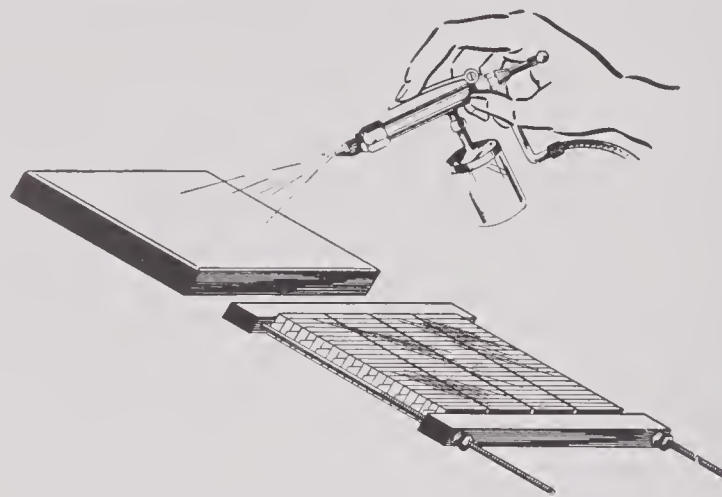


FIGURE 54. Spraying the initial 0.002-in. layer of bakelite cement on a porcelain backing plate and on a crystal array.

to within a very few thousandths of an inch. The grinding of the surface of a porcelain backing plate in order to assure that it was suffi-

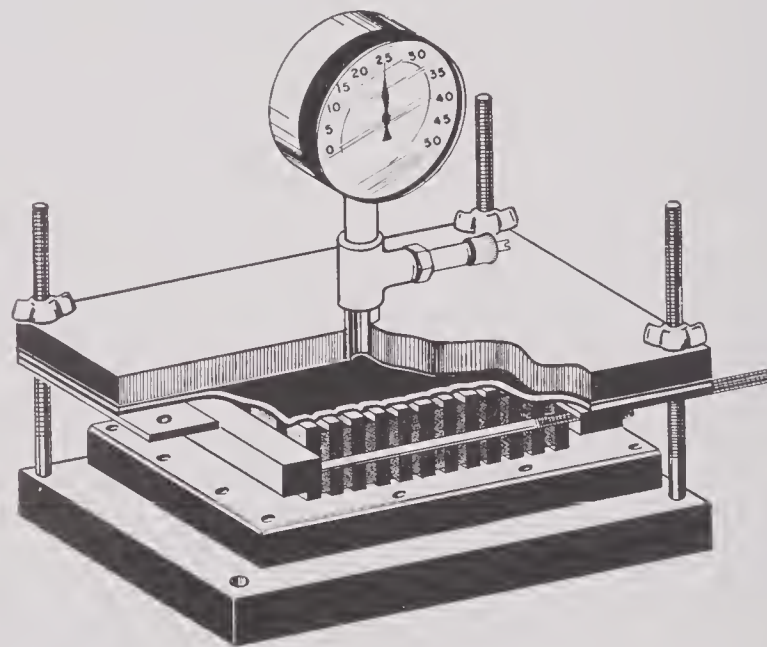


FIGURE 55. A constructional view of a laboratory pneumatic press as employed at UCDWR during the oven curing of an array bonded to a supporting structure.

ciently flat was discussed in Section 8.7.2. The lapping of the surface of the crystal array which is to be cemented to the backing plate is illustrated in Figure 53. For a tool, a sheet of

240-grit silicon carbide may be cemented to a piece of 1/2-in. plate glass or held as shown in the illustration. Since this fine grade of abrasive paper quickly becomes loaded with powdered ADP or RS, it should be cleaned frequently by means of a stream of compressed air. The lapping process should be continued until the face of the array is flat, as judged by a good quality surface plate.

In the light of past experience at UCDWR, the following cementing technique for attaching RS crystals to porcelain-coated backing plates is suggested. Both the porcelain surface of the backing plate and the face of the crystal array are covered with a 0.002-in. layer of bakelite or other appropriate cement. The detailed method of application of various cements has been discussed elsewhere but it may be pointed out here that a spray technique is to be preferred as illustrated in Figure 54. This initial coat of bakelite cement is allowed to dry quite thoroughly by exposure to the air for a minimum of 60 min. Just previous to the final assembly of the crystal array on the plate, an additional thin layer of cement should be sprayed on the porcelain only and allowed to dry until tacky. The crystals should then be positioned on the plate and held firmly in place with a uniform pressure of at least 25 psi. It may prove to be better to use a still higher pressure. This pressure is best applied by means of a pneumatic press. A press found suitable for this application at UCDWR is illustrated in Figure 55. Uniform pressure on each crystal is assured by this type of construction in which a layer of rubber is covered with a layer of heavy canvas and cemented around the edges to the top plate of the press. In addition, both are held against the top plate by a metal frame. After thoroughly warming the assembly of bars, crystals, and clamps to 115 F in an oven of low humidity, it should be placed in an oven at 115 F and 60 per cent relative humidity. The preliminary warming in a low humidity oven is essential in order to prevent condensation at the moment they are placed in the 60 per cent relative humidity oven. At the end of a period of at least 12 hr (24 hr is customary), the assembly should be removed from the oven and allowed to cool down to room temperature before the pres-

sure is released or the clamps are removed.

For ADP assemblies, the curing temperature may be increased to 80 C without reducing the curing time. Before attempting either RS or ADP bonding to backing plates, Sections 8.6.2 to 8.6.4 should be read.

For examples of crystal arrays mounted on porcelain backing plates, reference may be made to Figures 33 and 34 of Chapter 1. The former shows ADP crystals both on bars and on a plate in the same transducer; the latter shows a smaller motor of the UCDWR-type GD class. Still another example is Figure 49 of the present chapter, already discussed in connection with lobe suppression.

8.7.3

Other Supports

FRONTING PLATES

Owing to very meager experience with fronting plates at UCDWR it is difficult to comment on the methods of assembling crystal arrays for this type of transducer. However, it would seem that no new problems are involved as far as the mode of assembly of the crystal array is concerned that have not been discussed already in preceding sections in connection with backing plates.

The use of rubber windows as fronting plates will be discussed in the following section from the standpoint of inertia drive units. Plexiglas or Lucite has been used as a fronting plate in one or two instances. One such transducer is the Model 45-AX-1 high-power projector designed by BTL in which a 1/4-in. thick Plexiglas diaphragm was used as a fronting plate, apparently with the intention of imparting a broad-band characteristic to the radiation.

RUBBER (INERTIA DRIVE)

A number of inertia-drive transducers have been designed at UCDWR. One simple type, EP, produced in some quantity is illustrated in Figure 56. This unit consists of a large number of thin ADP crystals which have been bonded together in a solid block. Long strips of silver foil are cemented between adjacent rows of crystals to serve as electrodes. By having alternate strips protrude from opposite sides of the



crystal array the wiring arrangement has been very much simplified as is clearly brought out in the illustration. The jig which clamped this

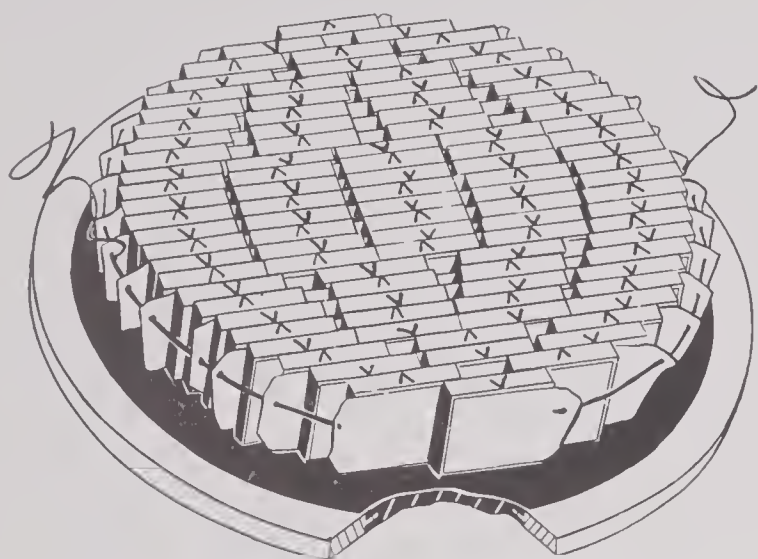


FIGURE 56. A flat inertia drive ADP array, bonded directly to a rubber window by the Cycle-Weld process. Note polarity marks, also the long silver foil strips which serve both as electrodes and as a means of wiring the array.

crystal assembly together while oven-curing the cement joints between the foils and the crystals is shown in Figure 37 of Chapter 1.

The entire crystal assembly was bonded as a unit to a rubber diaphragm by means of the

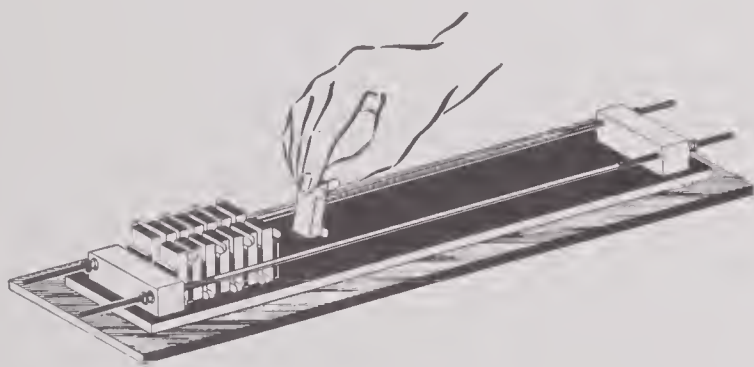


FIGURE 57. One stage in the construction of a cylindrical array. Assembling individual crystals in a jig prior to bonding them to a thin rubber mounting strip by the Cycle-Weld process. See Figure 58.

Cycle-Weld process described in Section 8.6.6. A part of the rim and diaphragm has been cut away in Figure 56 in order to show the manner in which the rubber diaphragm has been molded into the steel rim. The thickness of the neoprene diaphragm was $\frac{1}{8}$ in. In mounting this

crystal motor in its case, either an air space was provided immediately behind the crystals or they were permitted to rest against a layer of Cell-tite rubber. For assembly drawing, see Figure 82.

An interior view of a cylindrical inertia-drive transducer constructed on the same principle is photographed in Figure 40 of Chapter 1. In this case the crystals have been bonded to the interior of a reinforced rubber cylinder (see Figure 68) by means of the special jig illustrated in Figure 51. A further discussion on the construction of this particular transducer is contained in Section 8.7.1.

A third type of inertia-drive transducer designed at UCDWR is still in the trial stage. Since it possesses promising features from the standpoint of transducer construction, it will be briefly described. The crystals, either individually or grouped into strips, are bonded to a thin sheet of rubber by the Cycle-Weld process. One stage of the assembly process for an array consisting of individually foiled crystals is shown in Figure 57. After the array has been bonded to the rubber it may readily be formed into a circular contour as illustrated in Figure 58. In order to obtain inertia-drive characteristics, a sheet of Cell-tite rubber is placed be-

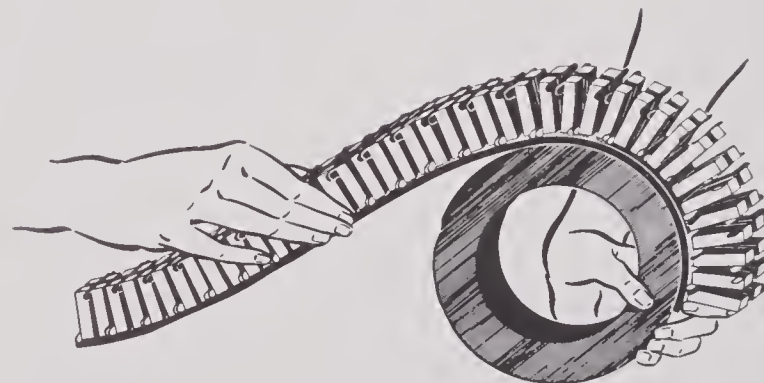


FIGURE 58. Forming the completed array of Figure 57 into a circular configuration. The addition of a layer of Cell-tite rubber beneath the solid rubber mounting strip results in an essentially inertia driven transducer.

neath the thin mounting strip of rubber to which the crystals are bonded. Another illustration which shows a completed transducer constructed on this principle occurs in Figure 62. After the strip containing the crystals had been coiled into a circular configuration and

cemented to a central metal core, additional support was given to the array by wrapping nylon thread about its circumference. The non-radiating edges of all crystals are blanked with Cell-tite rubber.

STACKS

A common type of stack transducer which has been built in large quantities at UCDWR is

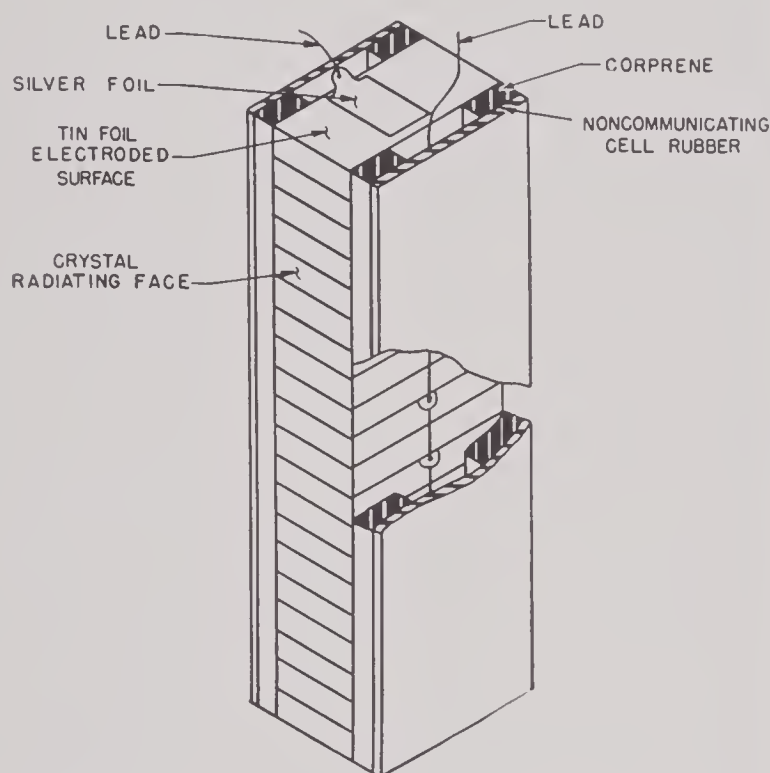


FIGURE 59. A typical stack crystal array as developed at UCDWR.

illustrated in Figure 59. The essential features have already been discussed in Section 8.7.1. For the most part stack-type arrays have been mounted within layers of Corprene and inserted in tin can cases of the kind discussed in Section 8.8.3. The stack unit is held securely in position in its cylindrical case by cementing to the top and bottom of the crystal-stack disks of rubber, plastic, or Corprene which have the same internal diameter as the can.

Blanking of the nonradiating faces of the crystals has been done usually by means of Corprene or Cell-tite rubber. The use of Corprene has been more common at UCDWR since it is somewhat more convenient to handle. By using narrow strips of Corprene along each edge of the crystal stack as shown in Figure 59, one reduces the area of contact between the Corprene

and the vibrating crystals. The wiring arrangement should be sufficiently clear from the figure. In similar stack units constructed at the Brush Development Company it has been the practice to have the sheets of Corprene lying flat against

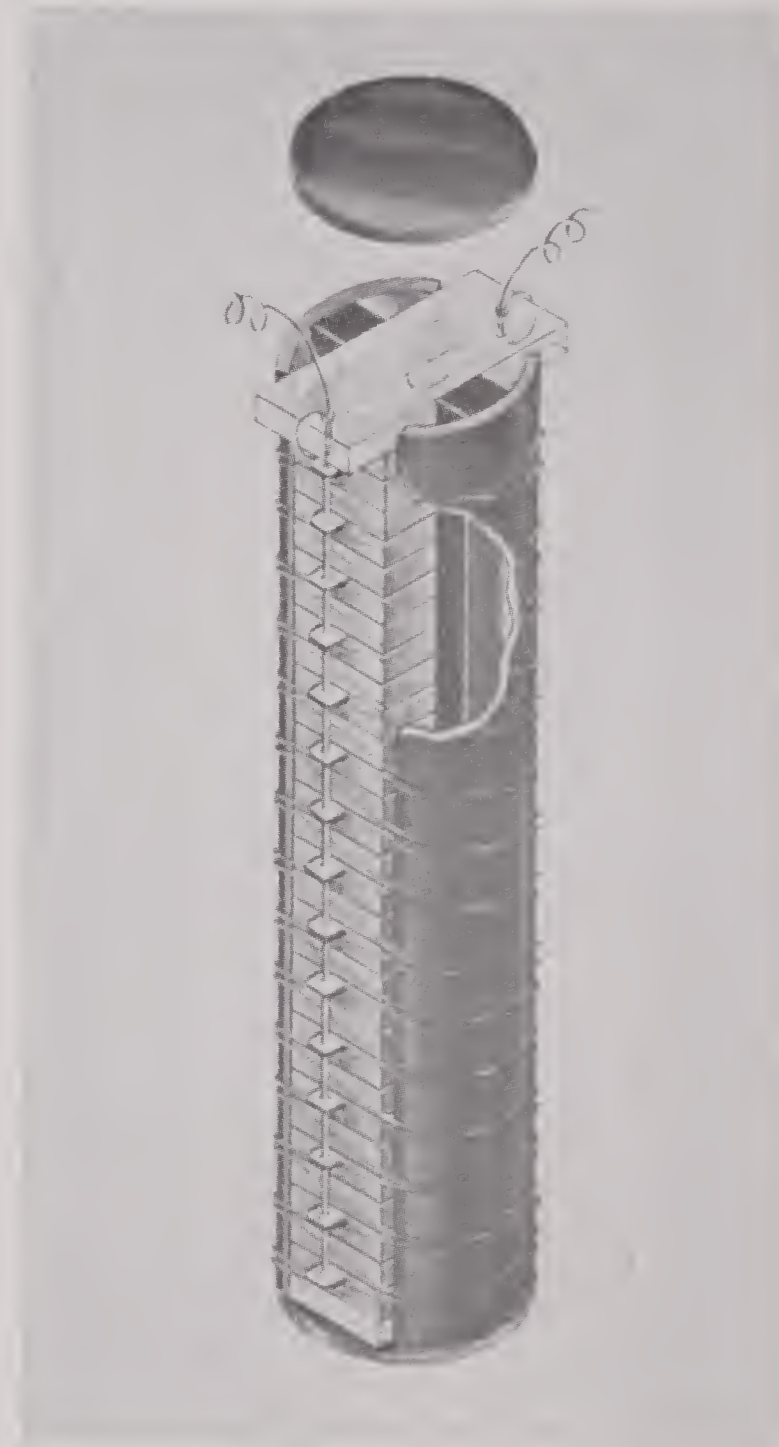


FIGURE 60. The UCDWR type 24C1Y1 (formerly CCZ10) stack transducer of Y-cut Rochelle salt crystals.

the nonradiating faces. Narrow slots cut in the Corprene sheets permit the foil ends to be brought out for soldering lugs. The tin-foil soldering tabs extend through the slots and are folded down and pressed against the outside of

the strip before the conducting wire is soldered to them.

Another example of a stacked array is shown in Figure 60. In this case the foil tabs are brought out along the radiating face, but the wire is so small that it does not interfere with the radiation field. Contact of the curved Corprene strip with the crystals has been avoided everywhere except at the central, relatively immobile, portion of the crystals by the use of a square Corprene rail. A Lucite plate having the same dimensions as one of the individual crystals is used at the bottom of the crystal stack and a similar Lucite plate except somewhat longer is used on top of the crystal stack. The additional length in the Lucite plate at the top has permitted holes to be drilled in it which act as supports for the lead wires. In addition to protecting the crystals on either end of the stack, these Lucite plates also serve to keep the narrow silver foil in contact with the end crystals. The narrow silver foils are cemented lightly between each pair of crystals, thus increasing the mechanical strength of the stack as well as anchoring the foils. An attempt to replace the tin-foil electrodes and the narrow foil strips in this transducer by a single silver foil between each pair of crystals proved unsuccessful in that it caused a lowering of the transducer output by several db. However, in this attempt all of the crystals in the stack were securely cemented together into a solid block. Further investigations along this line must be conducted before a final conclusion can be reached.

8.7.4

Wiring of Arrays

CHOICE OF MATERIALS

The principal factor governing the choice of wiring materials is resistance to corrosion in the presence of castor oil which is also in contact with rubber and RS or ADP crystals. Attention was focused on this problem in the early days of transducer design because it was observed that copper wire corroded in RS transducers. Whether this corrosion was due to interaction with the castor oil itself or to the additional presence of RS and/or rubber containing

sulfur is not known definitely to the writer. However, there is a well-established tradition that plain copper wire should not be used in transducers containing castor oil. Accordingly, it has been the custom to use well-tinned copper for this application. Silver wire has been used for wiring crystal assemblies at the UCDWR laboratory, apparently without any evidence of corrosive action.

Where the individual crystal electrodes are not furnished with tabs to permit soldering, it has been customary to connect the electrodes of the individual crystals with narrow strips of metal foil. The material used for these strips differs from one laboratory to another. Current practice at NRL is to use 0.002-in. nickel foil, at BTL 0.0007-in. gold-plated German silver which is given a ripple finish to improve the contact with the crystal electrode, at the Brush Development Company 0.001-in. gold-plated or tin-plated silver foil, and at UCDWR 0.0017-in. pure silver foil. Since all of these materials have been employed satisfactorily in existing equipment, any choice would seem to be a matter of individual preference. However, the quality of the electric contact is the most important consideration. In this respect, long experience at BTL has shown that gold forms the best low-resistance contact and the one least subject to corrosion. For high-power applications, the gold contacts may even prove essential.

ELECTRIC CONTACT STRIPS

The manner in which the electrodes of the individual crystals are connected by long strips of foil has already been discussed in Section 8.7.1 for one type of plane crystal array and relevant illustrations occur in Figures 47 and 61. Similarly, for stack-type arrays, Figure 59 will show clearly how silver strips which make contact with the tin-plated electrodes are brought out to permit soldering to the wire leads. Some other types of arrays may be quickly and easily built up in a similar manner.

Good electric contact to the electrode has been assured at UCDWR by imparting a sandpaper finish to the silver foils. This has been accomplished by laying the strips of silver foil on a piece of No. 2 emery cloth, placing a piece of Corprene approximately $\frac{1}{8}$ in. thick on the



foil, and pressing this assembly in a book press. An imprint of the many small protrusions on the emery paper is left in the foil. These sharp projections materially reduce the contact resistance between the silver and the tin-foiled surface of the crystal. Other laboratories have treated contacting foils in an analogous man-

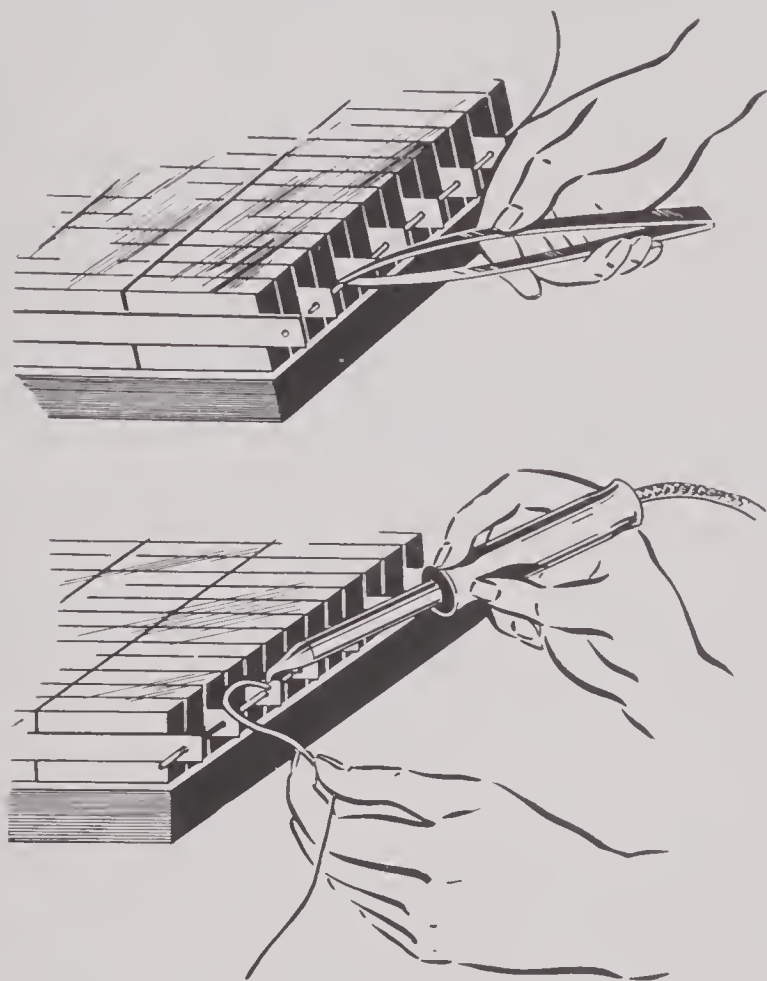


FIGURE 61. Two stages in the wiring of a crystal array. Above: Threading a wire through holes in the foil strips. Below: Soldering the foils to the wire. A minimum of solder should be used with a minimum of heat in order to avoid fracturing the crystals.

ner, using the materials mentioned in Section 8.7.4.

It is usual to cement these contacting foils to the electrodes in order to make their position secure. However, the cement layer should be extremely thin.

SOLDERING PRECAUTIONS

For soldering connections inside transducers a good grade of soft solder, preferably with the eutectic 63-37 composition, is recommended. But 60-40 or even 50-50 have been found satisfactory. Either rosin-core solder or a rosin-

alcohol flux should be employed. It is obvious that all solder connections should be done in such a fashion as to guarantee a permanent joint.

Since both RS and ADP crystals are quite readily fractured if subjected to large temperature gradients, soldering operations must be carried out carefully to prevent fracturing the crystals. This is particularly true for silver foils where the connecting wires are soldered directly to tabs on each individual crystal. The minimum of heat and the minimum of solder consistent with a reliable electrical connection should be the rule. It must be kept in mind, however, that transducers are subjected to mechanical vibration and also to depth charges; hence, the soldered connections must be mechanically rugged.

WIRING ARRANGEMENTS

In arranging the wiring for a crystal array, attention must be given to the questions of voltage insulation and wiring capacitance. In oil-filled transducers, voltage insulation does not usually constitute a major problem; in air-filled units which operate as a source and therefore at relatively high voltage, the problem may be important. The seriousness of the voltage insulation question depends also on the type of transducer design. For example, in a 2 to 1 lobe-suppressed array, illustrated in Figure 50, there is an intrinsic insulation difficulty which has had to be met by a wider spacing of the crystal groups between the two zones. This spacing in the array of Figure 50 amounts to $\frac{3}{8}$ in. For this reason, the 3 to 1 scheme of lobe suppression has been favored at UCDWR (see Figure 49, also Figure 33, of Chapter 1).

In most transducers the effect of the wiring capacitance on acoustic performance is probably negligible. In some small units, however, the wiring capacitance may play an important role. Since special cases of this kind must be studied individually, there is nothing particularly helpful which can be added on this topic in this section.

Since important technical considerations are frequently not involved, the arrangement of wiring in transducers is often dictated on the basis of simplicity arguments. Where space per-

mits the wiring may be arranged between rows or banks of crystals as in the lobe suppressed crystal array illustrated in Figure 50. Usually it is convenient to have the wiring near the edge of the crystal array as illustrated in Figure 56 or in Figure 33 of Chapter 1. In still other transducers it may be preferable to have the wires directly over the radiating face of the crystal array as in Figure 49 and Figure 60. Inasmuch as the diameter of the wires generally constitute a very small fraction of the wave-

This, however, does not constitute a practical solution to the problem for naval equipment operating at sea. The next best procedure would be to use a gas, preferably air, at the same pressure as its surroundings. This type of construction has been used in many different designs of transducers where air filling is permissible. In general, it is more difficult to secure a satisfactory watertight seal with air-filled transducers than with liquid-filled types, especially where the former operate at great depths in the water

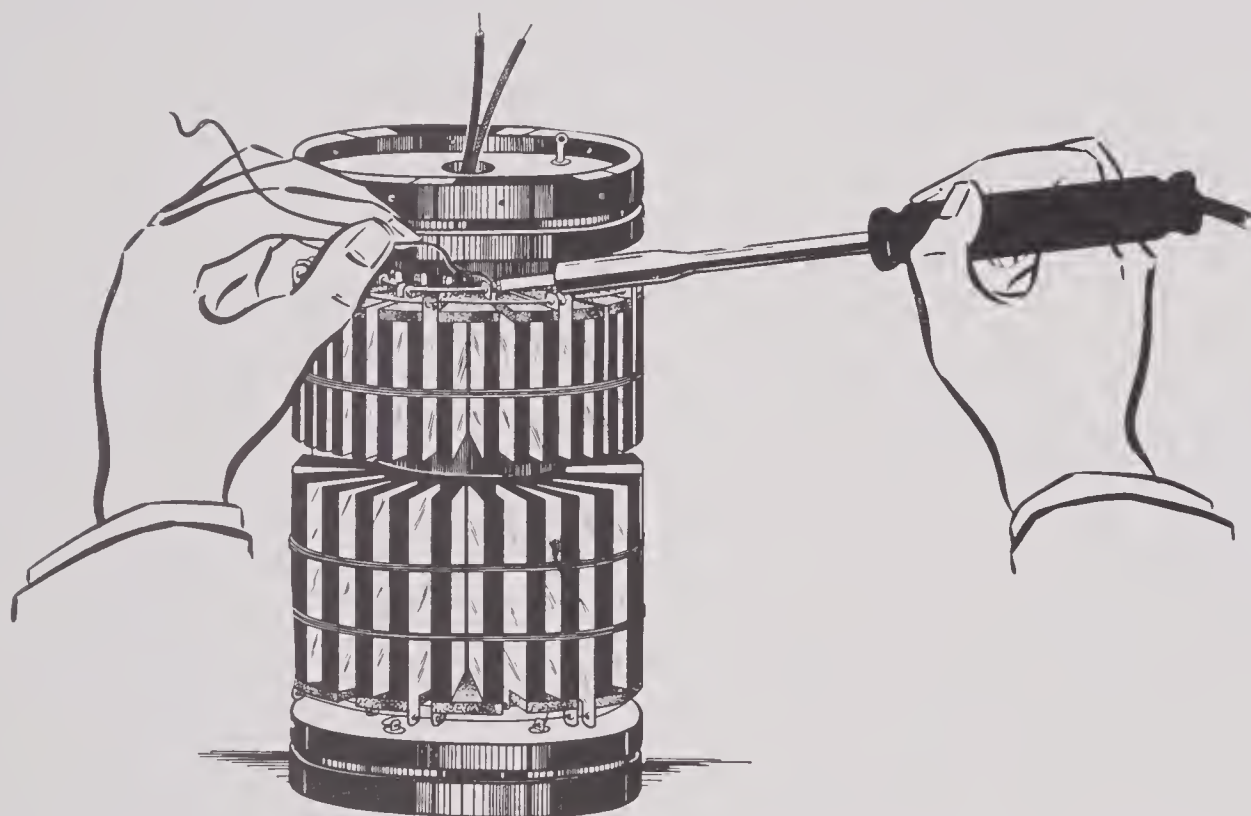


FIGURE 62. Soldering wires to the foil strips in a UCDWR cylindrical transducer. Note the use of metal-glass terminal seals; also the grooves provided for O-ring hydraulic gaskets with which to seal the completed assembly into its cylindrical housing.

length of the radiation, there does not seem to be any valid technical objection to this procedure, especially where bare wire is employed. The use of insulating material which might act as a pressure release immediately in front of the radiating face would be objectionable, of course.

8.7.5 Acoustic-Isolation Materials

FREE GAS

The highest degree of acoustic isolation obtainable within an array consists in having the individual crystal elements, except the radiating face, surrounded by an evacuated space.

and therefore are subjected to a large pressure differential. Attempts to equalize the pressure by various contrivances, while not unsuccessful, have usually led to complicated and awkward devices.

Gases other than air may prove desirable in special cases. Where voltage breakdown is a problem, for example, recourse may be had to Freon (dichloro-difluoro methane). Freon will withstand approximately three times as high a voltage as air at atmospheric pressure. While Freon has been tried in a few experimental transducers at UCDWR, its performance in the field remains unknown.



METAL-AIR CELLS

In liquid-filled transducers it is not feasible to surround the nonradiating faces of each crystal with air, but provision for acoustically isolating the ends opposite the radiating face may be met in any one of several ways. One relatively simple procedure is to provide an air layer sandwiched between two metal plates. These metal plates may be either a few thousandths of an inch thick and sealed by soldering around the edges or they may be sufficiently thick, perhaps $\frac{1}{2}$ in., to withstand relatively high pressures. Where thin metal walls are used it may be necessary to provide internal inserts which will prevent their collapse under conditions of high pressure. If these metal-air sandwiches must be subjected to a vacuum during the liquid-filling process of the transducer, it will probably be necessary to weld the inserts to prevent the walls from expanding.

A unique type of cellular construction in which an air layer is maintained in connection with a backing plate is shown in Figure 52. Constructional details of this backing plate unit have been discussed in Section 8.7.2.

CELLULAR RUBBER

Much of the advantage of an air layer for acoustic isolation may be obtained by the use of cellular rubber. That used at UCDWR had the trade name Cell-tite. In this material the air is



FIGURE 63. A Cell-tite rubber block completely sealed in a molded rubber sheath in order to prevent the diffusion of air from its cellular matrix. (Bell Telephone Laboratories.)

material may be readily cut with shears or a razor blade and is available in sheets a yard wide and in thicknesses ranging from $\frac{1}{32}$ in. to $\frac{1}{4}$ in. or more.

Two questions arise in connection with the use of cellular rubber in liquid-filled transducers. One involves its possible interaction with the liquid and the other involves the question of gaseous diffusion through the thin walls of the individual cells. The latter problem depends in part for its answer on the individual application. For transducers operating at great depths it is clear that the gas would be subjected to high hydrostatic pressures and it would seem only a question of time before an appreciable part of the gas could be lost by diffusion. In addition, one can envisage a loss of efficiency at great depths should the cellular rubber become unduly compressed.

Attempts have been made to reduce the likelihood of the gas escaping from the cellular structures by coating the rubber surface with a more impervious substance or by adding a thicker layer of rubber on the outside of the cellular matrix. In Figure 63 is shown a cross section of a sample resulting from one such attempt by BTL in which the cellular rubber has had an approximately $\frac{1}{32}$ -in. layer of solid rubber molded completely about it. Although this is a step in the right direction, efforts must still be exerted to find thinner layers of satisfactory cellular structures. To pursue this matter further it would be well to consider molding about the cellular matrix other materials which are even more impervious to gaseous diffusion. In particular, some of the synthetic materials such as butyl rubber or Koroseal should be tried.

In a great number of transducers designed at UCDWR it has been specified that strips of Cell-tite rubber be placed on all of the nonradiating edges of the crystals with the exception of the electrode faces. In order to hold the Cell-tite rubber in place, it has frequently been necessary to bond them to the crystals with some type of cement. For the most part bakelite cement has served this purpose. In attaching Cell-tite rubber on the narrow crystal surfaces between the electrode faces, particular attention must be paid to preserving high values for the electrical resistivity.

contained in small noncommunicating bubbles or cells incorporated into a rubber matrix. The



This electrical resistivity may be adversely affected in several ways.

1. The surface coating on the Cell-tite rubber may be contaminated with conducting materials. At UCDWR it has been found necessary to thoroughly wash and scrub the surface of the rubber with cheesecloth containing an organic solvent such as benzene.

2. It is important to avoid fingerprints, both on the surface of the rubber as well as on the crystals.

3. Any moisture which may be trapped beneath the surface of the crystal and either the layer of cement or the rubber may seriously increase the surface leakage.

This last point has been discussed in detail in Section 8.2.4, including the graph of Figure 3. The curves on this graph applied to an RS crystal which had been coated with Vulcalock cement and are not necessarily applicable to ADP. However, it has been found in voltage-testing ADP crystals that arcing is more likely to occur through the cement layer than across the somewhat greater air path around the insulating material. It would appear preferable if possible to avoid cement altogether in connection with Cell-tite rubber. This can be done in some transducers which have a proper spacing of the crystals merely by wedging the individual strips of Cell-tite rubber between them. There is little tendency for these strips to become dislodged in an oil-filled transducer.

In bonding cellular rubber to large surfaces, it should not be stretched. Otherwise it may pull away later and not cover the desired area completely. When heated under pressure, cellular rubber collapses. It is added to crystal arrays following the oven-curing processes.

CORK AND CORK-RUBBER COMPOSITIONS

The use of cork naturally suggests itself for purposes of acoustic isolation because it contains a large percentage of air. Although natural cork has been used to some extent for this application, a number of cork-rubber compositions are available which are much superior. This superiority arises from selecting a matrix material which is better than natural cork as regards its imperviousness to both gases and liquids. At the same time it is important to

select a cork-rubber composition which is resistant to the liquid involved and which possesses a high voltage-breakdown value. A commercial product which has been used to advantage at several laboratories has a neoprene-cork composition (Armstrong type DC-100). A sample $\frac{1}{32}$ in. thick has been known to withstand a breakdown test at 30 kc of 10,000 v rms.

These cork-rubber compositions are available in large sheets in thicknesses from $\frac{1}{32}$ to $\frac{1}{4}$ in. or more. They may be cut to any desired size very conveniently. No data are available as to whether any particular composition excels acoustically. It was felt by the designer at one laboratory that the best composition to use should have a Shore durometer test between 50 and 60.

The remarks in Section 8.7.5 with reference to the cementing of Cell-tite rubber to crystals are also applicable to cork and cork-rubber compositions.

8.7.6 Inspection and Test of Arrays

VISUAL INSPECTION

A careful visual inspection of completed arrays may result in the detection of faulty construction of several different kinds. One of the more important observations that can be made is an examination of the quality of the cemented bond. To facilitate inspection it is frequently advantageous to place a thin oil film on the radiating face of each crystal in order to obtain a clearer view of the bond. Where an appreciable number of the crystals are found to be improperly bonded, the entire array must be rebuilt. If only 1 or 2 per cent of the crystals in an array are improperly bonded, the unit would probably be considered acceptable. In some cases a few faulty crystals in an assembly can be replaced and rebonded satisfactorily without dismantling the whole unit, but this is usually difficult.

A thorough inspection should be made to see that all the electrical connections are secure and that there is an absence of solder or other loose dirt particles. Where polarity markings are such as to be visible, each crystal should be

checked to see that its polarity is correct. All isolating strips of Corprene or Cell-tite rubber specified in the design drawings should be checked for proper location.

The completed array must be thoroughly cleaned before it is permitted to pass inspection. Especially, excess cement and finger prints are likely to be present. It is not sufficient that crystals merely look clean, since conducting films or filaments may be quite invisible. If organic solvents are used to clean the crystals, proper regard must be paid to the solubility of the cemented bonds and other assembly components. This usually means that only a cloth dampened with solvent is employed for wiping the crystal surfaces, not an immersion of the entire assembly. The final check on the cleanliness of a crystalline array is the electrical testing for d-c resistance and voltage breakdown discussed in Section 8.7.6.

POLARITY OF CRYSTALS

Since the polarity of a crystal determines the phase relationship between electrical impulse and mechanical action, the polarity of each crystal is determined prior to its assembly into

quent wiring may be incorrect. It is therefore highly desirable to recheck the polarity of each crystal in its permanent position in the completed assembly.

This recheck of the polarity of each individual crystal may be accomplished in the manner shown in Figure 64. The indicating equipment for this purpose has already been described in Section 8.4.8. Each crystal is given a sudden push on its radiating face by means of a rubber-tipped pencil and the polarity indication is noted on the meter. In very large arrays, which may involve 100 to 500 or more crystals in parallel, the increased capacitance of the electrical circuit will tend to obscure somewhat the polarity indication which results from the voltage generated by the single crystal under test. If positive indications cannot be obtained when all the crystals of the complete array are in parallel, individual rows of crystals should be disconnected from the circuit and tested. Such an individual row of crystals under test is illustrated in Figure 64.

It should be pointed out that false indications of polarity may occur occasionally if the individual crystals under test are bonded to other crystals in a solid array. In assemblies where the crystals have been tightly packed, cases have been noted where the deflection of the polarity indicator made an individual crystal appear to be reversed in position. Removal and independent test of such a crystal has proved oftentimes that it had been correctly polarized, and also properly installed and wired in position. In cases of this kind, it must be assumed that pressure exerted on the end of the tested crystal resulted in distortion of its neighboring crystals to the extent that their out-of-phase output exceeded that of the crystal under test.

The correctness of the polarity of each crystal in a group can be determined also by using a probe microphone. The entire array of crystals is driven by an oscillator and the microphone probe is placed successively on the radiating face of each crystal of the array. A description of the probe-microphone equipment and the technique involved in its use occurs in detail in Section 9.2. Briefly, however, the probe microphone consists of two tiny piezoelectric crystals mounted in a small holder so that any mechan-

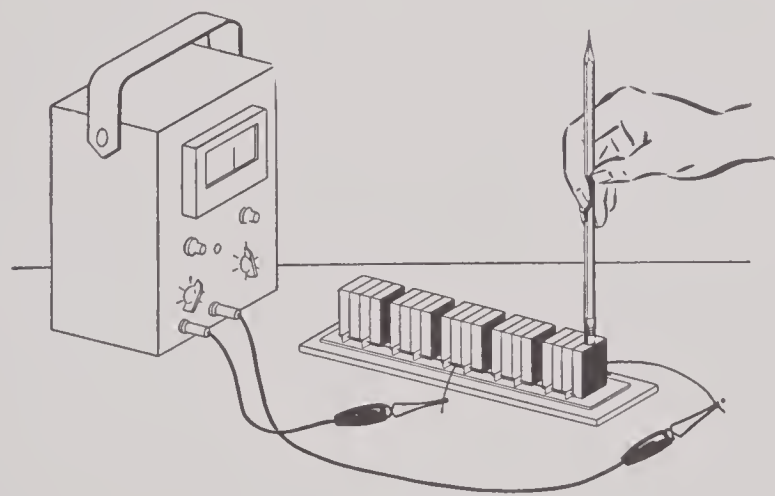


FIGURE 64. Inspecting the individual crystals on a backing bar for correct orientation by means of a polarity indicator.

an array as already discussed in Section 8.3.9. During the construction of large arrays, involving perhaps hundreds of crystals, numerous chances for errors arise. Apart from possible mistakes in the original polarity indications on each crystal, the crystals may be installed in an assembly in a reversed position or the subse-

ical pressure exerted on them can be amplified and read on electric meters which indicate both magnitude and phase.

At UCDWR the probe has been coupled mechanically to the radiating crystal surface by a thin film of castor oil. An oscilloscope coupled both to the probe and to the driving signal of the oscillator has been used to indicate phase relationship and thus to determine whether the individual crystals of the array are radiating in phase.

D-C RESISTANCE

The d-c resistivity of RS and ADP has been discussed in some detail in Sections 8.2.4, 8.2.8, and 8.5.7. It was seen that the d-c resistance varied with the temperature and humidity, particularly in the case of RS. In completed arrays consisting of a few hundred crystals the d-c resistance would be expected to depend in a known way on the circuit design and on both the dimensions and the number of crystals. Consequently a fair approximation to the d-c resistance expected for a particular transducer should be calculable from a knowledge of the kind of crystals, their dimensions and number, and their electrical connections. In practice, however, it will be found that the d-c resistance of a crystal array will vary markedly with the quality of the technique used in its assembly. For example, a large array of X-cut RS crystals may have a resistance as low as 20 megohms when constructed in a casual manner without special precautions. An identical crystal array, but constructed with care, may possess a d-c resistance as high as 1,000 megohms. To attain the higher value, it is especially important to refrain from touching the interelectrode surfaces of the crystals with the bare hands and to eliminate adsorbed moisture.

The presence of water vapor is a most important factor with RS. For instance, newly constructed arrays of RS crystals may have a very low resistance, perhaps only 100,000 or 200,000 ohms. When they are subjected to a vacuum for a time their resistance will gradually increase until it reaches a maximum value of perhaps 2,000 megohms or better. Upon being removed from the vacuum chamber this resistance value will drop somewhat but prob-

ably not below 100 megohms. In general, it is considered satisfactory if large RS transducers have a d-c resistance of 50 megohms or more when first constructed, although this value will be expected to increase upon being subjected to a vacuum. ADP crystals, however, are not so sensitive to relative humidity conditions so that little if any improvement can be expected in the d-c resistance of ADP arrays upon placing them in a vacuum chamber.

In addition to measuring the d-c resistance between the terminals of a crystal array, it is also desirable to check the resistance from each terminal to ground.

Resistance readings at UCDWR have been made usually with vacuum-tube ohmmeters. In general, precision is not an important consideration.

Discussion of the d-c resistance measurements to be made on transducers in their completed state will be discussed in Section 8.9.5.

CAPACITANCE

Capacitance values at 1,000 c (C_T) for individual crystals of RS and ADP were discussed in Section 8.5.4. From the information given it is possible to calculate the capacitance to be expected of an assembled array from the kind, number, and dimensions of the individual crystals and the manner in which they have been connected electrically. This calculated value may be checked with experimentally determined values for the completed crystal array. This type of check has not customarily been made at UCDWR except occasionally on transducers which have been finally cased and oil-filled.

ADMITTANCE

Admittance measurements on single crystals have been discussed in Section 8.5.5. The electric circuit for the determination of admittance characteristics was also given, together with a sample admittance curve for a single ADP crystal. It is true that admittance curves have greater significance in connection with single crystals than when they are determined for an assembly of many crystals bonded to a supporting structure and perhaps to each other. In some cases, nevertheless, a rough indication of the

efficiency of a crystal transducer can be obtained from an admittance curve, particularly if the efficiency is high. For a highly efficient transducer, a rise of 2 or 3 db in the admittance curve may occur at resonance. However, if no increase in slope of the admittance curve can be discerned at resonance, the transducer might still possess an efficiency of 50 per cent.

HIGH VOLTAGE

High-voltage specifications for individual crystals were discussed in Section 8.5.8. For a completed array, it seems to be too much to expect that the breakdown voltage of an entire assembly should be as high as the minimum breakdown voltage of the individual crystals which comprise it. In a number of experimental transducers constructed at UCDWR, the individual crystals used were tested at a voltage higher than that at which the completed transducer was to be operated, but near the expected breakdown voltage of individual crystals. It was found that in almost all cases the assembled arrays failed at voltages considerably below the test voltage for the single crystals. The explanation for this behavior probably lies in the contamination of some crystal surfaces during the course of construction, but, generally speaking, voltage breakdown is somewhat unpredictable.

Attempts have been made at UCDWR to determine maximum safe operating voltages for the three common piezoelectric crystals. Individual ADP crystals $\frac{1}{4}$ in. thick in oil were found to withstand 20,000 v rms in almost every case. Many of them tested higher than 30 kv and a few did not break down even at 40 kv. When failure occurred the breakdown usually took place through the body of the crystal. When the individual crystals are built into an array it might be expected that the array would withstand a test voltage of 20 kv. Nevertheless, this is not the case and, in general, it has been found for ADP crystals $\frac{1}{4}$ in. thick that approximately 5,000 v rms constitutes an upper limit for a safe operating voltage unless special precautions are taken during construction.

Unless special demands are to be placed upon ADP transducers, it would seem that voltage tests well in excess of the operating range should be made on the crystal array, *provided*

this test voltage does not exceed the specifications given in Section 8.5.8.

Single Y-cut RS crystals $\frac{1}{4}$ in. thick will normally withstand a test voltage of 20 kv rms. In practice, however, the maximum safe operating voltage for RS transducers has been in the neighborhood of 2,000 v. In several experimental transducers constructed at UCDWR, it was hoped that much higher operating voltages could be used as a consequence of the careful technique employed in their construction. As a matter of fact, breakdown voltages in excess of 6,000 v rms were obtained in one or two cases. As the result of much experience with RS transducers it has been found that the maximum safe operating voltage of 2,000 v rms is about as much as can be expected for $\frac{1}{4}$ -in. crystals. Crystals of other thicknesses would withstand proportional operating voltages.

It may be inconvenient to make an inspection test of assembled crystal arrays much above their rated operating voltage in that it will ordinarily be necessary to immerse them in a liquid. The use of most organic solvents for the immersion liquid, such as carbon tetrachloride mentioned in the specifications for testing individual crystals, is not permitted owing to their deleterious effect on most cement joints. One procedure would be to use the regular transducer liquid for this purpose, but this is inconvenient where further work on the array is contemplated. One possibility that suggests itself, if the test voltage is not appreciably higher than the air breakdown voltage for the spacings involved, is the use of a Freon atmosphere. The breakdown voltage of Freon at atmospheric pressure is approximately three times that of air.

8.8 HOUSINGS AND ACCESSORIES

8.8.1 Specifications and Tests

Several factors must be considered in the choice of a material for housing transducers. In general, the acoustic properties of the material selected are unimportant, except for the window through which the radiation enters the water. When crosstalk transmitted through the case proves to be a problem, as it has in some com-

plicated transducers which contain two or more transmitting and/or receiving units in the same housing, the acoustic properties of the case materials may have to be taken into consideration.

One of the most important requirements for transducer cases is that they must be free from leaks. It seems to be quite difficult to fabricate cases in such a manner that they can be guaranteed leakproof; only strict attention to detail during the course of manufacture will result in satisfactory performance. The quality of metal castings with respect to leaks will be discussed in Section 8.8.2. All transducer housings should be thoroughly tested for leaks before using. This is probably done most conveniently by using 60 to 70 psi air pressure inside the case and inspecting the outside for bubbles, either while immersed in water or while the exterior is wet with soap solution. Although the housing may be subjected to considerably higher pressures in actual use, it is too hazardous to test at a still higher pressure unless special precautions are taken to safeguard personnel.

Adequate mechanical strength in a transducer housing is a matter of design, but tests should be conducted to see that design specifications are met. Partial tests may be made by filling the cases with liquid at the required pressure. Usually the specifications as to strength will be such that the test equipment available in the ordinary laboratory may be inadequate. Actual tests in the field will then be required. As an illustration of the factors encountered, mention may be made of transducer cases intended for rocket launching or which are launched from high-speed aircraft so that they strike the water with tremendous velocity. It is clear that these conditions would be difficult to duplicate in the laboratory. Even in the case of ship-mounted transducers, which are subjected to rough seas and perhaps to depth charges, it will probably also be desirable to conduct tests under operating conditions.

Corrosion resistance will always be an important factor in the selection of materials for underwater operation. This problem may be attacked either by selecting a material which is least subject to corrosion, or by covering the transducer case with a corrosion resisting coating. The adoption of the latter practice, if satis-

factory, materially lessens the demands placed on the actual material of the housing. Corrosion resisting coatings and antifouling paints will be discussed in Section 8.8.5. Among workable metallic materials, best corrosion resistance at the present time is apparently found in some of the stainless steels and in the nickel-copper alloys, such as Monel and Inconel. Alloys containing more than 60 per cent copper are not likely to become fouled with marine organisms.¹⁸ The information in Table 2, which lists numerous elements and their alloys in a galvanic series for sea water, is reproduced from articles by LaQue¹⁸ and Cox.¹⁹ Further discussion and references on this important problem may be found in their articles. The importance of passive surface films on certain alloys is clearly demonstrated in this table.

TABLE 2. Galvanic series for sea water.

Magnesium	Lead
Magnesium alloys	Tin
Zinc	Muntz metal
Galvanized steel or galvanized wrought iron	Manganese bronze
Aluminum 52SH	Naval brass
Aluminum 4S	Nickel (active)
Aluminum 3S	Inconel (active)
Aluminum 2S	Yellow brass
Aluminum 53ST	Admiralty brass
Alclad	Aluminum bronze
Cadmium	Red brass
Aluminum A17ST	Copper
Aluminum 17ST	Silicon bronze
Aluminum 24ST	Ambrac
Mild steel	70:30 copper nickel
Wrought iron	Comp. G bronze (88% Cu, 10% Sn, 2% Zn)
Cast iron	Comp. M. bronze (88% Cu, 6.5% Sn, 4% Zn, 1.5% Pb)
Ni-resist	Nickel (passive)
13 per cent chromium stainless steel, type-410 (active)	Inconel (passive)
50-50 lead-tin solder	Monel
18-8 stainless steel, type-304 (active)	18-8 stainless steel, type-304 (passive)
18-8-3 stainless steel, type-316 (active)	18-8-3 stainless steel, type-316 (passive)

A streamlined transducer case which has been spun from sheet Inconel is photographed in Figure 65. The thick rubber window has been bonded inside a stainless-steel cylinder and has been given the contour of the Inconel housing. The qc rubber was Compound M-163, whose

composition occurs in Section 8.8.4. This transducer case is made to oscillate by a mechanism enclosed in the remainder of the gear.



FIGURE 65. A streamlined oscillating transducer housing of Inconel developed at UCDWR. The ADP crystals have been bonded to the thick neoprene window, whose cylindrical exterior surface is clearly shown in the photograph.

8.8.2

Metal Castings

Metal castings have been very widely used for transducer housings, partly for economical reasons, but also for the simplification of design which they permit. In general, castings would appear to be the best solution to the transducer housing problem except for their frequently poor quality with respect to porosity. Difficulty has been experienced in obtaining metal castings entirely satisfactory in this respect. Accordingly, all castings must be pressure tested in order to insure their freedom from leaks. Leaks may be detected usually by subjecting the castings to an air pressure of 70 psi while immersed in water or with the outside of the casting covered with a soap solution. This testing should be done immediately upon receipt of the castings, before any small cracks or holes have had a chance to become temporarily closed by oxide formation. Castings which contain small leaks should be discarded before any machining time has been wasted on them. Since most crystal motors involve an outlay of a few

hundred dollars, it is poor economy to try to salvage defective metal castings by attempts to make them waterproof. Only castings which are leak-free before and after machining by virtue of their own homogeneity should be used.

Iron alloys have found the widest application in castings. Meehanite, a patented alloy, is especially dense in structure and has desirable machining qualities as well. It has been used with considerable success in transducers. Numerous examples of iron castings will be found in photographs of transducer cases throughout this volume. One common type at UCDWR is shown in Figure 79.

Castings of stainless steel may prove an answer to this problem in the future, but they have seen very limited use so far. A photographic illustration of a stainless-steel casting occurs in Figure 21 of Chapter 1.

Castings of other metals have also been used for transducers, especially brass and bronze. These castings may be porous also and hence subject to leaks, particularly if the walls are thin. While it would seem simple to repair these leaks in the case of brass and bronze, again it seems undesirable to do so from an economic viewpoint. Exceptions to this conclusion might arise in the future, should better methods become available for the high-pressure impregnation of castings with plastic cements or other suitable substances.

Cast aluminum corrodes very rapidly in sea water unless coated with a satisfactory protective covering. The same is also true of pure aluminum and of many aluminum alloys. However, all these materials have found extensive use for expendable applications, where they need last but a few hours. For the position of aluminum and aluminum alloys in the galvanic series for sea water, refer to Table 2 which appears in Section 8.8.1.

8.8.3

Tin-Can Cases

Ordinary tin cans have been used extensively for housing expendable transducers. During the period 1941 to 1945 nearly 10,000 such transducers have been manufactured and used satisfactorily. These cans are subject to corrosion, if exposed to sea water an appreciable length of

time, but they are entirely acceptable for periods of a few hours, or, in the case of intermittent exposure, perhaps a few days. The wall thickness of the tin-plated steel used in these cans is approximately 0.010 in., so that the transmission loss is probably not more than a fraction of a decibel at frequencies lower than 80 kc. It has been observed that directivity patterns for the symmetrical-drive transducers housed in cans varied but slightly from the patterns obtained from identical crystal motors mounted in cylinders of qc rubber. Owing to the ease with which tin cans undergo minor deformation to accommodate variations in external pressure, they may be used at great ocean depths without difficulty.

In the early transducers of this type as developed at UCDWR, provision was made for two oil plugs on one end of the can; later, a single oil plug was used. In a number of instances these plugs were found to leak. It now appears that a great improvement in this respect is obtained by providing an approximately $\frac{1}{16}$ -in. diameter hole in one end of the can for oil filling. Following the evacuation of the can it is filled with DB castor oil and then this small hole is permanently sealed with a drop of solder. This procedure obviates the use of a standard oil plug and gives a simpler and more dependable seal. Electric leads to the crystal motor enter through metal-glass seals of the Sperti or Stupakoff type (see Section 8.8.6), which have been soldered into one end of the can lid. The sealing of the lid onto the can is done by means of commercial sealing machines. These are obtainable in small hand-operated models, which are well suited to experimental laboratory use.

A further discussion of one such transducer, UCDWR-type CY4, appears in Chapter 6 and a photographic illustration in Figure 22 of Chapter 6. A drawing showing construction is reproduced in Figure 59.

8.8.4 Rubber Windows and Cases

TYPES OF RUBBER

The physical properties of rubber which are important to the acoustic performance of trans-

ducers have been discussed in Section 3.7.3. It was pointed out that the density and the acoustic velocity must individually match that of sea water in order that sound waves may travel from rubber into sea water without suffering reflection or refraction. Samples of rubber which meet these two specifications have been referred to as qc rubber or sound rubber. In some transducers the window shape may necessitate the use of qc rubber if the window is not to interfere with the acoustical performance of the crystal motor, especially its directivity pattern. In transducers having flat rubber windows of uniform thickness an accurate impedance match to sea water is usually not necessary. Instead of qc rubber, it may be preferable to use neoprene or some other type which has more favorable mechanical properties.

Three different types of qc rubber have been made available. One, produced by the B. F. Goodrich Company, has been very widely used in the construction of underwater sound equipment. It carries their designation No. 79-SR-32. Its exact composition is unknown to the writer since it comes in the category of trade secrets. However, it is apparently of natural crude stock which has been very heavily loaded with castor oil. All samples have a very marked oily appearance and also an oily feel. Over long periods of exposure part of this oil is lost, at least from the surface layers. The rubber is quite soft and subject to tearing and eventually checks rather badly. In order to bond Goodrich qc rubber to metal it is necessary to interpose another type of rubber referred to in the trade as "tiegum." This will be discussed further on in this section.

A second type of qc rubber has been made available by BTL. Their sound transparent rubber, Compound M-163, has the following formula.

Smoked sheet	100.00 parts
Sulfur	3.00 parts
Zinc oxide	5.00 parts
Captax	0.50 parts
Stearic acid	0.50 parts
Heliozone	2.00 parts
Neozone D	1.00 parts
P 33 Black	0.50 parts

Uncured rubber stock having this composition

should be cured 30 min at 287 F for sheets 0.075 in. thick. Test data submitted by BTL indicates that rubber of this composition has a specific gravity of 0.975, a Shore A hardness of 35, and a tensile strength of at least 2,800 psi. A number of satisfactory transducer windows and cases at UCDWR have been made using this formula. Some of these were manufactured in commercial establishments; others, using uncured sheet stock obtained commercially, have been made in the UCDWR Transducer Laboratory (see Figure 68). As is clear from the formula, this compound is primarily crude natural rubber and contains no castor oil.

A third type of *qc* rubber has been compounded at NRL and carries the number F9-5. This particular brand of *qc* rubber is slate gray in appearance and is extremely oily. Although its exact composition is not known to the writer, it appears to be a crude rubber stock containing a very high percentage of castor oil. A few transducer cases having this composition were constructed for UCDWR through the courtesy of NRL.

Another rubber compound that is being used currently for underwater sound equipment is manufactured by the B. F. Goodrich Company and is known as Compound 8388. Acoustical data for this type of rubber as well as for many other kinds will be found in Table 4 of Section 3.8. It will be noted that Compound 8388 has an acoustic velocity close to that of sea water but that its specific gravity is 1.15. Where a strict *qc* match is not necessary, as in many flat windows, this compound may be useful in that it possesses superior abrasion resistance. Some additional information on types of rubber useful in transducers will be found in Section 3.8.

ACCEPTANCE TEST

In order to perform satisfactorily as a window for acoustic radiation, rubber must be free from small air pockets. Even when these air cavities possess microscopic dimensions, they may still be troublesome from the standpoint of acoustic transmission. Although some use has been made of X rays in attempting to analyze rubber windows, it would seem that X-ray techniques would not be satisfactory for this purpose.

The best test would appear to be one employing acoustic radiation. For ease in measurement it is desirable to use a very high frequency so that the dimensions of the testing equipment can be kept small. Equipment designed for such tests at NRL employed a frequency of 730 kc by using a transducer whose radiating dimensions provided a very sharp acoustic beam. Both the sending and receiving equipment were contained in a relatively small tank.

RUBBER METAL BONDS

In attaching rubber windows to transducer cases it is almost always advantageous to have the rubber bonded directly to a metal window frame, which in turn may be fastened to the

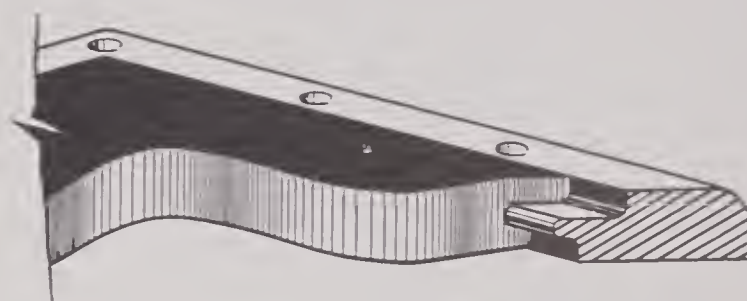


FIGURE 66. A cross section of the metal to rubber bond in the flat window of the UCDWR type GD case. The metal tongue protruding into the rubber results in a longer leakage path.

main case with a gasket seal. The most important exception is the use of cylindrical rubber tubes, often referred to in the language of the laboratory as "socks," and discussed in greater length in this section and Section 8.9.3. Although the art of bonding rubber to metal is quite old it seems to be the consensus that rubber-metal bonding must still be regarded as an art. Even experts with long experience in bonding rubber to metal will occasionally produce material that is distinctly inferior or even a complete failure. It apparently requires meticulous attention to detail.

There are several known methods for bonding rubber to metals of various types. One of the earliest methods required all metals except brass to be brass plated previous to the application of the rubber. This, too, is a very specialized technique requiring careful control and it would be out of place to discuss it further at this point. However, it does seem advisable to give a reference to a further source of information.²⁰

Perhaps one of the simpler methods of securing successful bonds between rubber and metal is to make use of an adhesive known as Ty-ply, a trademarked product of the R. T. Vanderbilt Company, 230 Park Avenue, New York. Ty-ply

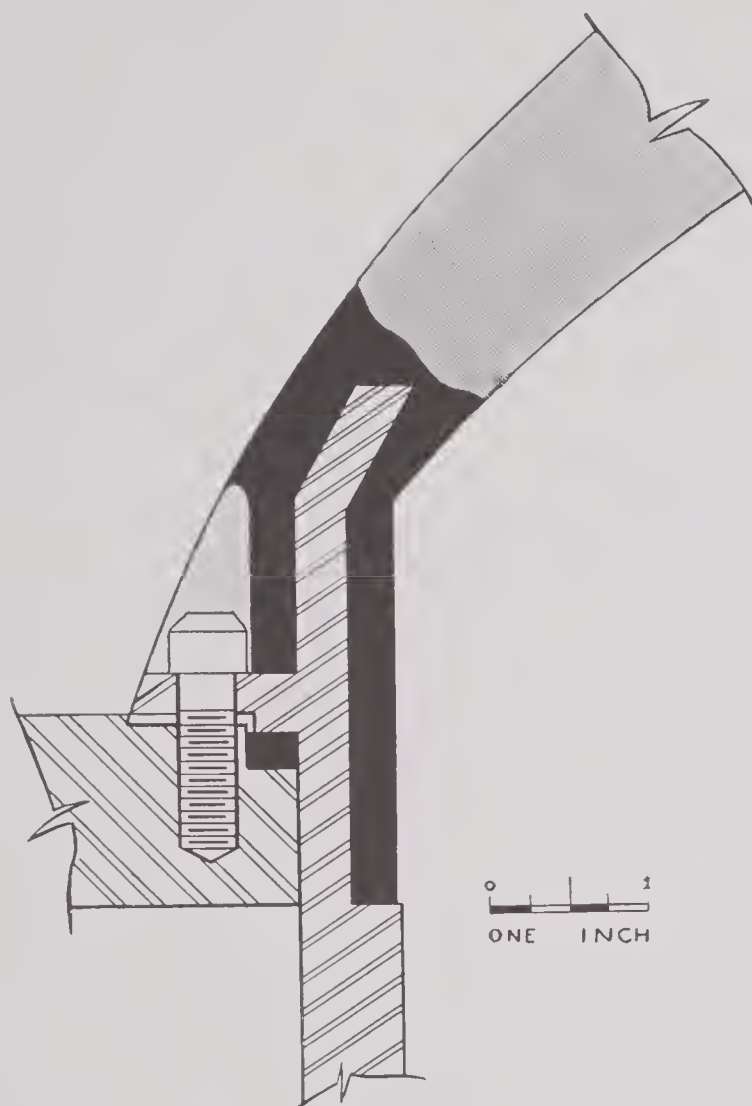


FIGURE 67. A cross section of the metal-rubber bond in the spherical JK transducer window. An extremely long water-to-liquid path is provided by the long metal tongue extending into the rubber. Note that the bonding of Goodrich qc rubber to metal has required an intermediate rubber layer; note also the presence of a rectangular shaped rubber gasket for sealing the transducer window to its case.

comes in several formulations intended for bonding various rubber compounds to practically any metal.

In bonding Goodrich Compound 79-SR-32 to metal it is first necessary to follow the coating of Ty-ply with a layer of intermediate rubber or tiegum. The uncured qc rubber stock is then placed on the intermediate layer and the whole assembly cured together.

This type of bond is illustrated in Figure 67 which depicts a cross section of the window for a spherical JK transducer. Of especial interest in this illustration is the length of path that water would have to travel in order to enter the transducer along the rubber-metal bond, a distance of approximately 5 in. A cardinal point in designing rubber metal bonds is to have this path as long as possible. It is also important to so design these bonds that there will be no regions of the rubber subjected to excessive tension. Another illustration of the design of a rubber metal bond is shown in Figure 66. This illustration represents a cross-sectional view of a UCDWR-type GD flat window. It will be noted that although the total thickness of this window is $\frac{1}{2}$ in. the minimum path along the bond between the two sides of the window is over an inch.

The Goodrich qc rubber window in the UCDWR-type CQ8Z transducer consists of a semicylindrical shell 2 in. thick. This window has been bonded by butt-jointing the rubber to a flat metal surface so that the minimum path between the two sides of the window is 2 in. (see Figure 33 of Chapter 1). Some difficulty has been experienced with the quality of the bonds in this particular transducer. It seems that zones of maximum stress, which result from the marked shrinkage of cured qc rubber upon cooling, occur at the external interface between the rubber and metal. Some breaking away of the rubber from the metal has occurred in this boundary region in a number of transducers, both in and out of service. It now seems clear that a superior design for this bond would have included a metal tongue which would have protruded into the rubber in a fashion analogous to that which obtains in Figure 67.

Another example of rubber-metal bonding occurs in Figure 68. In this case the rubber has been bonded to the metal at both ends of the cylindrical cage and also to the steel reinforcing rods. The uncured stock, Compound M-163, discussed in this section, was bonded directly to the steel with Ty-ply-Q cement.

CYLINDRICAL RUBBER CASES

Cylindrical rubber tubes are frequently a great convenience in the housing of experi-

mental transducers. This is often true even though the transducer is intended to radiate sound in only one direction. This convenience arises from two factors; (1) cylindrical tubing is either readily available in stock sizes or it can be made to order on short notice from commercial firms who maintain a supply of stock mandrels, and (2) a cylindrical rubber tube or sock may be advantageously installed by pulling it over the metal framework of a transducer and then made waterproof by clamping metal bands about it at each end. Methods of clamping such cylinders are discussed in some detail in Section 8.9.3.

Tubular cylinders of rubber may be formed easily in the laboratory with a minimum of processing equipment and without the necessity of designing expensive molds. To start with, a mandrel is prepared whose external diameter represents the desired internal diameter of the finished rubber cylinder. Upon this cylindrical mandrel, which is mounted temporarily between centers in a locked position, is wound the uncured rubber sheet. Layers of the uncured stock, about $\frac{1}{8}$ in. in thickness, are successively wound upon the mandrel until the desired diameter is reached. To allow for grinding this diameter should be about $\frac{1}{4}$ in. larger than the outside diameter of the finished product. Extreme precautions must be taken to prevent the inclusion of air between the rubber layers. The layers of rubber are held in place by wrapping the assembly as tightly as possible with thoroughly wetted cloth tape. When the rubber is later cured in a steam autoclave, great pressure is exerted on the rubber owing to the shrinkage of the cloth and to the thermal expansion of the rubber stock. The correct steam pressure and curing time depend on the type of rubber. Upon removal from the autoclave, the mandrel is again mounted between centers, the cloth tape removed, and the rubber cylinder ground to a smooth finish of the correct outside diameter. A high-speed lathe tool-post grinder is convenient for this operation.

A slight alteration of this technique which results in an improved rubber cylinder for some transducer applications, is to bond the rubber tube to metal end rings. These end rings are machined so that the final seal to the main body

of the transducer may be made with a gasket and gasket groove if desired. The design of the metal-rubber bond between the end rings and the rubber cylinder should follow the suggestions outlined in this section.

MOLDED-RUBBER CASES

Rather extensive use of molded-rubber cases has been made, especially for small transducers which are cylindrical in cross section. An example of a rubber window cap which may be included in this category is shown in Figure 21 of Chapter 1. For the most part, however, these cases consist essentially of a somewhat longer cylindrical tube with a molded bottom. They may be attached to transducers by the banding operation described in Section 8.9.3 or they may have a metal ring bonded to one end which permits a gasket seal to be made to the main body of the transducer.

While some rubber housings may be made by cloth-wrapping cylindrical mandrels in the manner described in Section 7.4.4, it is usually preferable to mold them under high pressure in order to render them free of occluded air. Flexibility of design with respect to shape is an important consideration, especially for streamlining small transducers.

STEEL-REINFORCED RUBBER

Transducer cases and windows in which the rubber has been reinforced by steel rods or bars have been found especially useful in the design of inertia-drive units where the crystals may be bonded directly to the rubber. This type of construction has been discussed in Section 8.7.3. The steel-reinforced rubber case for the transducer shown in Figure 40 of Chapter 1 is illustrated in Figure 68. In this transducer the location of the crystals is on the interior surface of the rubber cylinder midway between adjacent pairs of steel rods. A somewhat similar type of construction has been used in the UCDWR-type GD 34Z transducer window. Photographs and drawings of this window appear in Chapter 6. Instead of rods it contains rectangular steel bars 1 by $\frac{1}{8}$ in. in cross section.

Experience at NRL has shown that unusually strong, large sonar domes can be made of rubber by molding into the rubber a lattice work

of reinforced steel. By welding a meshwork of $\frac{3}{16}$ -in. steel rods together on $1\frac{1}{2}$ -in. centers an unusually strong structure can be fabricated and yet give little interference to sound radiation at frequencies of 24 kc and less. In order to obtain high transmission, the rubber molding and the bonding to metal must be done in such a manner as to avoid the inclusion of air in the rubber. This requires the use of very high pressure during the molding operation.



FIGURE 68. The reinforced rubber window used with inertia-drive transducers such as shown in Figure 40 of Chapter 1. Note the provision for capping the ends of this transducer by means of the grooves for O-ring hydraulic gaskets.

It appears to the writer that the use of reinforced steel in rubber windows for underwater sound applications has great possibilities and that much work should be devoted to its further development.

8.8.5 Corrosion-Resisting Coatings

The corrosion resistance of metals and alloys has been discussed in Section 8.8.1 in connection with Table 2, which listed these materials in an electromotive or galvanic series for sea water. Other things being equal, it would seem highly desirable to make use of one of the more highly resistant metals in the fabrication of transducer cases. Since this may not always be feasible, for economical or mechanical reasons, recourse must be had to methods of improving the corrosion resistance of the metals available.

In recent experience at UCDWR it has been

found that the most satisfactory coating for inhibiting corrosion in sea water is a plastic material sold under the trademark of Amercoat, a product of the American Pipe and Construction Company, Los Angeles 54, California. Amercoat is available in a number of types and colors. For best results the treatment consists of a priming coat, a body coat, and a seal coat. In order to be most effective it is quite important to apply Amercoat plastic coating in strict compliance with the detailed instructions furnished



FIGURE 69. A UCDWR type CQ transducer with its cylindrical rubber window covered with marine growth.

by the manufacturer. Hence, it seems unnecessary to enter into a further discussion of method at this point.

Transducer cases constructed of cold rolled steel (see Figure 33 of Chapter 1) have been painted with Amercoat at UCDWR in order to

make experimental observations of its effectiveness. A period of exposure to sea water of approximately 3 months has elapsed at this writing and the cases are still in excellent condition. There is reason to believe that Amercoat would also protect other metals, including aluminum. Although plastic coatings seem to offer the greatest promise at the present time as a corrosion resistant treatment, additional observations will have to be made over much longer periods of time.

The fouling of rubber windows by marine organisms is a problem of great concern in the construction of underwater sound equipment. An example of the appearance of a qc rubber window that has been badly coated with marine life during an exposure to sea water in the San Diego area for 3 to 4 months, is furnished by the photograph of a UCDWR-type CQ6Z transducer in Figure 69. Experimental measurements have shown that the transmission of sound radiation through such a window has been very materially reduced. This decrease in transmission has been ascribed not only to the presence of organisms themselves but also to the gas bubbles entrapped. The directivity patterns of the lobe suppressed receiving array in this transducer were very badly distorted owing to the marine growth.

Antifouling paints which are sufficiently flexible to be used on rubber have been under investigation at NRL. Their formulation NRL-P-10 antifouling paint is reported to prohibit successfully the attachment of marine growth to rubber windows. This paint has been made available commercially by the Akron Paint and Varnish Company of Akron, Ohio. It is understood that specifications covering this antifouling paint and its method of application are contained in BuShips specification No. 72Re78Z1149A. There has been no experience at UCDWR on the effect of this paint on transducer windows, either acoustically or biologically.

8.8.6

Miscellaneous Seals

GASKETS

Most transducers are sealed by means of gaskets. Although gaskets may be made of any one

of several different materials the most common composition for transducer applications consists of rubber. The quality of the rubber gasket where one is interested in a permanent seal is a very important matter. Only natural rubber stock should be used where transducers must be in service over very long periods of time. Materials which will take a set eventually upon being subjected to pressure will ultimately result in a failure of the seal. The best practice consists in confining the rubber gasket within a groove or other enclosure so that it is possible to maintain it permanently under high pressure. Such a groove or confined space occurs in numerous illustrations in this chapter, including Figures 67, 70 to 73, 81, and 82.

The most common type and size of rubber gasket used at UCDWR was a $\frac{1}{8}$ -in. diameter rod. This was bought in rolls and cut to length for each individual application, as illustrated in Figure 81. The standard groove had a width of $\frac{1}{8}$ in. and a depth of $\frac{5}{64}$ in. Neoprene gaskets have been used with satisfaction although they do take a permanent set. They are never re-used in case a transducer is opened for repair.

O-RING HYDRAULIC GASKETS

O-ring hydraulic gaskets have proved themselves very convenient for liquid-tight seals in transducer cases. An example of one transducer which was designed to be sealed with O-ring gaskets is illustrated in Figure 62. The two O-ring grooves of rectangular cross section are clearly evident in both the top and the bottom bulkhead. This unit was designed to fit into a cylindrical case consisting of a rubber sleeve bonded to metal end rings. The metal rings had a smooth interior finish which permitted them to slide over the O-rings in the assembly of Figure 62. The metal parts had a clearance of a few thousandths of an inch. The external appearance of the case for the transducer in Figure 62 was identical with that shown in the left half of Figure 68, but the rubber was not reinforced with rods. The metal ends of this cylindrical housing also contained grooves for the installation of O-rings so that the transducer case itself could be sealed on either end into sections of thin walled tubing. The tolerances for the grooves in which O-rings are to



be installed are fairly critical. For suitable design dimensions reference should be made to the standard Army-Navy specifications for O-ring hydraulic gaskets or to other appropriate sources of information. Further details on the correct installation of O-rings will be found in Section 8.9.3.

GLASS-METAL TERMINAL SEALS

In many transducers a junction box is provided in which the cable wires may be attached to the transducer terminals. It is customary to

trical and mechanical characteristics. In particular, tables of safe operating voltages as a function of relative humidity are essential for design.

In most cases these glass-metal terminals may be soldered directly into the bulkhead which separates the liquid compartment of the transducer from the air-filled junction box. Where the bulkhead material does not permit soldering, a method has been devised in which an O-ring hydraulic-rubber gasket may be employed. A hole in the metal bulkhead is made with its cross section as shown at the left in Figure 70, which also shows the O-ring in place and the glass-metal terminal partially inserted in the hole. A rim of metal about the hole has a beveled contour so that it can be easily pressed against the flange of the glass-metal terminal.

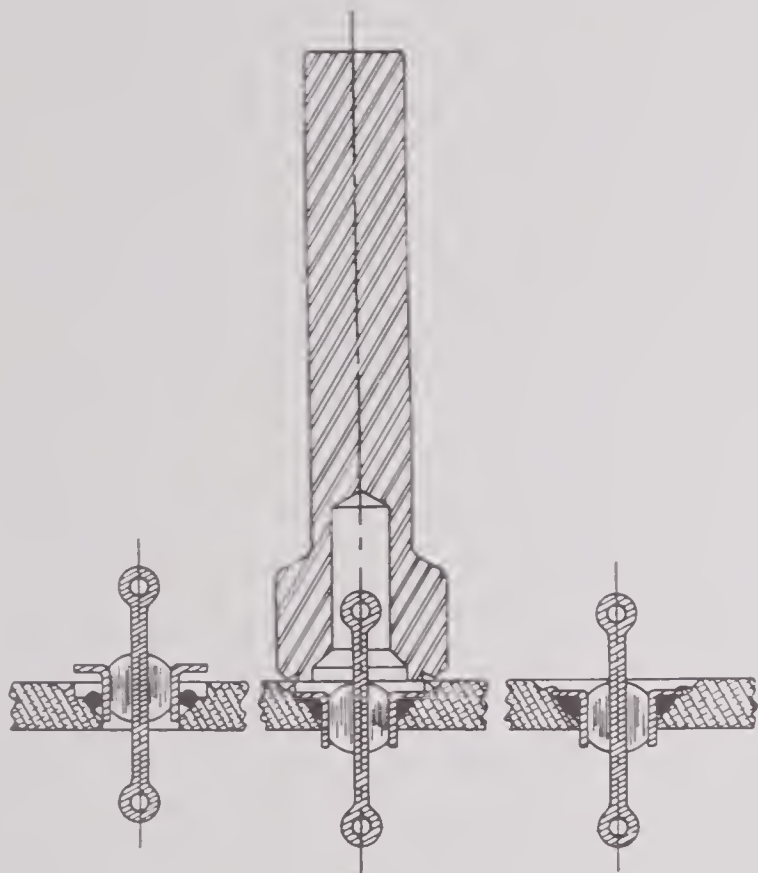


FIGURE 70. Three stages in the installation of a glass-metal terminal seal in a Dural bulkhead. See text for explanation.

have the junction box contain air at atmospheric pressure. This arrangement is much more convenient than one in which the cable enters directly into the oil compartment and obviates the use of oil-tight cables. The leads from the transducer motor are best brought out from the oil compartment by means of glass-metal seals. Such seals are available commercially from Sperti Incorporated, Cincinnati, Ohio, or from Stupakoff Ceramic and Manufacturing Company, Latrobe, Pennsylvania, in a variety of types and sizes. Extensive data are available from the manufacturers on their elec-

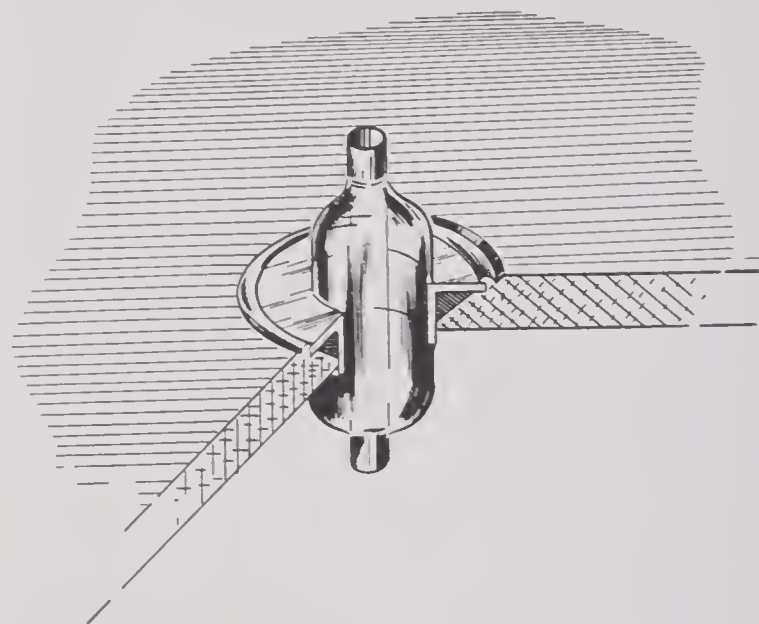


FIGURE 71. A view of a hollow glass-metal terminal seal installed in a Dural bulkhead with an O-ring gasket. A wire lead is first brought out through the hole and then soldered to the insulated metal tube.

It has proved very convenient to use a special burnishing tool for the installation of these terminals. A satisfactory tool is shown in section in the central drawing of Figure 70, just prior to contacting the metal for the burnishing operation. This tool rotates rapidly in a drill press which enables pressure to be applied at the same time. The final appearance of the glass-metal terminal seal in the bulkhead is shown in Figure 71. No difficulty has been experienced with glass-metal terminals installed

in this manner and many thousands of them have been used in expendable transducers made of Duralumin. In the glass-metal seal shown in Figure 71, a small tube comprises the conducting element. In some cases these are especially convenient in that the leads from the crystal motor may be brought out through these tubes and then soldered, thereby eliminating the additional length of wire which would be required if the soldered connection had to be made beneath the bulkhead before the latter was placed in position.

PACKING GLANDS FOR CABLES

Although several types of cable packing glands are in current use, all of them function on the same basic principle. A common design is illustrated in Figure 76. The essential feature is that the cable shall pass through a gland in which a rubber washer can be compressed until a tight seal results between the rubber and the cable, and between the rubber and the internal wall of the gland body. For best performance the dimensions and clearances provided for a given size cable are fairly critical. For this reason detail drawings and a table of dimensions for the cable-gland stuffing boxes used at UCDWR are reproduced in Figure 72. The most common size of cable employed had a diameter of 0.38 in.

Although the metal parts could conceivably be made of any one of several metals or their alloys, it has been the practice at UCDWR to use brass for the entire assembly. In most instances, the composition of the rubber washer is very important. In order to maintain a permanent seal, this washer should be made of a good grade of gum rubber. Otherwise, it is subject to decompression with a resultant loosening of the seal. It has been found convenient to cut the rubber washers from Garlock rubber tubing having approximately the inside and outside diameters listed in the table of Figure 72. The correct amount of tightening of the gland nut is a critical procedure. If too loose, water will leak past it; if fastened too tightly, there is danger of breaking the wires within the cable. In the limit the entire cable could be pinched in two. To start with, threads on packing gland nuts should permit the nut to turn very freely,

in other words, a loose fit is desirable. The object is to make it possible to gauge the extent to which the rubber is compressed by the torque required in turning the nut. Some experience in this connection seems to be an essential.

In some laboratories it is customary to prepare specially the cable at the point where it

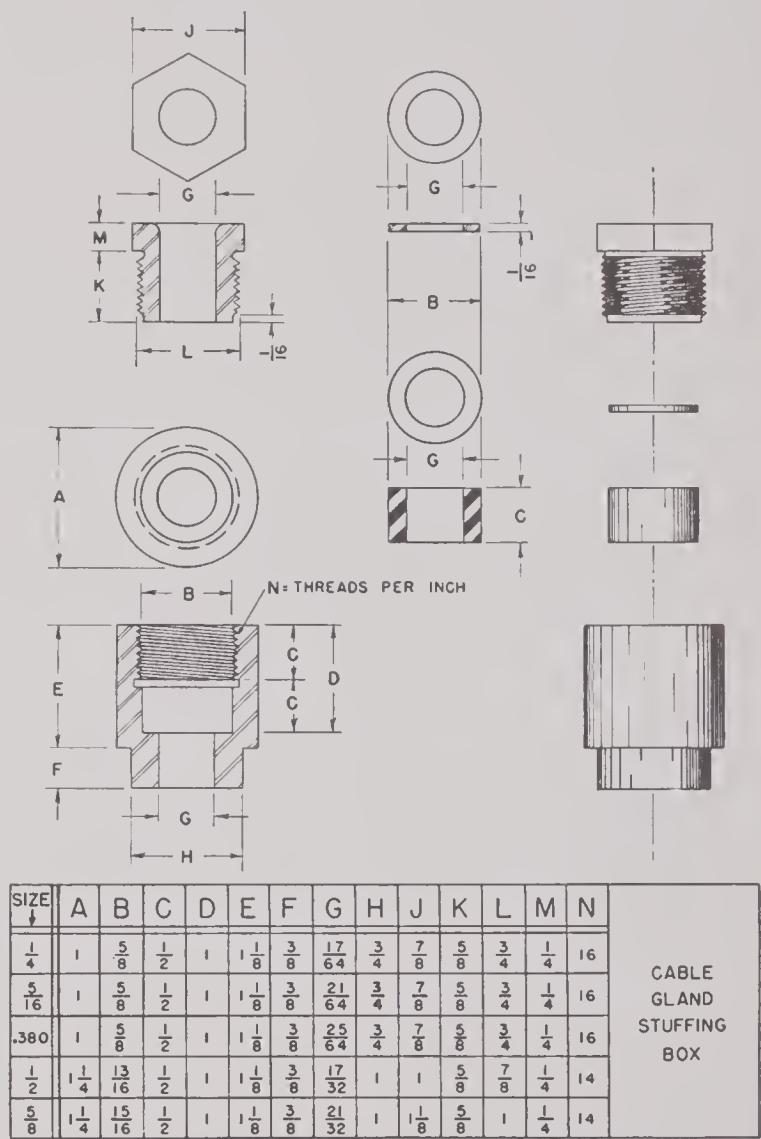


FIGURE 72. Shop drawing of the cable-gland stuffing boxes regarded as standard at UCDWR.

passes through the gland in order to avoid damaging the wires by overcompression of the rubber washer. This method is presented in detail in Section 8.8.8 and illustrated in Figure 75.

OIL PLUGS

The present method of installing tapered oil plugs at UCDWR has proved quite successful

and it is very seldom that failures occur involving them. Small plugs with standard iron pipe threads are used, preferably of brass and usually in a small size as $\frac{1}{8}$, $\frac{1}{4}$, or $\frac{3}{8}$ in. Current practice calls for carefully cleansing the oil plug in benzine and then immediately coating the clean plug with Glyptal paint before any contamination can take place. The concentration of the Glyptal is rather critical. It is somewhat too thin as it comes from the can but on exposure to the air gradually thickens. When

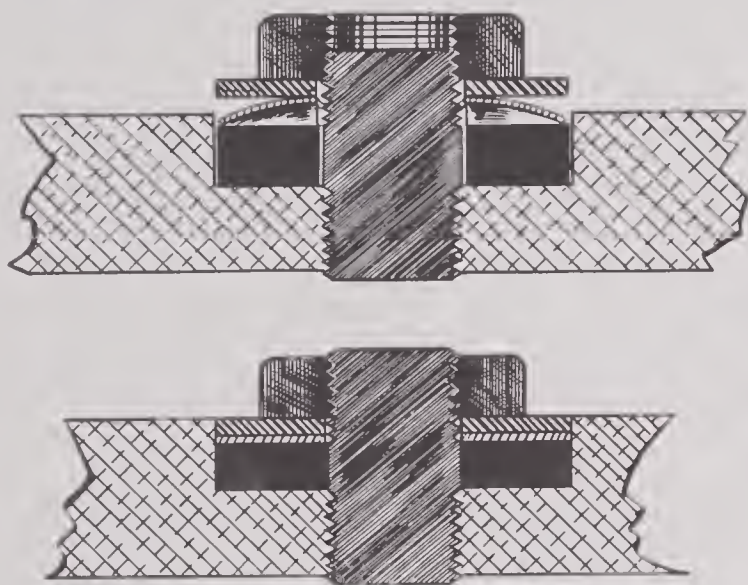


FIGURE 73. Cross section of the oil plug seals used by the Bell Telephone Laboratories. Above: before tightening. Below: after tightening.

too thick it does not adhere well, so it is better to be too thin than too thick. The recommended method of application is complete immersion of the threads in the Glyptal. The plug is then inserted in the oil plug hole. If the hole has been correctly tapped, the plug will begin to tighten after a few turns. The old rule, "tighten until you can't turn it any more and then give it another full turn," is not far wrong provided care is exercised to avoid stripping the threads. When done correctly the Glyptal adheres very tightly to both the plug and the case, making a very good seal. Units sealed in this manner have withstood depths of water up to 800 ft.

Considerable difficulty had been experienced in the past at UCDWR with tapered oil plugs. When an oil plug leaked, whether as a result of faulty design, defective materials, or improper installation, the crystal motor of the transducer often became a complete loss. In

the early history of UCDWR, the use of tapered oil plugs was so unreliable that every unit was water tested before it was considered ready for service. A pressure chamber designed for use up to 300 psi was used as a testing device to detect both defective oil plugs and stuffing glands. With electrical attachments on the pressure tank, resistance readings could be made continuously on the unit under test. If failure was indicated, the pressure was released quickly and the unit removed from the water before irreparable damage was done to the crystal motor.

To avoid the difficulties encountered in making watertight seals with tapered oil plugs, BTL have adopted a different type of seal. The details of their watertight seal are depicted in Figure 73. It depends on the compression of rubber between two surfaces. Since this type of seal has been used satisfactorily for cable packing glands and in numerous other applications, it should be entirely acceptable. The use of a cup-shaped spring washer insures a minimum clearance following the tightening of the top nut. The rubber washer should be of pure gum stock so that it will not take a permanent set. After filling the transducer with oil, the threaded rod is screwed into the hole; the rubber gasket, the spring washer and the flat washer are added in order and the top nut is turned down very tightly.

8.8.7 Sound Absorbing and Reflecting Pads

ABSORBING PADS

Materials discussed in Section 8.7.5 provide acoustic isolation because they act as good reflectors of sound radiation. In many applications it is highly desirable to absorb the acoustic energy. This, however, is quite difficult to achieve, especially in a small space. The problem has been investigated in great detail by W. P. Mason and reference may be made to two reports from BTL for a discussion of the factors involved,¹⁵ together with performance data on an acoustic measuring tank in which sound absorption materials were employed.²¹ The best attenuation reported by Mason resulted from the motion of a viscous liquid through small interstices in metallic wool pads or in fine-mesh

screen. In practice fine-mesh screen is superior to metallic wool in that it permits better control of the critical dimensions and makes fabrication less difficult. Viscous liquids by themselves must be used in too great thicknesses to be valuable as absorbing layers for underwater sound applications.

The screen type of construction is illustrated in Figure 74, where some 20 sheets of 100-mesh Monel screen, made of 0.004-in. wire, are shown separated by strips of coarse expanded metal.

obtainable from this type of construction, beyond which the addition of more screens does not result in increased absorption. This practical limit is in the neighborhood of 30 db for radiation reflected from the pad. Some improvement would naturally be expected from replacing the expanded metal by separator strips having more nearly the acoustic impedance of the liquid; with castor oil, narrow strips of gc rubber might be used. To make such a pad sufficiently strong mechanically, bonding of the

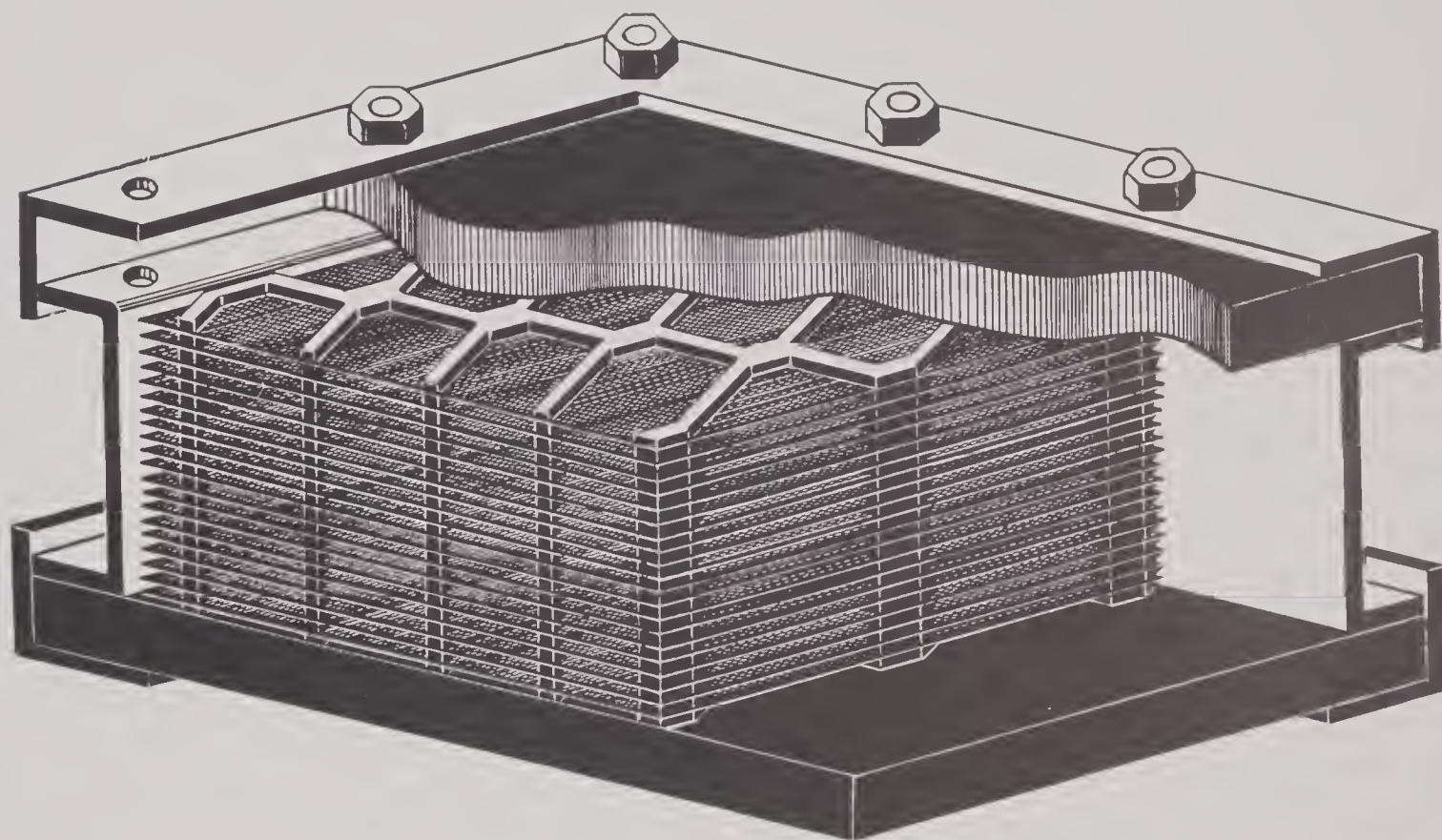


FIGURE 74. Wire mesh attenuator pad developed at the Bell Telephone Laboratories. See text for further details.

On reflection of sound waves from such a pad, an attenuation of about 20 db is obtained at frequencies over 20 kc. A useful rule-of-thumb indicates 0.5 db attenuation per screen for direct transmission or double that for reflection losses. A spacing of 5 to 10 screens per inch makes a satisfactory construction in the 20- to 100-kc range. Where special or critical applications are under consideration, calculations should be based on the equations in the articles cited^{15, 21} to determine optimum mesh size and spacing.

There is a practical limit to the attenuation

metal screen to the narrow rubber strips is suggested as highly desirable. Further improvement might also be sought in the direction of a better viscous liquid, particularly where temperature fluctuations are large during normal usage. Possibly some of the fluids used in hydraulic drive mechanisms might be adapted for this purpose, such as the Univis oils or the Union Carbide and Carbon Company's series HB Ucon 600 oils. The silicones should also be considered. In this connection, read also Section 8.8.9.

Since this type of attenuation pad is neces-



sarily bulky, its usefulness in small transducers is severely limited. The principal application to date has been in large acoustic domes in order to decrease interference from propeller noises and in the measuring tank already mentioned. Some of the large transducers might conceivably profit by these pads. They have been used in one transducer designed by BTL, as illustrated in Figure 11 of Chapter 1.

REFLECTING PADS

The fact that it has been difficult to secure adequate sound absorbing materials for transducer applications has led to the wide use of reflecting materials. Sound reflecting pads may be made of the acoustic-isolation materials discussed in Section 8.7.5. The most commonly used substance is either Corprene or cellular rubber. Since they are available in large sheets, they may be cut to size readily for covering areas of any size and shape which occur inside transducers.

In the transducer shown in Figure 4 of Chapter 6 the interior walls of the steel cylinder were lined with Cell-tite rubber. Since this particular transducer contained both a transmitting and a receiving unit it was also necessary to provide for acoustic isolation between them. This isolation was provided in part by the insertion of reflecting materials between the two crystal assemblies. The presence of the reflecting pads between the two units was not enough to eliminate crosstalk entirely since some transmission of sound occurred through the neoprene window. When substitution of qc rubber provided a better impedance match to the sea water, there was a noticeable decrease in crosstalk. In the later production model of this transducer (see Figure 33 of Chapter 1), the 2-in. thick qc cylindrical window had a steel member embedded in it to reduce the crosstalk through the rubber window.

The installation of sheets of either corprene or cellular rubber is accomplished simply by cementing the sheets to supporting structures. In the case of Cell-tite rubber it is important that the material not be stretched in applying it to an extended surface. Oftentimes, these reflecting pads may merely be laid in place or packed beneath the backing plate.

8.8.8

Electric Cables

SPECIFICATIONS AND TESTS

Electric cables for transducer applications must, generally speaking, satisfy two requirements, one electrical and the other mechanical. The electrical properties which are primarily important have been discussed at length in Section 5.2 of Chapter 5.

Mechanical considerations with regard to transducer cables have to do with ultimate tensile strength and freedom from liquid leaks. In short lengths of cable the mechanical strength of commercial materials is usually more than ample. Where extremely long cables are used, perhaps 500 or 1,000 ft in length, ordinary rubber covered cable may fail. For such applications it may be necessary to use cables with steel cores.

The most commonly used cable at UCDWR has been a two-conductor shielded cable known as Simplex 9061 (also AA60 or SA60). Its capacitance per foot and its power factor as a function of frequency have been given in Figure 3 of Chapter 5.

OIL-TIGHT CABLES

In transducers where the cable enters directly into the oil compartment, it is essential to provide an oil-tight cable. Although this may be accomplished in any one of a variety of ways, the most desirable procedure appears to be one employed at NRL. This consists in stripping off the insulation so that the conducting wires are completely laid bare, including the individual strands. The strands of wire in each conductor are then fluxed and soldered together to give a compact leakproof bundle. The conducting wires, which protrude about 2 in. from the insulated part of the cable, are now placed in a special mold, as illustrated in Figure 75. The rubber insulation of the cable next to the bare wires is now very carefully cleaned and roughened in order to insure that a good bond can be made to it with the uncured rubber which is about to be placed around the bare wires. Uncured rubber stock is now used to fill up the mold and the entire assembly is placed in a steam autoclave. Curing is done at the pressure and for the time recommended for the partic-

ular grade of rubber in question. Ty-ply-Q (see Section 8.8.4) is used on the bare wires and also on the rubber cable insulation in order to secure adequate bonding.

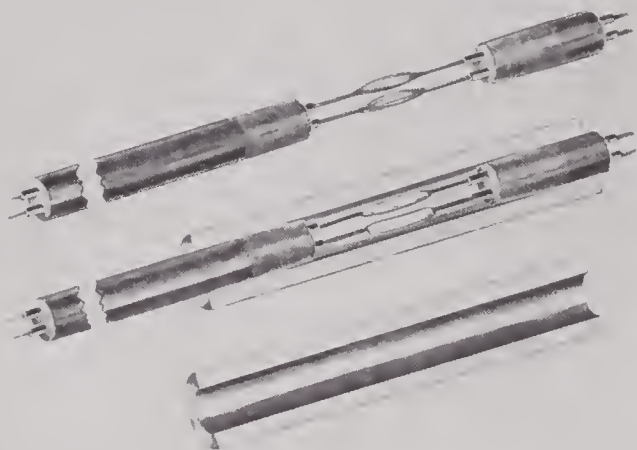


FIGURE 75. Stages in the preparation of a cable to make it liquid-tight by molding uncured rubber about stranded conductors. Above: Bare strands exposed and rubber sheath roughened. Below: Strands soldered together and cable placed in semicylindrical mold ready for addition of uncured rubber stock.

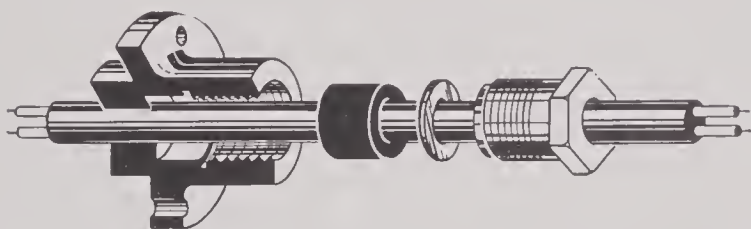


FIGURE 76. Cutaway view of the cable gland seal regularly employed at UCDWR. For standard dimensions, see Figure 72.

8.8.9

Filling Liquids

CHARACTERISTICS AND SPECIFICATIONS

The traditional liquid for filling underwater sound transducers is Baker's DB-grade of castor oil, a highly purified product prepared for electric capacitors by The Baker Castor Oil Company, Bayonne, New Jersey. The specific factors which enter into the choice of this particular liquid are not a matter of record as far as the writer is aware, but its selection could conceivably rest on several properties. Its impedance is a fairly close match to the impedance of sea water, castor oil having a density of 0.95 to

0.96 g per cu cm and an acoustic velocity of 1,540 m per sec. These values may be compared to a density of 1.03 g per cu cm and a velocity of 1,500 m per sec for sea water. DB castor oil is inert toward the many common components of a transducer, namely, ADP and RS crystals, natural and synthetic rubber, various types of adhesives, and many metals. It is relatively easy to dehydrate and to free from dissolved gases. However, the variation of the viscosity of castor oil as a function of temperature is very marked and an improvement in this respect could be obtained by adopting any one of several other liquids.

A systematic attempt to obtain a better liquid for filling transducers has been made by W. P.

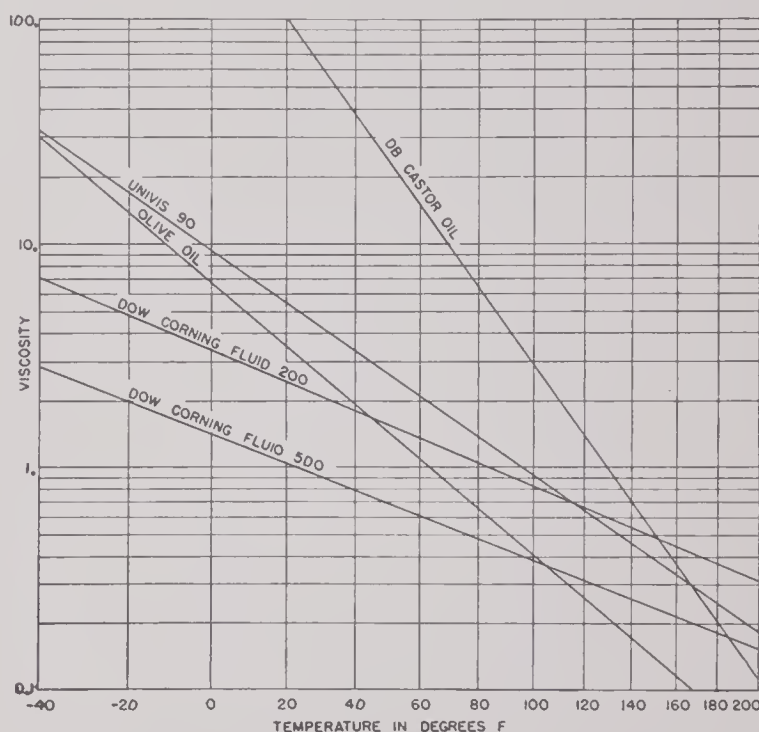


FIGURE 77. Viscosity-temperature curves for various liquids.

Mason and reference is made to his report¹³ for a complete discussion. Mason was interested particularly in increasing the power handling capacity of crystals and to this end he wished to have a liquid with a high cavitation level. Among the numerous liquids and vegetable oils investigated, dimethyl phthalate, olive oil, peanut oil, and sperm oil were definitely superior with respect to cavitation. With DB castor oil, RS crystals were nearly always destroyed by burning before any cavitation occurred. For increased power handling capacity and higher efficiency, the most desirable liquid to use ap-

pears to be one with a low viscosity. Olive oil, for example, which has a viscosity less than that of castor oil, can consistently radiate as much as 2 w per sq cm without cavitation. This may be compared to a reported value of 0.7 w per sq cm for castor oil. However, olive oil would necessitate that the window be not of rubber, which it attacks, and that a compatible cement, such as Acryloid, be used. Dimethyl phthalate will likewise stand 2 w per sq cm without cavitation, but this liquid softens Vulca-lock and Bakelite BC-6052 cement, although it does not attack rubber.

An acetylated castor oil known as Baker's grade P-8 has some desirable characteristics for use in transducer construction, but it has been found to deteriorate other transducer components, especially rubber. In a controlled study at UCDWR, it was found that neoprene swelled very badly when immersed a few days in the P-8 oil. This observation may be contrasted with the behavior of neoprene in the presence of DB oil, in which case no deterioration has been observed even after an exposure of 4 years duration. With neoprene cellular rubber stock in P-8 oil, it was found that the cellular spaces were penetrated and filled with oil after a month or two, thereby losing their value as an acoustic reflector. This experience conforms to that communicated in a letter to UCDWR from the Baker Castor Oil Company on July 10, 1945, in which they reported the effect of numerous liquids on a sample of rubber believed to have a natural-rubber base. The per cent increase in volume reported for P-8 oil under their test conditions was 28 compared to a value of 1 for AA grade castor oil (composition reported to be practically identical to DB grade).

Another liquid investigated for transducers by NRL is Ucon oil 50-HB-100, developed by the Union Carbide and Carbon Company. This material is noncorrosive to rubber and bakelite. Its impedance approaches that of castor oil and it is better from the standpoint of cavitation. This oil takes up water quite readily so that great care must be taken to see that it is kept dry. Dehydration offers some difficulty. When purchasing, it is important to insist on material which has a very low value of conductivity. Its electrical conductivity rises upon oxidation to

the point of becoming entirely useless, hence it must be protected from exposure to air.

Most promising of all as a transducer liquid are the two Dow-Corning fluids, type 200 and type 500. The freezing point of all these fluids is below -45°C , so that no concern need be had in this regard for the normal range of operation of sound equipment, even for topside mounting on submarines. In fact, some of these liquids have freezing points as low as -86°C (-123°F). The particular characteristic of importance for high-powered transducer operation is the comparatively slight change in viscosity as a function of temperature. This characteristic will be brought out clearly by an inspection of the curves in Figure 77, where graphic data for DB castor oil and various other liquids are given. These fluids do not deteriorate or soften natural rubber, synthetic rubber, or any of several types of plastic coating. Whether they have an influence on the cements hitherto used in transducer construction has not yet been tested. They are insoluble in water and the lower aliphatic alcohols but are soluble in most organic solvents. Their dielectric constant is approximately 2.8 over a frequency range of 10^3 to 10^8 c. In fact, the only known deterrent to their use at the present time is an economical one in that these fluids cost approximately 6 dollars per lb. However, it may be only a question of time until these production costs are materially reduced. These Dow Corning fluids are generally known as silicones. They are polymers composed of various combinations of organic radicals with silicon oxide.

DEHYDRATION

It has already been pointed out that owing to the solubility of RS and ADP crystals in water, dehydration of the liquid used for filling transducers is necessary. The design of equipment for this purpose is an engineering problem whose detailed solution may take many forms. Without making any claims for the superiority of the equipment used for this purpose at UCDWR, it will be discussed in order that the salient points may be better emphasized. A schematic diagram showing the essential parts of such a system appears in Figure 78.

In dehydrating a liquid with a viscosity as

high as that of castor oil, difficulty is experienced in securing adequate dehydration in a limited period of time. To hasten the removal of water, the liquid should be heated to about 90 F or higher. In addition it is essential to decrease the path which water vapor must traverse in order to escape from the body of the liquid. This can be done in either one of several ways. In the equipment shown in Figure 78 the castor oil is pumped to the top of a long

observed emerging from the liquid while still subjected to a vacuum, the castor oil is regarded as sufficiently dry. While no specific limits on the amount of moisture are specified, it can be noted that the average moisture content of DB castor oil is listed by the manufacturer as 0.01 per cent and the maximum as not over 0.02 per cent. However, there is no possibility of overdoing the dehydration process since ultimately the oil must take up the small amount of mois-

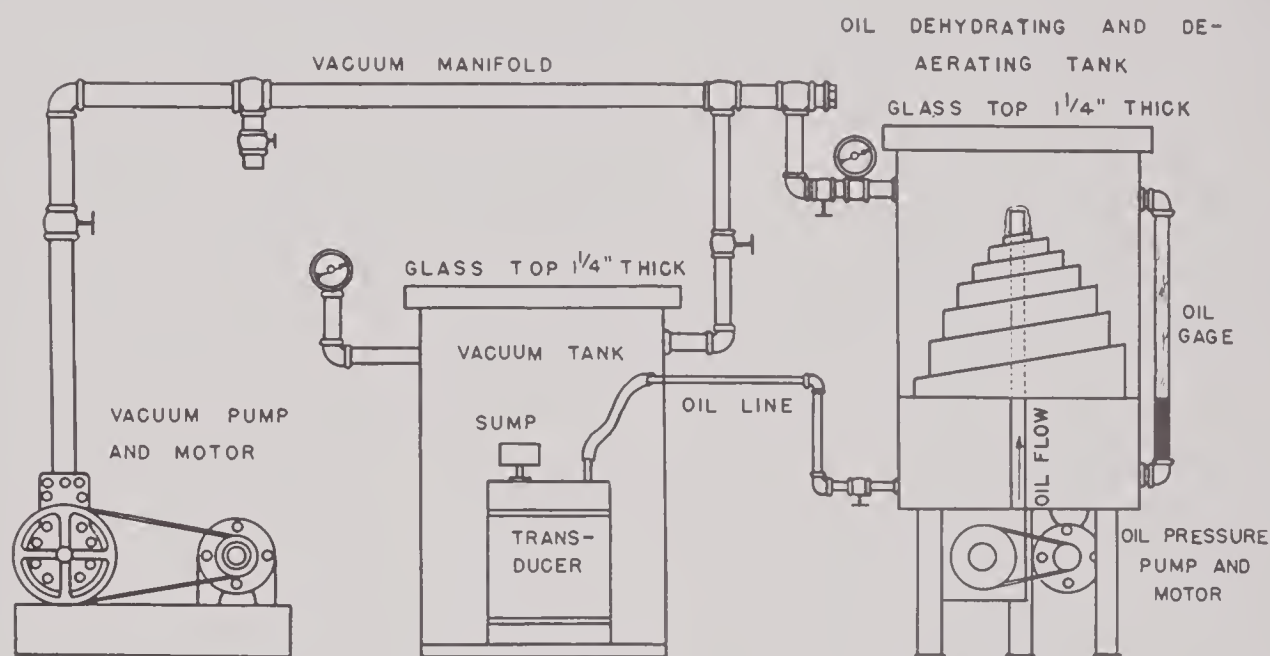


FIGURE 78. Schematic diagram of the UCDWR equipment for degassing and dehydrating castor oil; also the system used for evacuating and liquid-filling transducers.

spiral ramp from where it flows down in a thin sheet in an evacuated chamber and recirculates in this manner until the desired dehydration results. The dehydration system employed at the Brush Development Company achieves a similar aim by having the oil fall on rapidly rotating disks on which it spreads out in a thin layer and is then thrown off the whirling disk against the wall of the vacuum chamber. At BTL, dehydration is achieved by permitting small quantities of dry nitrogen at low pressure to bubble up through the castor oil contained in a series of 3-gallon bottles.

DB castor oil as purchased is not considered sufficiently dry for the direct filling of transducers. It is usually necessary to circulate it for a period of at least 8 hr in an evacuation system with a pressure of 1 cm of mercury or less. When no further bubbles of vapor are

observed emerging from the liquid while still subjected to a vacuum, the castor oil is regarded as sufficiently dry.

The glass top which covers the dehydrating tank in Figure 78 is regarded as a very desirable feature in that it permits direct observation of the condition of the oil. When the vacuum pump is initially started, following the introduction of a fresh sample of oil, intense foaming is likely to occur. This foaming can be held within proper limits by controlling the pressure while observing the behavior of the oil. While foaming has always been observed, even with new castor oil, it is likely to be much more pronounced in oil which has been reclaimed.

Where reclaimed castor oil is to be used again, as is often done in an experimental laboratory, it will be found desirable to incorporate a filter system into the oil processing equipment. Although no specific brand of equip-

ment can be recommended for this application, it is suggested that large oil filters of the type employed in commercial motor trucks should be satisfactory for this purpose.

For heating the castor oil, immersion type strip heaters have proved convenient. It has been the practice to heat castor oil to a temperature of 90 F, although there seems no sufficient reason why it could not be dehydrated at an appreciably higher temperature.

8.9 FINAL ASSEMBLY AND INSPECTION

8.9.1 Installation of Arrays

In the installation of crystal assemblies of the backing plate type into the transducer housing, provision should be made for both mechanical and acoustic isolation. In addition, it may be possible to prevent undesired modes of vibration in the backing plate by a careful consideration of the manner in which it is supported.

Although well-designed crystal arrays are quite rugged, yet some measure of protection for the assembly should be provided. It is suggested that a shock mounting be used when installing the assembly in its case. Such mountings are usually of a very simple type, often consisting of some type of rubber washer. In the UCDWR-type GD case illustrated in Figure 81 the backing plates are usually allowed to rest on a number of sheets of Corprene. By adding additional Corprene around the sides of the motor all metallic connections to the case are avoided. When the window is attached, it presses against a wide rail on the backing plate (see Figure 34 in Chapter 1) and holds the crystal motor in place. The radiating face of the crystal array is usually placed a short distance back of the window, perhaps $\frac{1}{8}$ of an inch. In packing Corprene in the type-GD case, channels must be provided to facilitate evacuation of the case and the subsequent liquid-filling operation.

The method of supporting backing-plate arrays with mounting brackets will be clear from Figure 49. The attachment of these mounting brackets to a transducer case can be visualized

by referring again to Figure 4 of Chapter 6 or to Figure 33 of Chapter 1.

According to the experience of BTL in mounting the crystal array shown in Figure 50, improved performance was obtained by attaching the supporting brackets some distance from the corners of the steel backing plate. This slight alteration in the point of support seemed to be effective in suppressing undesirable modes of vibration in the steel backing plate.

The problem of mounting inertia-drive crystal arrays solves itself for those units where the crystals are bonded directly to a rubber window. Examples of this type of mounting are to be seen in Figure 56 of this chapter and in Figure 40 of Chapter 1. The method of installing the inertia-drive window unit of Figure 56 in its case is illustrated in Figure 82 and discussed in Section 8.9.3. With inertia-drive units that are not bonded to windows some other provision must be made for mounting them in a case. An illustration of one such unit is shown in Figure 62, in which instance the assembly is inserted in a cylindrical rubber housing and sealed by means of an O-ring gasket. This process is discussed in somewhat greater detail in Section 8.8.6.

With stack-type crystal assemblies as developed at UCDWR up to the present time, their installation into a proper housing has been an exceedingly simple procedure. The stack unit illustrated in Figure 59 has circular disks of Corprene or rubber attached to each end of the crystal array, which center the assembly within a cylindrical tin can. These Corprene or rubber disks have the same diameter as the interior of the can and their thickness is selected so that they press lightly against either end of the can. It is usually also desirable to have the corners of the assembly, which in Figure 59 consist of Corprene and Cell-tite rubber, press lightly against the interior wall of the can.

The stack assembly in Figure 60 was mounted in its case by cementing thick rubber disks on either end of the unit and supporting the array between two rigid bulkheads, which were themselves attached to either end of a cylindrical rubber sock. However, to obtain sufficient strength in the housing and still permit radiation over a 360-degree angle, it was necessary

to couple the bulkheads with a cage made of expanded metal. In the frequency range of 60 to 90 kc, the expanded metal did not seriously interfere with either the directivity pattern or the output level of the transducer.

8.9.2 Matching Networks and Cables

Information pertinent to the design and construction of matching coils and/or transformers for transducers has been discussed at length in Chapter 5. In the design of transducer cases it is usually desirable to provide a satisfactory cavity in which these matching networks may be placed. From the standpoint of installation, few difficulties are likely to be encountered. Of principal concern is the necessity for securing adequate electrical insulation for the fairly high potentials to which these networks are subjected during operation. Where the tuning coil or the transformer is immersed in the transducer liquid, insulation is a very simple matter; for location in an air cavity, these components must be provided with the required insulation.

Perhaps the most common difficulty at UCDWR in connection with the installation of matching networks had to do with mistakes in connecting the leads of the network to the proper terminals of the transducer. Errors of this sort usually resulted from an improper or insufficient labeling of the leads. Further elaboration of this point need not be made since the remedy is well-known.

Since the inductance of either tuning coils or other matching network depends on the spatial relationships between the various windings and also on the proximity of the windings to neighboring metallic boundaries, special precautions may need to be taken at times, especially with uncased network components, in order to retain or attain the values of inductance called for in the specifications. In transducers designed for quantity production, this difficulty would probably be met by having all of the electrical networks permanently cased and provided with outside terminals so that the final check on their inductance could be made before their installation in the transducer housing.

In all except small transducers it has been

customary to provide a separate compartment where the electric terminals of the transducer can be attached to the cable. The wire leads from the crystal array or from the matching network are brought into this compartment through liquid-tight seals. This terminal compartment is usually air-filled in order to obviate the leakage of oil, which might otherwise occur through the main transducer cables. Between the main oil cavity of the transducer and the air-filled compartment, it will be found convenient to provide glass-metal terminal seals as

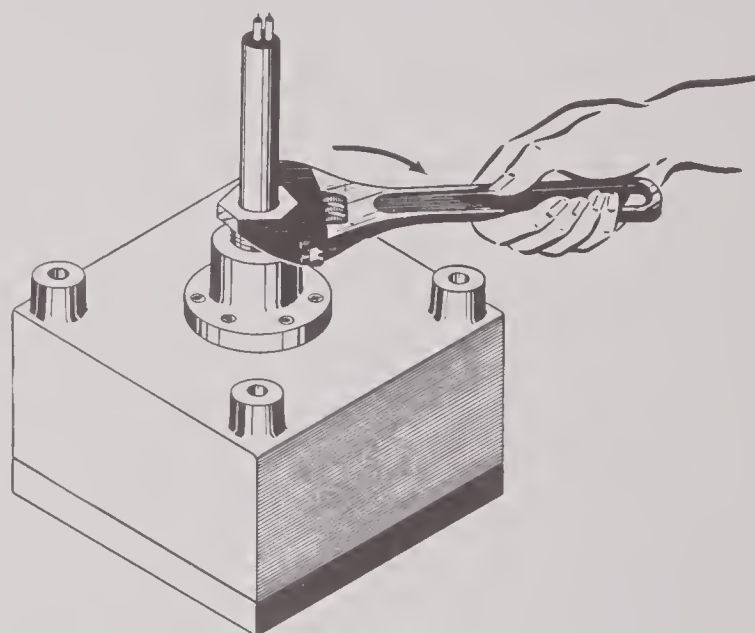


FIGURE 79. Tightening the packing gland nut on a UCDWR type GD transducer. See text for discussion.

described in Section 8.8.6. Another method of providing such a liquid-tight seal would be to use a modification of the cable-gland stuffing box shown in the shop drawing of Figure 72. Where cable is used for this type of connection, it is important to remember that the cable itself must be made oil-tight, perhaps by the method discussed in Section 8.8.8 and illustrated in Figure 75. It should be remembered also that for transducers which operate at great depths the differential pressure between the liquid compartment and the air-filled terminal-block compartment may amount to several hundred pounds per square inch.

In the installation of cable it is necessary to avoid manipulating it in such a way as to break any of the conductors. In particular one should avoid flexing the cable at sharp angles. In tight-

ening the nut of the cable-gland stuffing box it is possible to damage the cable by exerting too great a static pressure on the rubber washer. In extreme cases this can even result in breaking the conductors and thus causing an open circuit. The packing gland nuts should always be freely turning so that it is possible to judge the proper force necessary to tighten them to

8.9.3

Sealing Transducer Cases

BANDING RUBBER CYLINDERS

The suitability of cylindrical tubing as a housing for transducers has been discussed in Section 8.8.4. Much of the advantage derived from such cylindrical socks results from the ease with which waterproof seals may be made

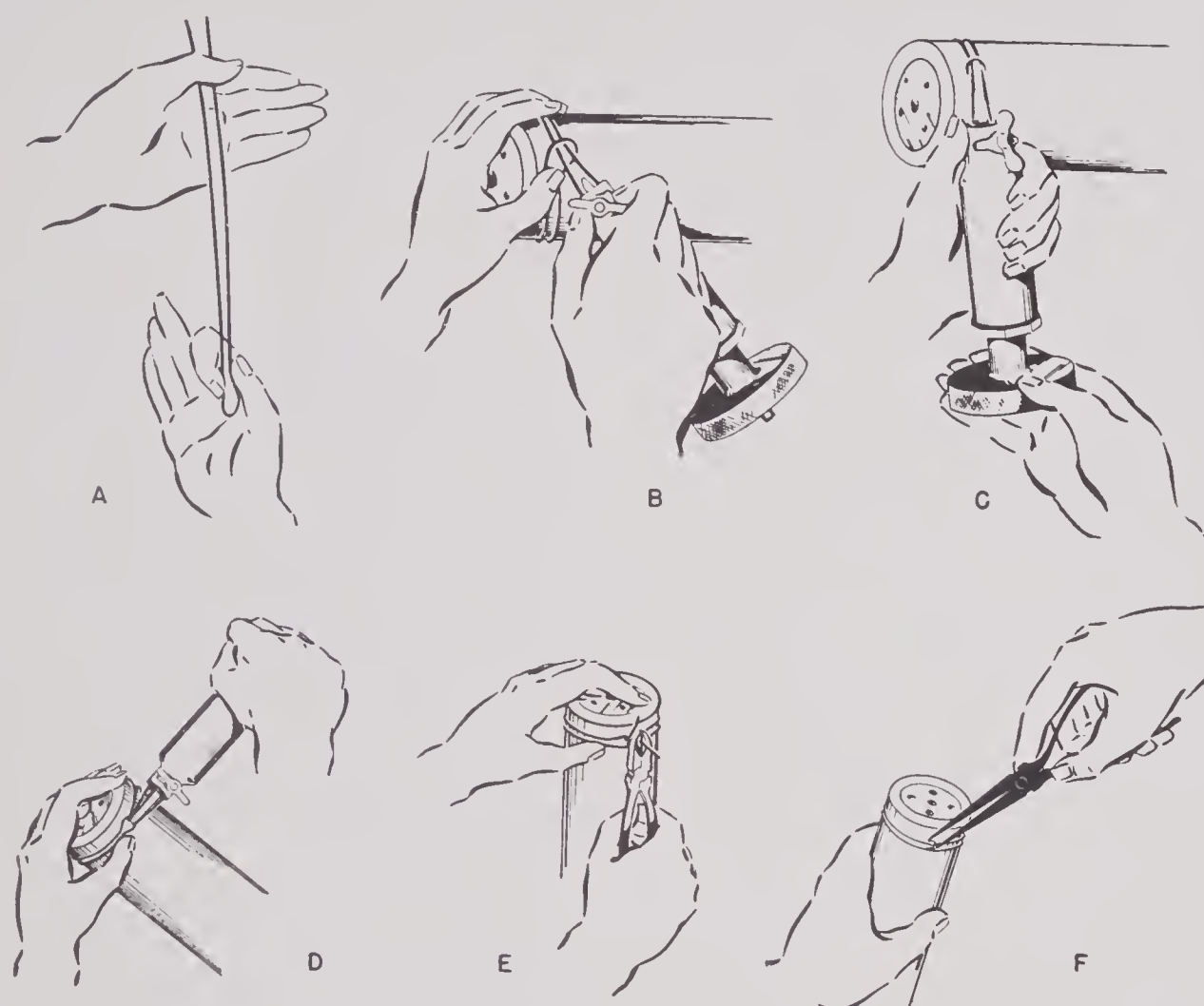


FIGURE 80. Stages in wire-banding a cylindrical rubber sleeve on a transducer. After the wire loop (A) is placed around the rubber cylinder, its ends are firmly gripped by the clamping tool (B) while the tongue of the tool engages the closed end of the wire loop (C). When the wire has been tightened sufficiently by turning the hand wheel (C), the wires are bent sharply around the loop (D), the tool removed and the wire ends cut down to proper length (E). The wire loop is secured by further bending of the wire ends with pliers (F).

the desired point. In the illustration of Figure 79, where a 0.38-in. cable stuffing box (see Figure 72) is being tightened with a wrench, a force of 30 lb at a distance of 7 in. from the cable is an approximately correct value. A little experience will enable one to judge the proper torque for satisfactorily tightening these glands.

to the underlying metal case of the transducer by a simple banding process. The metal ends of the transducer case should preferably possess a number of grooves or serrations. When metal bands are clamped tightly about the rubber cylinder, very high stresses will occur in the rubber in the region of these serrations, thus resulting in a dependable seal.



Cylindrical tubing in smaller sizes may be clamped by means of wires, preferably stainless steel. The several steps constituting an acceptable technique for wire banding are illustrated in Figure 80. A commercial tool designed for this process has been made available by the Chicago Pneumatic Tool Company. The proper length of wire required for a particular band is formed into a loop by bending it at its center (Figure 80A). The wire loop is curved about the rubber cylinder so that both ends of the wires extend through the loop and into holes in the special tool where they are clamped in place (Figure 80B). The wire band may be tightened now by turning the knurled head at the opposite end of the clamping tool until there is a marked depression formed in the rubber (Figure 80C). Judgment with regard to the proper amount of pressure on the rubber will be gained by experience. When the wire is considered sufficiently tight the tool is forced sharply backward as shown in Figure 80D and a finger should be held over the two wires to prevent them from unbending when the tool is removed with the other hand. While continuing to hold down the loose ends of the wires, one of them is clipped shorter with side cutting pliers (Figure 80E) and bent down securely as illustrated in Figure 80F. Then the excess length of the second wire is cut off and anchored securely in the same manner.

For cylindrical transducers whose diameters are greater than 4 in., the Punch-Lok type of band, manufactured by the Punch-Lok Company, Chicago 7, Illinois, is preferred. The Punch-Lok bands, which are $\frac{5}{8}$ in. wide and approximately either 0.020 or 0.030 in. thick, are available in various lengths and in several metals, including stainless steel. It is recommended that stainless steel be employed in instruments which are to remain in service under water an appreciable length of time, as ordinary iron bands would quickly deteriorate. A transducer utilizing this type of banding is shown in Figure 69. A special banding tool is essential for proper installation. The procedure involved is discussed in the manufacturer's direction sheets in sufficient detail. The only special comment required here is that serrations in the metal beneath the clamped region are recom-

mended, as outlined in the previous paragraph on wire banding. Again, experience will help in estimating the amount of compression required in the rubber for a waterproof seal.

A convenient method of tightening a stainless steel band on a transducer is illustrated in Figures 21 and 23 of Chapter 1. The stainless-steel bosses, which have been welded to the bands at either end, have been provided with a clamping-screw mechanism.

GASKET JOINTS

In sealing transducer cases it has been customary to use rubber gaskets to attach various lids and metal plates to the housing. Such metal surfaces occur where rubber windows have

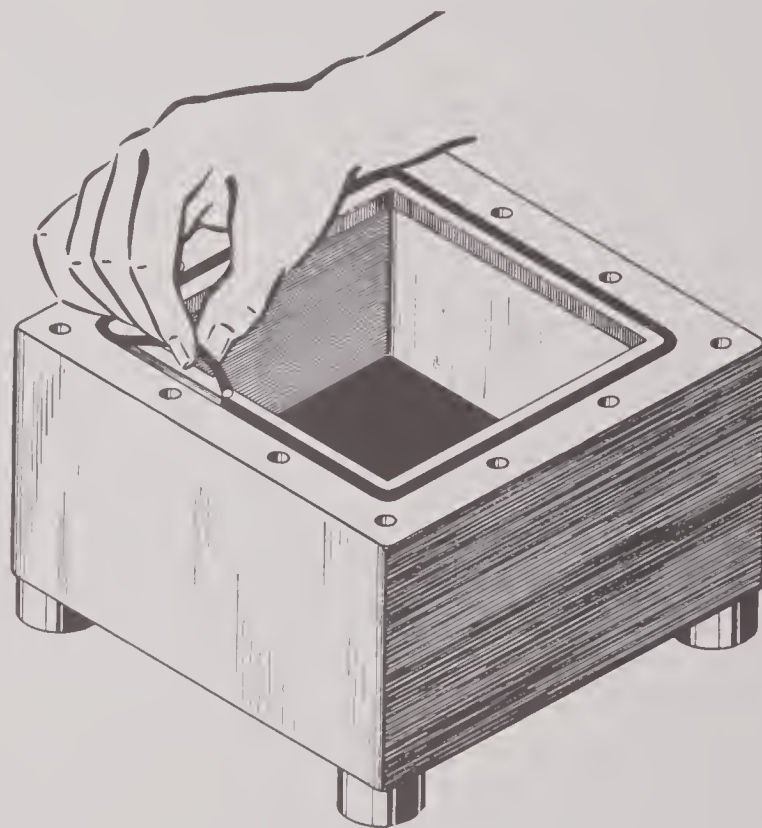


FIGURE 81. Inserting a rubber gasket in the rectangular groove of a UCDWR type GD transducer case so that the squarely cut ends of the round rubber rod meet under slight compression.

been bonded to metal frames, and where cover plates containing cable glands (see Figure 33 of Chapter 1) are used to seal the electric terminal compartment. In the installation of rubber gaskets in connection with any of various components there are two or three precautions to be observed. It has already been indicated in Section 8.8.6 that the dimensions of the gasket groove are rather critical since the object is to

force the gasket into a confined space. Similarly sufficient gasket material must be present with respect to length to fill the groove adequately. Where the $\frac{1}{8}$ -in. rubber gasket rod is cut to length it is recommended that it be cut slightly oversize so that the two cut ends will butt together firmly as depicted in Figure 81. These ends may be cut either perpendicular to the length or, provided the two ends match, at a slight angle.

In tightening a metal plate down on a gasket care must be exercised to see that approximately equal pressure is exerted along the en-

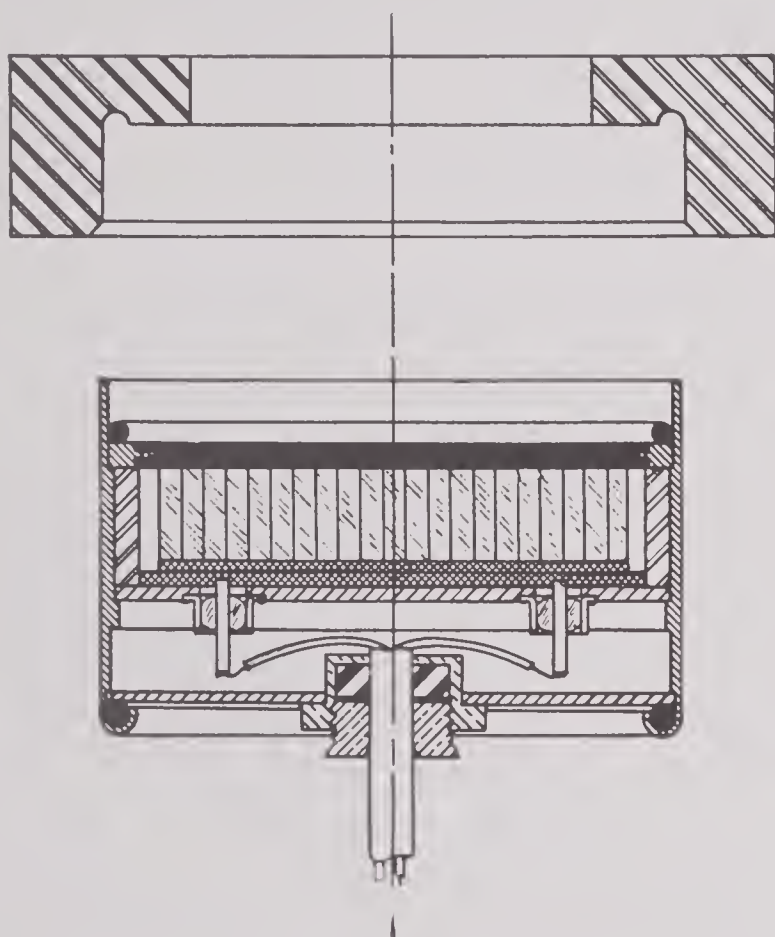


FIGURE 82. Closure of a UCDWR type EP transducer (also see Figure 56) with an upsetting die (above) which is forced down over the transducer case by means of a hydraulic press, thus curling the thinned steel wall of the cylindrical case around an O-ring gasket. A completed crimp seal appears on the bottom end of the case.

tire length of the gasket. This means that the individual bolts or screws should be tightened gradually and across diameters in order to avoid nonuniform compression of the gasket. An attempt should be made to inspect the gasket, if at all possible, during this tightening process to see that it has retained its correct position.

If a gasket groove possesses a circular contour whose length permits taking advantage of the availability of a wide range of closely graded sizes of O-ring gaskets, it may be preferable to do so instead of cutting a rubber rod to the proper length.

For the large spherical JK-type of transducer, photographs of which occur in Chapter 1, the spherical dome is sealed to the main body of the housing by a rubber gasket having a rectangular or square cross section. A cross-sectional view of this gasket appears in Figure 67 where the hemispherical window is shown bonded to the housing. It will be noted that the rectangular gasket is closely confined in a cavity near the bolt circle of the window frame and that it is compressed between the window frame and the flange of the housing. When the window is once placed in position it is not possible to inspect this gasket visually and a check on the tightness of the seal should be made by subjecting the transducer to internal air pressure or by actually testing it under water. The former procedure has been recommended, using an air pressure of 35 psi or less.

O-RING INSTALLATION

In closing transducers which contain O-ring hydraulic gaskets great care must be exercised to avoid damaging the rubber O-ring. It frequently is helpful to apply a small amount of oil to the gasket in order that the metal parts may slide over it more freely. In assembling transducers castor oil may be used for this purpose. Prior to their installation O-rings should be examined very carefully in order to eliminate those which contain any imperfections. Only perfect gaskets should be used.

Provision for proper clearance between metal transducer parts is a matter for the designer to handle. However, it should be pointed out that for a transducer seal which constitutes an essentially permanent installation, much less clearance should be provided for the O-ring than is specified in the standard Army-Navy specifications. This is owing to the fact that the specifications were set up for the case of rotating seals. Additional discussion of O-ring hydraulic gaskets is contained in Section 8.7.4. Apart from their use in sealing transducer cases of the type shown in Figure 62, they may also be

used for such applications as those pictured in Figures 70 and 82.

CRIMP-SEALING METHODS

In the construction of many thousands of expendable transducers, it has been found economical as well as entirely satisfactory, to obtain a liquid-tight closure by crimping the ends of the tubular metal housing. As an illustration, the transducer motor shown in Figure 56 can be very readily sealed into a cylindrical steel case in the manner illustrated in Figure 82. This sectional illustration depicts the approximate wall thickness required for a steel tube 3 in. in diameter. Above the transducer a special crimping die is in position, ready to be pressed down against the open end of the transducer. A rubber O-ring hydraulic gasket is in its place on top of the steel rim of the rubber window diaphragm. As the die is forced down over the transducer case, preferably by means of a hydraulic press, the thin steel wall curls around the O-ring. The appearance of a finished seal is illustrated in cross section at the opposite end of the same transducer case.

Another type of crimp seal has been discussed in Section 8.8.3, where the use of tin cans as transducer cases was presented.

8.9.4 Liquid-Filling Technique

EVACUATION

There may be two reasons for evacuating transducers before filling them with liquid. One reason is purely mechanical; with the filling equipment employed at UCDWR, it is much simpler to insure that the transducer is completely full of gas-free liquid if all air has been previously removed. Moreover, transducers may be filled with liquid much more rapidly when evacuated. The second reason for evacuating transducers is owing to the almost inevitable presence of moisture on the surfaces of the crystals. This is especially serious with RS crystals and has been discussed in the early sections of this chapter, particularly in Section 8.2.4.

In order to make certain that moisture has been removed from the crystals it has been customary at UCDWR to connect the terminals of the array to an external ohmmeter while the transducer is in the vacuum chamber. In this

manner the d-c resistance of the unit can be checked during the pumping process.

The evacuation of air and moisture from a transducer can take place by either one of two methods. One method is illustrated in Figure 78, in which the entire transducer is placed inside of a large vacuum tank. The principal advantage in this method is that it does not subject the walls of a transducer to the differential pressure of 1 atmosphere. This is usually an important consideration. In transducers which are capable of withstanding a differential pressure of 15 psi, it is somewhat simpler to provide them with two openings so that a vacuum line could be connected to one and, at the proper time, the liquid could flow into the transducer through the other.

FILLING WITH LIQUID

Where a transducer has been placed inside a vacuum tank for the evacuation process, it may be filled with liquid in the manner shown in Figure 78. In this equipment the dehydration of the castor oil takes place in an adjacent tank, which is coupled through the recirculating pump to the vacuum tank for this filling operation. By opening one valve and closing another (not shown), the purified castor oil is pumped through the oil line into the transducer. It is customary to provide a sump as shown so that oil may be allowed to run into the transducer until it appears in the sump. The object is to prevent air from entering the transducer when atmospheric pressure is established again inside the tank. After filling, the oil hole in the transducer is sealed according to the directions given in Section 8.8.6.

With transducer housings capable of supporting a differential pressure of 1 atmosphere, the evacuating and filling operation can be accomplished more simply by methods involving a system of valves. Further elaboration on such systems seems unnecessary in a volume of this kind.

8.9.5 Final Inspection and Testing

LEAKS

One of the troublesome factors in the construction of transducers is the frequent presence of liquid leaks in the final assembly. The

detection of leaks which may occur in the metal casting itself has already been discussed in Section 8.8.2. In the case of welded transducers, there is a still greater possibility that leaks may be present. Another possible source exists in bonds between metal and rubber. Leaks of these types may usually be investigated before the crystal array is mounted in the housing.

The gasket with which the major opening of the transducer is sealed may also be a troublesome cause of leaks. The stuffing-box seal for the cable gland may likewise be a source of annoyance. The proper procedure for the installation of cables has been discussed in Sections 8.8.6 and 8.9.2. When properly installed by an experienced worker, these cable glands should not fail.

The closure of the hole for liquid filling has been discussed in Section 8.8.6. As this usually constitutes the last opening in a transducer which is closed, there is normally no method of testing it for leaks. This is a fundamental difficulty in transducer design for which a remedy should be found. It seems that it should be possible to develop some type of small testing gadget by means of which a final inspection test of all sources of leaks could be made.

Previous to filling a transducer with oil, the entire housing and assembly may conveniently be tested for leaks by the use of dry compressed air, preferably introduced through the oil plug hole. After transducers are oil-filled, a test could be made by immersion in water over a sufficiently long period to see whether the housing actually leaked. This could be determined by a continuous d-c resistance measurement. In order to accelerate such a leak test, the transducer may be subjected to a hydrostatic pressure of several hundred pounds per square inch. Should leaks be present in the housing according to readings taken on the meter, the transducer may be immediately removed from the water and disassembled for repair before the crystal arrays are damaged.

D-C RESISTANCE

The quality of a transducer most frequently subjected to test both during and after construction is its d-c resistance. Not that the d-c resistance has an important bearing as far as the final operation of the transducer is con-

cerned, but largely owing to the fact that d-c resistance measurements are so easily made and yet furnish valuable indications of the quality of the construction. Since one is usually not interested in the absolute value of the d-c resistance, nor in the accuracy of its determination, the readings may be made on any vacuum-tube-type of ohmmeter. The voltage applied by such a meter should not be in excess of 500 v for general purpose use.

The d-c resistance to be expected from crystal arrays of either RS or ADP was indicated in Section 8.7.6. In a completely assembled transducer which may contain tuning coils or another type of matching network in addition to the crystal assembly, the d-c resistance may be unduly influenced by the network. Where a matching transformer is used, the d-c resistance would be expected to be comparatively low so that little or no indication of the condition of the crystal assembly could be obtained in this case by a d-c resistance measurement on the external terminals of the transducer.

In case a low resistance reading is obtained when a measurement is taken directly across the terminals of the crystal assembly itself, its cause may usually be assigned to contaminated crystal surfaces, especially to the presence of excess moisture, or to an individual crystal which has failed. In the latter event it may be possible to chip out the offending crystal without interfering with the behavior of the transducer as a whole.

Where d-c resistance measurements on the external terminals reveal a short circuit or a very low resistance, the cause may lie in any one of several directions. A systematic investigation of the possible sources which could contribute to a low resistance reading should be made. The cable should be removed and a check made for moisture in the stuffing box and in the terminal compartment. If these are satisfactory the terminal block should be tested, one terminal at a time, for proper insulation. If any indication of water is present, each terminal must be carefully cleaned. For transducers that have been immersed in sea water, warm water should be used for cleaning away the electrolytic deposit; then the terminals are dried thoroughly and retested.

In addition to measuring the d-c resistance between the two terminals of a transducer, it is also necessary to measure it between each one of the terminals and the ground connection; also between each individual terminal and the shield on the cable. The d-c resistance between the terminals and either ground or shield should be very high, the meter indicating anywhere from a few megohms upwards. Where low values of resistance are found, a thorough check of the insulation of the terminals should be made. The presence of soldering flux or too high a temperature during soldering is often to blame. The insulation may need to be carefully washed with warm water to remove the flux and then dried; or perhaps cleaned with some satisfactory organic solvent.

CALIBRATION

The numerous types of calibration data that may be obtained for transducers have been listed and discussed elsewhere in this volume. A preliminary presentation of the calibration measurements that may prove desirable was contained in Section 1.3. A more complete treatment of the complex impedance was given in Section 4.5 and the various steady-state responses have been considered in detail in separate subsections of Section 4.6. Directivity pat-

terns have been treated in several subsections under Section 4.3. Reference should be made to these sections for a thorough discussion of calibration subjects. With regard to methods of measurement and calibration equipment, it is the understanding of the writer that an entire volume in the series of Summary Technical Reports is being devoted to them.

In addition to indicating performance characteristics, calibration data are useful for indicating shortcomings both in design and in construction. Directivity patterns in some types of transducers are especially sensitive to constructional variations and hence serve as a check on correct assembly. This is true of stack-type transducers. Another example is the effect produced by the accidental inclusion of an X-cut crystal in a Y-cut RS array. Owing to the low impedance of the X-cut crystal, which receives most of the power, the pattern may resemble that of a point source instead of the Y-cut array.

Impedance measurements are most useful from the standpoint of construction in connection with determining the design values for matching networks and in checking their subsequent performance. Resonant frequencies of the transducer under water are also quickly obtained from impedance data.

RESEARCH TECHNIQUES AND APPARATUS

By *T. Finley Burke, Francis X. Byrnes, and Bourne G. Eaton*

9.1 ELECTRICAL MEASUREMENTS

IN BUILDING AND TESTING crystal transducers it is necessary to measure some of their electrical properties. Some of these properties are measured by tests that are essentially direct current in character, such as the simple push test for polarity and activity, and also the d-c resistance test. The methods and instruments used and the usual range of results obtained in making these tests are given in Chapter 8. The other electrical properties of great interest are the impedance of the transducer and the impedances of some of the electrical components used in the transducer. The methods and instruments used in measuring these impedances will be described in the following paragraphs.

9.1.1 Absolute Admittance

The simplest measure of the impedance of a network is a measurement of the absolute magnitude of its impedance. In actual practice, because of practical considerations in making the measurements, the quantity that comes directly out of the data is not impedance but the inverse quantity, absolute magnitude of the admittance of the circuit. The following discussion will therefore consider this measurement as an admittance measurement rather than an impedance measurement.

A measurement of the magnitude of the admittance of a completed crystal transducer, when it is loaded by the water, has a very limited use because of the very small changes in the magnitude of the admittance that are produced by significantly large changes in the magnitude of the various mechanical and acoustical admittances that are coupled into the crystal circuit. This is true because the magnitude of the admittances represented by the water impedance, and various other stray admittances, remain so low in comparison with the admit-

tance of the purely electrical capacitance of the crystal that they exert very little effect.

If a single crystal is measured in air, however, the admittance may be quite useful in checking many of the crystal's properties and in detecting defects in particular crystals. For example, the measured value of the admittance, as compared with the calculated value, measured at some frequency well below the first resonance, can be used to check whether or not the crystal has been cut out of the mother crystal at the correct angle. This is possible because of the fact that small errors in cutting angle will cause rather large changes in the capacitance and therefore the admittance of the crystal. This is especially true of Y-cut *Rochelle salt* [RS]. Other useful quantities that may be determined by an absolute admittance measurement are: (1) the maximum value of the admittance at resonance, (2) the minimum value of the admittance at antiresonance, and (3) the frequencies at which the resonance and antiresonance occur. Using these experimentally determined quantities in the following equations, the components in the first approximation equivalent circuit for a crystal may be determined. (See Figure A.)

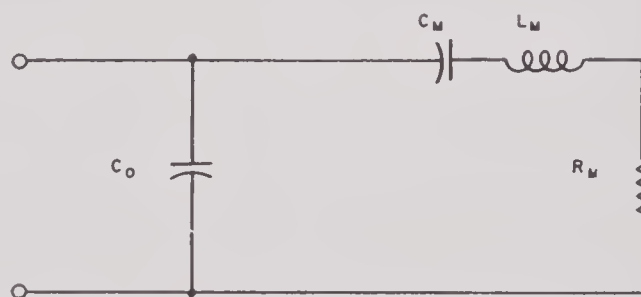


FIGURE A.

$$C_M \simeq \frac{2C_0(f_a - f_r)}{f_r},$$

$$L_M \simeq \frac{1}{8\pi^2 f_r (f_a - f_r) C_0},$$

$$R_M \simeq \frac{1}{Y_{\max} - Y_{\min}},$$

also

$$R_M \simeq \frac{1}{Y_{\max}},$$

$$r = \frac{C_0}{C_M} \simeq \frac{f_r}{2(f_a - f_r)},$$

where, $C_{\text{total}} = C_0 + C_M$ (which is the direct capacitance measured at a frequency well below the first resonance),

f_r = frequency of resonance
(Y = maximum),

f_a = frequency of antiresonance
(Y = minimum),

Y_{\max} = maximum value of the admittance ($f = f_r$),

Y_{\min} = minimum value of the admittance ($f = f_a$).

All the approximations given above hold quite well for small values of R_M . In particular, they hold quite well when the crystal is free, in air, and is mounted at the center with reasonable care to prevent damping.

Although a knowledge of the values of the elements in the equivalent circuit of a single crystal in air has a rather remote relationship with crystals built into a transducer operating in the water, it does furnish a method of determining some of the fundamental properties of crystals. By observing the changes in the observed values of the elements in the mechanical arm of the crystal circuit produced by attachments, the corresponding admittance measurements may be used to determine the properties of various attachments to the crystals, such as cement joints and the materials that are attached to the crystal by means of the cement joints.

The circuit used in a determination of the absolute admittance of a crystal is shown in Figure 1. The requirements of the various components in this circuit are as follows:

The oscillator should preferably have a low output impedance so that its output voltage will remain reasonably constant as its frequency approaches that at which the crystal is resonant. It must also have very low-harmonic content in its output, even when working into the very low impedance represented by the crystal at resonance. The maximum value that the first harmonic may have without causing appreciable

error will depend somewhat on the circumstances but may be taken as approximately $20\pi f_r C_0 R_M$ per cent. This expression will have a value as low as 0.1 per cent for quite commonly encountered values of C_0 and R_M . The higher harmonics should be even smaller in amplitude, falling off at a rate no lower than that at which the frequency increases.

No special characteristics are required of the voltmeter used to measure the output of the

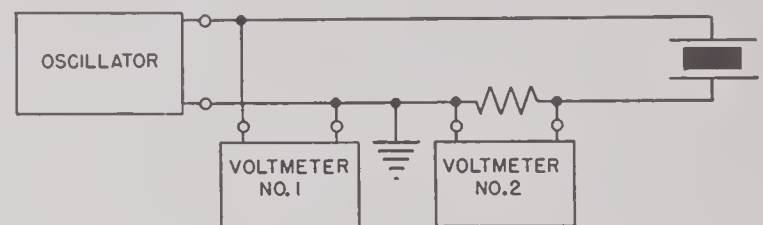


FIGURE 1. Circuit used for measuring the absolute admittance of crystal transducers or elements thereof.

oscillator. The meter used to indicate the voltage across the current resistor R , must be capable of accurate measurements over a large voltage range. This is because the current varies widely with frequency in passing from resonance to antiresonance. The voltage range requirements may be lessened appreciably by changing the value of the resistor R , in accordance with the change in the measured admittance. For example, when the admittance is measured at resonance the current is quite high and a small value of R may be used. When the admittance at antiresonance is being measured the current will be quite small and a much larger value of R will be helpful. Since the impedance of the crystal is very high at antiresonance the higher value of R may be used without introducing error caused by the voltage drop across it. It should be noted that the value R should never exceed one-tenth of the impedance $1/Y$ that is being measured. This is necessary because a valid correction for a large value of R cannot in general be made as one has no knowledge of the phase angle of Y .

The only requirements placed upon the other elements of the circuit, the wiring and the resistor, are that they contribute no reactance comparable to that of the crystal circuit even when the crystal is near resonance or antiresonance.

9.1.2 Complex Impedance of Two- and Three-Terminal Networks

A measurement of the absolute value of the electrical admittance is of great value in determining some properties of crystal transducers and of the components within the transducer, but it cannot yield all of the information which is required in the case of transducers which are radiating into water. Thus loaded, the resistive component is so large that there is very little change in the absolute value of admittance. However, bridge measurements of the real and imaginary terms of the admittance or impedance do give the necessary information under these conditions. The measurements are more tedious and it is usually advisable to first make a general survey by the absolute method and then conduct a more detailed study of the interesting regions with the aid of an impedance bridge.

With an ordinary impedance bridge two-terminal impedances may be measured, i.e., the unknown impedance has two terminals which are connected to the bridge, and the impedance between those terminals is measured. In the case of a crystal transducer this measurement is not always sufficient. Such two-terminal impedances are sometimes of value in predicting a transducer's performance when connected into a circuit, but such measurements can tell us very little about the arrangements of stray capacitances within the transducer. In some cases, these inactive capacitors together with their dissipation might actually be consuming a large part of the power being delivered to the transducer. In attempting the development or improvement of transducers it is very important to recognize this fact and, if large losses do occur in the purely electrical parts of the transducer, steps should be taken to change the dielectric materials or their geometry in order to reduce these losses.

It is possible to measure the direct impedance between any two terminals of the three-terminal network, represented by the two terminals of the transducer and ground, by means of the impedance bridge shown in Figure 2. This is a Schering bridge modified by the addition of a Wagner ground. The function of the Wagner

ground is to eliminate all capacitances to grounded terminals or to grounded shields. When the bridge, including the Wagner ground, is completely balanced, terminals *A* and *D* are both at ground potential. Under these condi-

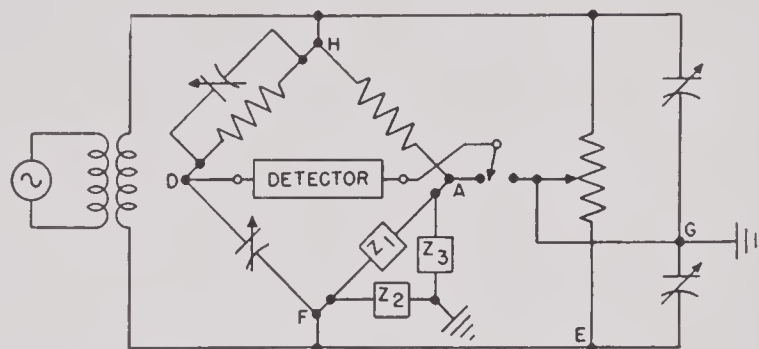


FIGURE 2. Circuit of Schering bridge with Wagner ground used for measuring the three-terminal impedance of crystal transducers.

tions, the capacitances to ground from terminals *A* and *F* cancel out and do not influence the indication of the bridge. The capacitance from *A* to ground merely appears as a shunt across the detector. The capacitance from *F* to ground is across the arm *E-G*. This is compensated for in the balancing of the Wagner-ground system, since the capacitor normally in the *E-G* arm is reduced by an amount sufficient to compensate for the *F-G* capacitor. The dissipations of the capacitances to ground are compensated for by adjustment of the variable resistor in the *E-G* arm. The procedure for balancing this bridge is first to connect the detector between *A* to *D*, adjust the capacitors *D-F* and *D-H* for a balance, then shift the detector from *A* to ground and readjust the elements from *E-G* for balance. The detector is then reconnected across *A-D* and the procedure repeated as often as may be necessary to obtain simultaneous balance of both the bridge and the Wagner ground.

In measuring the impedance of a transducer which has a nonmetallic backing plate, or none at all, the direct capacitance of the crystal motor may be measured by connecting the case of the transducer to the ground terminal *G* of the bridge. The two leads from the transducer should be connected to terminals *A* and *F*. The direct capacitance from either lead to case may be measured by grounding the other lead.

If the transducer has a metallic backing plate,

a lead must be brought out from the backing plate in order to make complete measurements on the total six capacitances to be found in the circuit. These are the capacitance of the crystals, the capacitances of the leads to ground and to the backing plate, and the capacitance of the backing plate to ground. Each of these six capacitances and their corresponding dissipation may be measured by grounding the two terminals not being used to point *G* on the bridge. A series of six measurements will thus give the values of all components of the circuit.

The capacitances from either lead to the case are very small and may be quite difficult to measure. All of the transducers developed by UCDWR have displayed such small capacitances to the case that they have been considered completely negligible. The capacitance from either lead to the backing plate and from the backing plate to the case may not be negligible. Furthermore, the dissipation of these capacitors may be large enough to cause an appreciable power loss and the consequent low efficiency of the transducer.

One factor to be considered in any measurement of the impedance of a transducer, especially when it is operating in water, is the cable to which it is connected. Because such measurements must be made at the end of this cable the effect of the cable must be taken into account. The method of handling this situation in the case of direct capacitance measurements is to connect the shield of the cable to the ground of the bridge and measure the direct impedance between the two conductors with the transducer disconnected. The measurement is then repeated with the transducer connected. These final measurements may be corrected by considering the direct capacitance of the cable to be in parallel with that of the transducer. The cable usually used with transducers developed at UCDWR is identified as Simplex No. 9061. The direct capacitance of this cable is approximately $5.0 \mu\text{f}$ per ft. This small capacitance is rarely an important factor except when dealing with very high impedance transducers.

As previously mentioned, it is sometimes desirable to measure the overall two-terminal impedance of the transducer as it will be seen by the power amplifier, regardless of the arrange-

ment of the internal capacitances. This measurement may be made using the balanced-to-ground arrangement, or it may be made with one side grounded. The one-side grounded measurement may be made with an ordinary impedance bridge, or the Schering bridge may be used. The more common arrangement, however, is to operate the transducer balanced to ground since the cable capacitances are thereby minimized and stray fields resulting from the cable current are kept at a low value. The calibration station at UCDWR employs the balanced system wherever possible and, to interpret their data, it is necessary to know the apparent impedance of the transducer as seen by a balanced line. For this purpose, a bridge of the hybrid-coil type has been devised which is similar to the Western Electric No. 4A, but which employs Western Electric Type-146A transformers. This hybrid-coil bridge is locally referred to as the "hy-bridge" and has proved very satisfactory. It is easily operated, requiring only one balance adjustment as compared to two in the case of the Schering-Wagner bridge, and the measurements are directly applicable to the calibration data taken on the sound field of the transducer. The circuit for this bridge is shown in Figure 3. The bridge is symmetrical at both

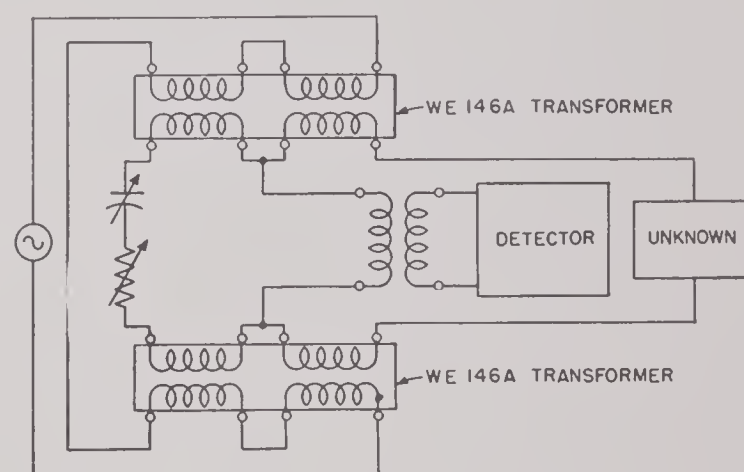


FIGURE 3. Circuit of the hybrid-coil bridge used for measuring the complex impedance of crystal transducers.

ends. A variable standard is connected at one end and the unknown impedance at the other. There is unity ratio between the two ends so that the unknown impedance may be read directly on the variable standards, providing that the transformers making up the bridge are well

balanced. The two transformers in the main loop must be of the very best quality, but the transformer leading to the detector is less critical.

A high-gain tuned amplifier is used as the detector with both the hybrid and Schering bridges. This circuit contains one or more high- Q coils and is equipped with variable capacitors so that it may be tuned to any frequency between 500 c and 500 kc. Suitable selectivity is obtained over the entire range.

The output of this tuned amplifier, or detector, is connected to the vertical deflection plates of a cathode-ray oscillograph [CRO]. The horizontal plates of this oscillograph are connected directly to the bridge oscillator so that a Lissajous figure results. At balance, in the absence of harmonics, the Lissajous figure reduces to a horizontal straight line. This method of detection has the advantage that it gives an indication of both the magnitude and the phase of the off-balance voltage with respect to that of the oscillator. If compensation is made for the

indication of which component, in the standards, resistive or reactive, needs adjustment. If the net phase shift through the system happens to be an odd multiple of 90 degrees instead of an even multiple, the effects of resistance and capacitance will be reversed, and the resistive changes will rotate the ellipse while the capacitive changes will alter the minor axis.

9.2

PROBE MICROPHONE

For many experimental purposes, an exceedingly small or point hydrophone that can be used either as a contact pickup or as a nondirectional pickup in a free sound field is a valuable tool. Because of its small size, acoustic measurements can be made with a minimum disturbance to the body under measurement. It can also follow very short pulses because of its necessarily high resonant frequency.

The most successful design developed is shown in Figure 4. Essentially the hydrophone

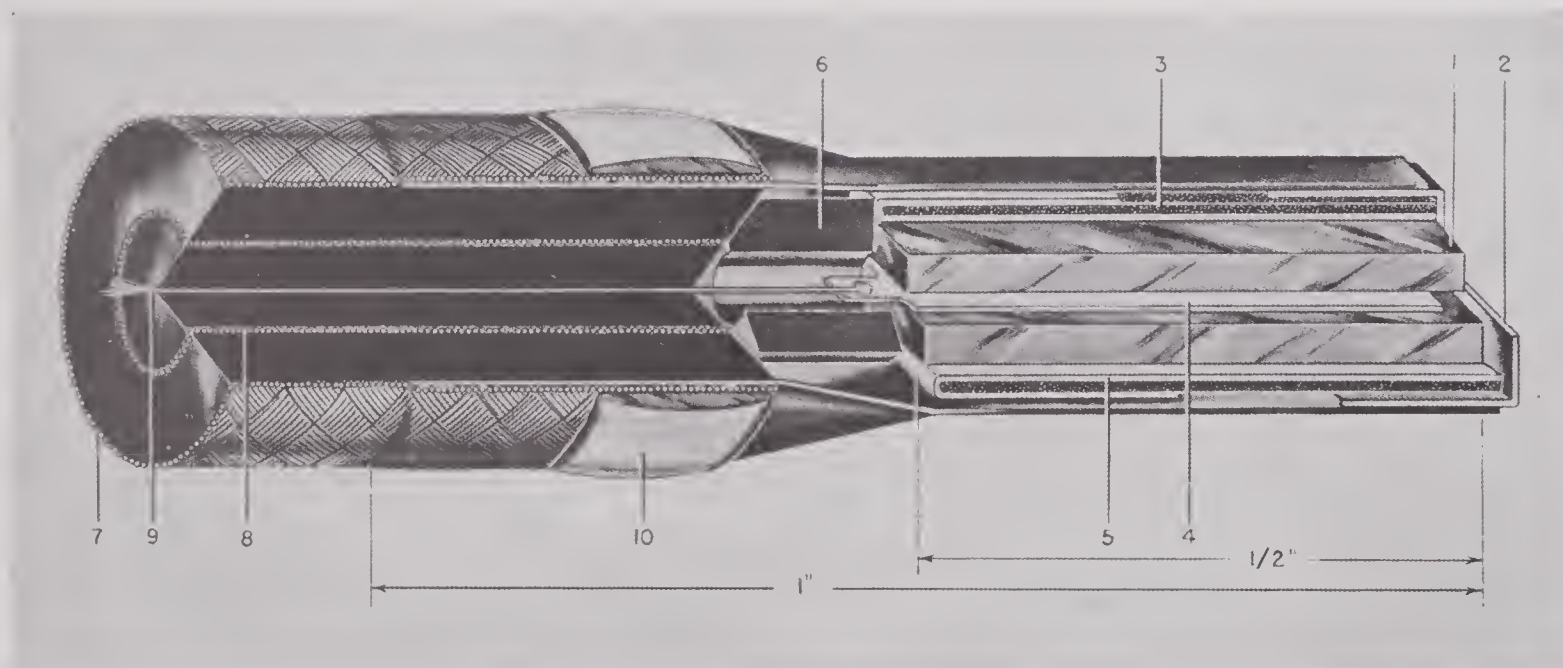


FIGURE 4. Cutaway of the probe hydrophone.

phase shift through the system (which is conveniently accomplished by a very slight detuning of the detector), then resistance changes will alter the axes of the ellipsoidal Lissajous figure while capacitive changes will rotate the ellipse about its center. This is especially convenient if the initial condition happens to be far from balance, since it gives the operator an in-

is just two ADP crystals ($0.4 \times 0.125 \times 0.06$ in.), inertia driven, with a metal case and end cap serving only for support and electrostatic shielding. Referring to the figure: (1) is the crystal motor; (2) is the end cap ($0.2 \times 0.2 \times 0.1$ in.), drawn from 0.001-in. silver foil; (3) is a foam rubber side support, serving to center the motor and to acoustically insulate it from the case;

(4) is the inside foil which is used as the high-potential lead; (5) is the outside electrode foil, curled around the foam rubber so as to contact the brass case which is at ground potential; (6) is a micarta spacer which transmits any mechanical thrust on the motor to the end of the cable thus relieving the delicate end cap; (7) is the external grounded shield; (8) is the interior guard shield, driven at the same voltage and phase as the central high-potential lead with a cathode follower; (9) is the central high-potential lead that connects to the grid of the cathode follower.

The inside guard shield is used because of the exceedingly low capacity of the crystal motor (about 10 μf). The capacity of low-capacity cable is usually at least 20 μf per ft so that a cable of 4- or 5-ft length would reduce seriously the already small signal from the crystal. If the guard shield surrounding the high-potential lead is driven with the same voltage and in phase with the lead, no current will flow from shield to lead, and the effective capacitance between lead and ground in the cable will be zero. This action is accomplished with a cathode-follower circuit shown in Figure 5. If a long

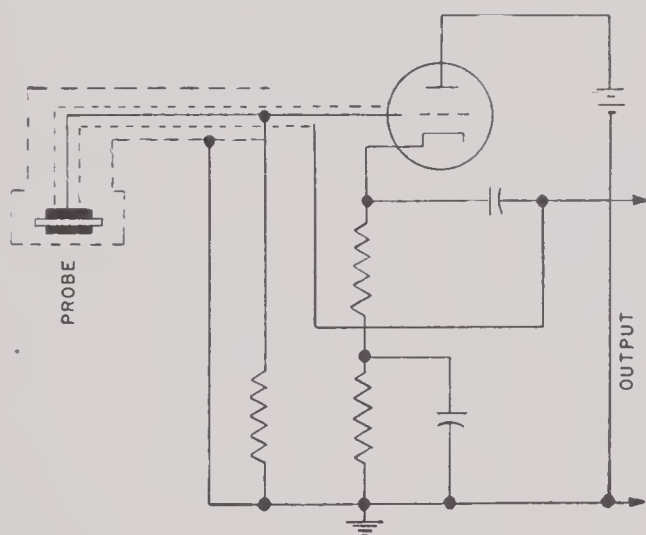


FIGURE 5. Cathode-follower guard circuit for use with probe hydrophone.

cable is necessary, this simple circuit must be replaced by several stages of a 100 per cent feedback amplifier that can furnish enough power to drive the guard.

The directivity pattern of the probe taken in a plane containing the center line of the motor is shown in Figure 7, and its sensitivity calibration in volts per dyne per sq cm pressure

in Figure 6. The voltage measured is that appearing across the cathode-follower terminals. For use as a contact pickup, the input imped-

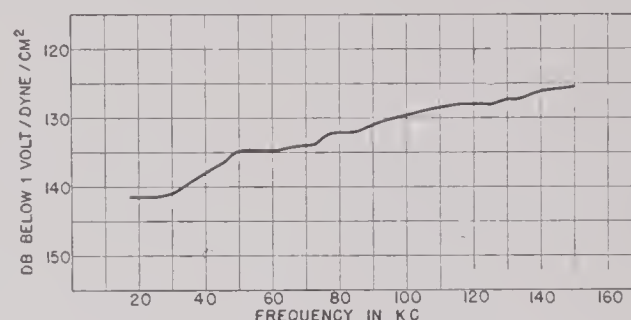


FIGURE 6. Frequency response of probe hydrophone in water (volts/dyne/cm²).

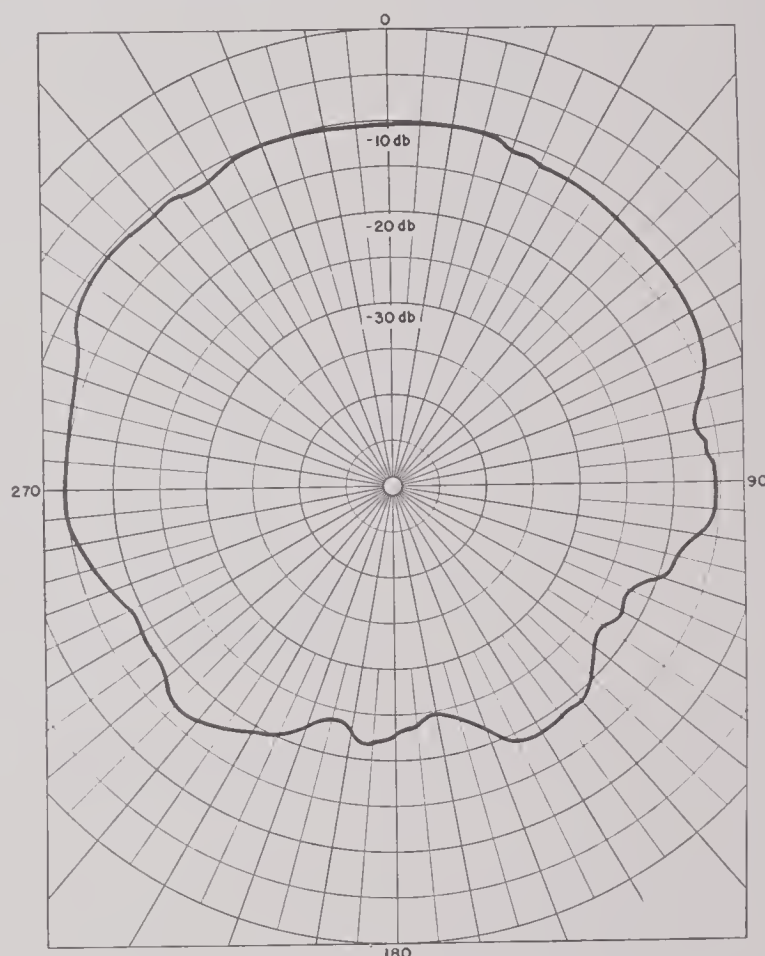


FIGURE 7. Directivity pattern of probe hydrophone (at 125 kc) in water, in a plane containing the axis.

ance was measured to be 4,700 mechanical ohms, which is low compared to 1.5×10^5 , the specific acoustic resistance of water. Thus, for contact measurements, it looks to the surface under measurement more like air than water loading. Absolute calibrations of the unit as a contact pickup are not measured. However, it is used principally for relative measurements, so that its linearity is of chief importance. This must be checked over the range used at the be-

ginning of every measurement, because these ranges are of the order of 30 db.

The complete vibration pattern of the surface of a transducer at a single frequency is obtained by scanning the probe over the surface, probe being coupled to the motor surface by a thin oil film (about 0.005 in. thick). A scanning machine that moves the transducer or motor under the probe is shown in Figure 8. This ma-

9.3 DIRECT-READING PHASE METER

Many methods of measuring phase differences between two circuits have been advanced; they can be divided generally in two classes, those which measure changes in magnitude of a resulting voltage with change of phase,¹ and those that measure directly the time difference between a certain point of a cycle of one circuit

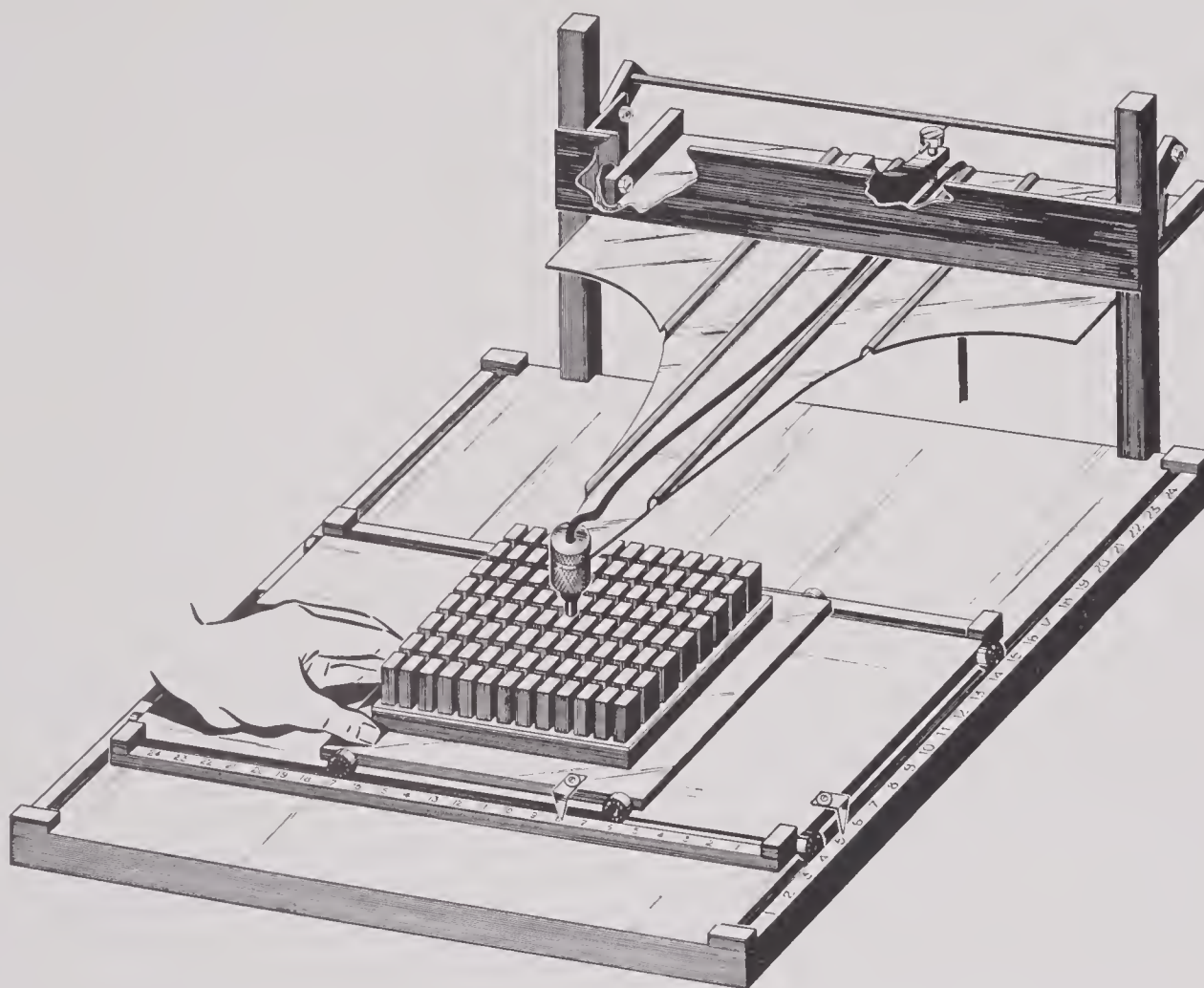


FIGURE 8. Jig for scanning transducer motors in air using a probe contact microphone.

chine keeps the probe spacing from the motor constant, and enables the operator to quickly scan a motor point by point. It can also be made automatic. Scanning under oil is shown in Figure 9. The results of a motor scanned both in air and oil are shown in Figure 21, Section 3.6. The phases indicated in that figure were measured by a phase meter described in Section 9.5. The oil bath for loading the motor must be free of standing waves that come from boundary reflections. This is accomplished by enclosing the oil in *gc* rubber case which is then immersed in a water tank that has acoustically absorbing walls, as illustrated in Figure 9.

and the corresponding point on a cycle of the other circuit.² The first method is essentially a point by point measurement, while the second can be made direct reading, and even recording. The present phase meter is based upon the second method and indicates phase differences directly with a d-c milliammeter. The overall operation is illustrated in Figure 10. Referring to the figure, each sine wave signal is squared and differentiated into successive positive and negative pips. These pips are used to trigger a flip-flop circuit (Figure 11) that works only on negative pips, each channel being fed into opposite sides of the circuit. The effect is that one

channel turns a tube on and the other channel turns the same tube off. The current through the tube thus flows only during the interval of

to use a flip-flop circuit that works with negative pulses instead of positive because in the latter type the square wave generated always

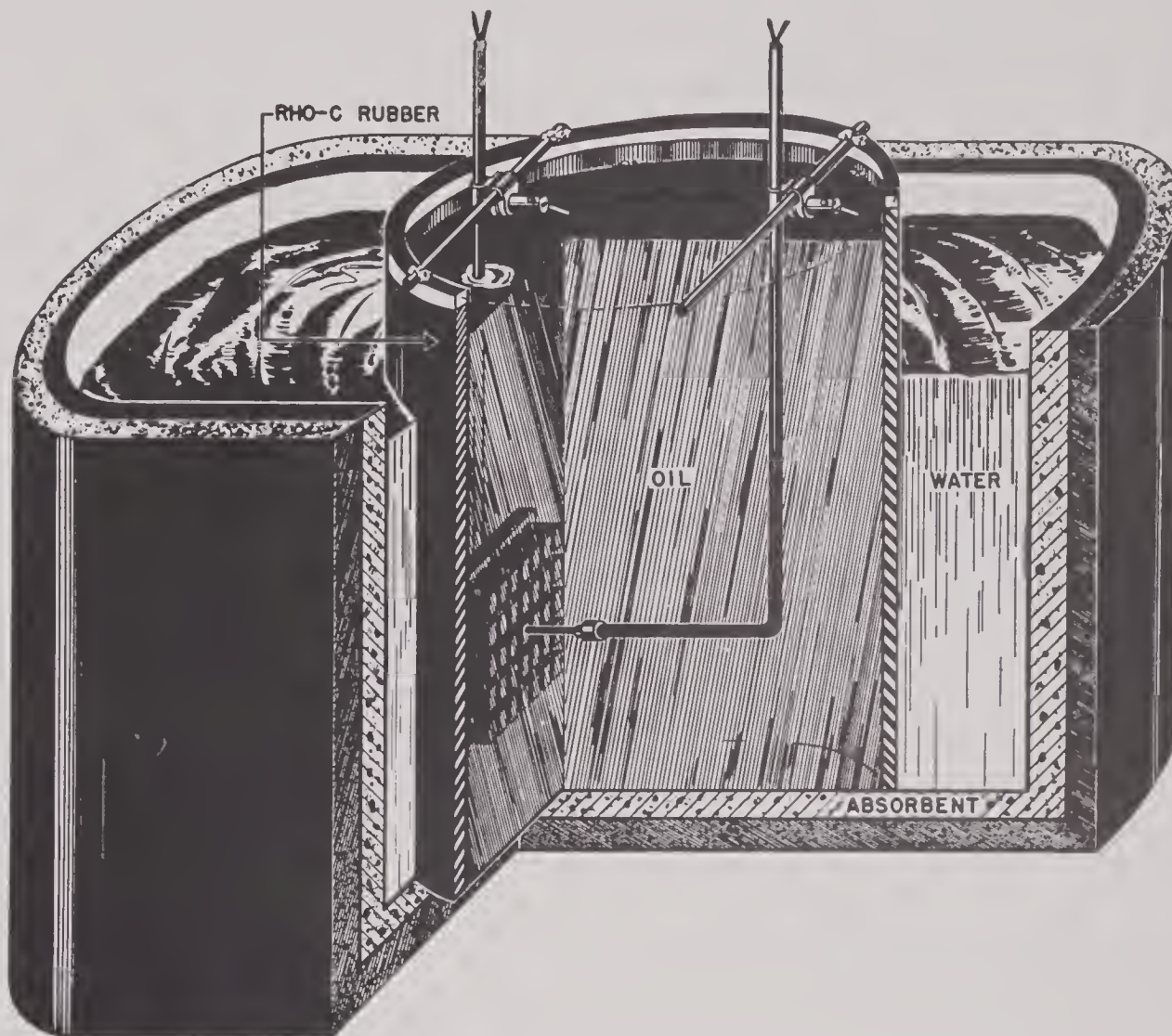


FIGURE 9. Cutaway, showing method of scanning transducer motor in oil using probe contact hydrophone.

time representing the difference in phase between the two circuits. These pulses are averaged in time with a d-c milliammeter whose readings are then directly proportional to phase differences in channels A and B. It is necessary

has a small initial pip superimposed at the beginning of each wave, and this perturbation introduces considerable error in a measurement

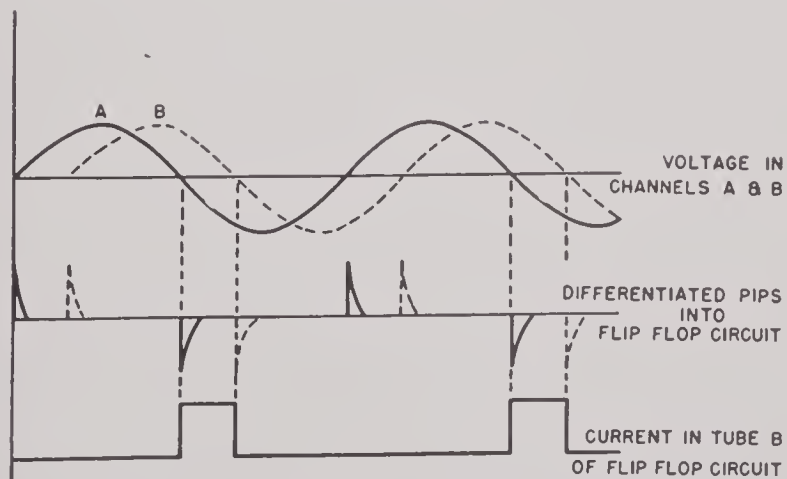


FIGURE 10. Wave form diagram showing overall operation of phase meter.

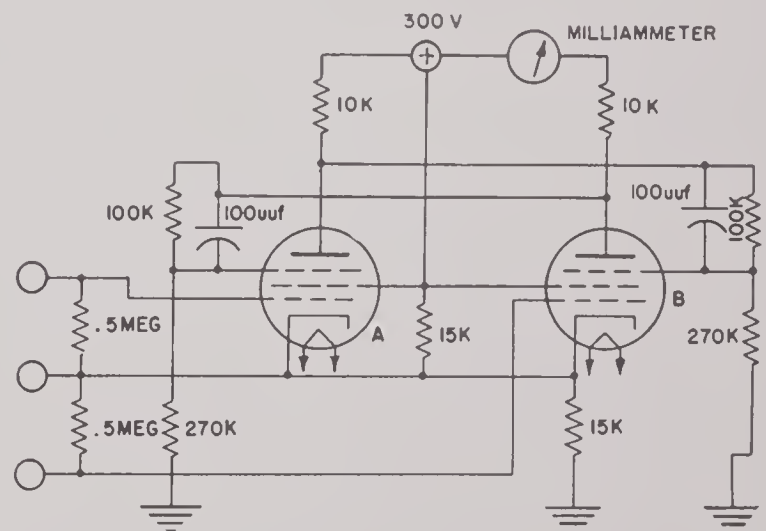


FIGURE 11. Flip-flop circuit employed in the phase meter which is sensitive to only negative impulses.

that depends upon short time intervals of constant current for its linearity. Also, the use of negative pips allows phase readings over a range of 0 to 360 degrees.

The operation of the circuit of Figure 11 is as follows. Assume tube *B* is conducting and *A* is shut off. The suppressor of *A* is about 50 volts less than the cathode so that a positive impulse at the grid of *A* will not disturb the plate current of the tube. Only by raising its suppressor can this tube be rendered conducting, and this happens when tube *B* is shut off. A negative

there will be beat frequencies of the form

$$E'_1 = \sin [(\omega_1 - \omega_2)T + \phi_1 + \theta],$$

$$E'_2 = \sin [(\omega_1 + \omega_2)T + \phi_2 + \theta],$$

and the phase difference between these signals is still $(\phi_1 - \phi_2)$.

Operating the flip-flop circuit at constant frequency gives two additional advantages in that phase variations with frequency in the amplifiers and in the standard phase shifter are eliminated.

Referring to Figures 12 and 13, the complete

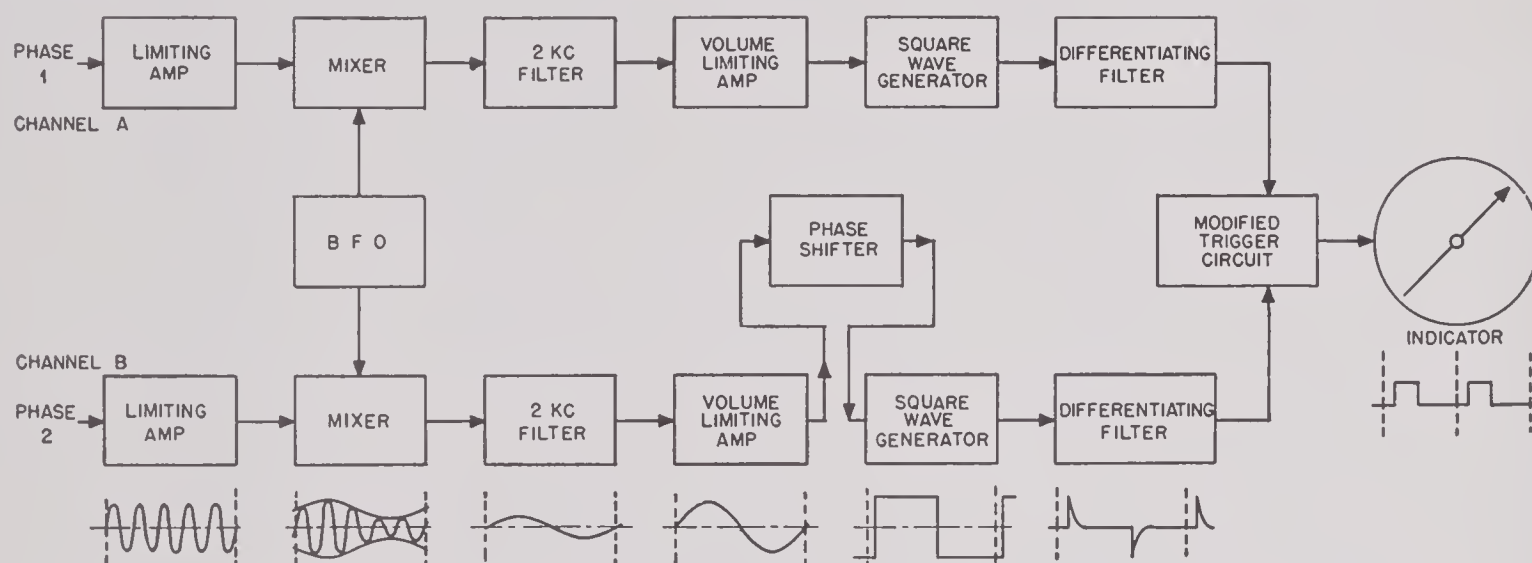


FIGURE 12. Block diagram of the phase meter.

pulse on the control grid of *B* will stop the flow of electrons through it momentarily whence its plate voltage rises, thus raising the suppressor of *A* and rendering it conducting. The plate of *A* now is depressed which depresses the grid of *B* thus keeping it shut off until a negative pip at the grid of *A* shuts it off thus allowing *B* to conduct again. At frequencies up to 10 kc the wave through tube *B* is perfectly square as indicated in Figure 10, but at higher frequencies the corners begin to round a little, which introduces errors in phase readings close to zero or 360 degrees. To extend this frequency range, the input signals in each channel are beat down to 2.2 kc with a common oscillator. This transformation does not change the phase relation between the channels, for if two signals of the same frequency but different phases

$$E_1 = \sin (\omega_1 T + \phi),$$

$$E_2 = \sin (\omega_1 T + \phi_2),$$

are beat with a second frequency

$$E_3 = \sin (\omega_2 T + \theta),$$

operation of the instrument is as follows: Each signal is fed into its respective channel through a high impedance input cathode follower input tube. The cathode follower then feeds into a limiting amplifier or *automatic volume control* [AVC] system which compensates for wide ranges in input-signal level. The resulting nearly constant signals are then mixed with a frequency from a tuned oscillator which changes their frequencies to 2.2 kc. The lower-frequency signals are then put through 2.2 kc tuned amplifiers to second-volume limiting amplifiers. The output of these second amplifiers is constant with about 30 db variation in the voltage of the input signal at the cathode follower. At this point channel *A* is fed directly into a square-wave generator, while *B* is fed through a standard phase shifter to a square-wave generator. This phase shifter allows phase compensation for the preceeding stages, accurate measurement of phase differences, and a means of adjusting for zero phase shift in the final circuits. From the square-wave generators



the signals are fed through differentiating filters to the final flip-flop measuring circuit.

The accuracy of the phase meter depends upon the linearity of the milliammeter, wave form of the flip-flop circuit square wave, sharp-

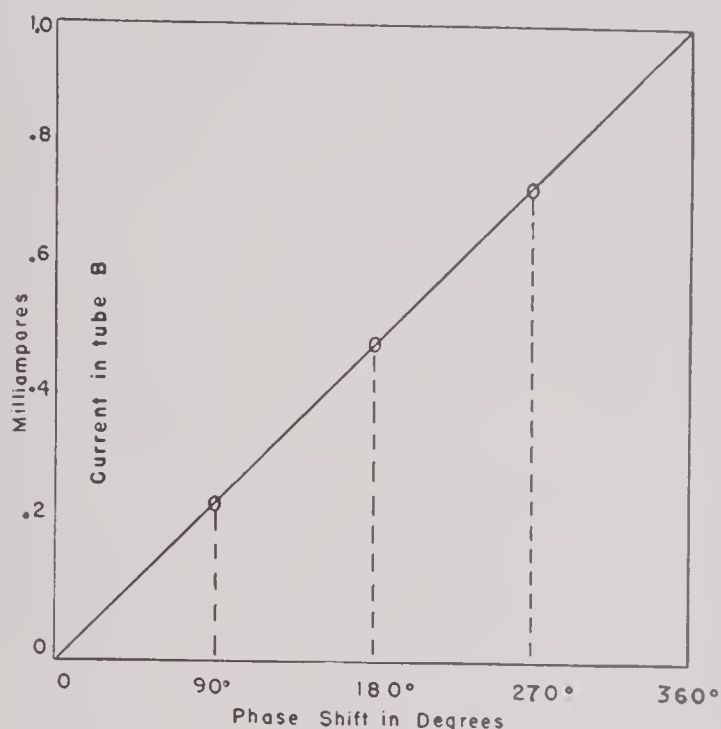


FIGURE 14. Five-point calibration of phase meter.

ness of the triggering pips to the flip-flop circuit, and readability of the indicating meter. In principle, all the factors can be held constant, so that a very accurate meter is theoretically

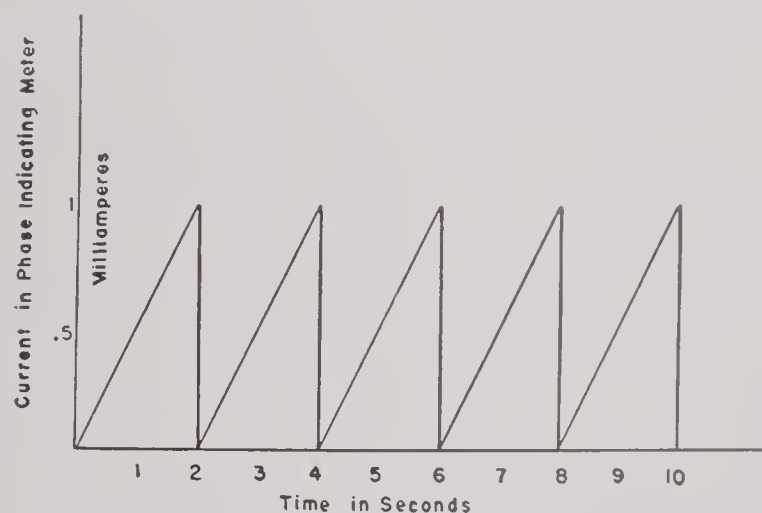


FIGURE 15. Calibration of phase meter by the two-oscillator method.

possible. In the calibration of the meter, three methods can be used and checked against each other.

1. Obviously, one method would simply compare the meter reading with a standard phase

shifter. At different frequencies, however, the calibration of such a shifter is in doubt, so that this method is restricted to the standard shifter incorporated in the meter that works at 2.2 kc.

2. The second method is as follows: Referring again to Figure 11, when tube *B* is conducting continuously, the corresponding phase shift should be 360 degrees and when it is shut off the shift should be 0 degrees. If the meter current is plotted for these two points, Figure 14, and connected with a straight line, the meter

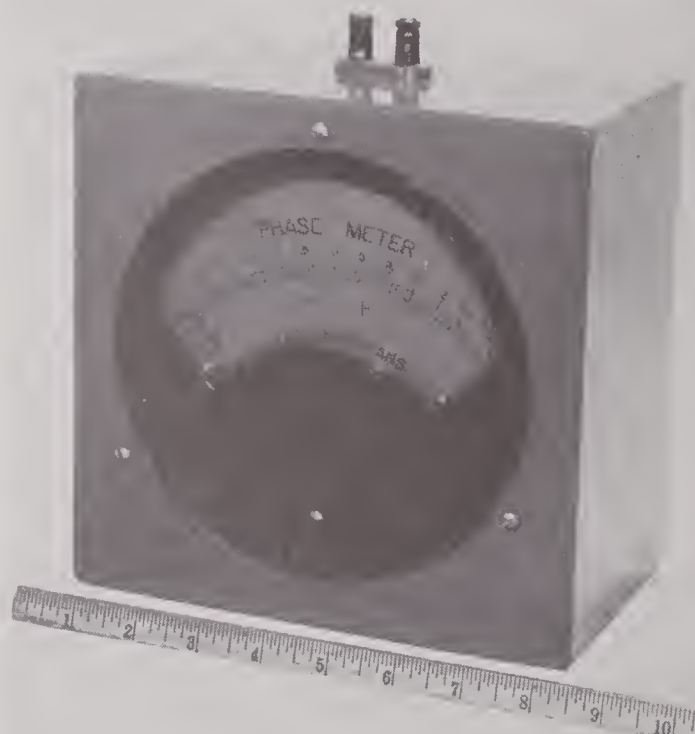


FIGURE 16. Large auxiliary indicator used with the phase meter.

reading for 180 degrees should lie on this line at half the distance between the zero and 360 degrees. A 180-degree phase shift in a high-frequency input signal is easily obtained from the secondary of a transformer by reversing the terminals. Actually, the 180-degree point lies exactly upon the curve as shown in Figure 14. Phase shifts of 90 and 270 degrees can be obtained from calibrated *RC* elements and, when used with the meter, fall exactly on the calibration line.

3. The third method requires two stable oscillators, one at each high-frequency input terminal, tuned at slightly different frequencies. With two such incommensurate frequencies, the phase difference in the two channels

varies linearly with the time (the linearity depending upon the stability of the oscillator). The meter reading should then vary linearly with time and experiments show that a very



FIGURE 17. Panel view of phase meter.

good linear variation with time is possible with this test. This calibration is illustrated in Figure 15.

Photographs of the phase meter, omitting the power supply, are shown in Figures 16, 17, and 18. Figure 16 is an auxiliary indicating meter

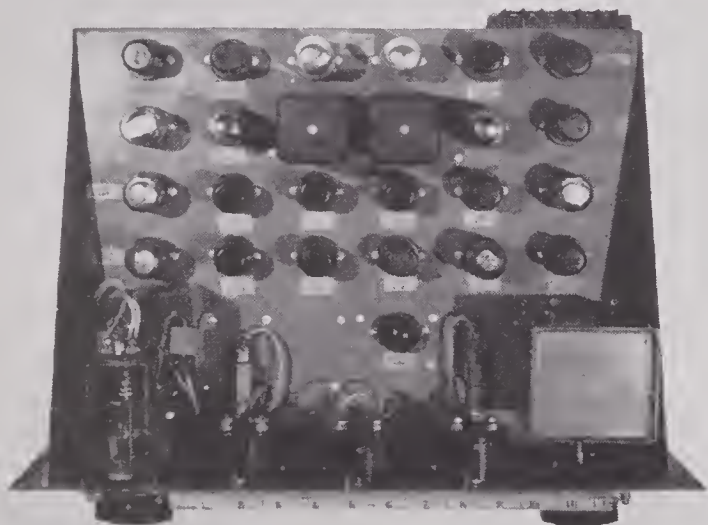


FIGURE 18. Chassis view of phase meter.

of a large type to give better scale readability. Figure 17 illustrates the controls of the phase meter. The operation is as follows: The oscillator dial on the right is first tuned to the input frequencies. Then the gain in each channel is turned to zero so that the zero- and the 360-degree currents in the indicating milliammeter can be adjusted with the knobs under the meter. These knobs operate shunting potentiometers across the meter as illustrated in Figure 13. Finally the gains in each channel are set so that

the two meters on each side of the central meter which read input signal to the square-wave generators read about half scale. It is necessary to keep the input signals strong enough to give good square waves but not so strong as to overload any of the amplifiers. Because of the two volume limiting controls, the levels of the input signals can vary through considerable range (0.023 to 5 v). Any phase-shift zero can now be set with the phase shifter, and the meter is ready to read or record phase differences. Zero phase can be set by paralleling the two input channels, and setting the phase indicating meter to zero with the standard phase shifter. Figure 18 illustrates the chassis of the meter.

9.4

PULSE MODULATOR

For direct investigations of the behavior of a circuit or transducer when being pulsed at short intervals with a given frequency, it is necessary to have a signal generator that will generate such pulses of controllable durations and repetition rates without transient build-up or

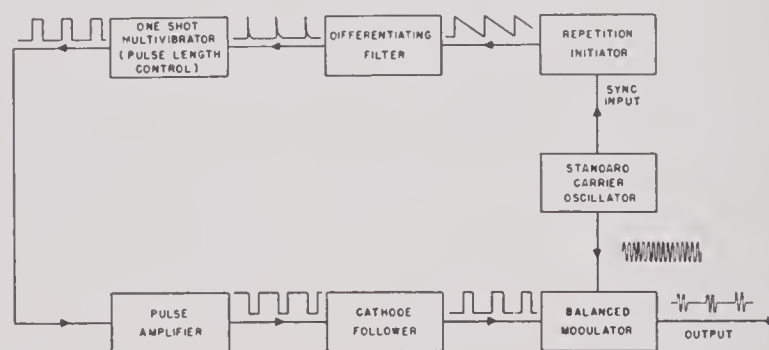


FIGURE 19. Block diagram of the pulse modulator.

decay perturbations. In addition it is desirable that the carrier frequency in the pulse be synchronized with the repetition rate of the pulse so that it will appear stationary when viewed on an oscilloscope screen.

All these controls are embodied in the present pulse modulator. Referring to the block diagram of Figure 19, the overall operation of the circuit is as follows: A repetition rate is first created by the pulse initiator, which is a saw-tooth oscillator synchronized to the carrier frequency in such a way that the sharp rise, or firing time, occurs only at a definite point on the positive swing of a carrier cycle. This rate may be

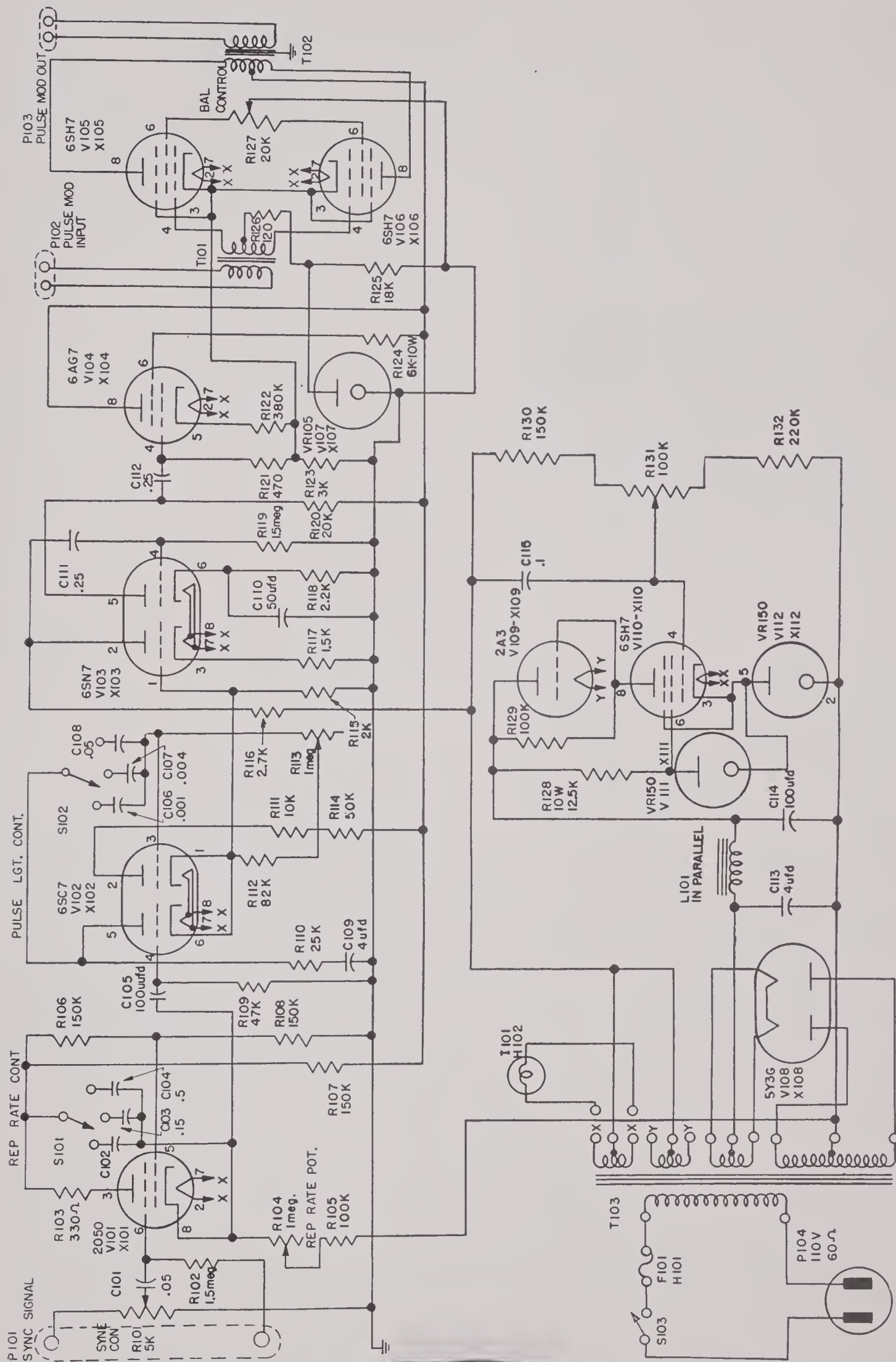


FIGURE 20. Schematic circuit diagram of the pulse modulator.

varied, but is always synchronized with some cycle of the carrier. This sawtooth signal is sharpened by a differentiating circuit, to allow for very short pulses, and used to trigger a "one-shot" multivibrator. The duration time of this multivibrator is determined by its resistance and capacitance, and is the duration of the final pulse. The multivibrator's square wave output is then amplified and used with a balanced modulator to shape a pulse of the carrier



FIGURE 21. Panel view of the pulse modulator.

signal having the desired duration and repetition rate.

The complete schematic circuit diagram appears in Figure 20. A sawtooth oscillator utilizing a 2050 tube is used for the pulse initiator because it synchronizes with the carrier over a much wider band of frequencies than do controlled multivibrators. The 2050 tube, whose screen is controlled by the carrier voltage, is used to discharge an RC charging circuit. The RC time constant controls the repetition rate generally, but the carrier voltage at the 2050 screen determines the precise time of discharge, thus synchronizing the square-wave modulating voltage with the carrier itself. The repetition rate is adjusted in large steps by capacity variations and in fine steps by a variable resistor. The one-shot multivibrator is likewise time controlled in large steps by a step-switch to capacitors, and in fine by a variable resistor. The usual type of multivibrator is inadequate to monitor very short pulse lengths in that it ceases to have a one-shot action and operates as a continuous multivibrator without control. (The cause of this instability at high frequencies lies in the high-impedance couplings between the grids and plates; low-impedance

loading upsets the frequency of the circuit.) A modified form of the conventional one-shot multivibrator using cathode output shown in the diagram is necessary if short pulses are to be produced. As the output of the multivibrator is low, it must be amplified, then fed to the modulator at low impedance. This is done with the amplifier and cathode-follower tubes following the multivibrator. The cathode-follower load resistor is common to the cathode resistor of the balanced modulator and keeps the modulator biased to cutoff except when there is a signal on the cathode follower. The carrier signal is fed push-pull through the modulator, and is chopped into packets determined by the cathode modulating square-wave voltage. It is necessary to connect the two screens in the modulator through a potentiometer to a source of very constant voltage as shown. This adjustment allows a very accurate balancing of the output signal to be made, which is necessary in order that the zero-voltage axis of the pulse be a straight line.

Photographs of the pulse modulator appear in Figures 21 and 22. Figure 21 illustrates the panel controls and Figure 22 illustrates the chassis. The synchronizing knob adjusts the input voltage to the screen of the 2050 tube that

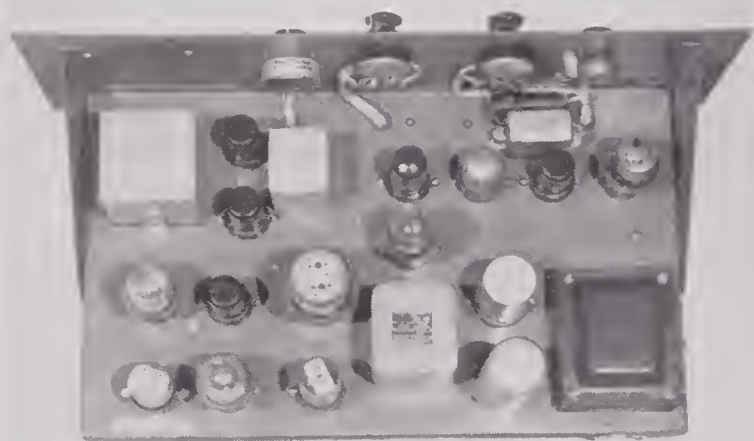


FIGURE 22. Chassis view of the pulse modulator.

acts as the pulse initiator, which adjustment is not critical. Two knobs are used on the repetition-rate control and two on the pulse-length control. In each case, the lower knob operates a capacitor step switch and the upper knob op-

erates a 1-megohm potentiometer. The balance control operates the potentiometer between the screens of the balanced modulator tubes. This control straightens out the horizontal axis of the pulse. An extra pair of terminals, not marked on the chassis, connects directly to the output of the differentiating circuit to give a synchronizing pip for use in synchronizing a single-sweep oscilloscope.

9.5 USE OF 45-DEGREE X-CUT RS AS A RESEARCH TOOL

It is well known that X-cut RS exhibits marked temperature dependence at temperatures commonly encountered in the oceans. This temperature dependence causes large changes in the dielectric constant K , electromechanical coupling coefficient k , velocity of sound in the crystal V , characteristic impedance Z_0 , and transformation ratio ϕ . For this reason 45-degree X-cut RS crystals are no longer used extensively in newly designed equipment. However, as will be discussed in the following text, there still remains an important possible use for these crystals in research, the results of which would allow the design of improved transducers using other more stable crystals.

9.5.1 Radiation Problems

An important class of transducer is that which has at least one dimension comparable to a wavelength. Our present theories of radiation all make use of an approximation that the transducer is either very large or very small compared with a wavelength; the inadequacy of this theory has been pointed out several times in this book (Sections 4.4.2 and 6.9.3). It is not now possible to calculate the directivity pattern, the point radiation impedance, or even the average radiation impedance of such transducers. The theoretical problems are very great, and no solutions are now in sight. The theoretical treatment would be aided greatly by experimental data for several typical radiators. These experimental data on directivity patterns are easily obtained, and much is now

available. However, there is available no information concerning radiation impedance.

The most natural way to obtain radiation-impedance information is from measurements made at the electric terminals of an efficient transducer. However, in both 45-degree Y-cut RS and 45-degree Z-cut ADP the electromechanical coupling coefficient is 0.3; consequently one cannot "see" the mechanical branch very well because of the low shunt impedance of C_0 . Even at resonance, the best available measurements of complex impedance allow very poor accuracy in computing the impedance of the mechanical branch. This situation would be improved by using a crystal having larger k .

9.5.2

X-Cut RS

According to Froman³ the apparent dielectric constant is not only temperature dependent but also very strongly field dependent, and neither

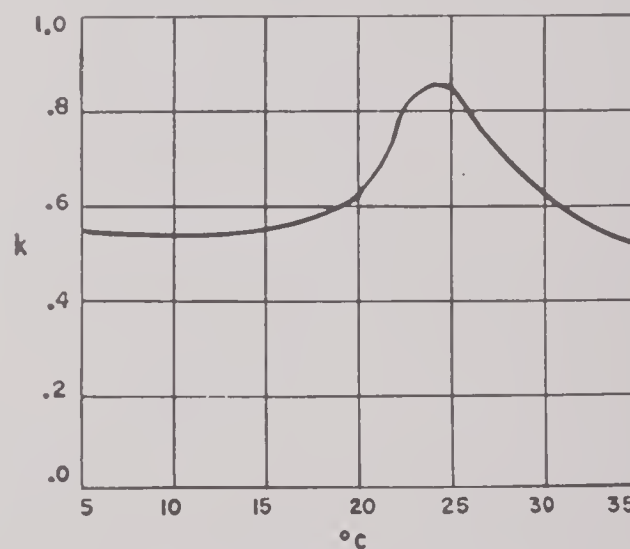


FIGURE 23. Electromechanical coupling coefficient k of 45° X-cut Rochelle salt crystals as a function of temperature.

dependence is monotonic at any value of the other variable. However, at low fields Froman observes the same temperature dependence as Mason,⁴ a smooth single-peaked curve. It is thought that at least within the Mason approximation at low fields the entire temperature dependence can be ascribed to K , the other quantities varying only as they are functions of K . If so, and if the available data on K versus temperature at low field are correct, we can

compute the behavior of 45-degree X-cut RS at any temperature and low field. In particular, we may compute k as a function of temperature; using Mason's data we obtain the curve shown in Figure 23.

The band width of a transducer, and also the

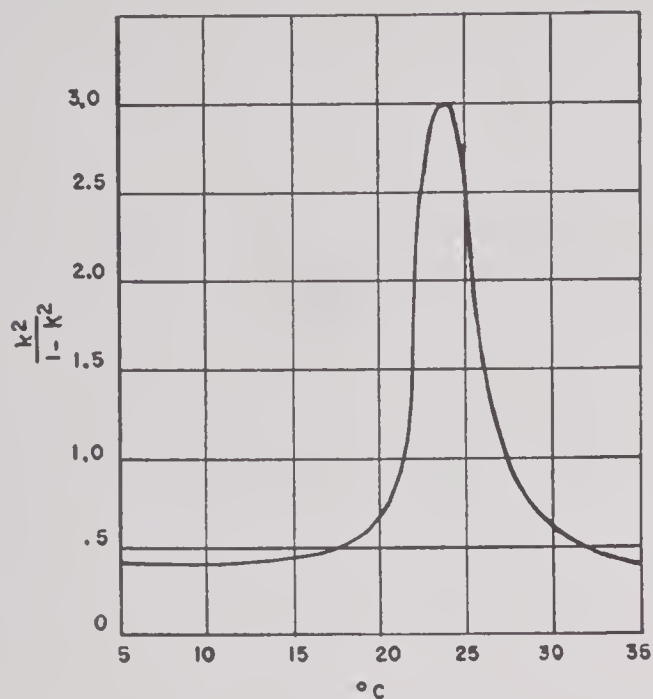


FIGURE 24. Figure of merit $\frac{k^2}{1-k^2}$ of 45° X-cut Rochelle salt crystals as a function of temperature.

sensitivity of measurements of the mechanical branch from the electric terminals, is governed primarily by the function

$$\frac{k^2}{1-k^2}.$$

Using the data in Figure 23, this function is shown in Figure 24.

It is seen from Figure 23 that at approximately 24 C, X-cut RS is an enormous improvement over Y-cut RS or Z-cut ADP.

9.5.3

Technique

The large values of k are found only over a very restricted temperature range. This is a temperature above that usually encountered at calibration stations, but not one difficult to obtain. It is suggested that test transducers be built using 45-degree X-cut RS. These could have radiating faces whose dimensions are of

interest. If these units and a large volume of water around them were maintained at very constant temperature near 24 C it should be possible to measure complex electrical impedances which allow calculation of the average radiation impedance as a function of frequency. These measurements would be done at low field where the assumed K should be correct. Under such conditions it is not uncommon that the mechanical arm be coupled so strongly that the transducer's series reactance go inductive above resonance.

9.5.4

Difficulties

Many difficulties present themselves, but none appears insurmountable, and the end appears to justify elaborate means of overcoming them.

The purely mechanical difficulties of maintaining a sufficiently large body of water different from ambient temperature are engineering problems whose solutions are straightforward. Some trouble may arise from reflections at the temperature interface; for this reason the interface should be as remote as possible.

Before this method can succeed the data on dielectric constant versus temperature and field must be checked and perhaps taken to greater accuracy. It is also necessary to show that all of the temperature dependence can be embodied in K .

Having computed the series impedance of the mechanical branch, it is then necessary to know that part caused by the crystal so it can be subtracted to determine the radiation impedance. For this it may be necessary to determine the constants in Camp's equivalent circuit.

The X-cut RS is not only temperature dependent, but it also shows marked nonlinearity and hysteresis. The nonlinearity may arise from the field dependence and may not be serious at low fields. The hysteresis introduces a resistive component, some of which may appear in the electrical branch. This resistance would have to be determined.

It is necessary to use highly efficient transducers and to know the values of the loss resistances. This may be difficult, but should be possible if gas-filled inertia drive is used. This

drive has the further advantage of lower electrical Q (Q_E).

9.6 ELECTRIC NETWORK SIMULATOR OF THE COMPLETE TRANSDUCER USING CONSTANT L , C , AND R ELEMENTS

The impedances appearing in the equivalent circuit for a piezoelectric crystal being transcendental functions, constant circuit elements of inductance, capacitance, and resistance can

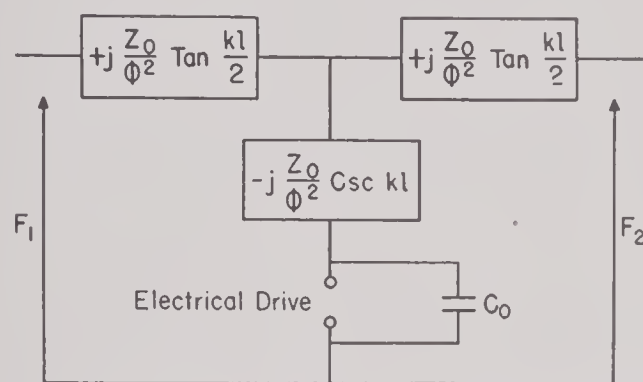


FIGURE 25. Equivalent circuit of a piezoelectric crystal (Mason⁴).

replace them directly at only one frequency in an electric simulating circuit. These functions are tangents, cotangents, and cosecants in non-dissipative systems and are the hyperbolic functions in dissipative systems. The problem of calculating a transducer's frequency response from an equivalent circuit of transcendental elements is very laborious, and it is more practical, and far more time saving, to build an equivalent circuit from constant L , C , and R elements, and measure its response with frequency. Transcendental impedance approximations using lumped circuit constants are derived in the following manner:

The dissipationless equivalent circuit of a piezoelectric crystal of length l and area A is^{4a} shown in Figure 25,

where $Z = \rho c A$; A is cross-sectional area,
 C_0 = capacity of blocked crystal,
 F_1 and F_2 = the longitudinal forces on the ends of the crystal,
 ϕ = piezoelectric-mechanical coupling coefficient.

The impedance elements in the T network can be approximated by considering the crystal bar

to be cut into short equal lengths l . Each length is represented by a T section in which the arguments kl are small. The equivalent circuit of the whole bar will then be a chain of these elements. The following approximations under these assumptions are valid:

$$\begin{aligned} \tan x &= x, \\ \csc x &= \frac{1}{x}. \end{aligned} \quad (1)$$

It can be shown that four sections of lengths $l/4$ are adequate to give excellent accuracy, so that the following approximations are valid:

$$\begin{aligned} \tan \frac{kl}{8} &= \frac{kl}{8}, \\ \sec \frac{kl}{4} &= \frac{kl}{4}. \end{aligned}$$

In the complete transducer of n crystals the electrical impedances are

$$\frac{\rho c A}{n \phi^2} \tan \frac{kl}{8} = \omega \frac{Al}{8n \phi^2},$$

and

$$\frac{\rho c A}{n \phi^2} \csc \frac{kl}{4} = \frac{1}{\omega \frac{n \phi^2 l}{4 \rho c^2 A}},$$

where

$$k = \frac{\omega}{c} = \frac{2\pi}{\lambda}.$$

From these approximations we see that constant inductances and capacitances

$$\begin{aligned} L &= \frac{\rho Al}{8n \phi^2}, \\ C &= \frac{n \phi^2}{4 \rho c^2 A}, \end{aligned} \quad (2)$$

can be used in the T branches of the bar elements. Each coil and condenser shown in Figure 26 have the values as given above.

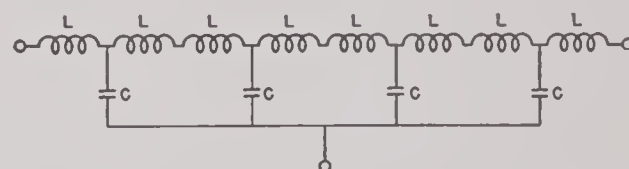


FIGURE 26. Four-section transmission line of constant L and C elements which is an approximation of a T network of transcendental elements.

With these four elements the short-circuited resonance (or free-free analog) occurs at $kl = 3.07$ which is to be compared to $kl = \pi$, the

short-circuited T network of three transcendental impedances. The complete transducer equivalent circuit using L and C constants for n crystals can be well represented up to the first free-free resonance by Figure 27.

If the transducer is inertia driven, the backing plate impedance is zero, or a short circuit. The radiation impedance is assumed to be pure

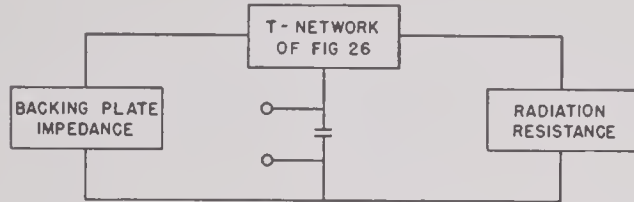


FIGURE 27. Approximate equivalent circuit of the complete crystal transducer.

resistance which in water is $\rho c A / \phi^2 n$ in cgs esu units. The backing plate being a transmission line terminated with zero impedance, its impedance could be represented by the circuit of Figure 26, short-circuited at the terminal end. The impedance of this circuit is, however, a single tangent function of the argument kl_b (l_b = thickness of the plate) and can be represented by only three or four L and C elements, using a partial fraction expansion.⁵

$$\tan x = \sum_{n=1}^{n=\infty} \frac{8x}{(2n-1)^2\pi^2 - 4x^2}, \quad (3)$$

or $Z = jZ_0 \tan kl$

$$= jZ_0 \sum_{n=1}^{n=\infty} \frac{8kl}{(2n-1)^2\pi^2 - 4(kl)^2}.$$

This expansion can be rewritten to represent an infinite sum of parallel LC circuits whose values are given in terms of Z_0 and the quarter-wave frequency f_0 of the plate. At this frequency $k_0 l = \pi/2$ so that $kl = k_0 l (k/k_0) = (\pi/2) \cdot (f/f_0)$, where f is any frequency up to f_0 .

Thus

$$Z = \sum_{n=1}^{n=\infty} \frac{j[4\pi(f/f_0)Z_0]/(2n-1)^2\pi^2}{1 - [f^2/f_0^2(2n-1)^2]}, \quad (4)$$

which may be written

$$Z = \sum_{n=1}^{n=\infty} j \frac{(\omega 2Z_0)/f_0(2n-1)^2\pi^2}{1 - [f^2/f_0^2(2n-1)^2]}.$$

Each term of this sum represents a parallel LC circuit whose impedance is given by

$$Z = \frac{\omega L}{1 - \left(\frac{\omega}{\omega_0}\right)^2},$$

and whose antiresonant frequency is $f'_0 = (2n-1)f_0$ and whose L and C constants are

$$L_n = \frac{2Z_0}{f_0(2n-1)^2\pi^2} = \frac{8M}{\pi^2(2n-1)^2}, \quad (5)$$

$$C = \frac{1}{(2\pi f'_0)^2 l Z_0} = \frac{1}{8f_0 Z_0} = \frac{L}{2\rho c A}, \quad (6)$$

where M is the mass of a section of area A in the plate. Equations (5) and (6) show that the capacitances do not vary with n , but the in-

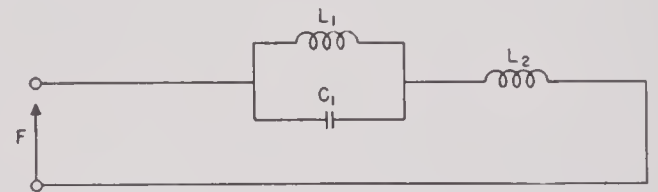


FIGURE 28. Approximate equivalent circuit of a backing resonator.

ductances decrease in ratios $1:1/9; 1/25; 1/49;$ etc., so that ultimately the capacitive reactance may be neglected without appreciable error. Since $f < f_0$ the denominators in equation (4) are appreciably one after the first term and equation (4) becomes

$$Z = \frac{2j\omega Z_0}{\pi^2 f_0 \left(1 - \frac{f^2}{f_0^2}\right)} + \sum_{n=1}^{\infty} \frac{2\omega Z_0}{F_0(2n-1)^2\pi^2}. \quad (7)$$

In terms of total mass of the section equation (7) can be written

$$Z = \frac{j\omega(8/\pi^2)M}{1 - (f^2/f_0^2)} + \sum_{n=2}^{\infty} j\omega \frac{8M}{\pi^2(2n-1)^2}, \quad (8)$$

which is the equation of one parallel LC circuit whose resonance is f_0 in series with a string of inductances of decreasing magnitude. The inductance of the first term is close to $8/\pi^2 = 0.813$ of the total mass since $f/f_0 < 1$ which leaves only 0.187 of the mass for the series elements. This approximation is exact at 0 and f_0 , and is

off less than 0.3 per cent at $f_0/2$. The resultant equivalent circuit for a backing plate is in Figure 28,

$$\text{where } L_1 = \frac{8}{\pi^2} M, \quad L_2 = 0.187M,$$

$$C_1 = \frac{1}{32f_0^2 M}.$$

The equivalent circuit for a complete transducer with a backing plate and radiating into

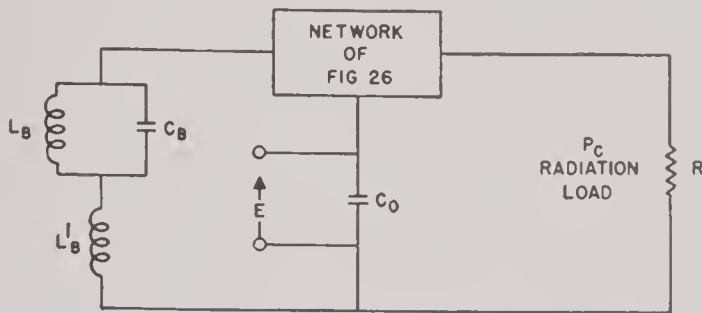


FIGURE 29. Approximate equivalent circuit of a complete transducer using a backing plate and radiating into water.

water can now be drawn. Using the network shown in Figure 29, the following equations can be set down:

$$C_0 = \frac{KA}{4n\pi l_c},$$

$$L_B = \frac{1}{n\phi^2} \frac{8\rho A l_B}{\pi^2},$$

$$C_B = n\phi^2 \frac{l_B}{2\rho c A},$$

$$L'_B = \left(1 - \frac{8}{\pi^2}\right) l_B$$

$$R = \frac{\rho c A}{n\phi^2}.$$

It now remains to be shown that the LC and R elements are practically realizable for a crystal. The resonant frequency of an LC element of Figure 26 can be calculated from equation (2) as

$$\frac{1}{LC} = 32 \left(\frac{c}{l_c}\right)^2 = \frac{128}{\pi^2} \omega_c^2,$$

where $\omega_c = (\pi/2) (C/l_c)$, the frequency of the first free-free resonance of the crystal bar, which occurs at $kl = \pi/2$. Thus each LC element must resonate at $8\sqrt{2}/\pi = 3.59$, instead of 4 times the resonance of a crystal blocked on one

end, which is certainly practical. As it is difficult to vary inductances and easy to vary capacitances, fixed inductors of a convenient size may be chosen, and different capacitors used to represent different transducers. The range of types is limited, however, by equation (2). Referring to this:

$$\ln A = \frac{8L}{\rho\phi^2} \text{ and } C = \frac{nl}{a} \frac{\phi^2}{4\rho c^2}.$$

Thus if L is fixed there is a definite relation $\ln A = \text{constant}$, which means that only two of the parameters n and A are independent. A convenient value of inductance equaling 3×10^{-3} h resonates with a capacitance c equaling $0.013 \mu\text{f}$ at 25.5×10^3 c. The circuit of Figure 26 using these values will represent a short-circuited line or tangent function whose characteristic impedance $Z_0 = 680$ ohms whose first resonance occurs at 7.08×10^3 c.

$$\text{For } Z_0 = \frac{cA}{n\phi^2} = 680 \text{ ohms,}$$

$$L = \frac{\rho A l}{8n\phi^2} = \frac{\rho A c}{n\phi^2} \frac{l}{8c}.$$

For the tangent function

$$k = \frac{2\pi f r^2}{C} = \frac{\pi}{2},$$

$$\frac{l}{C} = \frac{1}{4f_r}, \quad f_r = \frac{25.5 \times 10^3}{3.6} = 7.08 \times 10^3,$$

$$z_0 = 32f_r L = 680 \text{ ohms.}$$

A plot of the function

$$Z_0 = 680 \tan \left(\frac{f}{7.08 \times 10^3} \frac{\pi}{2} \right)$$

together with the measured impedance of the short-circuited transmission line is given in Figure 30. The agreement between the two is excellent up to 6.5 kc. Beyond that, the resistances in the inductances become effective, and throw the experimental values off somewhat.

If the transmission line be terminated in an open circuit, the input impedance will approximate a cotangent function. Figure 31 illustrates the experimental input impedance of this circuit together with the mathematical cotangent curve. The agreement between the measured

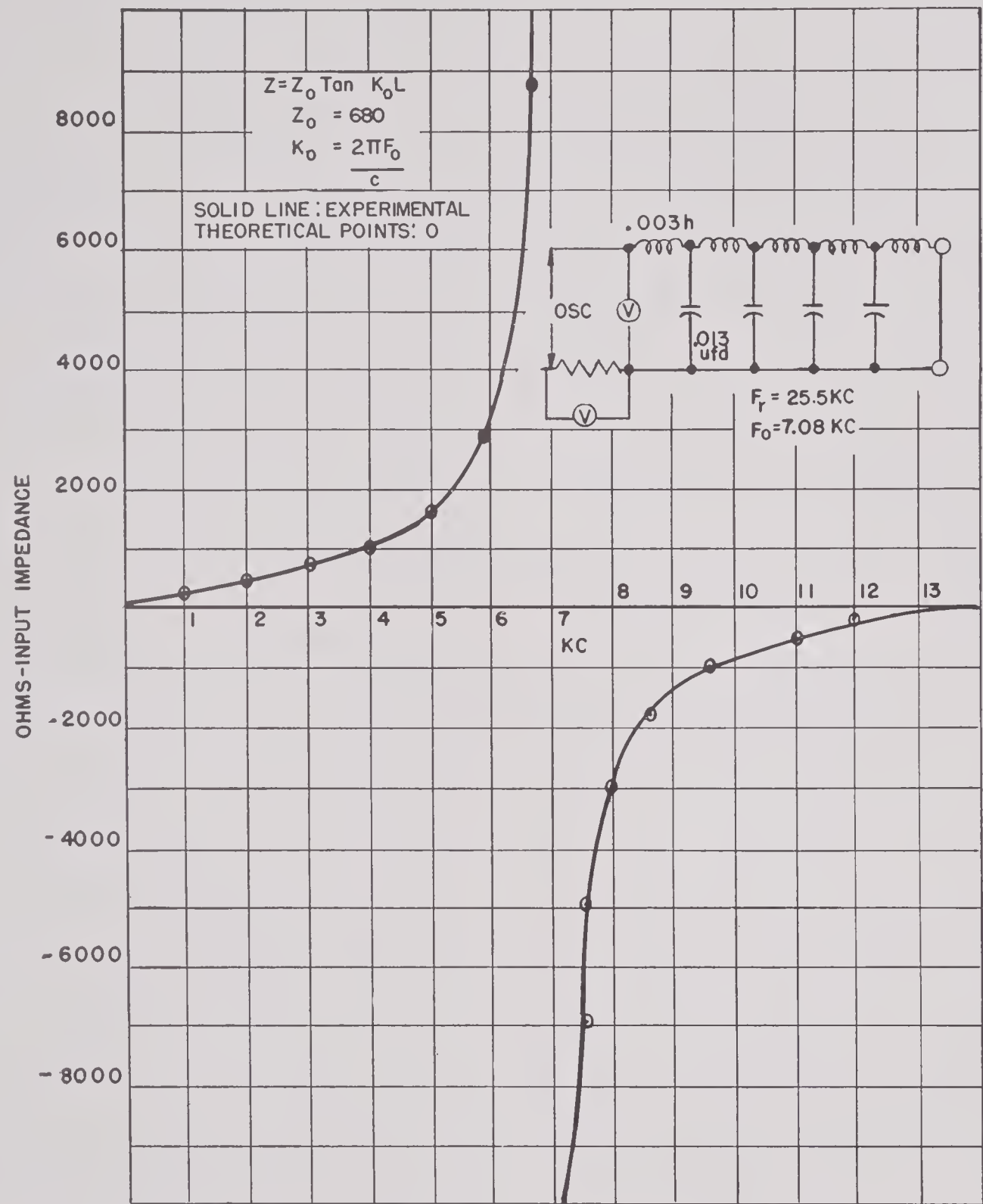


FIGURE 30. Experimental performance of the transmission line of Figure 26 connected so as to simulate the tangent function.

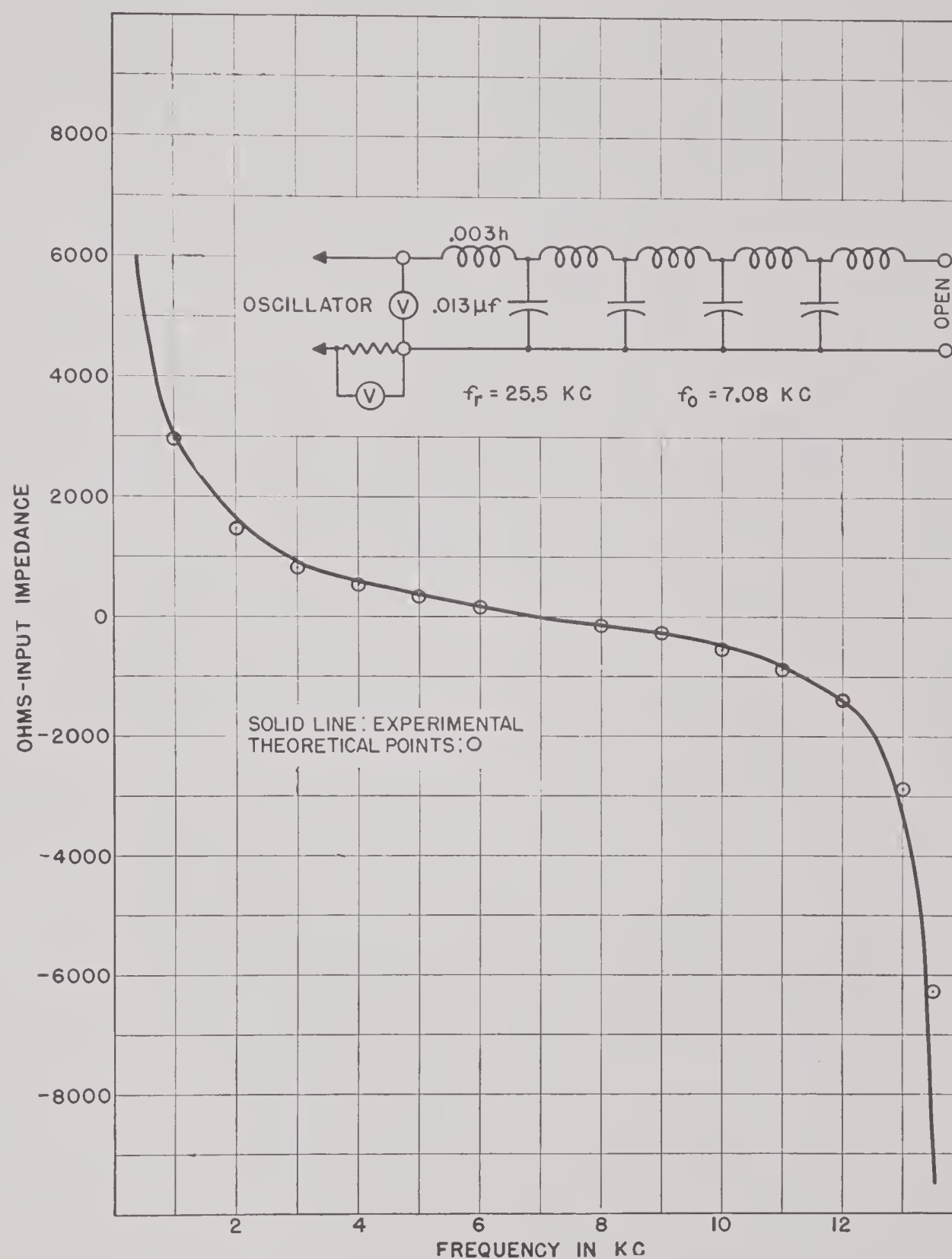


FIGURE 31. Experimental performance of the transmission line of Figure 26 connected so as to simulate the cotangent function.

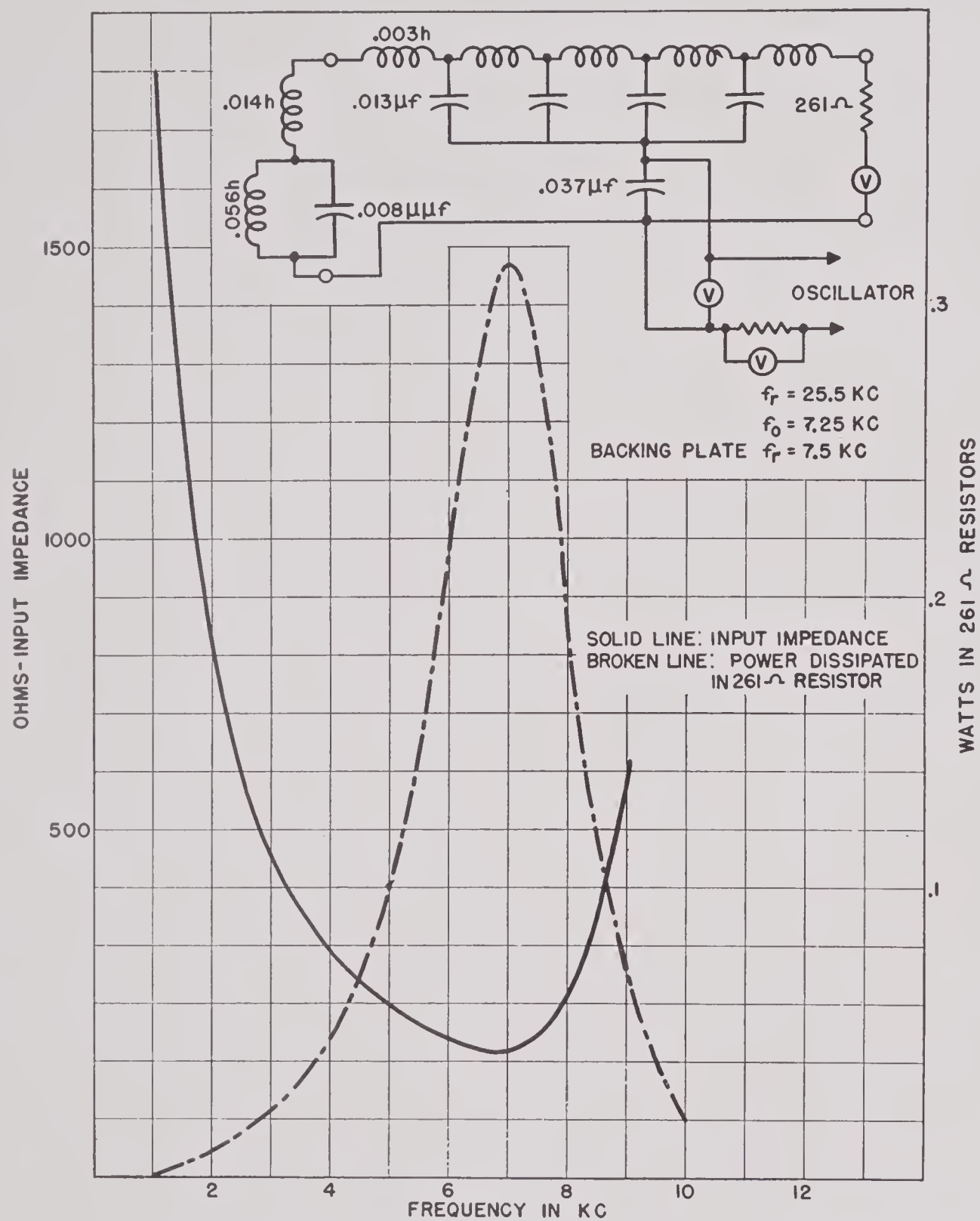


FIGURE 32. Application of the simulator for a backing plate transducer radiating into water.

impedances and the tangent function is remarkable.

A steel backing plate simulating circuit resonating at 7.5 kc can be built of two inductances of 0.014 and 0.056 h, and a capac-

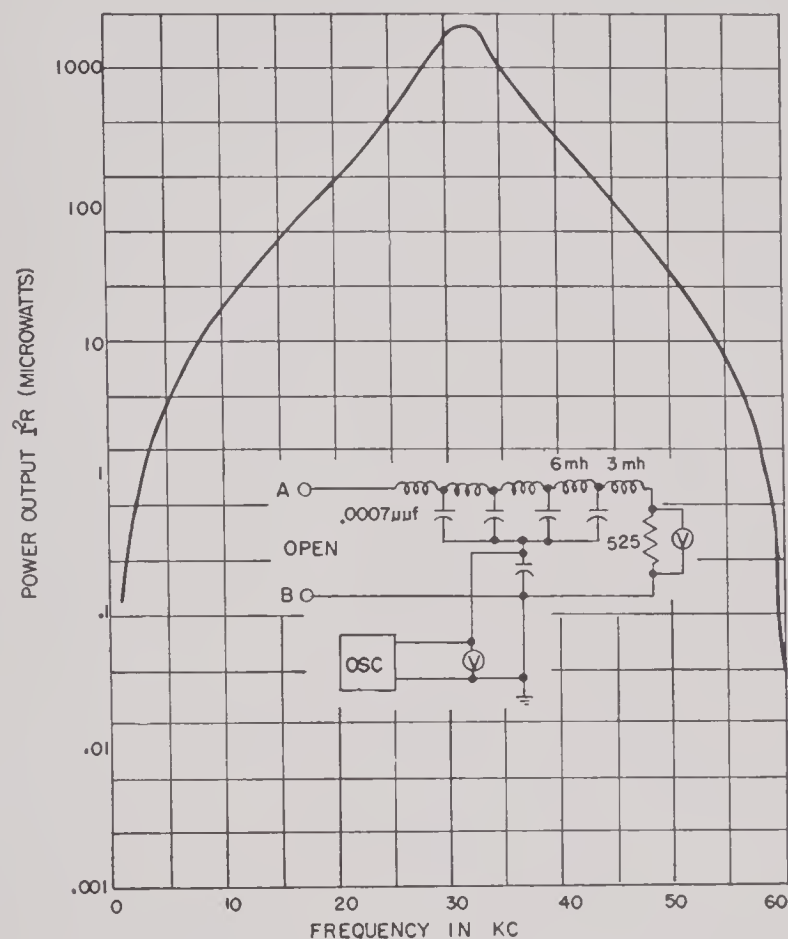


FIGURE 33. Application of the simulator for a hypothetical transducer, radiating into water, in which the back end of the crystals are blocked at all frequencies.

itance of $0.008 \mu\text{f}$ as shown in Figure 32. When the simulating circuit is loaded at one end with this circuit, and at the other with a resistance of 261 ohms, it represents a trans-

ducer whose crystals resonate at 14.15 kc, terminated at one end in a backing plate whose resonance is 7.5 kc, and radiating into water the resistance of which is $Z_0 = \rho c A / n \phi^2$, where A is the area of a single crystal. Curves of input impedance and velocity response at the radiating end of this circuit are shown in Figure 32. The resonant frequency is 7.02 kc which is just half that of the free-free crystal. The response shows a mechanical Q of about 3. The response of a real transducer is not as regular, of course, as this curve, because it is constructed of many crystals attached to a backing plate that has its own flexural modes through glue joints that are not uniform. The general overall response of a real unit does, however, resemble somewhat the response curve of the simulator. See Sections 4.5 and 4.6.

Figure 33 illustrates the simulation of a transducer whose calculated resonance is 30.5 kc when the crystals are blocked at all frequencies. Practically, this is not possible to achieve, because complete blocking can only be done with a quarter-wave resonator. However, the simulation represents the real transducer in the resonant region. The power dissipated in the water-loading resistor is plotted against frequency. As the power scale is logarithmic, the response appears to be quite broad. By shorting terminals A and B , the same circuit simulates the response of an inertia-driven transducer which resonates at 61 kc or double the resonant frequency shown in Figure 33 with terminals A and B open. The general shape of the response curves in both cases is theoretically the same but with the ordinate scale in a ratio of 2 to 1.

GLOSSARY

- ADP (CRYSTAL).** Ammonium dihydrogen phosphate crystal having marked piezoelectric properties.
- AMBIENT NOISE.** Noise present in the medium apart from target and own ship noise.
- BDI.** Bearing Deviation Indicator.
- BEARING DEVIATION INDICATOR.** A system which utilizes the outputs of the halves of a split transducer to provide accurate directional indication.
- BIMORPH (CRYSTAL).** A rigid combination of two Rochelle salt crystals designed to give improved coupling between the crystal element and low (mechanical) impedance devices, such as telephone diaphragms and loudspeaker mechanisms.
- BTL.** Bell Telephone Laboratories.
- CAVITATION.** The formation of gas or vapor cavities in a liquid, caused by sharp reduction of local pressure.
- CLAMPED DRIVE.** A condition in which the radiation impedance (water) is on one end of the crystal and a backing plate is on the other.
- CRYSTAL TRANSDUCER.** A transducer which utilizes piezoelectric crystals, usually Rochelle salt, ADP, quartz, or tourmaline.
- CUDWR.** Columbia University Division of War Research.
- CYCLE-WELD.** A commercial cement.
- DILATATION.** The increase in volume per unit volume of a very small undisplaced region of a substance.
- DIRECTIVITY FACTOR.** A measure of the directional properties of a transducer. It is the ratio between the average intensity, or response, over the whole sphere surrounding the transducer, and the intensity, or response, on the acoustic axis.
- DIRECTIVITY INDEX.** Directivity factor expressed in decibels.
- DOME.** A transducer enclosure, usually streamlined, used with echo-ranging or listening devices to minimize turbulence and cavitation noises arising from the transducer's passage through the water.
- EIGEN MODE.** Natural mode of vibration.
- ELECTRET.** The electrical analogue of a magnet.
- EUTECTIC ALLOY.** An alloy with the lowest melting point of all alloys containing the same constituents. Upon solidifying all the constituents crystallize simultaneously.
- HYDROPHONE.** Underwater microphone.
- INDUCTION FIELD.** The region, immediately surrounding a transmitter face, where the inverse square law does not hold.
- INERTIA DRIVE.** A condition in which the radiation impedance (water) is on one end of a crystal and zero impedance (air) is on the other.
- MATRIX (CRYSTAL).** An assemblage of crystals for use as a transducer.
- METASTABLE STATE.** A state, actually unstable, which appears stable because of the length of time it persists.
- MOTOR, CRYSTAL.** The crystal assembly and backing plate in a transducer.
- NEOPRENE.** Generic name for synthetic rubber made by polymerization of 2-chloro-1,3-butadiene. Vulcanizates are markedly resistant to oils, greases, chemicals, sunlight, ozone, and heat.
- NRL.** Naval Research Laboratory.
- OPTIC AXIS (Z-AXIS).** The direction in a doubly refracting crystal along which the ordinary and extraordinary light rays pursue the same path with the same velocity.
- ORTHORHOMBIC SYSTEM.** A system of crystals having three unequal axes at right angles to each other.
- PIEZOELECTRIC EFFECT.** Phenomenon exhibited by certain crystals in which mechanical compression produces a potential difference between opposite faces, or an applied electric field produces corresponding changes in dimensions.
- PING.** Acoustic pulse signal projected by an echo-ranging transducer.
- PROBE MICROPHONE.** A very small crystal microphone, used to study variations in sound output.
- RECIPROCITY PRINCIPLE.** The ideal transducer gives analogous performance in transmission and reception; for example, the directivity patterns are the same in both cases.
- REVERBERATION.** Sound scattered diffusely back towards the source, principally from the surface or bottom and from small scattering sources in the medium such as bubbles of air and suspended solid matter.
- ρc RUBBER.** A rubber compound with the same ρc (density times velocity of sound) product as water. Also called sound, or sound-water, rubber.
- ROCHELLE SALT.** Potassium sodium tartrate, $\text{KNaC}_4\text{H}_4\text{O}_6 \cdot 4\text{H}_2\text{O}$, piezoelectric crystal used in sonar transducers.
- RS CRYSTAL.** Rochelle salt crystal.
- SYMMETRIC DRIVE.** A condition in which the radiation impedance (water) is on both ends of a crystal.
- SOUND (SOUND-WATER) RUBBER.** See ρc rubber.
- TETRAGONAL SYSTEM.** A crystallographic system in which all the forms are referred to three axes at right angles; two are equal and are taken as the "horizontal" axes; the remaining "vertical" axis is either longer or shorter than the others.
- THERMOPLASTIC SUBSTANCE.** A substance which becomes plastic upon being heated.
- THERMOSETTING SUBSTANCE.** A substance which, upon the application of heat, acquires and retains new chemical and physical properties which subsequent application of heat does not alter.
- TRANSDUCER.** Any device for converting energy from one form to another (electrical, mechanical, or acoustical). In sonar, usually combines the functions of a hydrophone and a projector.
- UCDWR.** University of California Division of War Research.

VARISTOR. Nonlinear resistance whose value decreases with increasing applied voltage.

VEIL (CRYSTAL). Vacant or flawed region within the body of a crystal, caused by unfavorable saturation conditions in the solution during the growth of the mother bar.

WINDOW. The portion of a transducer case designed to permit the passage of acoustic waves.

X-CUT (45° X-CUT). A cut in which the electrode faces of a piezoelectric crystal are perpendicular to its *X*-, or electric, axis. In the 45° *X*-cut, the longest

dimension of the crystal is 45° from the *Y* and the *Z* axes.

Y-CUT (45° Y-CUT). A cut in which the electrode faces of a piezoelectric crystal are perpendicular to its *Y*-, or mechanical, axis. In the 45° *Y*-cut, the longest dimension of the crystal is 45° from the *X* and the *Z* axes.

Z-CUT (45° Z-CUT). A cut in which the electrode faces of a piezoelectric crystal are perpendicular to its *Z*-, or optic, axis. In the 45° *Z*-cut, the longest dimension of the crystal is 45° from the *X* and the *Y* axes.

BIBLIOGRAPHY

Numbers such as Div. 6-611.2-M3 indicate that the document listed has been microfilmed and that its title appears in the microfilm index printed in a separate volume. For access to the index volume and to the microfilm, consult the Army or Navy agency listed on the reverse of the half-title page.

Chapter 1

1. *Basic Methods for the Calibration of Sonar Equipment*, Summary Technical Report, Division 6, Vol. 10.
2. *Completion Report on Transducer Calibration Facilities and Techniques*, UCDWR U435.
3. *Principles and Applications of Underwater Sound*, Summary Technical Report, Division 6, Vol. 7.

Chapter 2

1. *The Absolute Differential Calculus*, Levi-Civita, Blackie and Sons, 1927.
2. *Mathematical Theory of Elasticity*, A. E. H. Love, Cambridge University Press, 1934, p. 44.
2a. *Ibid.*, p. 78.
2b. *Ibid.*, p. 102.
2c. *Ibid.*, p. 287 et seq., p. 428.
3. *Lehrbuch der Kristallphysik*, W. Voigt, B. G. Teubner, 1928.
3a. *Ibid.*, p. 167.
3b. *Ibid.*, pp. 218, 965.
3c. *Ibid.*, pp. 218, 915, 965, 978.
4. "Impedance Representation of Tangential Boundary Conditions," G. D. Camp, *The Physical Review*, Vol. 69, May 1946, p. 501.
5. *Vibration and Sound*, Philip M. Morse, McGraw-Hill Book Co., New York, 1936.
6. *Untersuchungen über das Logarithmische und Newtonische Potential*, C. Neumann, Leipzig, 1877.
7. "On the Acoustic Shadow of a Sphere," Lord Rayleigh and John William Strutt, baron, *Philosophical Transactions of the Royal Society (London)*, 1904.
8. "Über die von einer starren Kugel hervorgerufene Störung des Schallfeldes," Stenzel, *Electrische Nachrichten-Technik*, Vol. 15, No. 3, 1938.
9. *The Physical Review*, G. D. Camp [about September 1946].
10. "Absorption of Sound Waves," Epstein, *Theodore von Kármán Anniversary Volume*, California Institute of Technology.
11. *The Theory of Sound*, Vol. 2, Lord Rayleigh and John William Strutt, baron, Dover Publications, New York, 1945.
12. *Electromechanical Transducers and Wave Filters*, Warren P. Mason, D. Van Nostrand Co., New York, 1942, p. 200.
12a. *Ibid.*, pp. 315, 318.
12b. *Ibid.*, p. 205.
13. "Mathematics of the Physical Properties of Crystals," Walter L. Bond, *Bell System Technical Journal*, Vol. 22, January 1943.
13a. *Ibid.*, p. 22.

14. "On Dissipative Systems and Related Variational Principles," Bateman, *The Physical Review*, Vol. 38, p. 815.
15. *Nature*, Bateman, Vol. 131, 1933, p. 472.
16. *Journal für die Reine Angewandte Mathematik*, L. Pochhammer, Vol. 81, 1876, p. 324.
17. *Cambridge Philosophical Society Transactions*, C. Chree, Vol. 14, 1889, p. 278.

Chapter 3

1. *Electromechanical Transducers and Wave Filters*, Warren P. Mason, D. Van Nostrand Co., 1942, p. 200 et seq.
1a. *Ibid.*, Appendix C.
1b. *Ibid.*, p. 202.
2. *Dissipation of Energy in Crystal Transducers*, Parts A to C, Glen D. Camp, File 01.22, UCDWR Memorandum, Feb. 19, 1944. Div. 6-611.2-M3
3. *Electrical Measurements for 45° Z-cut ADP Crystals—Case 24769-8*, H. J. McSkimmin, Technical Memorandum MM-44-120-97, BTL, Oct. 6, 1944. Div. 6-611.1-M7
3a. Drawing No. BL 382365.
4. *The Design of Crystal Vibrating Systems*, William J. Fry, John M. Taylor, and B. W. Hennis, NRL, August 1945. Div. 6-611.2-M6
5. *Constants and Temperature Coefficients of ADP Crystals—Case 33222*, W. P. Mason and R. G. Kinsley, Technical Memorandum MM-43-160-38, BTL, Mar. 30, 1943, p. 15. Div. 6-611.1-M5
5a. *Ibid.*, p. 27.
6. *Properties of 45° Y-cut RS, and the Load Carrying Capacity of Liquids Used with Them*, OSRD 1308, NDRC 6.1-sr346-627, BTL, Dec. 15, 1942, p. 8. Div. 6-611.1-M3
7. *Vibration and Sound*, Philip M. Morse, McGraw-Hill Book Co., New York, 1936, p. 123.
8. *Theory of Sound*, Lord Rayleigh and John William Strutt, baron, Dover Publications, New York, 1945.
9. *Theoretical Physics*, Joos, G. E. Stechert and Co.
10. *Acoustics*, G. W. Stewart and R. B. Lindsay, D. Van Nostrand Co., New York, 1930.
11. "Der senkrechte und schräge Durchtritt einer in einem flüssigen Medium erzeugten ebenen Dilationen — Welle durch eine in diesem Medium befindliche planparallele feste Platte," H. Reissner, *Helvetica Physica Acta*, Vol. 11, 1938, pp. 140-144.
12. *Mechanical and Acoustic Attachments for Piezoelectric Crystals Used in Transducers*, NDRC 6.1-sr346-628, BTL, Dec. 15, 1942. Div. 6-611.2-M2
13. *Comparison of Two 54 Inch Domes*, Eginhard Dietze, NDRC 6.1-sr1130-1628, Service Project NS-139, CUDWR-USRL, June 19, 1944. Div. 6-555-M21

14. *Transmission of Sound Through Flat Plates* (Internal Memorandum), Edwin M. McMillan, [C4-sr30-025] UCDWR, Oct. 15, 1941. Div. 6-611.2-M1
15. *Technical Data on Plastics*, Plastics Materials Manufacturers' Association, Washington, D. C.

Chapter 4

1. *Electromechanical Transducers and Wave Filters*, Warren P. Mason, D. Van Nostrand Co., New York, 1942, p. 205.
 - 1a. *Ibid.*, p. 204 et seq.
 - 1b. *Ibid.*, p. 207.
 - 1c. *Ibid.*, p. 235.
2. *Principles and Applications of Underwater Sound*, Summary Technical Report, Division 6, Vol. 7.
3. *Vibration and Sound*, Philip M. Morse, D. Van Nostrand Co., New York, 1944, p. 260, Fig. 71.
4. *Methoden der Mathematischen Physik*, R. Courant and D. Hilbert, Vol. 1, J. Springer, Berlin, 1931, p. 412.
5. *Tables and Functions with Formulae and Curves*, Eugen Jahnke and Fritz Emde, B. G. Teubner, Leipzig and Berlin, 3rd Edition, [G. E. Stechert & Co., N. Y.] 1938.
6. *Journal of Mathematics*, Helmholtz, Vol. 57, 1859, p. 7.
7. *Mathematische Annalen*, Vol. 1, 1869, pp. 1-36.
8. *Mathematische Annalen*, A. Sommerfeld, Vol. 47, 1896, p. 317.
9. *Akustische Zeitschrift*, K. Osterhammel, Vol. 2, March 1941, p. 6.
10. *The Theory of Sound*, Vol. 2, Lord Rayleigh and John William Strutt, baron, Dover Publications, New York, 1945.
11. "Berechnung des Schallfeldes von Kreisförmigen Kolbenmembranen," *Electrische Nachrichten-Technik*, Vol. 4, 1927, p. 239.
12. *Mathematische Annalen*, K. Swartschild, Vol. 55, 1902.
13. "Das Schallfeld der Kreisförmigen Kolbenmembranen," H. Backhaus, *Annalen der Physik*, Vol. 5, 1930, p. 1.
14. "Acoustic and Inertia Pressure at any Point on a Vibrating Circular Disc," N. W. McLachlan, *Philosophical Magazine*, Vol. 14, Ser. 7, 1932, pp. 1012-1025.
15. *Annalen der Physik*, H. Stenzel, Vol. 4, 1942, p. 18.
16. "Acoustic Radiation Field of Piezoelectric Oscillator," L. V. King, *Canadian Journal of Research*, Vol. 11, August 1934, p. 135.
17. *Akustische Zeitschrift*, K. Menges, Vol. 6, 1941, p. 90.
18. *American Journal of Acoustics*, R. Clark Jones, Ser. 16, 1945, p. 147.
19. *Electrische Nachrichten-Technik*, H. Stenzel, Vol. 4, 1927, p. 239.
20. *Electrische Nachrichten-Technik*, H. Stenzel, Vol. 6, 1929, p. 165.
21. "The Impedance of Telephone Receivers as Affected

by the Motion of Their Diaphragm," Kennelly and Pierce, *Proceedings of the American Academy of Arts and Sciences*, September 1912.

Chapter 5

1. *Radio Engineering*, F. E. Terman, McGraw-Hill Book Co., New York, 1937, Ch. 7.
 - 1a. *Ibid.*, Sec. 43, Chap. 5; Sec. 55, Chap. 6.
 - 1b. *Ibid.*, Sec. 61, Chap. 7.
 - 1c. *Ibid.*, Sec. 5, par. 11; Sec. 3, par. 27.
2. "Circle Diagram in Tube Circuits," A. A. Nims, *Electronics*, Vol. 12, No. 3, May 1939, p. 23.
3. *Motion Picture Sound Engineering*, D. Van Nostrand Co., New York, 1938, Chaps. XVI, XVII.

Chapter 6

1. *Electromechanical Transducers and Wave Filters*, Warren P. Mason, D. Van Nostrand Co., New York, 1942, p. 202 et seq.
2. *Elements of Acoustical Engineering*, Harry F. Olsen, D. Van Nostrand Co., New York, 1940.

Chapter 7

1. *The Design of Crystal Vibrating Systems*, William J. Fry, John M. Taylor, and B. W. Hennis, U. S. Government Printing Office, NRL, August 1945. Div. 6-611.2-M6

Chapter 8

1. "The Growing of Crystals," R. W. Moore, *J. Am. Chem. Soc.*, Vol. 41, 1919, p. 1060.
2. U. S. Patent Reissues, 19697 (1935), 19698 (1935), B. Kjellgren.
3. German Patent 228, 246 (1908), F. Krueger and W. Finke.
4. "Dilations in Rochelle Salt," I. Vigness, *The Physical Review*, Vol. 48, 1935, pp. 198-202.
5. *Interelectrode Leakage of Rochelle Salt Crystals Used in Piezoelectric Devices*, H. J. McSkimin, Technical Memorandum MM-41-160-52, BTL, Oct. 14, 1941. Div. 6-611.1-M1
6. *Data on Piezoelectric PN Crystals* (Revised Edition), Hans Jaffe, Brush Development Company, Nov. 23, 1943. Div. 6-611.1-M6
7. *ADP Crystals, I. Growing ADP Crystals and Establishment of Pilot Plant, II. Processing ADP Crystals, III. Electrical Testing of ADP Crystals*, NXss-31643 and NXsr-46932, Task Nos. 7 and 8, BTL and BuShips, Dec. 15, 1945. Div. 6-611.1-M8
8. *The Electrical Resistivity of Crystals of Ammonium and Potassium Dihydrogen Phosphate*, J. B. Johnson and H. B. Briggs, Technical Memorandum MM-43-160-32, BTL, Mar. 20, 1943. Div. 6-611.1-M4
9. *Specification for ADP Crystal Plates*, NAVSHIPS (940-930D) Radio Division, Navy Department RE-13A-922A, Mar. 16, 1944. Div. 6-611.2-M4

10. *Piezoelectricity*, Walter G. Cady, McGraw-Hill Book Co., New York, 1946.
11. U. S. Patent 1,764,088, C. B. Sawyer; also Canadian Patent 302,568.
12. *Electrical Measurement for 45° Z-Cut ADP Crystals*, H. J. McSkimin, Technical Memorandum MM-44-120-97, BTL, Oct. 6, 1944. Div. 6-611.1-M7
13. *Properties of 45° Y-Cut Rochelle Salt Crystals, and the Load Carrying Capacity of Liquids Used with Them*, OSRD 1308, NDRC 6.1-sr346-627, BTL, Dec. 15, 1942. Div. 6-611.1-M3
14. *Fundamental Studies of X-Cut Rochelle Salt*, Darol K. Froman, NDRC C4-sr30-392, UCDWR, July 15, 1942. Div. 6-611.1-M2
15. *Mechanical and Acoustic Attachments for Piezoelectric Crystals Used in Transducers*, NDRC 6.1-sr346-628, BTL, Dec. 15, 1942. Div. 6-611.2-M2
16. *The Investigation of Adhesives for ADP Crystal Assemblies*, Bell Telephone Laboratories, Technical Memorandum 44-120-99, BTL, Oct. 10, 1944. Div. 6-611.2-M5
17. Letter from C. J. Frosch of Bell Telephone Laboratories to S. E. Urban of B. B. Chemical Company, Cambridge, Mass., Mar. 3, 1945.
18. "The Behavior of Nickel Copper Alloys in Sea Water," F. L. LaQue, *Journal of the American Society of Naval Engineers*, Vol. 53, February 1941, pp. 29-64.
19. "Some Observations of the Potentials of Metals and Alloys in Sea Water," F. L. LaQue and G. L. Cox, *Proceedings of the American Society of Testing Materials*, Vol. 40, June 1940.
20. "Brass Plating for Rubber Adhesion," H. P. Coats, *Monthly Review*, January 1937, pp. 5-26; "Brass Plating for Rubber Adhesion," W. Hayford and H. S. Rogers, *Monthly Review*, May 1945.
21. *Measuring Tank Suitable for Acoustic Measurements in Water*, 6.1-NDRC-836, BTL, Mar. 31, 1943. Div. 6-553.4-M2
22. *Absorption of Coated Steel Plates*, Eginhard Dietze, NDRC 6.1-sr1130-2146, Service Project NS-139, CUDWR-USRL, Apr. 5, 1945. Div. 6-552-M17

Chapter 9

1. *Electrical Communication*, M. Levy, Vol. 18, 1940, p. 206.
2. *Electronics*, T. P. Taylor, Vol. 12, 1934, p. 62.
3. *Fundamental Studies of X-Cut Rochelle Salt*, Darol K. Froman, NDRC C4-sr30-392, UCDWR, July 15, 1942. Div. 6-611.1-M2
4. *Electromechanical Transducers and Wave Filters*, Warren P. Mason, D. Van Nostrand Co., New York, 1942, p. 203.
4a. *Ibid.*, p. 205.
5. *Smithsonian Mathematical Formulae*, Smithsonian Institution, Washington, D. C., 1939, p. 129.

CONTRACT NUMBERS, CONTRACTORS, AND SUBJECT OF CONTRACTS

<i>Contract Number</i>	<i>Name and Address of Contractor</i>	<i>Subject of Contract</i>
OEMsr-30	The Regents of the University of California Berkeley, California	Maintain and operate certain laboratories and conduct studies and experimental in- vestigations in connection with submarine and subsurface warfare.
OEMsr-346	Western Electric Company, Inc. New York, New York	Studies and experimental investigations in connection with submarine and subsur- face warfare.

INDEX

The subject indexes of all STR volumes are combined in a master index printed in a separate volume. For access to the index volume consult the Army or Navy Agency listed on the reverse of the half-title page.

- AA60 transducer cable, 346
- Acheson 1008 (aqueous graphite suspension), 285
- Acoustic ammeter, 7
- Acoustic reciprocity principle, application to transducers, 152-161
 - calibration of transducers, 133-134
 - directivity index, 159-161
 - equivalent circuit, 59-61
 - lobe suppression, 154-159
 - theory, 132
- Acoustic windows
 - see* Windows, acoustic
- Acoustic-isolation materials, 125-126, 261-263, 328-330
 - Airfoam rubber, 257, 262-263
 - applications, 262-263
 - Cell-tite foam neoprene, 126
 - cellular rubber, 329-330, 346
 - cork and cork-rubber compositions, 330
 - Corprene, 125, 262, 265-266
 - dichloro-difluoro methane, 328
 - Foamglas, 125-126, 262
 - free gas, 328-329
 - Freon, 328
 - metal-air cells, 329
 - summary of types, 261-262
- Acryloid B-7 cement
 - application technique, 315-316
 - attaching tin-foils to crystals, 287
- Admittance, absolute, 162-163
- Admittance curves, 332
- Admittance measurements, transducer
 - see* Impedance measurements, transducer
- Admittance measuring circuit
 - crystal capacitance, 301-302
 - crystal resonance, 304
- Admittance specifications for crystals, 302-303, 332
- ADP crystals
 - see* Ammonium dihydrogen phosphate crystals
- Airfoam rubber
 - applications, 257, 262-263
 - comparison with Corprene, 262
- Akron Paint and Varnish Company, antifouling paints, 341
- Aluminum faces for transducer elements, 119, 284
- Amercoat (corrosion-resisting coating), 340-341
- American Pipe and Construction Company, Amercoat, 340-341
- Ammeter, acoustic, 7
- Ammonium dihydrogen phosphate crystals
 - advantages over Rochellesalt, 231-232
 - capacitance measurements, 300-301
 - characteristic impedance at zero width, 89
 - dielectric constant, 93
 - electromechanical coupling coefficient, 91-92
 - formula, 271-272
 - matrix formulation using crystallographic axes, 55-56
 - matrix formulation using rotated axes, 56-57
 - piezoelectric coupling coefficient, 91-92
 - solution of boundary-value problem, 64-72
 - summary of constants, 93
 - upper temperature limit, 306
- Ammonium dihydrogen phosphate crystals, characteristics
 - chemical properties, 271-272
 - electrical properties, 273-274
 - impedance measurements, 89
 - surface resistance, 273-274
 - thermal behavior, 273
 - volume-resistivity, 273
- Ammonium dihydrogen phosphate crystals, processing
 - bonding to rubber, 310-314
 - grinding, 289-291
 - growing process, 271-273
 - milling, 294-295
 - orientation of bars, 277-279
 - reflectoriascope, 278
 - rough-cutting from bars, 279-280
 - sawing, 292-294
 - spliced crystals, 281
 - surface finishing, 280-281
- Ammonium dihydrogen phosphate crystals, specifications
 - d-c volume resistivity, 305
 - electrical characteristics, 300
 - high voltage, 305
 - oscillatory characteristics, 304
- Amplifiers, transducer, 73, 217-226
 - effect of impedance-matching ratios, 220-223
 - effect of load magnitude and power factor, 218-219
 - for receiving transducers, 224-225
 - guard amplifier, 224-226
 - impedance-match, 224
 - preamplifier, 74
 - pulsed power, 224
 - transmitting response, 179
- Amplitude-directivity patterns, 130
- Antifouling paint, 341
- Antiresonance of crystals
 - definition, 303
 - electrical, 83-84
 - mechanical, 82
- Assembly and mounting of transducers, 95-97, 350-357
 - backing plates, 322-323
 - Benioff blocks, 97
 - cable installation, 351-352
 - cement joints, 95-96
 - crystal arrays, 316-319, 322-323, 350-351
 - crystal blocks, 96-97
 - liquid-filling technique, 355
 - matching networks and cables, 351
 - sealing cases, 352-355
 - unit-construction, 97
- B-7 cement, Acryloid
 - application technique, 315-316
 - attaching tin-foils to crystals, 287
- Backing plates, 75, 98-110
 - calculation of flexural modes, 98-99
 - calculation of impedance, 103-105, 360-361
 - coupling techniques, 98
 - criterion for determining minimum thickness, 105-106
 - effect on surface-velocity distributions, 108-110
 - frequency of flexure of a rectangular bar, 98
 - modal patterns for a square plate, 99
 - QBF-type, 102
 - slotted square bar, 102
 - spurious vibrations, 263
 - suppression of flexural modes, 101-102
- Backing plates, design, 262-264
 - acoustic-isolation materials, 262
 - insulation, 264
 - mounting technique, 322-323
 - multiple layers, 103-106, 263
 - thin plates, 264
 - use of silicone or Univis oil, 106
- Backing plates, materials, 319-322
 - aluminum, 119
 - Cerrobend, 110-111, 321
 - Duralumin, 322
 - glass, 122, 263, 321
 - lead, 121, 321-322
 - magnesium, 121
 - Meehanite, 120
 - plastic plates, 321
 - steel, 319-321
 - Wood's metal, 121
- Bakelite, use in transducers, 121
- Bakelite cement, use in transducers
 - application technique, 307-309
 - BC-6052 cement, 123, 286
 - effect of transducer filling liquid, 309
- Baker Castor Oil Company, oil filling for transducers, 347

- Bandwidth of crystals
 Benioff blocks, 97
 in constant-voltage drive crystals, 82-83
- BC-6052 Bakelite cement
 coupling of crystals, 123
 electroding crystals, 286
- BE transducer, 4
- Beam patterns
see Directivity patterns
- Beeswax, use in transducers, 124
- Bell Telephone Laboratories
 Butyl-C cement, 124, 309-310
 electrode of crystals, 93
 jacketed foam rubber, 262
 ρ c rubber, 264, 336-337
 transducer, 4
- Benioff blocks, 97
- BG transducer, 4
- Blocked crystal
 definition, 78
 resistance, 80
- Blocked impedance of transducers, 161
- Boundary-value problem, solution, 64-72
 approximation including all second-order moments, 69-72
 Mason approximation, 67-69
 piezoelectrics, 49-51
 steady-state, 61-62
- Brass, use in transducers, 119
- Bridge circuit for crystal capacitance measurement, 301
- Bridge methods for transducer impedance measurement, 360-362
 balanced-to-ground arrangement, 361-362
 effect of cable, 360-361
 "hy-bridge," 361-362
 metallic backing plate, 360-361
 nonmetallic backing plate, 360
 Schering bridge, 360
 three-terminal impedance, 360
 two-terminal impedance, 360
- Bronze for transducer cases, 119
- Brush Development Company
 milling equipment for processing crystals, 294
 synthetic Rochelle salt crystals, 269-270
 transducer, 4
- BTL (Bell Telephone Laboratories)
 Butyl-C cement, 124, 309-310
 electrode of crystals, 93
 jacketed foam rubber, 262
 ρ c rubber, 264, 336-337
 transducer, 4
- Butacite VF-7100 cement, 314
- Butyl phthalate for filling transducers, 124-125
- Butyl-C cement, use in transducers
 application technique, 309-310
 manufacturing process, 310
 properties, 310
- C-3 Cycle-Weld cement, 123-124
- Cable design, transducer, 73, 214-216, 346-347
 AA60; 346
 dielectrics, 214-215
 effect on impedance measurements, 360-361
 effect on performance, 215-216
 installation, 351-352
 Koroseal, 214-215
 oil-tight, 346-347
 packing glands, 343
 polythene, 214-215
 SA60; 346
 Simplex No. 9061; 346, 361
 specifications and tests, 346
 vinyl chloride plastics, 214-215
 Vinylite, 214-215
- Cadmium, use in transducers, 119
- Calcium chloride, use in transducers, 125
- Calibration of transducers
 application of data, 357
 complex impedance, 161-164
 directivity patterns, 22-25, 139-152
 impedance measurement methods, 177-178, 358-362
 reciprocity method, 133-134
 response measurements, 164-168, 235, 243-246, 251-254
 tests, 22-27
- Cases for transducers
see Housing for transducers
- Castor oil filling for transducers
 acetylated, 125
 Baker's DB-grade, 124-125
 characteristics and specifications, 347-348
 dehydration, 348-350
- Cavitation limit on transducer, 27, 171-172, 213
- Cavity modes in transducers, 113
- CD transducer, 7
- Cell-tite foam neoprene, use in transducers, 126
- Cell-tite rubber
 acoustic isolation, 329-330
 sound-reflecting pads, 346
- Cellular rubber
see Cell-tite rubber
- Cellulose acetate butyrate plastic for acoustic windows, 117
- Cement joints for crystals, 95-96, 305-306
- Cements used in transducers, 123-124, 305-316
 Acryloid B-7; 287, 315-316
 Bakelite, 123, 286, 307-309
 beeswax and rosin, 124
 Butacite VF-7100; 314
 Butyl-C, 309-310
 Cycle-Weld, 123-124, 312-314
 molten Rochelle salt, 124, 315
 Norace, 315
 sealing wax, 124
 thermoplastic, 281, 314-315
 Ty-ply, 338, 346-347
 urea formaldehyde, 315
 Vinylseal, 281
 Vulcalock, 123, 286, 307-309
- Cements used in transducers, application techniques, 305-307
 amount, 306
 condition of cemented surface, 306-307
 crystal blocks, 96-97
 curing, 307
 humidity, 307
 inertia-driven crystal, 256
 method, 306
 specifications, 305-306
- Ceramics and glasses used in transducers, 122-123, 263, 321
- Cerrobend transducer backing plates, 110-111, 321
- Chicago Pneumatic Tool Company,
 tool for banding rubber cylinders, 353
- Chrysler Corporation, Cycle-Weld cement, 123-124, 312-314
- Circuits, electronic
see also Equivalent circuits
 admittance measuring circuit, 301-302, 304
 bridge circuit for crystal capacitance measurement, 301
- CJ transducer, 7
- Clamped drive crystals, 173-176
 design, 255, 257, 259
 electrical Q, 423
 equivalent circuit, 173-174
 evaluation, 232
 groups of crystals, 257
 impedance, 178
 intensity, 180
 maximum short-circuit current, 181
 mechanical Q, 176
 radiation resistance, 177
 resonant frequency, 175
- Clamped drive transducers
 CP10Z, 236
 CQ4Z, 236
 CQ8Z, 4, 236, 338
 FG8Z, 236
 GA14Z, 236
 JB4Z, 236-246, 258-259
- Coatings, corrosion-resisting
 Amercoat, 340-341
 antifouling paints, 341

- Copolene for transducer cables, 214-215
- Copper, use in transducers, 119-120
- Corprene
 applications, 125, 265-266
 comparison with Airfoam rubber, 262
 sound-reflecting pads, 346
 use in blanking non-radiating faces of crystal, 325-326
- Corrosion-resisting coatings
 Amercoat, 340-341
 antifouling paints, 341
- Coupling between transducer sections
 backing plates, 98
 crystals, 123
 exterior case, 74
- CP10Z clamped drive transducer, 236
- CQ transducer, cylindrical crystal array, 318
- CQ4Z clamped drive transducer, 236
- CQ8Z clamped drive transducer
 acoustic window, 338
 crosstalk level, 4
 dual transducer, 236
- Crosstalk in transducers, 4, 265-266
- Crystal arrays, assembly, 316-319
 cylindrical and curved arrays, 318-319
 installation, 350-351
 mounting technique, 322-323
 simple flat arrays, 316-317
 stacked arrays, 319
- Crystal arrays, design, 259-260, 316-333
 acoustic-isolation materials, 328-330
 backing plates, 263-264, 319-323
 cylindrical source, 259
 fronting plates, 323
 lobe suppression, 159, 259, 317-318
 multiple motors, 259-260
 requirements, 234
 rubber diaphragm, 324-325
 stacked arrays, 325-326
- Crystal arrays, inspection techniques, 330-333
 admittance, 332
 capacitance, 332
 d-c resistance, 332
 high voltage, 333
 polarity of crystals, 331-332
 visual inspection, 330-331
- Crystal arrays, wiring techniques, 326-328
 choice of materials, 326
 electric contact strips, 326-327
 soldering precautions, 327
 wiring arrangements, 327-328
- Crystal blocks, design, 257-259
 cementing techniques, 96-97
 clamped drive, 255, 257, 258
 directivity patterns, 258
 foiling, 258
 inertia drive, 257-258
 size, 75
 symmetric drive, 258
- Crystal transducers
 see also Crystals
 applications, 27-29
 calibration tests, 22-27
 piezoelectricity, 1-4, 47-59
 power limitations, 27, 213
 typical units, 4-21
- Crystal transducers, component parts, 73-126
 acoustic windows, 113-119, 123, 336-338
 amplifiers, 74, 217-226
 backing plates, 75, 98-106, 263, 360-361
 cables, 214-216, 343, 346-347, 360-361
 case, 74-75, 333-350, 352-355
 crystal blocks, 75, 96-97, 257-259
 electronic system, 73
 inert materials, 119-126, 261-263, 319-321, 328-330
 liquids for filling, 124-125, 309, 347-350, 355
 matching network, 73-74, 351
 motor, 75, 107-112, 259-260
 single crystal plates, 75-95
 subassemblies, 95-97
- Crystal transducers, construction techniques, 267-357
 assembly and mounting, 95-97, 322-323, 350-357
 cements, 305-316
 GD28; 108-110
 housings and accessories, 333-350
 manufacturing requirements, 231
 precautions when handling crystals, 267-268
 preparation of arrays, 316-333
 preparation of individual crystals, 269-297
 storage conditions for crystals, 274-275
- Crystal transducers, design, 211-266
 see also Materials used in transducers
 application of Green's functions, 38-41
 application of Neumann boundary-value problem, 38-39
 application of reciprocity principle, 59-61, 132-134, 152-161
 backing plates, 103-106, 262-264, 322-323
 choice of basic design, 232-233
 choice of crystal material, 231-232
 clamped drive, 236-246, 258, 338
 crosstalk, 4, 265-266
 crystal array, 234, 259-260, 316-333
 crystal blocks, 75, 96, 257-259
 exterior case, 234-235
 groups of crystals, 257-259
 inertia drive, 246-249
 isolation material, 261-263
 lobe suppression, 142-145, 154-159, 259, 317-318
 response requirements, 235
 single crystals, 233-234, 255-257
 symmetric drive, 249-254
 tangential motion, 260-261
 windows, 264-265
- Crystal transducers, electronic design, 73, 211-229
 amplifiers, 74
 cables, 214-226, 343, 346-347, 360-361
 characteristics, 211-214
 equalizing networks, 226-229
 matching networks, 73-74, 216-217, 351
- Crystal transducers, general types, 4-7
 see also UCDWR transducers
 Bell Telephone Laboratories, 4
 Brush Development Company, 4
 clamped drive, 173-174, 236-246, 258, 338
 cylindrical, 134-139
 inertia drive, 173-174, 236, 246-249
 Submarine Signal unit, 4-7
 symmetric drive, 173-174, 236, 249-254
 unit-construction transducers, 97
- Crystal transducers, inspection techniques, 355-357
 see also Testing apparatus for transducers
 calibration, 357
 d-c resistance, 355-356
 leaks, 355-356
- Crystal transducers, performance limitations, 168-172
 cavitation, 27, 171-172, 213
 power, 27, 213
 receiving, 171
 transmitting, 168-171
- Crystal transducers, plane-radiating, 139-145
 directivity calculations, 140-142
 lobe suppression, 142-145
 sound field measurements, 142
- Crystal transducers, properties, 127-210
 analysis of equivalent circuits, 127-128, 173-182
 directivity, 139-152
 electrical characteristics, 211-214
 impedance, 85-87, 161-164, 177-178, 358-362
 modes, 98-102, 110-113, 257
 possible measurements, 128-129
 radiation theory, 129-139
 reciprocity, 152-161
 resonance, 112-113, 211-212
 response, 138-139, 164-168, 171, 235

- Crystal transducers, specific models
 BE, 4
 BG, 4
 CD, 7
 CJ, 7
 CP10Z, 236
 CQ4Z, 236
 CQ8Z, 4, 236, 338
 CY4; 7, 236, 249-254, 256
 EP, 7, 323-324
 FE2Z, 236, 246-249
 FG8Z, 236
 GA14Z, 236
 GD, 4
 GD22; 152
 GD28; 108-110
 GD34Z, 236
 JB, 4
 JB4Z, 236-246, 258-259
 JC2Z1; 110-112
 JK, 354
 KC, 4
 KC2; 236
 XCY8-1; 260-261
- Crystal transducers, specifications
 CY4; 249-250
 directivity, 230-231
 general requirements, 230-231
 impedance, 230
 JB4Z, 241
 manufacturing requirements, 231
 power, 230
 response, 230
- Crystals, 75-95
see also Ammonium dihydrogen phosphate crystals; Rochelle salt crystals
 electrodes, 93-95, 120, 282-287
 equivalent circuits, 77-87, 93, 173-174
 handling precautions, 267-268
 mounting techniques, 97
 processing techniques, 288-297, 305-306
 storage conditions, 274-275
 weakened crystals, 95
- Crystals, capacitance measurements, 300-304
 admittance measuring circuits, 301-302
 ammonium dihydrogen phosphate crystals, 300
 bridge circuit, 301
 dependent factors, 300
 formula for capacity ratio, 303-304
 frequency used, 300
 Rochelle salt crystals, 300-301
- Crystals, design
see also Ammonium dihydrogen phosphate crystals, processing; Rochelle salt crystals, processing
- clamped drive, 173-176, 178, 255, 257, 258
 coupling techniques, 123
 inertia drive, 173-178, 232-233, 256, 262-263
 optical orientation method for crystal bars, 278-279
 polarization, 287-288, 296, 331-332
 size of crystal, 233-234
 symmetric drive, 80, 173-180, 256, 258
 weakened crystals, 256-257
- Crystals, evaluation of constants, 87-93
 dielectric constant, 92-93
 effect of electrodes, 93-95
 piezoelectric coupling coefficient, 91-92
 resonance frequencies, 87-91
 summary, 93
- Crystals, properties, 268-275
 bandwidth, 82, 97
 chemical properties, 268-271
 crystallizing bars, 269, 272
 electrical properties, 270-271, 273
 impedance, 95
 low-frequency limit, 84-85
 resonance, 81-82, 108
 resonant frequency, 87, 175, 256-257, 303-305
 storage conditions, 274-275
 tangential motion, 260-261
 temperature limits, 306
 thermal behavior, 270, 273
- Crystals, specifications, 297-305
 admittance and Q , 302-303, 332
 capacitance, 300-302
 cement joints, 305-306
 d-c resistance, 305
 electrodes, 282
 geometric tolerances, 298
 high voltage, 305
 orientation, 298-300
 resonant frequencies, 303-305
 visible defects, 297
- Current-receiving response, 167, 181
 Current-transmitting response, 165-166, 179
- CY4 symmetric drive transducer, 7, 236, 249-254
 basic design, 250
 crystal, 250
 directivity pattern, 250-251, 256
 mechanical details, 251
 response, 251-254
 specifications, 249-250
- Cycle-Weld cement, use in transducers
 application technique, 312-314
 C-3; 123-124
- Cylindrical source, radiation resistance, 259
- Cylindrical transducers, radiation theory, 134-139
 directivity patterns, 135-136
 impedance, 136, 138
 incomplete arc, 136-138
 response, 138-139
- Damped resonance in transducers, 112
- Desiccants used in transducers, 125
- Design factors for transducers
see Crystal transducers, design
- Diaphragms for crystal arrays, 324-325
- Dichloro-difluoro methane for acoustic isolation, 328
- Dielectrics, theory, 44-47
 constant for crystals, 92-93
 dipole distribution, 44-46
 dissipation, 50-51
 linear, 46-47
- Dielectrics for transducer cables, 214-215
- Dimethyl phthalate for filling transducers, 347-348
- Dipole distribution in dielectrics, 44-46
- Directivity index
 calculation by reciprocity method, 159-161
 mathematical expression, 131
- Directivity of transducers, 139-152
 amplitude directivity, 130
 directivity factor, 22-25, 131, 148
 effect of case, 152
 effect of surface conditions, 151-152
 phasing, 145-148
 plane radiators, 139-145
 reciprocity theorem, 133
 specifications, 230-231
 theory, 40-41, 139
- Directivity patterns
 crystal blocks, 258
 CY4 transducer, 250-251, 256
 cylindrical transducer, 135-136
 effect of ρc rubber, 116
 GD22 transducer, 152
 intensity directivity, 22, 130
 pressure directivity, 22
- Direct-reading phase meter, 364-368
 accuracy, 367
 calibration, 367-368
 flip-flop circuit, 364-367
- Dow Corning fluids for filling transducers, 125, 348
- Duralumin backing plates, 322
- Echo ranging, transducer requirements, 28-29
- Efficiency of transducers, 159-161
- Elastics, nonviscous fluids, 37-42
 energy density and flux, 41-42
 field equations; boundary conditions, 37

- Green's functions, 38-41
 Neumann boundary-value problem, 38-39
 steady-state, 37-38
- Elastics, theory, 30-44
 application of Hooke's law, 35-36
 boundary conditions, 36-37
 displacement and strain, 31-34
 elastic stresses (equations of motion), 34-35
 energy density (generalized Hooke's law), 35-36
 intensity of crystal radiating into water, 30-31
 isotropic solids, 37
 physical principles, 31
 propagation of waves in a crystal-line medium having no sources, 35
- Elastics, viscous fluids, 42-44
 reflection conversion, 43-44
 steady-state boundary-value problem, 42-43
 tangential impedance, 43
- Electric analogues for crystals and transducers
see Equivalent circuits
- Electric network simulator (testing apparatus), 373-379
 inertia-driven, 374
 steel backing plate, 379
 transcendental impedance approximations, 373-374
- Electrical antiresonance of crystals, 83-84
- Electrical Q of transducer, 175-176, 212-213
- Electrodes for crystals, 282-287
 aluminum, 284-285
 effect on crystal constants, 93-95
 evaporated, 120, 282-284
 foils, 282, 285-286
 gold, 120, 282-284
 graphite, 285
 silver, 121, 284-286
 specifications, 282
 sprayed, 284-285
 tin-foil, 286-287
 use of cements, 286
- Electromechanical coupling coefficient, 91-92
- Electronic system of transducer, 211-229
 amplifiers, 74, 217-226
 cables, 214-216, 343, 346-347, 360-361
 characteristics, 211-214
 equalizing networks, 226-229
 matching networks, 73-74, 216-217, 351
- Energy density in piezoelectrics, 48-49
- EP transducer
 rubber diaphragm, 323-324
 window-coupled unit, 7
- Equivalent circuits for crystals, 77-87, 93, 173-174
 clamped drive, 173-174
 constant-voltage bandwidth, 82-83
 electrical antiresonance, transformation ratio, 83-84
 inertia drive, 173-174
 loaded rectangular crystal, 77-78
 low-frequency limit, 84-85
 mechanical arm, 78-79
 mechanical resonance and antiresonance, 81-82
 resistance and reactance, 79-81
 series-equivalent impedance, 85-87
 symmetrically driven, 173-174
- Equivalent circuits for transducers, 173-182
see also Network equivalent, transducer; Network simulator, transducer
 absolute magnitude of impedance, 181
 electrical Q , 175-177
 frequency, 175
 impedance, 177-178
 intensity, 180
 Mason circuit, 173
 mechanical Q , 176-177
 numerical values of constants, 181-182
 peak open-circuit voltage, 180
 peak short-circuit current, 181
 power factor, 181
 receiver responses, 180
 reciprocity principle, 59-61
 resistance, 177
 short-circuit response, 181
 theory, 127-128
 three basic drives, 173-174
 transmitter responses, 178-179
- Equivalent variational principle, 61-72
 boundary-value problem, 64-72
 steady-state boundary-value problem, 61-62
 theory, 62-64
- F9-5 μ c rubber, 264, 337
- Facings, transducer
see Materials used in transducers
- FE2Z inertia drive transducer, 236, 246-249
 crystals, 247-248
 design details, 248
 response, 248
- FG8Z transducer, 236
- Fillings for transducers
see Liquids for filling transducers
- Flexural modes in transducers, 98-102
 calculation, 98-99
 effect on overall response, 110-112
- groups of crystals, 257
 suppression, 101-102
- Fluids for filling transducers
see Liquids for filling transducers
- Foam rubber, 261-263
 Airfoam, 257, 262-263
 Cell-tite, 329-330, 346
 Cell-tite foam neoprene, 126
 elimination of cavity modes in transducer, 113
- Foamglas, use in transducers, 125-126, 262
- Formulas
 ammonium dihydrogen phosphate crystals, 271-272
 capacity ratio of crystals, 303-304
 directivity factor, 22-25, 148
 Rochelle salt, 268-269
- Four-terminal impedance, 163-164
- 45° Y-cut RS
see Rochelle salt crystals
- 45° Z-cut ADP
see Ammonium dihydrogen phosphate crystals
- Free-free crystal
 definition, 78
 resonance frequencies, 87
- Freon for acoustic isolation, 328
- Frequency, resonant
see Resonant frequency of crystals, measurement
- Frequency limit, low, of crystals, 84-85
- Frequency response of transducers
see Response of transducers
- GA14Z transducer, 236
- Galvanic series for sea water, 334
- GD transducer, 4
- GD22 transducer, directivity pattern, 152
- GD28 transducer
 construction, 108-110
 effect of backing plate on surface-velocity distributions, 108-110
 relative velocity of each crystal at resonance, 108
- GD34Z transducer, 236
- Geon for transducer cables, 214-215
- German silver, use in transducers, 121
- Glass backing plates
 advantages, 122, 263
 construction, 321
- Gold electrodes for crystals, evaporated, 120, 282-284
- Goodrich Company, B. F.
 compound 8388 rubber, 337
 μ c rubber, 123, 336
 Vulcalock, 123
- Graphite electrodes for crystals, 285
- Green's functions, application to transducer design, 38-41

- Hooke's law, application to elastics, 35-36
- Housing for transducers, 333-350
 acoustic-isolation material, 262
 bronze cases, 119
 corrosion-resisting coatings, 340-341
 coupling fluids, 74
 design, 234-235
 effect on directivity, 152
 function, 74
 metal castings, 335
 modes, 112-113
 rubber cases, 338-340
 seals, 341-344, 352-355
 sound-absorbing and -reflecting pads, 344-346
 tin-can cases, 335-336
- Housing for transducers, specifications, 333-335
 corrosion resistance, 334-335
 leakage, 333-334
 materials, 333-334
 mechanical strength, 334
- Huygens-Fresnel principle, application to transducer design, 39
- Hy-bridge (impedance bridge), 361-362
- Hydraulic gaskets for sealing transducer cases, 341, 354-355
- Hydrophone, equivalent circuit for low-frequency limit, 85
- Impedance measurements, transducer, 358-362
 absolute magnitude, 162-163, 181, 358-359
 boundary conditions, 36
 bridge methods for two- and three-terminal networks, 360-362
 circuit requirements, 359
 comparison with capacitor, 212-213
 effect of cable, 360-361
 equivalent circuits, 177-178
 rectangular crystal, 77
 series-equivalent impedance, 27, 85-87
 specifications, 230
 Young's modulus, 87-91
- Impedance of symmetrically-driven crystals, 178
- Impedance quantities characteristic of transducers
 blocked impedance, 161
 motional impedance, 161-162
 radiation impedance, 40-41, 131-132, 177, 259
 tangential impedance, 43
- Impedance transforming network, 217
- Inertia-driven crystals, design
 cementing requirements, 256
 determination of size, 233
 equivalent circuit, 173-174
 gas-filled unit, 262
 liquid-filled unit, 262
- Inertia-driven crystals, properties
 electrical Q , 176
 evaluation, 232-233
 groups of crystals, 257-258
 impedance, 178
 intensity, 180
 maximum short-circuit current, 181
 mechanical Q , 176-177
 resistance, 80-81, 177
 resonant frequency, 175
- Inertia-driven transducers
 FE2Z, 236, 246-249
 GD34Z, 236
 rubber diaphragm, 323-325
 simulated network, 374
- Intensity directivity pattern, 22, 130
- Intensity radiated from crystal faces, 30-31, 180
- Inverse piezoelectric effect, 1
- Iron, use in transducers, 120-121
- Isolation materials for transducers
see Acoustic-isolation materials
- Isotropic solids, theory, 37
- JB transducer, 4
- JB4Z transducer, 236-246
 choice of crystals, 241
 crystal size and shape, 241-242
 crystal spacing, 258
 design details, 241-242
 response, 243-246
 specifications, 241
- JC2Z1 transducer, response, 110-112
- JK transducer, 354
- KC transducer, 4
- KC2 transducer, 236
- Koroseal for transducer cables, 214-215
- Lead backing plates, 121, 321-322
- Liquids for filling transducers, 347-350
 butyl phthalate, 124-125
 castor oil, 124-125, 347-350
 characteristics and specifications, 347-348
 dehydration, 348-350
 dimethyl phthalate, 347-348
 effect on cements, 309
 filling technique, 355
 olive oil, 347-348
 petroleum oils, 125
 silicones, 106, 125, 348
 Ucon oil, 348
- Listening, transducer requirements, 27-28
- Lobe suppression in transducers, 154-159
 by crystal spacing, 145
 design requirements for crystal array, 259, 317-318
 effect on radiated power, 154-156
 effect on receiving response, 158
 method for circular arrays, 159
 plane radiators, 142-145
 series-parallel arrangements, 158
- Lucite acoustic windows, 116-117, 122
- M-163 ρ c rubber, 336-337
- Magnesium backing plates, 121
- Manufacturing requirements for transducers, 231
- Mason circuit
 approximation for boundary-value problem, 67-69
 equivalent for transducers, 173
- Matching networks for transducers
 design, 73-74, 216-217
 installation, 351
- Materials, crystal
see Ammonium dihydrogen phosphate crystals; Rochelle salt crystals
- Materials used in transducers
 acoustic-isolation materials, 125-126, 261-263, 265-266, 328-330
 cements, 95-96, 123-124, 287, 305-316
 desiccants, 125
 galvanic series for sea water, 334
 glasses and ceramics, 122-123, 263, 321
 liquids, 124-125, 309, 347-350
 magnesium, 121
 metals, 117-121, 319-321
 plastics, 117, 121-122, 321
 rubber, 114-116, 324-325, 329-330, 336-340
- Mechanical antiresonance of crystals, 82
- Mechanical Q of transducers, 176-177
- Mechanical resonance of crystals, 81-82
- Meehanite backing plates, 120
- Metal castings for transducer housings, 335
- Metals used in transducers, 119-121
 aluminum, 119, 284
 brass, 119
 bronze, 119
 cadmium, 119
 Cerrobend, 110-111, 321
 copper, 119-120
 Duralumin, 322
 German silver, 121
 gold, 120, 282-284
 iron, 120-121
 lead, 121, 321-322
 Meehanite, 120
 silver, 121, 284-286
 steel, 117-119, 319-321
 tin, 121, 286-287, 335-336
 Wood's metal, 121
 zinc, 121
- Modes in transducers, 110-113
 cavity, 113

- flexural, 98-102, 110-112, 257
 parasitic, 112-113
 vibrational, 98
- Molecular piezoelectricity, 1
- Monel screen (sound-absorbing pad), 345
- Motional impedance, transducer, 161-162
- Motor of transducer, probe examination techniques, 75, 107-112
 GD28 transducer, 108-110
 JC2Z1 transducer, 110-112
 measurements in air and oil, 107
 multiple, 259-260
 velocity distribution, 107
- Mountings for transducers
see Assembly and mounting of transducers
- Naval Research Laboratory
 mounting of crystals, 97
 ρ c rubber, 264, 337
- Neoprene
 acoustic windows, 116, 265
 Cell-tite foam neoprene, 126
- Network equivalent, transducer
see also Equivalent circuits for transducers
 equalizing, 226-229
 impedance transforming network, 217
 matching, 73-74, 216-217, 351
 power factor correcting network, 216
 two- and three-terminal, 360-362
- Network simulator, transducer, 373-379
 inertia-driven, 374
 steel backing plate, 379
 transcendental impedance approximations, 373-374
- Neumann boundary-value problem, application to transducer design, 38-39
- Norace cement, application technique, 315
- Norton Company, Norace cement, 315
- NRL (Naval Research Laboratory)
 mounting of crystals, 97
 ρ c rubber, 264, 337
- Nylon acoustic windows, 117
- Oil filling of transducers
 castor oil, 124-125, 347-350
 olive oil, 347-348
 petroleum, 125
 Ucon oil, 348
- Oil plugs for sealing transducer cases, 343-344
- Olive oil, disadvantages for filling transducers, 347-348
- Open-circuit response, transducer, 166-167, 180
- Optical orientation method for crystal bars, 278-279
- O-ring hydraulic gaskets for sealing transducer cases, 341, 354-355
- Paints, antifouling, 341
- Parasitic modes in transducers
 case modes, 112-113
 cavity modes, 113
 types of resonance, 112-113
- Petroleum oils for filling transducers, 125
- Phase meter, direct-reading, 364-368
 accuracy, 367
 calibration, 367-368
 flip-flop circuit, 364-367
- Phase variation of transducers, 145-148
- Phenomenological piezoelectricity, 1
- Piezoelectric coupling coefficient of crystals
 ammonium dihydrogen phosphate, 91-92
 Rochelle salt, 91-92
- Piezoelectrics, matrix formulations, 51-59
 ammonium dihydrogen phosphate crystals, 55-57
 matrices for rotated cuts, 56-59
 Rochelle salt crystals, 54-59
 strain matrix, 52
 stress matrix, 52
 symmetry reduction of the matrices, 54-56
- Piezoelectrics, theory, 1-2, 47-59
 direct and inverse effect, 1
 energy density, 48-49
 equations of propagation, 49
 equations of state, 48-49
 internal viscous and dielectric dissipation, 50-51
 molecular, 1
 phenomenological, 1
 surface dissipation, 49-50
- Pittsburgh-Corning Glass Company, foamglas, 125-126
- Plastics used in transducers
 Bakelite, 121
 Lucite, 116-117, 122
 Plexiglas, 122
 polystyrene, 122
 Polythene (polyethylene), 122, 214-215
 Tenite II; 117
- Plexiglas, properties, 122
- PN crystals
see Ammonium dihydrogen phosphate crystals
- Polarization, crystal equipment, 296
 inspection, 331-332
 marking, 288
 technique, 287-288
- Polystyrene, advantages for transducers, 122
- Polythene (polyethylene)
 for transducer cables, 214-215
 properties, 122
- Porcelain enamel, insulating material for transducers, 122
- Power factor correcting network, 216
- Power limitations, transducer, 27, 213
- Power output of transducers
 effect of lobe suppression, 154-156
 equivalent circuit, 181
 specifications, 230
 transmitting response, 166
- Power requirements for transducers, 230
- Pressure directivity pattern, 22
- Probe microphone for testing transducers, 7, 362-364
see also Motor of transducer, probe examination techniques
- Pulse modulator, 368-371
- Pulsed power amplifier, 224
- Punch-Lok Company, transducer bands, 353
- Q of crystal
 electrical, 175-176
 mechanical, 176
 specifications, 302-303
- Q of transducer, 175-177
 electrical, 175-176, 212-213
 mechanical, 176-177
- QBF-type-backing plates, 102
- Radiation impedance, 131-132
 clamped drive crystals, 177
 cylindrical source, 135-136, 138, 259
 dependent factors, 132
 method of measuring, 132
 symmetrically-driven crystals, 177
 theory of calculations, 40-41
- Radiation patterns
see Directivity patterns
- Radiation theory, 129-139
 cylindrical transducers, 134-139
 reciprocity, 132-134
 sound field, 129-131
- Reactance of crystals, equivalent circuit, 79-81
 blocked, 80
 inertia drive, 80-81
- Receiving patterns
see Directivity patterns
- Receiving response of transducers
 effect of lobe suppression, 158
 equivalent circuits, 180
 limitations, 171
 matched-receiver, 167
 open-circuit, 166-167

- short-circuit, 167
- voltage response, 166-167, 180
- Reciprocity principle, application to transducers, 132-134, 152-161
- calibration of transducers, 133-134
- directivity, 133
- directivity index, 159-161
- equivalent circuit, 59-61
- lobe suppression, 154-159
- theory, 132
- Rectangular crystal, equivalent circuit, 77-78
- Reflectoriascope for optical orientation of crystal bars, 278
- Resistance of crystals, equivalent circuit, 79-81
- blocked, 80
- inertia drive, 80-81
- symmetric drive, 80
- Resistance of transducer, equivalent circuit, 177
- Resonance of crystals
- mechanical, 81-82
- relative velocity at resonance, 108
- Rochelle salt, 98
- Resonance of transducers, 112-113, 211-212
- Resonant frequency of crystals, measurement
- admittance measuring circuit, 304
- clamped drive, 175
- definition, 303
- free-free crystal, 87
- inertia drive, 175
- method of lowering, 256-257
- specifications, 303-305
- symmetric drive, 80
- symmetrically driven crystals, 175
- Response of transducers
- calibration tests, 22-25
- curves, 212
- design requirements, 235
- effect of flexural modes, 110-112
- receiving, 158, 166-167, 171, 180, 181
- short-circuit, 167, 181
- specifications, 230
- system response, 167-168
- transient response, 168
- transmitting, 164-166, 178-179
- ρ c rubber, 336-337
- acoustic windows, 114-116, 123, 264
- Bell Telephone Laboratories (M-163 rubber), 336-337
- B. F. Goodrich Company (79-SR-32 rubber), 121, 336
- effect on directivity patterns, 116
- Naval Research Laboratory (F9-5 rubber), 264, 337
- Rochelle salt, molten (cement), 124, 315
- Rochelle salt crystals
- capacitance measurements, 300-301
- comparison with ammonium dihydrogen phosphate, 231-232
- formula, 268-269
- matrix formulations using crystallographic axes, 54-56
- matrix formulations using rotated axes, 57-59
- solution of boundary-value problem, 64-72
- summary of constants, 93
- synthetic, 269-270
- X-cut, use as research tool, 371-373
- Rochelle salt crystals, characteristics
- chemical properties, 268-269
- dielectric constant, 92-93
- dimensions required for resonance at 40 kc, 98
- electric properties, 270
- electromechanical coupling coefficient, 91-92
- impedance, 212-213
- leakage conduction, 273-274
- thermal behavior, 270
- upper temperature limit, 306
- Rochelle salt crystals, processing
- factors controlling successful crystallization, 269-270
- grinding, 288-289
- milling, 294
- orientation of bars, 275-276
- rough-cutting from bars, 276
- sawing, 291-292
- spliced crystals, 281
- surface finishing, 277
- Röhm and Haas, Acryloid B-7 cement, 287, 315-316
- Rosin, use in transducers, 124
- RS crystals
- see* Rochelle salt crystals
- Rubber acoustic windows, 336-338
- acceptance test, 337
- advantages, 114-116
- compound 8388; 337
- deterioration, 340-341
- metal bonds, 337-338
- neoprene, 116, 265
- ρ c rubber, 114-116, 123, 336-337
- steel reinforcements, 116
- Rubber cases, transducer, 338-340
- cylindrical cases, 338-339
- molded-rubber cases, 339
- steel-reinforced rubber, 339-340
- Rubber diaphragms for crystal arrays, 324-325
- Rubber materials used in transducers
- Airfoam rubber, 257, 262-263
- Cell-tite, 126, 329-330, 346
- compound 8388; 337
- ρ c rubber, 114-116, 123, 264, 336-337
- SA60 transducer cable, 346
- Schering impedance bridge, 360
- Sealing methods for transducer cases, 341-344, 352-355
- banding rubber cylinders, 352-353
- crimp-sealing, 355
- gaskets, 341, 353-354
- glass-metal terminal seals, 342-343
- oil plugs, 343-344
- O-ring hydraulic gaskets, 341, 354-355
- Punch-Lok bands, 353
- Sensitivity of transducers
- see* Receiving response of transducers
- Short-circuit response, transducer equivalent circuit, 181
- receiving, 167
- Silica gel, use in transducers, 125
- Silicones for filling transducers, 106, 125, 348
- Silver foil electrodes for crystals, 121, 284-286
- Simplex No. 9061 transducer cable, 346, 361
- Slotted square bar backing plates, 102
- Sound field, radiation theory, 129-131
- pressure, 130
- radiation zone, 130
- Sound field measurements, 142
- Sound-absorbing pads, 344-346
- Sound-reflecting pads, 346
- Sound-water rubber, 336-337
- acoustic windows, 114-116, 123, 264
- Bell Telephone Laboratories (M-163 rubber), 336-337
- B. F. Goodrich Company (79-SR-32 rubber), 123, 336
- effect on directivity patterns, 116
- Naval Research Laboratory (F9-5 rubber), 264, 337
- Specifications
- cables for transducers, 346
- crystals, 282, 297-306
- filling liquids for transducers, 347-348
- housing for transducer, 333-335
- transducers, 230-231, 241, 249-250
- Sperti Incorporated, glass-metal terminal seals for transducer cases, 342-343
- Sponge Rubber Products Company, Cell-tite foam neoprene, 126
- Stack transducers, crystal arrays
- assembly, 319
- design, 325-326
- Steel acoustic windows, 117-119
- angular variation in transmission, 118
- double-layer construction, 118-119
- transmission loss, 118

- Steel backing plates, construction, 319-321
- Steel-reinforced rubber transducer cases, 339-340
- Storage of crystals, 274-275
- Strain matrix for piezoelectrics, 52
- Stress formulas, elastic, 34-35
- Stress matrix for piezoelectrics, 52
- Stupakoff Ceramic and Manufacturing Company, glass-metal terminal seals for transducer cases, 342-343
- Submarine Signal transducer, 4-7
- Symmetrically-driven crystals, 173-180
design, 256
electrical Q, 175-176
equivalent circuit, 173-174
groups of crystals, 258
impedance, 178
intensity, 180
mechanical Q, 176
radiation resistance, 177
resistance, 80
resonant frequency, 175
- Symmetrically-driven transducers
CY4; 7, 236, 249-254, 256
KC2; 236
- Synthetic Rochelle salt crystals, 269-270
- Synthetic rubber (neoprene)
acoustic windows, 116, 265
Cell-tite foam neoprene, 126
- Tangential impedance of crystals, 43
- Tangential motion in crystals, 260-261
- Temperature limits of crystals, 306
- Tenite acoustic windows, 117
- Terminal box seals, transducer
see Sealing methods for transducer cases
- Testing apparatus for transducers, 316-379
see also Crystal transducers, inspection techniques
direct-reading phase meter, 364-368
electric network simulator, 373-379
probe microphone, 7, 362-364
pulse modulator, 368-371
use of 45-degree X-cut RS as a research tool, 371-373
- Theory of crystal transducers
see Piezoelectrics, theory
- Thermoplastic cements, 314-315
Butacite VF-7100; 314
Vinylseal, 281
- Three-terminal networks, transducer, 163-164, 360-362
- Tin, use in transducers
crystal electrodes, 286-287
metal plating, 121
transducer housing, 335-336
- Transducers
see Crystal transducers
- Transmitting limitations of transducers, 168-171
partially loaded transmitters, 170-171
short pings, 170
steady-state operation, 168-170
- Transmitting patterns
see Directivity patterns
- Transmitting response of transducers, 164-166
constant-current, 165-166, 179
constant-power, 166
constant-voltage, 164-165, 179
equivalent circuits, 178-179
idealized amplifier, 179
- Two-terminal networks, transducer, 163, 360-362
- Ty-ply, use in transducers, 338, 346-347
- UCDWR
acoustic ammeter, 7
probe microphone, 7, 362-364
- UCDWR transducers
BE, 4
BG, 4
CD and CJ, 7
CP10Z, 236
CQ, 318
CQ4Z, 236
CQ8Z, 4, 236, 338
CY4; 7, 236, 249-254, 256
EP, 7, 323-324
FE2Z, 236, 246-249
FG8Z, 236
GA14Z, 236
GD, 4
GD34Z, 236
JB, 4
JB4Z, 236-246, 258
KC, 4
KC2; 236
- Ucon oil 50-HB-100 for filling transducers, 348
- Underwater transducers
operation, 1
purpose, 1
types of crystals, 1-2
- Union Carbide and Carbon Company, Ucon oil, 348
- Unit-construction transducers, 97
- University of California Division of War Research
see UCDWR
- Univis oil, use in transducer backing plates, 106
- Urea formaldehyde cement, application technique, 315
- Variational principle, equivalent for transducers, 61-72
boundary-value problem, 64-72
steady-state boundary-value problem, 61-62
theory, 62-64
- Vibrational modes in transducer, 98
- Vinyl chloride plastics for transducer cables, 214-215
- Vinylite for transducer cables, 214-215
- Vinylseal cement for consolidating transducers, 281
- Voltage receiving response, 166-167, 180
- Voltage transmitting response, 164-165, 179
- Vulcalock cement, use in transducers
application technique, 307-309
density, 123
disadvantages, 309
effect of transducer liquid, 309
electroding crystals, 286
- Windows, acoustic, 113-119
design, 264-265
function, 113
Lucite, 116-117, 122
materials, 116
nylon, 117
rubber, 114-116, 123, 264, 336-338
steel, 117-119
Tenite, 117
transmission of plane waves, 113-114
- Wood's metal, use in transducers, 121
- XCU 16257 cement, 315
- X-cut Rochelle salt crystal, use as research tool, 371-373
limitations, 372-373
radiation problems, 371
technique, 372
- XCYS-1 transducer, 260-261
- Y-cut RS
see Rochelle salt crystals
- Young's modulus for crystal impedance, 87-91
- Z-cut ADP
see Ammonium dihydrogen phosphate crystals
- Zinc, use in transducers, 121

THIS ITEM CONTAINS SOME ILLUSTRATIONS WHICH
CANNOT BE REPRODUCED SATISFACTORILY BY EITHER
THE ELECTROSTATIC OR THE PHOTOSTATIC PROCESS.

THIS ITEM CONTAINS SOME ILLUSTRATIONS WHICH
CANNOT BE REPRODUCED SATISFACTORILY BY EITHER
THE ELECTROSTATIC OR THE PHOTOSTATIC PROCESS.

Xerox

~~11.00~~ 35.50
Neg 35-mm microfilm 11.00

NEG 6/64

LIBRARY OF CONGRESS



0 028 963 457 5